The Synthesis of Chromane Meroterpenoids via Biomimetic Cascade Reactions

Aaron John Day

B. sc. (Hons.)

A thesis submitted in total fulfilment of the requirements for the degree of Doctor of Philosophy

THE UNIVERSITY of ADELAIDE

2021

Department of Chemistry, The University of Adelaide

In Memory of My Dog Jasper

Man's Best Friend

I – Declaration

I certify that this work contains no material which has been accepted for the award of any other degree or diploma in my name, in any university or other tertiary institution and, to the best of my knowledge and belief, contains no material previously published or written by another person, except where due reference has been made in the text. In addition, I certify that no part of this work will, in the future, be used in a submission in my name, for any other degree or diploma in any university or other tertiary institution without the prior approval of the University of Adelaide and where applicable, any partner institution responsible for the joint-award of this degree.

I acknowledge that copyright of published works contained within this thesis resides with the copyright holder(s) of those works.

I also give permission for the digital version of my thesis to be made available on the web, via the University's digital research repository, the Library Search and also through web search engines, unless permission has been granted by the University to restrict access for a period of time.

I acknowledge the support I have received for my research through the provision of an Australian Government Research Training Program Scholarship.

___ 3/3/21

Aaron J. Day Date

II – Acknowledgements

The work presented in this thesis would not have been possible without the generous support of my supervisor Asoc. Prof. Jonathan George. Not only has Jonathan been the principal source of ideas for the projects which I have been fortunate to work on, he has also been a powerful source of inspiration with his infectious enthusiasm for synthetic organic chemistry. Thank you.

Secondly, I would like to thank my co-supervisors Prof. Simon Pyke and Dr. Christopher Newton for the advice they have given me throughout my PhD. I would also like to thank Dr. Thomas Fallon, who has been a wealth of knowledge and has always been willing to talk through chemistry problems and suggest experiments to overcome the many challenges that come with total synthesis.

I am also grateful to the various collaborators I have had the opportunity to work with over the past four years. Thank you to Asoc. Prof. Stephen Bell and Joel Lee for their chemoenzymatic experiments on the bruceol and rhodonoid projects. Thank you to Dr. Wolfgang Lewandrowski and Dr. Carole Elliott from Peth Botanic Gardens and Kings Park Authority for providing me with an enormous amount of *Philotheca brucei* plant material. Thank you to Dr. Gavin Flematti from the University of Western Australia for providing me with a fifty-year-old authentic sample of bruceol from its original isolation. And thank you to Dr. Adam Ametovsky from Prof. David Lupton's research group at Monash University for running analytical chiral HPLC on my behalf.

When I first joined the George group in 2016 my laboratory skills were virtually non-existent; I am truly in debt to the mentors I had, first as an honours student, then as an early PhD. Student. Thank you to Kevin, Justin, Adrian, and special thank you to Hilton and Henry for not only teaching me basic lab skills, but also for teaching me what it means to be a chemist.

Another special thank you goes to Oussama (SD) who brought a fresh burst of enthusiasm and vitality when he joined the university in 2018, but more importantly, has been a good friend and drinking buddy.

I would also like to thank Lauren, Stefania, and Laura who started their PhD.s with me in 2017. It has been a pleasure to share this experience with such a dynamic group of young scientists, it is wonderful to see how far we have come. A special thank you goes to Laura (TD), who work extensively on chromene chemistry alongside me and has become a true expert of the field. Working together on the rubiginosins project was an exciting and enjoyable “last dance” for my candidature.

I would like to thank JP (LD) who worked consistently with me as a placement student over almost two years. He is a true prodigy and I wish him the best of luck for the remainder of his PhD. with Jin-Quan Yu at the Scripps Research Institute in La Jolla, California.

To the newest members of the George group, Jacob, Tomas, Sarah, and Andreas, I wish you the best of luck with your PhD.s.

Lastly, I would like to thank my friends and family for their constant support throughout my candidature.

III – List of Abbreviations

Ac	acetyl
AIBN	azobisisobutyronitrile
Am	amyl (pentyl)
Bn	benzyl
bpy	bipyridyl
Bu	butyl
Bz	benzoyl
COSY	correlation spectroscopy
Cp	cyclopentadienyl
m-CPBA	*m*-chloroperoxybenzoic acid
CSA	camphorsulfonic acid
dba	dibenzylideneacetone
DCE	1,2-dichloroethane
DDQ	2,3-dichloro-5,6-dicyano-1,4-benzoquinone
DEAD	diethyl azodicarboxylate
DMAP	4-dimethylaminopyridine
DMAPP	dimethylallyl pyrophosphate
DMDO	dimethyldioxirane
DMF	*N*,*N*-dimethylformamide
DMP	Dess-Martin periodinane
Et	ethyl
EDDA	ethylenediamine diacetate
EDG	electron donating group
EWG	electron withdrawing group
FCC	flash column chromatography
fod	6,6,7,7,8,8,8-heptafluoro-2,2-dimethyl-3,5-octanedionato
GC	gas chromatography
HMDS	hexamethyldisilazide
HPLC	high performance liquid chromatography
HOMO	highest occupied molecular orbital
IBX	2-iodoxybenzoic acid
J	coupling constant
LED	light emitting diode
Me	methyl
m.p.	melting point
NADPH	nicotinamide adenine dinucleotide phosphate
NBS	*N*-bromosuccinamide
NCS	*N*-chlorosuccinamide
NIS	*N*-iodosuccinamide
NMR	nuclear magnetic resonance
Nu	any nucleophile
NOESY	nuclear Overhauser effect spectroscopy
[O]	oxidation
o-QM	*o*-quinone methide
PCC	pyridinium chlorochromate
PDC	pyridinium dichromate
Ph	phenyl
PHWE	pressurised hot water extraction
PPTS	pyridinium *para*-toluenesulfonate
Pr	propyl
R	radical, any carbon substituent
[R]	reduction
r.t.	room temperature
TBAB	tetrabutylammonium bromide
TBAF	tetrabutylammonium fluoride
Tf	trifluromethylsulfonyl
TLC	thin layer chromatography
TPP	tetraphenylporphyrin
UV	ultraviolet

IV – Abstract

In the current climate of synthetic organic chemistry the development of efficient, practical organic synthetic methodologies is of the utmost importance. Of particular interest is the rapid generation of molecular complexity. The field of biomimetic synthesis uses natural product biosynthesis as a guide, or source of inspiration for laboratory total synthesis. Nature often employs cascade or domino reactions which are chemically predisposed to occur. In this thesis the biomimetic synthesis of several chromane (benzopyran) natural products is reported.

Chapter 1 is an introductory essay on the development of biomimetic cascade reactions with several examples from the past 40 years. This chapter also introduces *ortho*-quinone methides, a reactive intermediate which visited frequently throughout this thesis.

Chapter 2 describes the three-step divergent synthesis of rhodonoid C and D, and synthesis of the related alkaloid murrayakonine D. Herein a new bioinspired acid-catalysed (3+2) epoxyolefin cycloaddition produced two rings, three stereocentres, one C-C bond, and one C-O bond in a single step.

In Chapter 3 the first asymmetric synthesis of (−)-bruceol – a caged pyranocoumarin meroterpenoid – is detailed. The concise three-step synthesis utilised a biomimetic cascade initiated by a chemoselective Jacobsen-Katsuki epoxidation (and kinetic resolution) as the key step. This reaction could also be catalysed by a bacterial cytochrome P450 monooxygenase enzyme. NMR analysis of synthetic bruceol lead to the discovery of isobruceol, an isomeric meroterpenoid which had been misidentified as bruceol. This was confirmed by re-isolation, total synthesis, and X-ray analysis of isobruceol.

Chapter 4 covers the synthesis of several bruceol related natural products via photochemical reactions. Chromenes are intrinsically good chromophores, and as such mild solar irradiation of the chromene precursors to bruceol and isobruceol completed the synthesis of the "cyclol" natural products eriobrucinol, isoeriobrucinol A, and isoeriobrucinol B by intramolecular [2+2] cycloaddition reactions. These chromenes also underwent singlet oxygen ene reactions to complete the synthesis of protobruceols II – IV.

Chapter 5 looks at the biosynthesis of seven unnamed prenylated bruceol derivatives. Speculating on the observed isolated compounds, it likely all seven natural products had the common precursor we coined "prenylbruceol A". It had previously been suggested the biosynthesis of these compounds involves what we consider to be an unlikely *C* alkylation. We put forth an alternative proposal involving *O* alkylation, followed by Claisen and Cope rearrangements to reach the correct connectivity for an intramolecular hetero-Diels-Alder reaction. This hypothesis was the basis for an attempted biomimetic synthesis of prenylbruceol A. After this approach was unsuccessful two alternative approaches were taken which were also ultimately unsuccessful. In lieu of a total synthesis, the isolation of the prenylbruceols was revisited through a mild extraction of *Philotheca myoporoides* using the pressurised hot water extraction technique. Gratifyingly, the extraction yielded prenylbruceol A proving that it is indeed a natural product. The natural prenylbruceol A was then used in a semisynthesis of three other members of the family (prenylbruceols B – D) using singlet oxygen chemistry.

V – List of Publications

The following journal articles were published based on work done during the candidature of this PhD.

1) **Aaron J. Day**; Hiu C. Lam; Christopher J. Sumby; Jonathan H. George. **2017** *"Biomimetic Total Synthesis of Rhodonoids C and D, and Murrayakonine D"*, *Org. Lett.*, *19*, 2463.

2) **Aaron J. Day**, Joel H. Z. Lee, Quang D. Phan, Hiu C. Lam, Adam Ametovski, Christopher J. Sumby, Stephen G. Bell, Jonathan H. George. *"Biomimetic and Biocatalytic Synthesis of Bruceol"*, *Angew. Chem. Int. Ed.* **2019**, *58*, 1427.

3) Jacob D. Hart, Laura J. Burchill, **Aaron J. Day**, Christopher G. Newton, Christopher J. Sumby, David M. Huang, Jonathan H. George *"Visible Light Photoredox Catalysis Enables the Biomimetic Synthesis of Nyingchinoids A, B and D, and Rasumatranin D"*, *Angew. Chem. Int. Ed.* **2019**, *58*, 2791.

4) **Aaron J. Day**, Christopher J. Sumby, Jonathan H. George *"Biomimetic Synthetic Studies on the Bruceol Family of Meroterpenoid Natural Products"*, *J. Org. Chem.* **2020**, *85*, 2103.

5) **Aaron J. Day**, Jonathan H. George, *"Isolation and Biomimetic Oxidation of Prenylbruceol A, an Anticipated Meroterpenoid Natural Product from Philotheca myoporoides"*, *J. Nat. Prod.* **2020**, *83*, 2305.

6) Laura Burchill, **Aaron J. Day**, Oussama Yahiaoui, Jonathan H. George *"Biomimetic Total Synthesis of the Rubiginosin Meroterpenoids"*, *Org. Lett.* **2021**, *23*, 578.

VI – Table of Contents

Chapter 1: Introduction

This chapter serves as a general introduction to the chemistry discussed throughout this thesis.

1.1 The Chemistry of Natural Product Synthesis

Organic synthesis is a sub-category of synthetic chemistry focused specifically on the reactions of organic molecules (carbon containing molecules). Broadly, there are two main facets of organic synthesis: synthetic methodology and total synthesis. Methodology is the development of synthetic reactions (reactions being the "tools" of the synthetic chemist), and total synthesis is the preparation of a chemical compound using synthetic methods. There has long been interplay between these sub-categories, as chemists wishing to synthesise molecules have needed to develop new reactions, and chemists working on methodologies have used total synthesis as a means to validate their new reactions.

In this era of 165 years of modern organic chemistry (marked arbitrarily by Perkin's 1856 synthesis of mauveine[1] and subsequent birth of the synthetic dye industry) almost any stable molecule imaginable could be synthesised given enough time and effort. Particularly in the mid-20th century organic chemistry had reached a level of maturity where the synthesis of the seemingly impossible became possible (Figure 1.1).

The legendary Robert Robinson said of his work on the attempted synthesis of brazilin (**1.1**) *"the synthesis of brazilin would have no industrial value; its biological importance is problematical, but it is worthwhile to attempt it for the sufficient reason that we have no idea how to accomplish the task."* This justification is summarised as "synthesis for the sake of synthesis" (often pejoratively). Robinson had worked on **1.1** as part of his doctoral thesis with W. H. Perkin Jr. (1905 – 1909) and continued this work throughout his life, completing the synthesis in 1970, 5 years before his death.[2]

The epitome of "synthesis for the sake of synthesis" is perhaps Woodward and Eschenmoser's landmark conquest over vitamin B12 (**1.3**). Here over 100 chemists were able to complete the "long and formidable" preparation of **1.3** in 73 steps.[3] The justification of such an endeavour is not immediately clear. B12 (**1.3**) is widely available from natural sources – a synthesis would never have any commercial use. Furthermore, the structure **1.3** had already been proven by X-ray diffraction in 1955.[4] Woodward saw beauty in what he described as this "exotic and marvellous natural product". New strategies were required to progress through this challenge, and the research here lead directly to the Woodward-Hoffman principles of orbital symmetry conservation and creation of the Eschenmoser sulfide contraction reaction.

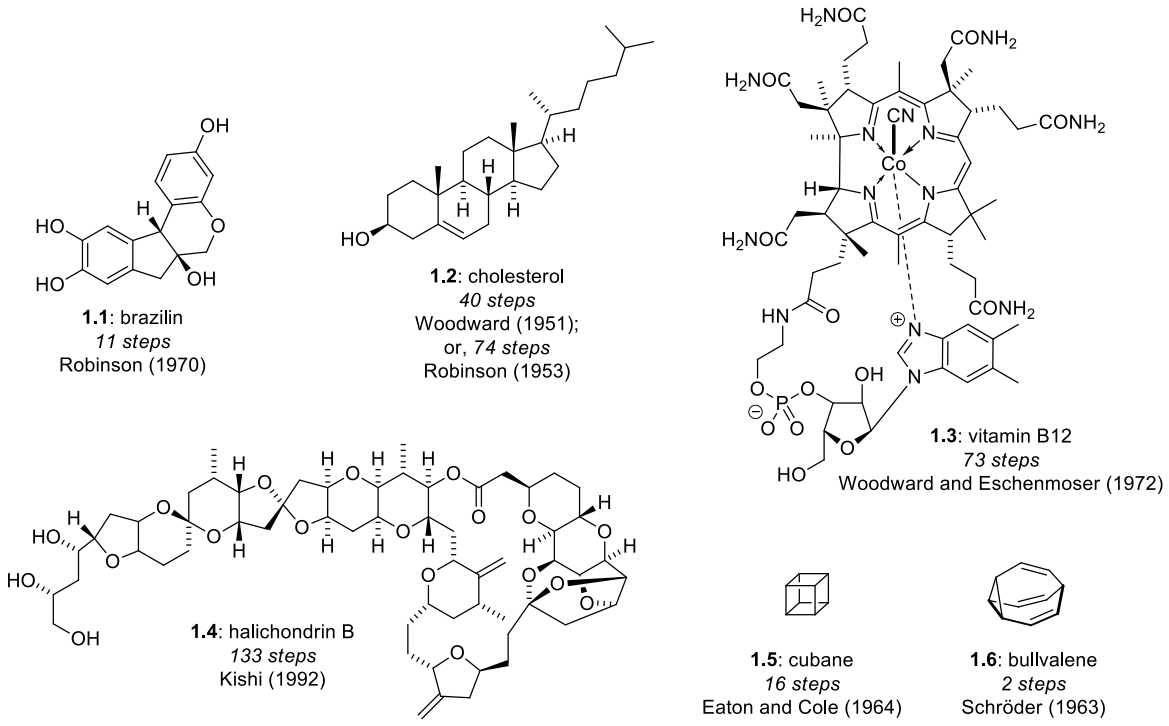

Figure 1.1: Natural and unnatural targets of total synthesis from the mid-20th century.

Further examples from Woodward and Robinson comes from their respective syntheses of cholesterol (**1.2**)[5], a terpenoid of major biological importance. Kishi and co-worker's synthesis of the marine sponge polyketide halichondin B (**1.4**)[6] not only completed a herculean challenge but also resulted in the development of eribulin,[7] an FDA approved anti-cancer drug who's structure contains the macrocycle of the right-hand side of **1.4** (as drawn). The reach of synthetic chemistry is not limited

to the molecules of nature, but indeed by the imaginations of chemists. Molecules of theoretical interest such as cubane (**1.5**)[8] or the perpetually fluctional bullvalene (**1.6**)[9] have been thrust to reality thanks to the dedication and planning of synthetic chemists.

These and the many other great feats of organic synthesis have only been possible through a keen understanding of chemical reactivity. The most broadly applicable reactions are those which occur universally and reliably on set functional groups. These allow the iterative and methodical manipulation of simple feed-stock chemicals to the impressive architecture of Figure 1.1 and beyond.

1.2 Cascade or Domino Reactions in Organic Synthesis

1.2.1: An Alternative to Classical Synthesis

The classical approach to synthesis is here defined as the stepwise transformation of one (often structurally similar) molecule using well defined reactions to form the synthetic target. This is exemplified nicely in Willsätter's 1911 synthesis of cyclooctatetraene (**1.10**) a molecule of importance to the understanding of anti-aromaticity (Scheme 1.2).[10] Here the semisynthetic amine **1.7** can be methylated and undergo Hoffman elimination to form cyclooctatriene (**1.8**). Dibromination and amine substitution allows a double Hoffmann elimination of **1.9** to the desired cyclooctatetraene **1.10**. Syntheses of this time were heavily limited by the lack of spectroscopic methods. This seemingly tedious sequence ensured the correct structure was formed.

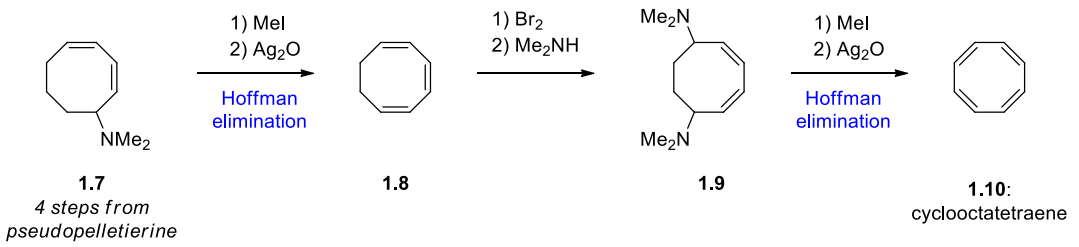

Scheme 1.1: Synthesis of cyclooctatetraene (**1.10**). Willsätter (1911)

While the arsenal of synthetic tools has greatly expanded since 1911, the adoption new synthetic philosophies has allowed magnificent advances in total synthesis. Cascade approaches use traditional synthetic methodologies to build toward a substrate which contains all or most of the atoms in the target molecule, and is engineered to *fall into place* in a single controlled cascade. There is an analogy to dominos which are carefully aligned on their ends – once pushed, one domino pushes the next and so forth until all the dominos fall in a spectacular single action. A benefit of this approach is that acyclic substrates are often easier to prepare than cyclic ones. This can lead to a more rapid generation of molecular complexity.

A great example of a cascade approach is Curran's 1985 synthesis of hirsutene (**1.15**) (Scheme 1.2).[11] The alkenyl-alkynyl-iodide **1.11** was prepared in 11 steps – the preparatory aligning of the dominos. After abstraction of the iodine atom with tributyltin radical to form intermediate **1.12** the cyclisation is very fast. 5-*exo*-trig cyclisation forms the A ring **1.13** and 5-*exo*-dig cyclisation forms the C ring **1.14**. Finally, hydrogen atom abstraction gives the tricyclic hydrocarbon target hirsutene (**1.15**) in 53% isolated yield.

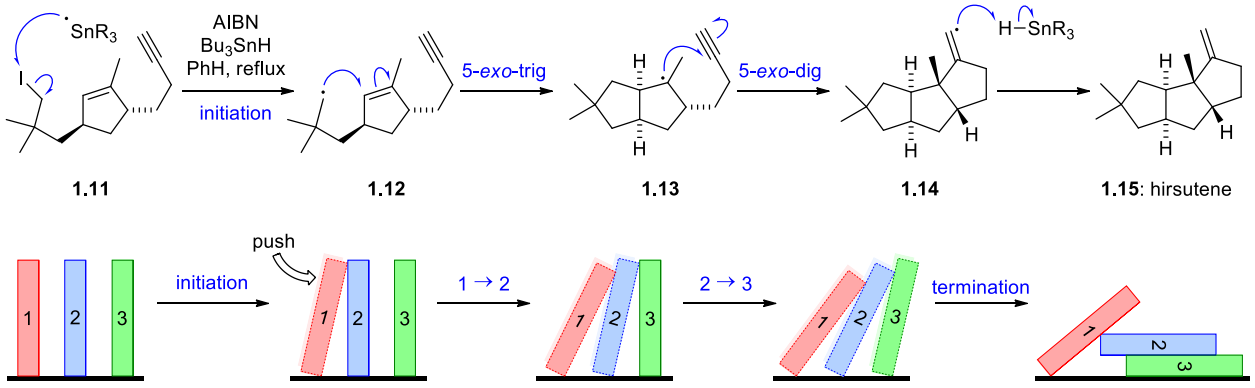

Scheme 1.2: "Domino" synthesis of hirsutene (**1.15**) via radical cascade reaction. Curran (1985)

Another excellent example of cascade synthesis is Smith's preparation of racemic morphine (**1.21**) (Scheme 1.3).[12] The highly functionalised dihydrobenzofuran **1.16** was prepared concisely in 6 steps and bares all the atoms of the target molecule. Treatment with Hoyveda-Grubb's 2nd generation

catalyst initiates a cyclisation cascade where first, ene-yne ring closing metathesis gives intermediate **1.17** which is poised to undergo a second ring closing metathesis reaction to give the *α*, *β*, *γ*, *δ*-unsaturated ketone **1.18**. At this point the reaction is telescoped with Boc- deprotection and intramolecular vinylogous Michael addition of the resultant amine to give an inconsequential mixture of **1.19** and **1.20**. This mixture was effectively converted into morphine (**1.21**) by simple functional group manipulations.

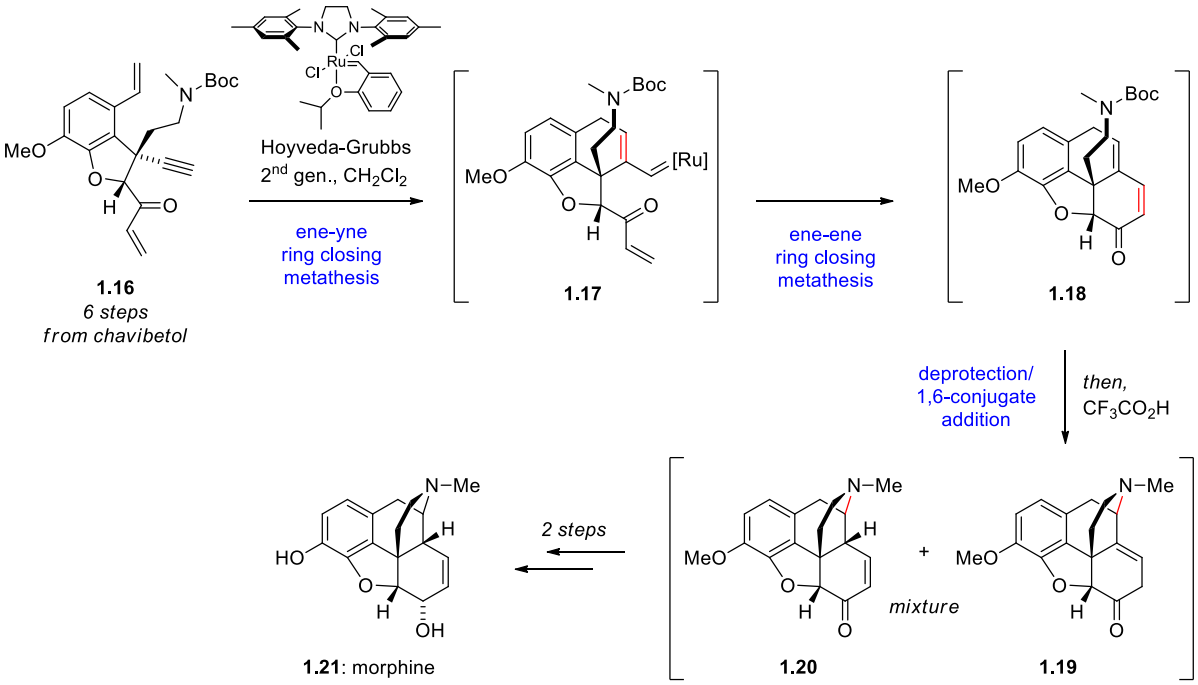

Scheme 1.3: Metathesis cascade synthesis of morphine (**1.21**). Smith (2016)

To develop domino reactions like Curran and Smith, a strong understanding and insight into chemical reactivity is needed. For Curran's synthesis of hirsutene (**1.15**) it was known that the 5-*exo*-trig cyclisation is favoured over 6-*endo*-trig, and the exact position of resulting tertiary radical would allow the second radical cyclisation. In Smith's synthesis of morphine (**1.21**) recognising intermediate **1.18** (which had previously been used in other morphine syntheses) could be disconnected by a tandem metathesis reaction guided the approach.

1.3 Biomimetic Synthesis

1.3.1: Nature Knows Best

Biomimetic chemistry is a philosophy behind the synthesis of natural products where consideration of the biosynthesis (the methods by which natural products are made in Nature) leads to the inspiration behind a synthetic plan.

Organisms (plant, fungi, bacteria, etc.) manufacture the same natural products that would take a skilled chemist weeks/months/years to prepare with exquisite efficiency and ease on a daily basis, with the limitation that reactions must occur in a functional cell (at biological pH, temperature etc.).

A myopic explanation for Nature's synthetic prowess is its ubiquitous use of enzymes; however, enzymes are created *a posteriori*. Rather, the natural variety of organisms may result in optimal conditions for a spontaneous reaction (production of building blocks, mineral content, peptide, or RNA sequence) which forms the basic skeleton of a natural product. If this is advantageous to the survival of the organism (e.g., for chemical defence), those which best produce these natural products will be chosen by natural selection. Over time, enzymes may be produced as a result of evolution to most efficiently produce this useful compound or diversify into different, more active compounds, but the key chemistry involved is nonetheless spontaneous and utilises *predisposed* reactivity.

1.3.2: Biomimetic Cascade Reactions

The power of biomimetic chemistry is best shown in its use to guide the development of cascade reactions. Nature has a plethora of cascade reactions which produce many of the organic compounds it possesses. As it is not always clear the methods which Nature uses. The first step in designing a biomimetic synthesis is the biosynthetic proposal.

What has become a very fruitful area in biomimetic synthesis is the synthesis of steroid molecules by polyene cascade reactions.[13] These cyclisation cascades are essentially extended forms of 1,5-diene cationic cyclisation reactions, the earliest example of which was in Krüger's 1893 synthesis of ionone (**1.25**) (Scheme 1.4). When pseudoionone (**1.22**)[14] is treated with acid, protonation gives the tertiary cation **1.23**. Cyclisation to **1.24** forms the 6-membered ring, and deprotonation gives ionone (**1.25**) as a mixture of isomers (only *β*-ionone is shown). This type of reactivity had been observed in many terpene molecules, and the regio- and stereochemical outcomes had been of great interest.[15]

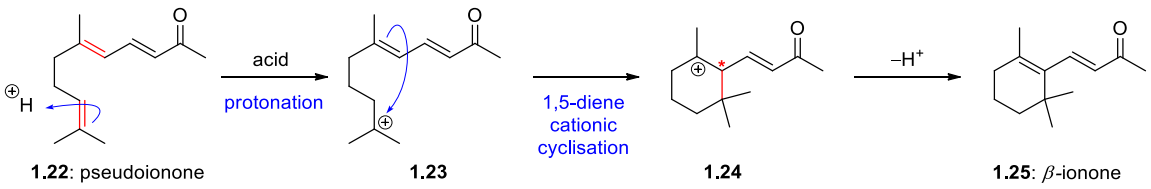

Scheme 1.4: Synthesis of ionone (**1.25**). Krüger (1893)

It had been postulated by Robinson as early as the 1930's that the steroids are derived from squalene (**1.26**), and the mechanism by which this can occur diasteroselectively was proposed independently by Stork[16] and Eschenmoser[17] in the early 1950's. Stork proposed that a stereoselective polyene cyclisation of squalene (**1.26**) initiated by oxidation of a terminal olefin (denoted as O^+) gives the tetracyclic carbocation **1.27** with an astounding 8 stereocentres formed at once (Scheme 1.5). Each cyclisation step results in a new tertiary carbocation, and the stereoselectivity is governed by chiral centres produced in the preceding steps. As such, this is a true example of domino synthesis, employed by Nature. The reaction can continue in a number of ways. For example, Meerwein-Wagner ring expansion to **1.28** and subsequent cyclisation gives lupeol (**1.29**). The advantages of this approach in Nature are significant. Terpenes, such as squalene (**1.26**), are very easily made, as the building blocks come from major pathways, ubiquitous to life. By utilising the intrinsic, predisposed reactivity of polyenes, very complex molecules can be made with minimal effort.

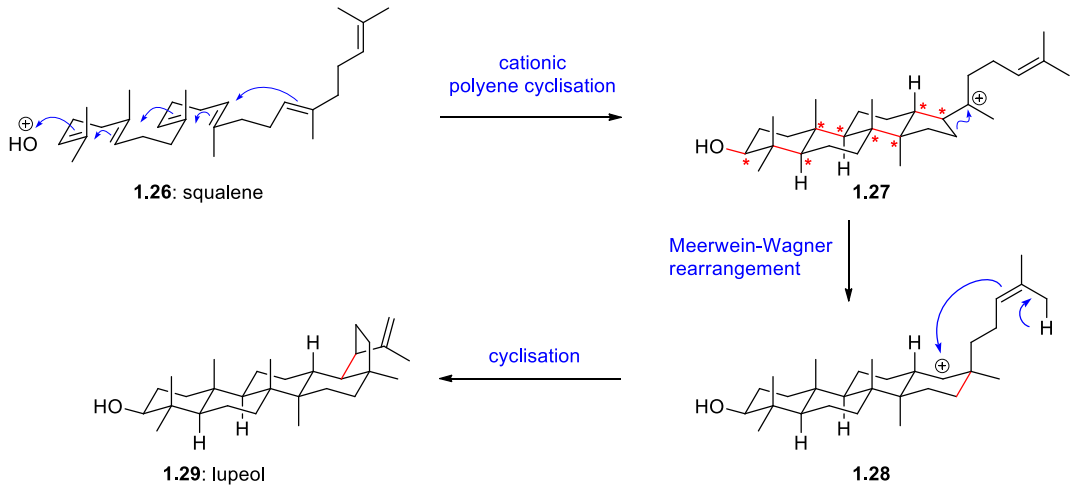

Scheme 1.5: Proposed biosynthesis of lupeol (**1.29**). Stork (1955).

The biological methods of producing the sterols can serve as clues to how a similar domino sequence could be emulated in the laboratory. For example, the female sex hormone progesterone (**1.33**) was synthesised by Johnson and co-workers by a "bioinspired" polyene cascade approach (Scheme 1.6).[18] The polyene (**1.30**) was prepared in 11 steps, the cascade is triggered by acid promoted elimination of the tertiary alcohol, tandem 1,5-diene cyclisation furnishes the B and C rings with high stereoselectivity, and alkyne cyclisation completes the D ring (5 membered ring). The ultimate vinylcarbocation is quenched with ethylene carbonate, which after hydrolysis gives the product **1.31**. 6 contiguous stereocentres, 3 rings, and 3 C-C bonds were formed in a single step! To complete the synthesis, ozonolysis of **1.31** gives the triketone **1.32** which after an intramolecular aldol condensation affords the natural product progesterone (**1.33**).

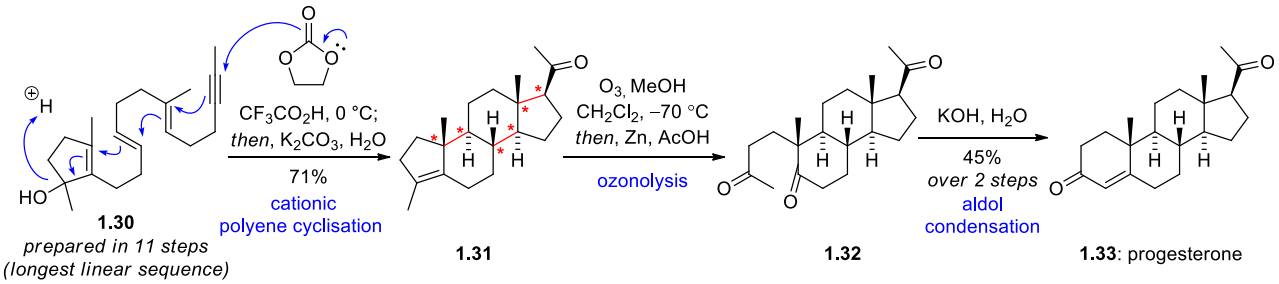

Scheme 1.6: Bioinspired cascade synthesis of progesterone (**1.33**). Johnson (1971)

The power of biomimetic principles is not limited to cascade reactions involving unfunctionalized terpenes, and indeed have been applied to all classes of natural product. Recently, the amino acid derived meroterpenoid brevianamide (**1.38**) was synthesised by Lawrence (Scheme 1.7).[19] Combining synthetic equivalents of the natural building blocks **1.34**, **1.35**, and **1.36** gave dehydrodeoxybrevianimide E (**1.37**) in only 5 steps. Chemoselective oxidation using *m*-CPBA, and treatment with hydroxide in water at ambient temperature facilitated a 1,2-shift/hetero-Diels-Alder cascade. Demonstrating that this reaction can occur under such mild and biologically relevant conditions countered the previously held belief that a Diels-Alderase enzyme was required for the formation of **1.38**.

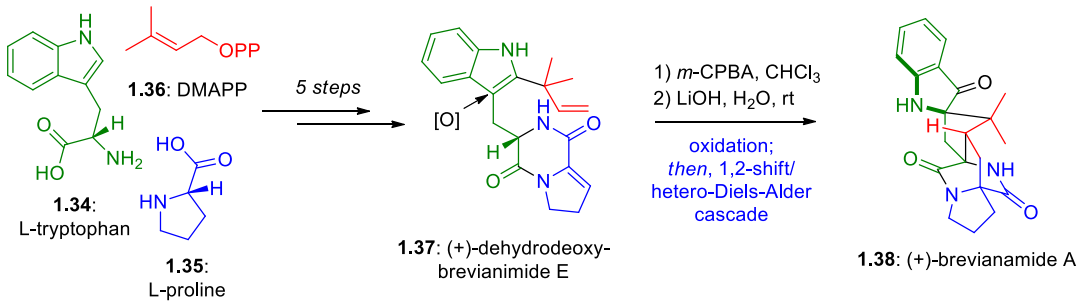

Scheme 1.7: Biomimetic cascade syntheses of (+)-brevianimide (**1.38**). Lawrence (2020)

A strong indication that a natural product is formed by non-enzymatic pathways is its optical purity. The polycyclic endiandric acid A (**1.41**) was prepared by an impressive pericyclic cascade from the linear polyene **1.39** (Scheme 1.8a).[20] Similarly, the pseudodimeric caged epicolactone (**1.45**) was prepared from the planar *o*-quinones **1.42** and **1.43** (Scheme 1.8b).[21] The endiandric acids and epicolactone were both isolated as racemic mixtures, despite boasting impressive densities of contiguous chiral centres. This is a valuable clue to their biosynthesis, which in both cases is not immediately obvious – all of the stereogenic centres are formed from achiral starting materials, and the sequence in which chirality is formed does not require enzymes. This greatly simplifies the total synthesis plan.

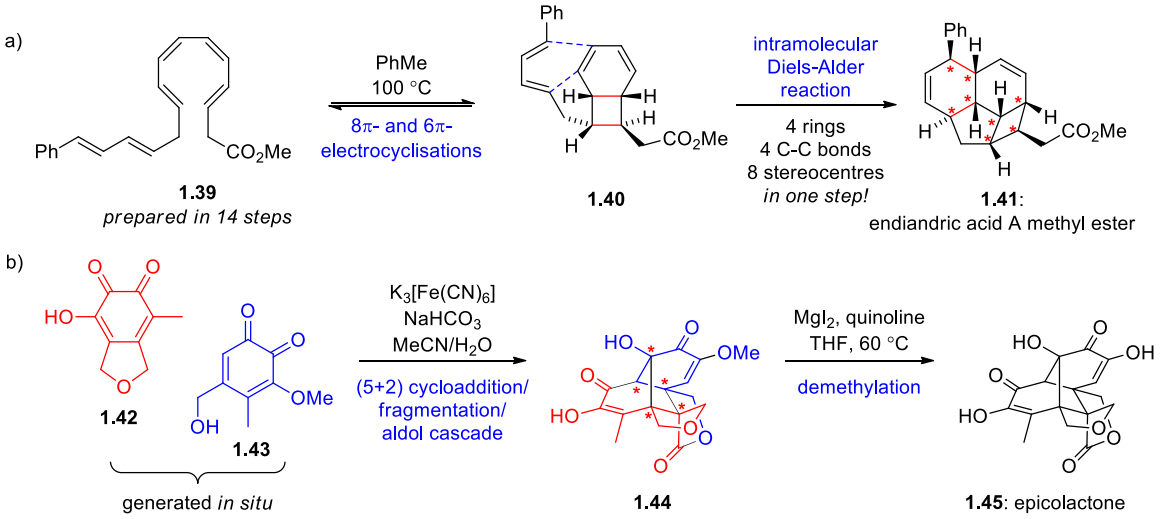

Scheme 1.8: Biomimetic synthesis of: a) endiandric acid A methyl ester (**1.41**). Nicolaou (1982); and b) epicolactone (**1.45**). Trauner (2015)

1.4 The Chemistry of *ortho*-Quinone Methides

1.4.1 Reactions Involving *ortho*-Quinone Methides

ortho-Quinone methides (*o*-QMs) are a class of reactive compounds.[22] The simplest *o*-QM is derived by the oxidative dearomatisation of hydroxytoluene (**1.46**) (Scheme 1.9). *o*-QMs are heavily polarised and have a strong driving force to rearomatise, which dictates their reactivity. The main reactions of *o*-QMs are nucleophilic addition reactions (those which form **1.48**) and more importantly hetero-Diels-Alder reactions (those which form **1.49**).

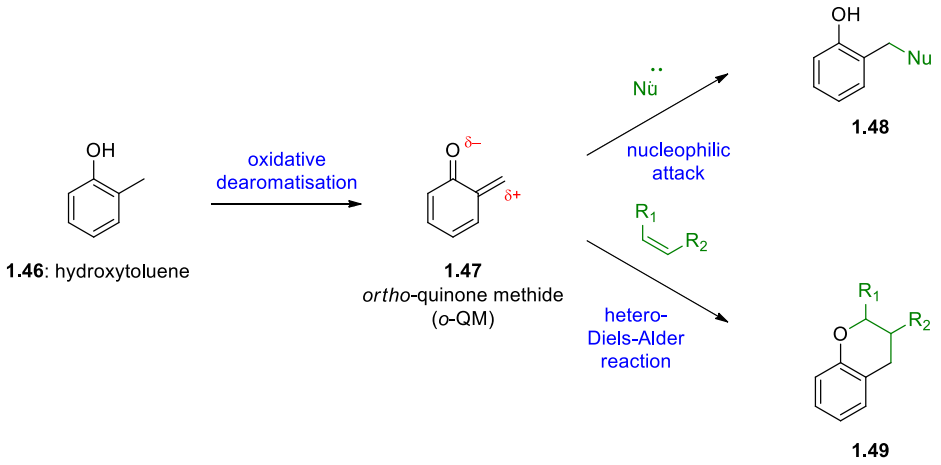

Scheme 1.9: Main reactivity of *ortho*-Quinone Methides.

Lee and Lawrence used an intermolecular hetero-Diels-Alder cycloaddition of an *o*-QM in their biomimetic synthesis of guajadial (**1.53**) and psidial (**1.54**) (Scheme 1.10).[23] Here a three component, one-pot reaction was developed where diformylphloroglucinol (**1.51**) undergoes Knoevenagel condensation with benzaldehyde to give the *o*-QM intermediate **1.52**. hetero-Diels-Alder reaction with caryophyllene (**1.50**) then proceeds to give a mixture of guajadial (**1.53**), psidial (**1.54**) and **1.55**. Selectivity is low because *o*-QM **1.52** is made as a mixture of *cis* and *trans* isomer, and caryophyllene (**1.50**) has a number of stable conformations it can react in.

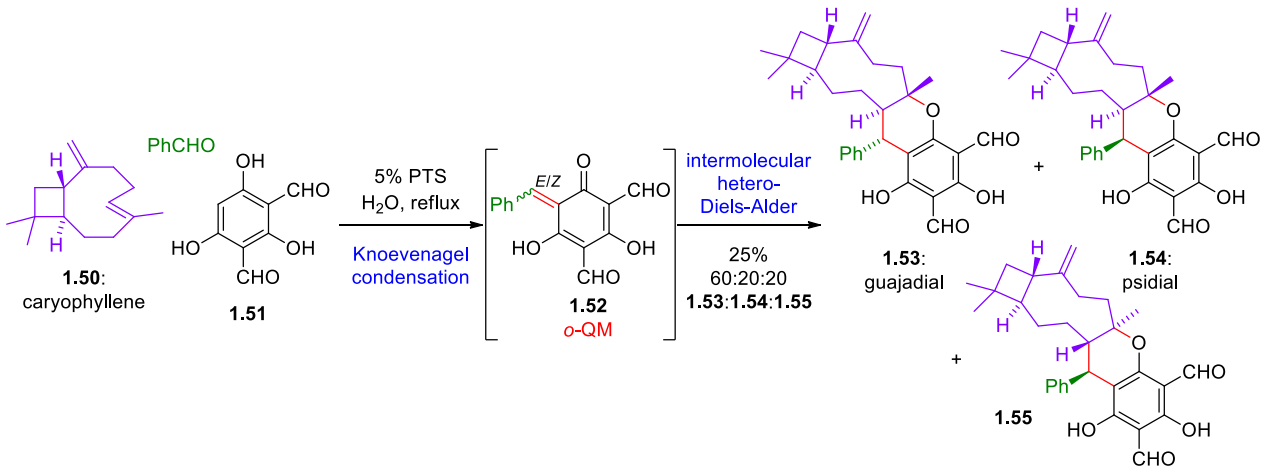

Scheme 1.10: One-pot biomimetic synthesis of guajadial (**1.53**). Lawrence and Lee (2010)

Like Diels-Alder reactions in general, the selectivity problem of hetero-Diels-Alder reactions of *o*-QMs is greatly reduced in the intramolecular mode. For example, Trauner and co-workers completed an elegant bioinspired synthesis of the pseudodimeric naphthoquinone rubiocolin B (**1.59**) from the tethered ester **1.56** (Scheme 1.11).[24] Removal of the silyl ether protecting groups and oxidation with $PhI(OAc)_2$ creates the *o*-QM **1.57** *in situ*. Due to the limited length of the linker, only the *Z* isomer of **1.57** can undergo intramolecular cyclisation with the *o*-QM and benzofuran, giving **1.58** as a single diastereoisomer. The synthesis of rubiocolin B (**1.59**) was completed by simple methyl deprotection using BBr_3.

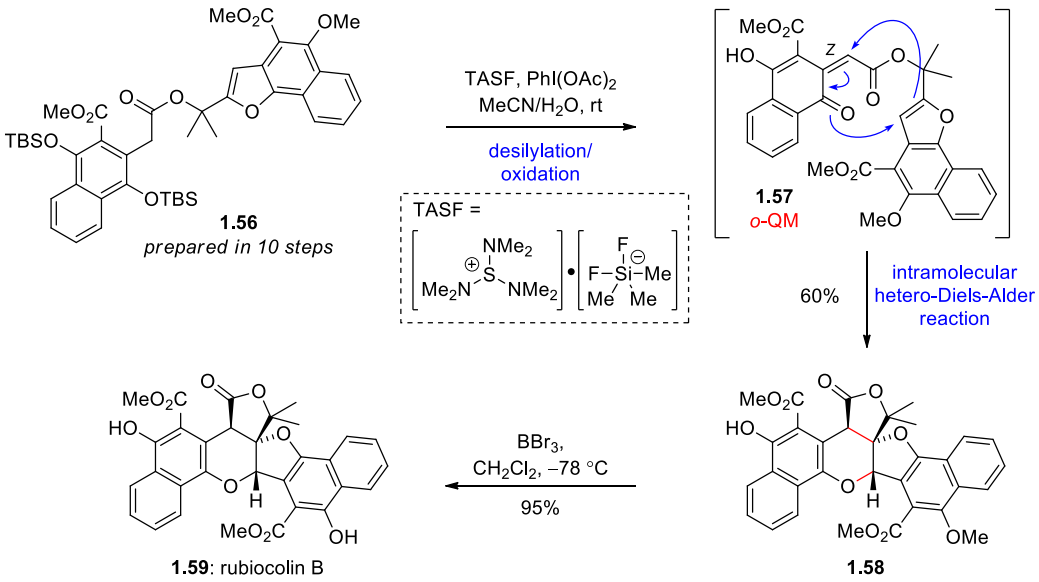

Scheme 1.11: Total synthesis of rubiocolin B (**1.59**). Trauner (2008)

1.5 The Chemistry of Chromenes

1.5.1: Chromene (Bio)Synthesis

2H-Chromene (**1.60**) is a common moiety in naturally occurring meroterpenoids (compounds of mixed terpene biosynthesis) (Figure 1.2). The "tail" length of the chromene is a defining feature of the chromene, coming from the number of isoprene (C_5) units. As such, chromenes can be hemimeroterpenoid (**1.61**), monomeroterpenoid (**1.62**), sesquimerotepenoid (**1.65**), and so forth.

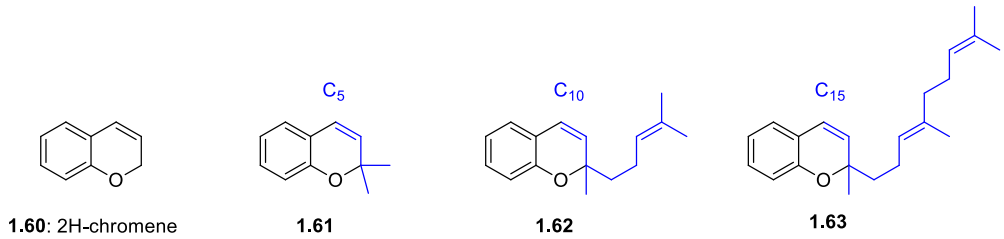

Figure 1.2: Chromene structure. Terpene fragment shown in blue.

In nature, chromenes are derived from phenols of various biogenetic origin (polyketide, flavin, amino acid, etc.). Alkylation with DMAPP (or GPP, FPP etc.) gives **1.65**, which after oxidation gives the *o*-

QM **1.66** poised to undergo oxa-6π-electrocyclisation affording a chromene **1.67** (Scheme 1.12a). In the laboratory, chromenes are usually prepared from the corresponding terpene aldehyde (Scheme 1.12b). Here the starting materials are already in the correct oxidation state. Knoevenagel condensation of **1.64** with the corresponding aldehyde forms the *o*-QM **1.66** directly, and subsequent electrocylisation gives **1.67** in a single step. This reaction is sometimes called the Crombie chromenylation, especially when pyridine is used as the base and solvent. The chiral centre of the chromene (indicated by a red star) is formed during the electrocyclisation step, as such the chromenylation reaction is difficult to control enantioselectively.

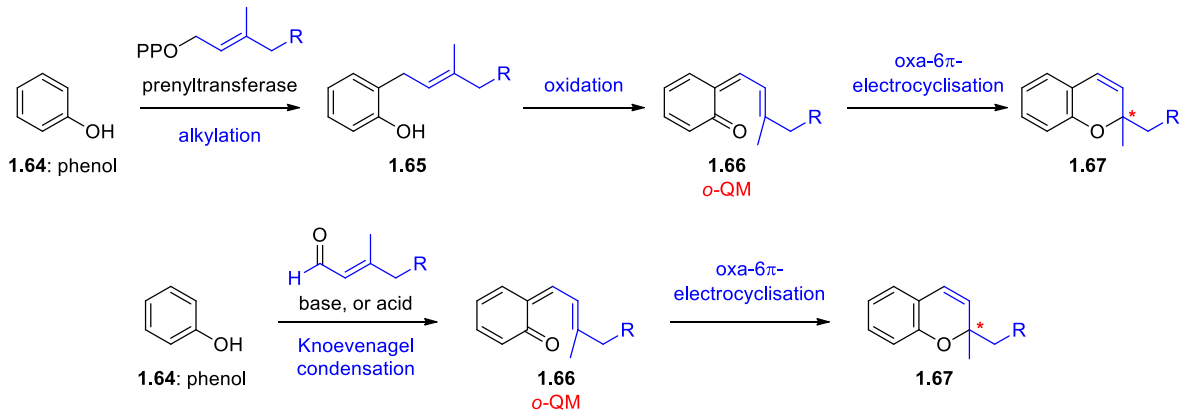

Scheme 1.12: a) Typical biosynthesis of chromenes; b) Crombie chromenylation.

Trost and Toste prepared a protocol for the preparation of chrial chromanes (reduced chromenes) (Scheme 1.13).[25] The phenol (**1.68**) underwent an asymmetric Tsuji-Trost allylation with geranyl methylcarbonate using catalytic Pd_2dba_3 and the Trost ligand **1.69**. The resultant linaloyl ether **1.70** was formed in good yield and modest enantiomeric excess (e.e. = 76%). Cyclisation of **1.70** was achieved by chemoselective hydroboration of the terminal olefin followed by electrophilic aromatic substitution, triggered by triflation of the intermediate primary alcohol. The chromane formed **1.71** shared the nucleus of vitamin E (**1.72**) which is found enantiopure in nature.

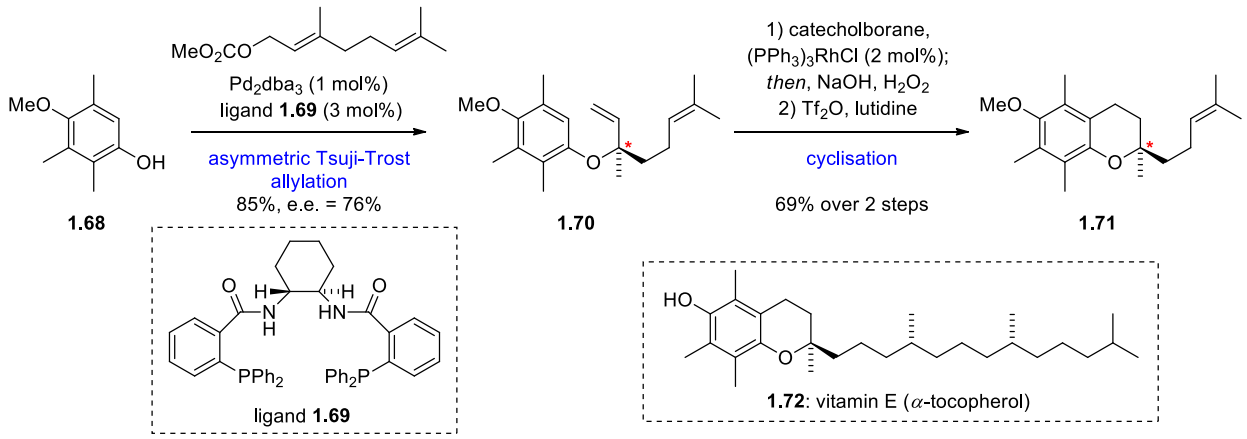

Scheme 1.13: Enantioselective synthesis of the vitamin E nucleus (**1.71**). Trost and Toste (1998)

An alternative asymmetric procedure was used by Woggon and Liu in their enantioselective synthesis of the C_{15} chromene confluentin (**1.76**) (Scheme 1.14).[26] Asymmetry was achieved by an enantioselective vinylogous aldol / oxa-Michael cascade reaction of farnesal and benzaldehyde **1.73** using the proline organocatalyst **1.74**. The resulting caged lactol **1.75** was converted into the chromene **1.76** in a cumbersome 8 steps, but with excellent enantioenrichment (e.e. = 97%). Racemic confluentin (**1.76**) has been prepared previously in a single step by chromenylation of orcinol (5-methylresorcinol) in 65% yield.[27]

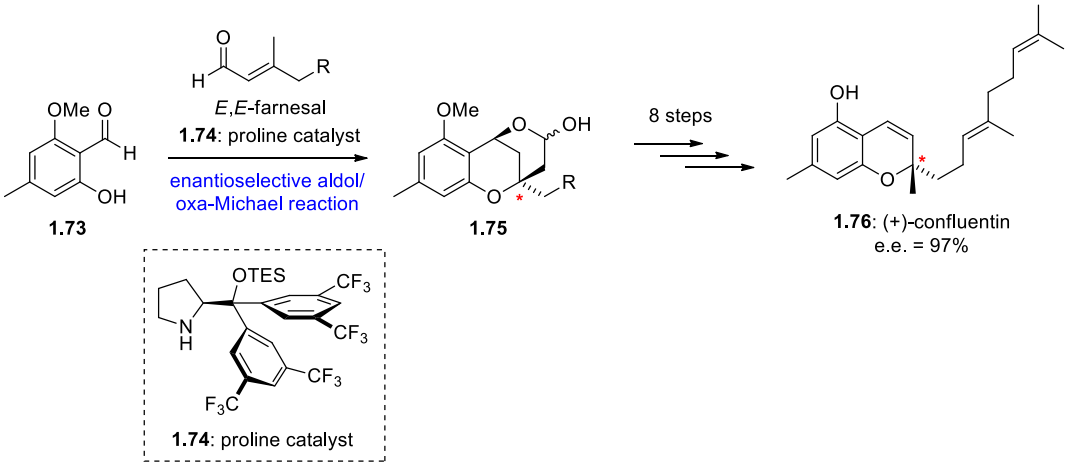

Scheme 1.14: Enantioselective synthesis of (+)-confluentin (**1.76**). Woggon (2010)

1.5.2: The Reactivity of Chromenes

Chromenes exhibit unique reactivity. A simple C_{10} chromene contains two nucleophilic centres, one on the chromene alkene, this is made more nucleophilic through *ortho* or *para* electron donating groups such as phenols. The second nucleophilic site is on the "tail" olefin (Scheme 1.15). Addition of these electrophiles reveals either a carbocation (path a) or an *o*-QM (path b) which in turn allow intramolecular reactivity between the remaining nucleophile, and the newly formed electrophile. This type of reactivity is explored in the synthesis of rhodonoid C (**1.77**) and D (Chapter 2) and the synthesis of bruceol (**1.78**) and isobruceol (Chapter 3).

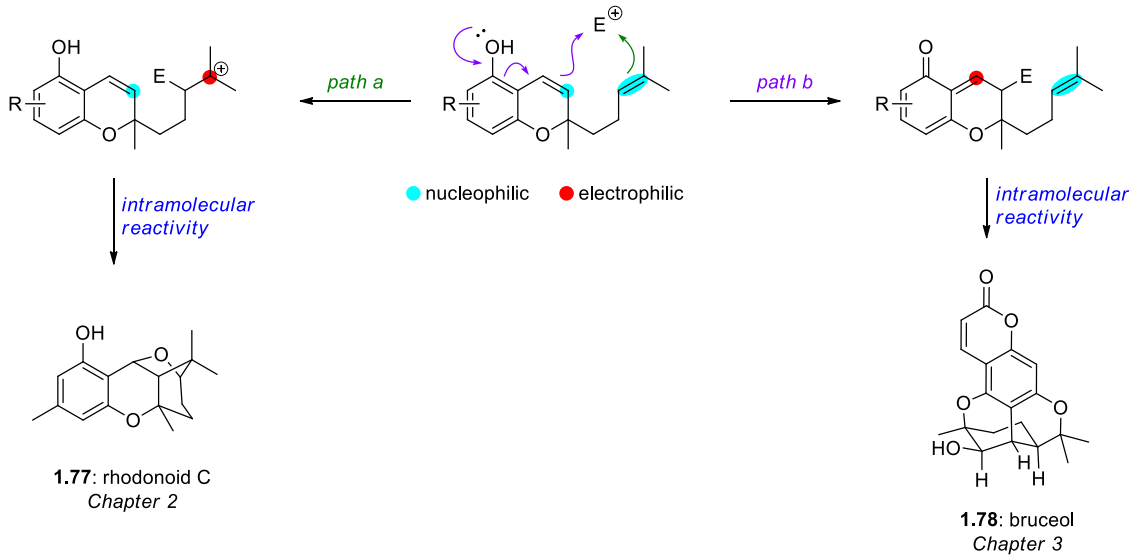

Scheme 1.15: Reactivity of chromenes with electrophiles (E = H^+, or O^+).

1.6 Aims

The aim of the work presented in this thesis was to explore the predisposed reactivity of chromenes and develop biomimetic cascade reactions to complete concise syntheses of chromane merotepenoids.

1.7 References

[1] For the original patent of mauveine: a) Patent No. 1984 UK, August 26 1856; for a retrospective account on the preparation of mauveine: b) Perkin, W. H. *J. Chem. Soc. Trans.* **1879**, *35*, 717.

[2] Morsingh, F.; Robinson, R. *Tetrahedron* **1970**, *26*, 281.

[3] The exact step count is debatable. Woodward and Eschenmoser's synthesis had many points of convergence, and multiple preparations of key fragments.

[4] Crowfoot-Hodgkin, D. Pickworth, J.; Robertson, J. H.; Trueblood, K. N.; Prosen, R. J.; White, J. G. *Nature*, **1955**, *176*, 325.

[5] a) Woodward, R. B.; Sondheimer, F.; Taub, D.; Heusler, K.; McLamore, W. M. *J. Am. Chem. Soc.* **1952**, *74*, 4223. b) Cardwell, H. M. E.; Conforth, J. W.; Duff, S. R.; Holtermann, H.; Robinson, R. **1953**, *J. Chem. Soc.* 361.

[6] Aicher, T. D.; Buszek, K. R.; Fang, F. G.; Forsyth, C. J.; Jung, S. H.; Kishi, Y.; Matelich, M. C.; Scola, P. M.; Spero, D. M.; Yoon, S. K. *J. Am. Chem. Soc.* **1992**, *114*, 3162.

[7] Kremer, A.; Tarassoff, P.; Olivo, M.; He, Y.; Guo, M.; Savulski, C. **2014**, US Patent: W0 2014087230A1.

[8] Eaton, P. E.; Cole, T. W. *J. Am. Chem. Soc.* **1964**, *86*, 3157.

[9] Schröder, G. *Angew. Chem. Int. Ed.* **1963**, *2*, 481.

[10] Willsätter, R.; Waser, E. *Chem. Ber.* **1911**, *44*, 3423.

[11] Curran, D. P.; Rakiwicz, D. M. *J. Am. Chem. Soc.* **1985**, *107*, 1448.

[12] Chu, S.; Münster, N.; Balan, T.; Smith, M. D. *Angew. Chem. Int. Ed.* **2016**, *55*, 14306.

[13] For a review of biomimetic polyene cyclisations: a) Yoder, R. A.; Johnston, J. N. *Chem. Rev.* **2005**, *105*, 4730. For a recent review of polyene cyclisation reactions with unusual termination steps: b) Feilner, J. M.; Haut, F. -L.; Magauer, T. *Chem. Eur. J.* **2021**, *27*, 7017.

[14] Pseudoionone (**1.22**) is made in a single step by the condensation of citral and acetone, Russel, A.; Kenyon, R. L.; Smith, L. I.; Renfrow, W. B.; De Mytt, L. E. *Org. Synth.* **1943**, *23*, 78.

[15] Hibbit, D. C.; Linstead, R. P. *J. Chem. Soc.* **1936**, 470.

[16] Stork, G.; Burgstahler, A. W. *J. Am. Chem. Soc.* **1955**, *77*, 5068.

[17] Eschenmoser, A.; Ruzicka, L.; Jeger, O.; Arigoni, D. *Helv. Chim. Acta*, **1955**, *38*, 1890.

[18] Johnson, W. S.; Gravestock, M. B.; McCarry, B. E. *J. Am. Chem. Soc.* **1971**, *93*, 4332.

[19] Godfry, R. C.; Green, N. J.; Nichol, G. S.; Lawrence, A. L. *Nature Chem.* **2020**, *12*, 615.

[20] Nicolaou, K. C.; Petasis, N. A.; Zipkin, R. E. *J. Am. Chem. Soc.* **1982**, *104*, 5560.

[21] Ellerbrock, P.; Armanino, N.; Ilg, M. K.; Webster, R.; Trauner, D. *Nature Chem.* **2015**, *7*, 879.

[22] For a review on the use of *o*-QMs in natural product synthesis: Willis, N. J.; Bray, C. D. *Chem. Eur. J.* **2012**, *18*, 9160.

[23] Lawrence, A. L.; Adlington, R. M.; Baldwin, J. E.; Lee, V.; Kershaw, J. A.; Thompson, A. L. *Org. Lett.* **2010**, *12*, 1676.

[24] Lumb, J. -P.; Choong, K. C.; Trauner, D. *J. Am. Chem. Soc.* **2008**, *130*, 9230.

[25] Trost, B. M.; Toste, D. *J. Am. Chem. Soc.* **1998**, *120*, 9074.

[26] Liu, K.; Woggon, W. -D. *Eur. J. Org. Chem.* **2010**, 1033.

[27] Lee, R. Y.; Wang, X.; Noh, S. K.; Lyoo, W. S. *Synth. Commun.* **2006**, *36*, 3329.

Chapter 2: Biomimetic Synthesis of Rhodonoid C, D and Murrayakonine D

The work presented in this chapter was performed alongside colleague Dr. Hiu Chun Lam who contributed equally to this project.

2.1 Introduction

2.1.1: Rhodonoid Natural Products

Between 2015 and 2017 seven orcinol (5-methylresorcinol) derived meroterpenoid natural products were isolated from the aerial parts of *Rhododendron capitatum*; a deciduous flowering shrub native to China (Figure 2.1)[1,2]. *R. capitatum* has been used traditionally in Tibetan folk medicine as a treatment for inflammation, gastric cold, and abdominal pain. All seven rhodonoid meroterpenoids (A-G, **2.1**-**2.7**) were isolated as scalemic mixtures (partial racemates) despite containing four to six stereocenters – suggesting the biosynthesis of the rhodonoids may occur by predisposed, non-enzymatic reactions.

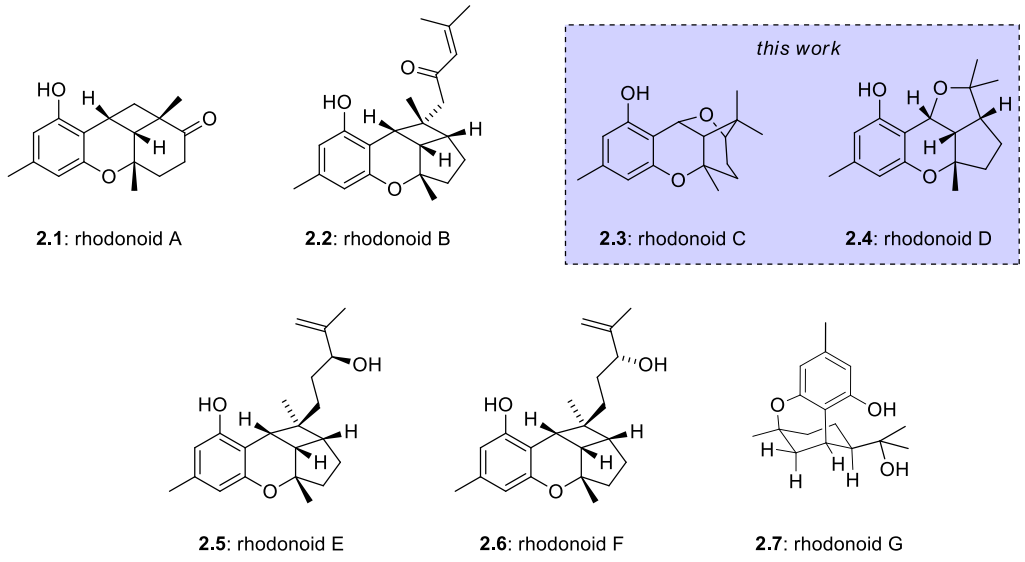

Figure 2.1: Rhodonoid natural products from *R. Capitatum*. Hou (2015, 2017)

2.1.2: Isolation of Related *Rhododendron* Natural Products

Rhododendron plants have been a source of a diverse range of chromane meroterpenoids. Figure 2.2 shows a range of *Rhododendron* natural products with particular emphasis on the relationship with their parent chromenes (**2.8** – **2.11**) (shown in the dotted box).

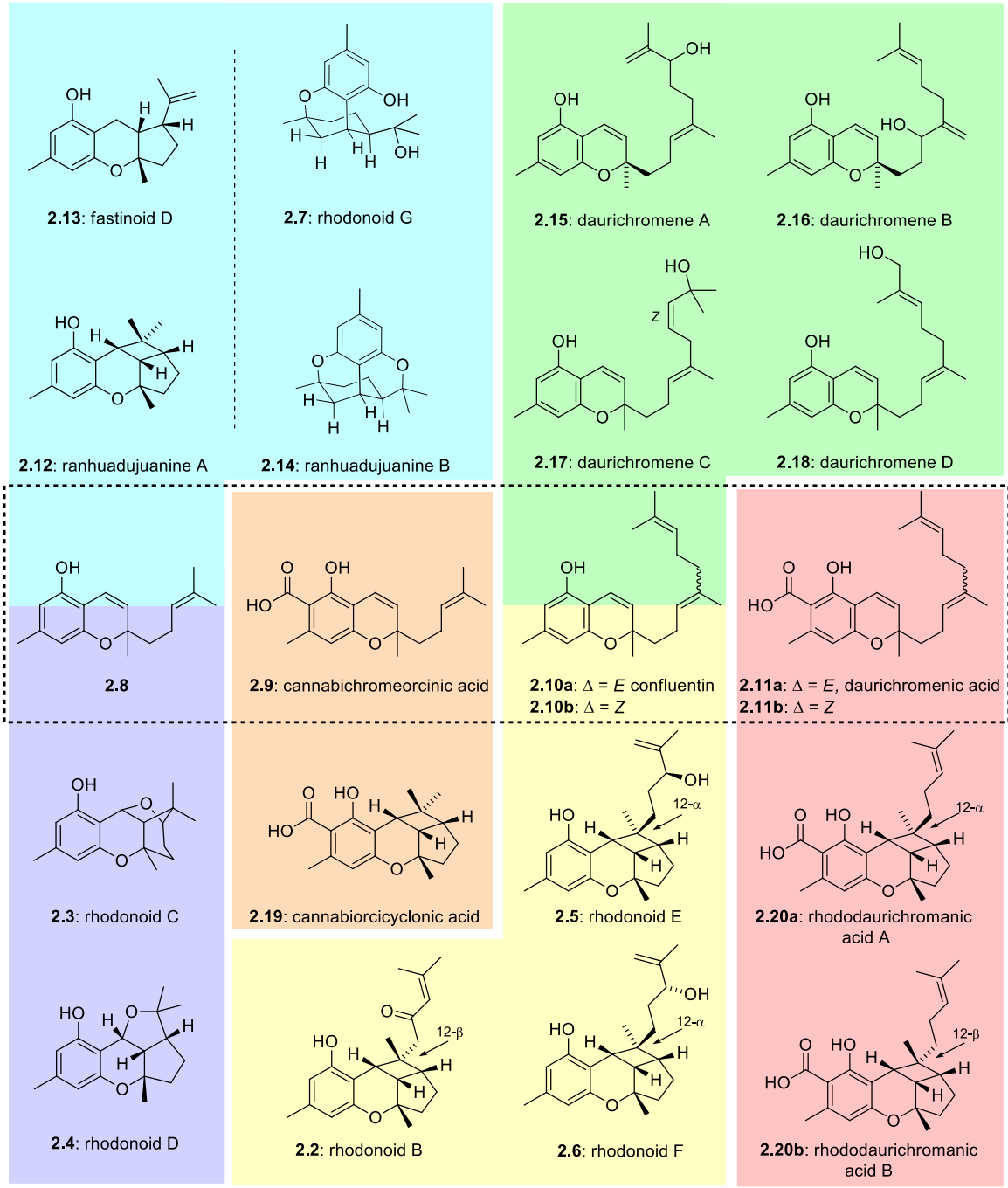

Figure 2.2: *Rhododendron* natural products from *R. capitatum* (**2.2** – **2.7**), *R. dauricium* (**2.11**, **2.15** – **2.18**, **2.20**), *R. anthopogonoides* (**2.8**, **2.9**, **2.12**, **2.14**, **2.19**), and *R. fastigium* (**2.13**).

Starting from the unnamed C_{10} chromene **2.8** (isolated from *R. anthopogonoides*) redox neutral transformations could occur (cyan box). [2+2] cycloaddition would give the "cyclol" ranhuadujuanine A (**2.12**), or an interrupted [2+2], or formal ene reaction could give fastionoid D (**2.13**). Alternatively, tautomerisation of **2.8** and hetero-Diels-Alder cycloaddition could give the "citran" ranhuadujuanine B (**2.14**), and if this process were interrupted by addition of water, rhodonoid G (**2.7**) is formed. The cyclol and citran classes of molecules are common motifs in the chemistry of chromenes. Citran molecules are discussed in greater depth in Chapter 3.

Singlet oxygen ene reaction (often called the Schenck ene reaction, this reaction is discussed further in Chapter 4) of the C_{15} chromene confluentin (**2.10a**) gives daurichromenes A – C[3] (**2.15** – **2.17**) through a transient hydroperoxide and mild reduction to the allylic alcohols (green box). As the Schenck ene reaction is notoriously non-selective in linear unfunctionalised systems like this,[4] it is possible that there are several alternative daurichromene natural products which are yet to be discovered. The *Z* geometry of daurichromene C (**2.17**) is unusual, in analogous systems the *E* isomer predominates. Daurichromene D (**2.18**) is again slightly different, it is the direct allylic oxidation product, possibly formed by a cytochrome P450 mono-oxygenase enzyme.

From confluentin (**2.10a**), [2+2] cyclisation and Schenck ene oxidation could give rhodonoid E (**2.5**) and F (**2.6**) (yellow box). These could also be the direct product of [2+2] reaction of daurichromene A (**2.15**), differing by the undefined stereocentre of the allylic alcohol. Rhodonoid B (**2.2**) is also product of a [2+2] cycloaddition, but of the *Z* version of confluentin (**10b**). **10b** has not been isolated in Nature as of yet but is necessary for the formation of the β configuration of the prenyl group. The necessary oxidation to the ketone must occur at some point.

Another common theme in these natural products is repetition of structures differing only by a carboxylic acid. Cannabichromeorcinic acid (**2.9**)[5] is an analogue of **2.8** and can also cyclise to give the cyclol cannabiorcicyclonic acid (**2.19**)[6] (orange box). Likewise, *E* and *Z* daurichromenic acid

(**2.11a** and **2.11b**)[7] gives the cyclols rhododaurichromenic acid A and B (**2.20a** and **2.20b**) respectively (pink box).[8]

Of the natural products shown here, rhodonoids C (**2.3**) and D (**2.4**) were thought to be the most fascinating (blue box). Simple cyclols like **2.12** and **2.20** have been synthesised by biomimetic photochemical [2+2] reactions for over 50 years. While the interesting oxidation patterns of daurichromene A – D (**2.15** – **2.18**) and rhodonoids B, E, and F (**2.2**, **2.5**, and **2.6**) posed an interesting problem for synthesis (and was later addressed by our group), the challenge of the unique carbon scaffold of rhodonoid C (**2.3**) and rhodonoic D (**2.4**) (none synthesised at this point) was the most enticing initially.

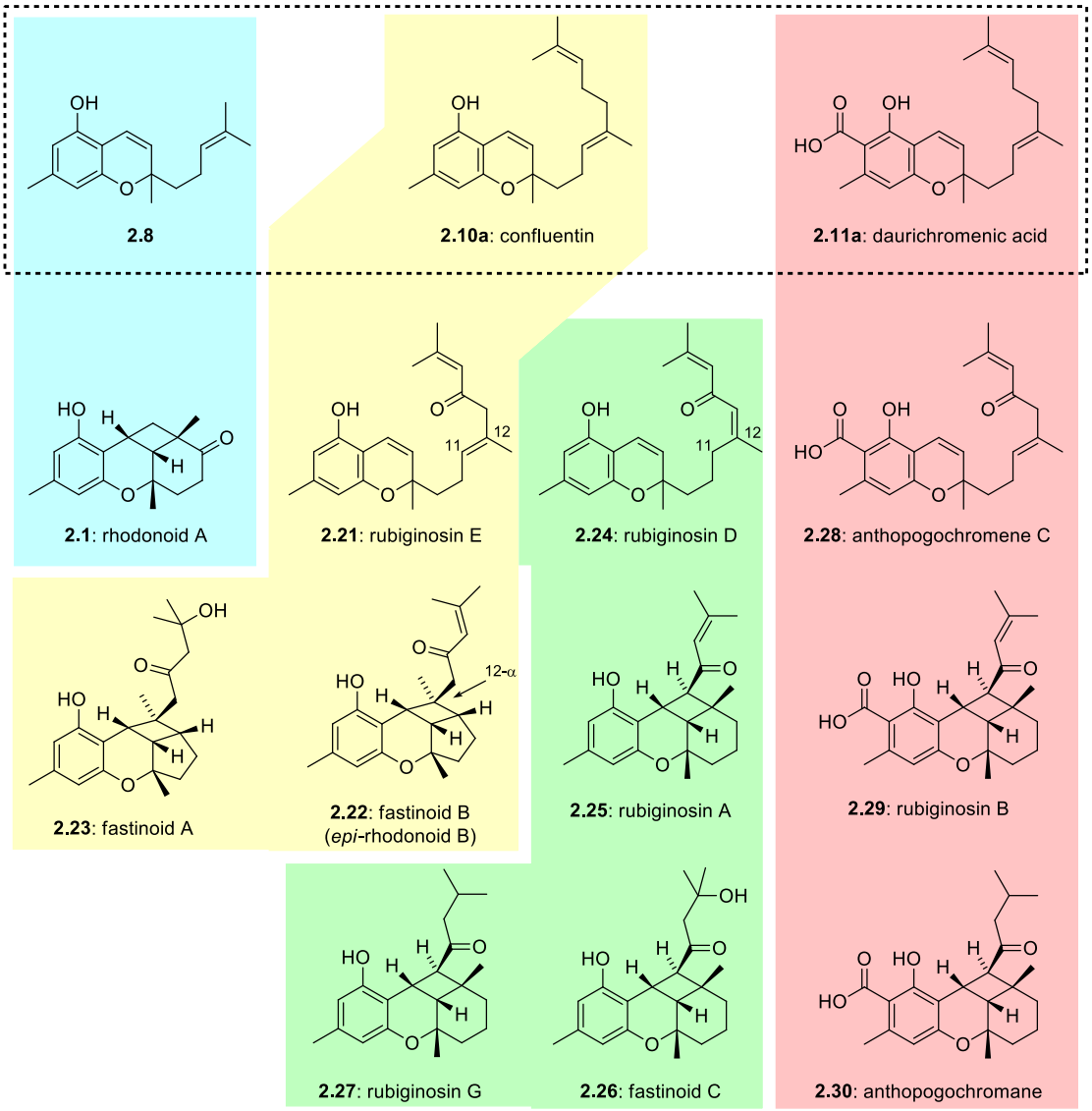

Figure 2.3: 6-6-6-4 cyclobutane containing meroterpenoids from *Rhododendron* species.

The last class of natural products discussed here will be the 6-6-6-4 cyclobutane containing molecules (Figure 2.3). The simplest of these is rhodonoid A (**2.1**). As in the cyclols, this scaffold is forged by a [2+2] cycloaddition, however the alkene double bond must migrate, and oxidation must occur (cyan box). This transformation was explored within our group and will be briefly discussed later.

Confluentin (**2.10a**) could be oxidised to the ketone rubiginosin E (**2.21**) (yellow box). Our familiar [2+2] cycloaddition would give fastinoid B (**2.22**)[9] (N.B. the *Z* isomer of **2.21** would give rhodonoid B (**2.2**)). Hydration of the α,β-unsaturated ketone gives fastinoid A (**2.23**).

Rubiginosin E (**2.21**) could undergo a bond tautomerisation ($\Delta^{11} \rightarrow \Delta^{12}$) to the more conjugated rubiginosin D (**2.24**).[10] [2+2] cycloaddition could occur in a stepwise (and thermally allowed) double conjugate addition fashion giving rubiginosin A (**2.25**). Fastinoid C (**2.26**) and rubiginosin G (**2.27**) are the products of hydration and reduction of the olefin respectively. As with the cyclols, these natural products also have carboxylic acid analogues (pink box). From daurichromenic acid (**2.11a**) oxidation gives anthopogochromene C (**2.28**).[11] Tautomerisation to an analogue of rubiginosin D (yet to be discovered) and formal [2+2] cyclisation gives the 6-6-6-4 cyclobutane rubiginosin B (**2.29**) and finally anthopogochromane (**2.30**) by reduction.

The rubiginosins, fastinoids, and anthopogochromane pose as an intriguing problem, and to date, no synthesis of these molecules (or any containing this 6-6-6-4 system) has been reported. This is currently an active area of research in our group.[12]

The connection between confluentin (**2.10a**) and rubiginosin E (**2.21**) is curious. The likely biosynthesis would proceed by an enzymatic C-H oxidation, either on confluentin (**2.10a**) itself or prior to prenylation. Naya and co-workers have proposed a similar pathway to occur within species of sweet potatoes (Scheme 2.1).[13]

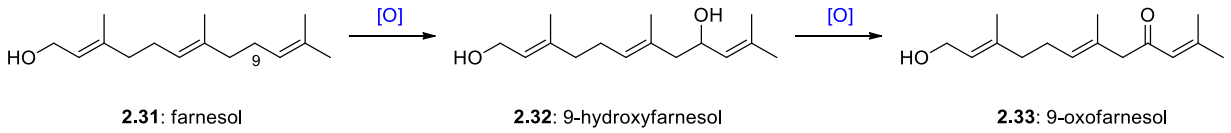

2.31: farnesol **2.32**: 9-hydroxyfarnesol **2.33**: 9-oxofarnesol

Scheme 2.1: Biosynthesis of 9-oxofarnesol in *Ipomoea batatas*; a sweet potato. Naya (1984)

Closer to this family, we also see similarly oxidised orcinol meroterpenoids in grifolinone A (**2.35**) and its dimer grifolinone B (**2.36**) isolated within the fungus *Albatrellus confluens* (Figure 2.4)[14] showing oxidation at C-9 to not be uncommon.

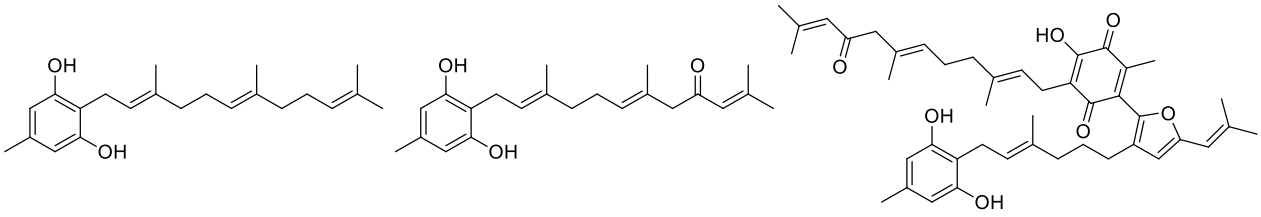

2.34: grifolin **2.35**: grifolinone A **2.36**: grifolinone B

Figure 2.4: 9-Oxofarnesal orcinol meroterpenoids grifolinone A (**2.35**) and dimer B (**2.36**) from *A. confluns*. Yang (2008)

Analysis of the compounds isolated in these closely related plant species, as well as understanding of commonly employed biosynthetic tactics allows us to speculate on the biosynthesis occurring to form this diverse natural product family. Our basic assumption is the processes used in these plants are by necessity very efficient processes, and this will serve as a guide to our total synthesis plan.

2.1.3: Biosynthesis of Rhodonoids C (**2.3**) and D (**2.4**)

Before looking at the key terpene oxidation / cyclisations which forge the rhodonoids C (**2.3**) and D (**2.4**) meroterpenoid skeletons, we will briefly discuss the polyketide biosyntheisis of the aromatic portion of these molecules.

Orcinol (**2.37**), which provides the foundation of rhodonoids A – G (**2.1** – **2.7**) and other *Rhododendron* meroterpenoids, is made in nature from a polyketide pathway. Taura, Morita, and co-workers explored the biosynthesis within *R. dauricum* using gene mining strategies and were able to identify a new polyketide synthase, "orcinol synthases".[15] Their experiments showed in the presence of orcinol synthase, acetyl-CoA (**2.38**) can oligomerise to form tetraketide **2.39**. Without any other enzymes **2.39** will release into solution and spontaneously cyclise, forming orcinol (**2.37**) as the major product. Small amounts of orsellenic acid (**2.40**), phloroacetophenone (**2.41**), and other building blocks also formed, but not enough to explain the amount of orsellenic acid derived compounds present in *R. dauricum*. However, when the authors add olivetolic acid cyclase (from *Cannabis sativa*) the amount of orsellenic acid (**2.40**) formed dramatically increases.

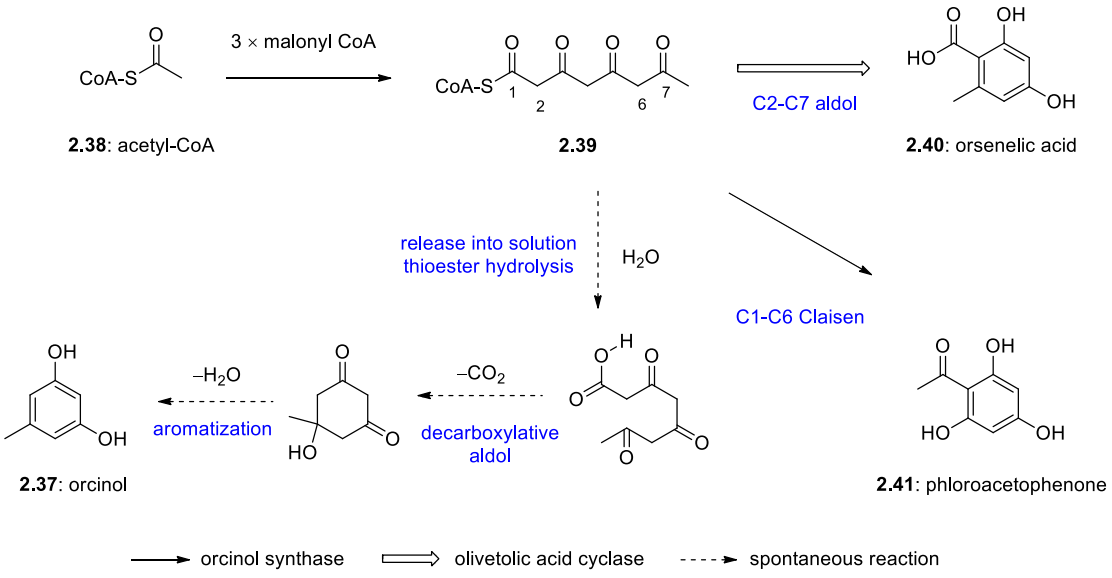

Scheme 2.2: Biosynthetic studies of orcinol (**2.37**) and orsellenic acid (**2.40**) in *R. dauricum*. Taura and Morita (2019)

Within the same group, the enzyme responsible for the biosynthesis of daurichromenic acid (**2.11**) in *R. dauricum*, named DCA synthase (Scheme 2.3) was identified[16]. This enzyme, and/or very similar enzymes, provide the mechanism by which chromenes are formed in *Rhododendron* plants. First alkylation occurs via an appropriate prenyl transferase, then DCA synthase converts the linear meroterpenoid to a chromene by oxidation, using dissolved oxygen as the terminal oxidant. The 6-π-

electrocyclization is a very spontaneous transformation and is the origin of chirality in chromane meroterpenoids. The rhodonoids being isolated as partial racemates can be rationalised by the cyclisation substrate having only a weak association with its respective "DCA" synthase.

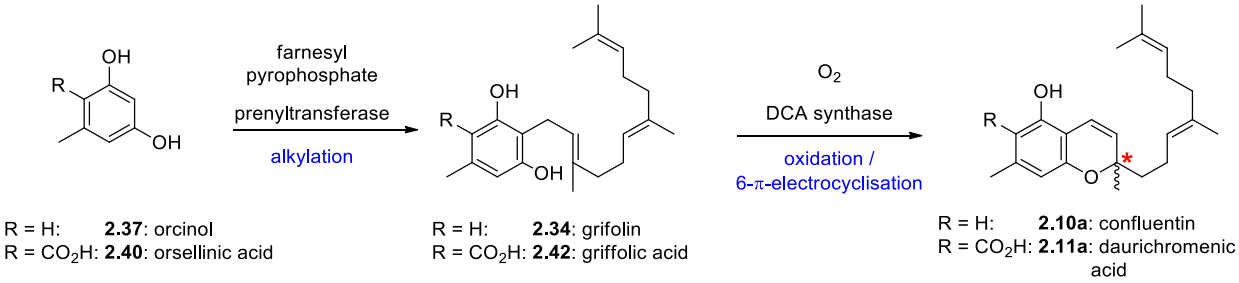

Scheme 2.3: Biosynthesis of daurichromenic acid (**2.11a**) in *R. dauricum*. Taura (2014)

Rhodonoids C (**2.3**) and D (**2.4**) have a shared biosynthesis. Oxidation occurs on the pendant prenyl chain of chromene **2.8** and the resultant epoxide **2.43** can ring open by the vinylogous enol attacking either C-12 (path a) or C-11 (path b) (Scheme 2.4). In path a, the 6-*endo*-tet provides *ortho*-quinone methide (*o*-QM) **2.44** which after a rapid 5-*exo*-trig affords the caged rhodonoid C (**2.3**). Similarly, the 5-*exo*-tet in path b forms *o*-QM **2.45** which gives rhodonoid D (**2.4**) after an analogous 5-*exo*-tet cyclisation. In anionic conditions, path b is predicted to be more favoured using Baldwins rules[17] (5-*exo*-tet vs 6-*endo*-tet); however, these rules do not apply to cationic cyclisations, and in this case the relative stability of the carbocations **2.46** and **2.47** would be more critical.

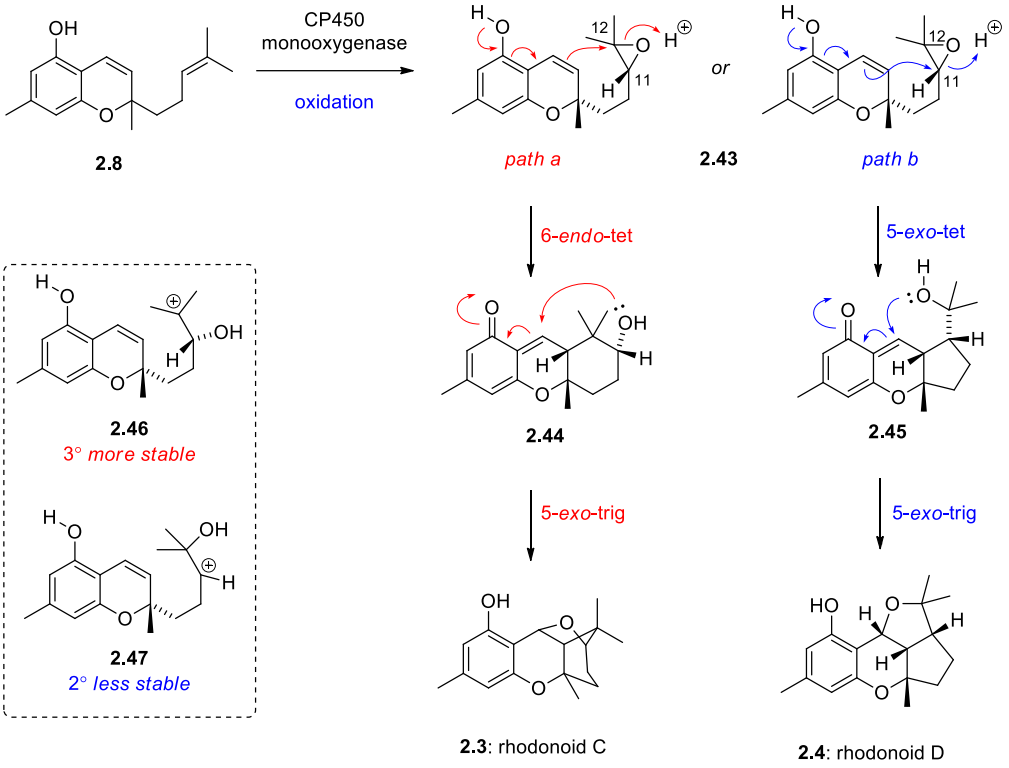

Scheme 2.4: Proposed biosynthesis of rhodonoid C (**2.3**) and D (**2.4**).

This process is of particular interest to us because at the time, no molecules of this scaffold had been prepared synthetically before; and we believed we could emulate the biosynthesis in the laboratory.

We discovered after a simple SciFinder search of our target scaffold that a carbazole alkaloid named murrayakonine D (**2.48**) was the only known naturally occurring analogue of rhodonoid C (Figure 2.4). Murrayakonine D (**2.48**) was isolated only year before rhodonoid C (**2.3**) in the aerial parts of *Murraya koenigii*, the curry-leaf tree.[18] *M. koenigii* has been a rich source of bioactive carbazole meroterpenoids. Coisolated with murrayakonine D (**2.48**) was the precursor chromene mahanimbine (**2.49**), and by analogy, the biosynthesis of **2.3** occurs via the intermediate epoxide **2.50**. Assuming the biosynthesis mirrors that of rhodonoid C, we also believed it would be possible an analogue of rhodonoid D (**2.4**) could also be formed, leading us to propose speculatively that rhodonoid D analogue (**2.51**) may be an undiscovered natural product. As such, we sought these natural products as secondary targets to our investigations of the *Rhododendron* meroterpenoids.

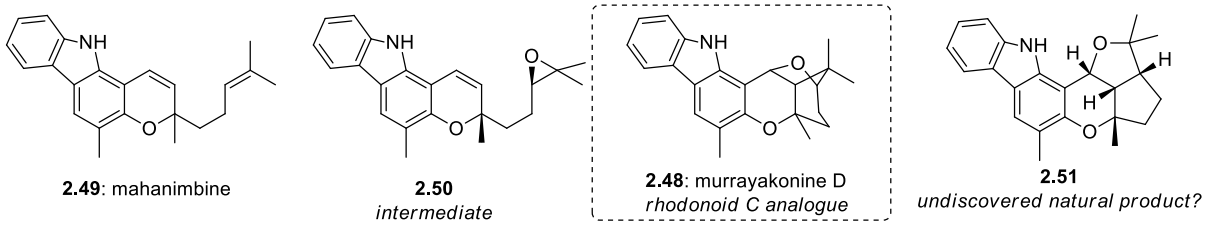

Figure 2.4: Analogue of rhodonoid C (**2.3**), murrayakonine D (**2.48**) isolated from *M. koenigii*, co-isolated with chromene mahanimbine (**2.49**). Also shown is the presumed intermediate **2.50**, and theorhetical rhodonoid D analogue **2.51**.

2.1.4: Previous Syntheses of Orcinol Chromane/Chromenes

Many of the chromane natural products discussed hitherto have been the targets of total synthesis. Their concentrated complex scaffolds and subtle differences warrant synthetic investigations.

The earliest example of a synthesis of an orcinol chromane natural product was by Crombie in 1975. Crombie has been a pioneer in the area of chromene and chromane natural products synthesis, whose achievements include the structural elucidation of the citran scaffold. In an effort of natural product anticipation, a series of small-scale reactions (coined "miniaturised synthesis") were performed to rapidly generate a diverse library of cannabinoid analogues, analysed by GLC.[19] Within this study the citran ranhuadujuanine B (**2.14**) was synthesised 35 years before its first isolation! (Scheme 2.5)

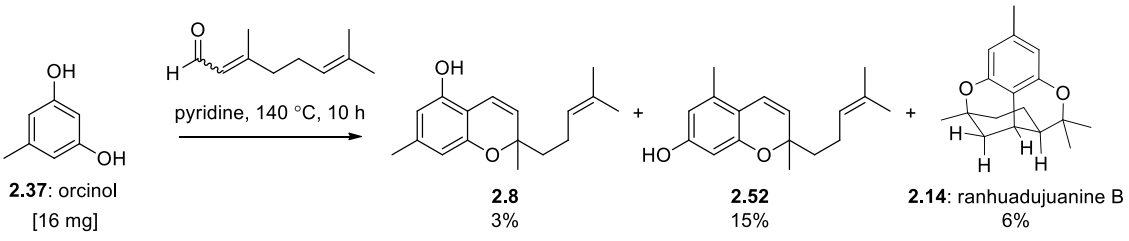

Scheme 2.5: "Miniature" synthesis of orcinol cannabinoid analogues. Crombie (1975).

These experiments were reproduced by Kane, Martin, and co-workers several years later for the purpose of gathering ^{13}C NMR data of cannabinoids and analogues thereof (Scheme 2.6) Kane achieved more favourable yields and also observed the cyclol ranhuadujuanine A (**2.12**) during these investigations.[20]

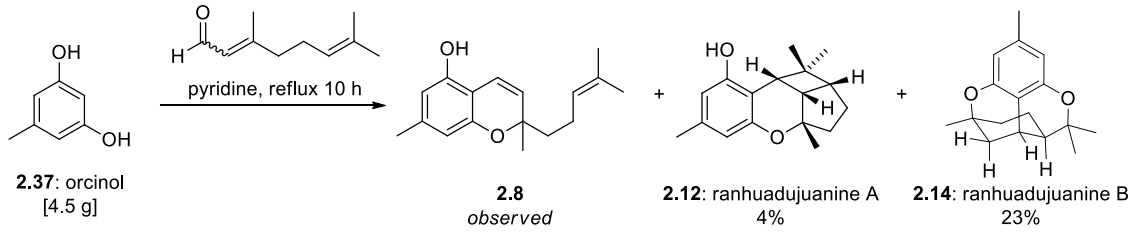

Scheme 2.6: Synthesis of ranhuadujuanine A (**2.12**) and B (**2.14**). Kane and Martin (1984)

The first of the C_{15} terpene *Rhododendron* meroterpenoids tackled was the rhododaurichromanic acids A (**2.20a**) and B (**2.20b**) by Hsung and coworkers in 2003 (Scheme 2.7).[21] The synthesis began with chromenylation of 5-methyl-1,3-cyclohexanedione (**2.53**) with *E*-farnesal in the presence of piperidine, and Ac_2O. Addition of Mander's reagent (**2.55**) to the enolate of **2.54** gave ester **2.56**; which after oxidative aromatisation with DDQ gave the methyl ester of daurichromenic acid **2.57**.

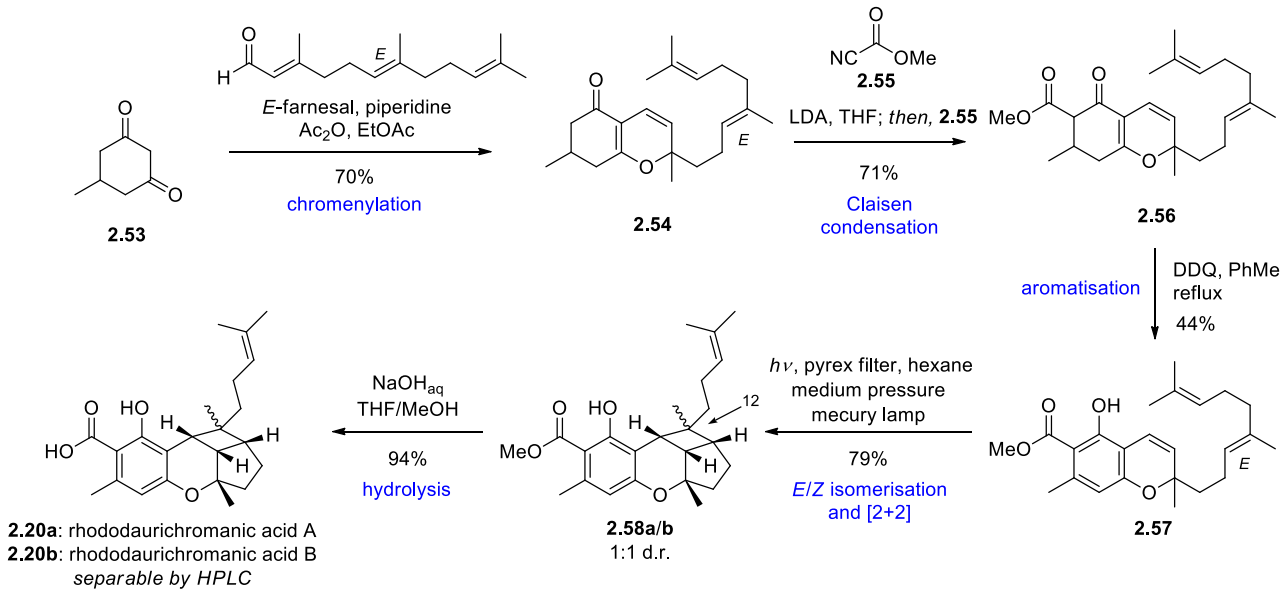

Scheme 2.7: Synthesis of rhododaurichromanic acids A (**2.20a**) and B (**2.20b**). Hsung (2003).

The [2+2] cycloaddition of ester **2.57** was achieved photochemically with a medium pressure mercury lamp with a Pyrex filter. The relative stereochemistry of C-12 cyclol **2.58** was completely lost (1:1 d.r.); showing that photochemical isomerisation of the alkene is much faster than the cycloaddition reaction. Finally, hydrolysis of the methyl ester gave a 1:1 mixture of rhododaurichromanic acids A (**2.20a**) and B (**2.20b**) which were separable by HPLC.

In the same year, a second synthesis of rhodochromanic acids A (**2.20a**) and B (**2.20b**) was completed by Jin and co-workers (Scheme 2.8).[22] The syntheses differ principally by the choice of orsellenic acid (**2.40**) as a starting material. The acid **2.40** was protected as a *β*-trimethylsilyl ethyl ester (**2.59**) by Mitsunobou reaction, subsequent chromenylation to **2.60** occurred smoothly using the group's optimised microwave conditions. Mild deprotection with TBAF afforded daurichromenic acid (**2.11a**) in good yield. Finally, UV irradiation using a low-pressure mercury vapour lamp gave a separable mixture of rhododaurichromanic acid A (**2.20a**) (40% BRSM) and B (**2.20b**) (20% BRSM). It is not clear what the authors mean exactly when reporting yields based on recovered starting material exactly, and no detailed experimental procedures are provided. But Jin observes a preference for **2.20a**, the product of *E*-daurichromenic acid without isomerisation.

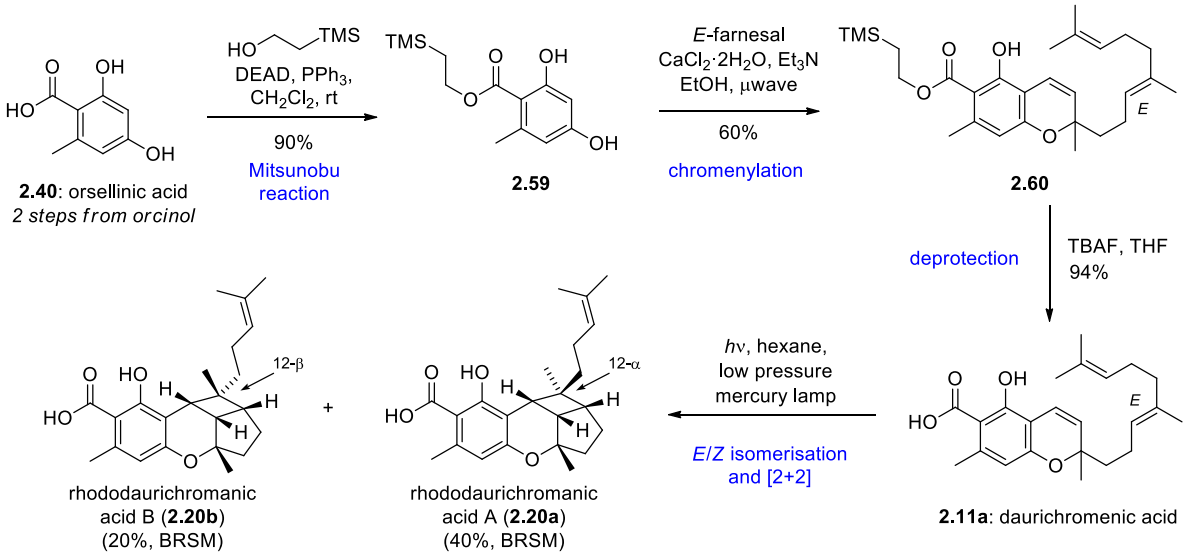

Scheme 2.8: Synthesis of rhododaurichromanic acids A (**2.20a**) and B (**2.20b**). Jin (2003).

This synthesis inspired a third approach, where the carboxylic acid is added after chromenylation by Lee.[23] Hsung's approach led to a derivitisation protocol developed by Wilson and co-workers.[24]

Work on rhodonoids A – G (**2.1** – **2.7**) was done in both the labs of Hsung and Tang and our own group at around the same time. To put things in context: Hsung and Tang completed the first synthesis of rhodonoid A (**2.1)** and B (**2.2**)[25] shortly before rhodonoids C – G (**2.3** – **2.7**) were reported in the literature. Then our group published the first synthesis of rhodonoid C (**2.3**) and D (**2.4**)[26] (*this chapter*) which was followed by Hsung and Tang publishing a second paper,[27] again reporting C (**2.3**) and D (**2.4**) as well as the remaining rhodonoids E – G (**2.5** – **2.7**). Two years later our group reported revised syntheses of rhodonoids A (**2.1**), B (**2.2**), E (**2.5**), and F (**2.6**).[28]

The first point of difference is the manner in which the chromenes are made. Hsung formed *E* and *Z*-confluentin (**2.10a** and **2.10b**) separately, from *E* and *Z*-farnesal (**2.62a** and **2.62b**) respectively; using the same conditions to form chromene (**2.8**) from citral (**2.61**) (Scheme 2.9).

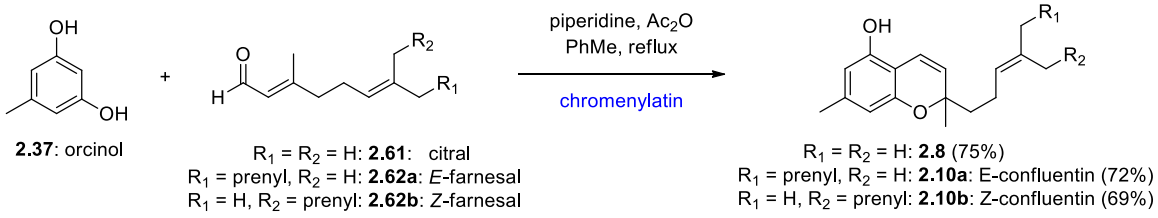

Scheme 2.9: Piperidine/acetic anhydride catalysed chromenylation. Hsung and Tang (2017)

With **2.10a** and **2.10b** separated, Hsung could optimise [2+2] cycloaddition conditions which minimise loss of *E*/*Z* stereochemistry; an issue which caused a difficult separation in their previous synthesis of rhododaurichromenic acid A (**2.20a**) and B (**2.20b**) when UV light was used. Hsung found Lewis acid promoted [2+2] cycloaddition using $Fe(OTf)_3$ to be effective and capable of stereoretention at low temperatures. At room temperature, selectivity is lost due to Lewis acid catalysed isomerisation of the alkene (Scheme 2.10).

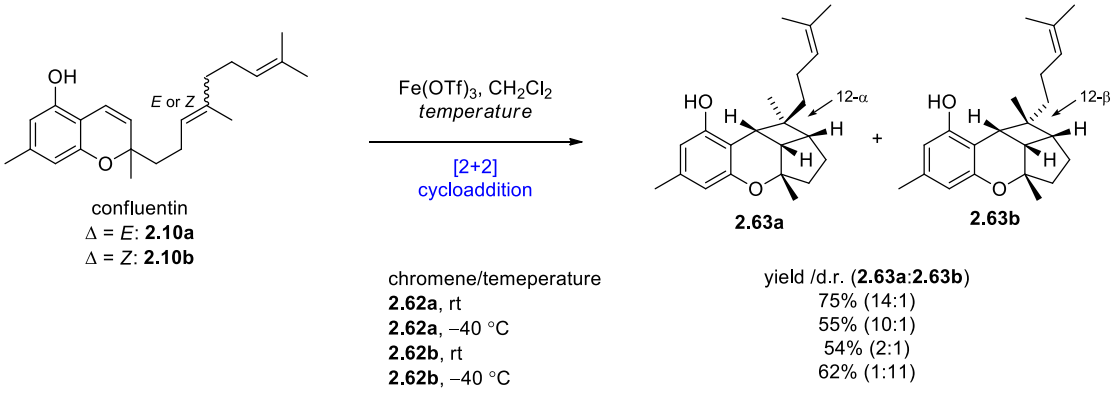

Scheme 2.10: $Fe(OTf)_3$ catalysed [2+2] cycloadditdion optimisation. Hsung (2017)

Hsung's approach had the distinct advantage of selectivity; at the time of this work the only natural product with the skeleton **2.63a**/**2.63b** (excluding the carboxylated rhododaurichromenic acids A (**2.20a**) and B (**2.20b**)) was rhodonoid B (**2.2**), as such a method of selectively synthesising **2.63b** was seen as important. When our group pursued the synthesis of rhodonoids B (**2.2**), and rhodonoids E (**2.5**) and F (**2.6**), both **2.63a** and **2.63b** were equally desired, so a non-specific approach was taken. Chromenylation of a mixture of *E* and *Z* farnesal (**2.62**), followed by non-selective [2+2] cycloaddition using Hsung's $Fe(OTf)_3$ conditions gave a separable mixture of **2.63a/b** (Figure 2.11). The advantage of this approach is one of convenience: both diastereomers are made in a single fell swoop, and *E*/*Z* farnesal (**2.62a/b**) is more readily available (by trivial oxidation of commercially cheap *E*/*Z* farnesol).

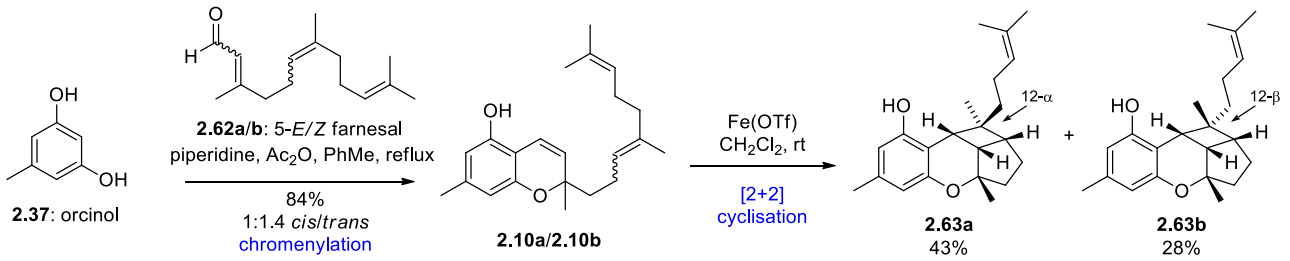

Scheme 2.11: Divergent synthesis of cyclols **2.63a** and **2.63b**. George (2020)

With access to the unfavoured cyclol **2.63b** the only remaining challenge to Hsung was the deceptively difficult oxidation at C-12 which required 9 functional group manipulations (Figure 2.12).

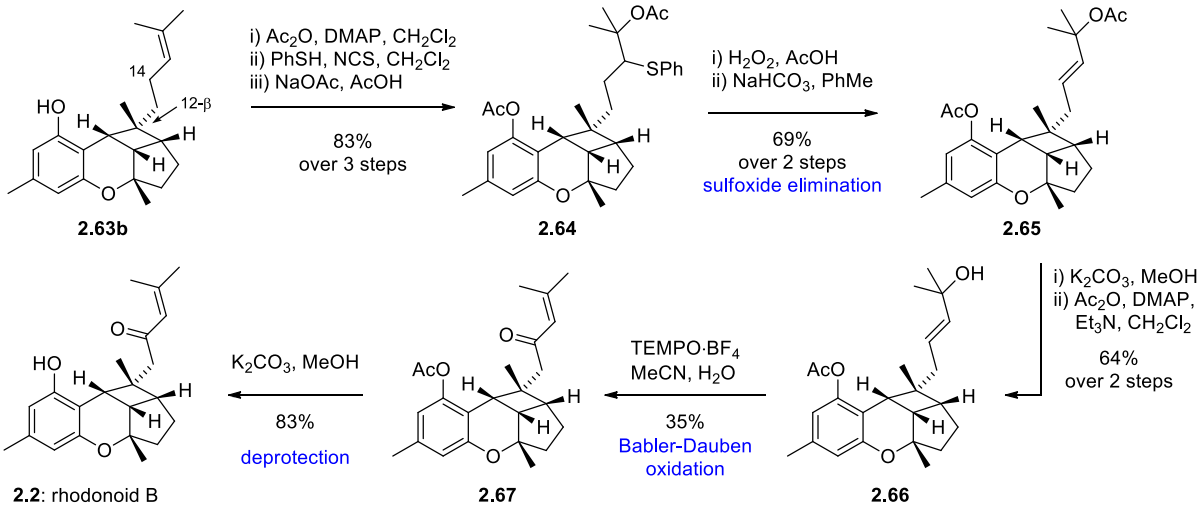

Scheme 2.12: Total synthesis of rhodonoid B (**2.2**). Hsung (2017)

After protection of the phenol of cyclol **2.63b**, Markovnikov addition of benzensulfenyl choride (generated *in situ*) across the pendant olefin, and displacement of the resultant tertiary chloride with sodium acetate gave the 1,2 acetoxy thioether **2.64**. Oxidation and sulfoxide elimination to **2.65** then global deacetylation, followed by selective re-acetylation of the phenol gave the key allylic alcohol **2.66**, primed to undergo a Babler-Dauben reaction. Standard conditions such as PCC, or PDC failed in their hands, but TEMPO·BF_4 facilitated the desired oxidative transposition to *α*,*β*-unsaturated ketone **2.67**. Deacetylation with standard conditions afforded rhodonoid B (**2.2**) in 10.6% overall yield from the cyclol **2.63**.

This same sequence was performed on the more favoured C-12*α* epimer **2.63a** (Scheme 2.13). Protection, then oxidation of the pendant olefin with benzenesulfenyl chloride then S_N1 substitution with NaOAc gave **2.68**. Again, sulfoxide elimination to **2.69** followed by protecting group manipulations gave the key allylic alcohol **2.70**. Babler-Dauben oxidative transposition on this system

was successful under classical PDC conditions, giving a better (though still modest) yield of **2.71**. The synthesis was completed again by deacetylation with normal conditions to give "*epi*-rhodonoid B" (**2.22**), two years before it was isolated and given the name fastinoid B,[9] in another example of rational natural product anticipation.

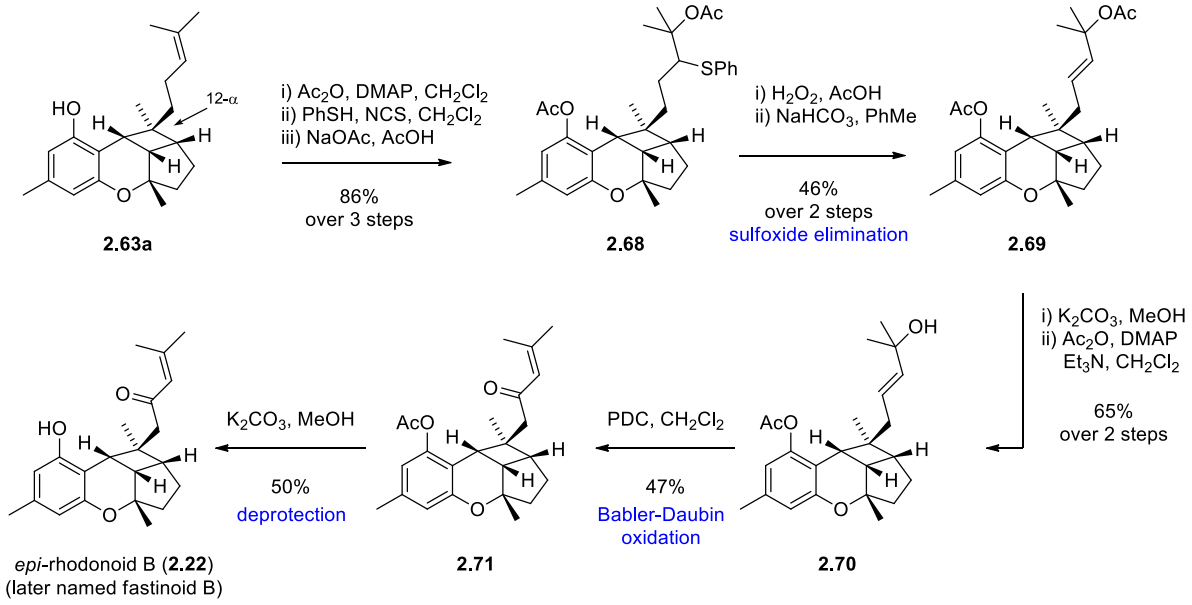

Scheme 2.13: Pre-emptive synthesis of fastinoid B (**2.22**). Hsung (2017)

George's addition to the synthesis of rhodonoid B (**2.2**), as well as rhodonoid A (**2.1**) and E and F (**2.5** and **2.6**), was the elegant use of singlet oxygen as a chemical oxidant. In the synthesis of rhodonoid B (**2.2**) (Scheme 2.14) the protected cyclol **2.72** was synthesised by the same method as Hsung. The Schenck ene reaction was carried by bubbling oxygen through a solution of **2.72** (with TPP as a sensitiser) and irradiating with visible light. The hydroperoxide products were reduced *in situ* to provide a non-discriminant mixture of regioisomers **2.73** (as a 1:1 mixture of diastereoisomers) and Hsung's intermediate **2.66** in good overall yield. Use of singlet oxygen here reduces Hsung's sequence by 5 steps.

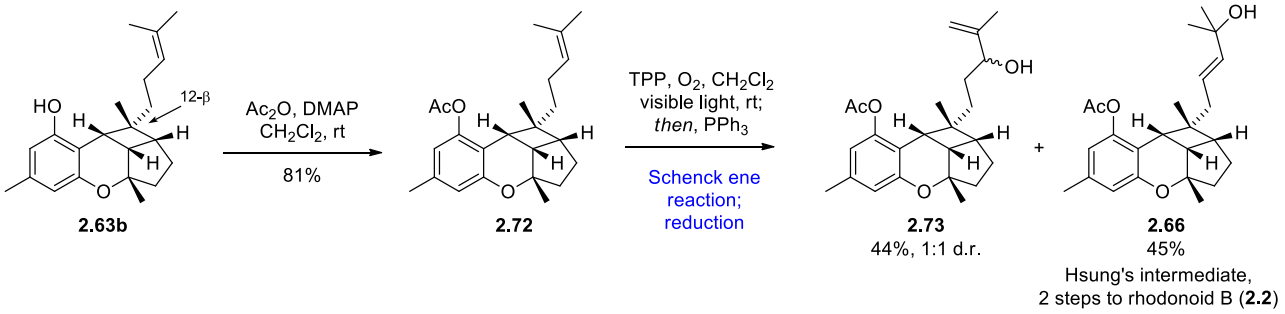

Scheme 2.14: Formal synthesis of rhodonoid B (**2.2**). George (2020)

In Hsung's second report of rhodonoid natural product synthesis rhodonoids E (**2.5**) and F (**2.6**) were targeted (Scheme 2.15).[25] Cyclol **2.63a** (used in their previous synthesis of *epi*-rhodonoid B (**2.2**)) was protected as silyl enol ether **2.74**. Epoxidation and Lewis acid mediated ring opening of the epoxide selectively gave allylic alcohols with a terminal olefin as a 1:1 mixture of epimers **2.75** and **2.76**. These were separated and individually deprotected using TBAF, completing the synthesis of rhodonoid E (**2.5**) and F (**2.6**).

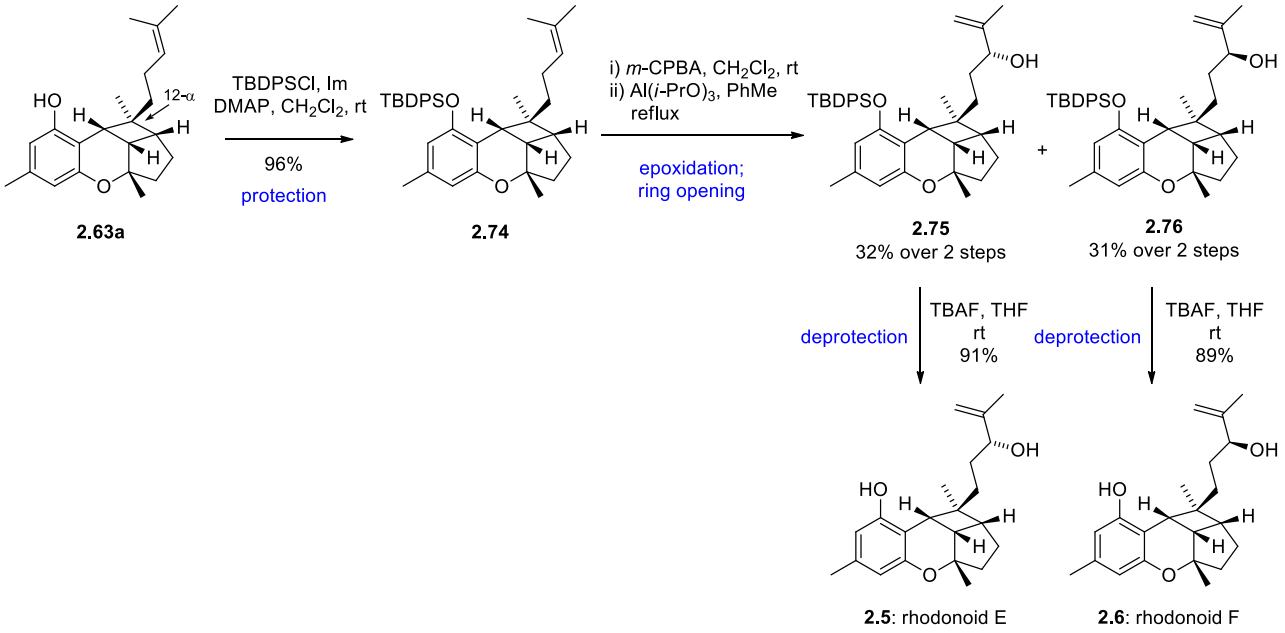

Scheme 2.15: Synthesis of rhodonoid E (**2.5**) and F (**2.6**). Hsung (2017)

Again, George utilised singlet oxygen as an improvement to accessing these molecules. From cyclol **2.63a** Schenck ene reaction and reduction forms rhodonoid E (**2.5**) and F (**2.6**) as well as the intermediate in Hsung's synthesis of *epi*-rhodonoid B (fastinoid B, **2.22**) in a single pot, without the

need for protecting groups (Figure 2.16). The only flaw of this approach is the low selectivity and difficult separation of **2.5**, **2.6**, and **2.70**.

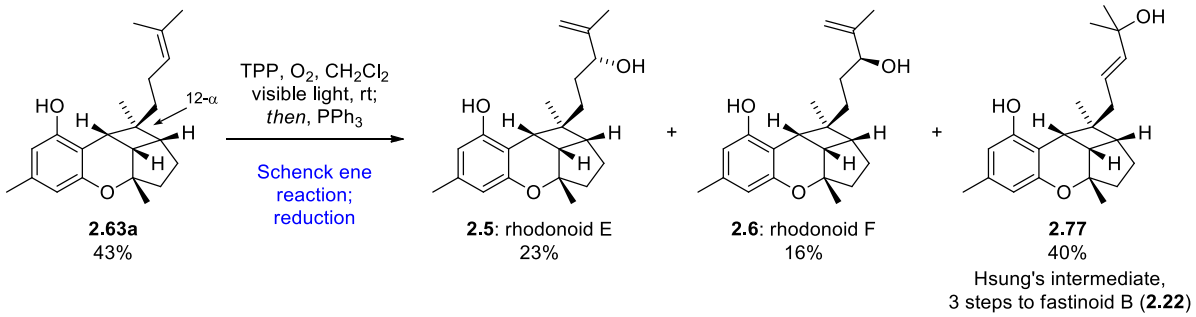

Scheme 2.16: Divergent synthesis of rhodonoid E (**2.5**) and F (**2.6**); and formal synthesis of fastinoid B (**2.22**). George (2020)

Moving to the C_{10} terpene rhodonoids, Hsung utilised the same epoxide opening method in his earlier synthesis of rhodonoid A (**2.1**) (Scheme 2.17). Following protection of **2.8** as a benzyl ether, and epoxidation to **2.78**, Al(O*i*-Pr)$_3$ was used to open the epoxide regioselectively to the terminal allylic alcohol **2.79**. After Dess-Martin oxidation to *α,β*-unsaturated ketone **2.80,** photochemical [2+2] cyclisation was achieved using a high pressure mercury vapour lamp, securing the cyclobutane scaffold **2.81** in modest yield. Removal of the benzyl ether occurred smoothly by hydrogenation, completing the synthesis of rhodonoid A (**2.1**) from chromene **2.8** in 6 steps and 10% overall yield.

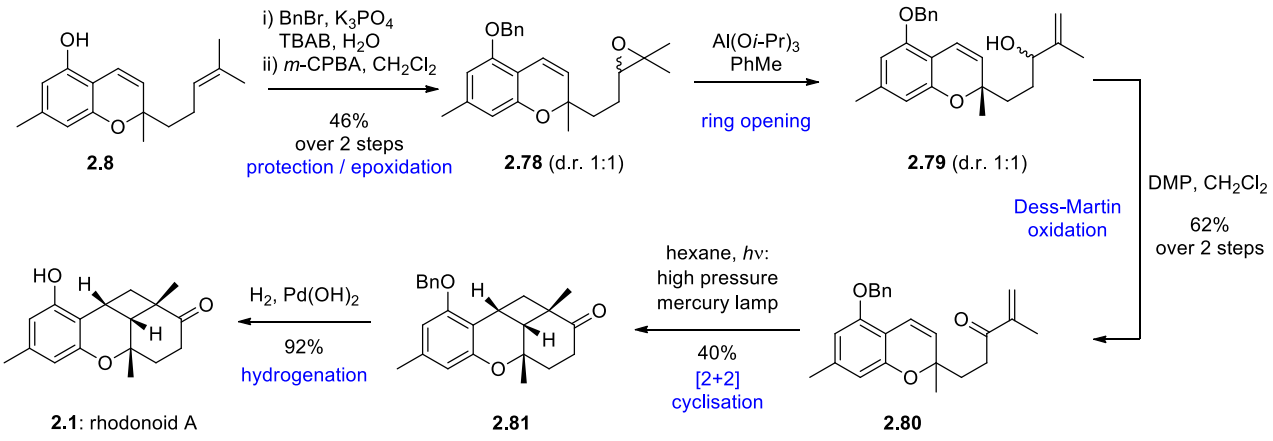

Scheme 2.17: Synthesis of rhodonoid A (**2.1**). Hsung (2017)

In a similar manner as in the synthesis of rhodonoid E (**2.5**) and F (**2.6**), our group again used the Schenck ene reaction to greatly reduce the step count of the synthesis of rhodonoid A (**2.1**) (Scheme 2.18).

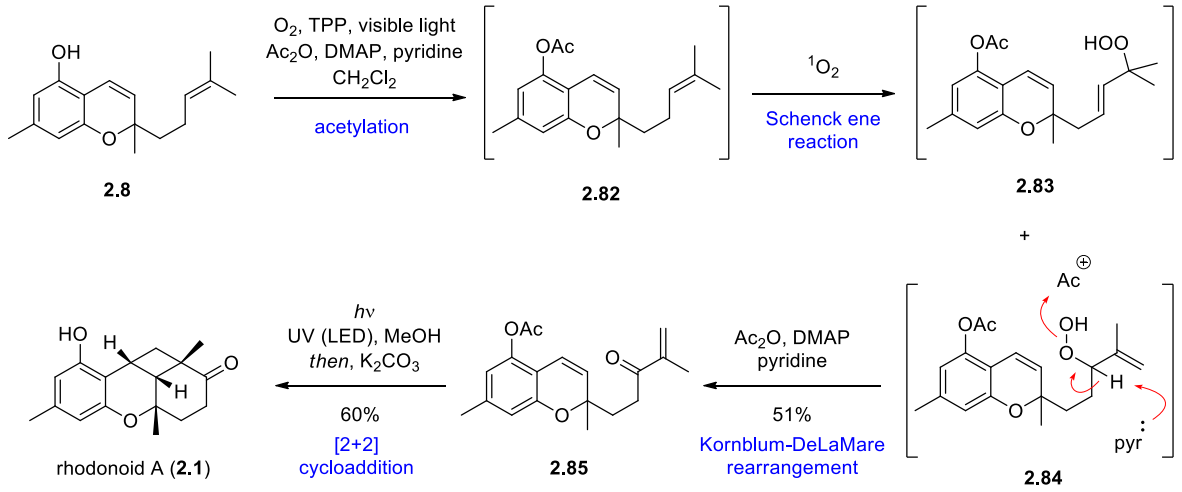

Scheme 2.18: Biomimetic synthesis of rhodonoid A (**2.1**). George (2020)

In a dextrous example of synergy in functional group manipulations, the conditions of the Schenck ene reaction (visible light, O_2, and TPP sensitiser) and the Kornblum-DeLaMare rearrangement were combined. Initially, **2.8** will react with acetic anhydride to form the acetate protected chromene **2.82**. Schenck ene peroxidation will form a roughly equal mixture of regioisomeric allylic hydroperoxides **2.83** and **2.84**: only hydroperoxide **2.84** which contains a peroxymethine proton can undergo the Kornblum-DeLaMare rearrangement giving α,β-unsaturated ketone **2.85** in 51% yield. This tandem reactivity of Schenck ene/ Kornblum-DeLaMare can referred to as a "duet" (the acetate protection is not counted) using the definitions of Jones and Stoltz.[29] Photochemical [2+2] cycloaddition of **2.85** in MeOH and deprotection by subsequent addition of K_2CO_3 in one pot afforded rhodonoid A (**2.1**).

The last of the rhodonoid syntheses discussed here is Hsung's synthesis of rhodonoid G (**2.7**) (Scheme 2.19). Hsung's aim was to intercept the intermediate tertiary cation **2.87** of the stepwise cationic hetero Diels-Alder reaction (path a) to form ranhuadujuanine B (**2.14**) with water. To this end, *p*-TsOH·H_2O was found to be the best after a screening a library of protic acids.

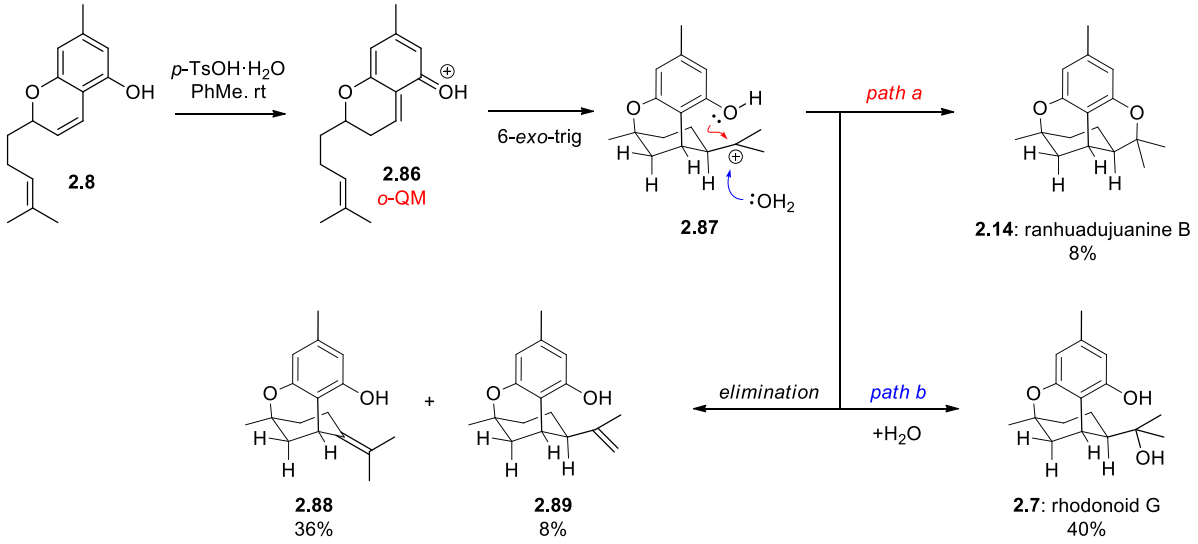

Scheme 2.19: Synthesis of rhodonoid G (**2.7**). Hsung (2017)

Mechanistically, chromene **2.8** is protonated, forming *o*-QM **2.86** which after 6-*exo*-trig cyclisation gives the key tertiary cation **2.87**. Simple ring closing by the nearby phenol (path a) gives citran **2.14**; and alternatively, elimination of either the tertiary methine proton (Zaitsev), or the gem dimethyl protons (anti-Zaitsev) would give alkenes **2.88** or **2.89**, respectively. Addition of water to the tertiary carbocation gives rhodonoid G (**2.8**) (path B). It is worth noting the isolated yields reported by Hsung represent the equilibrium of this reaction, as each product forming step is reversible. Hsung performed experiments where each isolated product **2.7**, **2.14**, **2.88**, and **2.89** was resubjected to the reaction conditions separately, and the products consistently redistributed to the same ratio.

2.1.4: Previous Epoxide Cyclisation Cascade Reactions

Returning to the biosynthesis of rhodonoid C (**2.3**) and D (**2.4**) (as well as murrayakonine D (**2.48**)), our proposal shows a stepwise, ionic cyclisation occurring. If we were to simplify this process, it can be classified as a formal (3+2) cycloaddition (Scheme 2.20a). Hypothetical cleavage of the C-O bond in the epoxide reveals a 1,3-zwitterion (Scheme 2.20b), this dipolar cyclisation is analogous to the more common 1,3-dipolar cycloaddition of a nitrone and an alkene (2.20c).

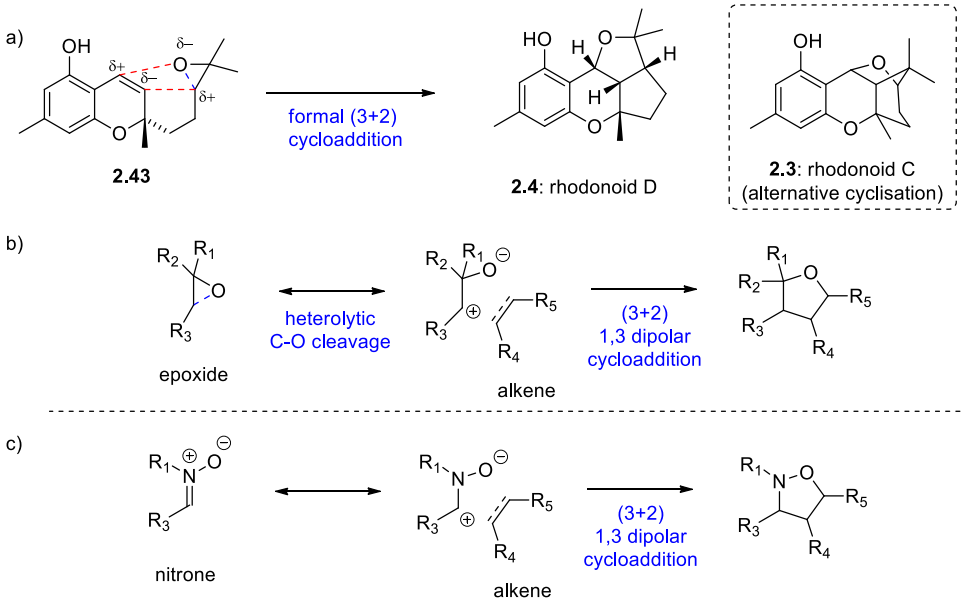

Scheme 2.20: a) Desired rhodonoid cyclisation. b) epoxy-olefination shown as a formal (3+2) cycloaddition. c) (3+2) cycloaddition of a nitrone and an olefin.

With this model in mind, there are very few examples of this transformation occurring in the literature; specifically, the formal (3+2) cyclisation of an epoxide with an alkene.

A closely related palladium catalysed methodology was reported by Yamamoto in 1998.[30] Here, an elegant Tsuji-Trost / coupling cascade of allylic epoxides and electron poor olefins gave an assortment of substituted tetrahydrofurans (Scheme 2.21). Palladium (0) (as $Pd(PPh_3)_4$ in the initial report) forms π-allyl species **2.91** with allylic epoxide **2.90**. Conjugate addition of the resultant alkoxide with Michael acceptor **2.92** (EWG = CN, CO_2Et, or SO_2Ph) gives the zwitterion **2.93**. Finally, cyclisation to **2.94** followed by *β*-hydride elimination affords tetrahydrofuran **2.95** and regenerates Pd (0), completing the cycle.

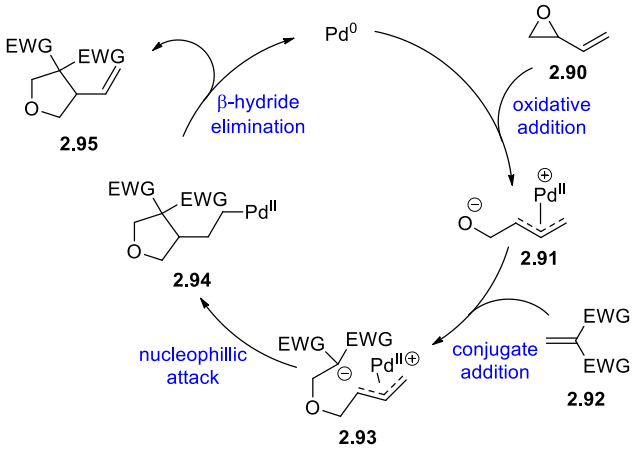

Scheme 2.21: Pd Catalysed (3+2) Epoxy-olefin Cycloaddition. Yamamoto (1998)

In this report, diastereoselectivity was generally very poor with substituted Michael acceptors. Later work, independently by Hou[31], and Song and Ni[32], further developed this methodology by using the bulky, chiral phosphine ligand BINAP which gave both high diasetereoselectivity and enantioselectivity. The substrate scope was also expanded to include *α,β*-unsaturated ketones, and aryl imines as Michael acceptors.

This methodology is essentially the *umpolung* variant of our proposed cyclisation for rhodonoids C (**2.3**) and D (**2.4**). In place of a Michael acceptor, we proposed a vinylogous enol, and the order of the stepwise cyclisation is reversed (C-C bond, then C-O bond).

A relatively recent example of this transformation is from Song's synthesis of 2-hydroxy-*α*-cyclogeraniol (**2.97**).[33] Song treated epoxide **2.96** against a selection of Lewis acids with the intention of selectively forming **2.97** without the *exo* alkene **2.98**. In several of the conditions screened the unwanted byproduct **2.99** was observed. Although no mechanism was presented by the author, it is most likely formed in a process analogous to the synthesis of rhodonoid C (**2.3**) by a strongly cationic pathway (Scheme 2.22).

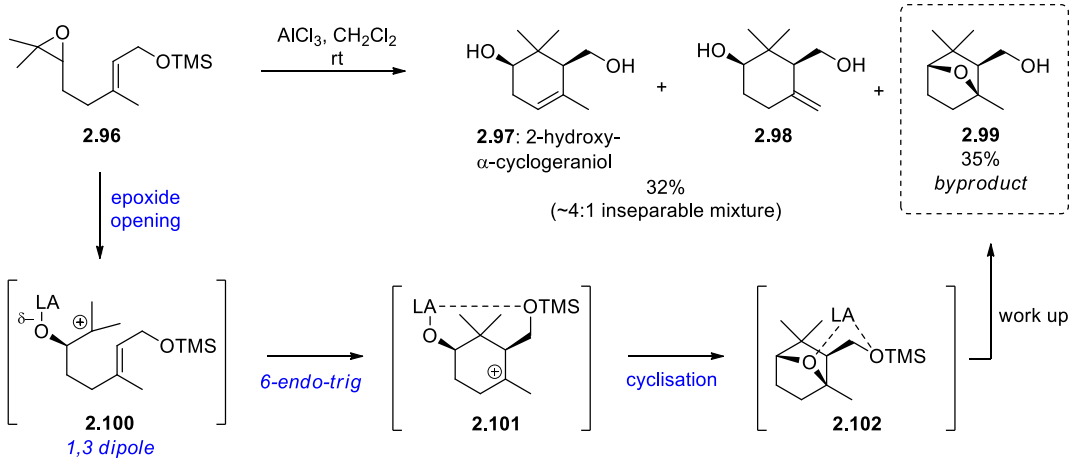

Scheme 2.22: Unwanted formal (3+2) cyclisation during optimisation of the synthesis of 2-hydroxy-*α*-cyclogeraniol (**2.97**). Song (2016)

Epoxide **2.96** is opened by the Lewis acid ($AlCl_3$) to the more stable tertiary carbocation **2.100**, cyclisation from the alkene (6-*endo*-trig) gives the carbocation **2.101**, which can eliminate to give either **2.97** or **2.98**, or cyclise from the alcohol giving the bicycle **2.102** (**2.99** after work up).

In a more complex setting, this method was attempted by the Trost group toward an asymmetric synthesis of siccanin (**2.104**).[34,35] Siccanin (**2.104**) is a meroterpenoid derived from *H. siccans* (Dreschler), a parasitic plant fungus.[36] Trost proposed a biomimetic synthesis using a formal (3+2) cycloaddition, or as he coined "epoxyolefin cyclization" from the epoxide sicannochromene B (**2.105**) (Scheme 2.23). Unfortunately, Trost's attempts at this catalysed epoxyolefin cyclisation, or formal (3+2) cycloaddition, failed with all Lewis acid conditions screened (including: $BF_3{\cdot}OEt_2$, $TiCl_4$, $SnCl_4$, $FeCl_3$, $Yb(OTf)_3$, etc.); resulting only in decomposition, or formation of aldehyde **2.112** via a Meinwald rearrangement.

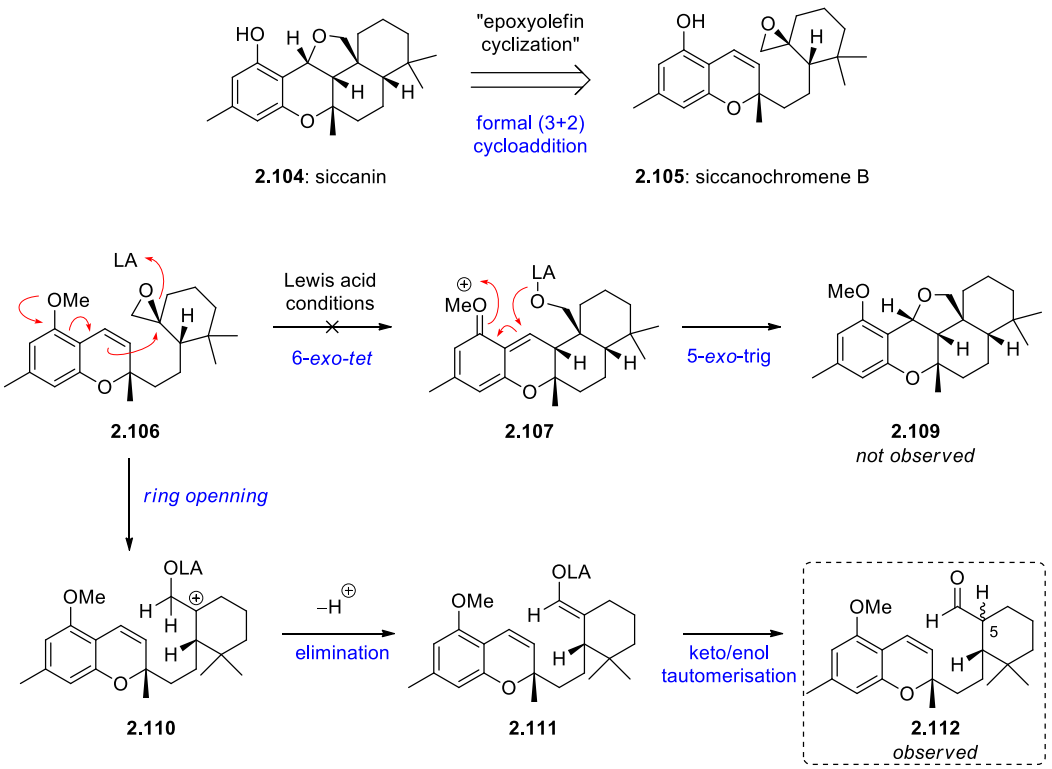

Scheme 2.23: Biomimetic disconnection of siccanin (**2.104**) to siccanochromene B (**2.105**) and unsuccessful attempts under Lewis acid conditions. Trost (2003)

Not discouraged, Trost turned to radical cyclisation conditions. Cp_2TiCl, a Titanium (III) single electron reductant, had been used with epoxides in either stereo- and regioselective reduction to alkenes, and in intramolecular alkene-epoxide cyclisations; both proceeding by reductive ring opening of the epoxide to the most stable carbon centred radical.[37]

With the same epoxide **2.106** in hand, the Trost group used Cp_2TiCl (generated *in situ* from Cp_2TiCl_2 with elemental Manganese) to complete the endgame of the synthesis of siccanin (**2.104**) (Scheme 2.24). Single electron reduction and ring opening of **2.106** gave the tertiary radical **2.113**, ablating the stereoconfiguration at C-5. This prochiral radical can cyclise with the chromene olefin (6-*exo*-tet) in two ways. In the top pathway, a trans-decalin **2.116** intermediate is formed. **2.116** is arranged such that subsequent radical cyclisation back to oxygen is possible, giving **2.117**; this is a formal (3+2) cyclisation). Demethylation of **2.117** gave the C-5 epimer of siccanin (**2.118**). Alternatively, **2.113**

can cyclise to give a cis-decalin **2.114**, but rather than further cyclising like the first pathway, further reduction occurs giving **2.115** after protonation as the major product. The final ring of siccanin (**2.104**) was made by oxidative dearomatisation of alcohol **2.115** to an *o*-QM like benzylic cation, and nucleophilic addition of the alcohol.

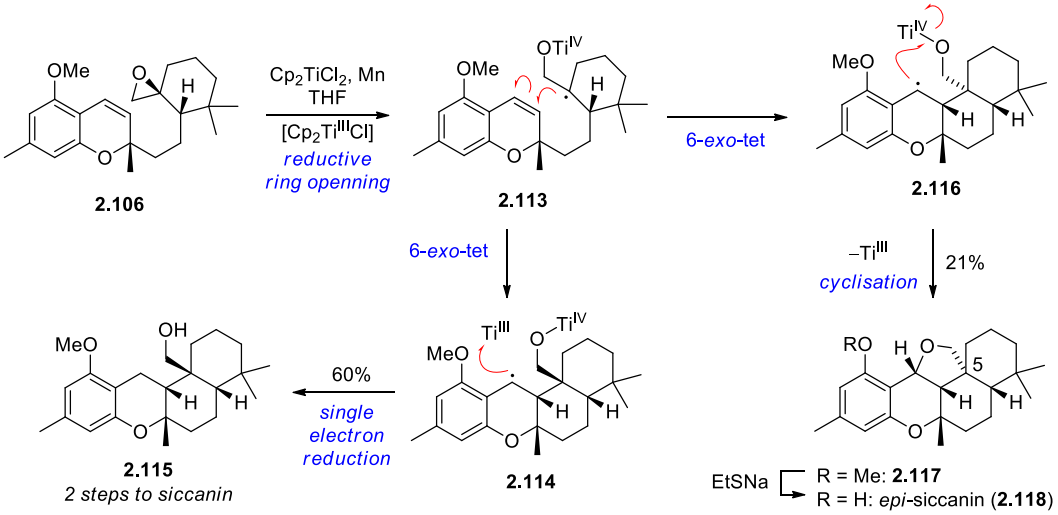

Scheme 2.24: Successful radical cyclisation approach to siccanin (**2.104**). Trost (2003)

Trost's biomimetic synthetic investigations raised questions as whether the true biosynthesis occurs by either radical or cationic pathways. These same questions apply to our synthesis of rhodonoid C (**2.3**) and D (**2.4**). It is unclear if the results of the cationic experiments would be different if non-methylated siccanochromene B (**2.105**) was used instead of **2.106**.

2.2 Results and Discussion

2.2.1: Biomimetic Synthesis of Rhodonoids C (**2.3**) and D (**2.4**)

Access to the key cyclisation substrate **2.43** was trivial by chromenylation of orcinol (**2.37**) followed by epoxidation using *m*-CPBA (Scheme 2.25). For the chromenylation, conditions using catalytic EDDA (popularised by Lee[38]) were preferred over Hsung's conditions (piperidine and Ac_2O) due to ease. The amount of EDDA used could be reduced to <5 mol% while maintaining yields comparable

to Hsung (75%, Scheme 2.9) and work up was greatly simplified to just removal of the solvent, and column chromatography. The epoxidation was stubborn; never going to completion. Attempts to improve conversion by longer reaction time, increasing equivalents of *m*-CPBA, adding *m*-CPBA portion-wise, adding $NaHCO_3$, gently warming, or cooling with longer reaction time gave no improvement to the yield; and in most cases led to decreased purity of the product. The pragmatic solution was to deliberately stop the reaction before completion and recover the remaining starting material for future use.

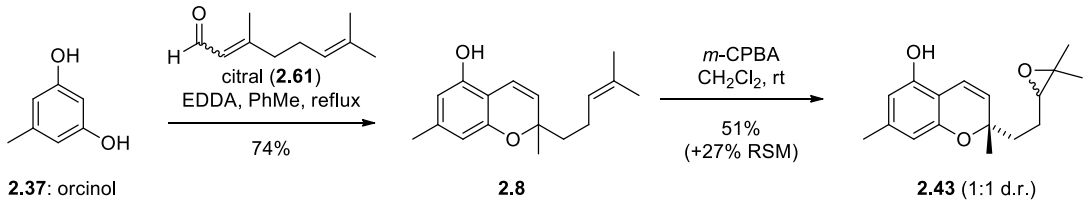

Scheme 2.25 Synthesis of epoxide **2.43**.

With this method we could readily make multiple grams of the epoxide **2.43**. Our attention was placed toward developing our proposed cyclisation cascade. Initially we were unsure if the cascade would best occur through an anionic or cationic pathway. Our hope was to see some selectivity toward rhodonoid C (**2.3**) or D (**2.4**) depending on reagent used (e.g. C as major product when a Lewis acid is used, D as major product when base is used).

Whilst screening cyclisation conditions (Table 2.1) it was quickly found the reaction only worked in acidic (Lewis or Brønstead-Lowry) conditions; though some rhodonoid C (**2.3**) was formed when heated to reflux "on" water. The best conditions we found were using $SnCl_4$, giving rhodonoid C (**2.3**) and D (**2.4**) in 32% and 5% yield, respectively, alongside the ketone by-product (**2.119**) (Scheme 2.26).

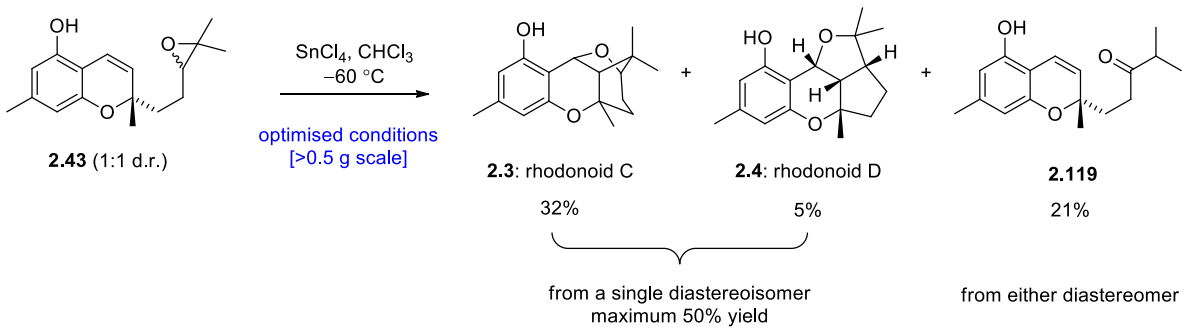

Scheme 2.26: Synthesis of rhodonoids C (**2.3**) ad D (**2.4**) by epoxy-olefin cyclisation cascade.

The ketone **2.119** was formed in almost all acidic conditions tried. It is similar to aldehyde (**2.112**) in Trost's cationic approach to siccanin (*vide supra*, Scheme 2.23) being formed by a Meinwald rearrangement of the epoxide (Scheme 2.27).

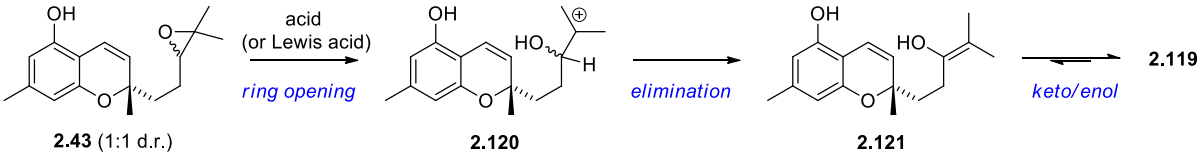

Scheme 2.27: Meinwald rearrangement of **2.43** to form ketone **2.119**.

A short coming of this approach is the epoxide **2.43** is formed as a 1:1 mixture of diastereoisomers. As both rhodonoid C (**2.3**) and D (**2.4**) come from the same epoxide (**2.43a**), the maximum yield possible from 1:1 d.r. **2.43** is only 50%. The ketone **2.119** however can be formed from either isomer of **2.43**.

Table 2.1: Conditions for epoxy-olefin (3+2) cyclisation.

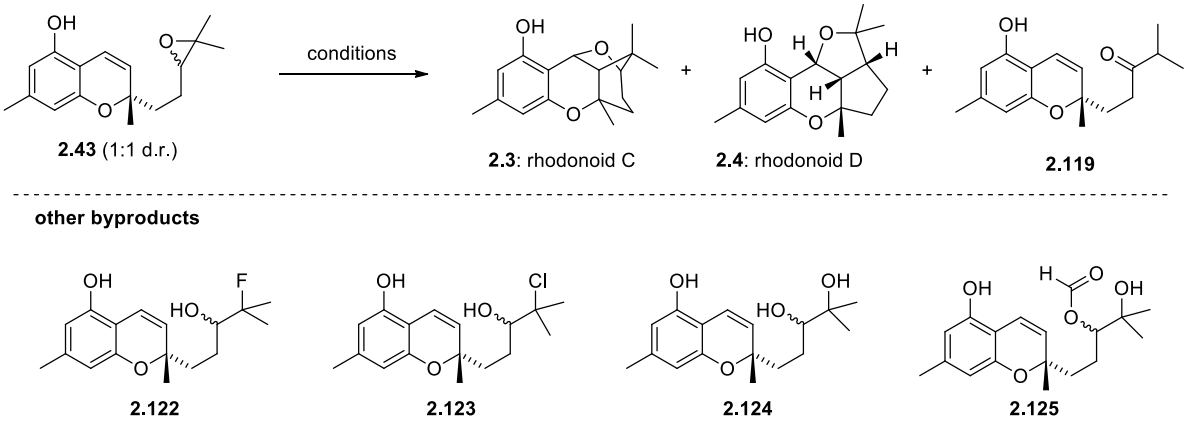

	reagent (eq.)	conditions	**2.3**	**2.4**	**2.119**	other
Brønsted-Lowry acids	*p*-TsOH (1.0)	CH_2Cl_2, rt, 10 min	12%	1%	2%	-
	p-TsOH (1.0)	CH_2Cl_2, –78 ˚C, 1 h	no reaction			
	p-TsOH (1.0)	CH_2Cl_2, –78 ˚C→rt, 1 h	15%	2%	4%	-
	p-TsOH (1.0)	$CHCl_3$, rt, 15 min	13%	2%	5%	-
	p-TsOH (0.1)	$CHCl_3$, rt, 30 min	21%	2%	5%	-
	p-TsOH (1.0)	DMF, rt, 30 min	0%	-	2%	**2.125**: 28%
	PPTS (1.0)	CH_2Cl_2, rt, 5 h	11%	3%	6%	-
	CSA (1.0)	CH_2Cl_2, 0 ˚C, 10 min	21%	2%	-	-
	TFA (1.0 eq)	CH_2Cl_2, 0 ˚C, 15 min	20%	-	28%	-
	AcOH (1.0)	CH_2Cl_2, rt, 3 d	no reaction			
	1.0 M HCl	EtOH (1:1), rt, 15 min	-	-	-	**2.123**: 26% **2.124**: 9%
Lewis acids	$SnCl_4$ (1.0)	$CHCl_3$, –60 ˚C, 30 min	32%	5%	21%	-
	$SnCl_4$ (1.0)	CH_2Cl_2, –78 ˚C, 10 min	25%	0%	6%	-
	$SnCl_4$ (0.5)	CH_2Cl_2, –78 ˚C, 15 min	26%	3%	29%	-
	$TiCl_4$ (1.0)	CH_2Cl_2, –78 ˚C, 5 min	26%	-	15%	**2.123**: 17%
	$FeCl_3$ (0.5)	CH_2Cl_2, –78 ˚C, 75 min	25%	2%	35%	-
	$FeCl_3 \cdot 6H_2O$ (1.0)	CH_2Cl_2, –78 ˚C to 0 ˚C	23%	-	40%	**2.123**: 4%
	$BF_3 \cdot OEt_2$ (1.0)	CH_2Cl_2, –78 ˚C, 30 min	-			**2.122** 18%
bases	$Ca(OH)_2$ (1.0)	EtOH, rt, 1 d	no reaction			
	$Ni(OH)_2$ (1.0)	EtOH, reflux, 1 d	no reaction			
	NaH (1.0)	THF, rt, 16 h	no reaction			
	K_2CO_3 (1.0)	DMF, rt, 3 d	no reaction			
	t-BuOK (1.0)	THF, 0 ˚C to rt, 1 d	no reaction			
	t-BuOK (1.0)	*t*-BuOH, reflux, 1 d	no reaction			
nil	-	PhMe, reflux, 16 h	no reaction			
	-	H_2O, 100 ˚C, 16 h	4%	-	3%	**2.124**: 44%

We also considered a radical cyclisation approach, similar to those used by Trost. This approach would be mechanistically different to the cationic pathway, and as such might give us different selectivity. To this end, Cp_2TiCl (generated *in situ*) was employed. The only observed product was **2.126**, as a 1:1 mixture of epimers (retained from the starting mixture). **2.126a** contains the 6-6-6 rings of rhodonoid C (**2.3**); but the second cyclisation event did not occur. This is similar to what occurred in the major product of Trost's synthesis of siccanin (**2.104**) (*vide supra*, Scheme 2.24).

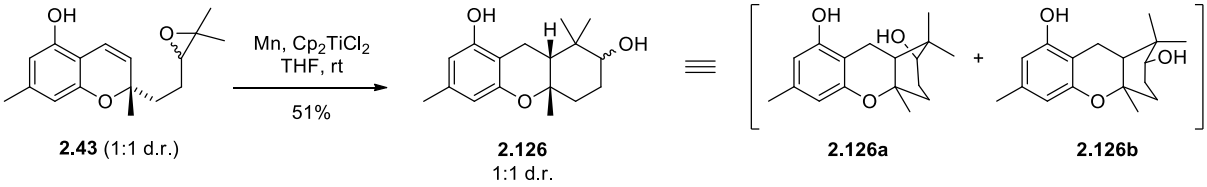

Scheme 2.28: Reductive cyclisation of epoxide **2.43** using $Cp_2Ti^{III}Cl$.

2.2.2: Kinetic Separation of Epoxide **2.43**

Our hypothesis was that only half of the epoxide **2.43** (**2.43a**) had the correct configuration to cyclise to either rhodonoid C (**2.3**) or D (**2.4**). This could be supported if we separated the isomers and repeated the reaction on each isomer separately. The correct isomer (**2.43a**) should give a much higher (theoretically double) yield; and the incorrect isomer (**2.43b**) should give a much lower (theoretically zero) yield under the same reaction conditions. Unfortunately, the epimeric epoxides were practically inseparable using flash column chromatography with SiO_2 or silver nitrate impregnated SiO_2 (SNIS)[39], or semipreparative HPLC.

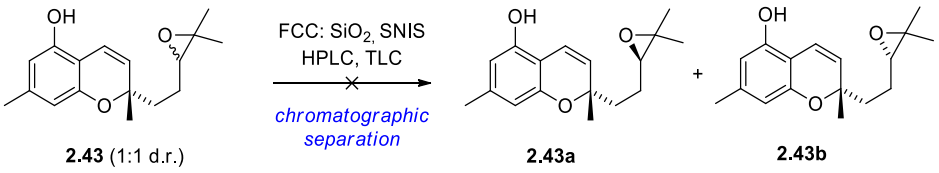

Figure 2.29: Failed chromatographic separation of **2.43**.

A solution to this problem was initially found by accident. When scaling up the best conditions ($SnCl_4$, $CHCl_3$, −60 °C) a reaction was unintentionally quenched prematurely, and after chromatography, the product distribution showed only slightly lowered yields for rhodonoids C (**2.3**) and D (**2.4**), and a significantly lowered yield of the ketone **2.119**. The epoxide (**2.43**) recovered from this reaction was no longer an equal mixture, now an enriched to d.r. 1:3.3 (Scheme 2.30). This is interpreted as a difference in reaction rate. The natural epoxide **2.43a** reacts to form rhodonoid C and D more rapidly than it does to form the ketone. As the unnatural epoxide **2.43b** cannot form C or D, it can only react to form the ketone, at the same slower rate. So, at the half-point of the reaction, most of the natural epoxide **2.43a** has been consumed, leaving mostly **2.43b**.

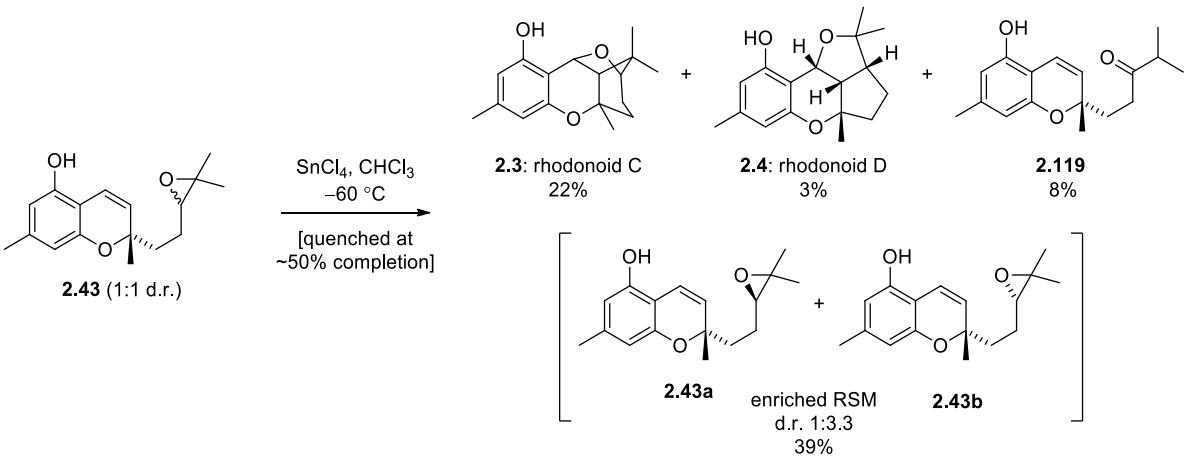

Scheme 2.30: Serendipitous kinetic separation of epoxide **2.43**.

This difference is quite subtle as the majority of ^1H NMR signals are perfectly overlapped. However, the change in ratio can be seen in one of the chromene peaks (Figure 2.5).

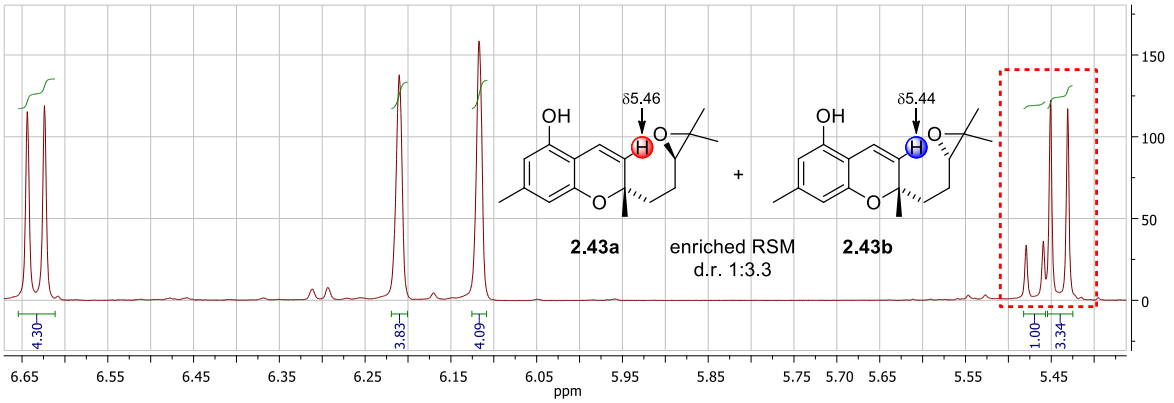

Figure 2.5: Integration of enriched mixture of epoxide **2.43** (^{1}H NMR, 500 MHz, $CDCl_3$)

To solidify our claim the epoxide was enriched with the unwanted epimer **2.43b** this 1:3.3 mixture was resubjected to the same reaction conditions (Scheme 2.31). As expected, the yield of rhodonoid C (**2.3**) was dramatically reduced (13%, from 32%), and rhodonoid D was not observed (presumably formed but not isolated). The ketone **2.119** now dominated as the major product (32% from 20%) and the chloride **2.123**, which was only previously observed in trace amounts, formed in 13% as a single isomer (presumably with the configuration of **2.43b**).

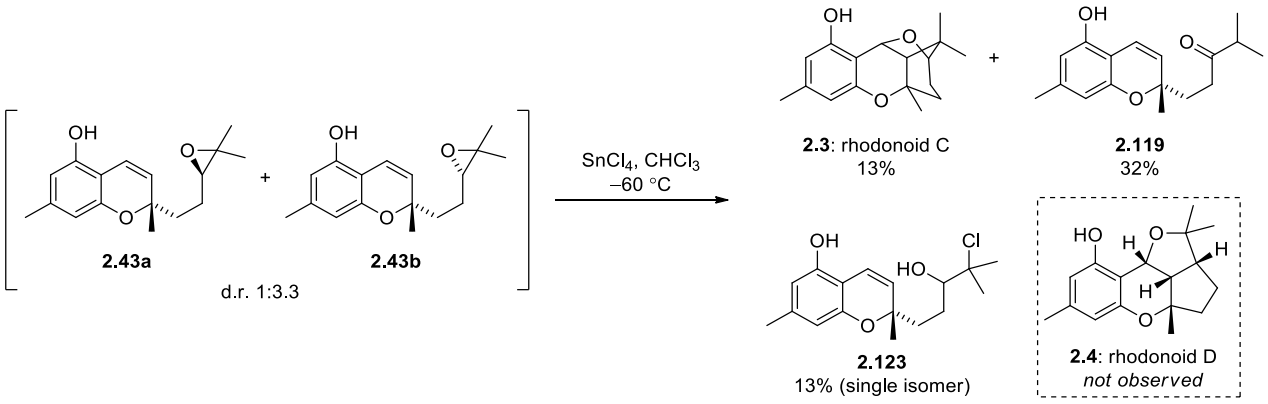

Scheme 2.31: Resubjecting epoxide enriched with **2.43b** to standard cyclisation conditions.

2.2.3: Biomimetic Synthesis of Murrayakonine D (**2.48**)

After the completion and optimisation of the rhodonoid C and D synthesis in the simple and readily accessible orcinol system our eyes were set on the slightly more complex rhodonoid C carbazole

analogue murrayakonine D (**2.48**). We were particularly interested in how a more electronically deficient chromene would fare in the key step, and if we could synthesise the theoretical rhodonoid D carbazole analogue.

A published preparation of the chromene mahanimbine (**2.49**) by Knölker[40] was followed to begin our synthesis (Scheme 2.32). Starting from 2-methyl-5-nitrophenol (**2.127**), benzyl protection to **2.128** and nitro reduction with iron powder gave the aniline **2.129** in good yield. The carbazole **2.131** could be completed by Buchwald-Hartwig amination and intramolecular oxidative Heck reactions. Knölker had originally used PhBr with $Pd(OAc)_2$ and the ligand XPhos in the presence of Cs_2CO_3 for the Buchwald-Hartwig amination step. We opted for the palladium-free procedure of Dethe *et al.* using $PhB(OH)_2$ and catalytic $Cu(OAc)_2$[41], mainly because this alternative procedure seemed more practical, and didn't require XPhos. Following Dethe's procedure gave poor conversion and low yield in our hands; however, simply changing the amount of $Cu(OAc)_2$ to a superstoichiometric amount (2 equiv.) dramatically improved the reaction to 69% **2.130**. Following this, the intramolecular oxidative Heck reaction to carbazole **2.131** proceeded smoothly with Knölker's conditions of catalytic Pd (II) in molten pivalic acid open to air.

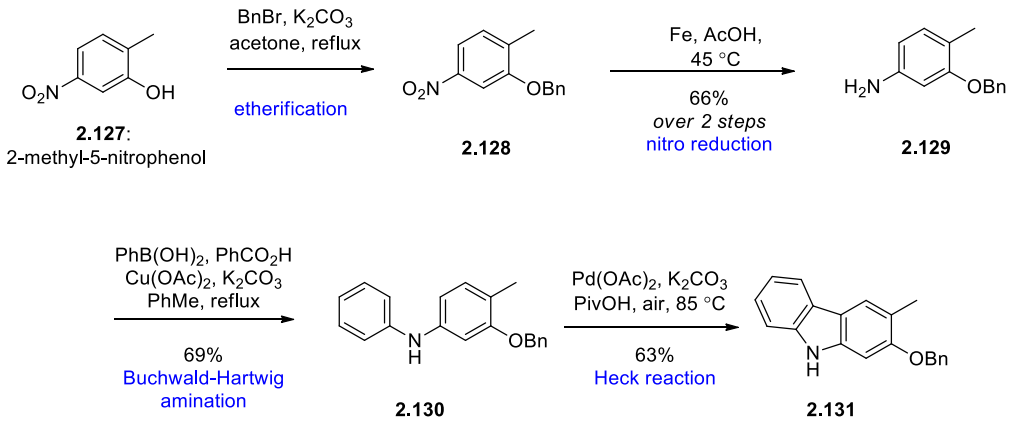

Scheme 2.32: Synthesis of carbazole **2.131** *en route* to mahanimbine (**2.49**).

An alternative protocol was tried using a methodology from Wang and co-workers[42] where anilines were coupled with cyclohexanones to form carbazoles in a single step (Scheme 2.33). In this reaction

cylohexanone and anliline **2.129** condense to form an imine (**2.132**, enamine tautomer) which adds to Pd (II) (as $Pd(OPiv)_2$). The cyclohexyl ring aromatised by successive β-hydride eliminations, and the carbazole **2.131** is formed by a final intramolecular Heck reaction. Palladium is used catalytically, with $Cu(OAc)_2$ acting as the terminal oxidant.

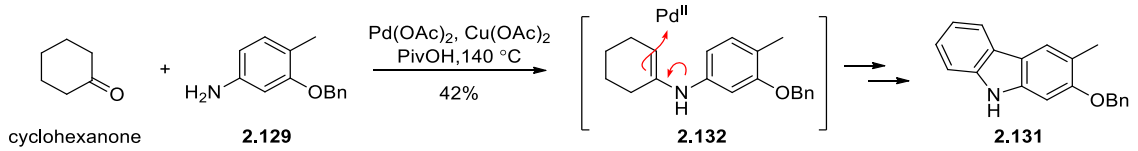

Scheme 2.33: One-pot carbazole formation.

The one-pot procedure occurred with full conversion, and only one major product; however isolated yields were consistently poor to modest (30 – 50%). The main problem of this method was purification. Removing the large amounts of pivalic acid and copper proved difficult, especially when scaled up, and the poor solubility of the product made chromatography cumbersome. In practice, we mainly used the first (two-step) method as it was more consistent and easier to scale; however, the second protocol (one-step) had more potential, though we were unsuccessful in harnessing it.

The complete furnishing the mahanimbine skeleton, Knölker's procedure was followed closely (Scheme 2.34). Hydrogenation of carbazole **2.131** gave phenol **2.133**, and chromenylation with the Lewis acid $Ti(O\textit{i}\text{-}Pr)_4$ gave mahanimbine (**2.49**) in good yield. In our hands, we found residual citral difficult to remove after the chromenylation by chromatography. To circumvent this, we reduced it to geraniol/nerol using $NaBH_4$ to increase the separation.

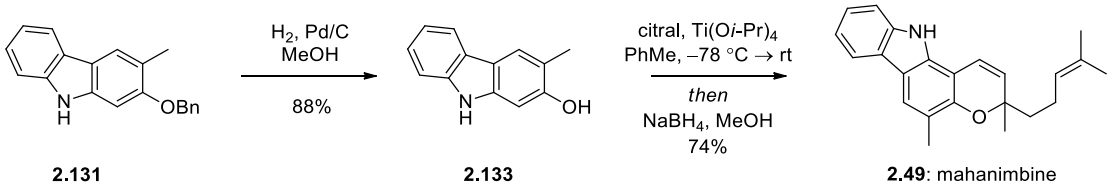

Scheme 2.34: Deprotection and chromenylation to mahanimbine (**2.49**).

With this chromene (**2.49**) we carried out the same cyclisation methods as in the rhodonoid system (Scheme 2.35). Only our best conditions from the previous system were screened as material was much more limited.

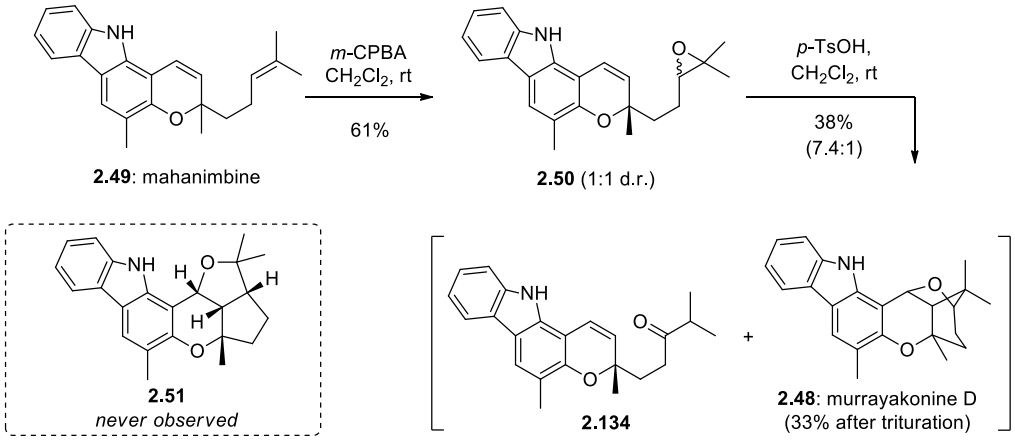

Scheme 2.35: Biomimetic epoxy-olefination to murrayakonine D (**2.48**)

With the carbazole system, no rhodonoid D-type compound (**2.51**) was ever observed. This is attributed to poorer electron donation from the pyrrole-like nitrogen (*cf.* a phenol) making the chromene olefin a poorer nucleophile. As such, this reaction proceeds completely by *path a* (Scheme 2.4), and by a more cationic process. A ketone **2.134** (analogous to **2.119** in the rhodonoid system) was also formed, which had the same R_f as murrayakonine D **2.48** and could not be separated by standard flash column chromatography on SiO_2 or SNIS. The solution we found was to isolate **2.48** and ketone **2.134** as mixture by chromatography, then selectively remove **2.134** by careful trituration in cold MeOH. A clean sample of the ketone was produced by further purification of the filtrate. The residual solid was pure, and recrystallisation gave a single crystal of **2.48** suitable for X-ray diffraction.

2.2.4: Later Synthesis of Rhodonoids C (**2.3**) and D (**2.4**)

Shortly after our synthesis of rhodonoids C and D, and murrayakonine D (**2.48**) was published, the Hsung group reported a second synthesis (Scheme 2.36).[27] To overcome the modest yield of the epoxidation, Hsung evoked an acetyl protecting group (as he had in the synthesis of rhodonoid B (**2.2**), Scheme 2.12). Subsequent oxidation and deprotection occurred smoothly, giving an increased overall yield of **2.43** (*vide supra*, Scheme 2.12). Finally, for the cyclisation step, by refluxing epoxide **2.43** in toluene in the presence of SiO_2 gel the rearrangement occurred in a lower combined yield, but with increased ratio of rhodonoid D (**2.4**) compared to rhodonoid C (**2.3**); the highest yield of rhodonoid D in any synthesis to date. SiO_2 gel promoted rearrangements of chromenes have been reported previously in the synthesis of THC like compounds and showed to give different selectivity than more standard Lewis acids (e.g. $FeCl_3$).[43,44]

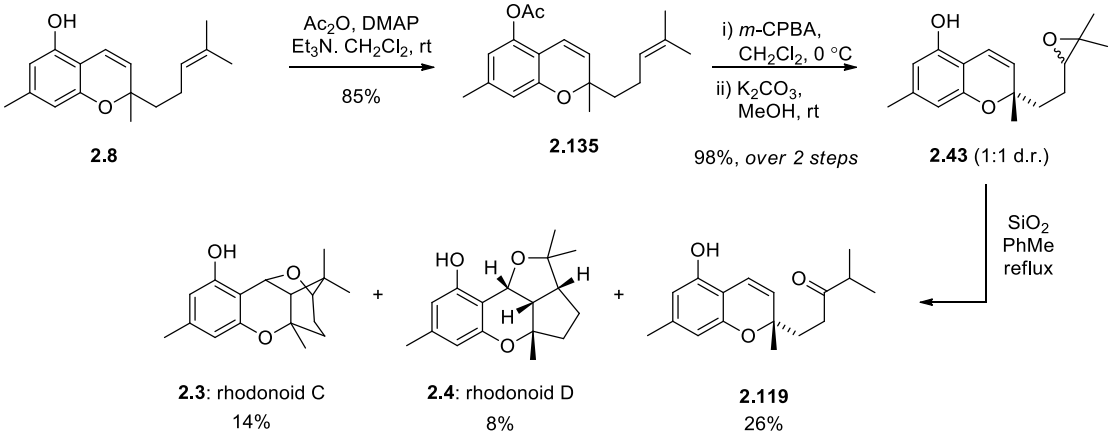

Scheme 2.36: Biomimetic synthesis of rhodonoids C (**2.3**) and D (**2.4**). Hsung (2017)

2.3 Summary and Conclusion

In summary a divergent total synthesis of rhodonoid C (**2.3**) and D (**2.4**) was achieved in three steps from commercially available starting materials. This synthesis represents the first total synthesis of these molecules, and to the best of our knowledge, contains the first cationic (3+2) epoxy-olefin cyclisation used in total synthesis. This methodology was also applied to the total synthesis of the alkaloid murrayakonine D (**2.48**).

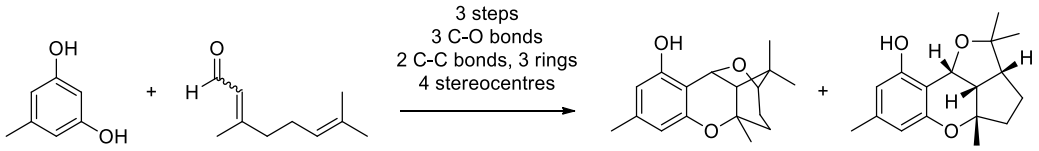

2.37: orcinol **2.61**: citral **2.3**: rhodonoid C **2.4**: rhodonoid D

Scheme 2.37: Summary of rhodononoid C (**2.3**) and D (**2.4**) synthesis.

2.4 Experimental

2.4.1: General methods

All chemicals used were purchased from commercial suppliers and used as received. All reactions were performed under an inert atmosphere of N_2. All organic extracts were dried over anhydrous $MgSO_4$. TLC was performed using aluminium sheets coated with silica gel F_{254}. Visualization was aided by viewing under a UV lamp and staining with ceric ammonium molybdate (CAM) stain followed by heating. All R_f values were measured to the nearest 0.05. Flash column chromatography was performed using 40-63 micron grade silica gel. Melting points were recorded on a digital melting point apparatus and are uncorrected. Infrared spectra were recorded using an FT-IR spectrometer as the neat compounds. High field NMR spectra were recorded using a 500 MHz spectrometer (^{1}H at 500 MHz, ^{13}C at 125 MHz). Solvent used for spectra were $CDCl_3$ unless otherwise specified. ^{1}H chemical shifts are reported in ppm on the δ-scale relative to TMS (δ 0.0) and ^{13}C NMR are reported in ppm relative to $CDCl_3$ (δ 77.00). Multiplicities are reported as (br) broad, (s) singlet, (d) doublet, (t) triplet, (q) quartet, (quin) quintet, (sext) sextet, (hept) heptet and (m) multiplet. All *J*-values were rounded to the nearest 0.1 Hz. ESI high resolution mass spectra were recorded on a ESI-TOF mass spectrometer.

2.4.2: Experimental Procedures

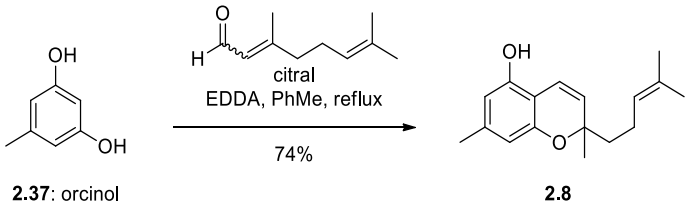

2.37: orcinol **2.8**

To a solution of orcinol (**2.37**) (15.0 g, 121 mmol) in PhMe (400 mL) at room temperature was added citral (18.4 g, 121 mmol) and EDDA (440 mg, 2.42 mmol). The reaction was stirred at reflux for 5 h. The mixture was cooled to room temperature, then concentrated *in vacuo*. The residue was purified by flash column chromatography on SiO_2 (8:1, petrol/EtOAc) to give chromene **2.8** as an orange oil (23.1 g, 74%). Data for **2.8** matched that previously reported in the literature.

Data for **2.8**:

^{1}H NMR (500 MHz, $CDCl_3$): δ 6.61 (d, *J* = 10.0 Hz, 1H), 6.24 (s, 1H), 6.11 (s, 1H), 5.49 (d, *J* = 10.0 Hz, 1H), 5.10 (t, *J* = 7.1 Hz, 1H), 4.71 (br s, 1H), 2.20 (s, 3H), 2.13 – 2.07 (m, 2H), 1.72 (dd, *J* = 10.7, 5.9 Hz, 1H), 1.66 (s, 3H), 1.66 – 1.63 (m, 1H), 1.58 (s, 3H), 1.37 (s, 3H)

^{13}C NMR (125 MHz, $CDCl_3$): δ 154.1, 151.0, 139.5, 131.6, 127.2, 124.2, 117.0, 109.9, 108.3, 106.7, 78.2, 41.1, 26.2, 25.7, 22.7, 21.5, 17.6

R_f 0.40 (5:1 petrol/EtOAc)

IR (neat): 3387, 2970, 2924, 2857, 1625, 1578, 1509, 1450, 1377, 1330, 1250 cm^{-1}

HRMS (ESI): calculated for $C_{17}H_{21}O_2$ 257.1547 $[M-H]^-$, found 257.1539

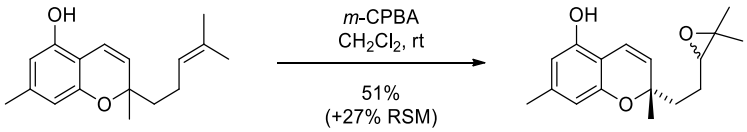

2.8 **2.43** (1:1 d.r.)

To a solution of chromene **2.8** (5.60 g, 21.7 mmol) in CH_2Cl_2 (250 mL) at room temperature was added *m*-CPBA (77%, 3.92 g, 22.8 mmol). The reaction was stirred at room temperature for 30 min. The solution was washed sequentially with saturated $Na_2S_2O_3$ solution (2 × 200 mL) and saturated $NaHCO_3$ solution (2 × 200 mL). The organic layer was washed with brine (200 mL), dried over $MgSO_4$, filtered, and concentrated *in vacuo*. The residue was purified by flash column

chromatography on SiO_2 (5:1 → 3:1 petrol/EtOAc) to give recovered **2.8** as an orange oil (1.51 g, 27%). Further elution gave epoxide **2.43** (d.r. = 1:1) as a brown oil (3.00 g, 51%).

Data for **2.43**:

^{1}H NMR (500 MHz, $CDCl_3$): δ 6.64 (d, *J* = 10.0 Hz, 2H), 6.20 (s, 2H), 6.12 (s, 2H), 5.46 (d, *J* = 10.0 Hz, 1H), 5.43 (d, *J* = 10.0 Hz, 1H), 5.33 (br s, 2H), 2.77 (t, *J* = 6.2 Hz, 1H), 2.75 (t, *J* = 5.8 Hz, 1H), 2.19 (s, 6H), 1.83 (t, *J* = 8.1 Hz, 2H), 1.75 – 1.66 (m, 6H), 1.38 (s, 3H), 1.37 (s, 3H), 1.30 (s, 3H), 1.29 (s, 3H), 1.25 (s, 3H), 1.24 (s, 3H)

^{13}C NMR (125 MHz, $CDCl_3$): δ 153.9, 153.8, 151.34, 151.32, 139.6, 126.6, 126.3, 117.4, 117.3, 109.6, 109.5, 108.50, 108.46, 106.7, 106.5, 78.0, 77.6, 64.8, 64.5, 59.1, 58.9, 37.9, 37.4, 26.6, 26.1, 24.8, 23.9, 23.6, 21.5, 18.63, 18.57

R_f 0.35 (5:1 petrol/EtOAc)

IR (neat): 3348, 2969, 2925, 2857, 1624, 1579, 1452, 1452, 1425, 1380, 1329, 1272 cm^{-1}

HRMS (ESI): calculated for $C_{17}H_{21}O_3$ 273.1496 $[M-H]^-$, found 273.1495

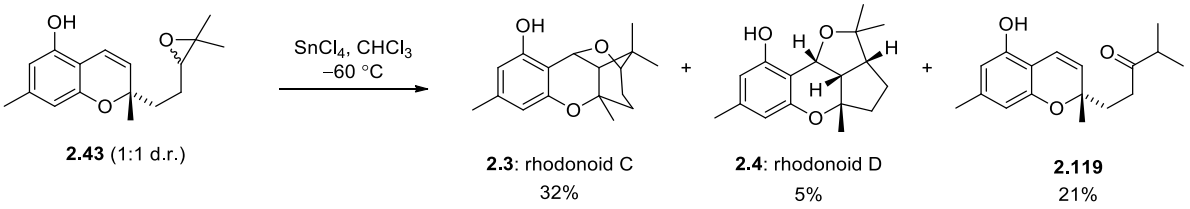

To a solution of **2.43** (d.r. = 1:1) (685 mg, 2.50 mmol) in $CHCl_3$ (40 mL) at –60 ºC was added $SnCl_4$ (0.29 mL, 2.50 mmol) dropwise. The reaction was stirred at –60 ºC for 30 min, then quenched with saturated $NaHCO_3$ solution (50 mL) and warmed to room temperature. The layers were separated, and the organic phase was washed with saturated $NaHCO_3$ solution (2 × 50 mL), dried over $MgSO_4$, filtered and concentrated *in vacuo*. The residue was purified by flash column chromatography on SiO_2 (5:1 → 3:1 petrol/EtOAc gradient elution) to give rhodonoid D (**2.4**) as a white solid (33 mg, 5%). Further elution gave ketone **2.119** as a white solid (144 mg, 21%). Further elution gave rhodonoid C (**2.3**) as a white solid (218 mg, 32%).

Data for rhodonoid C (**2.3**):

^{1}H NMR (500 MHz, $CDCl_3$): δ 6.30 (s, 1H), 6.26 (s, 1H), 5.64 (br s, 1H), 5.05 (d, *J* = 4.2 Hz, 1H), 3.85 (s, 1H), 2.23 (s, 3H), 1.87 – 1.81 (m, 2H), 1.73 – 1.69 (m, 2H), 1.64 (s, 3H), 1.49 (dd, *J* = 14.6, 5.7 Hz, 1H), 1.29 (s, 3H), 1.26 (s, 3H)

^{13}C NMR (125 MHz, $CDCl_3$): δ 155.6, 152.6, 140.2, 109.8, 108.5, 107.8, 82.0, 77.5, 68.9, 51.1, 42.6, 30.1, 27.9, 27.6, 27.0, 23.0, 21.5

R_f 0.20 (2:1 petrol/EtOAc)

IR (neat): 3259, 2927, 2869, 1628, 1593, 1456, 1421, 1380, 1327, 1266, 1144, 1126 cm^{-1}

m.p.: 196 – 198 ºC.

HRMS (ESI): calculated for $C_{17}H_{21}O_3$ 273.1496 $[M-H]^-$, found 273.1490

Data for rhodonoid D (**2.4**):

^{1}H NMR (500 MHz, $CDCl_3$): δ 6.92 (s, 1H**),** 6.35 (s, 1H), 6.29 (s, 1H), 4.92 (d, *J* = 9.1 Hz, 1H), 2.82 (t, *J* = 8.5 Hz, 1H), 2.56 (ddd, *J* = 9.9, 8.0, 3.8 Hz, 1H), 2.23 (s, 3H), 1.85 – 1.78 (m, 1H), 1.75 – 1.72 (m, 1H), 1.67 – 1.61 (m, 1H), 1.48 (s, 3H), 1.44 – 1.40 (m, 1H), 1.33 (s, 3H), 1.29 (s, 3H)

^{13}C NMR (125 MHz, $CDCl_3$): δ 156.1, 151.7, 139.9, 110.0, 109.2, 107.3, 83.2, 82.9, 68.8, 51.6, 51.5, 34.9, 28.0, 27.5, 24.13, 24.07, 21.5

R_f 0.55 (2:1 petrol/EtOAc)

IR (neat): 3435, 2970, 2921, 2853, 1636, 1586, 1460, 1370, 1326, 1299, 1278, 1190 cm^{-1}

m.p.: 162 – 165 ºC

HRMS (ESI): calculated for $C_{17}H_{21}O_3$ 273.1496 $[M-H]^-$, found 273.1489

Data for ketone **2.119**:

^{1}H NMR (500 MHz, $CDCl_3$): δ 6.63 (d, *J* = 10.0 Hz, 1H), 6.22 (s, 1H), 6.12 (s, 1H), 5.41 (d, *J* = 10.0 Hz, 1H), 4.71 (br s, 1H), 2.68 – 2.54 (m, 3H), 2.20 (s, 3H), 1.99 – 1.94 (m, 2H), 1.36 (s, 3H), 1.07 (d, *J* = 7.1 Hz, 6H)

^{13}C NMR (125 MHz, $CDCl_3$): δ 214.8, 153.9, 151.2, 139.7, 126.4, 117.5, 109.7, 108.5, 106.4, 77.9, 41.0, 35.3, 34.9, 26.6, 21.5, 18.33, 18.27

R_f 0.50 (2:1 petrol/EtOAc)

IR (neat): 3387, 2970, 2924, 2854, 1698, 1623, 1579, 1510, 1450, 1368, 1329, 1280 cm^{-1}

m.p.: 116 – 121 ºC.

HRMS (ESI): calculated for $C_{17}H_{23}O_3$ 275.1642 $[M+H]^+$, found 275.1642

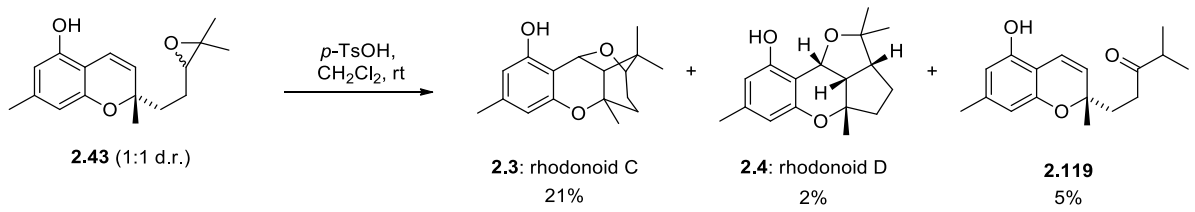

To a solution of **2.43** (d.r. = 1:1) (66 mg, 0.24 mmol) in $CHCl_3$ (10 mL) at room temperature was added *p*-TsOH·H_2O (4.6 mg, 0.024 mmol). The reaction was stirred at room temperature for 30 min, then quenched with saturated $NaHCO_3$ solution (10 mL). The organic layer was separated, and the aqueous layer was extracted with CH_2Cl_2 (2 × 10 mL). The combined organic extracts were washed with brine (10 mL), dried over $MgSO_4$, filtered, and concentrated *in vacuo*. The residue was purified by flash column chromatography on SiO_2 (5:1 → 3:1 petrol/EtOAc gradient elution) to give rhodonoid D (**2.4**) as a white solid (1.5 mg, 2%), further elution gave ketone (**2.119**) as a colourless oil (3 mg, 5%), further elution gave rhodonoid C (**2.3**) as a white solid (14 mg, 21%). Data for **2.3**, **2.4**, and **2.119** matched what was previously obtained.

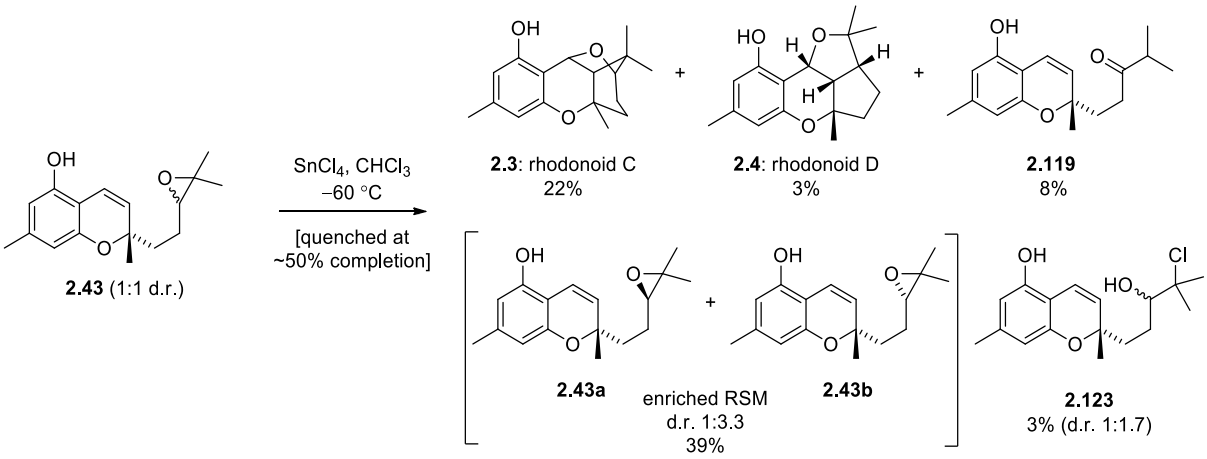

To a solution of **2.43** (d.r. = 1:1) (2.02 g, 7.24 mmol) in $CHCl_3$ (50 mL) at –60 ºC was added $SnCl_4$ (0.42 mL, 3.62 mmol) dropwise. The reaction was stirred at –60 ºC for 30 min, then quenched with saturated $NaHCO_3$ solution (50 mL), warmed to room temperature. The mixture was filtered through a pad of Celite, washed thoroughly with CH_2Cl_2. The layers were separated, and the organic phase was washed with saturated $NaHCO_3$ solution (2 × 50 mL), dried over $MgSO_4$, filtered and concentrated *in vacuo*. The residue was purified by flash column chromatography on SiO_2 (5:1 → 3:1, petrol/EtOAc gradient elution) gave in order of increasing polarity: rhodonoid D (**2.4**) as a white solid (69 mg, 3%), ketone **2.119** as a white solid (152 mg, 8%), enriched recovered epoxide **2.43** (d.r. = 1:3.3) as a brown oil (792 mg, 39%), **2.123** (d.r. = 1:1.7) as a brown oil (77.3 mg, 3%), and

rhodonoid C (**2.3**) as a white solid (443 mg, 22%). Data for **2.3**, **2.4**, and **2.119** matched what was previously obtained.

NMR data for **2.43b** (major diastereomer):

^{1}H NMR (500 MHz, $CDCl_3$): δ 6.63 (d, *J* = 10.0 Hz, 1H), 6.21 (s, 1H), 6.12 (s, 1H), 5.44 (d, *J* = 10.0 Hz, 1H), 4.97 (br s, 1H), 2.75 (t, *J* = 6.2 Hz, 1H), 2.20 (s, 3H), 1.82 (d, *J* = 8.1 Hz, 1H), 1.74 – 1.64 (m, 3H), 1.38 (s, 3H), 1.28 (s, 3H), 1.23 (s, 3H)
^{13}C NMR (125 MHz, $CDCl_3$): δ 153.9, 151.2, 139.7, 126.4, 117.3, 109.6, 108.4, 106.5, 78.0, 64.6, 58.8, 37.9, 26.6, 24.9, 23.9, 21.5, 18.7

NMR data for **2.43a** (minor diastereomer):

^{1}H NMR (500 MHz, $CDCl_3$): δ 6.63 (d, *J* = 10.0 Hz, 1H), 6.21 (s, 1H), 6.12 (s, 1H), 5.47 (d, *J* = 10.0 Hz, 1H), 4.97 (br s, 1H), 2.73 (t, *J* = 5.9 Hz, 1H), 2.20 (s, 3H), 1.84 (d, *J* = 8.0 Hz, 1H), 1.74 – 1.64 (m, 3H), 1.38 (s, 3H), 1.29 (s, 3H), 1.24 (s, 3H)
^{13}C NMR (125 MHz, $CDCl_3$): δ 153.8, 151.2, 139.6, 126.7, 117.2, 109.7, 108.4, 106.5, 77.7, 64.4, 58.7, 37.5, 26.1, 24.9, 23.6, 21.5, 18.6

Data for **2.123** (chloride):

^{1}H NMR (500 MHz, $CDCl_3$): δ 6.64 (d, *J* = 10.1 Hz, 1H), 6.23 (s, 2 H), 6.12 s, 2H), 5.48 (d, *J* = 10.0 Hz, 1H), 5.47 (d, *J* = 10.0 Hz, 1H), 4.97 (br s, 2H), 3.54 – 3.49 (m, 2H), 3.43 – 3.40 (m, 2H), 2.20 (s 6H), 2.07 – 1.97 (m, 3H), 1.84 – 1.77 (m, 3H), 1.75 – 1.70 (m, 1H), 1.58 (s, 3H), 1.54 (s, 3H), 1.51 (s, 3H), 1.48 – 1.42 (m, 1H), 1.37 (s, 3H), 1.37 (s, 3H)
^{13}C NMR (125 MHz, $CDCl_3$): δ 153.9, 153.8, 151.2, 139.7, 139.6, 127.2, 126.7, 117.3, 117.2, 109.8, 109.7, 108.6, 108.5, 106.8, 106.7, 79.3, 79.2, 78.4, 78.0, 38.4, 37.9, 29.4, 29.2, 27.1, 26.9, 26.6, 26.4, 26.0, 25.9, 21.5, 16.1
R_f 0.45 (2:1 petrol/EtOAc)
IR (neat): 3342, 2974, 2922, 1624, 1579, 1511, 1452, 1370, 1330 cm^{-1}
HRMS (ESI): calculated for $C_{17}H_{24}ClO_3$ 311.1408 $[M+H]^+$, found 311.1410

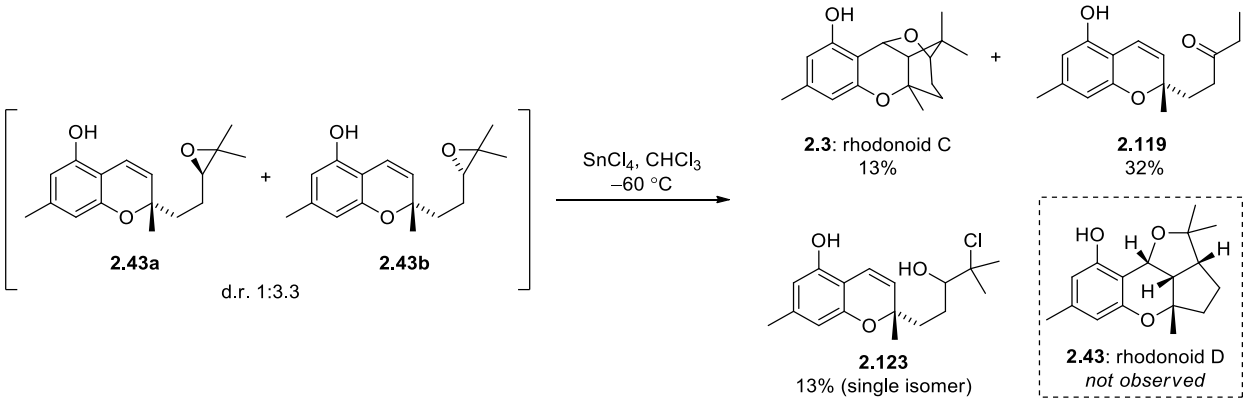

To a solution of **2.43** (d.r. = 3.3:1) (99 mg, 0.36 mmol) in $CHCl_3$ (5 mL) at −60 ºC was added $SnCl_4$ (0.04 mL, 0.36 mmol) dropwise. The reaction was stirred at −60 ºC for 15 min, then quenched with saturated $NaHCO_3$ solution (5 mL), warmed to room temperature. The aqueous layer was separated, and the organic extract was washed with saturated $NaHCO_3$ solution (2 × 10 mL), brine (10 mL), dried over $MgSO_4$, filtered and concentrated *in vacuo*. The residue was purified by flash column chromatography on SiO_2 (4:1 → 2:1, petrol/EtOAc gradient elution) to give ketone **2.119** as a white solid (32 mg, 32%). Further elution gave **2.123** (single isomer) as a brown oil (26.7 mg, 13%). Further elution gave rhodonoid C (**2.3**) as a white solid (13 mg, 13%). Data for **2.3**, **2.119**, and **2.123** matched what was previously obtained.

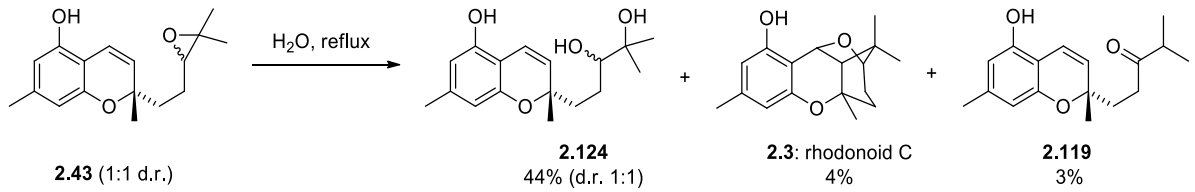

A solution of **2.43** (d.r. = 1:1) (97 mg, 0.35 mmol) in water (10 mL) was heated to reflux for 16 h. the reaction was cooled to rt, then extracted with Et_2O (2 × 10 mL). The combined organic extracts were dried over $MgSO_4$, filtered, and concentrated *in vacuo*. The residue was purified by flash column chromatography (5:1 → 2:1 petrol/EtOAc, gradient elution) to give ketone **2.119** as a white solid (3 mg, 3%). Further elution gave rhodonoid C (**2.3**) as a white solid (4 mg, 4%). Further elution gave diol **2.124** as a white solid (45 mg, 45%). Data of **2.3** and **2.119** matched what was previously obtained.

Data for diol **2.124**:

^{1}H NMR (500 MHz, $CDCl_3$): δ 6.63 (d, *J* = 10.0 Hz, 2H), 6.31 (br s, 2H), 6.19 (s, 2H), 6.13 (s, 2H), 5.44 (d, *J* = 9.9 Hz, 1H), 5.42 (d, *J* = 9.9, 1H), 3.37 (t, *J* = 9.6 Hz, 2H), 2.80 (br s, 2H), 2.45 (br s, 2H), 2.17 (s, 6H), 2.10 – 1.90 (m, 2H), 1.80 – 1.64 (m, 4H), 1.50 – 1.39 (m, 2H), 1.35 (s, 3H), 1.34 (s, 3H), 1.17 (s, 3H), 1.14 (s, 3H), 1.13 (s, 3H)

^{13}C NMR (125 MHz, $CDCl_3$): δ 153.6, 153.5, 151.6, 139.6, 139.5, 126.9, 126.5, 117.4, 109.4, 108.8, 108.7, 106.9, 106.8, 78.9, 78.6, 78.4, 78.1, 73.51, 73.47, 38.2, 37.9, 26.43, 26.38, 26.36, 26.31, 25.89, 25.87, 23.3, 23.2, 21.5

R_f 0.05 (2:1 petrol/EtOAc)

IR (neat): 33.42, 2971, 2929, 2865, 1623, 1510, 1450, 1421, 1329 cm^{-1}

m.p.: 55 ºC.

HRMS (ESI): calculated for $C_{17}H_{25}O_4$ 293.1747 $[M+H]^+$, found 297.1747

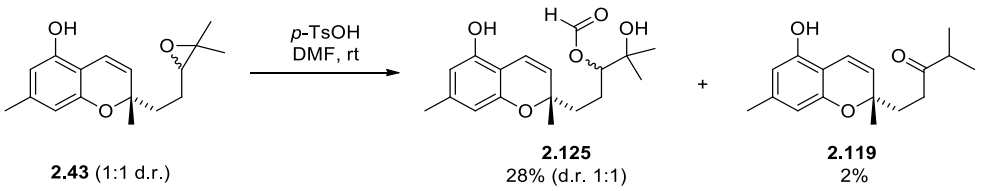

To a solution of **2.43** (d.r. = 1:1) (124 mg, 0.45 mmol) in DMF (5 mL) was added *p*-TsOH (86 mg, 0.45 mmol) and the resultant mixture was stirred at room temperature for 30 min. The reaction diluted with water (10 mL) and extracted with Et_2O (4 × 10 mL). The combined organic extracts were dried over $MgSO_4$, filtered, and concentrated *in vacuo*. The residue was purified by flash column chromatography on SiO_2 (5:1 → 1:1 petrol/EtOAc, gradient elution) to afford ketone **2.119** as a white solid (3 mg, 2%), further elution gave formate **2.125** as a colourless oil. Data of **1.119** matched that which was previously obtained.

Data for formate **2.125**:

^{1}H NMR (500 MHz, $CDCl_3$): δ 8.18 (s, 1H), 8.18 (s, 1H), 6.64 (d, *J* = 10.0 Hz, 1H), 6.62 (d, *J* = 10.0 Hz, 1H), 6.21 (s, 1H), 6.20 (s, 1H), 6.12 (s, 2H), 5.43 (d, *J* = 10.0 Hz, 1H), 5.30 (d, *J* = 10.0 Hz, 1H), 4.89 – 4.87 (m, 2H), 2.19 (s, 6H), 1.90 – 1.62 (m, 8H), 1.21 (s, 6H), 1.20 (s, 3H), 1.19 (s, 3H)
^{13}C NMR (125 MHz, $CDCl_3$): δ 161.5, 161.4, 153.8, 15.7, 151.31, 51.30, 139.7, 126.5, 126.2, 117.6, 117.4, 109.62, 109.56, 108.55, 108.51, 106.60, 106.57, 80.4, 80.2, 78.0, 77.7, 72.47, 72.46, 37.7, 37.5, 26.54, 26.47, 26.2, 24.9, 24.9, 24.8, 24.3, 24.0, 21.5
R_f 0.20 (2:1 petrol/EtOAc)
IR (neat): 3387, 2976, 2924, 1714, 1624, 1579, 1452, 1378, 1330, 1266 cm^{-1}
HRMS (ESI): calculated for $C_{18}H_{25}O_5$ 321.1697 $[M+H]^+$, found 321.1699

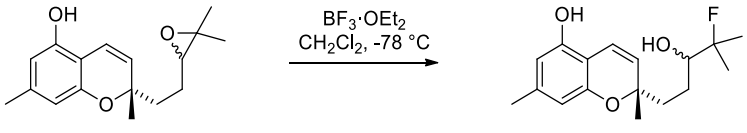

2.43 (1:1 d.r.) **2.122** 28% (d.r. 1:1)

To a solution of **2.43** (d.r. = 1:1) (123 mg, 0.45 mmol) in CH_2Cl_2 (15 mL) at −78 °C was added $BF_3{\cdot}OEt_2$ (0.05 mL, 0.45 mmol) dropwise. The reaction was stirred at −78 °C for 30 min, then quenched with sat. $NaHCO_3$ solution (15 mL) and warmed to room temperature. The organic layer was separated, and the aqueous layer was extracted with CH_2Cl_2 (20 mL). The combined organic extracts were washed with sat. $NaHCO_3$ solution (3 × 20 mL), water (40 mL), dried over $MgSO_4$, filtered, and concentrated *in vacuo*. The residue was purified by flash column chromatography on SiO_2 (2:1 petrol/EtOAc) to afford **2.122** (d.r. = 1:1) as a colourless oil (21 mg, 18%).

Data for **2.122**:

^{1}H NMR (500 MHz, $CDCl_3$): δ 6.64 (d, *J* = 10.0 Hz, 2H), 6.22 (s, 1H), 6.12 (s, 1H), 5.46 (d, *J* = 10.0 Hz, 2H), 5.27 (br s, 2H), 3.58 (t, *J* = 11.0 Hz, 2H), 2.19 (s, 6H), 2.02 – 1.96 (m, 2H), 1.83 – 1.77 (m, 2H), 1.89 – 1.64 (m, 2H), 1.45 – 1.39 (m, 2H), 1.36 (s, 6H), 1.34 (s, 3H), 1.33 (s, 3H), 1.29 (s, 3H), 1.28 (s, 3H)
^{13}C NMR (125 MHz, $CDCl_3$): δ 153.8, 151.3, 139.6, 126.6, 117.3, 109.6, 108.5, 106.7, 98.8, 97.5, 78.4, 77.2, 38.2, 26.6, 26.12, 26.08, 23.8, 23.6, 21.5, 21.2, 21.0
^{19}F NMR (470 MHz, $CDCl_3$): δ −144.69 (hept, *J* = 22.3 Hz), −144.72 (hept, *J* = 22.3 Hz)
R_f 0.15 (2:1 petrol/EtOAc)

IR (neat): 3356, 274, 2927, 1623, 1579, 1451, 1376, 1330, 1246 cm^{-1}

HRMS (ESI): calculated for $C_{17}H_{22}FO_3$ 293.1558 $[M+H]^+$, found 293.1559

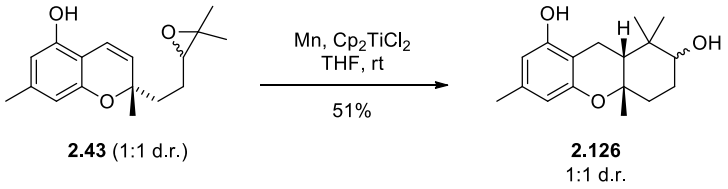

2.43 (1:1 d.r.) **2.126** 1:1 d.r.

A suspension of Cp_2TiCl_2 (168 mg, 0.68 mmol) and powdered Manganese (149 mg, 2.71 mmol) in dry THF (5 mL) was stirred at room temperature until the colour changed from orange to dark green (~1.5 h). A solution of **2.43** (d.r. = 1:1) (93 mg, 0.34 mmol) in dry THF (3 mL) was added and the resultant mixture was stirred at room temperature for 2 h. The mixture was filtered through a pad of Celite, washed through with EtOAc (20 mL), and the filtrate was concentrated *in vacuo*. The residue was purified by flash column chromatography on SiO_2 (2:1 petrol/EtOAc) to afford **2.126** (d.r. = 1:1) as an orange oil (48 mg, 51%).

Data for **2.126**:

^{1}H NMR (500 MHz, $CDCl_3$): δ 6.21 (s, 2H), 6.17 (s, 2H), 5.62 (br s , 2H), 3.38 (dd, *J* = 11.8, 3.7 Hz, 1H), 2.80 – 2.65 (m, 4H), 2.19 (s, 6H), 2.16 (ddd, *J* = 11.8, 4.1, 2.1 Hz, 1H), 2.08 – 2.03 (m, 2H), 1.99 (dd, *J* = 14.1, 4.3 Hz, 1H), 1.93, 1.87, (m, 2H), 1.81 – 1.77 (m, 1H), 1.67 – 1.58 (m, 3H), 1.46 (d, *J* = 7.7 Hz, 1H), 1.21 (s, 3H), 1.17 (s, 3H), 1.08 (s, 3H), 1.05 (s, 3H), 0.69 (s, 3H), 0.64 (s, 3H)

^{13}C NMR (125 MHz, $CDCl_3$): δ 155.03, 155.00, 153.38, 15.36, 136.8, 136.7, 110.09, 110.05, 107.4, 107.3, 106.3, 78.4, 76.4, 74.9, 74.3, 43.5, 39.5, 37.90, 37.86, 37.3, 32.1, 27.3, 27.1, 26.44, 26.40, 26.38, 24.6, 21.8, 21.2, 17.8, 17.8, 17.4, 14.0

R_f 0.45 (2:1 petrol/EtOAc)

IR (neat): 3342, 2971, 2929, 1623, 1578, 1510, 1450, 1421, 1366, 1329 cm^{-1}

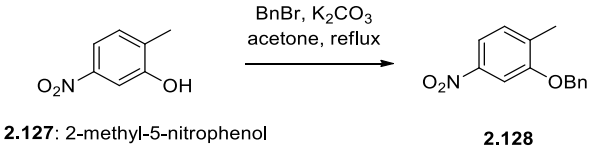

2.127: 2-methyl-5-nitrophenol

2.128

To a solution of 2-methyl-5-nitrophenol (**2.127**) (10.0 g, 65.3 mmol) and K_2CO_3 (13.5 g, 98.0 mmol) in acetone (100 mL) was added BnBr (8.1 mL, 68.6 mmol). The mixture was heated to reflux for 3h, then cooled to rt, and diluted with CH_2Cl_2 (100 mL). The organic phase was separated and washed with water (2 × 100 mL), brine (100 mL), dried over $MgSO_4$, filtered through a pad of SiO_2 washed through with EtOAc (100 mL). The filtrate was concentrated *in vacuo* to give **2.128** as a pale cream solid (15.9), which was used without further purification. Data for **2.128** matched what was reported in the literature.[40]

Data for **2.128**:

^{1}H NMR (500 MHz, $CDCl_3$): δ 7.78 (d, *J* = 8.2 Hz, 1H), 7.75 (s, 1H), 7.46 (d, *J* = 7.0 Hz, 1H), 7.46 (s, 1H), 7.42 (t, *J* = 7.6 Hz, 2H), 7.37 – 7.35 (m, 1H), 7.29 (d, *J* = 8.2 Hz, 1H), 5.17 (s, 2H), 2.36 (s, 3H)

R_f 0.45 (5:1 petrol/EtOAc)

IR (neat): 1713, 1594, 1511, 1451, 1416, 1355, 1254, 1221 cm^{-1}

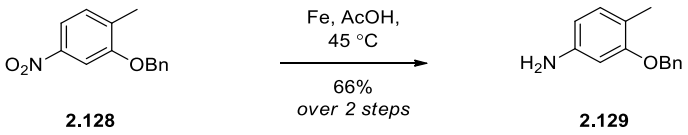

2.128 **2.129**

To a solution of crude **2.128** (15.9 g) in AcOH (200 mL) was added iron powder (36.5 g, 65.3 mmol). The mixture was heated to 45 °C for 14 h, then cooled to room temperature and diluted with EtOAc (200 mL). The resultant slurry was filtered through a pad of Celite, washed through with EtOAc (2 × 100 mL). The filtrate was concentrated *in vacuo* and the residue was purified by flash column chromatography on SiO_2 (3:1 petrol EtOAc) to afford aniline **2.129** as a red oil (9.14 g, 66% over 2 steps). Data for **2.129** matched what was reported in the literature.[40]

Data for **2.129**:

^{1}H NMR (500 MHz, $CDCl_3$): δ 7.44 (d, *J* = 7.6 Hz, 1H), 7.44 (s, 1H), 7.39 (t, *J* = 7.6 Hz, 2H), 7.32 (t, *J* = 7.3 Hz, 1H, 6.93 (d, *J* = 7.8 Hz, 1H), 6.29 (d, *J* = 2.1 Hz, 1H), 6.24 (dd, *J* = 7.9, 2.0 Hz, 1H), 5.03 (s, 2H), 3.58 (br s, 2H), 2.18 (s, 3H).

^{13}C NMR (125 MHz, $CDCl_3$): δ 157.6, 145.4, 138.6, 131.0, 128.5, 127.7, 127.0, 117.0, 107.2, 100.0, 69.7, 15.5.

R_f 0.45 (1:1 petrol/EtOAc)

IR (neat): 3348, 3366, 3072, 2924, 1709, 1616, 1588, 1512, 1454, 1436, 1361 cm^{-1}.

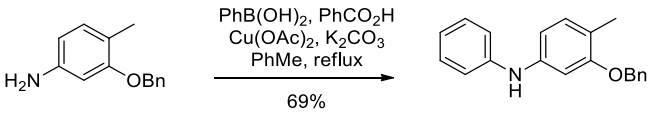

2.129 **2.130**

2.129 (9.14 g, 42.9 mmol), phenylboronic acid (13.1 g, 107 mmol), $Cu(OAc)_2$ (15.6 g, 85.7 mmol), benzoic acid (5.93 g, 42.9 mmol), and K_2CO_3 (5.90 g, 42.9 mmol) were combined in PhMe (200 mL) and heated to reflux for 12 h. The reaction was cooled to room temperature and filtered through a pad of Celite, washed through with EtOAc (200 mL). The filtrate was concentrated *in vacuo* and the residue was purified by flash column chromatography on SiO_2 (10:1 → 2:1 petrol/EtOAc) to afford **2.130** as a yellow solid (8.57 g, 69%). Data for **2.130** matched what was reported in the literature.[40]

Data for **2.130**:

^{1}H NMR (500 MHz, $CDCl_3$): δ 7.42 (d, *J* = 7.2 Hz, 1H), 7.42 (s, 1H), 7.39 (t, *J* = 7.5 Hz, 2H), 7.32 (t, *J* = 7.3 Hz, 1H), 6.67 (d, *J* = 2.0 Hz, 1H), 6.59 (dd, *J* = 7.9, 2.1 Hz, 1H), 5.61 (br s, 1H), 5.04 (s, 2H), 2.24 (s, 3H)

^{13}C NMR (125 MHz, $CDCl_3$): δ 157.3, 143.7, 141.7, 137.4, 131.1, 129.3, 128.5, 127.7, 127.0, 120.3, 120.0, 117.0, 110.8, 103.1, 69.7, 15.8

R_f 0.50 (5:1 petrol/EtOAc)

IR (neat): 3400, 3036, 2925, 2857, 1712, 1633, 1609, 1498, 1458, 1361, 1344, 1307 cm^{-1}

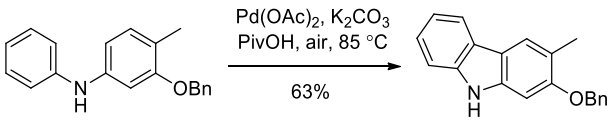

2.130 **2.131**

To a solution of **2.130** (6.39 g, 22.0 mmol) in molten pivalic acid (30 mL) was added K_2CO_3 (304 mg, 2.20 mmol), and $Pd(OAc)_2$ (450 mg, 2.20 mmol). The mixture was heated to 85 °C in an open flask for 20 h, then was cooled to room temperature, and sat. K_2CO_3 solution (50 mL) was added. The resultant mixture was filtered through a pad of SiO_2, and washed through with EtOAc (200 mL). The filtrate was washed with sat. K_2CO_3 solution (100 mL), brine (100 mL), dried over $MgSO_4$, filtered, and concentrated *in vacuo*. The residue was purified by flash column chromatography on SiO_2 (10:1 petrol/EtOAc) to afford **2.131** as a white solid (4.00 g, 63%). Data for **2.131** matched what was reported in the literature.[40]

Data for **2.131**:

^{1}H NMR (500 MHz, $CDCl_3$): δ 7.95 (d, *J* = 7.7 Hz, 1H), 7.86 (br s, 1H), 7.82 (s, 1H), 7.50 (d, *J* = 7.4 Hz, 2H), 7.41 (t, *J* = 7.5, 2H), 7.37 – 7.30 (m, 3H), 7.21 – 7.17 (m, 1H), 6.91 (s, 1H), 5.17 (s, 2H), 2.44 (s, 3H)

^{13}C NMR (125 MHz, $CDCl_3$): δ 153.4, 139.2, 139.0, 137.5, 128.5, 127.8, 127.1, 124.2, 123.5, 121.6, 119.7, 119.4, 119.3, 116.5, 110.2, 84.0, 70.2, 16.9

R_f 0.35 (3:1 petrol/EtOAc)

IR (neat): 3381, 3032, 2924, 1710, 1615, 1560, 1510, 1496, 1454, 1411, 1362 cm^{-1}

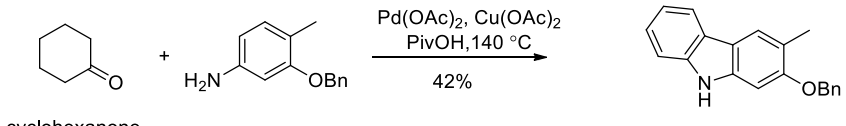

cyclohexanone **2.129** **2.131**

To a solution of **2.129** (5.00 g, 23.4 mmol) and cyclohexanone (2.42 g, 24.6 mmol) in molten pivalic acid (40 mL) was added $Cu(OAc)_2$ (23.3 g, 129 mmol), and $Pd(OAc)_2$ (526 mg, 2.34 mmol). The mixture was heated to 140 °C for 7 h, cooled to room temperature and diluted with EtOAc (150 mL), and then sat. K_2CO_3 solution (50 mL) was added. The mixture was filtered through a pad of Celite, washed through with EtOAc (200 mL). The aqueous layer was removed from the filtrate and the organic layer was washed with EDTA solution (7 g in 100 mL) and sat. K_2CO_3 solution (3 × 100 mL). The organic phase was dried over $MgSO_4$, filtered, and concentrated *in vacuo*. The residue was

purified by flash column chromatography on SiO_2 (20:1 CH_2Cl2_2/EtOAc) to give **2.131** as a black solid, which after trituration with petroleum ether became a pale brown solid (2.80 g, 42%). Data for **2.131** matched what was previously obtained.

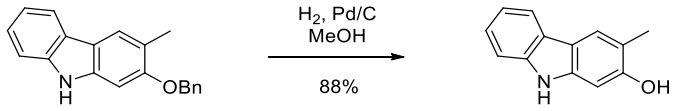

2.131 **2.133**

To a solution of **2.131** (4.39 g, 15.3 mmol) in MeOH/CH_2Cl_2 (3:1, 100 mL) at room temperature was added Pd/C (5%, 800 mg, 0.376 mmol). The mixture was stirred under an atmosphere of H_2 for 36 h, then filtered through a pad of Celite, washed through with EtOAc (150 mL). The filtrate was concentrated *in vacuo* and the reside was purified be flash column chromatography on SiO_2 (4:1 → 2:1 petrol/EtOAc) to give **2.133** as a pale yellow solid (2.65 g, 88%). Data for **2.133** matched what was reported in the literature.[40]

Data for **2.133**:

^{1}H NMR (500 MHz, $CDCl_3$): δ 9.92 (br s, 1H), 8.23 (br s, 1H), 7.92 (d, *J* = 7.8 Hz, 1H), 7.77 (s, 1H), 7.37 (d, *J* = 8.0 Hz, 1H), 7.22 (t, *J* = 7.6 Hz, 1H), 7.07 (t, *J* = 7.5 Hz, 1H), 6.96 (s, 1H), 2.34 (s, 3H)

R_f 0.15 (2:1 petrol/EtOAc)

IR (neat): 3639, 3532, 3403, 1699, 1637, 1613, 1459, 1437, 1416, 1309, 1248 cm^{-1}

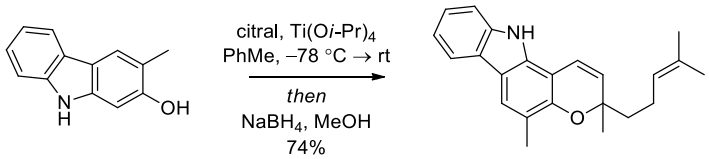

2.133 **2.49**: mahanimbine

To a solution of carbazole **2.133** (500 mg, 2.54 mmol) and citral (443 mg, 5.08 mmol) in PhMe (10 mL) at –78 ˚C was added Ti(O*i*-Pr)$_4$ (3.00 mL, 10.1 mmol). The solution was stirred at –78 ˚C for 15 min, then warmed to room temperature and stirred for 16 h. The reaction was quenched with saturated hydroxylamine hydrochloride solution (10 mL). The mixture was filtered through Celite, then washed with EtOAc (20 mL). The filtrate was washed sequentially with 1 M HCl solution (30 mL), brine (30 mL), dried over $MgSO_4$, filtered, and concentrated *in vacuo*. The residue was re-dissolved in MeOH

(10 mL), and $NaBH_4$ (182 mg, 5.08 mmol) was added to reduce unreacted citral that is difficult to separate from **2.49**. The reaction was stirred at room temperature for 30 min, then quenched with 1 M HCl solution (20 mL). The solution was extracted with Et_2O (2 × 30 mL). The combined organic extracts were washed with brine (30 mL), dried over $MgSO_4$, filtered, and concentrated *in vacuo*. The residue was purified by flash column chromatography on SiO_2 (4:1 petrol/EtOAc) to give mahanimbine (**2.49**) as a yellow oil (662 mg, 74%). Data for **2.49** matched what was reported in the literature.[40]

Data for mahanimbine **2.49**:

^{1}H NMR (500 MHz, $CDCl_3$): δ 7.89 (d, *J* = 7.7 Hz, 1H), 7.78 (br s, 1H), 7.64 (s, 1H), 7.31 – 7.27 (m, 2H), 7.16 (td, *J* = 6.5, 1.2 Hz, 1H), 6.54 (d, *J* = 9.8 Hz, 1H), 5.59 (d, *J* = 9.8 Hz, 1H), 5.11 (t, *J* = 7.1 Hz, 1H), 2.32 (s, 3H), 2.20 – 2.11 (m, 2H), 1.75 (dd, *J* = 8.6, 8.1 Hz, 2H), 1.65 (s, 3H), 1.57 (s, 3H), 1.43 (s, 3H)

^{13}C NMR (125 MHz, $CDCl_3$): δ 149.9, 139.2, 134.8, 131.6, 128.4, 124.18, 124.16, 123.9, 121.1, 119.4, 119.2, 118.3, 117.5, 116.6, 110.4, 104.2, 78.1, 40.8, 25.8, 25.6, 22.7, 17.6, 16.1.

R_f 0.45 (2:1 petrol/EtOAc)

IR (neat): 3423, 1968, 2920, 2853, 1645, 1610, 1491, 1458, 1440, 1307 cm^{-1}

HRMS (ESI): calculated for $C_{23}H_{26}NO$ 332.2009 $[M+H]^+$, found 332.2004

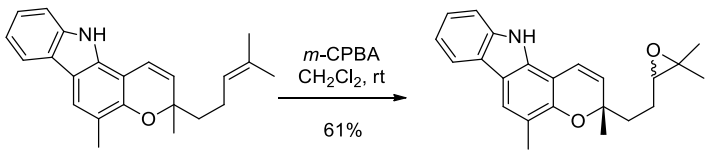

2.49: mahanimbine **2.50** (1:1 d.r.)

To a solution of mahanimbine (**2.49**) (623 mg, 1.88 mmol) in CH_2Cl_2 (10 ml) at room temperature was added *m*-CPBA (77%, 509 mg, 2.07 mmol). The reaction was stirred at room temperature for 10 min, then quenched with saturated $Na_2S_2O_3$ solution (10 mL). The organic layer was separated, then washed sequentially with saturated $NaHCO_3$ solution (10 mL), brine (10 mL), dried over $MgSO_4$, filtered and concentrated *in vacuo*. The residue was purified by flash column chromatography on SiO_2 (4:1 petrol/EtOAc) to give epoxide **2.50** (d.r. = 1:1) as a grey solid (400 mg, 61%).

Data for epoxide **2.50**:

^{1}H NMR (500 MHz, $CDCl_3$): δ 8.01 (s, 2H), 7.90 (d, *J* = 7.6 Hz, 2H), 7.65 (s, 1H), 7.64 (s, 1H), 7.34 (d, *J* = 8.1 Hz, 2H), 7.31 (t, *J* = 7.6 Hz, 2H), 7.16 (t, *J* = 7.4 Hz, 2H), 6.64 (d, *J* = 9.7 Hz, 2H), 5.61 (d, *J* = 9.8 Hz, 1H), 5.57 (d, *J* = 9.8 Hz, 1H), 2.78 (t, *J* = 6.2 Hz, 1H), 2.74 (t, *J* = 6.1 Hz, 1H), 2.31 (s, 3H), 2.30 (s, 3H), 1.92 – 1.85 (m, 4H), 1.79 – 1.71 (m, 4H), 1.44 (s, 3H), 1.43 (s, 3H), 1.28 (s, 3H), 1.27 (s, 3H), 1.23 (s, 6H)

^{13}C NMR (125 MHz, $CDCl_3$): δ 149.6, 149.5, 139.5, 134.9, 128.1, 127.6, 124.25, 124.22, 123.8, 121.31, 121.30, 119.43, 119.41, 119.27, 119.26, 118.2, 118.14, 118.13, 117.9, 116.8, 116.7, 110.39, 110.37, 104.1, 103.9, 78.0, 77.7, 64.5, 64.3, 58.7, 58.6, 37.7, 37.1, 26.3, 25.6, 24.84, 24.83, 24.0, 23.7, 18.63, 18.57, 16.04, 16.03

R_f 0.20 (4:1 petrol/EtOAc)

IR (neat): 3333, 2972, 2925, 2853, 1646, 1612, 1459, 1441, 1405, 1323, 1214 cm^{-1}

HRMS (ESI): calculated for $C_{23}H_{26}NO_2$ 348.1958 $[M+H]^+$, found 348.1959

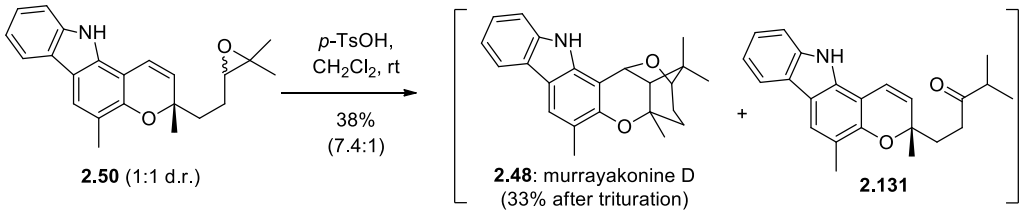

To a solution of **2.50** (d.r. = 1:1) (200 mg, 0.58 mmol) in CH_2Cl_2 (5 mL) at room temperature was added *p*-TsOH·H_2O (11 mg, 0.058 mmol). The reaction was stirred at room temperature for 1 h, then quenched with H_2O (5 mL). The organic layer was separated, and the aqueous phase was extracted with CH_2Cl_2 (5 mL). The combined organic extracts were washed with brine (10 mL), dried over $MgSO_4$, filtered, and concentrated *in vacuo*. The residue was purified by flash column chromatography on SiO_2 (5:1 petrol/EtOAc) to give a 7.4:1 mixture of murrayakonine D (**2.48**) and ketone **2.131** (76 mg). This mixture was triturated with MeOH to give murrayakonine D (**2.48**) as a white solid (65 mg, 33%). Small quantities of ketone **2.131** were obtained for characterisation purposes after repeated purification of the filtrate.

Data for murrayakonine D **2.48**:

^{1}H NMR (500 MHz, $CDCl_3$): δ 8.28 (br s, 1H), 7.93 (d, *J* = 7.7 Hz, 1H), 7.75 (s, 1H), 7.36 (d, *J* = 8.07 Hz, 1H), 7.29 (t, *J* = 7.3 Hz, 1H), 7.17 (t, *J* = 7.4 Hz, 1H), 5.29 (d, *J* = 4.2 Hz, 1H), 3.90 (d, *J* = 4.2 Hz, 1H), 2.32 (s, 3H), 1.97 (d, *J* = 3.9 Hz, 1H), 1.95 – 1.90 (m, 1H), 1.81 – 1.75 (m, 1H), 1.74 (s, 3H), 1.72 – 1.67 (m, 1H), 1.53 (dd, *J* = 14.5, 7.1 Hz, 1H), 1.38 (s, 3H), 1.32 (s, 3H)
^{13}C NMR (125 MHz, $CDCl_3$): δ 149.0, 139.6, 138.4, 123.97, 123.95, 121.3, 119.3, 119.2, 118.5, 115.9, 110.6, 105.0, 82.1, 77.8, 70.4, 51.0, 42.7, 30.4, 28.1, 27.6, 27.1, 23.0, 16.3
R_f 0.45 (2:1 petrol/EtOAc)
IR (neat): 3280, 2964, 2931, 2853, 1633, 1613, 1460, 1313, 1215 cm^{-1}.
m.p.: 244 ºC
HRMS (ESI): calculated for $C_{23}H_{26}NO_2$ 348.1958 $[M+H]^+$, found 348.1958

Data for 2.131:

^{1}H NMR (500 MHz, $CDCl_3$): δ 7.92 (br s, 1H), 7.91 (s, 1H), 7.67 (s, 1H), 7.38 (d, *J* = 8.0 Hz, 1H), 7.31 (t, *J* = 7.6 Hz, 1H), 7.18 (t, *J* = 7.8 Hz, 1H), 6.68 (d, *J* = 9.8 Hz, 1H), 5.60 (d, *J* = 9.8 Hz, 1H), 2.73 (ddd, *J* = 17.4, 9.2, 6.3 Hz, 1H), 2.65 (ddd, *J* = 16.9, 8.6, 5.8 Hz, 1H), 2.59 (hept, *J* = 6.9 Hz, 1H), 2.32 (s, 3H), 2.08 – 2.04 (m, 2H), 1.43 (s, 3H), 1.07 (d, *J* = 6.9 Hz, 6H)
^{13}C NMR (125 MHz, $CDCl_3$): δ 214.6, 149.6, 139.5, 134.8, 127.8, 124.3, 123.8, 121.4, 119.5, 119.3, 118.24, 118.21, 116.8, 110.4, 103.9, 77.9, 41.1, 35.3, 34.7, 26.2, 18.33, 18.27, 16.1
R_f 0.45 (2:1 petrol/EtOAc)
IR (neat): 3369, 2971, 2926, 1703, 1646, 1611, 1459, 1443, 1405, 1310, 1265 cm^{-1}
HRMS (ESI): calculated for $C_{23}H_{26}NO_2$ 348.1958 $[M+H]^+$, found 348.1954

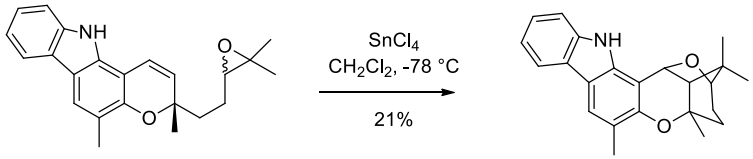

2.50 (1:1 d.r.) **2.48**: murrayakonine D

To a solution of **2.50** (d.r. = 1:1) (200 mg, 0.58 mmol) in CH_2Cl_2 (15 mL) at –78 ˚C was added $SnCl_4$ (0.06 mL, 0.58 mmol). The reaction was stirred at –78 ˚C for 15 min. The reaction was quenched with saturated $NaHCO_3$ solution (10 mL). The organic layer was separated, and the aqueous phase was extracted with CH_2Cl_2 (3 × 5 mL). The combined organic extracts were washed with brine (2 × 10 mL), dried over $MgSO_4$, filtered, and concentrated *in vacuo*. The residue was triturated with MeOH to give murrayakonine D (**2.48**) as a white solid (42 mg, 21%). Data for **2.48** matched that which was previously reported.

2.4.3: NMR Spectra

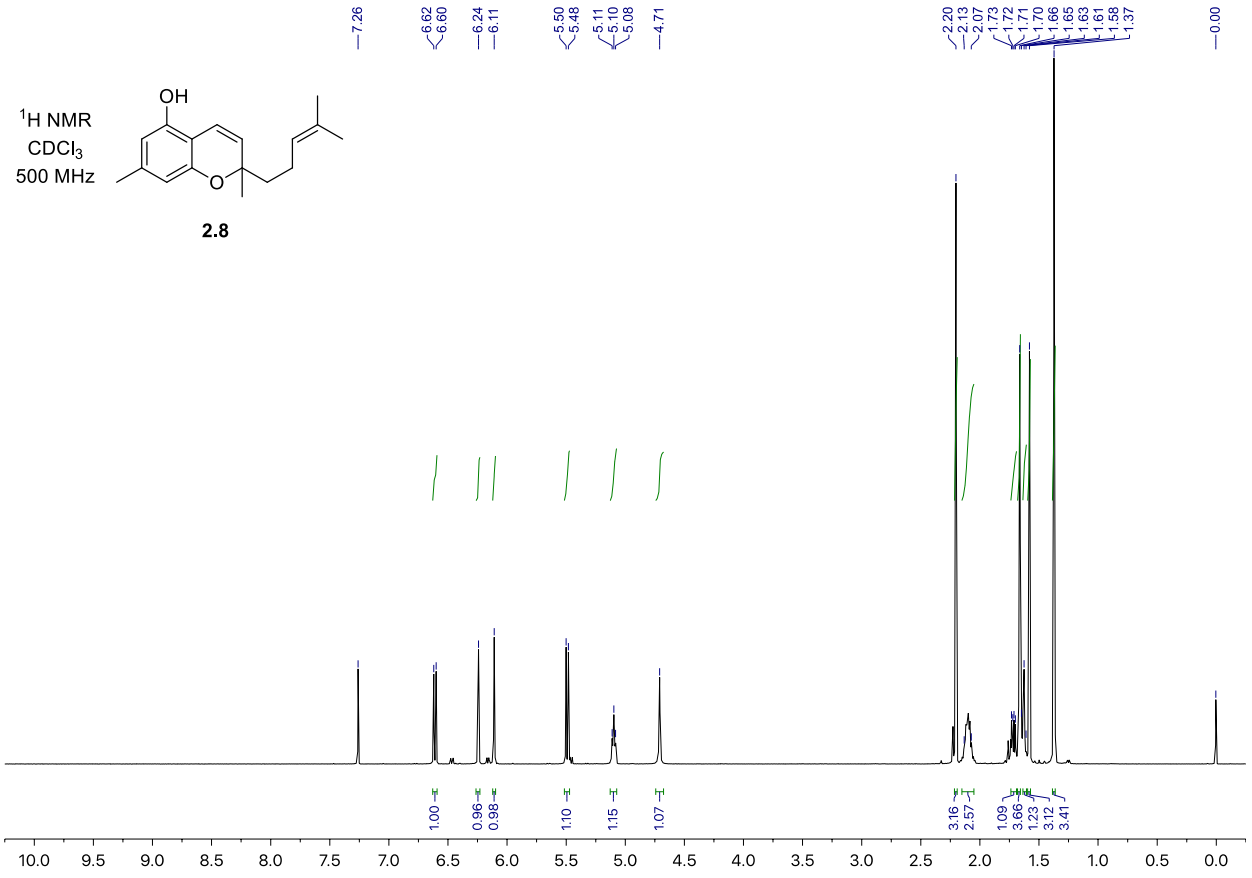

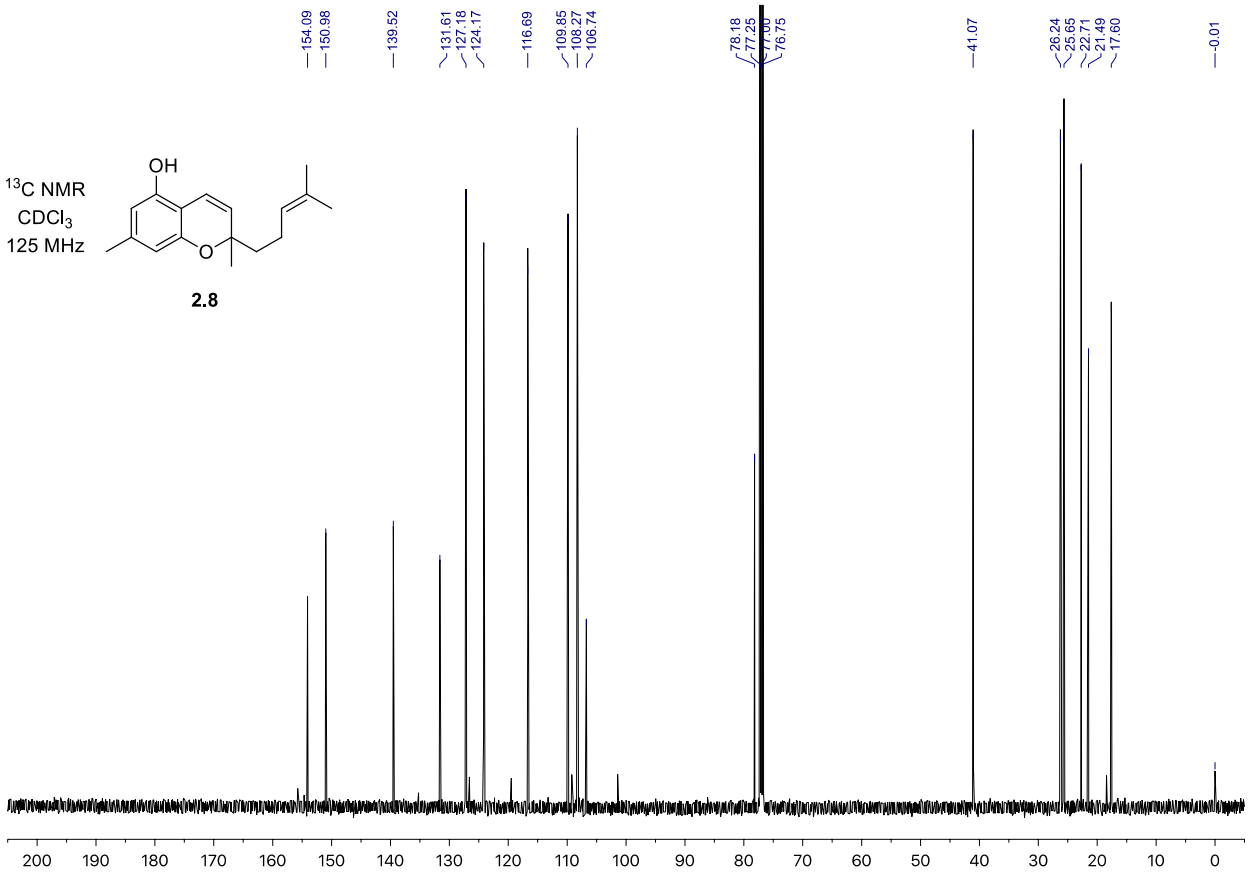

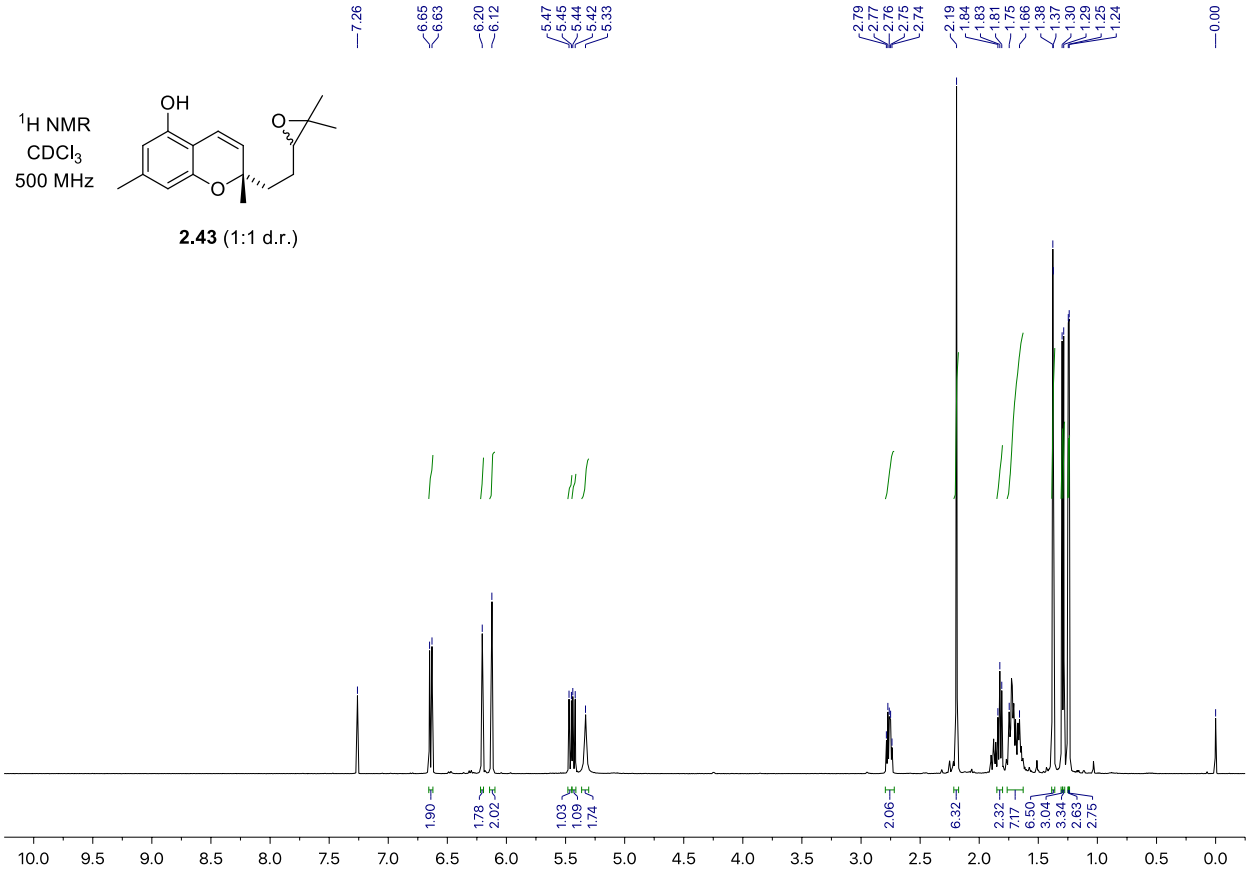

^{1}H NMR
$CDCl_3$
500 MHz

2.43 (1:1 d.r.)

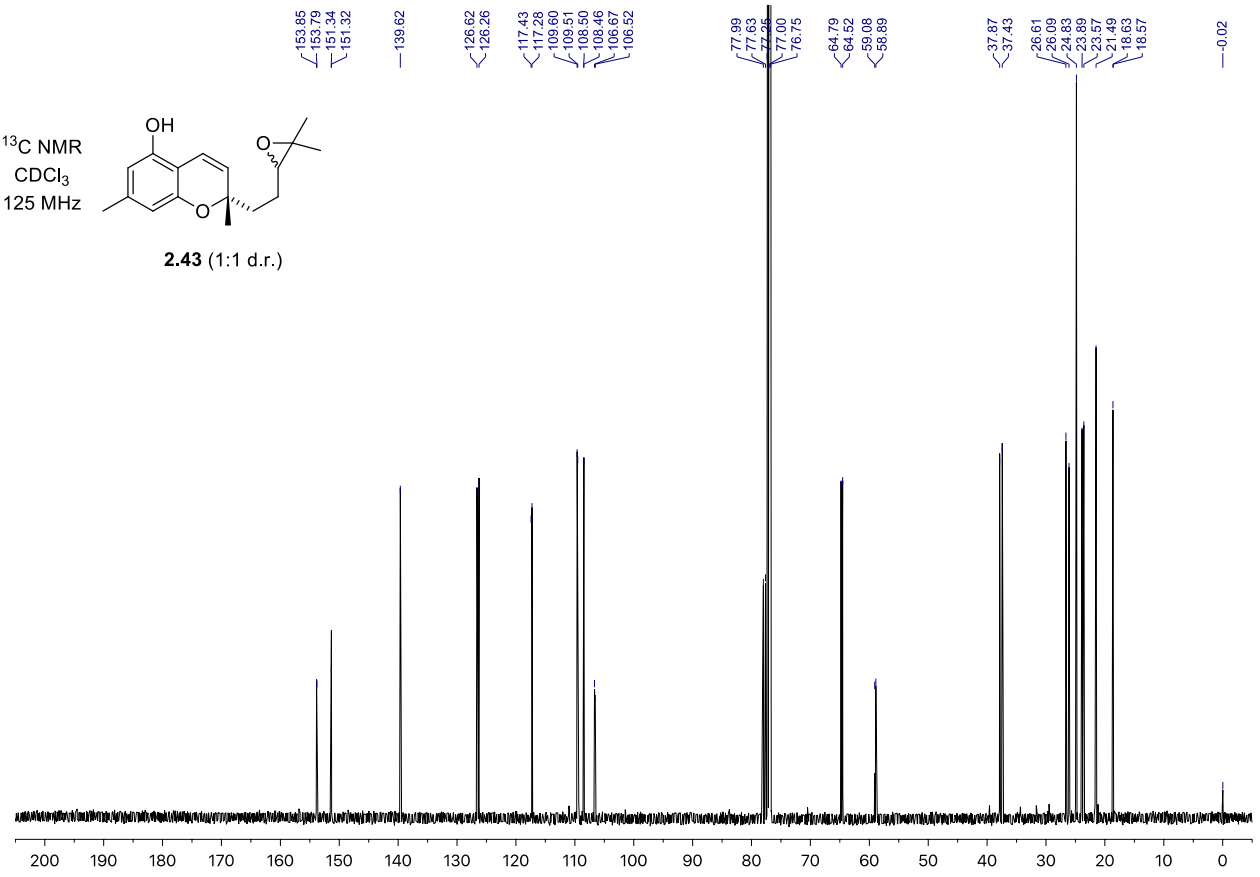

^{13}C NMR
$CDCl_3$
125 MHz

2.43 (1:1 d.r.)

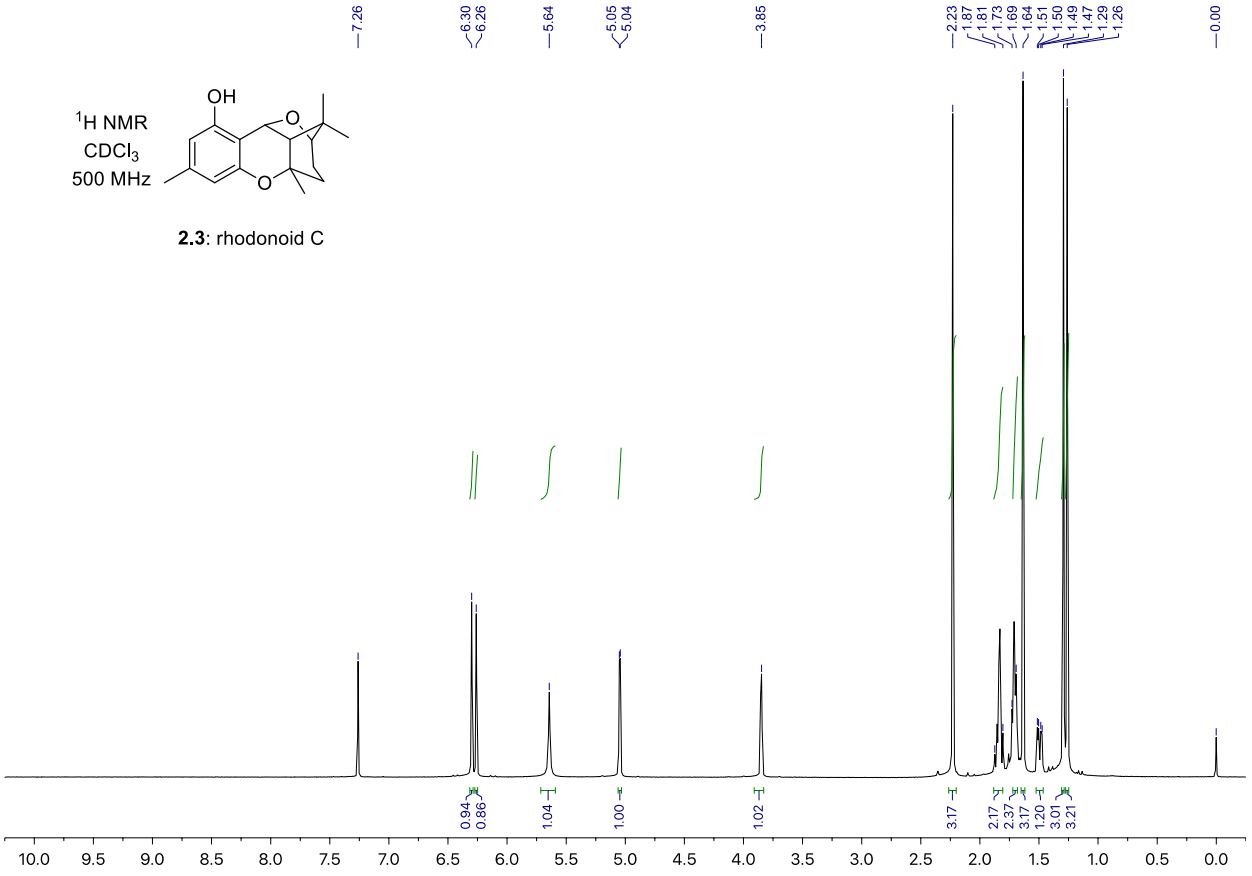

2.3: rhodonoid C

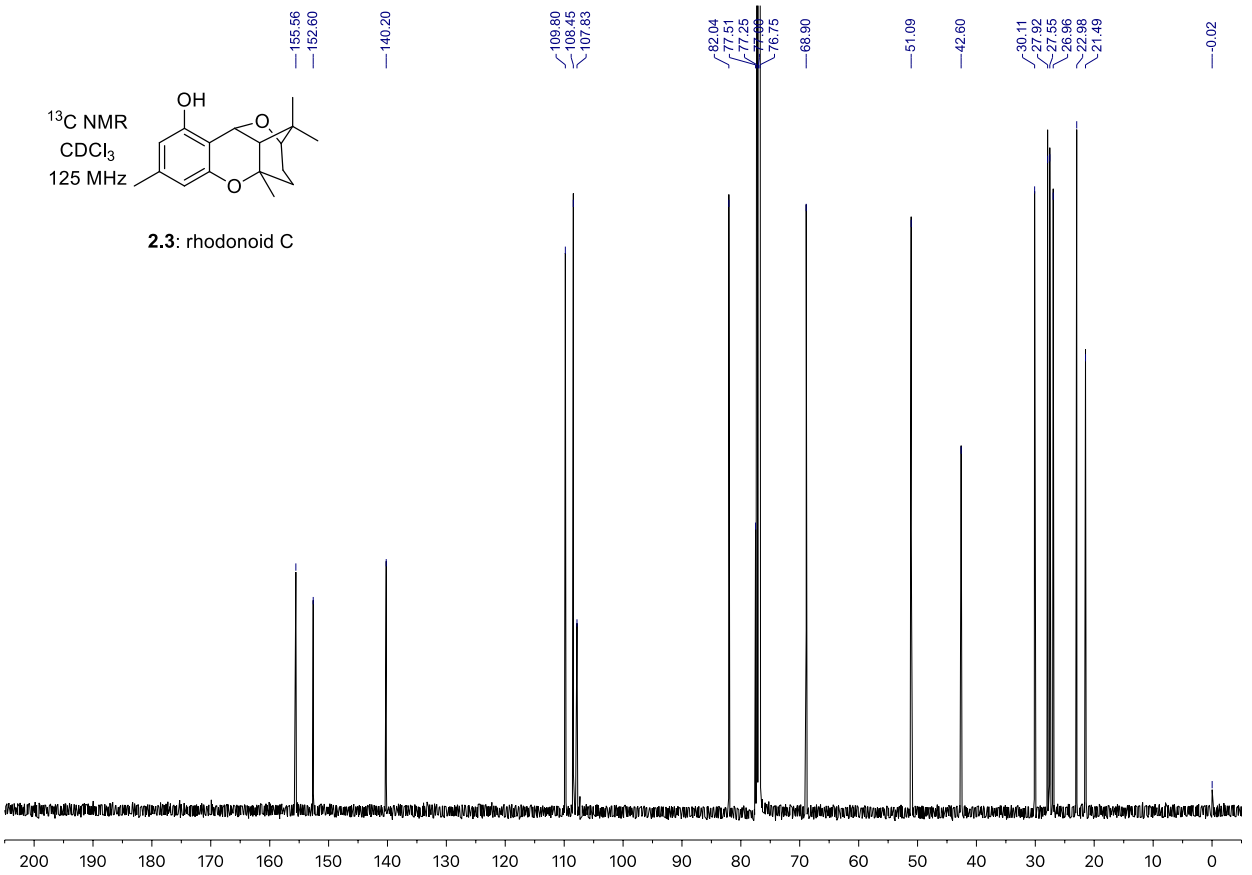

2.3: rhodonoid C

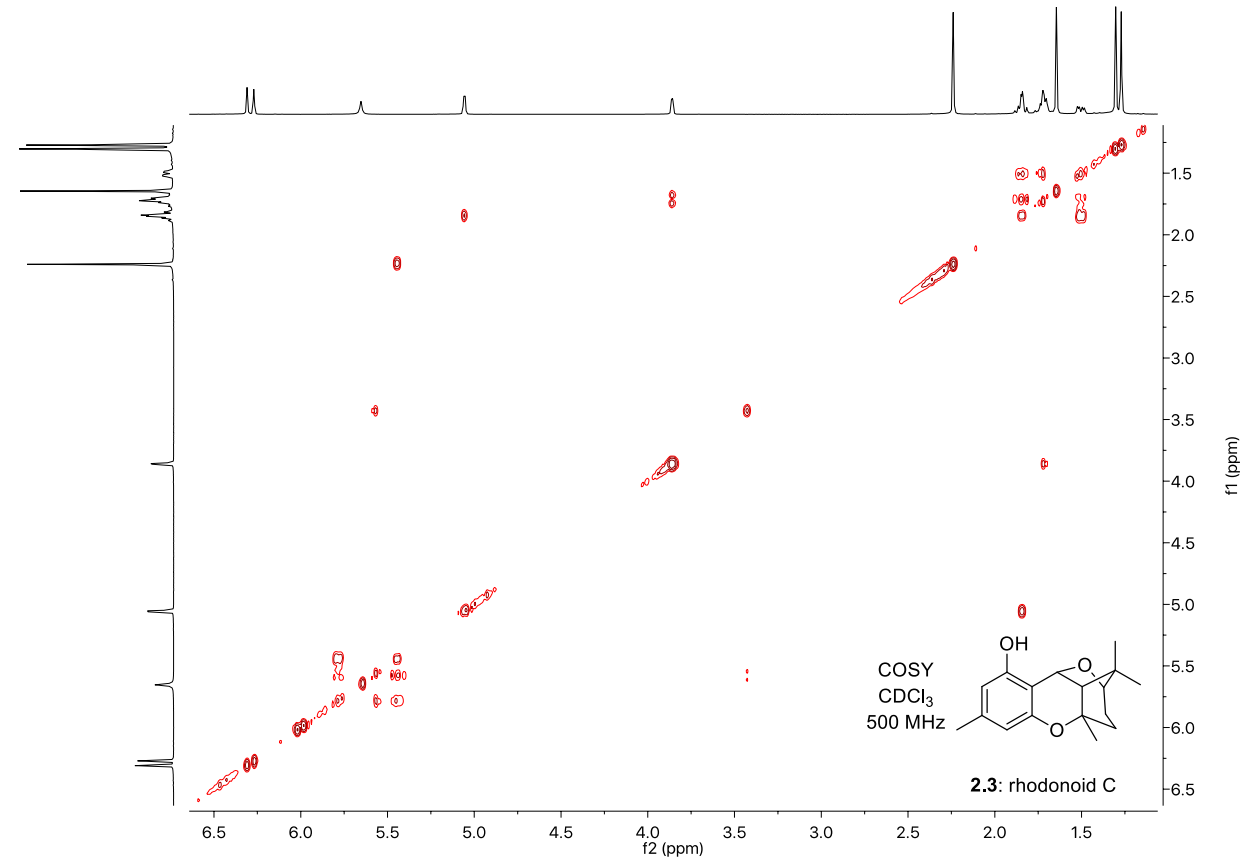
COSY
CDCl3
500 MHz
OH
O
O
2.3: rhodonoid C
f2 (ppm)
f1 (ppm)

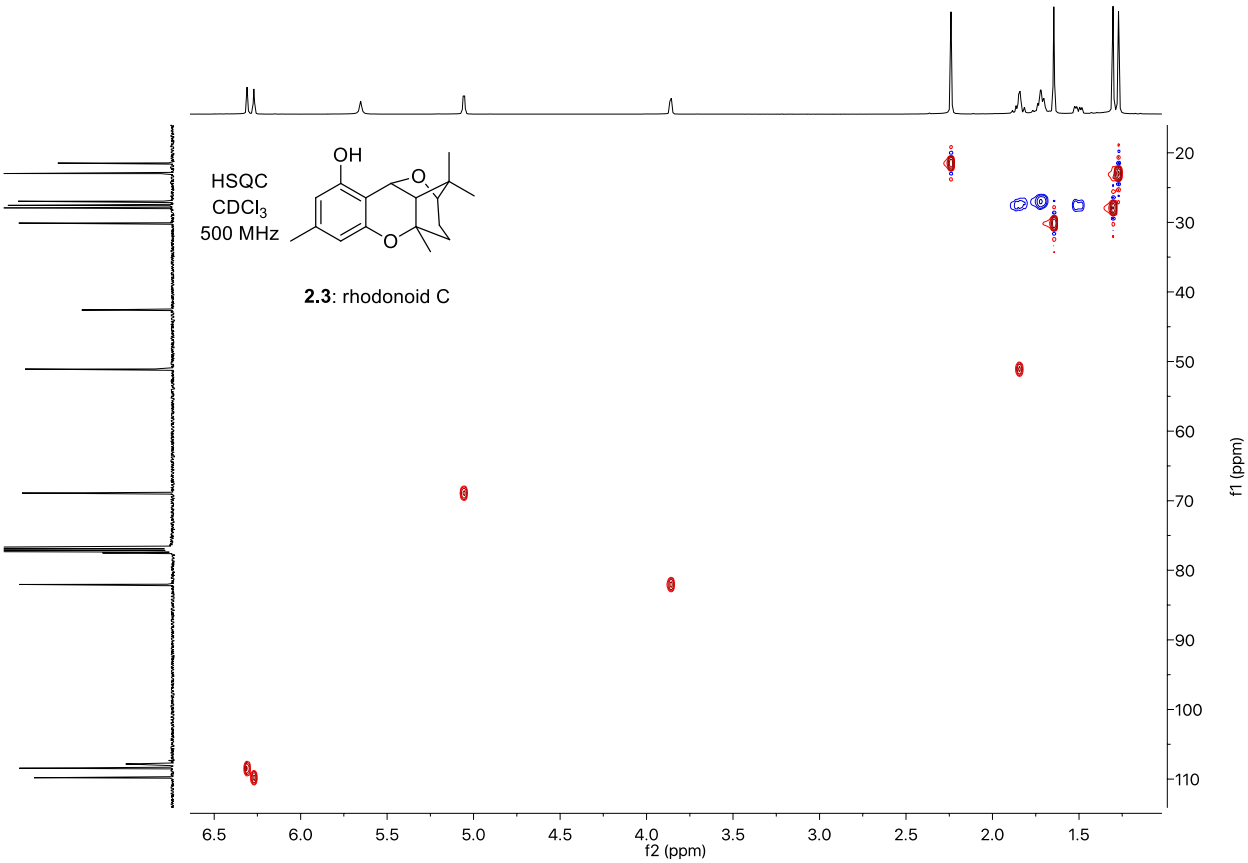
HSQC
CDCl3
500 MHz
OH
O
O
2.3: rhodonoid C
f2 (ppm)
f1 (ppm)

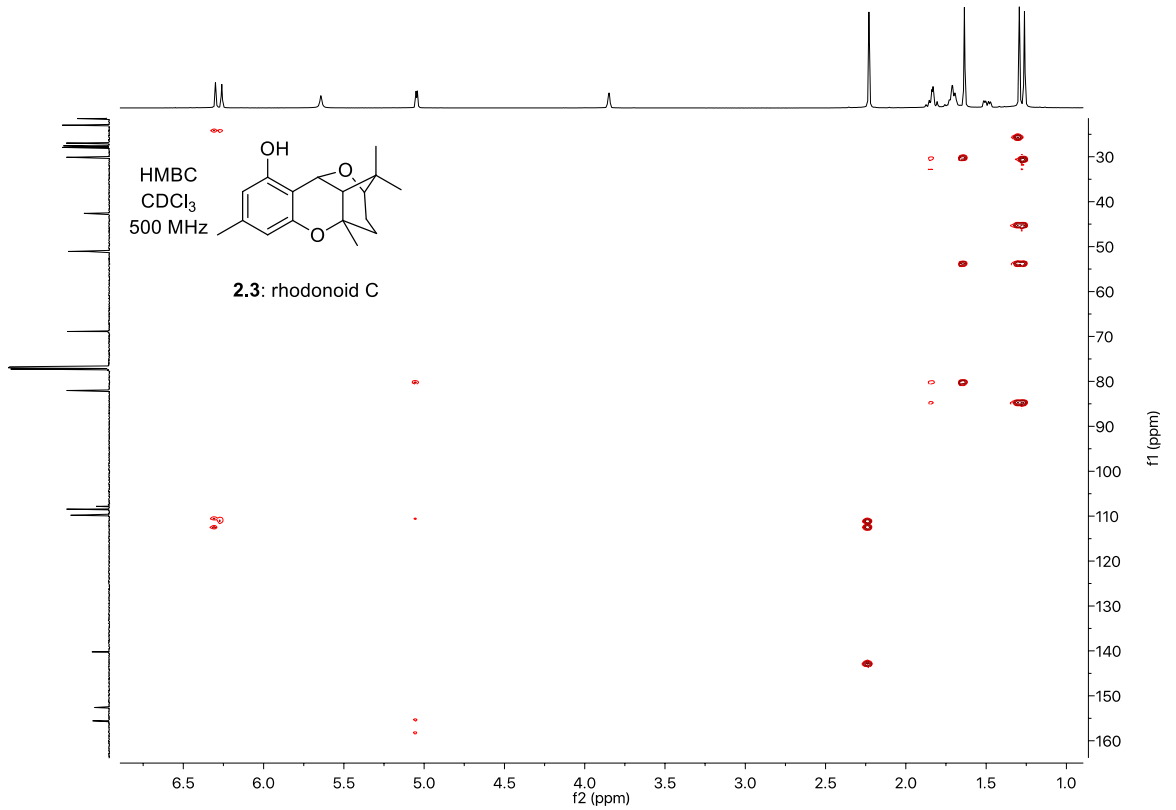
HMBC
CDCl3
500 MHz
OH
O
O
2.3: rhodonoid C
f2 (ppm)
f1 (ppm)

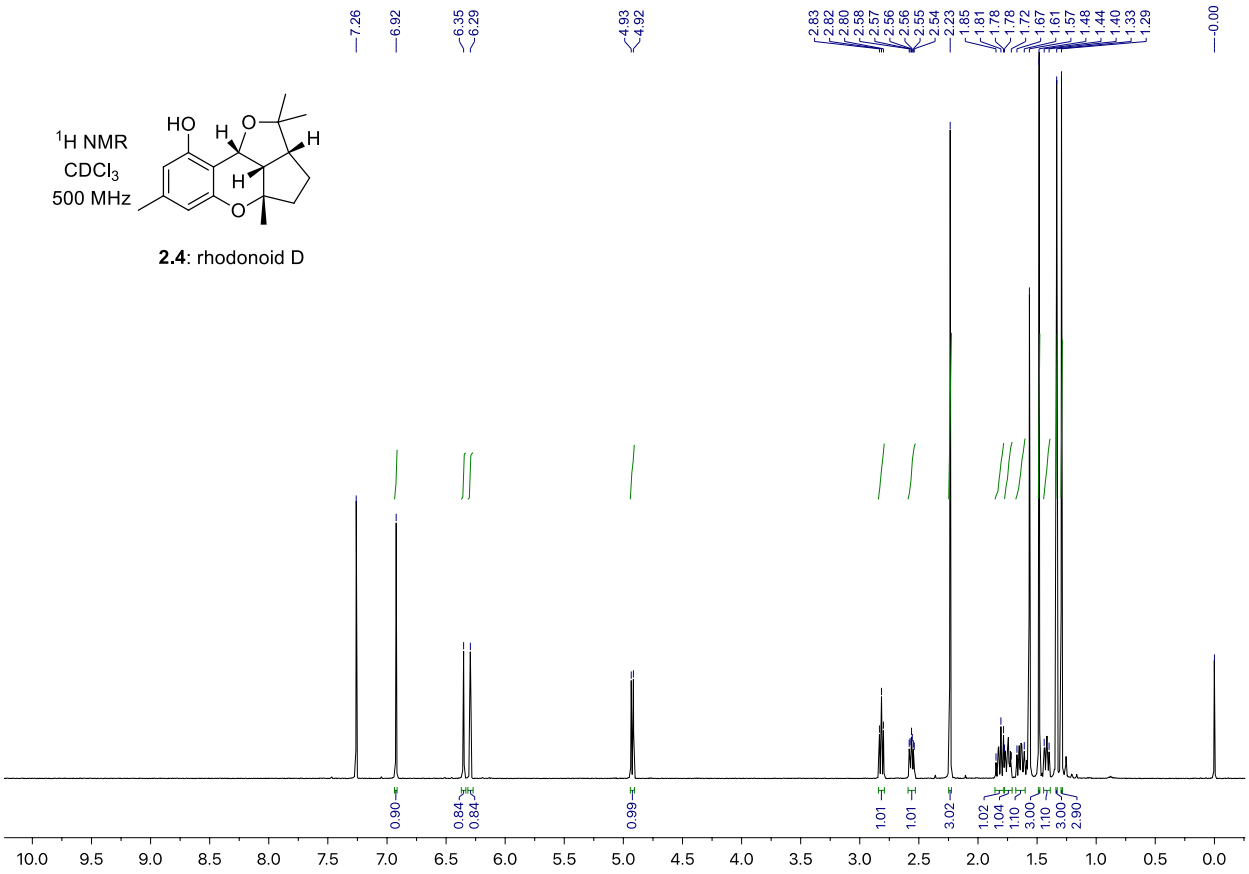
1H NMR
CDCl3
500 MHz
HO
H
O
H
H
O
2.4: rhodonoid D

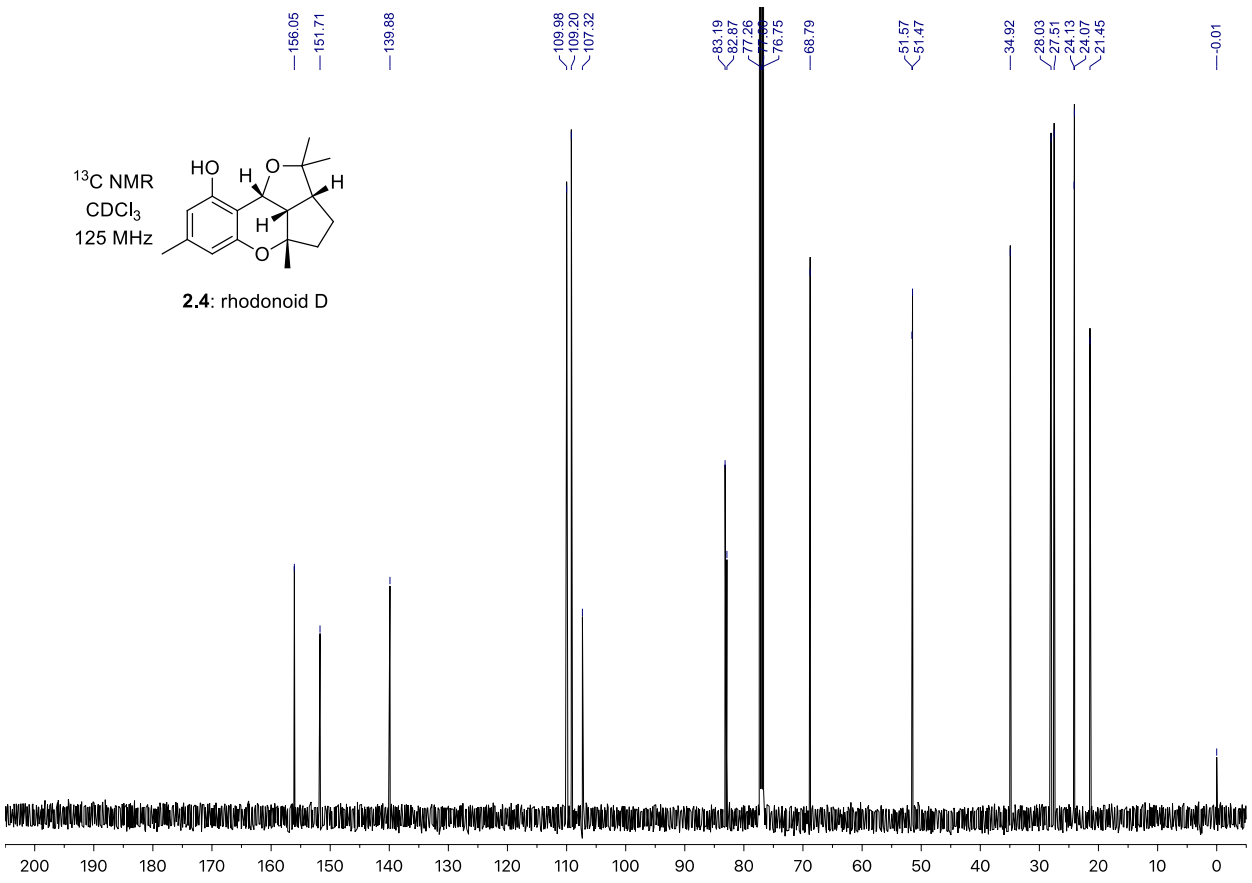
156.05
151.71
139.88
109.98
109.20
107.32
83.19
82.87
77.26
76.75
68.79
51.57
51.47
34.92
28.03
27.51
24.13
24.07
21.45
0.01
^{13}C NMR
$CDCl_3$
125 MHz
HO
H
O
H
H
O
2.4: rhodonoid D
200
190
180
170
160
150
140
130
120
110
100
90
80
70
60
50
40
30
20
10
0

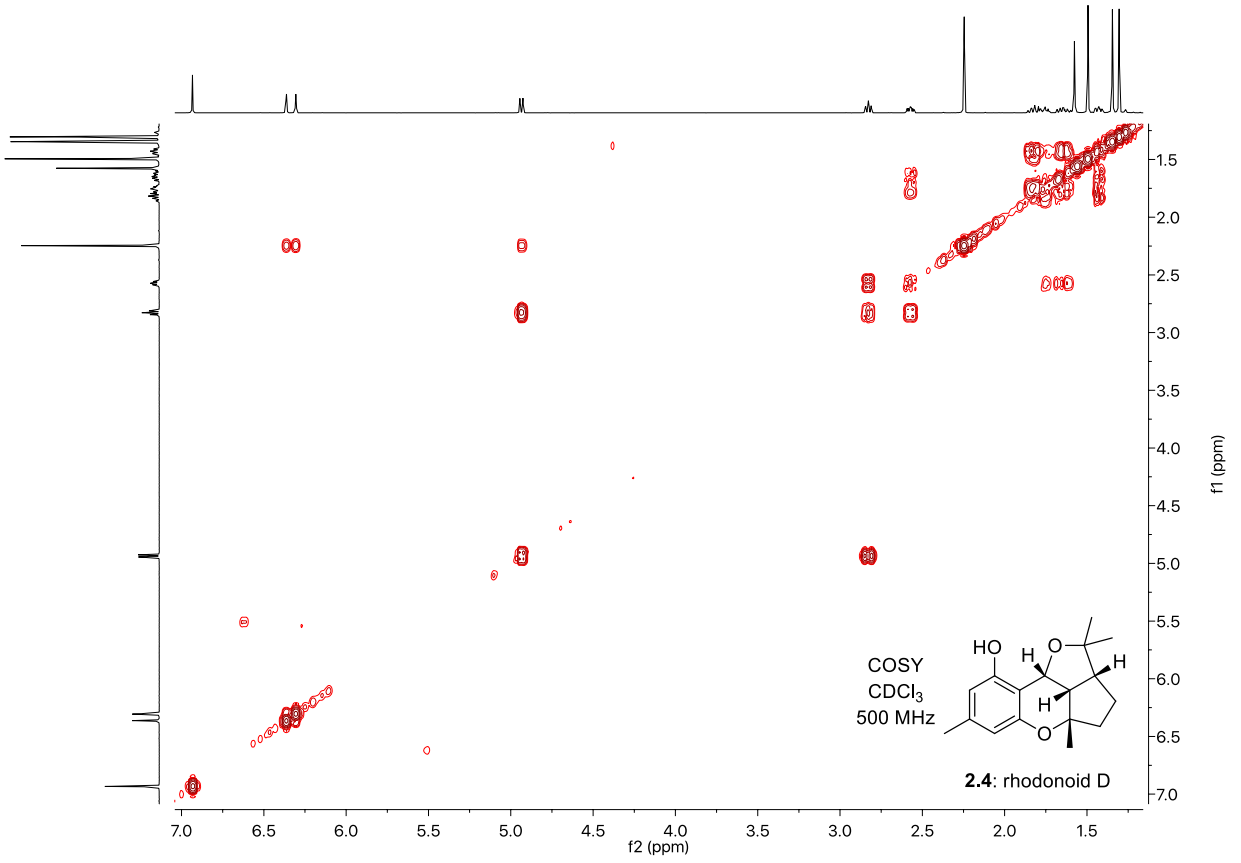
COSY
$CDCl_3$
500 MHz
HO
H
O
H
H
O
2.4: rhodonoid D
f1 (ppm)
f2 (ppm)
1.5
2.0
2.5
3.0
3.5
4.0
4.5
5.0
5.5
6.0
6.5
7.0

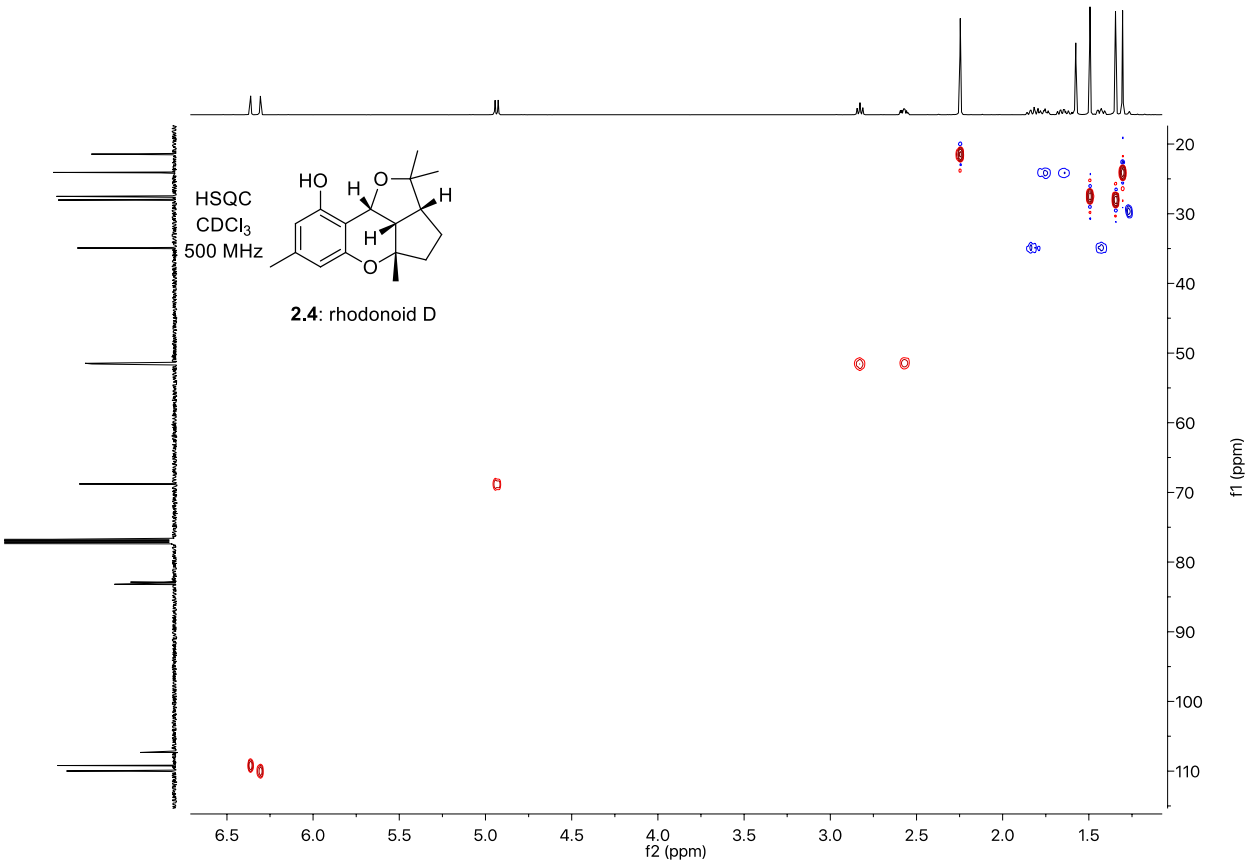
HSQC
CDCl3
500 MHz
HO
H
O
H
H
O
2.4: rhodonoid D
f2 (ppm)
f1 (ppm)

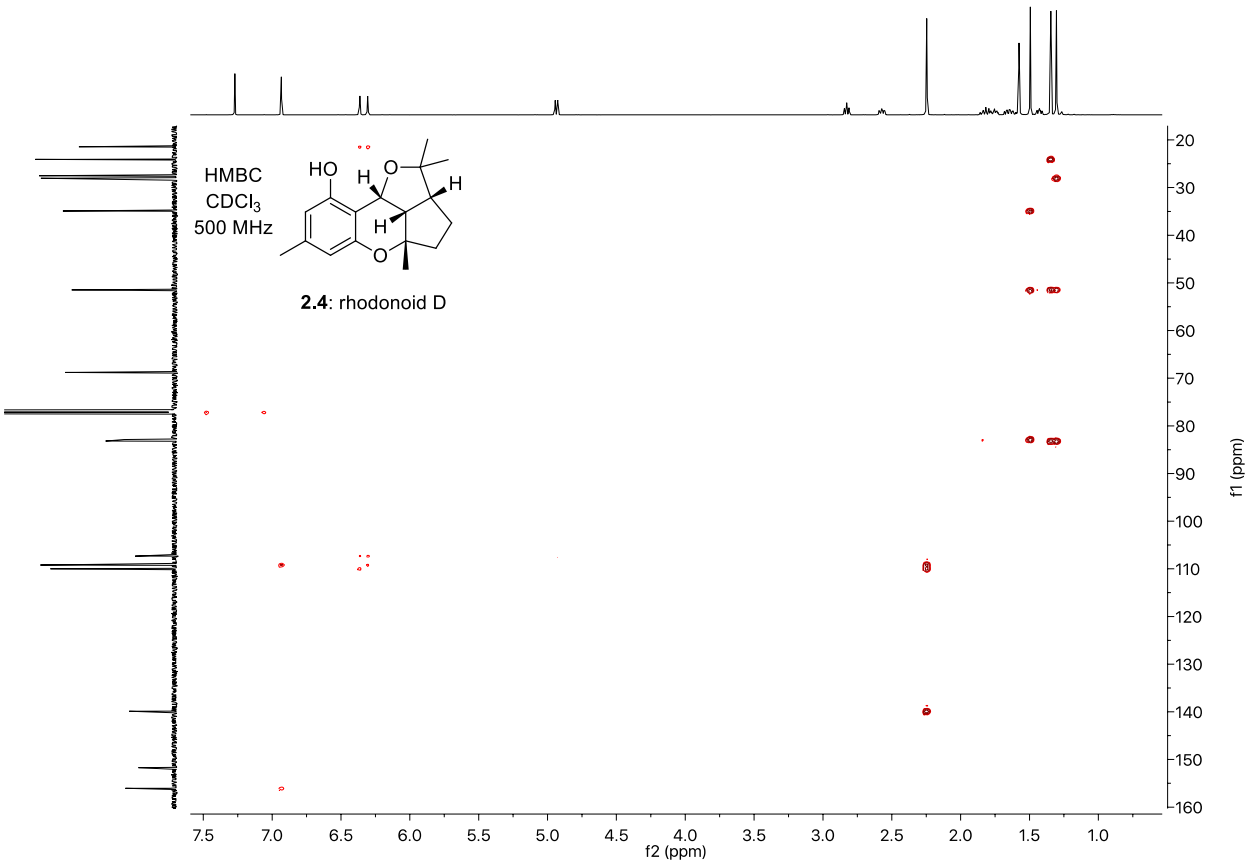
HMBC
CDCl3
500 MHz
HO
H
O
H
H
O
2.4: rhodonoid D
f2 (ppm)
f1 (ppm)

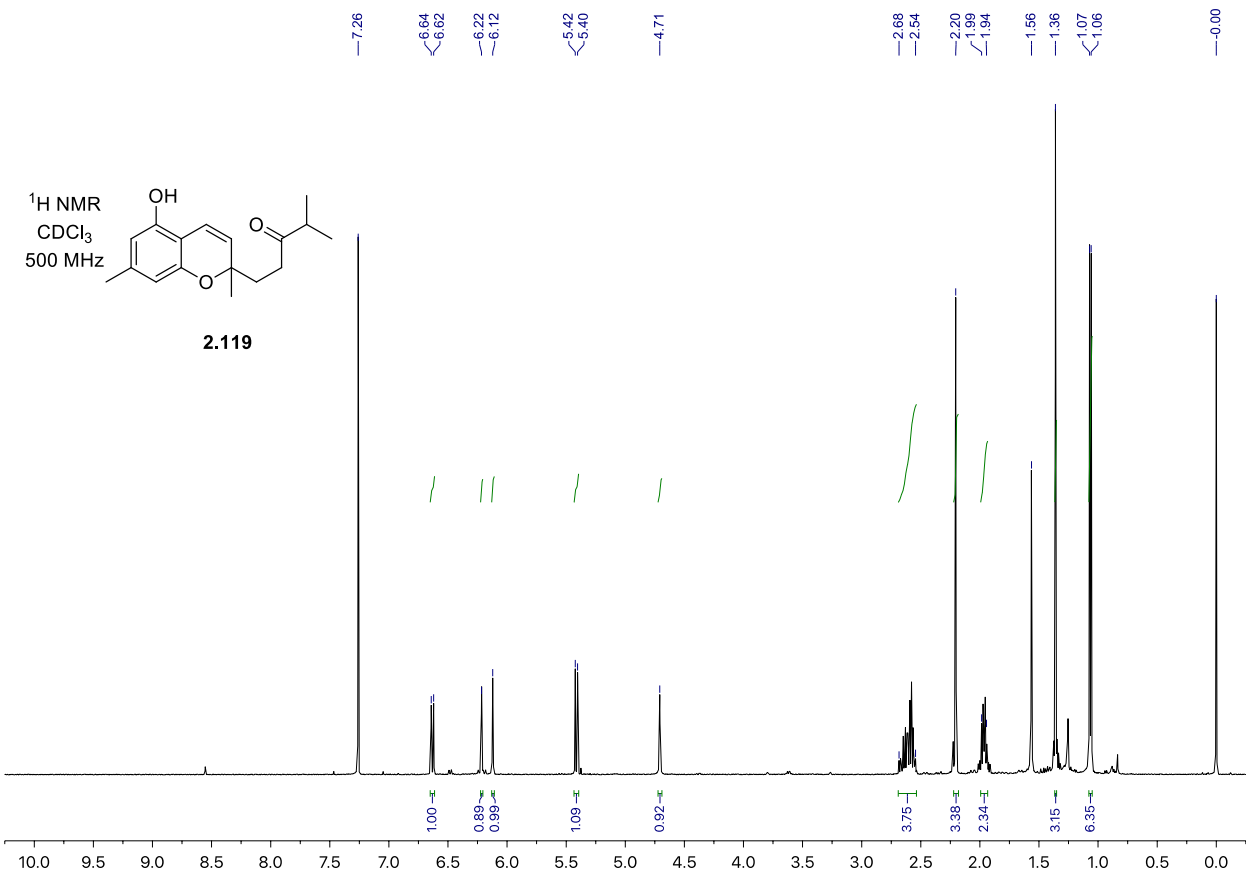
7.26
6.64
6.62
6.22
6.12
5.42
5.40
4.71
2.68
2.54
2.20
1.99
1.94
1.56
1.36
1.07
1.06
0.00
1H NMR
CDCl3
500 MHz
OH
O
O
2.119
1.00
0.89
0.99
1.09
0.92
3.75
3.38
2.34
3.15
6.35
10.0
9.5
9.0
8.5
8.0
7.5
7.0
6.5
6.0
5.5
5.0
4.5
4.0
3.5
3.0
2.5
2.0
1.5
1.0
0.5
0.0

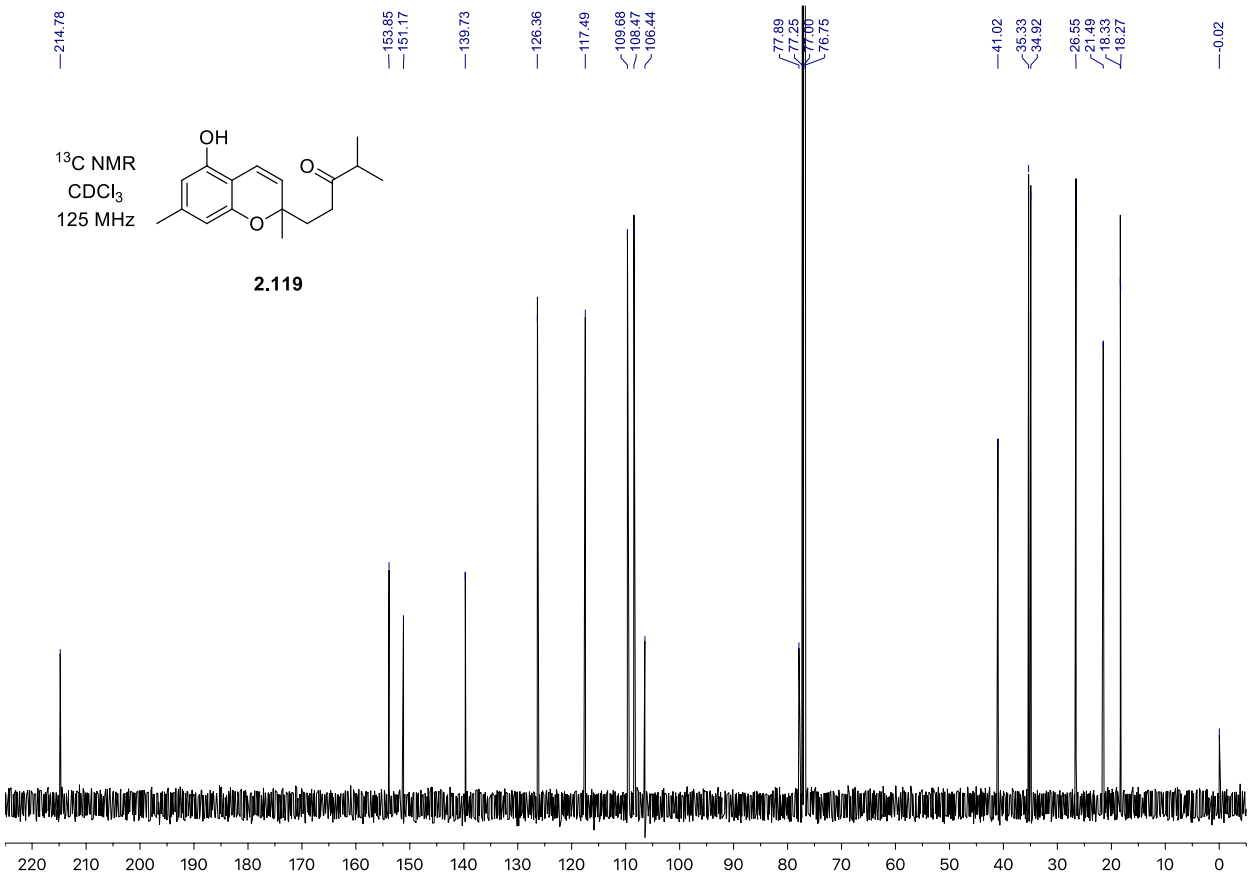
214.78
153.85
151.17
139.73
126.36
117.49
109.68
108.47
106.44
77.89
77.25
77.00
76.75
41.02
35.33
34.92
26.55
21.49
18.33
18.27
0.02
13C NMR
CDCl3
125 MHz
OH
O
O
2.119
220
210
200
190
180
170
160
150
140
130
120
110
100
90
80
70
60
50
40
30
20
10
0

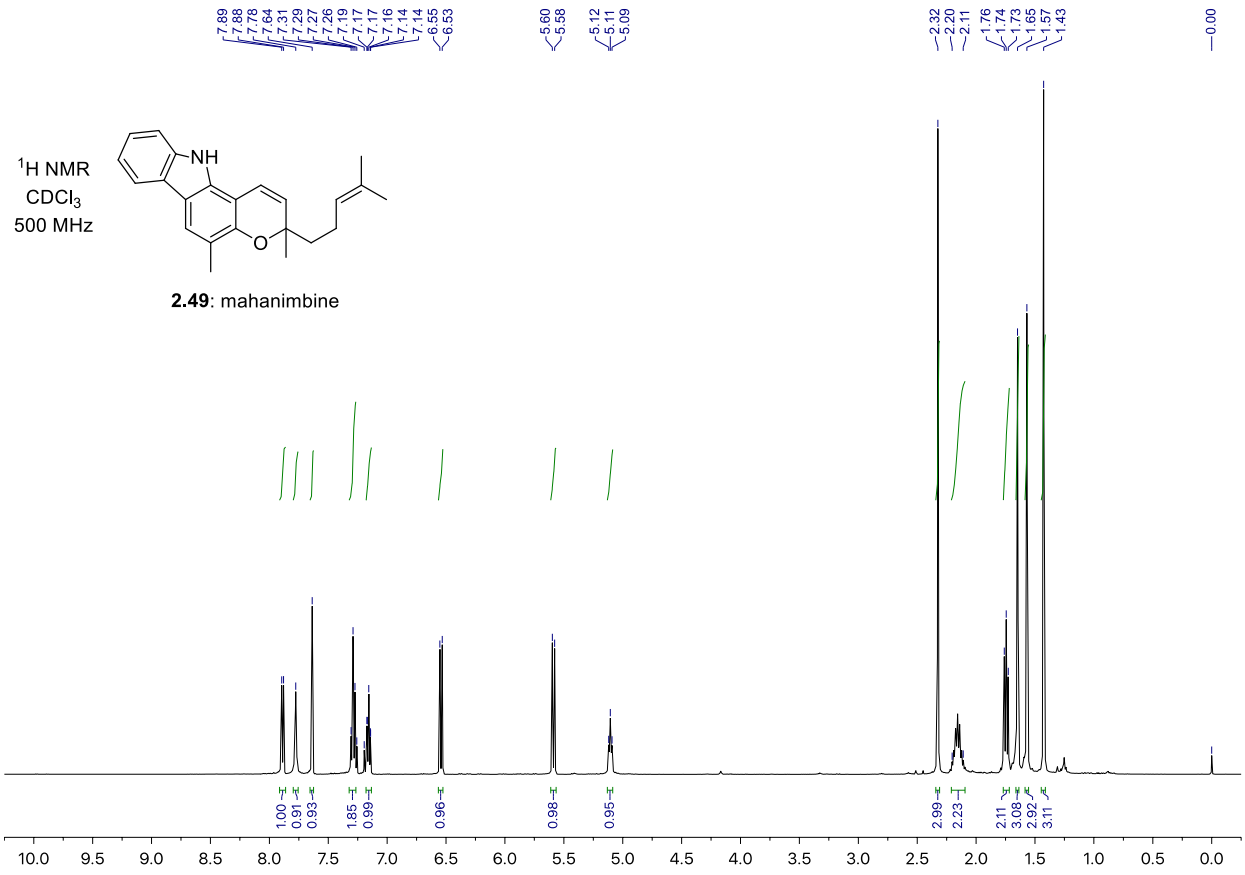
7.89
7.88
7.78
7.64
7.31
7.29
7.27
7.26
7.19
7.17
7.17
7.16
7.14
7.14
6.55
6.53
5.60
5.58
5.12
5.11
5.09
2.32
2.20
2.11
1.76
1.74
1.73
1.65
1.57
1.43
0.00
1H NMR
CDCl3
500 MHz
NH
O
2.49: mahanimbine
1.00
0.91
0.93
1.85
0.99
0.96
0.98
0.95
2.99
2.23
2.11
3.08
2.92
3.11
10.0
9.5
9.0
8.5
8.0
7.5
7.0
6.5
6.0
5.5
5.0
4.5
4.0
3.5
3.0
2.5
2.0
1.5
1.0
0.5
0.0

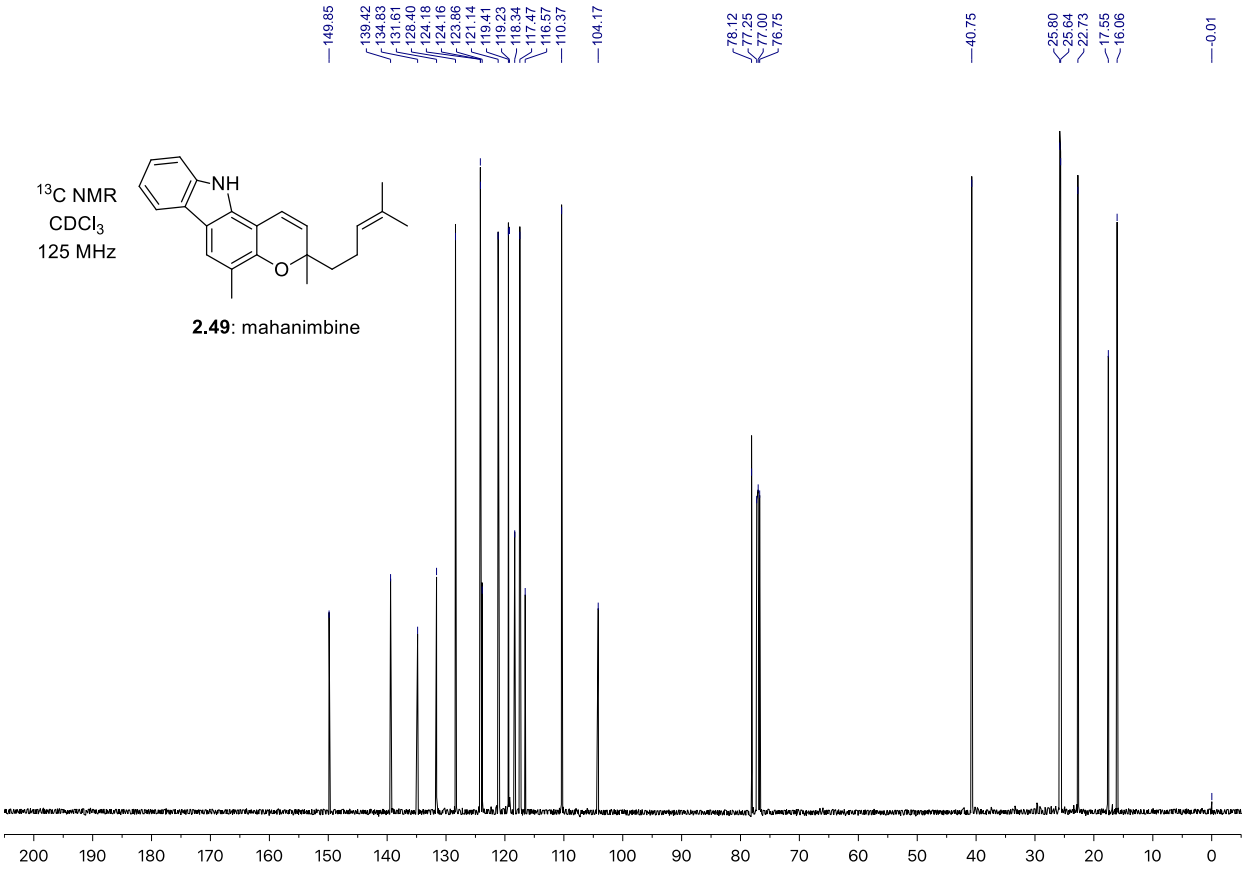
149.85
139.42
134.83
131.61
128.40
124.18
124.16
123.86
121.14
119.41
119.23
118.34
117.47
116.57
110.37
104.17
78.12
77.25
77.00
76.75
40.75
25.80
25.64
22.73
17.55
16.06
0.01
13C NMR
CDCl3
125 MHz
NH
O
2.49: mahanimbine
200
190
180
170
160
150
140
130
120
110
100
90
80
70
60
50
40
30
20
10
0

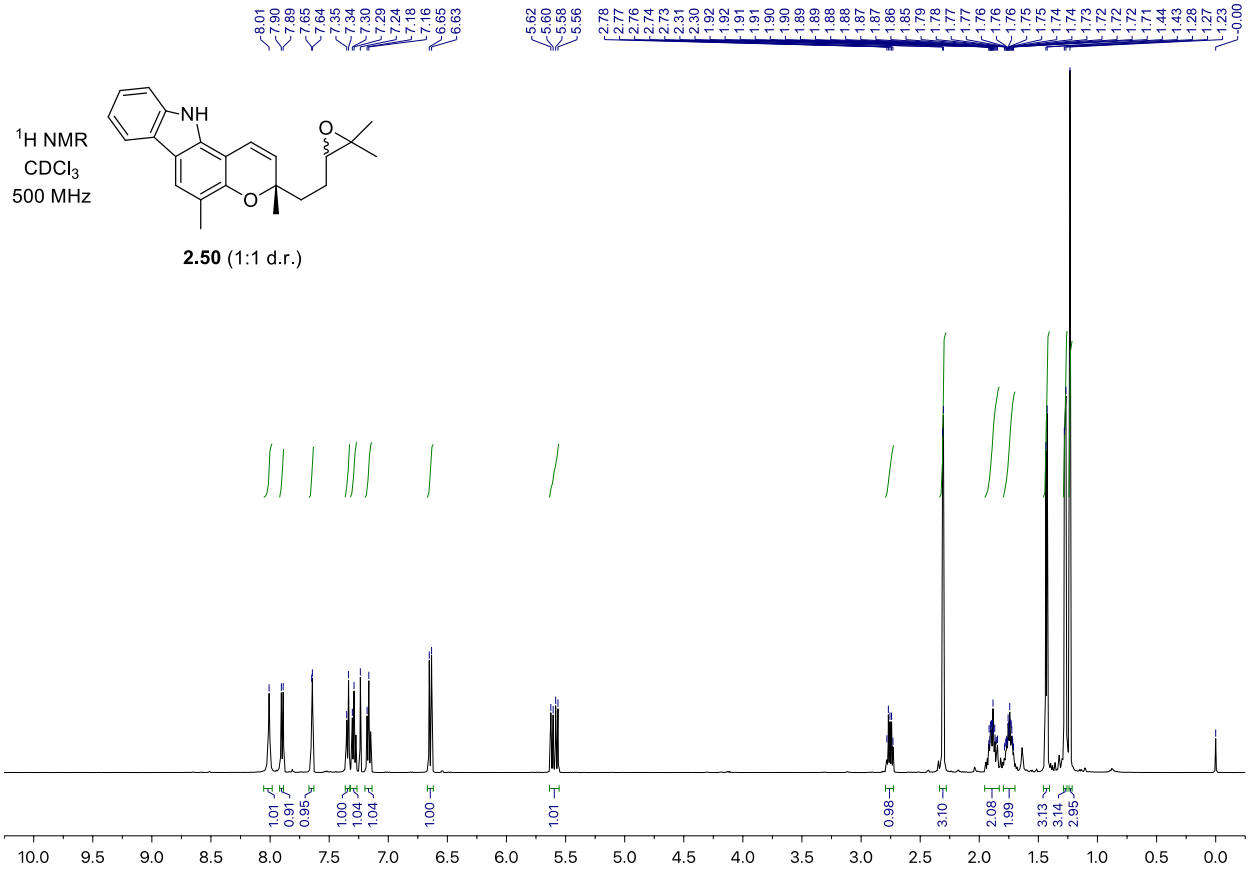
^{1}H NMR
$CDCl_3$
500 MHz
NH
O
O
2.50 (1:1 d.r.)

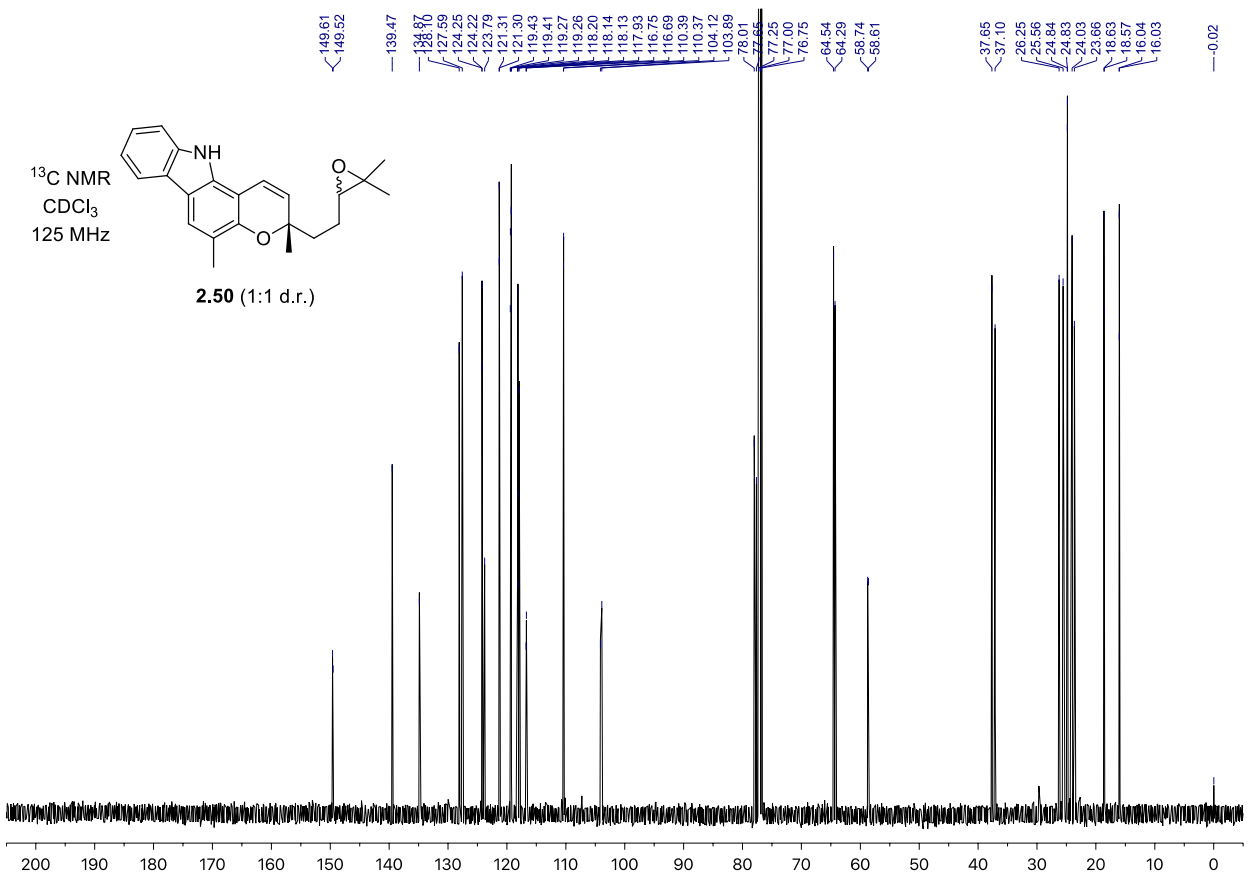
^{13}C NMR
$CDCl_3$
125 MHz
NH
O
O
2.50 (1:1 d.r.)

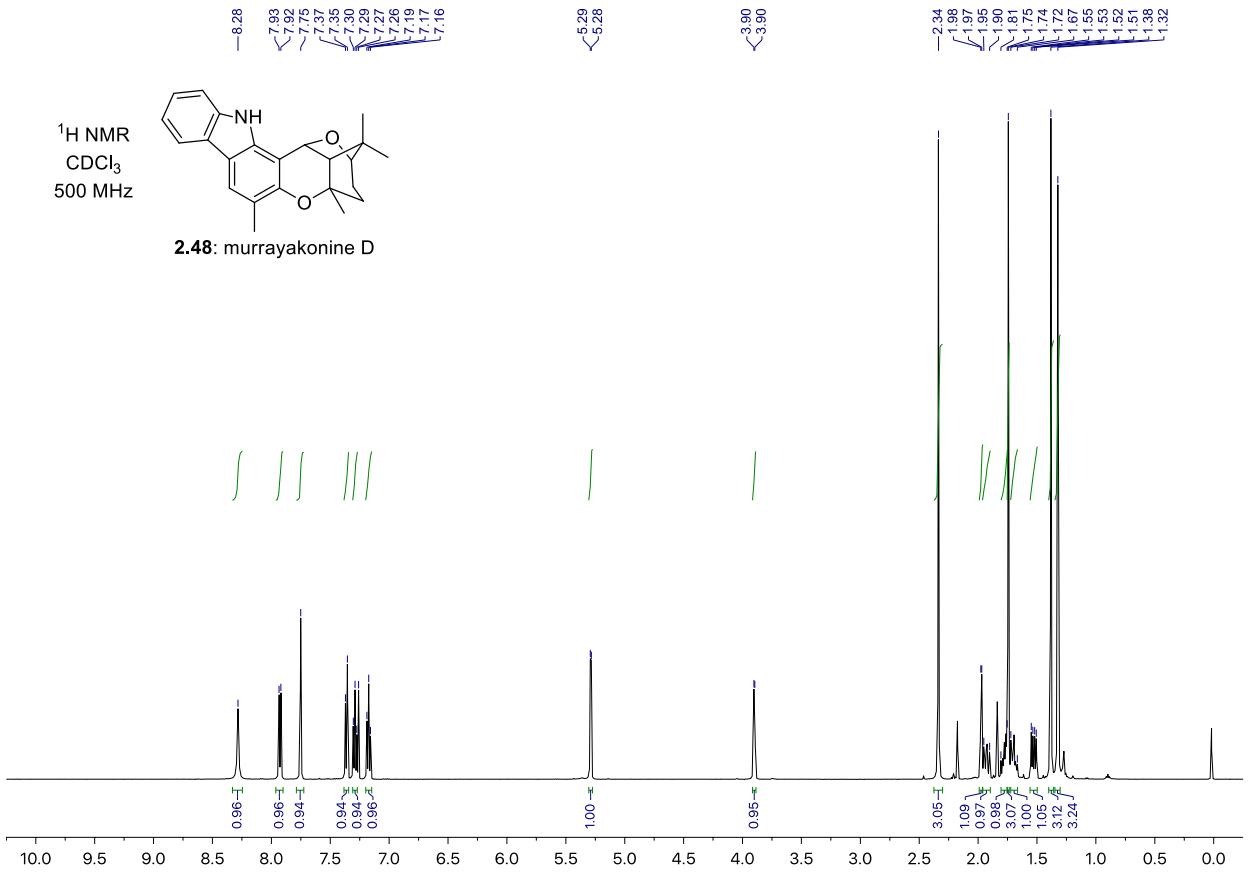

2.48: murrayakonine D

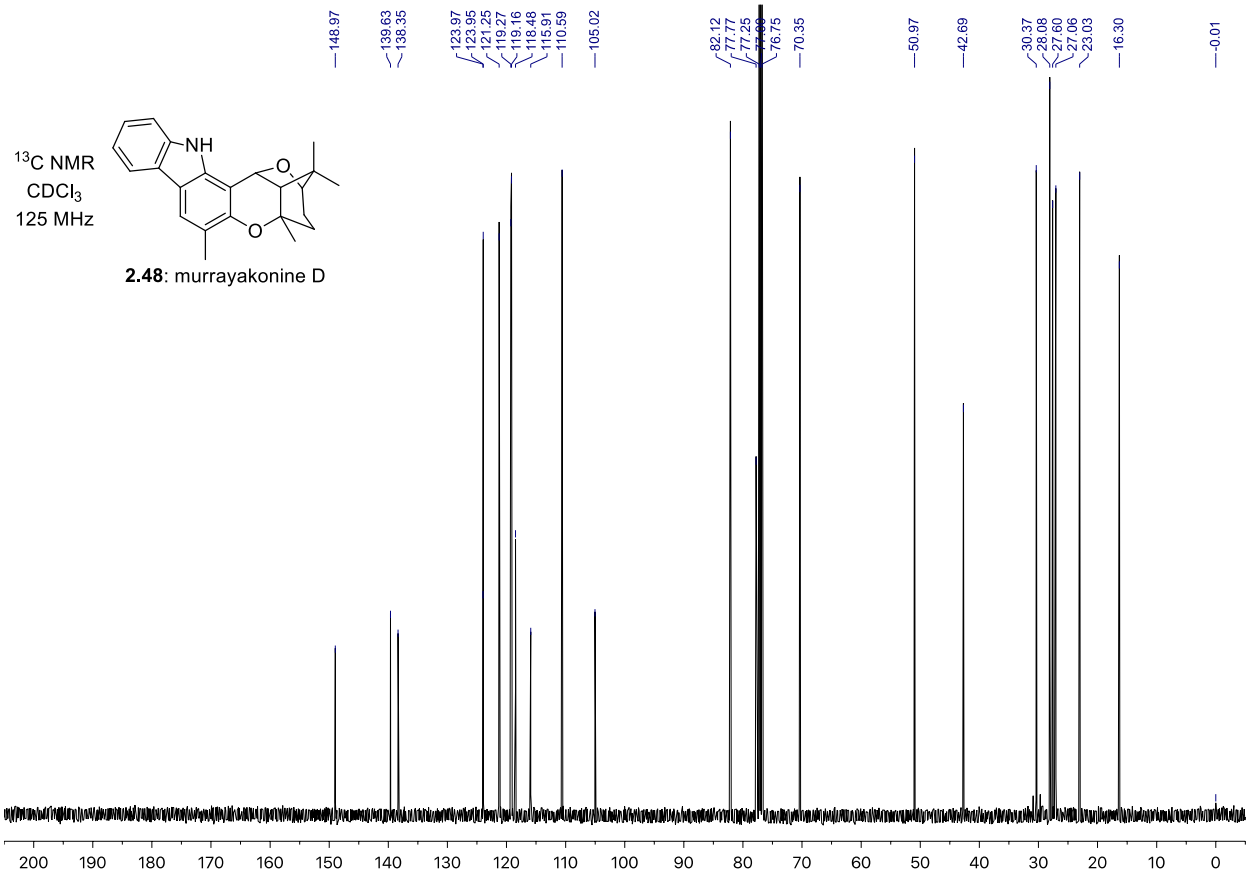

2.48: murrayakonine D

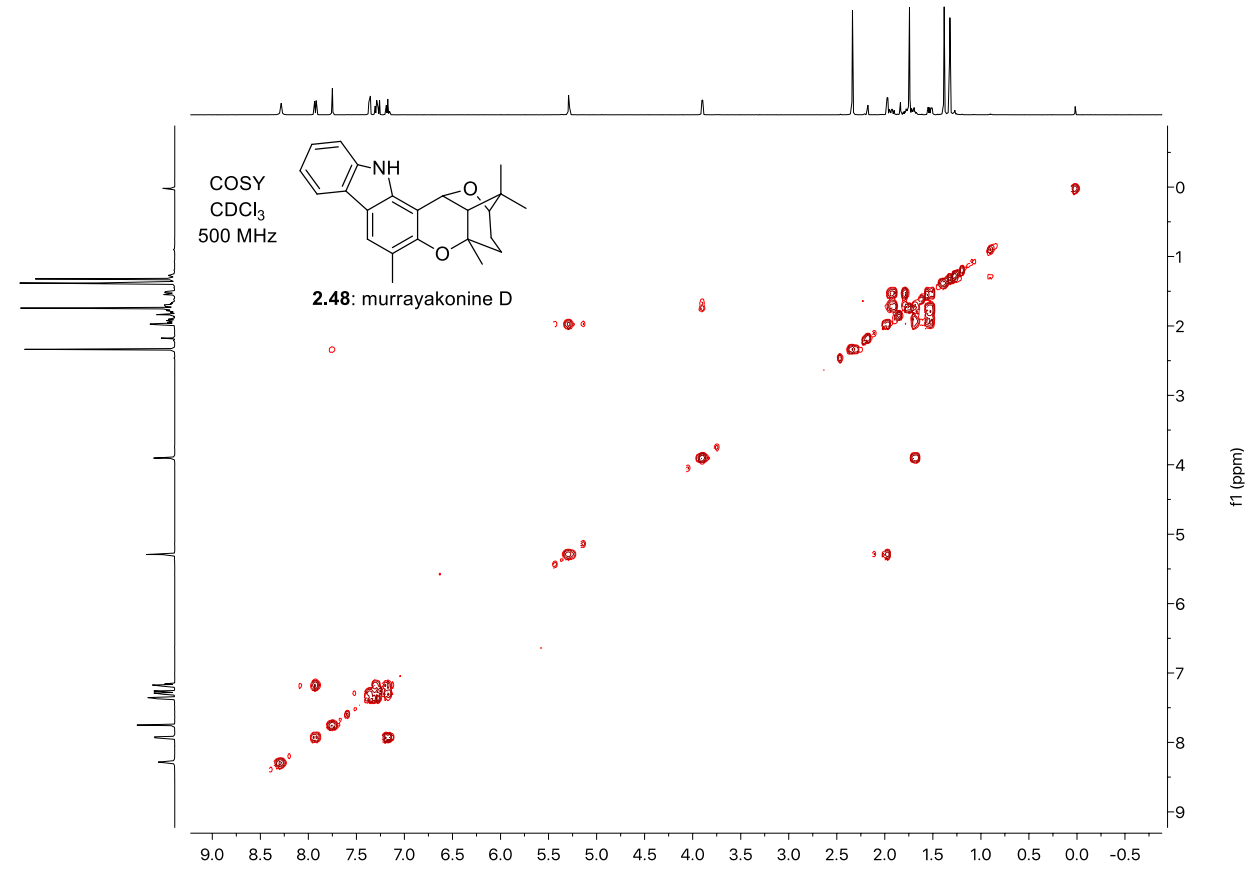
COSY
CDCl3
500 MHz
NH
O
O
2.48: murrayakonine D
f1 (ppm)

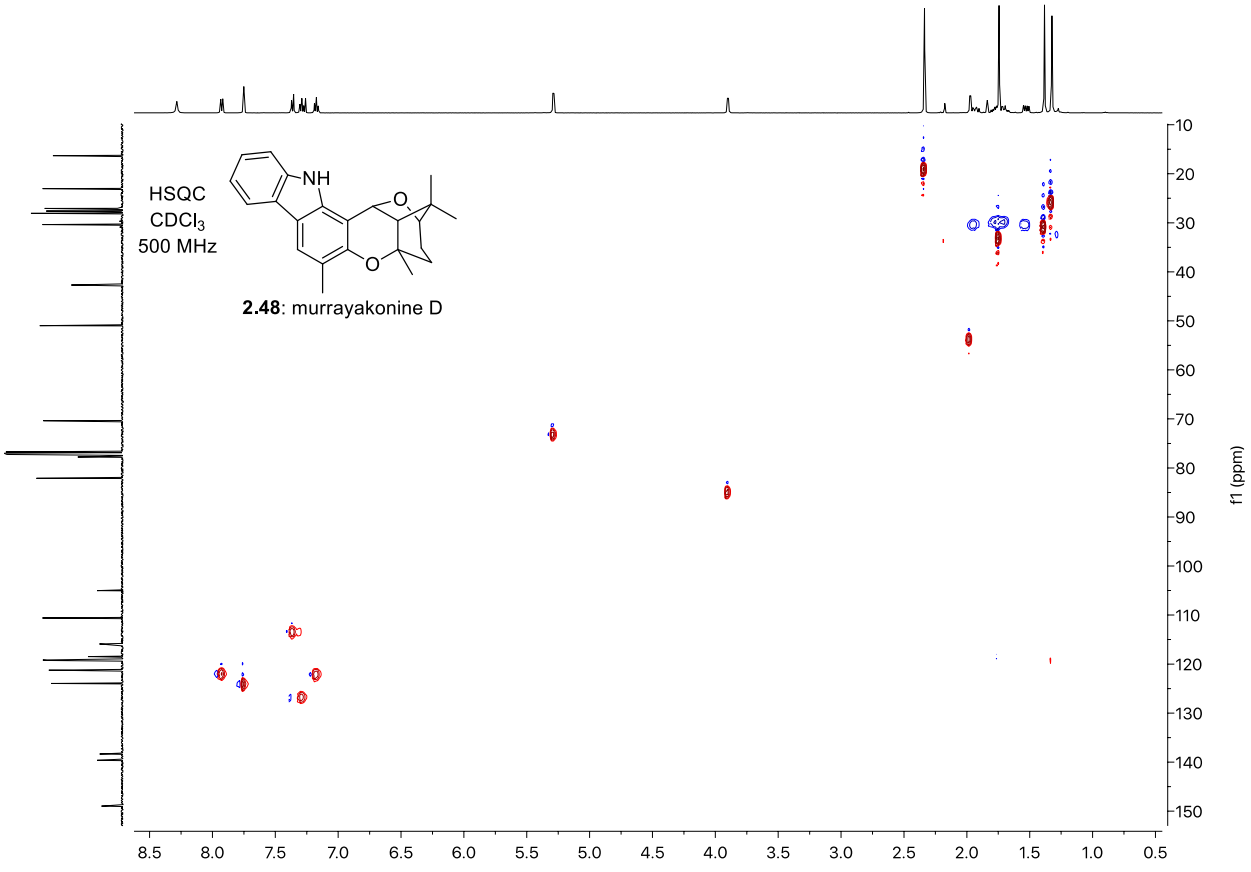
HSQC
CDCl3
500 MHz
NH
O
O
2.48: murrayakonine D
f1 (ppm)

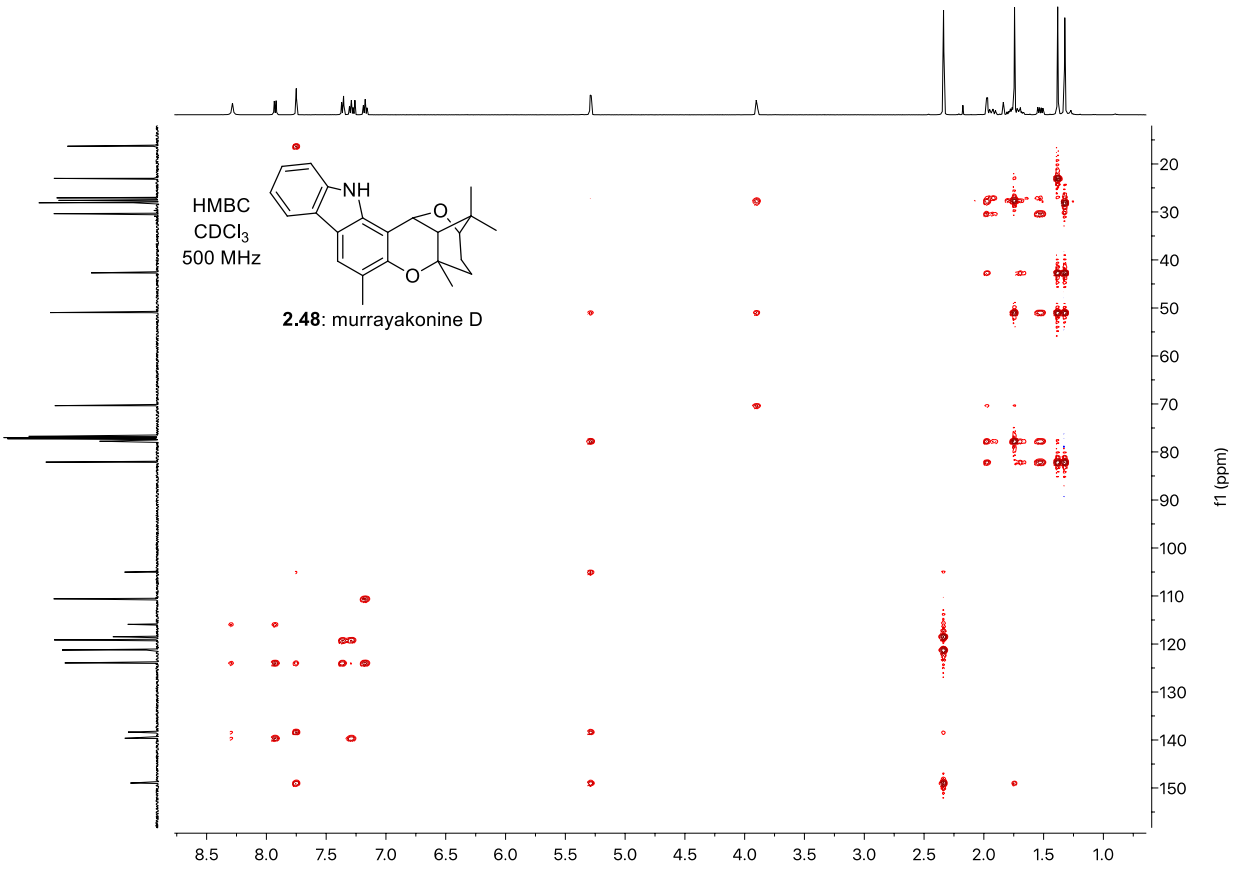
HMBC
CDCl3
500 MHz
NH
O
O
2.48: murrayakonine D
f1 (ppm)

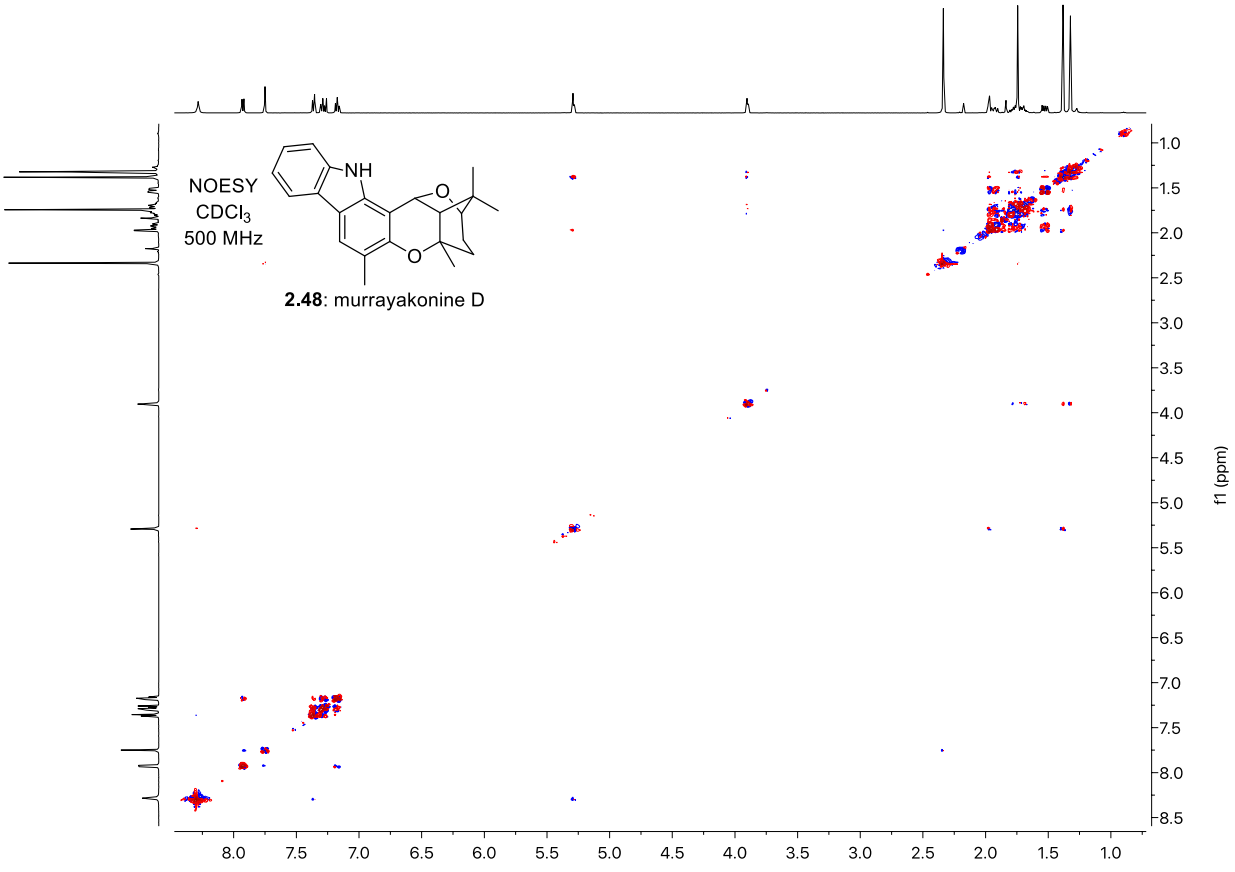
NOESY
CDCl3
500 MHz
NH
O
O
2.48: murrayakonine D
f1 (ppm)

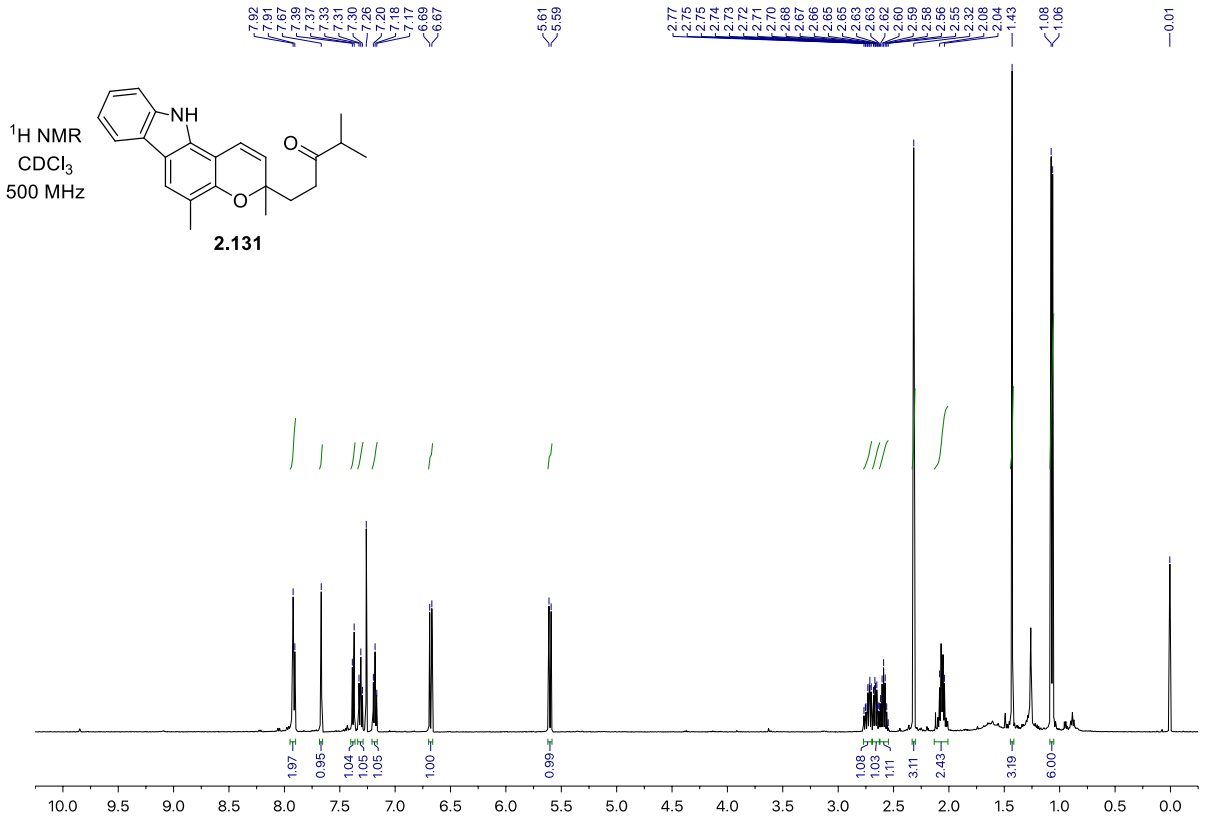
7.92
7.91
7.67
7.39
7.37
7.33
7.31
7.30
7.26
7.20
7.18
7.17
6.69
6.67
5.61
5.59
2.77
2.75
2.74
2.73
2.72
2.71
2.70
2.68
2.67
2.66
2.65
2.65
2.63
2.63
2.62
2.60
2.59
2.58
2.56
2.55
2.32
2.08
2.04
1.43
1.08
1.06
0.01
1H NMR
CDCl3
500 MHz
NH
O
O
2.131
1.97
0.95
1.04
1.05
1.05
1.00
0.99
1.08
1.03
1.11
3.11
2.43
3.19
6.00
10.0
9.5
9.0
8.5
8.0
7.5
7.0
6.5
6.0
5.5
5.0
4.5
4.0
3.5
3.0
2.5
2.0
1.5
1.0
0.5
0.0

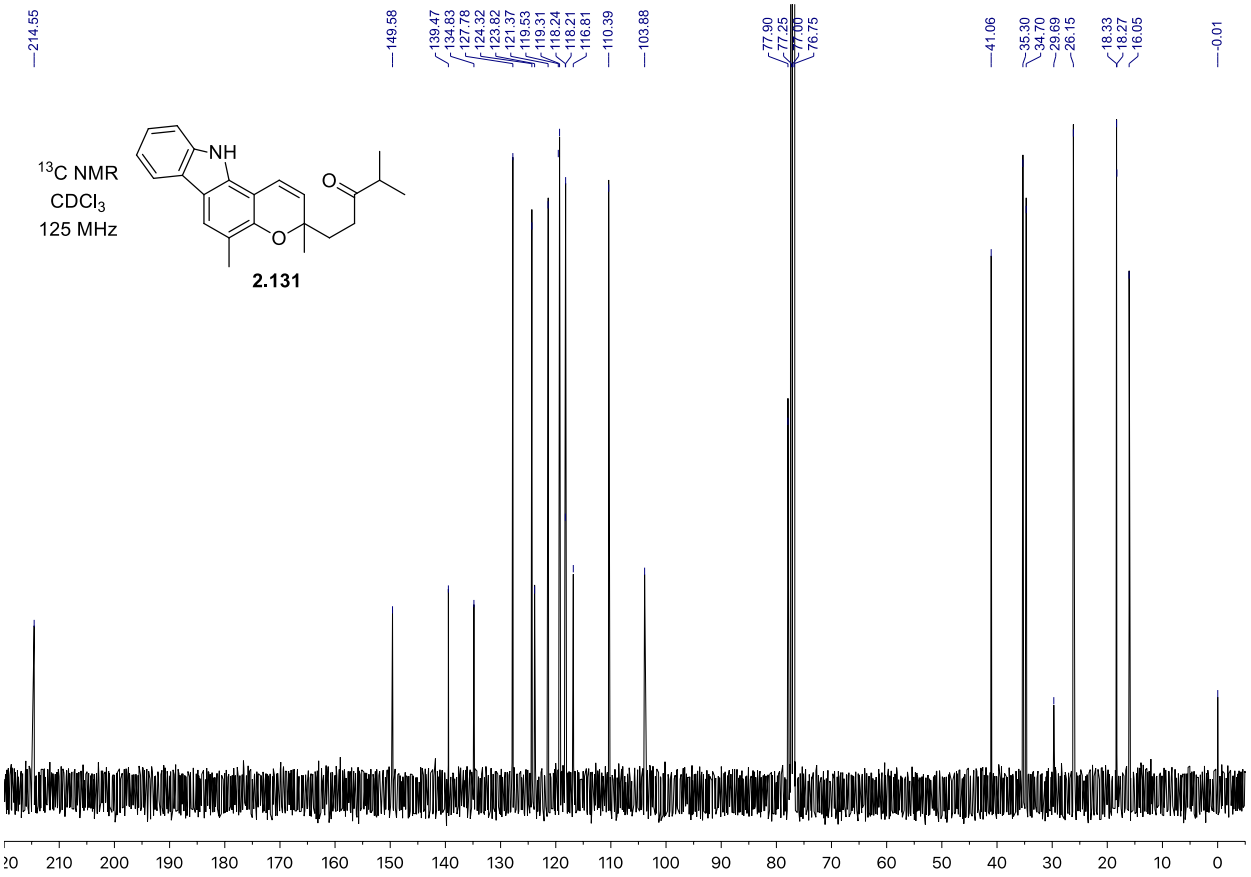
214.55
149.58
139.47
134.83
127.78
124.32
123.82
121.37
119.53
119.31
118.24
118.21
116.81
110.39
103.88
77.90
77.25
77.00
76.75
41.06
35.30
34.70
29.69
26.15
18.33
18.27
16.05
0.01
13C NMR
CDCl3
125 MHz
NH
O
O
2.131
210
200
190
180
170
160
150
140
130
120
110
100
90
80
70
60
50
40
30
20
10
0

2.4.4: ^{1}H and ^{13}C NMR Comparison Tables

Table 2.2: Comparison of the ^{1}H and ^{13}C NMR spectra of natural[2] and synthetic rhodonoid C.

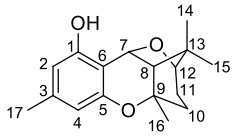

2.3: rhodonoid C

	Natural **2.3** ^{1}H NMR, $CDCl_3$ (400 MHz)	Synthetic **2.3** ^{1}H NMR, $CDCl_3$ (500 MHz)	Natural **2.3** ^{13}C NMR, $CDCl_3$ (150 MHz)	Synthetic **2.3** ^{13}C NMR, $CDCl_3$ (125 MHz)
1	-	-	155.7	155.6
2	6.30 br s	6.30 s	108.6	108.5
3	-	-	140.4	140.2
4	6.26 br s	6.26 s	110.0	109.8
5	-	-	152.8	152.6
6	-	-	108.0	107.8
7	5.04 d (4.3)	5.05 d (4.2)	69.1	68.9
8	1.83 d (4.3)	1.87 – 1.81 m	51.3	51.1
9	-	-	77.7	77.5
10	1.82 dd (13.7, 6.0) 1.49 dd (13.7, 6.0)	1.87 – 1.81 m 1.49 dd (14.6, 5.7)	27.7	27.6
11	1.71 m	1.73 – 1.69 m	27.1	27.0
12	3.85 br s	3.85 s	82.2	82.0
13	-	-	42.8	42.6
14	1.29 s	1.29 s	28.1	27.9
15	1.26 s	1.26 s	23.1	23.0
16	1.63 s	1.64 s	30.3	30.1
17	2.23 s	2.23 s	21.6	21.5
1-OH	-	5.64 br s	-	-

Table 2.3: Comparison of the ^{1}H and ^{13}C NMR spectra of natural[2] and synthetic rhodonoid D.

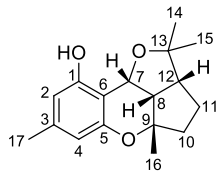

2.4: rhodonoid D

	Natural **2.4** ^{1}H NMR, $CDCl_3$ (400 MHz)	Synthetic **2.4** ^{1}H NMR, $CDCl_3$ (500 MHz)	Natural **2.4** ^{13}C NMR, $CDCl_3$ (150 MHz)	Synthetic **2.4** ^{13}C NMR, $CDCl_3$ (125 MHz)
1	-	-	156.2	156.1
2	6.35 br s	6.35 s	109.3	109.2
3	-	-	140.0	139.9
4	6.30 (br s)	6.30 s	110.1	110.0
5	-	-	151.9	151.7
6	-	-	107.5	107.3
7	4.92 d (9.0)	4.92 d (9.1)	68.9	68.8
8	2.82 (9.0)	2.82 t (8.5)	51.7	51.6
9	-	-	83.0	82.9
10	1.80 m 1.42 m	1.85 – 1.78 m 1.44 – 1.40 m	35.0	34.9
11	1.74 m 1.64 m	1.75 – 1.72 m 1.67 – 1.60 m	24.3	24.12
12	2.56 m	2.56 ddd (9.9, 8.0, 3.8)	51.6	51.6
13	-	-	83.3	83.2
14	1.33 s	1.33 s	28.2	28.0
15	1.29 s	1.29 s	24.2	24.08
16	1.48 s	1.48 s	27.6	27.5
17	2.24 s	2.24 s	21.6	21.5
1-OH	6.94 br s	6.92 br s	-	-

Table 2.4: ^{1}H and ^{13}C NMR spectra of natural[18] and synthetic murrayakonine D (**2.48**).

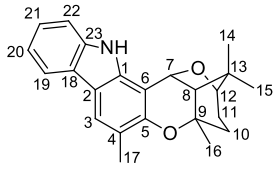

2.48: murrayakonine D

	Natural **2.48** ^{1}H NMR, $CDCl_3$ (400 MHz)	Synthetic **2.48** ^{1}H NMR, $CDCl_3$ (500 MHz)	Natural **2.48** ^{13}C NMR, $CDCl_3$ (150 MHz)	Synthetic **2.48** ^{13}C NMR, $CDCl_3$ (125 MHz)
1	-	-	138.4	138.4
2	-	-	115.9	115.9
3	7.67 s	7.75 s	121.2	121.3
4	-	-	118.5	118.5
5	-	-	149.0	149.0
6	-	-	105.0	105.0
7	5.22 d (4.2)	5.29 d (4.2)	70.4	70.4
8	1.91 d (4.2)	1.97 d (3.9)	51.0	51.0
9			77.8	77.8
10	1.88 – 1.80 m 1.48 – 1.42 m	1.95 – 1.90 m 1.53 dd (14.5, 7.1)	27.6	27.6
11	1.55 s**	1.81 – 1.74 m 1.72 – 1.67 m	27.1	27.1
12	3.82 d (3.9)	3.90 d (4.2)	82.2	82.1
13	-	-	42.7	42.7
14	1.31 s	1.38 s	28.1	28.1
15	1.25 s	1.32 s	23.1	23.0
16	1.67 s	1.74 s	30.4	30.4
17	2.25 s	2.34 s	16.3	16.3
18	-	-	124.0	123.97
19	7.85 d (7.0)	7.93 d (7.7)	119.3	119.3
20	7.09 t (7.4)	7.17 t (7.4)	119.2	119.2
21	7.22 d (8.0)	7.29 t (7.3)	124.0	123.95
22	7.31 d (8.0)	7.36 d (8.0)	110.6	110.6
23	-	-	139.7	139.6
1-NH	8.21 s	8.28 s	-	-

* ^{1}H spectrum is incorrectly referenced (our chemical shift values for synthetic **3** are 0.07-0.09 ppm higher than for natural **3**).

** Misassigned water peak.

2.4.5: Single Crystal X-ray Data

A single crystal was mounted in paratone-N oil on a plastic loop and X-ray diffraction data were collected at 150(2) K on an Oxford X-Calibur single crystal diffractometer (λ = 0.71073 Å). Data was corrected for absorption using a multi-scan method, and the structure solved by direct methods using SHELXS-97[45] and refined by full-matrix least squares on F2 by SHELXL-2014,[46] interfaced through the program X-Seed.[47] All non-hydrogen atoms were refined anisotropically and hydrogen atoms were included as invariants at geometrically estimated positions. X-ray experimental data is given below. CIF data have been deposited with the Cambridge Crystallographic Data Centre, CCDC reference number CCDC 1538308 (murrayakonine D).

X-Ray experimental data for murrayakonine D (**2.48**): $C_{23}H_{25}NO_2$, F_w 347.44, monoclinic, *I*2/*a*, *a* 20.969(3), *b* 10.2106(14), *c* 17.083(3) Å, *β* 99.423(16)º, Vol. 3608.3(9) Å^3, *Z* = 8, density (calc.) 1.279 Mg/m^3, abs. coefficient 0.081 mm^{-1}, F(000) 1488, crystal size 0.34×0.18×0.11 mm^3, θ range 3.36 to 28.47°, reflns collected 12832, Obs. reflns 1910 [R(int) = 0.1658], GoF^2 0.974, R_1 [I>2σ(I)] 0.0927, wR_2 (all data) 0.3054, Largest diff. peak and hole 0.339 & -0.459 e.Å^{-3}.

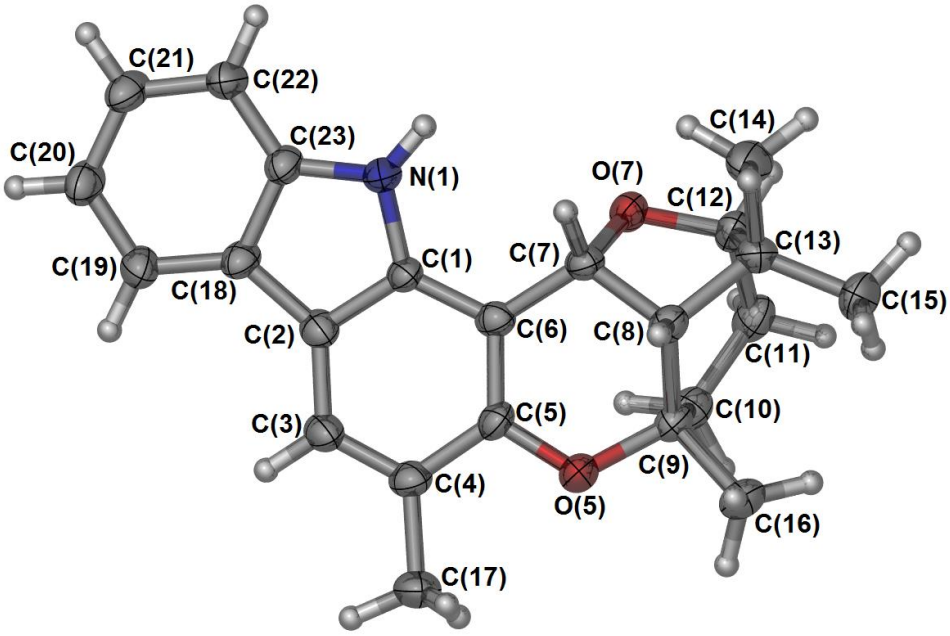

Figure 2.6: A representation of the structure of murrayakonine D (**2.48**) with ellipsoids shown at the 50% probability level (carbon – grey; hydrogen – white; nitrogen – blue; oxygen – red).

2.5 References

[1] Liao, H.-B.; Lei, C.; Gao, L.-X.; Li, J.-Y.; Li, J.; Hou, A.-J. *Org. Lett.* **2015**, *17*, 5040.

[2] Liao, H.-B.; Huang, G.-H.; Yu, M.-H.; Lei, C.; Hou, A.-J. *J. Org. Chem.* **2017**, *82*, 1632.

[3] Iwata, N.; Wang, N.; Yao, X.; Kitanaka, S. *J. Nat. Prod.* **2004**, *67*, 1106.

[4] For a review on the regioselectivity of the Schenck ene reaction: Stratakis, M.; Orfanopoulos, M. *Tetrahedron* **2000**, *56*, 1595.

[5] Zhou, X.-L.; Wu, N.-Z.; Huang, S.; Wang, C.-J.; Wang, Y.-S.; Zhang, Y. *Chin. Pharm. J.* **2012**, *47*, 95.

[6] Iwata, N.; Kitanaka, S. *Chem, Pharm, Bull.* **2011**, *59*, 1409.

[7] Japan, JP57028080 A 1982-02-15

[8] Kashiwada, Y.; Yamazaki, K.; Ikeshiro, Y.; Yamagishi, T.; Fujioka, T. Mihashi, K.; Mizuki, K.; Cosentino, L. M.; Morris-Natschke, S. L.; Lee, K-. H. *Tetrahedron* **2001**, *57*, 1559.

[9] Huang, G.-H.; Lei, C.; Zhu, K.-X.; Li, J.-Y.; Li, J.; Hou, A.-J. *Chin. J. Nat. Med.* **2019**, *17*, 963.

[10] Yang, Y.-X.; Wang, J.-X.; Wang, Q.; Li, H.-L.; Tao, M.; Luo, Q.; Liu, H. *Fitoterapia* **2018**, *127*, 396.

[11] Kitanaka, S.; Iwata, N. *J. Nat. Prod.* **2010**, *73*, 1203.

[12] This work was published during the writing of this thesis: Burchill, L. Day, A. J.; Yahiaoui, O.; George, J. H. *Org. Lett.* **2021**, *23* 578.

[13] Schneider, J. A.; Lee, J.; Naya, T.; Nakanishi, K.; Oba, K.; Uritani, I. *Phytochemistry* **1984**, *23*, 759.

[14] Yang, X.-L.; Qin, C.; Wang, F.; Dong, Z.-J.; Liu, J.-K. *Chem. Biodivers.* **2008**, *5*, 484.

[15] Taura, F.; Iijima, M.; Yamanaka, E; Takahashi, H.; Kenomku, H.; Saeki, H.; Morimoto, S.; Asakawa, Y.; Kurosaki, F.; Morita, H. *Front. Plant Sci.* **2016**, *7*, 1452

[16] Taura, F.; Iijima, M.; Lee, J.-B.; Hashimoto, T.; Asakawa, Y.; Kurosaki, F. *Nat. Prod. Comm.* **2014**, *9*, 1329.

[17] Baldwin, J. E. *J. Chem. Soc., Chem. Comm.* **1976**, 734.

[18] Nalli, Y.; Khajuria, V.; Gupta, S.; Arora, P.; Riaz-Ul-Hassam, S.; Ahmed, Z.; Ali, A. *Org. Biol. Chem.* **2016**, *14*, 3322.

[19] Crombie, L.; Crombie, W. M. L. *Phytochemistry* **1975**, *14*, 213.

[20] Kane, V. V.; Martin, A. R.; Peters, A. R.; Crews, P. *J. Org. Chem.* **1984**, *49*, 1793.

[21] Kurdyumov, A. V.; Hsung, R. P.; Ihlen, K.; Wang, J. *Org. Lett.* **2003**, *5*, 3935.

[22] Kang, Y.; Mei, Y.; Du, Y.; Jin, Z. *Org. Lett.* **2003**, *5*, 4481.

[23] Lee, Y. R.; Wang, X.; Noh, S. K.; Lyoo, W. S. *Syn. Comm.* **2006**, *36*, 3329.

[24] Hu, H.; Harrison, T. J.; Wilson, P. D. *J. Org. Chem.* **2004**, *69*, 3782.

[25] Wu, H.; Hsung, R. P.; Tang, Y. *J. Org. Chem.* **2017**, *82*, 1545.

[26] Day, A. J.; Lam, H. C.; Sumby, C. J.; George, J. H. *Org. Lett.* **2017**, *19*, 2463.

[27] Wu, H.; Hsung, R.P. Tang, Y. *Org. Lett.* **2017**, *19*, 3505.

[28] Burchill, L.; George, J. H. *J. Org. Chem.* **2020**, *85*, 2260.

[29] Jones, A. C.; May, J. A.; Sarpong, R.; Stoltz, B. M. *Angew. Chem. Int. Ed.* **2014**, *53*, 2556.

[30] Shim, J. -G.; Yamamoto, Y. *J. Org. Chem.* **1998**, *63*, 3067.

[31] Suo, J.-J.; Du, J.; Liu, Q. -R.; Chen, D; Ding, C.-H.; Peng, Q. Hou, X. -L. *Org. Lett.* **2017**, *19*, 6658.

[32] Song, X.; Gu, M.; Chen, X.; Xu, L.; Ni, Q. *Asian J. Org. Chem.* **2019**, *8*, 2180.

[33] Wang, Z.; Qi, Q.; Yan, Y.; Hu, Y.; Song, L. *Syn. Comm.* **2016**, *23*, 1932.

[34] Trost, B. M.; Shen, H. C.; Surivet, J.-P. *Angewandte*, **2003**, *42*, 3943.

[35] Trost, B. M.; Shen, H. C.; Surivet, J.-P. *J. Am. Chem. Soc.* **2004**, *126*, 12565.

[36] Hirai, K.; Nozoe, S.; Tsuda, K.; Itaka, Y.; Ishibashi, K.; Shirasaka, M. *Tetrahedron Lett.* **1967**, *23*, 2177.

[37] RajanBabu, T. V.; Nugent, W. A. *J. Am. Chem. Soc.* **1994**, *116*, 986.

[38] Lee, Y. R.; Choi, J. H.; Yoon, S. H. *Tetrahedron Lett.* **2005**, *46*, 7539.

[39] For a review of chromatography using SNIS: Mander, L. N.; Williams, C. M. *Tetrahedron*, **2016**, *72*, 1133.

[40] Hesse, R.; Gruner, K. K.; Kataeva, O.; Schmidt, A. W.; H. -J. Knölker *Chem. Eur. J.* **2013**, *19*, 14098.

[41] Dethe, D. H,; Das, S.; Dherange, B. D.; Mahapatra, S. *Chem. Eur. J.* **2015**, *21*, 8347.

[42] Wen, L.; Tang, L.; Yag, Y.; Zha, Z.; Wang, Z. *Org. Lett.* **2016**, *18*, 1278.

[43] Riveira, M. J.; La-Venia, A.; Mischne, M. P. *J. Org. Chem.* **2016**, *81*, 7977.

[44] Coleman, M. A.; Burchill, L.; Sumby, C. J.; George, J. H. *Org. Lett.* **2019**, *21*, 8776.

[45] G. M. Sheldrick *Acta Cryst.* **1990**, *A46*, 467.

[46] G. M. Sheldrick *Acta Cryst.* **2015**, *C71*, 3.

[47] L. J. Barbour *J. Supramol. Chem.* **2001**, *1*, 189.

Chapter 3: Biomimetic Synthesis of Bruceol and the Discovery and Synthesis of Isobruceol

The work presented in this chapter was the beginning of what became a continued investigation of *Philotheca* coumarin-meroterpenoids: these studies are continued in chapters 4 and 5.

3.1 Introduction

3.1.1: The Isolation of Bruceol (**3.1**)

Bruceol (**3.1**) is a pentacyclic coumarin monomeroterpenoid first isolated from the Western Australian shrub *Philotheca brucei* (formerly *Eriostemon*) in 1963 by Duffield and Jefferies.[1] Its densely complex structure consists of a fused heterocyclic coumarin and a caged "citran" moiety (Figure 3.1). Bruceol (**3.1**) occurs is Nature as the enantiopure (−) isomer. Its absolute configuration was determined almost 20 years after its initial isolation by Ghisalberti and White by single crystal X-ray diffraction (SC-XRD) of chloro- and iodo-acetate derivatives of bruceol at C-2'.[2]

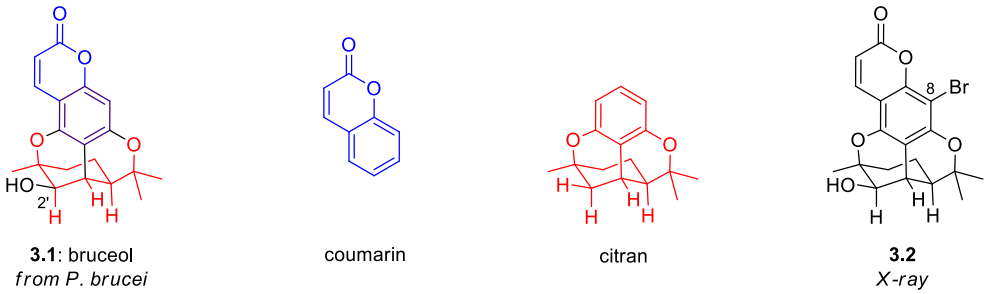

Figure 3.1: The structure of bruceol (**3.1**) and key moieties: coumarin (in blue) and citran (in red). bromo-derivative used for X-ray diffraction **3.2**. Duffield and Jefferies (1963)

The structural determination of bruceol (**3.1**) occurred at an exciting time in chemistry history. What are now considered very low-resolution methods such as I.R. and U.V. spectroscopy had become well established, insightful techniques after the Second World War; and alongside elemental analysis, and chemical degradation – these (mostly) obsolete methods were in their peak in utility and importance to structure determination. New high-resolution techniques NMR and SC-XRD were very much in

their infancy. This was only 20-30 years after Dorothy Crowfoot Hodgkin's pioneering work, using SC-XRD on small molecules such as cholesterol, penicillin, and vitamin B-12;[3] and 7 years after R. B. Woodward declared with great foresight: "Nuclear Magnetic Resonance is even now on the horizon, and we shall be surprised if it does not permit another great step forward".[4] Indeed, John D. Roberts' famous early text on the analysis of ^{1}H NMR of organic molecules was published only two years prior,[5] and this was only 6 years after he and Caltech purchased the first ever commercial NMR machine sold to a university in 1955.[6] With this in mind, Duffield and Jefferies work can be considered somewhat progressive: utilising both NMR and SC-XRD, relying primarily on X-ray of the C-8 bromo-derivative (**3.2**). However, only half of the ^{1}H NMR signals were reported; presumably due to poor resolution of the early 60 MHz machine used, and the inclusion of NMR added little to their structural assignment. Indeed, it was not until 1992 (29 years later) until the full NMR spectrum of what was believed to be bruceol (**3.1**) was reported by Waterman and co-workers.[7]

3.1.2: Proposed Biosynthesis of Bruceol (**3.1**)

Speculation on the mechanism for the biosynthesis of bruceol (**3.1**) has been reported independently in two reviews by Ghisalberti[8] and Trauner[9] respectively (Scheme 3.1). The agreed mechanism involves protobruceol-I (**3.3**), which was co-isolated in *P. brucei*.[10] Stereoselective oxidation of the less hindered face of the chromene olefin would give epoxide **3.4**. The free phenol can push the fragmentation of the epoxide to give the reactive *ortho*-quinone methide (*o*-QM) **3.5** which is poised to undergo an intramolecular hetero-Diels-Alder cycloaddition reaction furnishing the complete bruceol structure **3.1**. The absolute stereochemistry of bruceol is defined by the initial stereocentre in protobruceol-I (**3.3**) (found enantiopure in Nature), and the stereoselective oxidation, which functions as a trigger for this cascade, is presumably enacted by a cytochrome P450 monooxygenase enzyme.

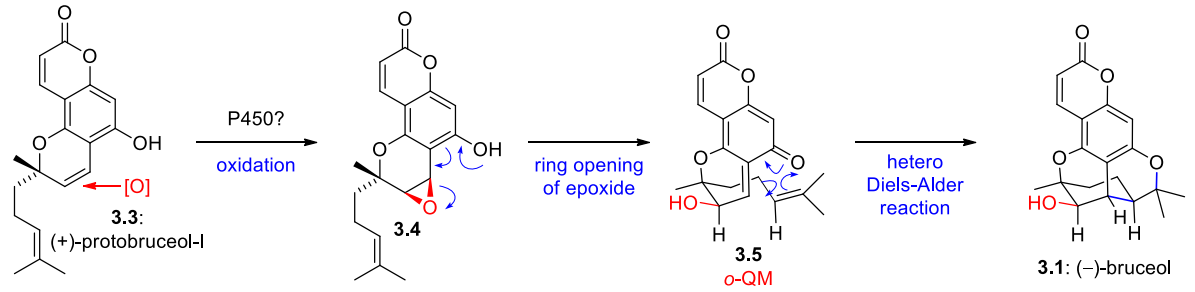

Scheme 3.1: The putative biosynthesis of bruceol (**3.1**). Ghisalberti (1997) and Trauner (2005).

Protobruceol-I (**3.3**) itself is derived from a cinnamic acid pathway (Scheme 3.2), as are the greater majority of coumarins found in *Rutacae*.[11] Starting from the amino acid tyrosine (**3.6**) (itself being formed via the shikimic acid pathway, from sugars), deamination by phenylalanine ammonia lyase (PAL) affords *p*-coumaric acid (**3.7**).[12] Oxidation and glycosylation *ortho* to the cinnamyl group gives **3.8**, and isomerisation to the necessary cis-acid **3.9** allows cyclisation to the coumarin umbelliferone (**3.10**). At this point it is worth noting the C-7 position is oxidised in all coumarins found in *Rutacae* (with very few exceptions).[13,14]

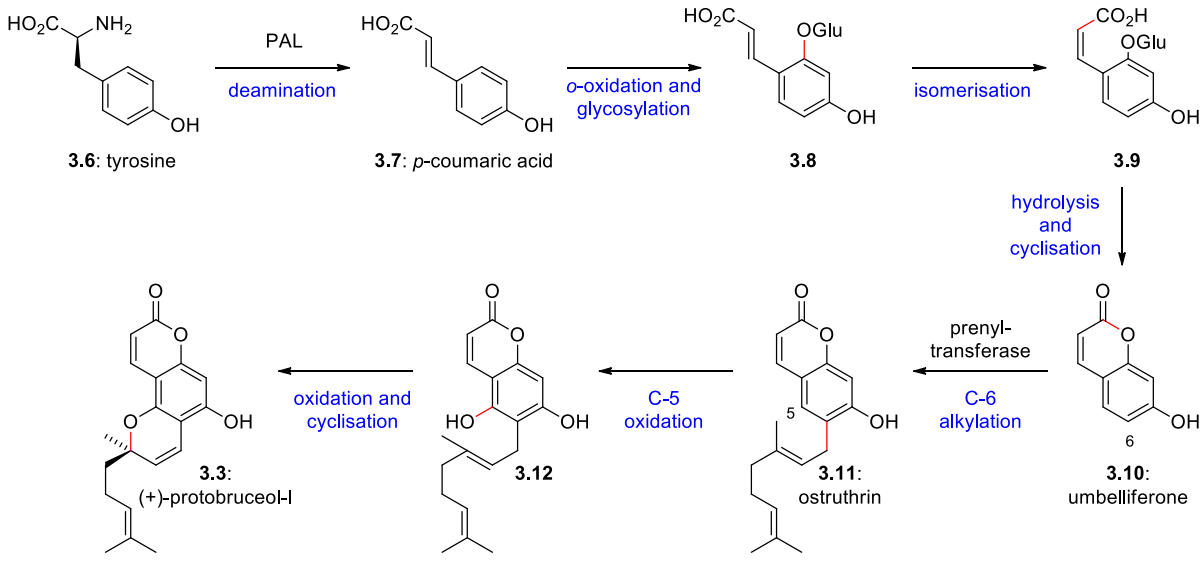

Scheme 3.2: Biosynthesis of protobruceol-I (**3.3**) via a cinnamic acid pathway

Alkylation of the **3.10** with a geranylpyroposphate (GPP) dependant prenyltransferase gives ostruthin (**3.11**) which has been co-isolated in *P. brucei*. Monooxygenation at C-5 gives **3.12**, and finally

oxidation and cyclisation occurs, perhaps by a similar enzyme mediated aerobic process as the cannabichromene in *Cannabis sativa* (discussed in Chapter 2.1.3) to afford the enantiopure protobruceol-I (**3.3**).

3.1.3: Previous Work on "Citran" Containing Compounds

Bruceol (**3.1**) was the first molecule containing the citran moiety found in Nature. However, this scaffold had been produced synthetically (at least unwittingly) 60 years prior to its isolation. The first man-made "citran" (and where the term is derived) was citrylidene malonic acid (**3.17**) – the product of the condensation of citral with malonic acid. Verley reported this one-step reaction occurring in good yield in 1899 (Scheme 3.3)[15]; however, the product was initially misidentified as **3.14**, the simple product of the Knoevenagel condensation. At the same time, Grünhagen made the same compound, but by initial Knoevenagel condensation of diethylmalonate followed by acidification and heating.[16] He, incorrectly, identified the product as the *β,δ*-dilactone **3.15**. The Nobel Prize recipient Richard Kuhn and student Hoffer entered **3.16** as a more plausible structure;[17] however, it wasn't until 1960 that Crombie correctly elucidated its true structure **3.17**.[18]

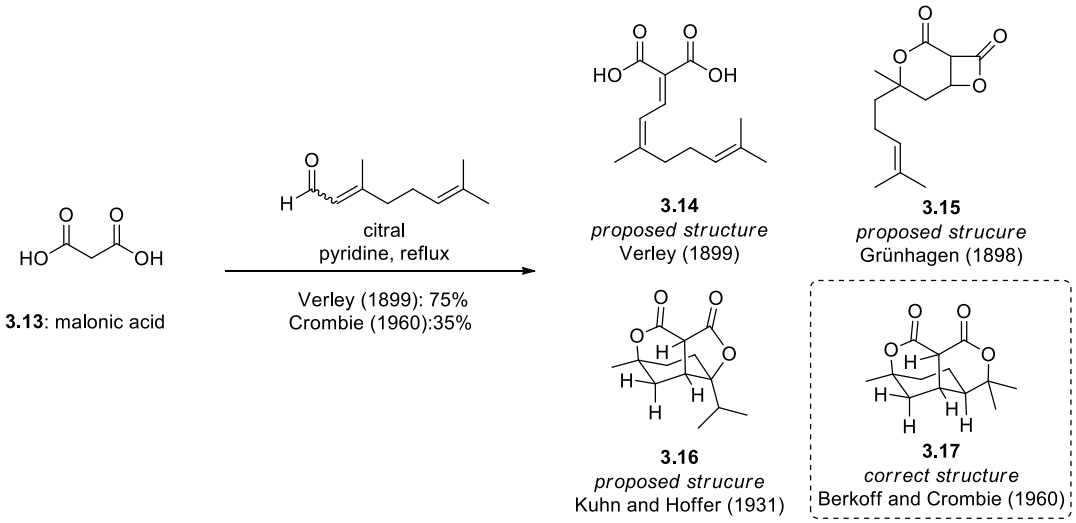

Scheme 3.3: One-pot synthesis of citrylidene malonic acid, with various previously assigned structures (**3.14** – **3.17**) . Verley (1899)

It is worth noting structural elucidation was much more difficult in the early 20th century. As John D. Roberts bluntly stated, "[before] the 1940s, the main laboratory instrument was the thermometer".[19] As citrylidene malonic acid showed no significant absorption in the UV spectrum, and did not form acetone upon ozonolysis, Crombie could quickly rule out structures **3.14** and **3.15**. To determine its true structure, an interesting combination of IR spectroscopy and degradation/derivatisation studies were employed. Again, this was before NMR was routine in synthetic chemistry laboratories.

The basic approach was to decarboxylate **3.17** giving isomeric compounds he called hydroxylactone A (**3.18**) and B (**3.19**). A key factor in his assignment was both products contain δ-lactones (from IR analysis). Formal dehydration of hydroxylactone A (**3.18**) gave isomeric products **3.20** and **3.21** which release formaldehyde and acetone respectively upon ozonolysis, suggesting the isopropyl group and ruling out Kuhn and Hoffers' structure **3.16**. Analysis of the phenylhydrazone derivatives of **3.22** and **3.23** both show the δ-lactone ring was untouched. Similar degradation and analysis of hydroxylactone B (**3.19**) allowed Crombie to successfully deduce the structure of **3.17** (Scheme 3.4).

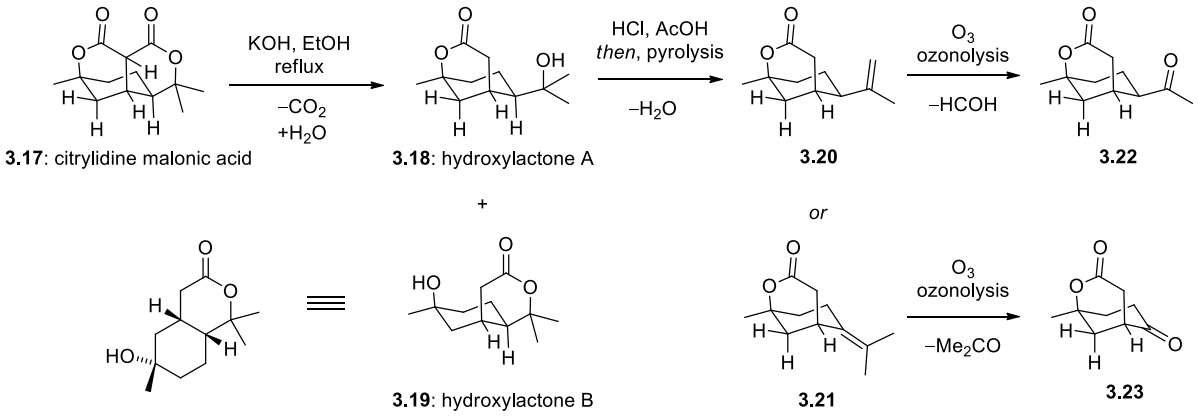

Scheme 3.4: Degradation studies used for the structural elucidation of **3.17**. Crombie (1960)

With the revised structure in mind, the name "citrylidene malonic acid" has become something of a misnomer, as **3.17** contains neither citrylidene nor malonic acid moieties (but derivatives thereof).

In this work Crombie also proposed a plausible mechanism for the formation of **3.17** (Scheme 3.5).

Initial Knoevenagel condensation of malonic acid (**3.13**) with citral gives Verley's structure **3.14**. The reaction continues by oxa-6π-electrocyclisation to afford lactone **3.24**, and further cyclisation by a stepwise hetero-Diels-Alder reaction through carbocation **3.24** finally gives the caged dilactone citylidene malonic acid (**3.17**).

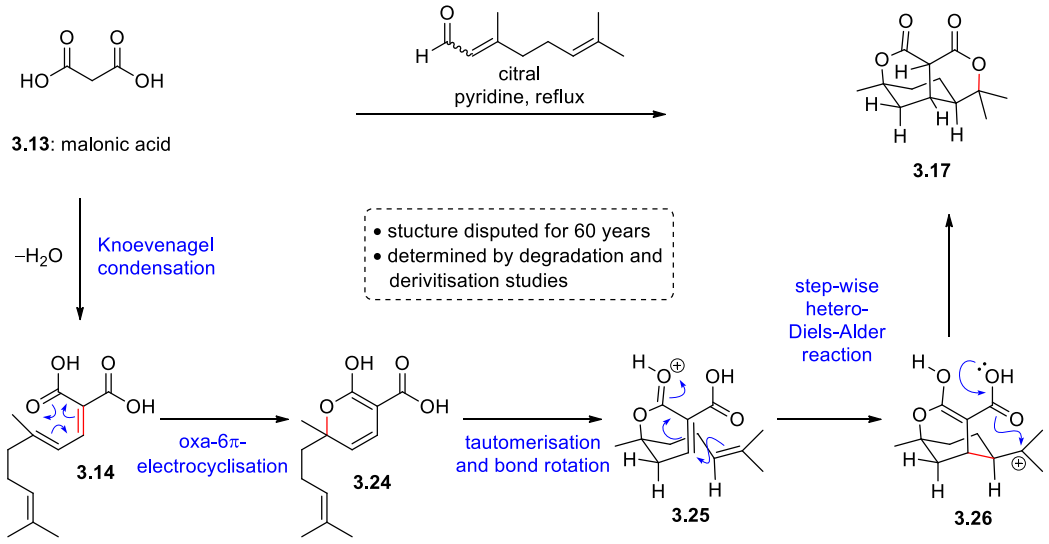

Scheme 3.5: Proposed mechanism for the formation of **3.17**. Crombie (1960)

Crombie, seeing potential in this very rapid generation of the caged polycylclic scaffold (which he coined "citran"), sought to apply this type of cascade reaction in the total synthesis of a natural product. Sometime after the report of bruceol (**3.1**) in 1963 Crombie had learnt of an analogue of bruceol lacking the hydroxyl group: "deoxybruceol" (**3.27**) coisolated with **3.1** (Figure 3.2).[20]

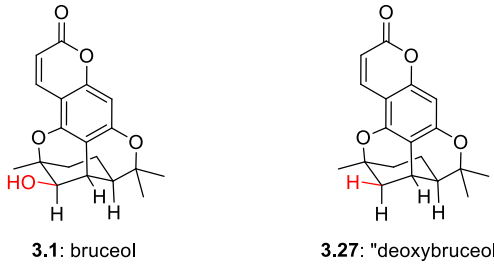

Figure 3.2: Comparison of bruceol (**3.1**) and deoxybruceol (**3.27**).

In 1968 Crombie completed an astonishingly short biomimetic synthesis of "deoxybruceol".[21] By refluxing 5,7-dihydroxycoumarin (**3.29**), which is made in a single step from phloroglucinol (**3.28**),[22]

with citral in the presence of pyridine; Crombie and Ponsford synthesised what they believed to be deoxybruceol **3.27** (Scheme 3.6).

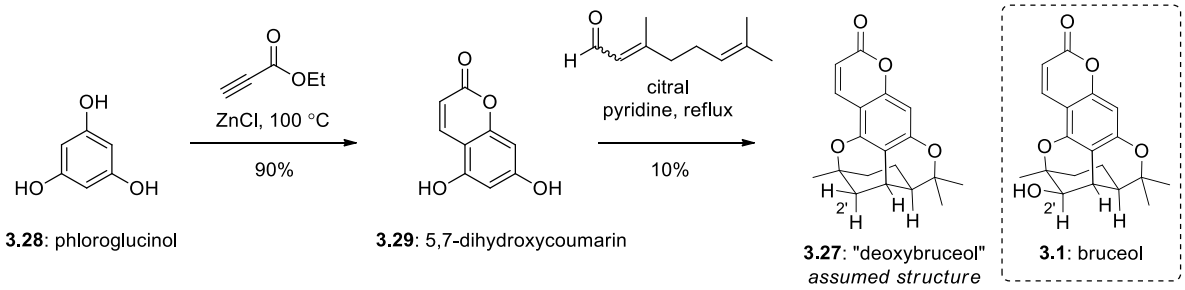

Scheme 3.6: Biomimetic total synthesis of "deoxybruceol". Crombie (1968)

Later studies involving X-ray analysis showed that what was actually synthesised was the isomer **3.31** (Figure 3.3).[23] Crombie and others have continued to refer to the reassigned structure as "deoxybruceol" despite the name being misleading. This becomes increasingly confusing as the deoxygenated bruceol structure **3.27** also continued to be referred to as "deoxybruceol". To rectify this, we coined (and strongly recommend) using the name "deoxyisobruceol" for the natural product **3.31**, and suggest using the name "deoxybruceol" for **3.27**.

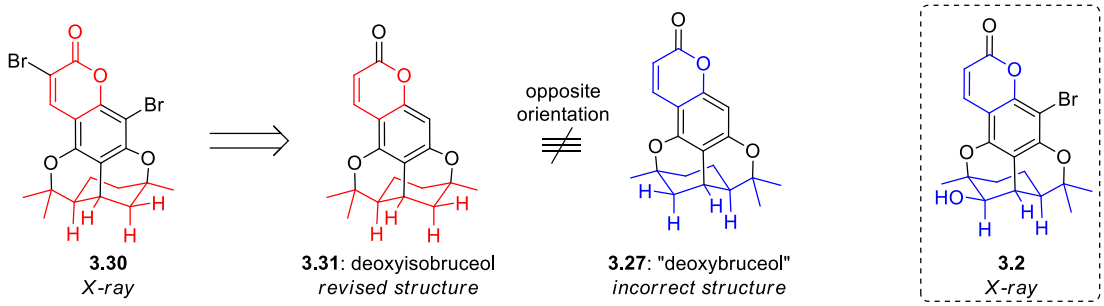

Figure 3.3: X-ray studies of **3.30** showing Crombie's deoxyisobruceol contains the opposite configuration of the citran to bruceol (**3.1**). Crombie (1976)

During his investigations, Crombie found stopping the cascade reaction after 12 hours the chromenes could be isolated. Interestingly, out of three possible chromene products that could form from coumarin **3.29** only the angular chromenes protobruceol-I (**3.3**) and **3.32** formed; the linear chromene (**3.33**) which goes to form the observed product deoxyisobruceol (**3.27**) is not isolated (Scheme 3.7).

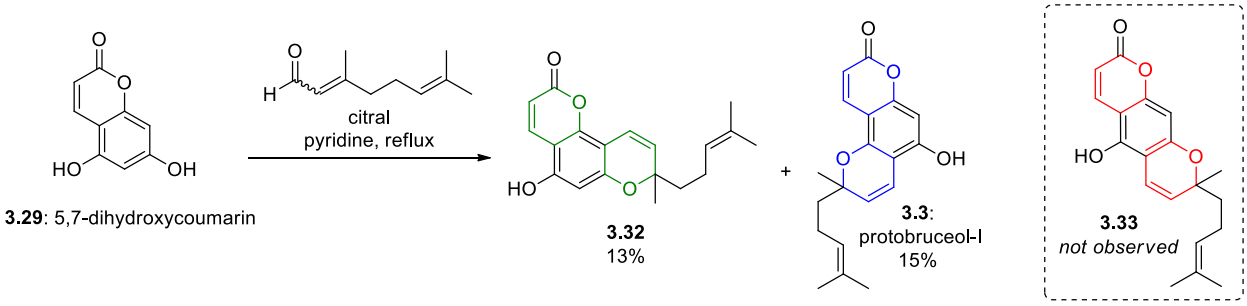

Scheme 3.7 Chromenylation of 5,7-dihydroxycoumarin (**3.29**). Crombie (1976)

However, by resubjecting the purified protobruceol-I (**3.3**) to refluxing pyridine for a further 4 days deoxyisobruceol (**3.31**) was afforded, and as the major product compared to **3.27** (Scheme 3.8). The ratio of products was not reported.

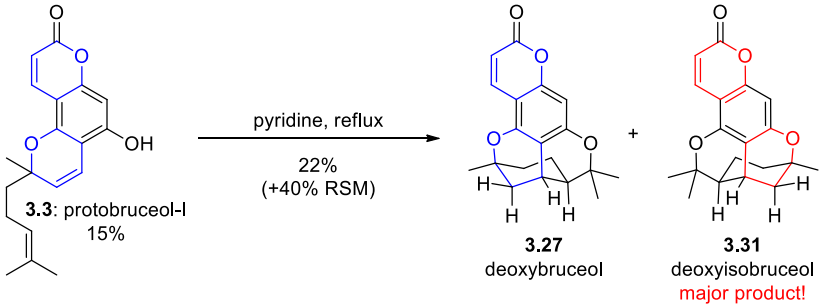

Scheme 3.8: Product of resubjecting **3.3** to cascade conditions. Crombie (1976)

Crombie provided a simple explanation for this isomerisation which is an elegant example of the Curtin-Hammett principle (Scheme 3.9).[24] Starting from protobruceol-I (**3.3**), the minor product, deoxybruceol (**3.27**) is formed by first tautomerisation to *o*-QM **3.34**, followed by a [4+2] cycloaddition. **3.34** is a high energy intermediate for two reasons: 1) it contains an *o*-QM motif, and more critically 2) the lactone ring of the coumarin is no longer aromatic. Alternatively, protobruceol-I (**3.3**) can revert to *o*-QM **3.35** by a retro oxa-6π-electrocyclisation, and by tautomerisation to **3.36**, the required chromene **3.33** is formed after re-cyclisation. Now the barrier between the linear chromene **3.33** and deoxyisobruceol (**3.31**) is smaller than that of protobruceol-I (**3.3**) and deoxybruceol (**3.27**) as the intermediate *o*-QM **3.34**, which we can approximate to be similar in

energy to the transition state (Hammond's postulate) retains aromaticity in the lactone ring. This is why deoxyisobruceol is the major product of the reaction. This also explains why protobruceol-I (**3.3**) is formed in the chromenylation reaction and not **3.33**. *o*-QM **3.35** is lower in energy than **3.36** so the equilibrium will favour **3.3**.

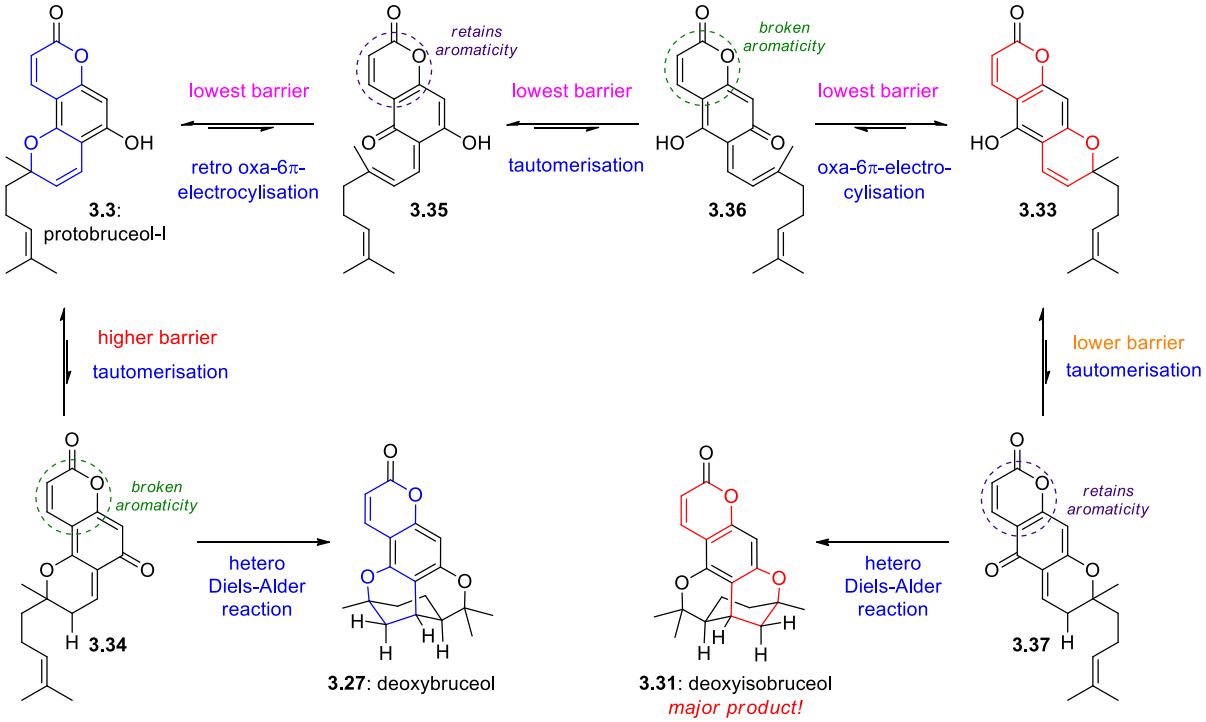

Scheme 3.9: Mechanistic explanation for the formation of deoxyisobruceol (**3.31**). Crombie (1976)

Beyond the bruceol-coumarin system, Crombie showed recurring interest with citrans in his on-going investigations of chromane natural products. In addition, more citran natural products have been discovered, and synthesised by other groups since his initial studies.

In each case, subsequent syntheses of citran natural products have been largely derivative of Crombie's work. In Figure 3.4 several of these natural products are shown. The chalcone-citrans rubraine (**3.39**)[25], sumadain (**3.40**) and respective isomers **3.41** and **3.42** from *Alpinia katsumadai*[26] share a similar story to the selectivity of deoxyisobruceol (**3.31**) and isomer deoxybruceol (**3.27**).

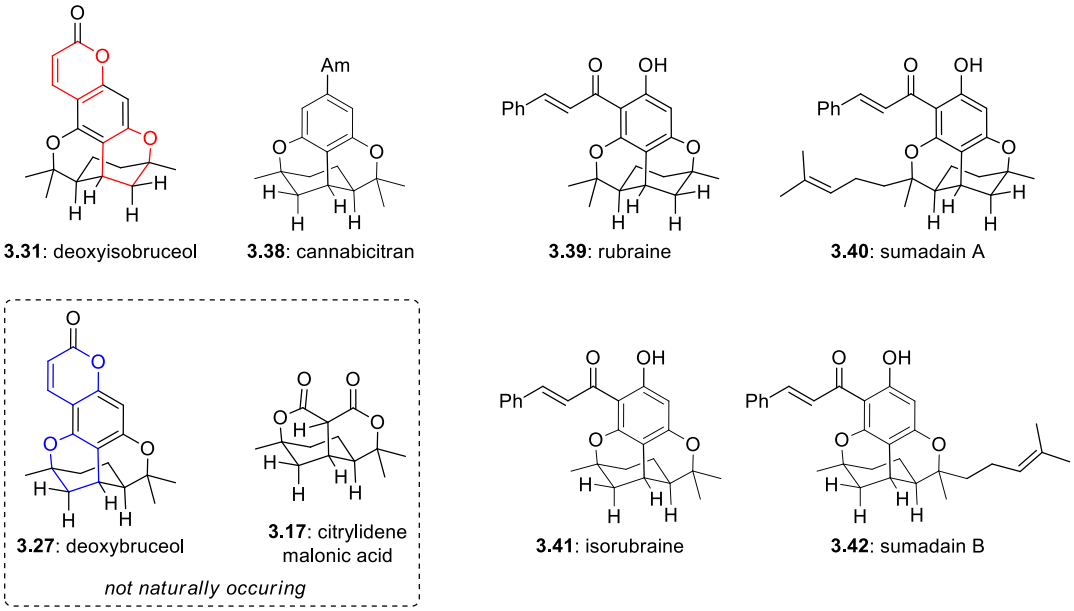

Figure 3.4: Several citran containing natural products and synthetic compounds.

The first chalcone-citran synthesis was Kane and Grayeck's two step synthesis of rubraine (**3.39**) (Scheme 3.10).[27] Starting from acetophenone **3.43** the usual conditions, citral in pyridine, gave the desired citran **3.44** in good yield and was completely regioselective. The structure corresponding to isorubraine (**3.45**) (bruceol-type) was not observed. The acetophenone was successfully converted to the chalcone moiety by simple aldol condensation with benzaldehyde in excellent yield, completing the synthesis of **3.39**.

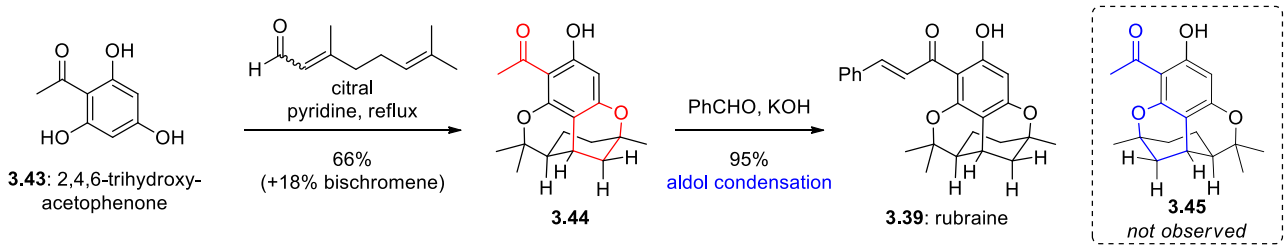

Scheme 3.10: First total synthesis of rubraine (**3.39**). Kane and Grayeck (1971)

More recently, this synthesis was revisited by Lee and co-workers.[28] Lee's interest laid primarily in demonstrating the use of EDDA in chromenylation reactions, and/or subsequent citran formation. For

rubraine (**3.39**) a one-pot method was employed (Figure 3.11a). From the chalcone **3.46**, condensation and cyclisation with citral in the presence of EDDA gave the desired **3.39** albeit in modest yield.

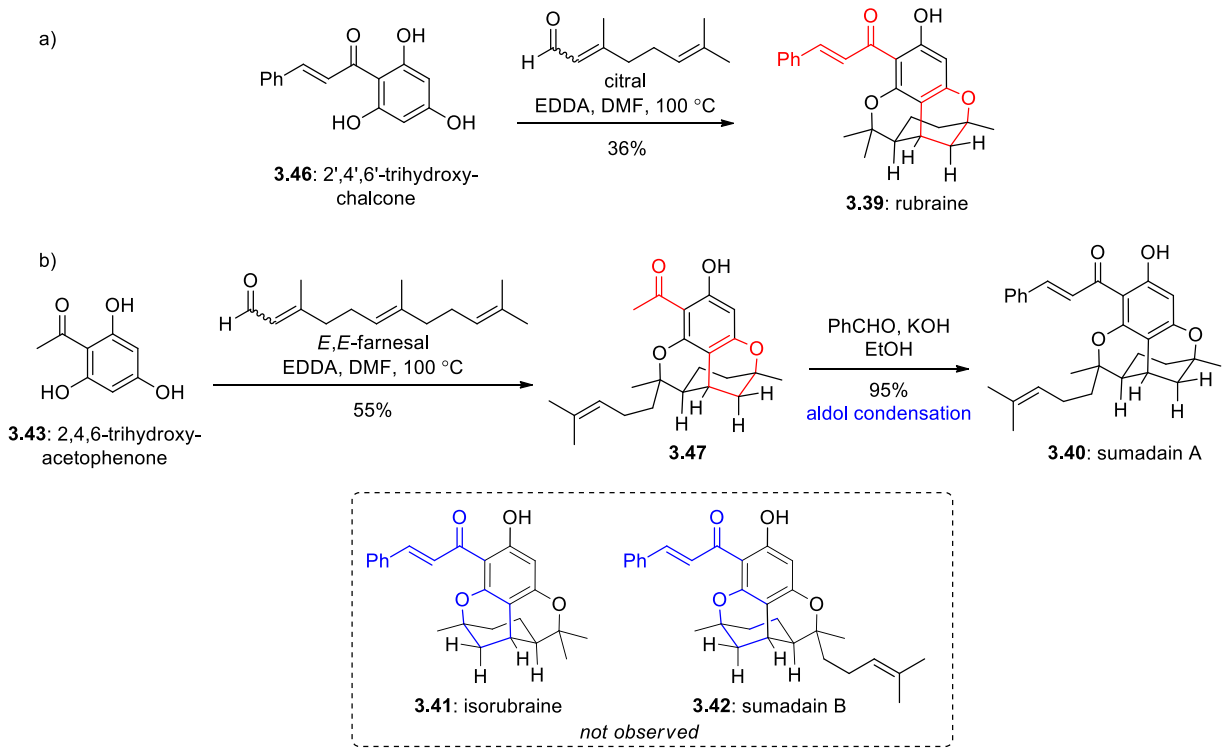

Figure 3.11: a) One-pot synthesis of rubraine (**3.39**) b) two-step synthesis of sumadain A (**3.40**). Lee (2009)

For the analogous sesquimerotepenoid sumadain B (**3.40**) Lee returned to a two-step protocol (Figure 3.11b). The cascade of acetophenone **3.43** with *E,E*-farnesal afforded the citran **3.47**, and subsequent aldol condensation with benzaldehyde afforded sumadain A (**3.40**). In both cases the citran of the opposite orientation to bruceol (**3.1**) is formed exclusively, with the isomers isorubraine (**3.41**) and sumadain B (**3.42**) not observed.

Lee also offered a modification of Crombie's total synthesis of deoxyisobruceol (**3.31**)[29]. Using this EDDA the cascade reaction proceeded in an improved 55% (Scheme 3.12).

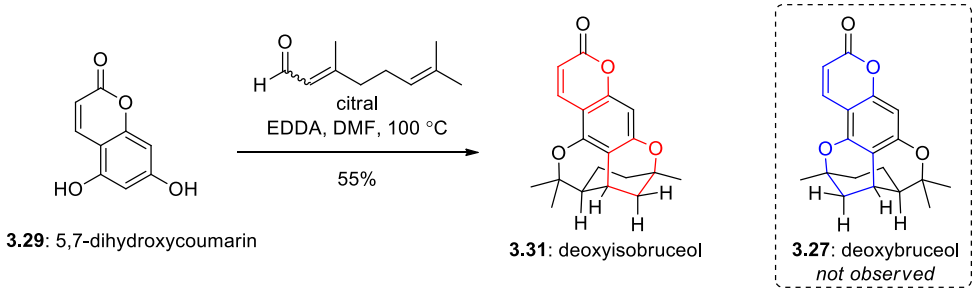

Scheme 3.12: Improved conditions for the synthesis of deoxyisobruceol (**3.31**). Lee (2007)

3.1.4 Chemoselective Oxidations of Styrenes

Returning to the problem at hand, a biomimetic synthesis of bruceol (**3.1**) contains a serious chemoselectivity problem from the outset. Protobruceol-I (**3.3**) contains three potentially reactive olefins (Figure 3.5). The first olefin (green) can mostly be ignored. It is the most stable as it is part of an aromatic ring, and further, it is electron poor: distinguishing it chemically from the other olefins. The second olefin (red) is very electron rich styrene, with electron density donated from the highly oxygenated aromatic ring. Desired oxidation at this position will give the key epoxide **3.4**, triggering the cyclisation cascade. The last olefin (blue) is also election rich. It is a trisubstituted alkene. This will pose a serious threat to the synthesis of bruceol (**3.1**) and a way to differentiate the two alkenes must be found. Oxidation of this "tail" olefin will give the epoxide **3.49**, analogous to the epoxides utilised in the rhodonoids synthesis (Chapter 2).

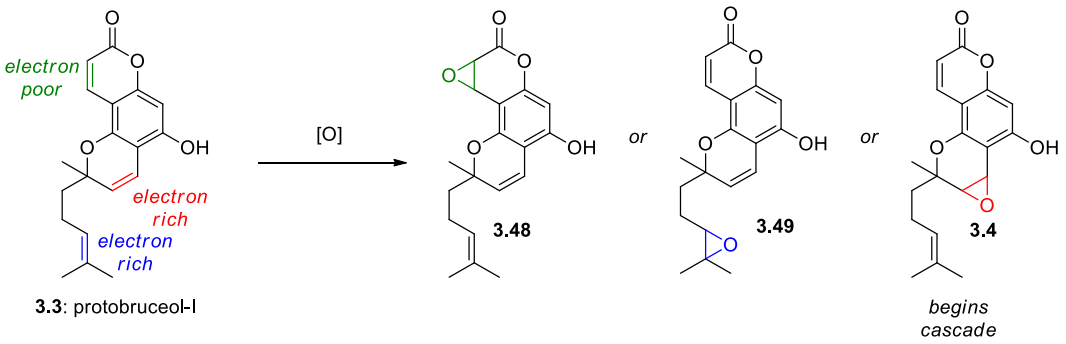

Figure 3.5: Reactive olefins in protobruceol-I (**3.3**).

In itself, oxidation of the chromene olefin is trivial. For example, Lee and co-workers were able to epoxidise the pyranocoumarin hemimeroterpenoid seselin (**3.50**) using the usual electrophilic epoxidation reagent *m*-CPBA (Scheme 3.13).[30] In this simpler system the coumarin is untouched and the epoxide **3.51** can be isolated. The epoxide is extremely susceptible to nucleophilic attack: treatment with a variety of alcohols and thiols gave the scaffold **3.52** in good to excellent yields.

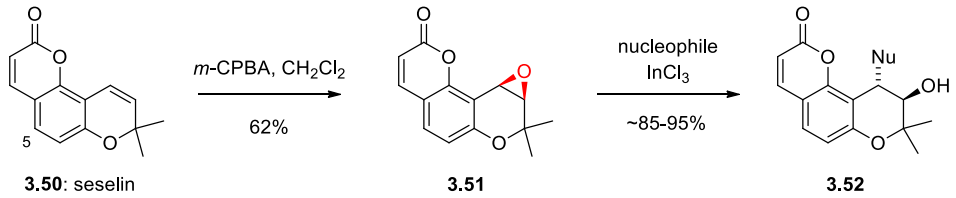

Scheme 3.13: Epoxidation of seselin (**3.50**). Lee (2005)

Palladium (II) has also been used to oxidise chromenes by the Tsuji-Wacker reaction. This is exemplified in Knölker's total synthesis of the carbazole euchestrifoline (**3.55**). (Scheme 3.14)[31] Chromene **3.53** is oxidised to the chromanone **3.54** using classic Tsuji-Wacker conditions, catalytic $Pd(OAc)_2$ and $Cu(OAc)_2$ open to air. The reaction does not stop here as an intramolecular Heck reaction is also possible, furnishing the carbazole moiety of **3.55**.

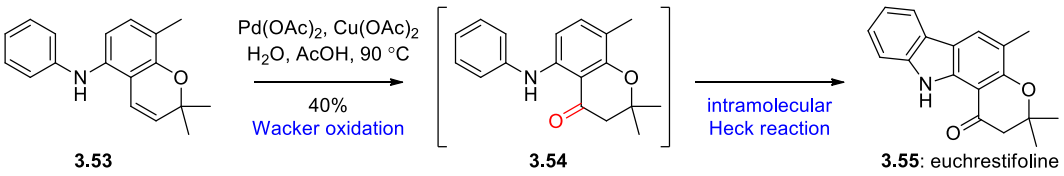

Scheme 3.14: Wacker oxidation in the synthesis of euchrestifoline (**3.55**). Knölker (2008)

Another possible oxidation at this position was shown by Magiatis and co-workers while exploring the antibacterial effects of pyranocoumarins (Scheme 3.15).[32] Upjohn oxidation conditions (using catalytic OsO_4 and stoichiometric NMO) gave the *cis*-diol **3.56** from 5-methoxyseselin (**3.57**).

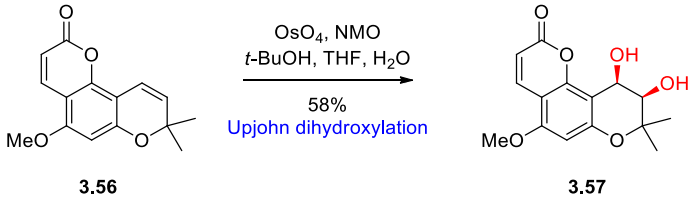

Scheme 3.15: Uphohn oxidation of 5-methoxyseselin (**3.56**). Magiatis (2005)

The three examples shown here of oxidation at the chromene olefin do not have competing electron rich alkenes as in the bruceol system. In fact, during our literature search there was only one oxidant which has shown to effectively make this distinction. Jacobsen's chiral Mn(salen) catalyst (**3.62**) has shown selectivity in similar systems: this is best shown in his asymmetric synthesis of (+)-teretifolione B (**3.61**) (Scheme 3.16).[33] In this synthesis, Jacobsen used his catalyst to enact chiral resolution. The chromene **3.58** was subjected to the standard reaction conditions and proceeded to about ~80% conversion before quenching. This was essential as **3.62** shows poor substrate selectivity (but good catalyst selectivity), **3.58** was enriched to 91% e.e. (95.5:4.5 e.r.) of the desired enantiomer. The resolution works because epoxidation on the same face as the methyl group (to form **3.59**) is slightly faster than epoxidation on the same face as the homoprenyl group (to form **3.60**).

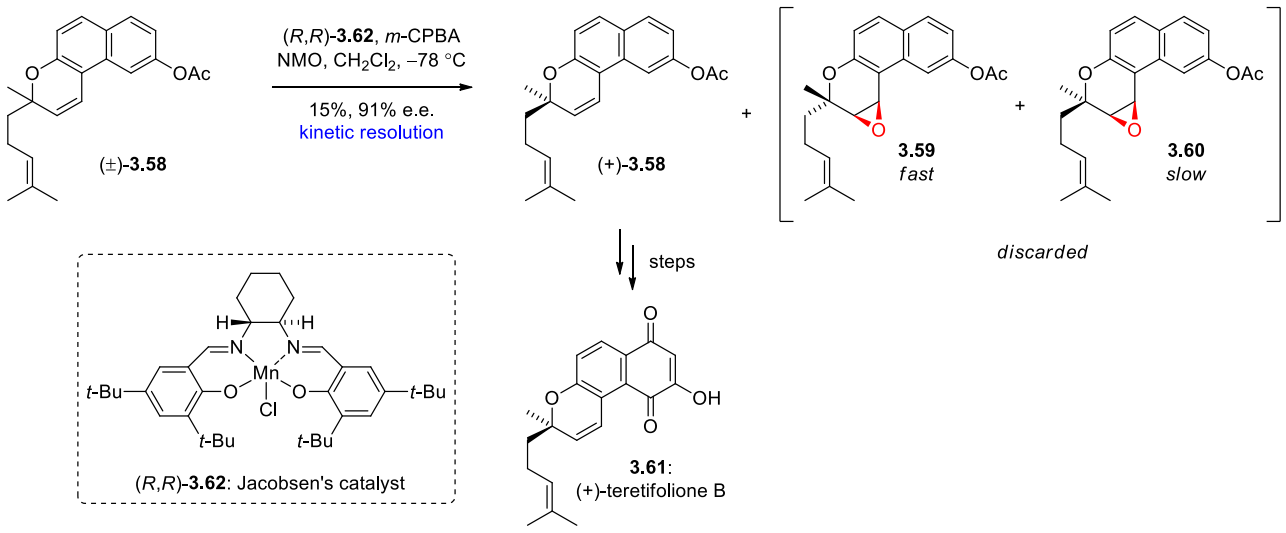

Scheme 3.16: Asymmetric synthesis of (+)-teretifolione B (**3.61**). Jacobsen (1995)

Jacobsen's catalyst (**3.62**) is a pre-catalyst. In the reaction, the stable Mn(III) complex is temporarily oxidised to Mn(V) (**3.63**) by a stoichiometric oxidant: typically *m*-CPBA in anhydrous conditions, or NaOCl in hydrolytic conditions.[34] Although exact details of the mechanism are not completely understood, the explanation for enantioselectivity is simply that the bulky chiral salen ligand restricts the approach of the substrate such that one prochiral face of the olefin is favoured over the other. The active catalyst **3.63** has been likened to iron-porphyrin complexes that exist in Nature, such as those present in cytochrome P450 enzymes. A fortunate result of this sterically encumbered complex (**3.63**) for us is that *cis*-olefins are preferred substrates. This is why Jacobsen did not observe oxidation at the "tail" alkene in his resolution of the chromene **3.58**.

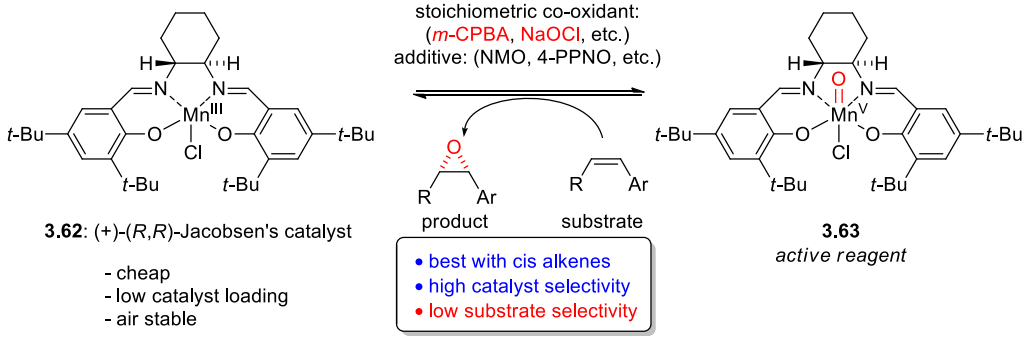

Scheme 3.17: Mechanism of the Jacobsen-Katsuki oxidation.

In our synthetic plan, Jacobsen-Katsuki oxidation looked the most promising and had the added bonus of being asymmetric, suggesting a late stage enantio-divergent process could be possible. Although the epoxide was discarded in the previous example, high enantioselectivity has been shown in hemiterpene chromenes (Scheme 3.18).[35] Here Jacobsen uses a slightly different TIPS catalyst (**3.66**) than the usual *t*-butyl catalyst **3.62** which is now commercially available. The TIPS catalyst has been shown to have superior difference in relative rate constants when used for kinetic resolution (for systems similar to Scheme 3.16).[33] For the simple chromene substrate **3.64**, epoxidation occurs to give **3.65** in great yield with excellent enantioselectivity.

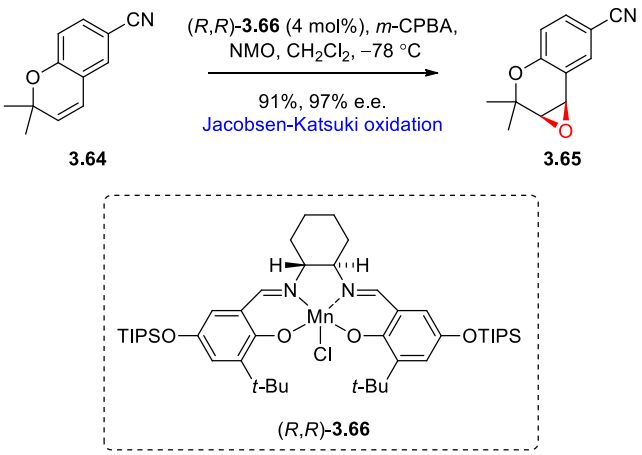

Scheme 3.18: Highly enantioselective epoxidation of **3.64**. Jacobsen (1995)

The selectivity of the catalyst is highly predictable for styrenes (Figure 3.19). To synthesise (−)-bruceol (**3.1**) an *R,R*, version of the catalyst **3.62** is needed.

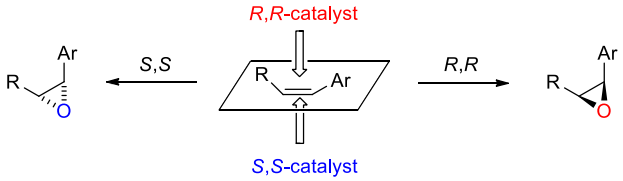

Figure 3.6: Model for the enantioselectivity of Jacobsen-Katsuki epoxidation.

3.2 Results and Discussion

3.2.1: Orcinol Model System

Initial attempts of the epoxidation cascade began on the slightly simpler orcinol chromene **3.67** which was readily accessible to us: this was immediately after completing work on the rhodonoids (Chapter 2).

Subjecting **3.67** to Jacobsen's standard epoxidation conditions (10 mol% catalyst, 1.5 equiv. *m*-CPBA, 5 equiv. NMO) gave promising results, affording the bruceol analogue **3.70** in 23% yield and good (92:8 e.r.) enantioselectivity (Scheme 3.19). The epimer **3.73** arises from the opposite

enantiomer of chromene **3.67**, as we begin with a racemate. Enantioselective epoxidation of the racemic **3.67** gives diastereomeric epoxides **3.68** and **3.71**. These open to *o*-QMs **3.69** and **3.72** which in turn furnish the citrans **3.70** and **3.73** by hetero-Diels-Alder cycloaddition. While the relative stereochemistry differs only at the C-2' position, each of the other stereocenters differ in absolute configuration, making them pseudo-enantiomers. These compounds are oxygenated derivatives of ranhuadujuanine B (**3.74**).

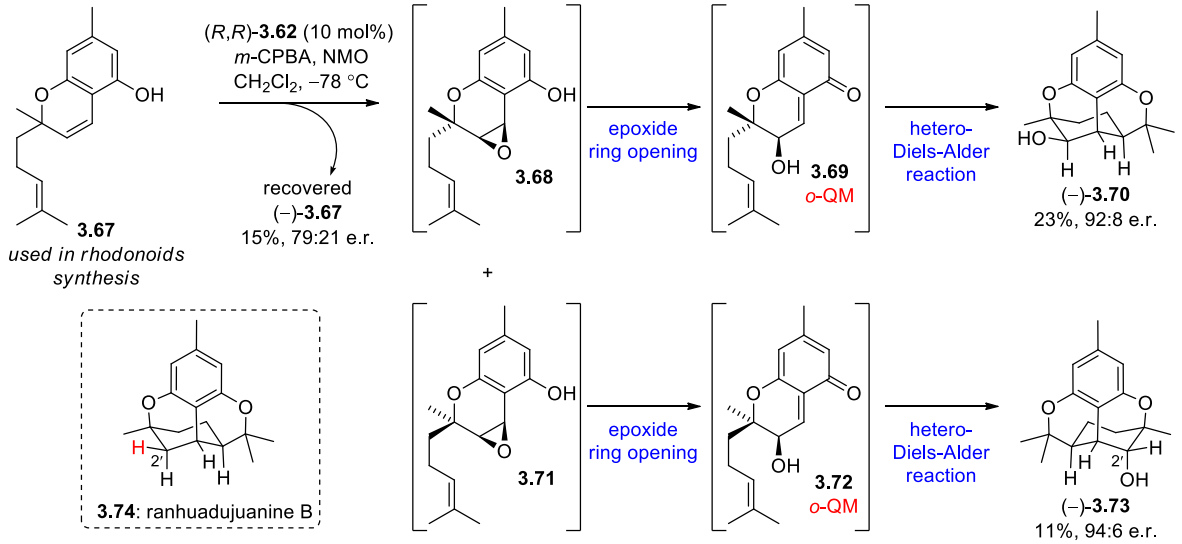

Scheme 3.19: Model system for the synthesis of bruceol (**3.1**).

This experiment was repeated using the opposite catalyst (*S*,*S*)-**3.62** which gave very similar results; differing only by the absolute stereochemistry of the three products (Scheme 3.20). This absolute configuration was predicted by the generalised trends of Jacobsen epoxidation, (*vide supra*). The modest enrichment of the recovered **3.67** (77:23 e.r.) demonstrates the low substrate selectivity of the catalyst.

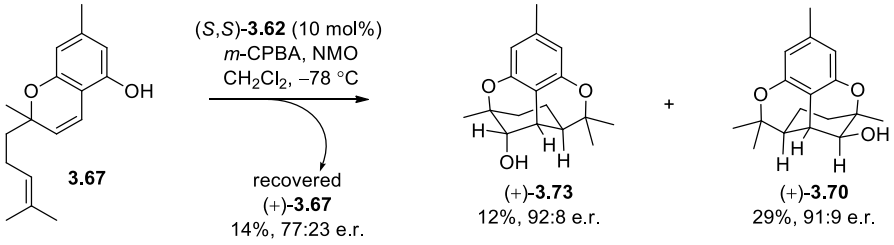

Scheme 3.20: Model system for the synthesis of *ent*-bruceol ((+)-**3.1**).

A problem with the epoxidation cascade reaction was it would never go to completion. Elongated reaction time, increased equivalents of *m*-CPBA, or the catalyst (**3.62**) gave a reduced yield, and using a 50:50 mixture of (*R*,*R*)- and (*S*,*S*)-**3.62** in the hope of having a racemic synthesis with improved ratio of **3.70** to enantiomer **3.73** only resulted in loss of enantioselectivity. A practical issue was that only one chiral HPLC columns was available to us for analysing e.r. and this was poorly suited for these compounds. Only the most polar compound (**3.70**) could be analysed in house; the remainder, **3.67** and **3.73** (as well as several other compounds from this project) were sent to Monash University in Victoria where Adam Ametovski from the Lupton group performed the HPLC analysis.

Other reaction conditions were screened (Scheme 3.21). As shown in Chapter 2, oxidation with *m*-CPBA occurred exclusively at the tail olefin, as does OsO_4/NMO (Upjohn conditions). Whilst oxidative dearomatisation using $PhI(OAc)_2$ led only to decomposition.

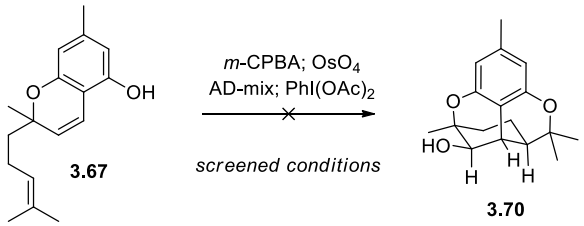

Scheme 3.21: Failed conditions for the bruceol model system (**3.70**)

3.2.2: The Synthesis of Bruceol (**3.1**)

With a successful model study completed, we embarked on the asymmetric synthesis of bruceol (**3.1**). Preparation of our key precursor protobruceol-I (**3.3**) would be simple, following literature methods.

The synthesis of the coumarin (**3.29**) by combination of phloroglucinol (**3.28**) and ethyl propiolate in the presence of $ZnCl_2$ (Scheme 3.22) went smoothly.[22] Early on, an alternative procedure which differed only in using 1,4-dioxane as reaction solvent, and a modified purification procedure was

considered.[36] This was primarily due to mechanical issues with running neat reaction (uneven heating, mixing, glassware cracking, product caking/burning etc.). However, after some practice, the neat method showed clear superiority in both yield and ease of operation. The reaction was scaled up to 50 g with good yield; however, as the reaction is highly exothermic care must be taken to prevent thermal runaway. Anecdotally, a summer placement student performing this reaction once neglected to remove the heat source after the exothermic phase began resulting in a small explosion!

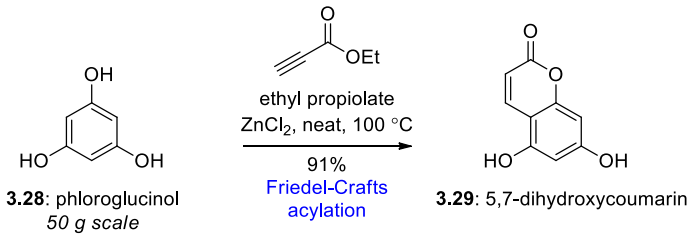

Scheme 3.22: Preparation of 5,7-dihydroxycoumarin (**3.29**).

The chromenylation followed Crombie's method, only with a modified purification (Scheme 3.23). The problem with this reaction is the chromene products protobruceol-I (**3.3**) and **3.32** can both further react in these conditions. When forced closer to completion various undesired by products are observed. This would eventually decrease the total yield of chromenes, but also sacrifice purity as the purification becomes more difficult. On the other hand, stopping the reaction early also causes issues in the purification as the starting material (**3.29**) is not soluble in solvents typically used for work-up, or flash column chromatography. The pragmatic solution found was to use shorter reaction time and omit a conventional work up and instead subject the crude reaction mixture to a fast-eluting column directly; the aim being to remove most **3.29**, pyridine, citral, and bischromene **3.75**. The result would be quick access to a mixture of mostly chromenes **3.3** and **3.32** which could be separated by a second more careful column.

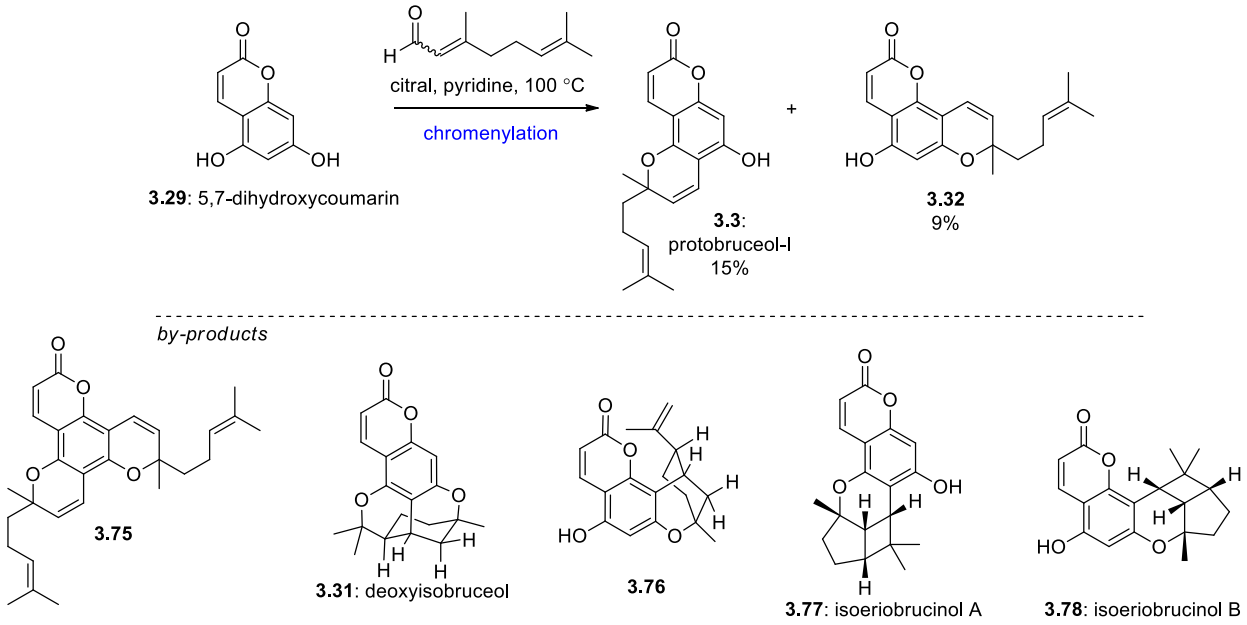

Scheme 3.23: Chromenylation of coumarin **3.29** and observed by-products.

Alternative chromenylation conditions were considered ($Ca(OH)_2$/EtOH; $PhB(OH)_2$/PhMe; EDDA/PhMe etc.) but none showed any immediate advantage to Crombie's conditions. Many suffered from the poor solubility of the starting material. As our sequence was so short, and we had a practical method of preparing protobruceol-I (**3.3**) already we saw little value in further optimising this reaction.

With protobruceol-I (**3.3**) we tried our conditions from the model study (Scheme 3.19). Again, indiscriminate epoxidation of both enantiomers of protobruceol-I (**3.3**) gives a mixture of diastereomeric epoxides **3.4** and **3.79**, which open to reveal *o*-QMs **3.5** and **3.80** furnishing the natural product bruceol (**3.1**) and the C-2' epimer **3.81** by intramolecular hetero-Diels-Alder cycloaddition (Scheme 3.24). Again, this reaction was very stubborn and could not be pushed beyond ~50% completion. Despite the poor yield (11%), good enantiopurity (e.r. = 98:2) was achieved. The reaction was also performed with (*S*,*S*)-**3.62** catalyst to give the unnatural (+)-bruceol (**3.1**).

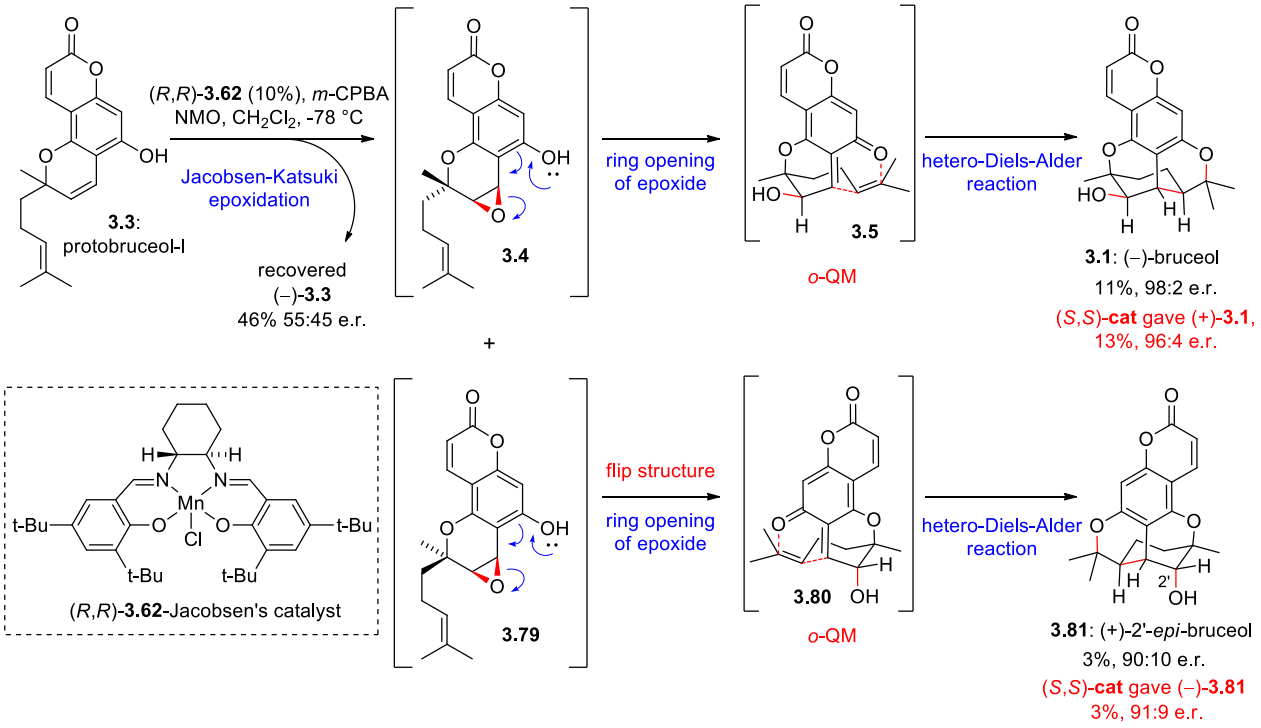

Scheme 3.24: Synthesis of bruceol (**3.1**) by asymmetric epoxidation cascade.

The yield of this reaction was noticeably lower than that of the model system. These losses are associated with the stunted action of the catalyst. In an attempt to mitigate this, we explored other variants of manganese-salen catalysts.

Firstly, the TIPS catalyst (**3.66**) seen previously in Scheme 3.18 was synthesised in 4 steps[37] (Scheme 3.25). We hoped that this version might give better results. The preparation went smoothly, silylation of *t*-butyl hydroquinone (**3.82**) with TIPSCl gave **3.83** quantitatively. Formylation to benzaldehyde **3.84** and Schiff base formation with *trans*-diaminocyclohexane gave the salen ligand **3.85**. Finally, metalation and aerobic oxidation completed catalyst **3.66**. Both (*R*,*R*)- and (*S*,*S*)-**3.66** catalysts were prepared using this method.

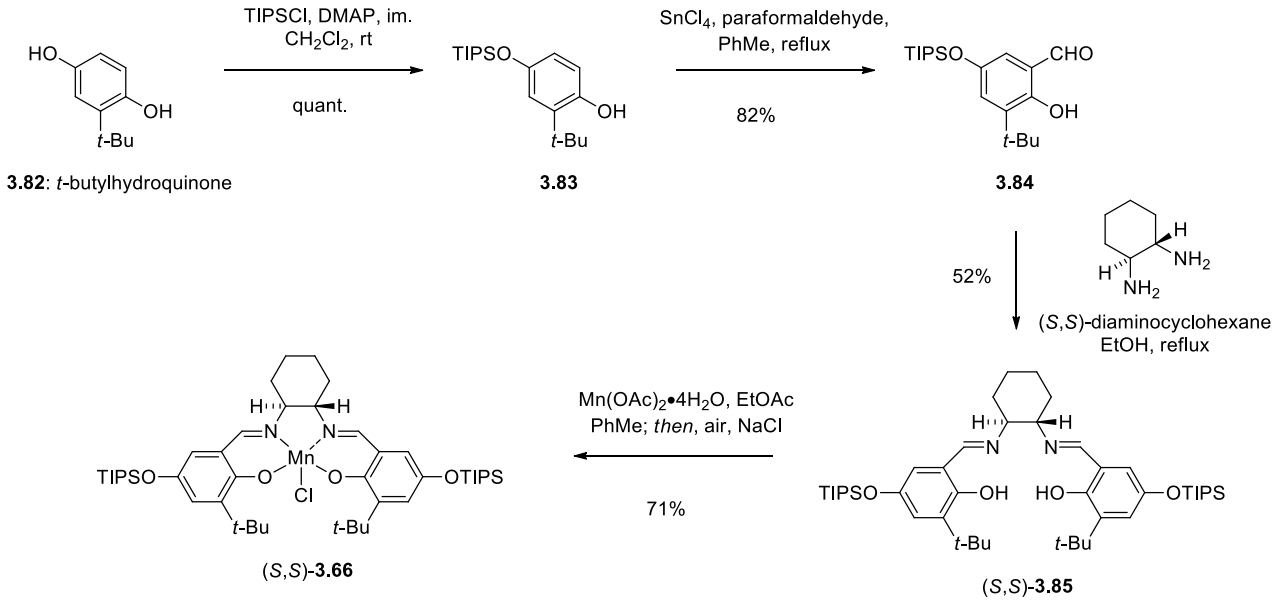

Scheme 3.25: Preparation of TIPS variation of Jacobsen's catalyst (**3.66**).

The second catalyst prepared was a very simple achiral version of the catalyst (Scheme 3.26).[38] The salen ligand **3.86** was prepared directly from commercially available salicylaldehyde and diaminoethane. This was metalated and oxidised to the achiral catalyst **3.87**.

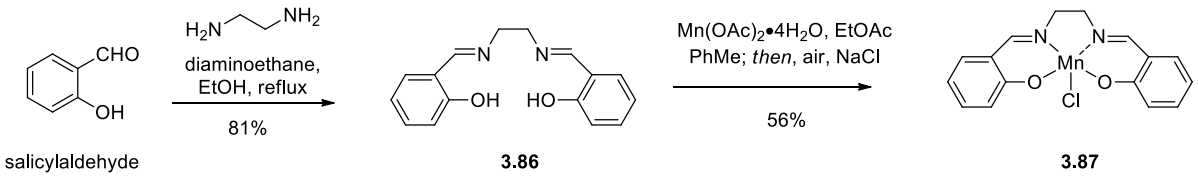

Scheme 3.26: Preparation of achiral manganese-salen catalyst **3.87**.

Representative reactions are shown (Table 3.1). Our goal here was to increase the yield of bruceol (**3.1**). The TIPS catalyst (**3.66**) (entry 2) and the achiral catalyst (**3.87**) (entry 3) act much the same as the commercially available (**3.62**) (entry 1). Using *m*-CPBA without any catalyst (entry 4) gave only epoxidation at the tail olefin (**3.89**), just like the orcinol model (**3.67**).

Shi's fructose derived diketal organocatalyst (**3.88**) (entry 5) was also tried. This goes through a dioxirane active catalyst and is known to work best with *trans* and tri-substituted olefins.[39] There are alternative versions of this catalyst which reportedly work best on *cis* alkenes, but none were commercially available to us at the time. Shi epoxidation gave small amounts of bruceol (**3.1**) and the epoxide (**3.89**). This reaction required a more complicated set up: a biphasic reaction with two reagents added simultaneously by syringe pump. The partial success of this led us to try DMDO[40] (entry 6), however this only gave the epoxide **3.89**. Poor conversion could be due to degradation of the reagent and hence inaccurate measurement of DMDO. Qualitatively, no bruceol (**3.1**) was formed, so this was not further explored.

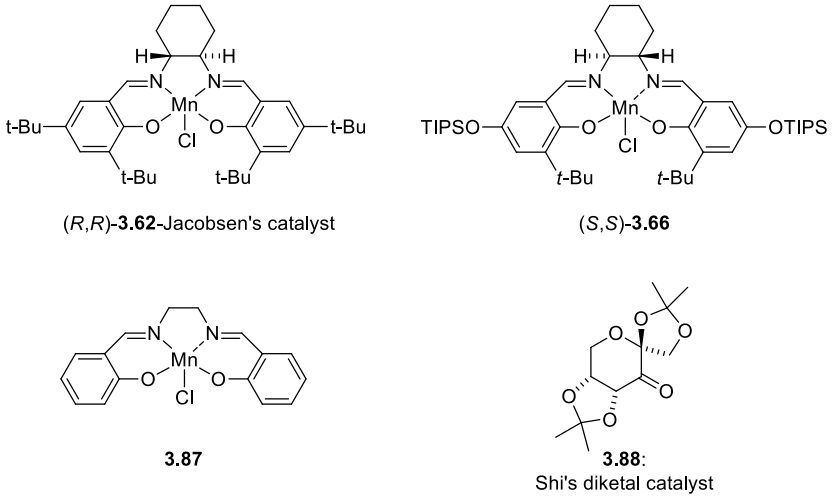

Figure 3.7: Catalysts screened for the synthesis of bruceol (**3.1**).

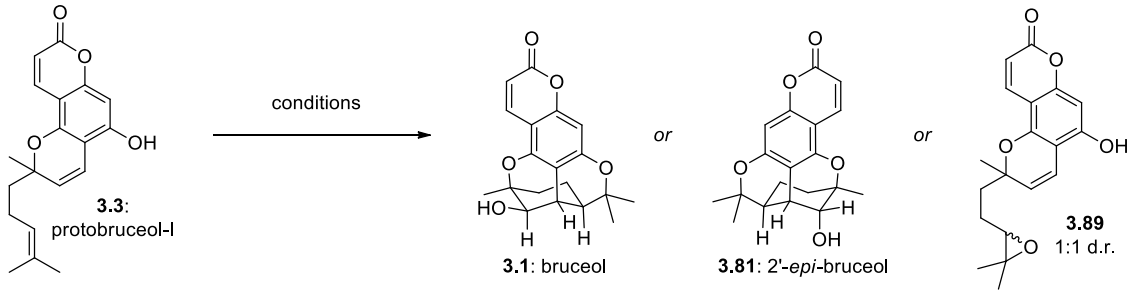

Table 3.1: Oxidation catalysts screened for the bruceol synthesis.

	Catalyst (mol%)	Oxidant(s) (equiv.)	Conditions	Products (yield)
1	(*R*,*R*)-**3.62** (10%)	*m*-CPBA (1.5), NMO (5.0)	CH_2Cl_2, −78 °C, 30 min	bruceol (**3.1**) (11%) epimer (**3.81**) (3%) RSM (**3.3**) (46%)
2	(*R*,*R*)-**3.66** (10%)	*m*-CPBA (1.5), NMO (5.0)	CH_2Cl_2, −78 °C, 45 min	bruceol (**3.1**) (11%) epimer (**3.81**) (5%) RSM (**3.3**) (31%)
3	**3.87** (10%)	*m*-CPBA (1.5), NMO (5.0)	CH_2Cl_2, −78 °C, 1 h	bruceol (**3.1**) (10%) epimer (**3.81**) (4%) RSM (**3.3**) (13%)
4	-	*m*-CPBA (1.1)	CH_2Cl_2, 0 °C → rt	epoxide (**3.89**) (71%) (no reaction at 0 °C)
5	Shi's diketal catalyst (**3.88**) (15%)	Oxone (1.8)	K_2CO_3 (4.0), Bu_4NSO_4 (cat.), 0.2 M K_2CO_3/AcOH buffer, H_2O/3:1 DME/DMM 0.4 mM EDTA, −10 °C, 5 h	bruceol (**3.1**) (3%) epoxide (**3.89**) (4%) RSM (**3.3**) (45%)
6	-	DMDO (1.0)	acetone, −78 °C	epoxide (**3.89**) (21%) RSM (**3.3**) (75%)

3.2.3: Misidentification of Bruceol (**3.1**)

An immediate issue after first synthesising bruceol (**3.1**) which has been ignored up to this point is that the NMR spectra of our synthetic bruceol did not match what was reported in the literature[7] by Waterman in 1992. We quickly dismissed any question of failure by obtaining SXCD of our synthetic material, confirming we had made the same structure (**3.1**) as Jefferies' bruceol from the original isolation in 1963.

Additionally, we were generously donated a crystalline 60-year-old sample (~1 g) of natural bruceol from the original isolation at the University of Western Australia (UWA) by Dr. Gavin Flematti, a natural products chemist currently working there. Gavin had inherited his lab from his former Ph.D. supervisor Emilio Ghisalberti[41], who in turn inherited the lab from his former Ph.D. supervisor Phil Jefferies; over three generations their libraries of natural products have been preserved, and fortunately bruceol (**3.1**) was not lost to time.[42] We were extremely thrilled and grateful to be donated some of this historic sample and of course, the NMR spectrum of the 60-year-old sample matched our synthetic bruceol perfectly! (Table 3.2)

Table 3.2: ^{1}H NMR Comparison of bruceol (**3.1**). *J* in brackets (Hz), n.r. = not reported

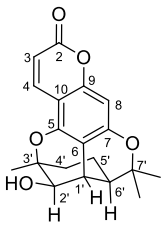

bruceol (**3.1**)


60 year old sample

Position	Natural bruceol (**3.1**) (1963) (60 MHz)[7]	Waterman's "bruceol" (1992) (400 MHz)[7]	Natural bruceol (**3.1**) (500 MHz)	Synthetic bruceol (**3.1**) (500 MHz)
3	6.10 d (10)	6.11 d (9.6)	6.17 d (9.6)	6.17 d (9.6)
4	7.90 d (10)	7.84 dd (9.6, 0.6)	7.96 dd (9.6, 0.6)	7.96 d (9.6)
8	6.40 s	6.48 d (0.6)	6.46 d (0.6)	6.47 br s
1'	2.90 t ("weak")	2.88 t (2.2)	2.93 t (2.4)	2.93 d (2.4)
2'	3.85 d (n.r.)	3.83 dd (7.1, 2.2)	3.85 dd (8.4, 2.1)	3.85 dd (8.4, 2.0)
2'-OH	2.60	2.38 d (7.2)	2.12 d (8.4)	2.07 d (8.5)
3'-Me	1.50 s	1.46 s	1.50 s	1.50 s
4'-ax.	n.r.	1.48 ddd (13.2, 11.5, 5.3)	1.51 ddd (16.2, 14.4, 7.6)	1.51 ddd (15.5, 13.3, 6.9)
4'-eq.	n.r.	1.90 dd (13.2, 5.3)	1.91 dd (15.6, 6.3)	1.92 dd (15.6, 6.2)
5'-ax	n.r.	0.54 dtd (13.4, 11.5, 5.3)	0.59 tdd (13.5, 11.5, 6.3)	0.59 tdd (13.6, 11.7, 6.2)
5'-eq.	n.r.	1.20 dt (13.4, 5.3)	1.25 ddd (13.0, 7.0, 5.3)	~1.2 mult (overlap)
6'	n.r.	2.31 ddd (11.5, 5.3, 2.2)	2.30 ddd (11.6, 5.4, 2.7)	2.30 ddd (11.6, 5.4, 2.6)
7'-Me	1.60 s	1.59 s	1.58 s	1.58 s
7'-Me	1.10 s	1.09 s	1.07 s	1.07 s

Now we were confident we had succeeded in our synthesis the question became: why did Waterman's spectra not match? The simplest answer being: Waterman must not have isolated bruceol (**3.1**). As our spectra were so similar, we proposed Waterman might have isolated "isobruceol" (**3.90**); which bears the same configuration as deoxyisobruceol (**3.31**) (Figure 3.8).

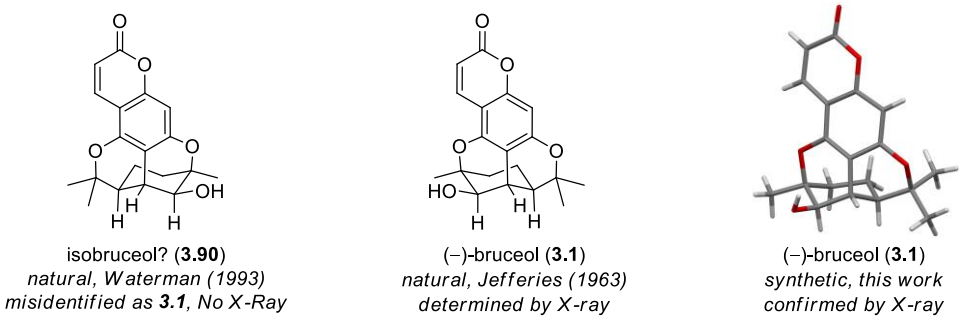

Figure 3.8: SXRD of synthetic bruceol (**3.1**), proposed structure of Waterman's "bruceol" (**3.90**).

This hypothesis should be easily testable; if we could produce the proposed structure of "isobruceol" (**3.90**), its NMR spectra should match Waterman's.

3.2.4: Isolation of Isobruceol (**3.90**)

The initial plan was to synthesise isobruceol (**3.90**); but for a long time, this did not work. The requisite chromene **3.33** (we sometimes referred to as "protoisobruceol") eluded us. Somewhat defeated, our attention turned to the idea of isolation. Our thought process being, if we cannot make it, perhaps we can find it.

Both Jefferies and Waterman performed their extractions of *P. brucei* (formerly *E. brucei*), which is native to Western Australia. We considered travelling to Perth and simply trying to find the plant in the wild as it is supposedly quite common; but with our lack of expertise of plant taxonomy to correctly identify the species, and without any permission from landowners, we decided to ask for help. By inquiring with the Perth Botanic Gardens and Parks Authority I came into contact with ecologists Dr Carole Elliott and Dr Wolfgang Lewandrowski who very generously agreed to find and harvest *P. brucei* from the Koolyanobbing Range (~500 km west of Perth) on our behalf during an upcoming field trip. They sent us ~5 kg of plant material by express post, more than enough for our extraction, and submitted voucher specimens to the Perth Herbarium.

Figure 3.9: Left: *P. brucei* shrub as Found in rural Western Australia. Right: plant material used for the re-isolation of isobruceol (**3.90**).

With the plant material in hand the isolation work was first performed by carefully following the procedures of both Jefferies and Waterman. Jefferies extracted 9 kg of *P. brucei* by maceration in Et_2O for 7 days followed by acid and base washes; bruceol (**3.1**) crystallising out of the remaining Et_2O. Waterman extracted 460 g by with petroleum ether by Soxhlet apparatus followed by chromatography. Both methods were employed, the maceration on 1 kg and the Soxhlet extraction on 600 g, hoping differences in the natural products isolated might be observed.

The maceration and Soxhlet procedures had similar results: after extraordinarily long and painful work-up, and equally difficult flash column chromatography impure natural bruceol (**3.1**) was obtained (Scheme 3.27). Both extractions gave very complex mixtures, and synthetic bruceol was used as a guide for the search and after repeated chromatography, the now modestly pure **3.1** had what appeared to be isobruceol (**3.90**) as its main impurity (~11:1 mixture). This impurity was consistent with the spectra of Waterman's "bruceol". The bruceol mixture obtained from the Soxhlet process was noticeably less pure; this is likely due to degradation occurring after prolonged heating, and the fact no acid/base work-up was done. But in both cases the ratio was the same. From 1 kg of *P. brucei* only 500 mg of this mixture was produced.

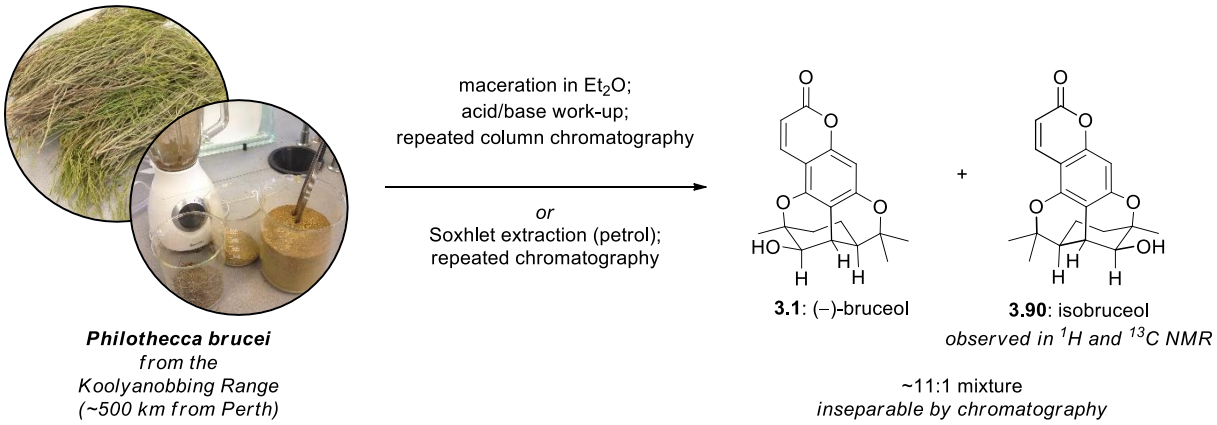

Scheme 3.27: Maceration and Soxhlet extraction of *P. brucei*.

We also tried using the pressurised hot water extraction (PHWE) method. A simple description of this process is water is pumped from a reservoir and heated as it passes through a coil in an oven (temperature >100 °C), and the superheated water goes through the sample matrix to be extracted (e.g. plant material). At the end of the apparatus is a regulator which maintains a high pressure built up from pumping into a partially closed system and the extract flows continuously out the end (Figure 10a).[43] This has been seen as a green (environmentally friendly) alternative to traditional approaches using organic solvents. This works partly because at high pressure the dielectric constant of water changes slightly, becoming more similar in polarity to that of the lower alcohols and dissolving organic molecules which are otherwise insoluble in water.

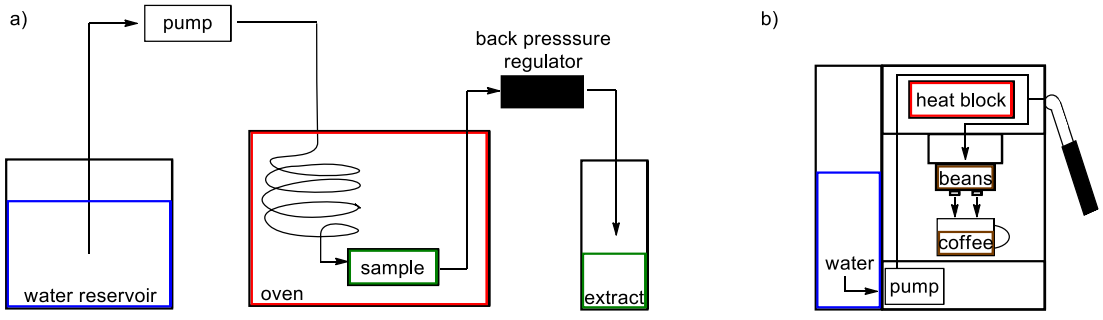

Figure 3.10: a) Schematic of a typical pressurised hot water extraction (PHWE) apparatus; and b) a conventional espresso coffee maker.

This typically requires an expensive custom-built extractor, but there are great similarities to PHWE schematic and a conventional household espresso maker (Figure 3.10b). In a coffee machine, water is pumped over a metal heating block to ~100 °C and into packed ground coffee beans, the coffee slows the flow of hot water and builds up pressure, and as the hot, pressurised water passes through, extracting with it the many prized aroma and flavour molecules, and of course caffeine.

The use of an espresso machine for PHWE in natural product isolation and bioprospecting has been championed by Professor Jason Smith from the University of Tasmania who praises its ease operation, fast extraction time, and selectivity for small molecule natural products while excluding large ones (cf. lignans, chlorophylls etc.) which complicate purification.[44] With an old, disused coffee machine in hand I reached out to Jason who was extraordinarily forthcoming and helpful answering questions on how to best do PHWE. Further, by fortunate coincidence Jason was visiting his family in Adelaide over the Christmas break soon after I had contacted him, and he kindly offered to personally demonstrate the process and gave tips on technique. The main difference to this operation and actually making coffee is EtOH is added to the water; this helps extract less polar molecules.

A limiting factor with the coffee machine is that only a small amount of plant can be extracted at a time (~10-15 g). After some initial test runs, the PHWE was scaled up to 100 g by repeating the process 10 times. The extract here was still complex, but much, much simpler. Large amounts of the natural product hydroxyeriobrucinol (**3.91**) were found (0.44% w/w), as well as small amounts of isoimperatorin (**3.92**) which had not previously been reported in *P. brucei*. The amount of bruceol mixture from this procedure was relatively much higher. This is undoubtedly thanks to the much simpler purification. SCXRD of natural (−)-**3.91** allowed its absolute stereochemistry to be determined to be as it is shown, this agrees with a previous tentative assignment.[45]

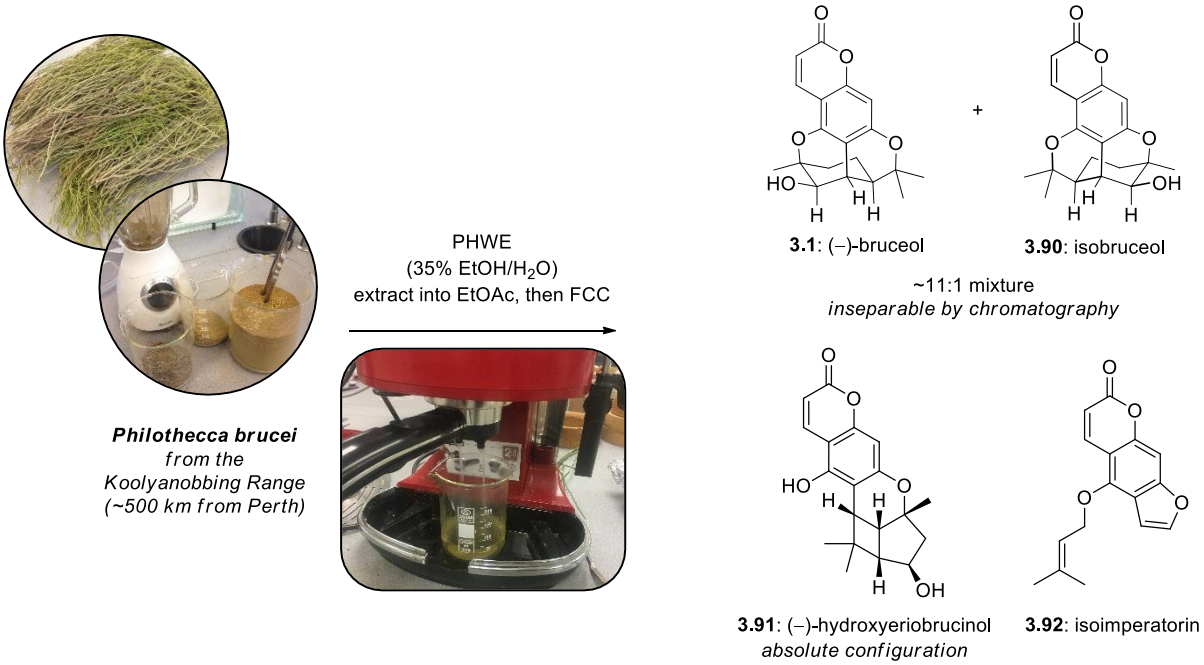

Scheme 3.28: Pressurise hot water extraction (PHWE) of *P. brucei*.

As said previously, the mixture of bruceol (**3.1**) and isobruceol (**3.90**) was completely inseparable by flash column chromatography. But the much more abundant bruceol (**3.1**) could be selectively crystalised out of the mixture, enriching the remaining filtrate with isobruceol (**3.90**). This was repeated until an enriched mixture of ~2:1 was achieved, and no further crystallisation would occur. For the final purification we turned to semi-preparative HPLC. The two compounds were so similar, separation could only just be achieved with the column under-loaded. After many repeated HPLC runs only a few milligrams of pure isobruceol was obtained (~10 mg). The full ^{1}H and ^{13}C NMR spectra of our isobruceol (**3.90**) were in full agreement with Waterman's "bruceol". To confirm our hypothesis, a single crystal of the natural **3.90** was grown and SCXRD was in complete agreement with our proposed structure, proving isobruceol (**3.90**) is the compound Waterman isolated in 1992.

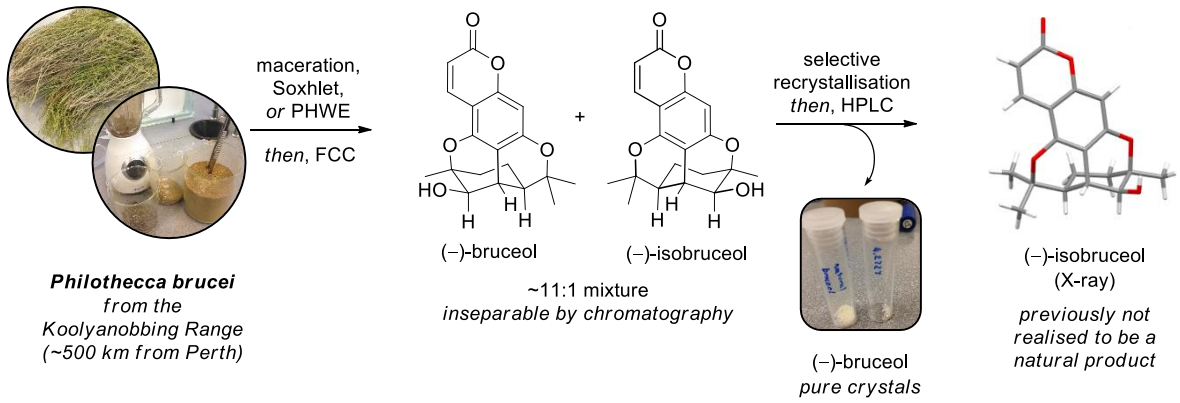

Scheme 3.29: Purification of mixture of natural bruceol (**3.1**) and isobruceol (**3.90**).

3.2.5: Total Synthesis of Isobruceol (**3.90**)

As stated previously, the initial attempts of synthesising isobruceol (**3.90**) were unsuccessful. The spirit of the early approaches was quite logical (Scheme 3.30); as the coumarin ring is what prevented chromenylation to give **3.33** (see Crombie's work, Scheme 3.7), we thought if we formed the chromene first (**3.93**) and the coumarin second, we should get a statistical mixture of the three possible chromenes **3.3**, **3.32**, and most importantly **3.33**. All attempts here failed as the relatively harsh Lewis-acidic conditions for a Friedel-Crafts reaction would quickly destroy the reactive, electron rich chromene. We pre-functionalised the chromene to contain a formyl group (**3.94**) in the hopes a milder, and potentially more selective coumarin formation would be possible. Unfortunately, all attempts by Wittig/HWE olefination, or Perkin reaction failed. Again, the fragility of the chromene is likely to blame – no reaction occurred at room temperature, and when heated, the starting material degraded.

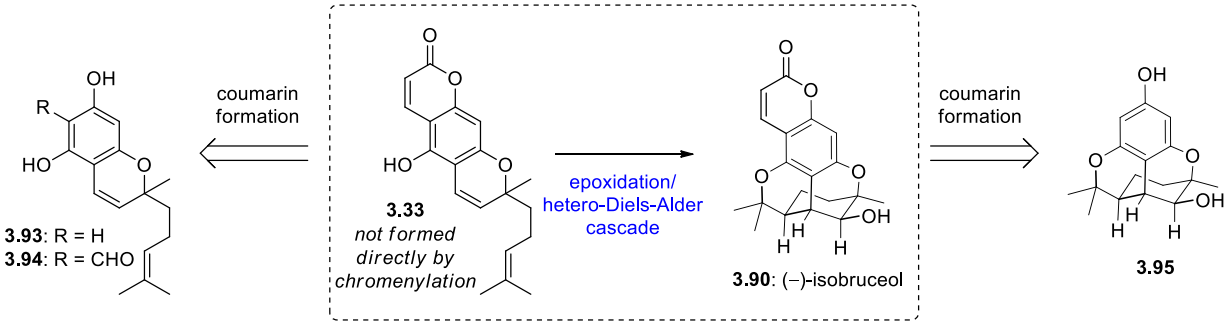

Scheme 3.30: Unsuccessful initial approach to synthesise isobruceol (**3.90**).

The chromene moiety seemed to be the problem, so we tried pre-forming the bruceol citran scaffold **3.95** for a late stage coumarin formation. This approach had similarities to Hsung's synthesis of eriobrucinol.[46] However, this Friedel-Crafts reaction also did not work.

It was only after our successful isolation work that the synthesis was revisited with fresh eyes and we were able to develop a viable solution. The answer came from some of the work of R. D. H. Murray on the pyranocoumarins (Scheme 3.31)[47]. The reverse prenylated (*α*,*α*-dimethylallyl) merohemiterpenoid **3.96** was made by an interesting aromatic Claisen rearrangement. Methanolysis of **3.96** would not only remove the acetate, but also cleave the lactone ring of the coumarin. Now the ester **3.97** can recombine on *either* free phenol position; in this system there is a preference for the linear pyranocoumarin nordentatin (**3.98**), presumably influenced by the bulky reverse prenyl group.

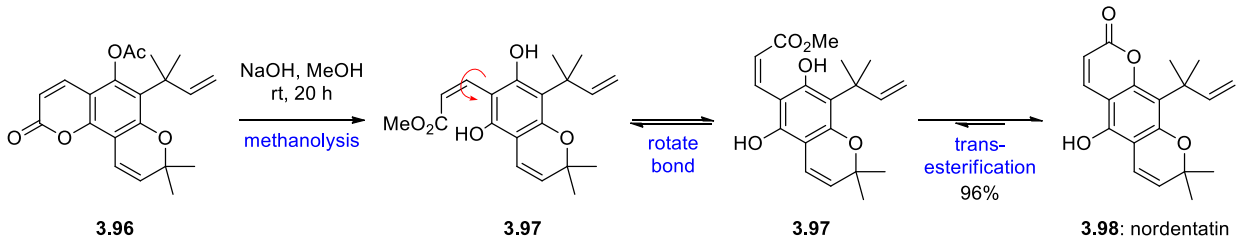

3.96 **3.97** **3.97** **3.98**: nordentatin

Scheme 3.31: Coumarin rearrangement in the synthesis of nordentatin (**3.98**). Murray (1984)

After finding this paper we eagerly applied the tactic to our own problem (Scheme 3.32). Conveniently, **3.32** had already been synthesised as a by-product of the protobruceol-I (**3.3**) preparation (*vide supra*) and I had pooled this, up until now, "undesired" chromene until ~10 g was accumulated; at this point subsequent material was regrettably discarded. The reaction was successful, giving a 1:1 mixture of starting material **3.32** and product **3.33** – an equilibrium mixture where there is no thermodynamic preference.

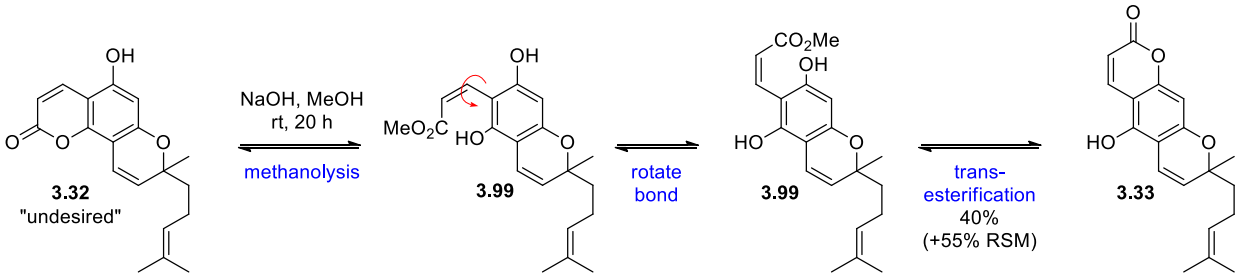

Scheme 3.32: Preparation of chromene **3.33** by coumarin rearrangement.

It was hoped that by changing solvent or counterion the ratio might be skewed to favour **3.33**. MeOH was found to be unique in causing this transformation. NaOH/H_2O and NaOH/DMSO both caused complete decomposition; NaOH/EtOH and $Ca(OH)_2$/EtOH had little/no reaction. A convenient discovery was that the reaction could also be performed substituting KOH for NaOH. This showed no difference in reactivity but is considerably more soluble in MeOH, meaning scaled up reactions could be performed using less solvent. The mixture of chromenes could be separated and resubjecting the starting material **3.32** to the isomerisation conditions could force conversion to mostly **3.33** over several iterations.

With a convenient preparation of the requisite chromene **3.33**, isobruceol (**3.90**) could be synthesised by the same biomimetic epoxidation/hetero-Diels-Alder cascade as bruceol (**3.1**) (Scheme 3.33). Subjecting **3.33** to our optimal conditions gave (−)-isobruceol (**3.90**) in a low 5% yield and modest enantiopurity (93:7 e.r.). Jacobsen had observed epoxidation of linear tricycles (naphthalene derived) to perform poorly.[33] To prepare the natural enantiomer of **3.90** the opposite catalyst ((*S*,*S*)-**3.62**) is used to that in the bruceol (**3.1**) synthesis. This shows that (−)-bruceol and (−)-isobruceol are in fact pseudoenatiomers and **3.90** has the absolute configuration shown. The reaction was repeated with (*R*,*R*)-**3.62** to give the unnatural (+)-isobruceol (**3.90**) in similar yield and e.r.

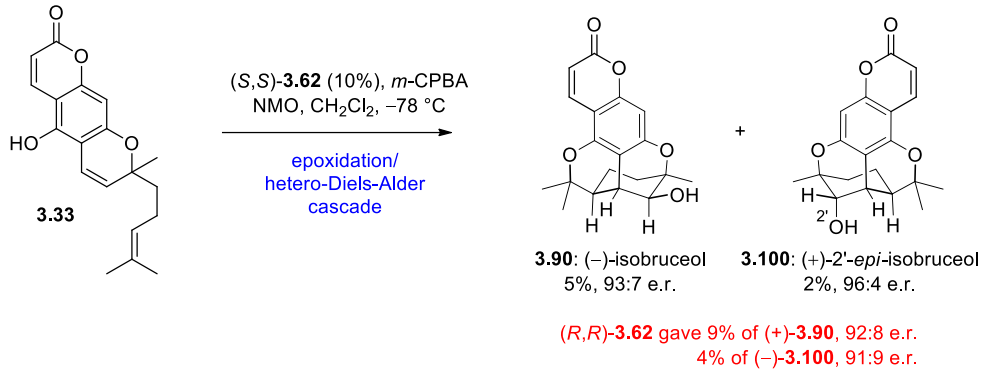

Scheme 3.33: Biomimetic asymmetric synthesis of (−)-isobruceol (**3.90**).

3.2.6: Biocatalytic Synthesis of Bruceol (**3.1**) and Isobruceol (**3.90**)

At the University of Adelaide, our colleague Assoc. Prof. Stephen Bell specialises in biocatalysis - using cytochrome P450 enzymes as catalysts for oxidation reactions. Much of this work involves engineering mutant P450s and finding new substrates/new applications. Since many of the projects we were working on at the time involved key biomimetic steps which we proposed required oxidation by a P450 enzyme in Nature; and there were similarities to our substrates and the ones used by the Bell group (Scheme 3.34), we felt this lent itself naturally to collaboration.

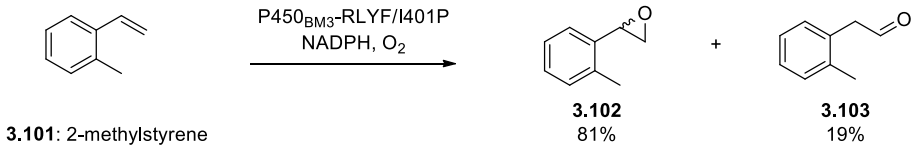

Scheme 3.34: An example of P450 oxidation from the Bell Group. Bell (2017)[48]

The collaboration was initially proposed by our senior Ph.D. student Hilton Lam, while we were working on the Rhodonoids project (Chapter 2). Joel Lee, who was Stephen's Masters student screened our orcinol chromene **3.67** against a small library of P450 enzymes:[49] CYP101B1, CYP101C1, and variants of CYP102A1 ($P450_{BM3}$). $P450_{BM3}$-A74G/F87V/L188Q ("GVQ") was the only enzyme tested which gave desired product: a mixture of the model bruceol analogue **3.70** and

the epoxide **3.104** (Figure 3.11). The GVQ variant has previously been shown to oxidise a range of hydrophobic terpenes and terpenoids.[50]

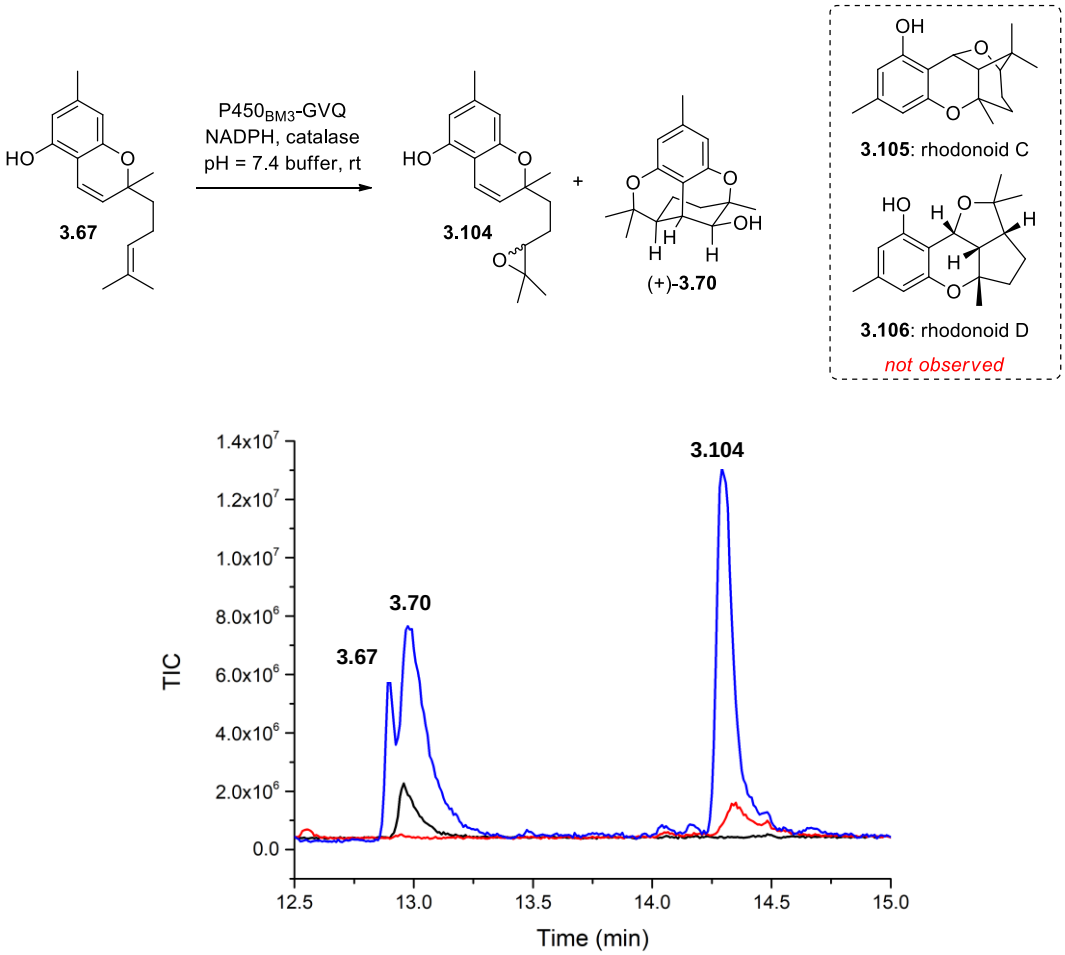

Figure 3.11: GC-MS trace showing conversion of chromene **3.67** to bruceol analogue **3.70**.

Chiral HPLC showed the (+)-**3.70** enantiomer with high enantioselectivity. Although these experiments failed to produce any of the rhodonoids (C, **3.105**, or D, **3.106**), the reasonably good conversion of chromene **3.67** to citran **3.70** was very promising for a biocatalytic synthesis of bruceol **3.1** or isobruceol (**3.90**).

A challenge to overcome would be accommodating the relatively large protobruceol-I (**3.3**) and **3.33**. Variants of $P450_{BM3}$ which had mutations F87A of F87V as this increases the size of the active site and has been shown to allow larger substrates.[51,52] A total of six mutants P450s were screened, and

the highest level of conversion to either bruceol (**3.1**) or isobruceol (**3.90**) was from the variant KSK19/I263A/A328I (KSK19 = F87A/H171L/Q307H/N319Y). Unfortunately, **3.1** and **3.90** standards gave poor traces on GC-MS making it unsuitable for analysis of the enzymatic reaction, so the formation of product was observed by analytical HPLC (Figure 3.12). The conversion was poor, this is perhaps because our substrate was still too large for the active site. However, we could demonstrate the epoxidation/Hetero-Diels-Alder cascade reaction could be enacted by a P450 enzyme (albeit a promiscuous bacterial P450) as we believe this supports a proof of concept for our biosynthetic proposal.

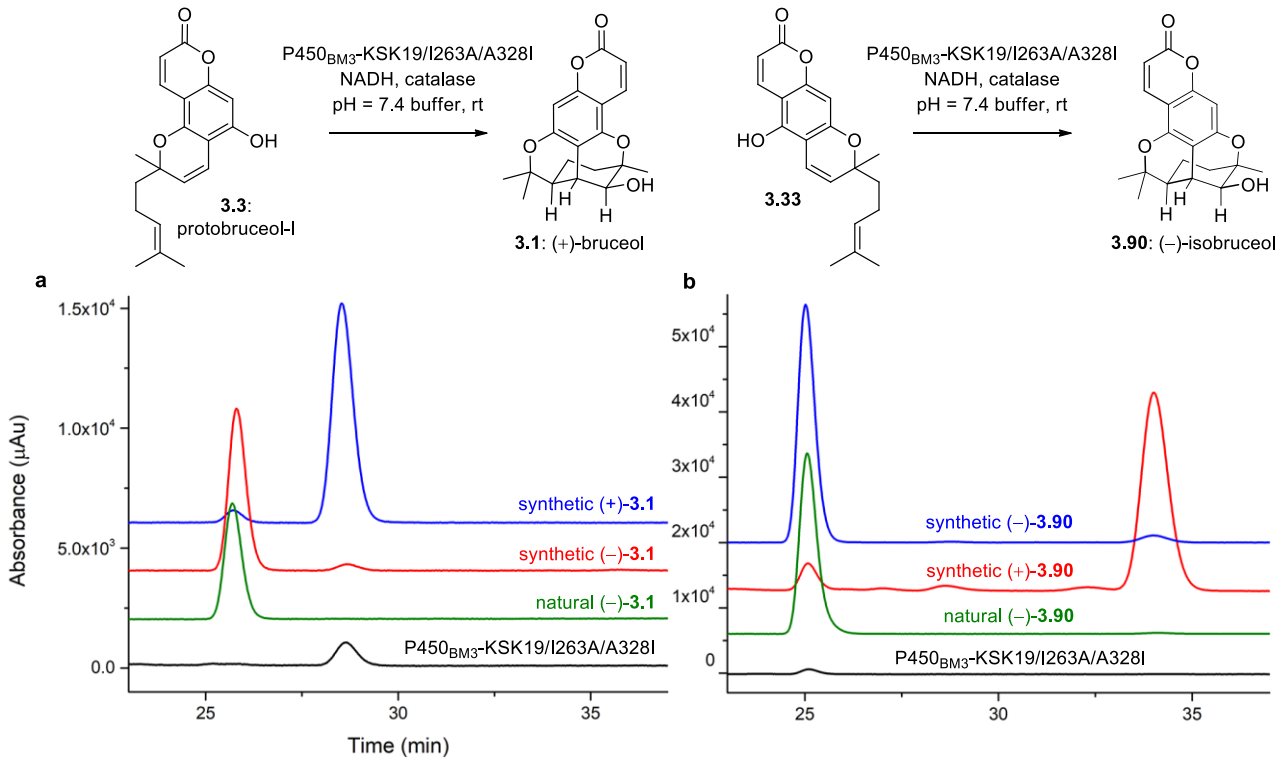

Figure 3.12: HPLC traces of enzymatic syntheses of a) bruceol (**3.1**) and b) isobruceol (**3.90**).

3.3 Summary and Conclusion

Overall, a concise 3 step total synthesis of bruceol (**3.1**) was achieved by a biomimetic epoxidation/hetero-Diels-Alder cascade initiated using Jacobsen's asymmetric epoxidation as a final stereodivergent step. Synthesis of **3.1** revealed a separate natural product isobruceol (**3.90**) was

previously isolated and mistakenly identified as bruceol. This was confirmed by reisolation of both bruceol (**3.1**) and isobruceol (**3.90**) from *Philotheca brucei*. A total synthesis of isobruceol (**3.90**) was also completed, using the same biomimetic cascade reaction, but on the isomeric chromene **3.33**. This required the development of the first preparation of **3.33** which used a dextrous isomerisation of a waste product of the bruceol synthesis, resulting in a highly divergent sequence. Lastly, to probe our biosynthetic proposal, the biomimetic epoxidation/hetero-Diels-Alder cascade reaction was demonstrated to be possible using $P450_{BM3}$-KSK19/I263A/A328I, a mutant bacterial cytochrome P450 monooxygenase enzyme.

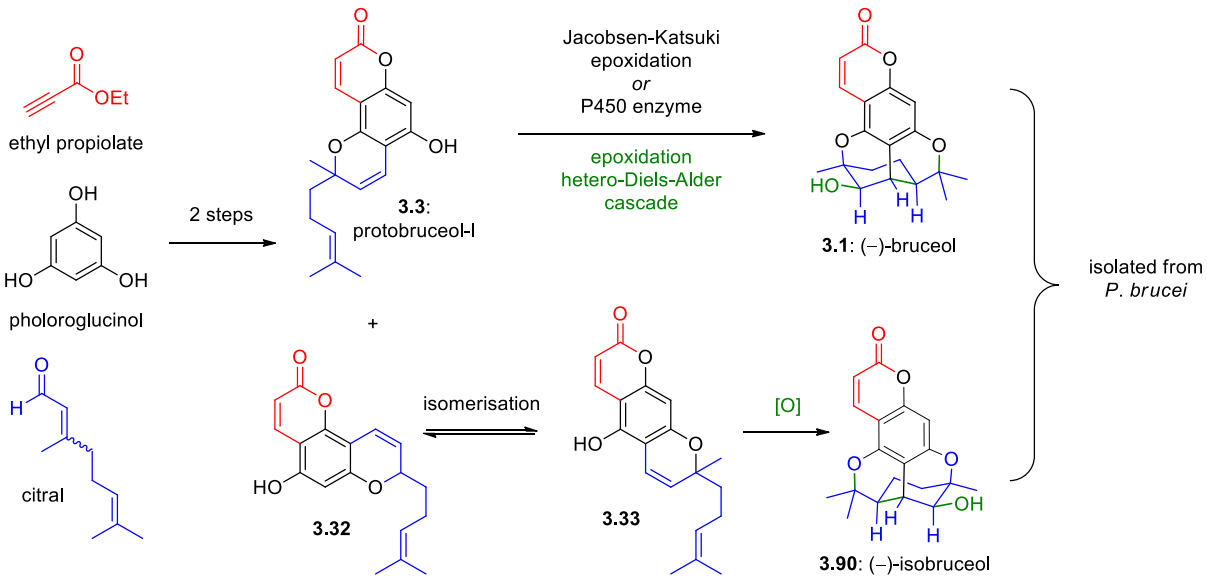

Scheme 3.35: Summary of the bruceol project

This project demonstrates an opportunistic and multifaceted approach to science which relied on collaboration. A combination of biosynthetic speculation, total synthesis, asymmetric catalysis, natural product isolation, and biocatalysis was necessary to complete this project in the way that we did.

3.4 Experimental

3.4.1: General Methods

All chemicals were purchased from commercial suppliers and used as received. All reactions were performed under an inert atmosphere of N_2. All organic extracts were dried over anhydrous magnesium sulfate. Thin layer chromatography was performed using aluminium sheets coated with silica gel F_{254}. Visualization was aided by viewing under a UV lamp and staining with ceric ammonium molybdate stain followed by heating. All R_f values were measured to the nearest 0.05. Flash column chromatography was performed using 40-63 micron grade silica gel. Melting points were recorded on a digital melting point apparatus and are uncorrected. Infrared spectra were recorded using an FT-IR spectrometer as the neat compounds. High field NMR spectra were recorded using either a 500 MHz spectrometer (^{1}H at 500 MHz, ^{13}C at 125 MHz) or 600 MHz spectrometer (^{1}H at 600 MHz, ^{13}C at 150 MHz). The solvent used for NMR spectra was $CDCl_3$ unless otherwise specified. ^{1}H chemical shifts are reported in ppm on the δ-scale relative to TMS (δ 0.00) or $CDCl_3$ (δ 7.26) and ^{13}C NMR chemical shifts are reported in ppm relative to $CDCl_3$ (δ 77.16). Multiplicities are reported as (br) broad, (s) singlet, (d) doublet, (t) triplet, (q) quartet, (quin) quintet, (sext) sextet, (hept) heptet and (m) multiplet. All *J*-values were rounded to the nearest 0.1 Hz. ESI high resolution mass spectra were recorded on an ESI-TOF mass spectrometer. Optical rotations were recorded on an Anton Paar Modular Circular Polirimeter at 20 °C.

3.4.2: Synthetic Procedures

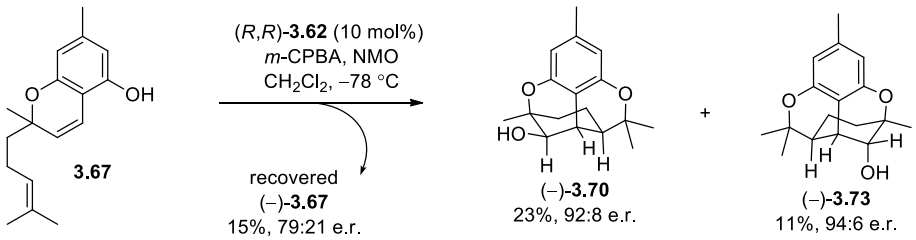

To a solution of (±)-**3.67** (1.32 g, 5.09 mmol) in CH_2Cl_2 (45 mL) at −78 °C was added (*R,R*)-**3.62** (Jacobsen's catalyst) (323 mg, 0.509 mmol), followed by NMO (2.98 g, 25.5 mmol). Then *m*-CPBA (77%, 1.70 g, 7.64 mmol) was added in portions over 20 min. The mixture was stirred at −78 °C for a further 30 min. The reaction was quenched with Me_2S (1 mL), and warmed to room temperature. The resultant mixture was filtered through a pad of SiO_2, and flushed with excess Et_2O (300 mL) and the solvent was removed *in vacuo*. The residue was redissolved in Et_2O (100 mL) and washed sequentially with $NaHCO_3$ solution (75 mL × 4), water (75 mL), then brine (75 mL), dried over

$MgSO_4$, filtered, and concentrated *in vacuo*. The residue was purified by flash column chromatography (2:1 → 1:1 petrol/Et_2O) to afford recovered (−)-**3.67** as an orange oil (119 mg, 15%, **$[\alpha]^{20}_D$ =** −63.9 ($CHCl_3$, c = 1.07), e.r. 79:21). Further elution afforded (−)-**3.73** as a light orange oil (157 mg, 11%, e.r. 94:6), then (−)-**3.70** as a light brown oil (322 mg, 23%, e.r. 92:8).

Data for (−)-**3.73**:

^{1}H NMR (500 MHz, $CDCl_3$) δ 6.31 (d, *J* = 1.2 Hz, 1H), 6.29 (d, *J* = 0.9 Hz, 1H), 4.24 (d, *J* = 4.8 Hz, 1H), 2.94 (dd, *J* = 4.9, 2.8 Hz, 1H), 2.46 (ddd, *J* = 11.6, 5.5, 2.8 Hz, 1H), 2.25 (s, 3H), 1.82 – 1.74 (m, 1H), 1.58 (dd, *J* = 15.1, 6.2 Hz, 1H), 1.51 (s, 3H), 1.38 (s, 3H), 1.21 – 1.15 (m, 1H), 1.03 (s, 3H), 0.55 (tdd, *J* = 13.4, 11.6, 6.2 Hz, 1H)
^{13}C NMR (125 MHz, $CDCl_3$) δ 157.1, 155.6, 138.0, 113.4, 111.1, 109.5, 83.8, 76.8, 70.7, 39.8, 34.5, 31.8, 29.7, 25.2, 24.0, 21.8, 21.4
$[\alpha]^{20}_D$ = −35.5 ($CHCl_3$, c = 1.24)
IR (neat) $\bar{\nu}$ 3468, 2975, 1914, 1620, 1588, 1493, 1455, 1370, 1335, 1314, 1251, 1212, 1179 cm^{-1}
R_f 0.25 (3:1 petrol/EtOAc)
HRMS (ESI) Calculated for $C_{17}H_{23}O_3$ 275.1642 $[M+H]^+$, found 275.1633

Data for (−)-**3.70**:

^{1}H NMR (600 MHz, $CDCl_3$) 6.34 (s, 1H), 6.31 (d, *J* = 1.3 Hz, 1H), 3.71 (d, *J* = 6.7 Hz, 1H), 2.87 (d, *J* = 2.5 Hz, 1H), 2.25 (s, 3H), 2.19 (ddd, *J* = 11.5, 5.4, 2.7 Hz, 1H), 1.83 (ddd, *J* = 15.5, 6.2, 1.3 Hz, 1H), 1.52 (s, 3H), 1.44 – 1.37 (m, overlapped, 1H), 1.40 (s, 3H), 1.16 – 1.10 (m, 1H), 1.00 (s, 3H), 0.47 (tdd, *J* = 13.5, 11.5, 6.3 Hz, 1H)
^{13}C NMR (150 MHz, $CDCl_3$) δ 157.6, 155.3, 137.9, 111.6, 111.6, 109.9, 83.7, 77.6, 71.5, 47.8, 36.6, 36.3, 29.7, 24.7, 23.8, 21.8, 21.7
$[\alpha]^{20}_D$ = −1.1 ($CHCl_3$, c = 1.49)
IR (neat) $\bar{\nu}$ 1380, 2974, 2933, 1620, 1587, 1492, 1452, 1369, 1333, 1313 cm^{-1}
R_f 0.15 (3:1 petrol/EtOAc)
HRMS (ESI) Calculated for $C_{17}H_{23}O_3$ 275.1642 $[M+H]^+$, found 275.1640

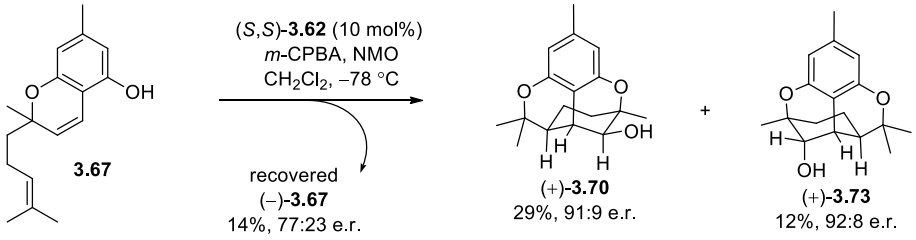

To a solution of (±)-**3.67** (1.30 g, 5.05 mmol) in CH_2Cl_2 (60 mL) at −78 °C was added (*S*,*S*)-**3.62** (Jacobsen's catalyst) (320 mg, 0.505 mmol), followed by NMO (2.96 mg, 25.2 mmol) and then *m*-CPBA (77%, 1.30 mg, 5.81 mmol) in portions over 5 min. The reaction mixture was stirred at −78 °C for 1 h, then quenched with $Na_2S_2O_3$ (5 g) and warmed to room temperature. Water (100 mL) was added and the layers were separated. The organic phase was diluted with CH_2Cl_2 (100 mL) and washed sequentially with saturated $NaHCO_3$ solution (100 mL × 2), water (100 mL), and brine (100 mL). The solvent was dried over $MgSO_4$, filtered, and removed *in vacuo*, and the residue was purified by flash column chromatography on SiO_2 (8:1 → 4:1 petrol/EtOAc) to give recovered (+)-**3.62** as a dark orange oil (185 mg, 14%, $[\alpha]^{20}_D$ = +48.6 (c = 1.0, $CHCl_3$), e.r. 77:23). Further elution gave (+)-**3.70** as a yellow oil (160 mg, 12%, $[\alpha]^{20}_D$ = +33.9 (c = 1.0, $CHCl_3$), e.r. 92:8), followed by (+)-**3.70** as an orange oil (402 mg, 29%, $[\alpha]^{20}_D$ = +1.7 (c = 1.0, $CHCl_3$), e.r. 91:9).

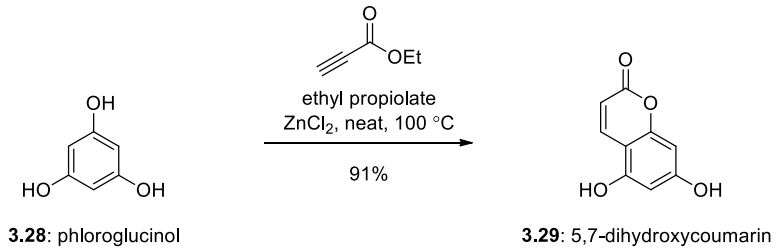

Phloroglucinol (**3.28**) (50.0 g, 396 mmol), powdered anhydrous $ZnCl_2$ (26.9 g, 198 mmol), and ethyl propiolate (50.6 g, 602 mmol) were combined and mixed until consistent. The mixture was heated to 100 °C until a violent exotherm occurred, at this point the heat source was removed. A water-cooled condenser was used to limit the loss of unreacted ethyl propiolate. After the exotherm subsided (~10 min) heating was resumed and continued at 100 °C for 1 h. 10% HCl solution (200 mL) was added to the resultant clay-like solid and was manually mixed thoroughly. The solid was collected by filtration, washed with boiling water (200 mL × 2), and oven dried at 110 °C overnight to afford 5,7-dihydroxycoumarin (**3.29**) as a orange/brown powder (64.2 g, 91%).

Data for **3.29**:

^{1}H NMR (500 MHz, d_6-DMSO) δ 10.68 (br s, 1H) , 10.40 (br s, 1H), 7.95 (d, *J* = 9.59, 1H), 6.25 (s, 1H), 6.18 (s, 1H), 6.03 (d, *J* = 9.60)

^{13}C NMR (125 MHz, d_6-DMSO) δ 162.1, 160.9, 156.5, 1560, 139.6, 108.7, 101.7, 98.3, 94.1

R_f 0.20 (15:1 CH_2Cl_2/MeOH)

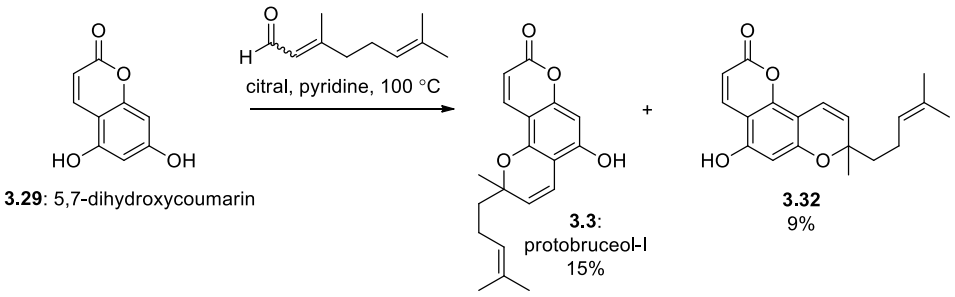

5,7-Dihydroxycoumarin **3.29** (10.0 g, 56.1 mmol) and citral (9.6 mL, 56.1 mmol) were heated in pyridine (9.0 mL, 112 mmol) at 90 °C for 18 h. The reaction mixture was purified by flash column chromatography on SiO_2 (1:1 petrol/Et_2O). A second flash column on SiO_2 (20:1 CH_2Cl_2/EtOAc) gave chromene **3.23** as a yellow solid (1.41 g, 8%). Further elution gave protobruceol-I **3.33** as a tan solid (2.72 g, 15%).

Data for **3.23**:

^{1}H NMR (500 MHz, $CDCl_3$) δ 8.04 (d, *J* = 9.6 Hz, 1H), 7.10 (br s, 1H), 6.79 (d, *J* = 10.1 Hz, 1H), 6.26 (s, 1H), 6.15 (d, *J* = 9.5 Hz, 1H), 5.50 (d, *J* = 10.1 Hz, 1H), 5.07 (t, *J* = 7.0 Hz, 1H), 2.07 (q, *J* = 8.0 Hz, 2H), 1.80 – 1.70 (m, 2H), 1.65 (s, 3H), 1.55 (s, 3H), 1.40 (s, 3H)

^{13}C NMR (125 MHz, $CDCl_3$) δ 162.6, 158.0, 153.9, 151.0, 140.0, 132.1, 126.7, 123.9, 115.5, 109.9, 103.2, 102.7, 99.4, 80.6, 41.7, 27.1, 25.8, 22.8, 17.8

IR (neat) $\bar{\nu}$ 3064, 1673, 1620, 1598, 1466, 1349, 1261, 1147, 1122, 1074, 1006, 840 cm^{-1}

m.p. 144 – 148 °C

R_f 0.30 (1:1 petrol/Et_2O)

HRMS (ESI) Calculated for $C_{19}H_{19}O_4$ 311.1289 $[M-H]^-$, found 311.1292

Data for protobruceol-I **3.3**:

^{1}H NMR (500 MHz, $CDCl_3$) δ 7.97 (d, *J* = 9.6 Hz, 1H), 6.66 (d, *J* = 10.1 Hz, 1H), 6.45 (s, 1H), 6.35 (br s, 1H), 6.15 (d, *J* = 9.6 Hz, 1H), 5.53 (d, *J* = 10.1 Hz, 1H), 5.08 (t, *J* = 6.9 Hz, 1H), 2.11 (dq, *J* = 11.4, 6.1 Hz, 2H), 1.85 – 1.67 (m, 2H), 1.65 (s, 3H), 1.56 (s, 3H), 1.44 (s, 3H)

^{13}C NMR (125 MHz, $CDCl_3$) δ 163.0, 156.3, 155.4, 151.2, 139.8, 132.1, 126.6, 123.9, 116.7, 110.2, 106.1, 103.5, 95.7, 80.5, 41.4, 26.7, 25.8, 22.8, 17.8

IR (neat) $\bar{\nu}$ 3180, 1690, 1615, 1587, 1442, 1365, 1257, 1209, 1182, 1088, 990 cm^{-1}

m.p. 119 – 126 °C

R_f 0.20 (1:1 petrol/Et_2O)

HRMS (ESI) Calculated for $C_{19}H_{19}O_4$ 311.1289 $[M-H]^-$, found 311.1293

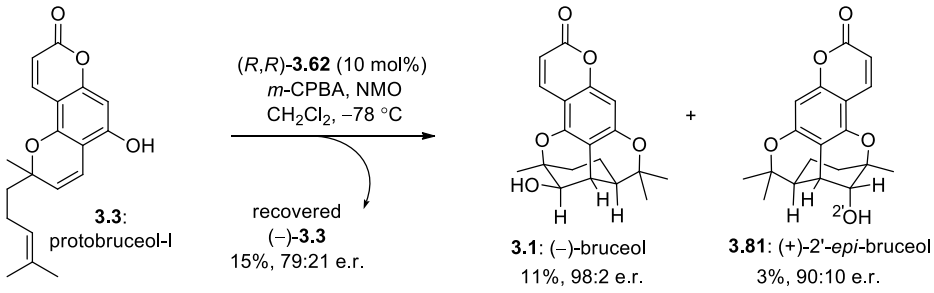

To a solution of protobruceol-I (**3.3**) (204 mg, 0.652 mmol) in CH_2Cl_2 (10 mL) at −78 °C was added (*R*,*R*)-**3.62** (Jacobsen's catalyst) (41.4 mg, 0.0652 mmol), followed by NMO (382 mg, 3.26 mmol) and by *m*-CPBA (77%, 219 mg, 0.975 mmol). The reaction was stirred for a further 30 min then quenched with Me_2S (0.5 mL), and warmed to room temperature. 1 M NaOH (3 mL) was added and the mixture was stirred for 5 min before acidifying with 1 M HCl (5 mL). The mixture was filtered through a pad of SiO_2, flushed with excess Et_2O (100 mL × 3), concentrated *in vacuo* and dissolved in Et_2O (80 mL). The organic phase was washed sequentially with $NaHCO_3$ (50 mL × 4), water (50 mL), and brine (50 mL), dried over $MgSO_4$, filtered, and concentrated *in vacuo*. The residue was purified by flash column chromatography on SiO_2 (1:1 → 0:1 petrol/Et_2O) to afford recovered (−)-**3.3** as a white solid (93.7 mg, 46%, $[\alpha]^{20}_D$ = −21.7 ($CHCl_3$, c = 1.04), e.r. 55:45). Further elution afforded (+)-**3.81** as a white solid (7.1 mg, 3%, e.r. 90:10), followed by (−)-bruceol (**3.1**) as a light brown solid (24.1 mg, 11%, e.r. 98:2).

Data for (+)-**3.81**:

^{1}H NMR (600 MHz, $CDCl_3$) δ 7.92 (d, *J* = 9.5 Hz, 1H), 6.44 (s, 1H), 6.16 (d, *J* = 9.5 Hz, 1H), 4.28 (t, *J* = 4.6 Hz, 1H), 2.99 (dd, *J* = 4.9, 2.8 Hz, 1H), 2.56 (ddd, *J* = 11.6, 5.5, 2.8 Hz, 1H), 2.16 (d, *J* = 4.3 Hz, 1H), 1.87 (ddd, *J* = 15.3, 13.1, 7.0 Hz, 1H), 1.64 (dd, *J* = 15.3, 6.2 Hz, 1H), 1.59 (s, 3H), 1.46 (s, 3H), 1.28 (dt, *J* = 13.7, 6.5 Hz, 1H), 1.09 (s, 3H), 0.63 (tdd, *J* = 13.4, 11.7, 6.2 Hz, 1H)
^{13}C NMR (150 MHz, $CDCl_3$) δ 162.0, 160.1, 155.3, 151.8, 138.7, 111.1, 111.0, 104.0, 98.9, 86.0, 78.7, 69.9, 39.1, 34.1, 32.1, 29.6, 24.9, 24.3, 21.3
IR (neat) $\bar{\nu}$ 3435, 1713, 1615, 1567, 1448, 1355, 1241, 1122 cm^{-1}
$[\alpha]^{25}_D$ = +61.9 ($CHCl_3$, c = 0.36)
R_f 0.40 (1:1 petrol/EtOAc)
HRMS (ESI) Calculated for $C_{19}H_{20}O_5Na$ 351.1203 $[M+Na]^+$, found 351.1204

Data for (−)-bruceol (**3.1**):

^{1}H NMR (500 MHz, $CDCl_3$) δ 7.96 (d, *J* = 9.6 Hz, 1H), 6.47 (s, 1H), 6.17 (d, *J* = 9.6 Hz, 1H), 3.85 (dd, *J* = 8.4, 2.0 Hz, 1H), 2.93 (d, *J* = 2.4 Hz, 1H), 2.30 (ddd, *J* = 11.6, 5.4, 2.6 Hz, 1H), 2.07 (d, *J* = 8.5 Hz, 1H), 1.92 (dd, *J* = 15.6, 6.2 Hz, 1H), 1.58 (d, *J* = 2.5 Hz, 3H), 1.56 – 1.47 (m, 1H), 1.50 (s, 3H), 1.30 – 1.19 (m, 2H), 1.07 (s, 3H), 0.59 (tdd, *J* = 13.6, 11.7, 6.2 Hz, 1H)
^{13}C NMR (125 MHz, $CDCl_3$) δ 161.6, 160.5, 155.1, 151.4, 138.3, 111.2, 109.4, 104.0, 99.2, 85.5, 79.3, 70.9, 47.0, 36.8, 35.9, 29.5, 24.2, 23.9, 21.6
IR (neat) $\bar{\nu}$ 3529, 3457, 2971, 1702, 1615, 1566, 1447, 1360, 1248, 1196 cm^{-1}
$[\alpha]^{25}_D$ = −178.7 ($CHCl_3$, c = 0.51)
R_f 0.20 (1:1 petrol/EtOAc)
m.p. 197 – 209 °C (amorphous)
HRMS (ESI) Calculated for $C_{19}H_{19}O_5$ 327.1238 $[M-H]^-$, found 327.1235

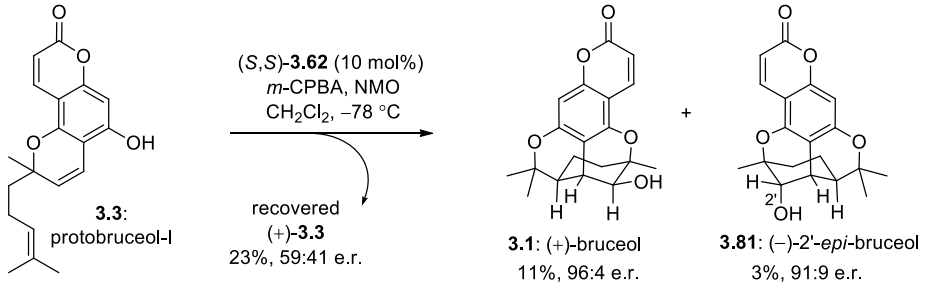

To a solution of protobruceol-I (**3.3**) (312 mg, 0.999 mmol) in CH_2Cl_2 (15 mL) at −78 °C was added (*S*,*S*)-**3.62** (Jacobsen's catalyst) (63.5 mg, 0.0999 mmol), followed by NMO (585 mg, 5.00 mmol) and *m*-CPBA (77%, 258 mg, 1.50 mmol). The reaction mixture was stirred at −78 °C for 30 min, then quenched with Me_2S (1 mL) and warmed to room temperature. 1 M NaOH solution (5 mL) was then added and the resultant mixture was stirred at room temperature for 30 min. The mixture was dried over $MgSO_4$, filtered through a pad of Celite and flushed with excess CH_2Cl_2 (30 mL). The solvent was removed *in vacuo* and the residue was purified by flash column chromatography on SiO_2 (3:1 → 1:1 petrol/Et_2O) to afford recovered (+)-protobruceol-I (**3.3**) as a white solid (70.8 mg, 23%, $[\alpha]^{20}_D$ = +25.6 ($CHCl_3$, c = 0.94), e.r. 59:41). Further elution gave (−)-**3.81** as a white solid (9 mg, 3%, $[\alpha]^{20}_D$ = −96.5 ($CHCl_3$, c = 0.24), e.r. 91:9), followed by (+)-bruceol (**3.1**) as a white solid (41.5 mg, 13%, $[\alpha]^{20}_D$ = +190.1 ($CHCl_3$, c = 0.23), e.r. 96:4). Data for **3.81** and **3.1** matched what was previously reported.

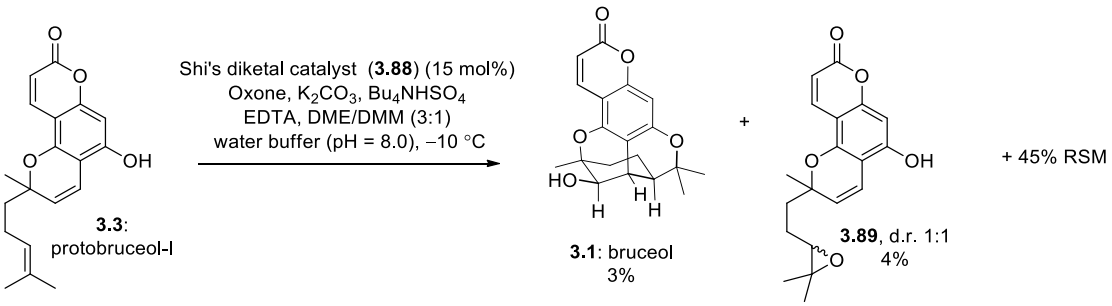

A biphasic mixture of **3.3** (156 mg, 0.500 mmol) in 1,2-dimethoxyethane/dimethoxymethane (3:1, 7.5 mL), and Shi's catalyst (**3.88**) (19.4 mg, 0.075 mmol) and Bu_4NHSO_4 (7.5 mg, 0.040 mmol) in 0.2 M aqueous AcOH/K_2CO_3 buffer solution (5 mL, pH = 8.0) containing EDTA (0.4 mM) was cooled to −10 °C and stirred. Two separated aqueous solutions, one is Oxone (0.212 M, 4.2 mL, 0.89 mmol) containing EDTA (0.4 mM); the other is K_2CO_3 (0.479 M, 4.2 mL, 2.0 mmol) containing EDTA (0.4 mM) were added dropwise simultaneously to the biphasic mixture by syringe pump over 5 h. After the addition was complete the layers were separated, and the aqueous phase was extracted with EtOAc (10 mL × 3). The combined organic extracts were washed with water (10 mL), and brine

(10 mL), dried over $MgSO_4$, filtered, and concentrated *in vacuo*. The residue was purified by flash column chromatography on SiO_2 (2:1 → 1:1 petrol/EtOAc) to give recovered **3.3** (70.7 mg, 45%), epoxide **3.89** as an orange oil (6.7 mg, 4%), and bruceol (**3.1**) as a discoloured solid (4.6 mg, 3%). Data for bruceol (**3.1**) what was previously reported.

NB: This reaction was inconsistent regarding conversion. In the best case, 22% of epoxide **3.89** was achieved using similar conditions.

Partial data for epoxide **3.89** (1:1 mixture of diastereoisomers):

^{1}H NMR (500 MHz, $CDCl_3$) δ 8.32 (br s, 2H), 7.96 (d, *J* = 9.6 Hz, 2H), 6.71 (d, *J* = 10.1 Hz, 2H), 6.53 (s, 2H), 6.13 (d, *J* = 9.58 Hz, 2H), 5.50 (d, *J* = 9.6 Hz, 1H), 5.48 (d, *J* = 9.6 Hz, 1H), 2.78 (t, *J* = 6.0 Hz, 2H), 2.00 – 1.64 (m, 8H), 1.54 (s, 6H), 1.30 (s, 3H), 1.28 (s, 3H), 1.24 (s, 6H)
R_f 0.50 (neat Et_2O)

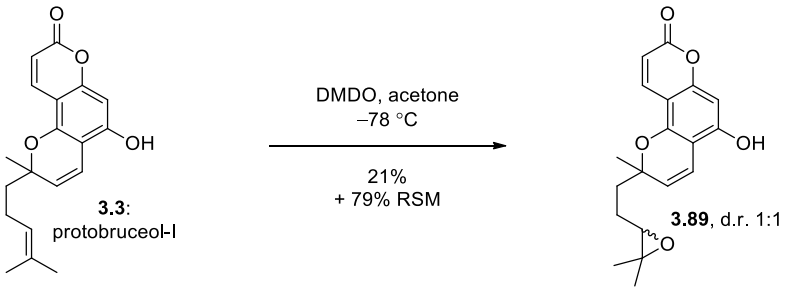

To a solution of protobruceol-I (**3.3**) (89.8 mg, 0.268 mmol) in acetone (5 mL) cooled to −78 °C was added DMDO (44 mM in acetone, 6.1 mL, 0.268 mmol) dropwise. The reaction was stirred for 30 min at −78 °C, then quenched with Me_2S (1 drop) and warmed to room temperature. The solvent was removed *in vacuo* and the residue was purified by flash column chromatography on SiO_2 (1:1 → 1:2 petrol/Et_2O) to afford recovered **3.3** (71.3 mg, 79%), and epoxide **3.89** as a clear colourless oil (18.9 mg, 21%). Data for **3.89** matched that previously synthesised.

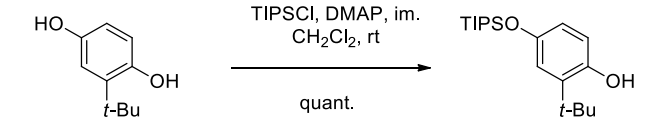

3.82: *t*-butylhydroquinone **3.83**

To a solution of *t*-butylhydroquinone (**3.82**) (5.00 g, 30.1 mmol) in CH_2Cl_2 (150 mL) was added imidazole (2.66 g, 39.1 mmol), then DMAP (1.83 g, 15.1 mmol), and finally TIPSCl (1.83 mL, 36.1 mmol) slowly. The reaction was stirred at room temperature for 15 h, then quenched by the addition of sat. NH_4Cl solution (50 mL). The layers were separated, and the organic phase was washed with sat. NH_4Cl solution (50 mL), then water (50mL), dried over $MgSO_4$, filtered, and concentrated *in vacuo*. The residue was purified by flash column chromatography on SiO_2 (10:1 petrol/EtOAc) to afford **3.83** as a pale yellow oil (10.6 g, quant.).

Data for **3.83**:

^{1}H NMR (500 MHz, $CDCl_3$) δ 6.91 (d, *J* = 2.9 Hz, 1H), 6.57 (dd, *J* = 2.9, 8.4 Hz, 1H), 6.50 (d, *J* = 8.44 Hz), 4.42 (br s, 1H), 1.37 (s, 9H), 1.25 – 1.18 (m, 3H), 1.09 (d, *J* = 7.2 Hz, 18H), 1.05 (s, 12H)
R_f 0.30 (15:1 petroleum ether/EtOAc)

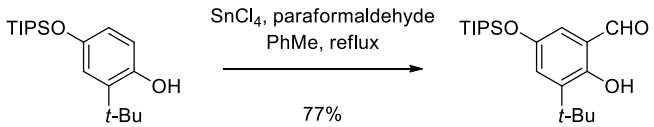

3.83 **3.84**

To a solution of **3.83** (4.45 g, 13.8 mmol) in PhMe (125 mL) was added 2,6-lutidine (1.9 mL, 16.6 mmol), then $SnCl_4$ (0.47 mL, 4.10 mmol). The mixture was stirred at room temperature until a yellow suspension formed, then paraformaldehyde (1.66 g, 55.2 mmol, formaldehyde) was added. The resultant mixture was heated to reflux for 6 h. The reaction was cooled to room temperature and Et_2O (125 mL) and water (125 mL) were added. Solids were removed by filtering through a pad of celite, and the pad was washed with Et_2O (~50 mL). The layers were separated and the organic phase was washed with water (100 mL), then brine (100 mL), dried over $MgSO_4$, filtered, and concentrated *in vacuo*. The residue was purified by flash column chromatography on SiO2 (10:1 petrol/EtOAc) to afford **3.84** as a yellow oil (3.72 g, 77%).

Data for **3.84**:

^{1}H NMR (500 MHz, $CDCl_3$) δ 11.40 (s, 1H), 9.77 (s, 1H), 7.13 (d, *J* = 2.9 Hz), 6.83 (dd, *J* = 3.0, 14.4 Hz, 1H), 1.40 (s, 9H), 1.26 – 1.20 (m, 3H), 1.11 (d, *J* = 7.27, 18H)

R_f 0.60 (10:1 petroleum ether/EtOAc), 0.75 (6:1 petrol/EtOAc)

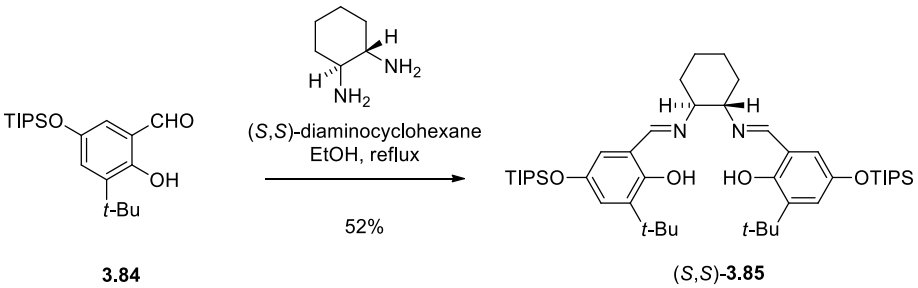

3.84 (S,S)-**3.85**

3.84 (1.60 g, 4.56 mmol) and (*S*,*S*)-diaminocyclohexane (0.260 mg, 2.28 mmol) were dissolved in EtOH (40 mL) and heated to reflux for 2 h. The reaction was slowly cooled to room temperature to crystalise, and the crystals were collected by vacuum filtration, giving the Schiff base (*S*,*S*)-**3.85** as yellow needles (930 mg, 52 %).

Data for **3.85**:

^{1}H NMR (500 MHz, $CDCl_3$) δ 13.38 (br s, 2H), 8.16 (s, 2H), 6.84 (d, *J* = 1.8 Hz, 2H), 6.47 (d, *J* = 1.8 Hz, 2H), 3.30 – 3.25 (m, 2H), 1.97 (d, *J* = 12.7 Hz, 2H), 1.87 (d, *J* = 9.2 H), 1.78 – 1.66 (m, 3H), 1.48 – 1.42 (m, 3H), 1.38 (s, 18H), 1.18 – 1.12 (m, 6H), 1.04 (d, *J* = 7.16 Hz, 36H)

^{13}C NMR (125 MHz, $CDCl_3$) δ 165.5, 154.7, 147.1, 122.3, 119.0, 72.5, 34.9, 33.2, 29.5, 24.4, 18.1, 12.7

R_f 0.65 (8:1 petrol/EtOAc)

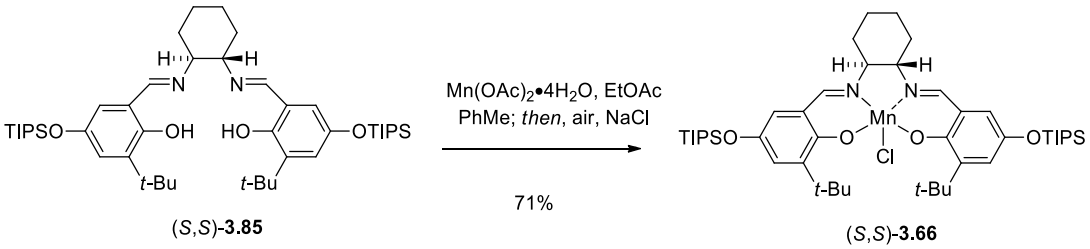

(S,S)-**3.85** (S,S)-**3.66**

To a refluxing solution of $Mn(OAc)_2 \cdot 4H_2O$ (877 mg, 3.58 mmol) in EtOH (10 mL) was added a solution of (*S*,*S*)-**3.85** (930 mg, 1.19 mmol) in PhMe (10 mL) dropwise. Additional PhMe (5 mL) was used to rinse the dropping funnel. Air was then bubbled through the solution as the reaction was

heated at reflux for 1.5 h, after which brine (5 mL) was added, and the mixture was cooled to room temperature. PhMe (30 mL) was added and the layers were separated. The organic phase was washed with water (20 mL × 3), then brine (20 mL), dried over Na_2SO_4, filtered, and concentrated *in vacuo*. The residue was dissolved in CH_2Cl_2 (5 mL), and *n*-heptane (5 mL) was carefully added. The mixture was left to slowly evaporate CH_2Cl_2 and crystalise out the product. **3.66** was collected by filtration as small brown granular crystals (746 mg, 71%).

Data for **3.66**:

NMR Not applicable (paramagnetic)
IR (neat) $\bar{\nu}$ 2951, 2906, 1605, 1533, 1431, 1388, 1314, 1251, 1174, 1033, 838 cm^{-1}
R_f 0.00 (10:1 petrol/EtOAc)

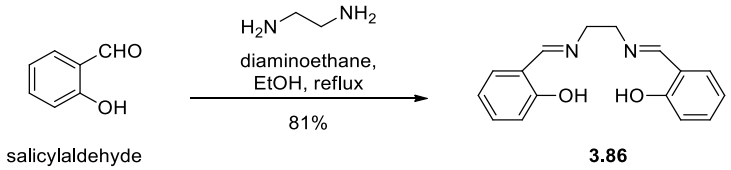

To a solution of salicylaldehyde (2.1 mL, 20.0 mmol) in EtOH (40 mL) was added ethylenediamine (1.3 mL, 10.0 mmol). The mixture was heated to reflux for 1 h, then cooled slowly to 0 °C to crystallise. The crystals were collected by vacuum filtration to afford the Schiff base **3.86** as yellow flakes (2.11 g, 81%).

Data for **3.86**:

^{1}H NMR (500 MHz, $CDCl_3$) δ 13.19 (br s, 2H), 8.35 (s, 2H), 7.29(t, *J* = 7.8 Hz, 2H), 7.22 (d, *J* = 7.6 Hz, 2H), 6.94 (d, *J* = 8.3 Hz, 2H), 6.85 (t, *J* = 7.5 Hz, 2H), 3.93 (s, 4H)

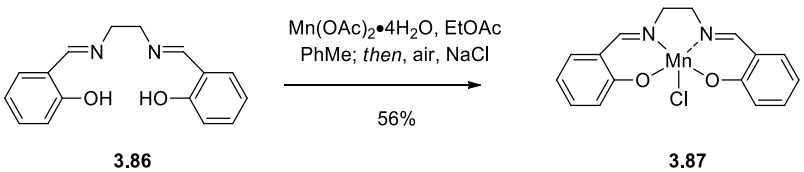

To a refluxing solution of **3.86** (160 mg, 0.596 mmol) in 95% EtOH (10 mL) was added $Mn(OAc)_2 \cdot 4H_2O$ (292 mg, 1.19 mmol) and the resultant mixture was stirred at reflux for 30 min. The reaction was then cooled to room temperature and CH_2Cl_2 (25 mL) was added. The mixture was

extracted with brine (10 mL × 3) and the aqueous phase was filtered to give **3.87** as a dark brown/black solid (120 mg, 56%).

Data for **3.87**

NMR Not applicable (paramagnetic)

IR (neat) $\bar{\nu}$ 3378, 1660, 1623, 1598, 1539, 1469, 1443, 1333, 1287, 1201, 1129, 1050 cm^{-1}

R_f 0.00 (10:1 petrol/EtOAc)

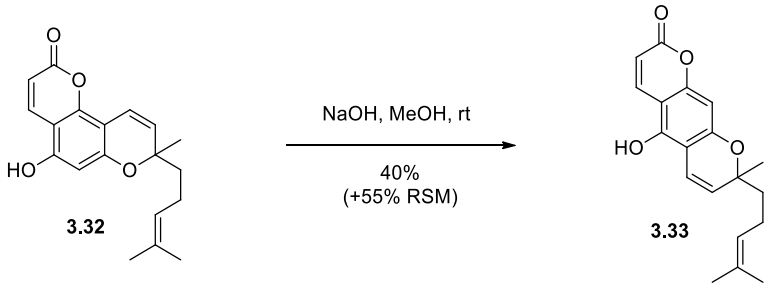

To a suspension of chromene **3.32** (1.01 g, 3.23 mmol) in MeOH (10 mL) was added 1% NaOH in MeOH (25 mL, 6.25 mmol) and the resultant solution was stirred at room temperature for 26 h. The reaction mixture was then acidified by careful addition of 1 M HCl solution (~10 mL) at 0 °C until precipitate formed. Brine (30 mL) was added and the mixture was extracted with Et_2O (30 mL × 3). The combined organic extracts were dried over $MgSO_4$, filtered, and concentrated *in vacuo*. The residue was purified by flash column chromatography on SiO_2 (2:1 → 1:1 petrol/Et_2O) to give recovered **3.32** as a pale yellow solid (554 mg, 55%). Further elution gave chromene **3.33** as a white solid (400 mg, 40%).

Data for **3.33**:

^{1}H NMR (600 MHz, $CDCl_3$) δ 8.11 (d, *J* = 9.6 Hz, 1H), 7.48 (br s, 1H), 6.71 (d, *J* = 10.2 Hz, 1H), 6.36 (s, 1H), 6.15 (d, *J* = 9.6 Hz, 1H), 5.62 (d, *J* = 10.2 Hz, 1H), 5.06 (tt, *J* = 7.1, 1.5 Hz, 1H), 2.07 (h, *J* = 5.7 Hz, 2H), 1.75 (ddd, *J* = 14.0, 10.3, 6.4 Hz, 1H), 1.68 – 1.62 (m, overlapped, 1H) 1.64 (d, *J* = 1.6 Hz, 3H), 1.55 (d, *J* = 1.3 Hz, 3H), 1.40 (s, 3H)

^{13}C NMR (150 MHz, $CDCl_3$) δ 163.1, 158.3, 155.7, 149.0, 140.3, 132.9, 128.6, 123.7, 115.6, 110.1, 106.1, 104.0, 97.4, 79.9, 41.4, 26.8, 25.8, 22.7, 17.8

IR (neat) $\bar{\nu}$ 3282, 2970, 2925, 1685, 1612, 1565, 1451, 1406, 1353, 1195, 1084 cm^{-1}

R_f 0.20 (2:1 petrol/EtOAc), 0.10 (1:1 petrol/Et_2O), 0.25 (20:1 CH_2Cl_2/EtOAc)

m.p. 121 – 130 °C

HRMS (ESI) Calculated for $C_{19}H_{20}O_5Na$ 313.1434 $[M+H]^+$, found 313.1437

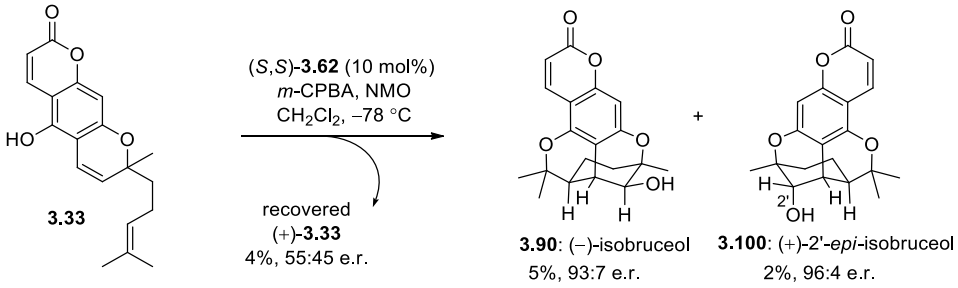

To a solution of (±)-**3.33** (210 mg, 0.672 mmol) in CH_2Cl_2 (10 mL) at −78 °C was added (*S*,*S*)-**3.62 (**Jacobsen's catalyst) (43.0 mg, 0.0670 mmol). After 2 min, NMO (157 mg, 1.34 mmol) was added, followed by *m*-CPBA (77%, 165 mg, 0.740 mmol). The reaction mixture was stirred at −78 °C for 30 min. The reaction mixture was quenched with solid $Na_2S_2O_3$ (1 g) and 1 M NaOH solution (5 mL) and then stirred for 10 min at room temperature. The mixture was filtered through Celite and concentrated *in vacuo*, then dissolved in Et_2O (20 mL) and washed with 1 M NaOH (10 mL), water (10 mL) and brine (10 mL). The organic phase was dried over $MgSO_4$, filtered and concentrated *in vacuo*. The residue was dissolved in Et_2O and filtered through a short pad of SiO_2, flushed through with excess Et_2O (150 mL), and concentrated *in vacuo*. The residue was purified by flash column chromatography on SiO_2 (1:1 → 1:3 petrol/Et_2O) to afford recovered (+)-**3.33** as a white solid (7.4 mg, 4%, **$[\alpha]^{20}_D$ =** +21.0 ($CHCl_3$, c = 21.01), e.r. 55:45). Further elution gave (+)-**3.100** as a white solid (5.4 mg, 2%, e.r. 93:7), followed by isobruceol (−)-**3.90** as a white solid (9.9 mg, 5%, e.r. 96:4).

Data for (+)-**3.100**:

^{1}H NMR (600 MHz, $CDCl_3$) δ 7.87 (d, *J* = 9.5 Hz, 1H), 6.46 (br s, 1H), 6.13 (d, *J* = 9.5 Hz, 1H), 4.28 (t, *J* = 4.4 Hz, 1H), 2.97 (dd, *J* = 5.0, 2.8 Hz, 1H), 2.59 (ddd, *J* = 11.7, 5.5, 2.7 Hz, 1H), 2.02 (d, *J* = 4.4 Hz, 1H), 1.85 (ddd, *J* = 15.2, 13.1, 7.0 Hz, 1H), 1.65 (dd, *J* = 15.4, 6.2 Hz, 1H), 1.60 (s, 3H), 1.43 (s, 3H), 1.26 (dt, *J* = 11.9, 6.0 Hz, 1H), 1.10 (s, 3H), 0.60 (tdd, *J* = 13.1, 11.6, 6.2 Hz, 1H)
^{13}C NMR (150 MHz, $CDCl_3$) δ 162.0, 158.6, 154.9, 153.6, 138.3, 111.8, 111.2, 105.6, 96.8, 86.7, 78.5, 69.7, 39.3, 34.3, 31.8, 29.5, 24.9, 24.5, 21.2
$[\alpha]^{20}_D$ = +133.1, ($CHCl_3$, c = 0.12)
IR (neat) $\bar{\nu}$ 3434, 2976, 1714, 1617, 1568, 1447, 1390, 1348, 1314, 1257, 1187, 1142, 1077 cm^{-1}
R_f 0.55 (neat Et_2O)
HRMS (ESI) Calculated for $C_{19}H_{21}O_5$: 329.1384 $[M+H]^+$, found: 329.1383

Data for (−)-isobruceol (**3.90**):

^{1}H NMR (500 MHz, $CDCl_3$) δ 7.85 (d, *J* = 9.5 Hz, 1H), 6.50 (s, 1H), 6.13 (d, *J* = 9.6 Hz, 1H), 3.83 (s, 1H), 2.90 (t, *J* = 2.5 Hz, 1H), 2.31 (ddd, *J* = 11.6, 5.4, 2.7 Hz, 1H), 2.16 (s, 3H), 1.91 (dd, *J* = 15.3, 5.9 Hz, 1H), 1.48 (ddd, *J* = 15.1, 13.3, 7.0 Hz, 1H), 1.46 (s, 3H), 1.22 (dt, *J* = 13.3, 6.7 Hz, 1H), 1.07 (s, 3H), 0.55 (tdd, *J* = 13.5, 11.6, 6.3 Hz, 1H)

^{13}C NMR (125 MHz, $CDCl_3$) 161.8, 158.3, 154.8, 154.2, 138.1, 111.6, 110.1, 105.9, 97.3, 86.5, 79.3, 71.0, 47.4, 36.7, 36.3, 29.6, 24.4, 24.3, 21.6

$[\alpha]^{20}_D$ = −87.1 ($CHCl_3$, c = 0.57)

IR (neat) $\bar{\nu}$ 3434, 2977, 2936, 1719, 1617, 1569, 1446, 1388, 1338, 1315, 1258, 1142, 1077 cm^{-1}

R_f 0.20 (2:1 petrol/EtOAc), 0.35 (neat Et_2O)

HRMS (ESI) Calculated for $C_{19}H_{20}O_5Na$: 351.1203 $[M+Na]^+$, found: 351.1206

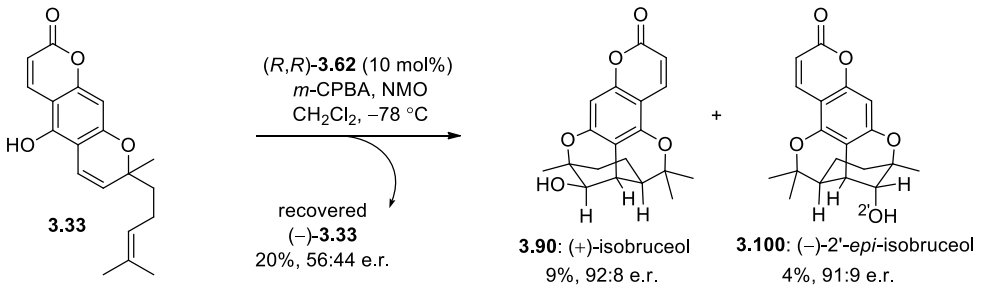

To a solution of **3.33** (261 mg, 0.836 mmol) in CH_2Cl_2 (5 mL) at −78 °C was added (*R*,*R*)-**3.62** (53.0 mg, 0.0856 mmol) followed by NMO (489 mg, 4.18 mmol) in three portions. Then *m*-CPBA (77%, 281 mg, 1.25 mmol) was added in portions over 5 min. The mixture was stirred for a further 10 min, then quenched with Me_2S (0.5 mL), warmed to room temperature, and filtered through a pad of SiO_2, flushed with excess Et_2O (400 mL), and concentrated *in vacuo*. 1 M NaOH (5 mL) was added to the residue and stirred, followed by 1 M HCl (8 mL). The resulting mixture was extracted with Et_2O (75 mL). The organic phase was washed sequentially with $NaHCO_3$ (20 mL × 4), water (20 mL), then brine (20 mL), dried over $MgSO_4$, filtered, and concentrated *in vacuo*. The residue was purified by flash column chromatography on SiO_2 (1:1 → 0:1 petrol/Et_2O) to give recovered (−)-**3.33** (53.9 mg, 20%, **$[\alpha]^{20}_D$** = −22.8, ($CHCl_3$, c = 1.08), e.r. 56:44). Further elution gave (−)-**3.100** (9.7 mg, 4%, **$[\alpha]^{20}_D$ =** −68.8 ($CHCl_3$, c = 0.18), e.r. 91:9), followed by (+)-isobruceol (**3.90**) (25.9 mg, 9% **$[\alpha]^{20}_D$** = +74.3 ($CHCl_3$, c = 0.45), e.r. 92:8). Data for **3.90** and **3.100** matched what was previously reported.

3.4.3 Extraction of *Philotheca brucei* Procedures

Philotheca brucei was collected from the Koolyanobbing Range (approx. 500 km east of Perth, GPS location E749300 N6581700). Voucher specimens were donated to the Perth Herbarium.

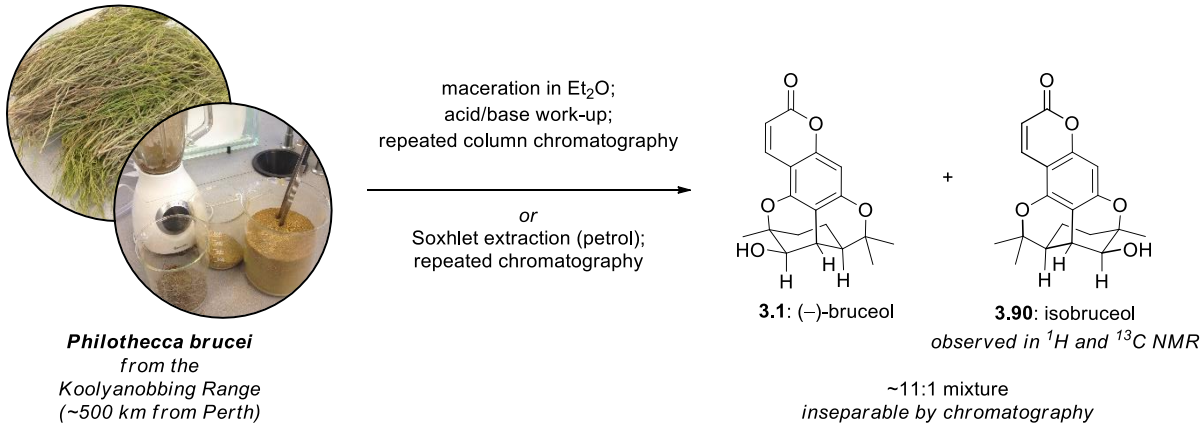

Fresh *P.* brucei (1.0 kg) was cut into a crude mulch and macerated in Et_2O (~3 L) for 5 days with intermittent stirring. The extract was filtered and concentrated to ~750 mL, then washed sequentially with 5% HCl (500 mL × 2), 8% $NaHCO_3$ (500 mL × 2), and 5% NaOH (500 mL × 2). The organic phase was dried over anhydrous $MgSO_4$, filtered and the solvent was removed *in vacuo*, giving a green, fragrant oil. The volatiles (mostly eucalyptol) were removed by vacuum distillation. The residue was purified by sequential flash column chromatography on SiO_2 (10:1 → 1:1 petrol/EtOAc, then 2:1 petrol/EtOAc) to give a mixture of bruceol **3.1** and isobruceol **3.90** (500 mg, 11:1 in favour of **3.1**). The mixture was then recrystallised from petrol/EtOAc to afford pure **3.1** as colourless prisms (140 mg), and the residue was repurified by flash column chromatography to afford an enriched mixture of bruceol **3.1** and isobruceol **3.90** (300 mg, 4.5:1 in favour of **3.1**). Further recrystallization from petrol/EtOAc afforded more **3.1** as colourless prisms (36 mg). The residue was repurified by flash column chromatography (2:1 petrol/EtOAc) to afford a further enriched mixture of bruceol **3.1** and isobruceol **3.90** (200 mg, 2:1 in favour of **3.1**). No more bruceol **3.1** in the residue could be removed by crystallization. The residue was then purified by semi-preparative reverse phase HPLC on an Ascentis ® C18 column (25 cm × 10 mm, 5 μm) (MeCN/H_2O, gradient elution) to afford isobruceol **3.90** as a white solid (11 mg). A single crystal was obtained by recrystallization from $CHCl_3$/Et_2O.

Data for isobruceol (**3.90**):

^{1}H NMR (500 MHz, $CDCl_3$) δ 7.85 (d, *J* = 9.6 Hz, 1H), 6.51 (s, 1H), 6.14 (d, *J* = 9.5 Hz, 1H), 3.83 (s, 1H), 2.91 (t, *J* = 2.4 Hz, 1H), 2.32 (ddd, *J* = 11.7, 5.6, 2.7 Hz, 1H), 2.14 (s, 1H), 1.92 (dd, *J* = 15.5, 6.2 Hz, 1H), 1.62 (s, 3H), 1.50 (ddd, *J* = 15.0, 13.3, 7.2 Hz, 1H) 1.47 (s, 3H), 1.23 (dt, *J* = 13.2, 6.4 Hz, 1H), 1.07 (s, 3H), 0.56 (tdd, *J* = 13.6, 11.7, 6.2 Hz, 1H)

^{13}C NMR (125 MHz, $CDCl_3$) δ 161.8, 158.3, 154.7, 154.2, 138.1, 111.6, 110.1, 105.9, 97.3, 86.5, 79.3, 71.0, 47.4, 36.7, 36.2, 29.6, 24.4, 24.3, 21.6

IR (neat) $\bar{\nu}$ 3422, 2925, 1718, 1617, 1568, 1446, 1387, 1338, 1315, 1258, 1214, 1193 cm^{-1}

R_f 0.20 (1:1 petrol/EtOAc)

HRMS (ESI) Calculated for $C_{19}H_{19}O_5$ 329.1384 $[M+H]^+$, found 329.1386

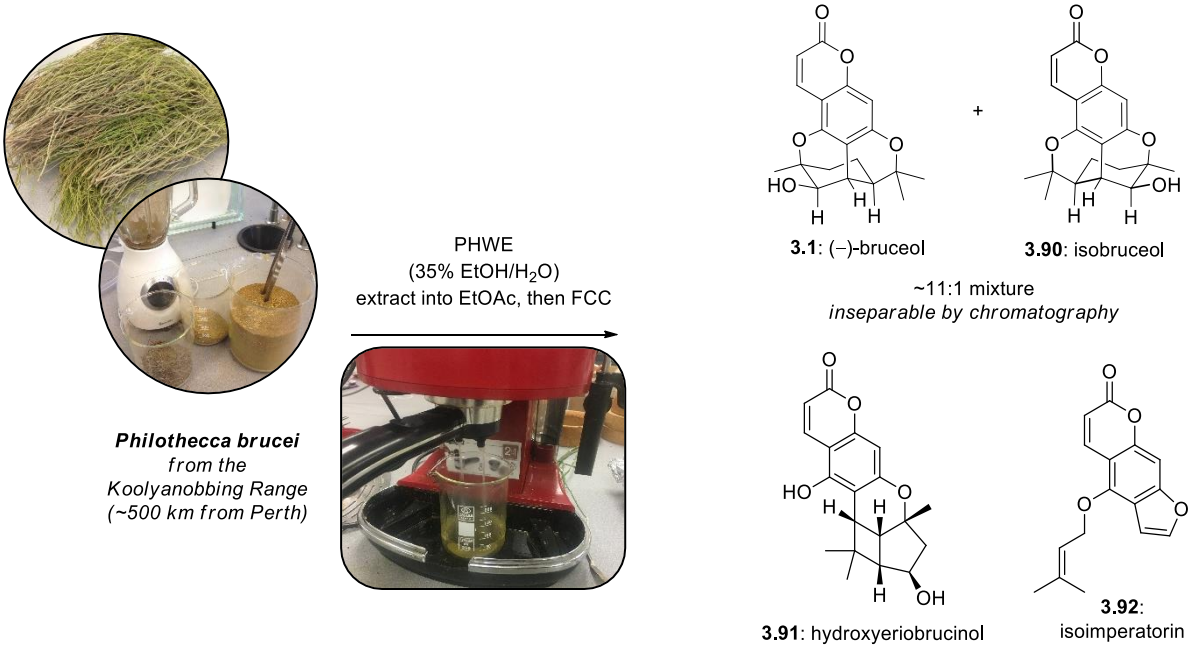

Dried and finely powdered *Philotheca brucei* (10.0 g) was mixed with sand (3.5 g), placed in the portafilter (sample compartment) of a conventional, unmodified espresso machine and extracted with 35% EtOH in water (100 mL × 2). The process was repeated nine times (100 g total plant material). The combined extracts were concentrated to ~200 mL on a rotary evaporator (40 °C bath) and the aqueous phase was extracted with EtOAc (200 mL × 4). The combined organic extracts were washed with brine (200 mL × 2), dried over $MgSO_4$, and concentrated *in vacuo*. The residue was initially purified by flash column chromatography on SiO_2 (10:1 → 1:1 petrol/Et_2O, gradient elution) giving fractions containing a non-polar fragrant oil, shown to be mostly eucalyptol (254 mg), a brown oil containing a complex mixture of compounds (944 mg), and a mixture of (–)-bruceol (**3.1**), (–)-isobruceol (**3.90**), and (–)-hydroxyeriobrucinol (**3.91**) as well as other minor impurities (1.1 g). Flash

column chromatography on SiO_2 (4:1 petrol/EtOAc) of the brown oil gave crude isoimperatorin (**3.92**) as a brown solid (55 mg), which was recrystallised (petrol/EtOAc) to afford **3.92** as white needles (18.1 mg, 0.018% w/w).. Trituration of the mixture containing **3.1**, **3.90**, and **3.91** with $CHCl_3$ (20 mL) gave (–)-hydroxyeriobrucinol (**3.91**) as a white powder (438 mg, 0.44% w/w).

Data for isoimperatorin (**3.92**):

^{1}H NMR (600 MHz, $CDCl_3$) δ 8.16 (dd, *J* = 9.8, 0.7 Hz, 1H), 7.60 (d, *J* = 2.3 Hz, 1H), 7.16 (t, *J* = 0.8 Hz, 1H), 6.96 (dd, *J* = 2.3, 1.0 Hz, 1H), 6.27 (d, *J* = 9.8 Hz, 1H), 5.54 (tt, *J* = 7.0, 1.5 Hz, 1H), 4.92 (dt, *J* = 7.1, 0.9 Hz, 2H), 1.80 (s, 3H), 1.70 (s, 3H)
^{13}CNMR (150 MHz, $CDCl_3$) δ 161.5, 158.3, 152.8, 149.1, 145.0, 140.0, 139.8, 119.2, 114.3, 112.7, 107.7, 105.2, 94.4, 69.9, 26.0, 18.4
IR (neat) 3026, 2997, 2667, 1603, 1507, 1460, 1443, 1286, 1238, 1229, 1179, 1039 cm^{-1}
m.p. 98.2 – 99.2 °C (*lit.*[53] 110 °C)
R_f 0.40 (1:1 petrol/Et_2O)
HRMS (ESI) calculated for $C_{16}H_{15}O_4$ 271.0968 $[M+H]^+$, found: 271.0971

Data for hydroxyeriobrucinol (**3.91**):

^{1}H NMR (500 MHz, d_5-pyridine) δ 8.29 (d, *J* = 9.6 Hz, 1H), 6.73 (s, 1H), 6.25 (d, *J* = 9.6 Hz, 1H), 4.51 (d, *J* = 5.0 Hz, 1H), 3.47 (d, *J* = 9.7 Hz, 1H), 2.92 (dd, *J* = 9.7, 7.5 Hz, 1H), 2.75 (d, *J* = 7.4 Hz, 1H), 2.52 (dd, *J* = 14.0, 5.2 Hz, 1H), 2.25 (d, *J* = 13.9 Hz, 1H), 1.87 (s, 3H), 1.53 (s, 3H), 0.99 (s, 3H)
^{13}C NMR (125 MHz, d_5-pyridine) δ 161.6, 158.7, 155.6, 154.9, 140.1, 111.1, 111.0, 105.1, 98.7, 85.6, 73.4, 57.2, 48.7, 39.0, 38.7, 36.6, 34.5, 29.9, 19.0; IR (neat) 3289, 2972, 2936, 1683, 1605, 1562, 1446, 1405, 1357, 1283, 1253, 1146, 1107
$[\alpha]_D^{25°C}$ −181 (MeOH, c = 1.0)
m.p. 245 – 249 °C (decomposes) (needles from EtOH)
R_f 0.15 (1:1 petrol/EtOAc)
HRMS (ESI) calculated for $C_{19}H_{21}O_5$ 329.1384 $[M+H]^+$, found: 329.1384.

3.4.4: Biochemical Methods

Orcinol model (**3.67**)

The *in vitro* reactions of the CYP101 enzymes were carried out in a 2 mL mixture of the following: P450 (1 µM), ferredoxin (Arx, 2.5 µM), ferredoxin reductase (ArR, 1 µM), Catalase (12 µL of 10 mg mL^{-1} stock in glycerol), NADH (8 mM), tris buffer (50 mM, pH 7.4) and (±)-**3.67** (500 µM). For the $P450_{BM3}$ variants, reactions were carried out in a 2 mL mixture of the following: P450 (2 µM), Catalase (12 µL of 10 mg mL^{-1} stock in glycerol), NADPH (8 mM), tris buffer (50 mM, pH 7.4) and (±)-**3.67** (500 µM). All enzymatic reactions were carried out at room temperature and in 10 mL conical flasks shaken at 50 rpm. The reactions were extracted with EtOAc (2 x 500 µL) and analysed by GC-MS. The $P450_{BM3}$-GVQ variant was the only enzyme tested that gave product formation.

Chromene (±)-**3.67:**

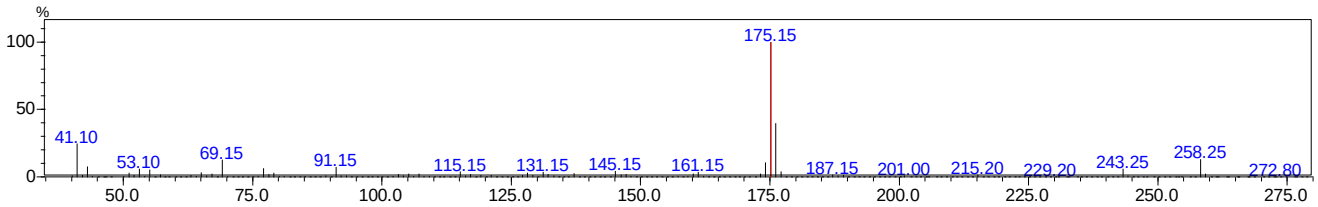

(a) **(**±)-**3.67** synthetic control with expected mass of 258 (m/z = 258.25). T_R = 12.9 min.

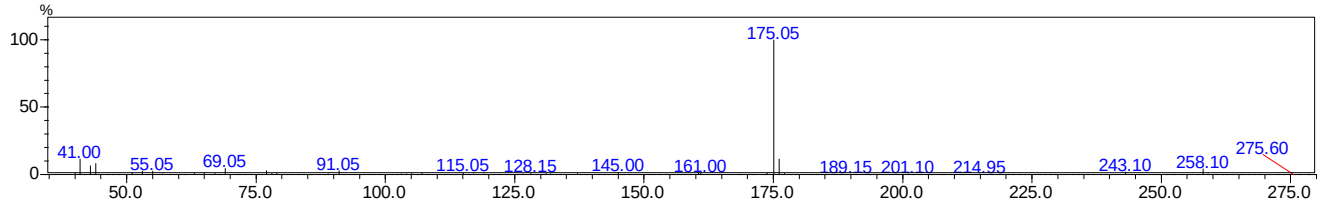

(b) Unreacted (±)-**3.67** from enzyme turnover with expected mass of 258 (m/z = 258.1). T_R = 12.9 min.

Bruceol analogue (+)-**3.70**:

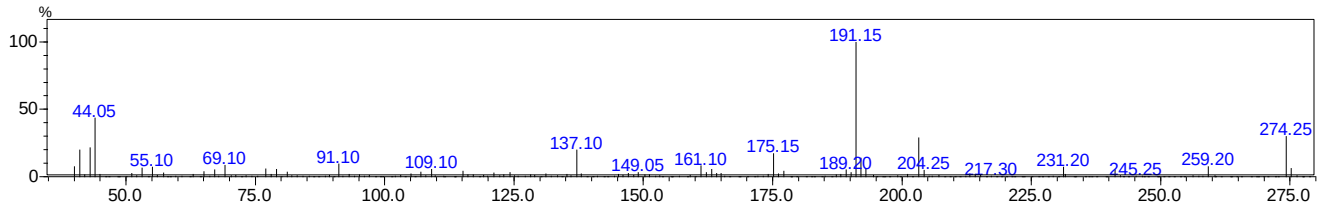

(a) Bruceol analogue (+)-**3.70** synthetic control with expected mass of 274 (m/z = 274.25). T_R = 13.0 min.

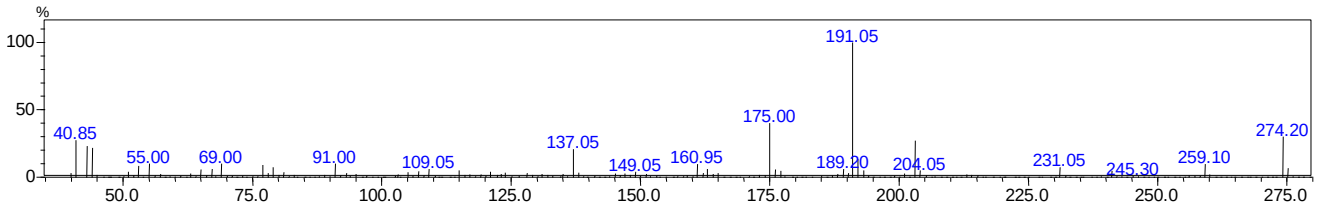

(b) Bruceol analogue (+)-**3.70** from enzyme turnover with expected mass of 274 (m/z = 274.2). T_R = 13.0 min.

Chromene epoxide **3.104**:

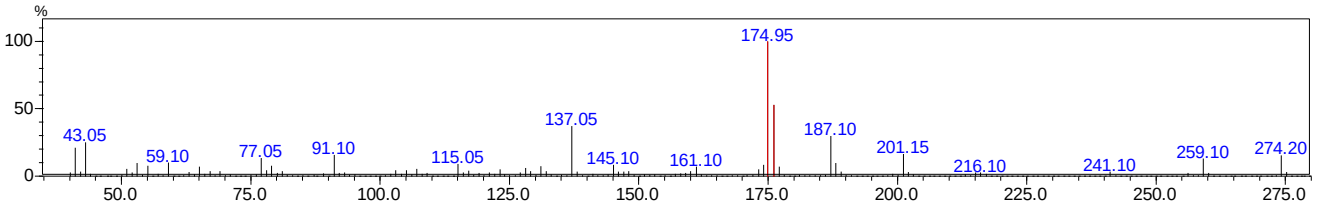

(a) Chromene epoxide **3.104** synthetic control with expected mass 274 (m/z = 274.2). T_R = 14.3 min.

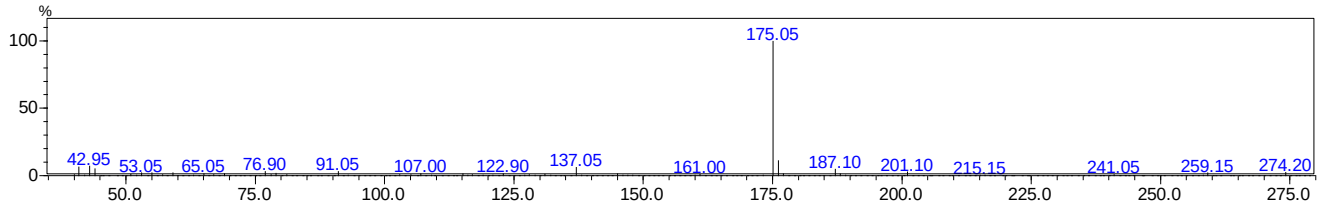

(b) Chromene epoxide **3.104** from enzyme turnover with mass 274 (m/z = 274.20). T_R = 14.3 min.

Figure 3.14: MS data for the products of $P450_{BM3}$-GVQ turnover with (±)-**3.67**.

Bruceol (**3.1**) and Isobruceol (**3.90**)

Several variants of $P450_{BM3}$ were tested with (±)-**3.3** and (±)-**3.33** as listed below:

Plasmid	**$P450_{BM3}$ Mutants**	**Antibiotic**
pET22	R47L/Y51F/F87A	ampicillin
pET28	R47L/Y51F/F87A/I401P R47L/Y51F/F87V/E267V/I401P KSK19/I263A/A328I KSK19/I259V KSK19/Q403P	kanamycin
KSK19 ≡ F87A/H171L/Q307H/N319Y		

Table 3.3: $P450_{BM3}$ Mutants tested with (±)-**3.3** and (±)-**3.33**.

The plasmids listed in Table S1 were transformed in competent BL21(DE3) cells and grown on Luria-Bertani (LB) agar plates containing ampicillin (100 μg mL^{-1}) or kanamycin (30 μg mL^{-1}) depending on the vector used. A single colony from the plates was used to inoculate 100 mL of LB containing the appropriate antibiotic and 300 μL of trace elements solution. The culture was the allowed to grow at 37 °C and 120 rpm for 6 h, which was followed by lowering the incubation temperature to 18 °C for 30 min. Benzyl alcohol (0.02 % v/v) and EtOH (2 % v/v) were then added to the culture. The culture was left for 30 min and protein expression was then induced by adding IPTG (0.1 mM). The culture was then left for 16 h at 18 °C and 90 rpm. The cells were harvested via centrifugation (5000 *g*, 15 min). The cells pellets were re-suspended in 40 mL of tris buffer. Sonication was used to lyse the cells Autotune CV334 Ultrasonic Processor equipped with a standard probe (136 mm x 13 mm; Sonics and Materials, US) using 5 x 5 s pulses at 0 °C. Cell debris was then removed using centrifugation (18000 g, 30 min, 4 °C). The supernatant was concentrated using ultrafiltration (30 kDa exclusion membrane) to a volume of 5 mL and the concentration of the P450 enzyme was determined by measuring the UV-visible absorbance spectrum of the supernatant (ε_{418} = 95 mM^{-1} cm^{-1}). Reactions of all $P450_{BM3}$ variants with (±)-**3.3** was carried out in a 2 mL mixture of the following: P450 (2 μM), Catalase (12 μL of 10 mg mL^{-1} stock in glycerol), NADH (8 mM), tris buffer (50 mM, pH 7.4) and (±)-**3.3** (500 μM). Reactions of $P450_{BM3}$ variants KSK19/I263A/A328I and KSK19/I259V with (±)-**3.33** was carried out in a 2 mL mixture of the following: P450 (2 μM), Catalase (12 μL of 10 mg mL^{-1} stock in glycerol), NADH (8 mM), Tris Buffer (50 mM, pH 7.4) and (±)-**3.67** (500 μM). The reactions were extracted with EtOAc (2 x 500 μL) and analysed by chiral

analytical HPLC. Variants KSK19-I263A-A328I showed the highest levels of product formation with both (±)-**3.3** and (±)-**3.33**.

3.4.5: HPLC Methods

Chiral normal phase HPLC analysis of compounds (±)-**3.1**, (±)-**3.90**, and (±)-**3.70** were carried out on a Shimadzu system equipped with a DGU-20A5R degasser, 2 x LC-20AR pumps, SIL-20AC HT autosampler, SPD-M20A photodiode array detector and a CT0-20AC column oven. Separation of the chiral products was carried out using a CHIRALPAK® IG column (5 μm particle size, 4.6 mm diameter x 150 mm; Daicel Chemical Industries Ltd.) equipped with a Chiralpak® IG guard column (5 μm particle size, 4.0 mm diameter x 10 mm; Daicel Chemical Industries Ltd.). The injection volume was 10 μL. Flow rate was kept constant at 0.5 mL/min

For bruceol (±)-**3.1** and isobruceol (±)-**3.90** HPLC analysis was carried out by eluting at 10% *i*-PrOH in hexane for 5 min and increased to 40% *i*-PrOH in hexane over 1.0 min then held at 40% *i*-PrOH for over 30 minutes. Retention times are as follows: (+)-**3.1** 28.5 min, (−)-**3.1** 25.8 min, (−)-**3.90** 25.1 min, (+)-**3.90** 34.1 min.

For (±)-**3.70** HPLC analysis was carried out operating in isocratic mode eluting at 20% *i*-PrOH in *n*-hexane over 30 minutes. Retention times are as follows: (+)-**3.70** 12.3 min, (−)-**3.70** 13.3 min.

Chiral normal phase HPLC analysis of compounds (±)-**3.3**, (±)-**3.33**, (±)-**3.81**, (±)-**100**, (±)-**3.67**, and (±)-**3.73** were carried out on an Agilent Technologies 1260 infinity system. Separation of the chiral products was carried out using a Chiralpak AD-H column (5 μm particle size, 4.6 mm x 250 mm; Daicel Chemical Industries, Ltd). The injection volume was 10 μL. Flow rate was kept constant at 1 mL/min.

For (±)-**3.73** and (±)-**3.100** HPLC analysis was carried out by eluting at 10% *i*-PrOH in hexane over 30 min. Retention times are as follows: (−)-**3.73** 21.5 min, (+)-**3.73** 23.5 min, (−)-**3.100** 16.8 min, (+)-**3.100** 18.5 min.

For (±)-**3.33**, (±)-**3.3**, (±)-**3.67**, and (±)-**3.73** HPLC analysis was carried out by eluting at 5% *i*-PrOH in hexane over 30 min. Retention times are as follows: (+)-**3.33** 11.2 min, (−)-**3.33** 12.6 min, (−)-**3.3** 6.2 min, (+)-**3.3** 9.3 min, (+)-**3.67** 8.5 min, (−)-**3.67** 10.5 min, (+)-**3.73** 8.5 min, (−)-**3.73** 9.0 min.

3.4.6: NMR Spectra

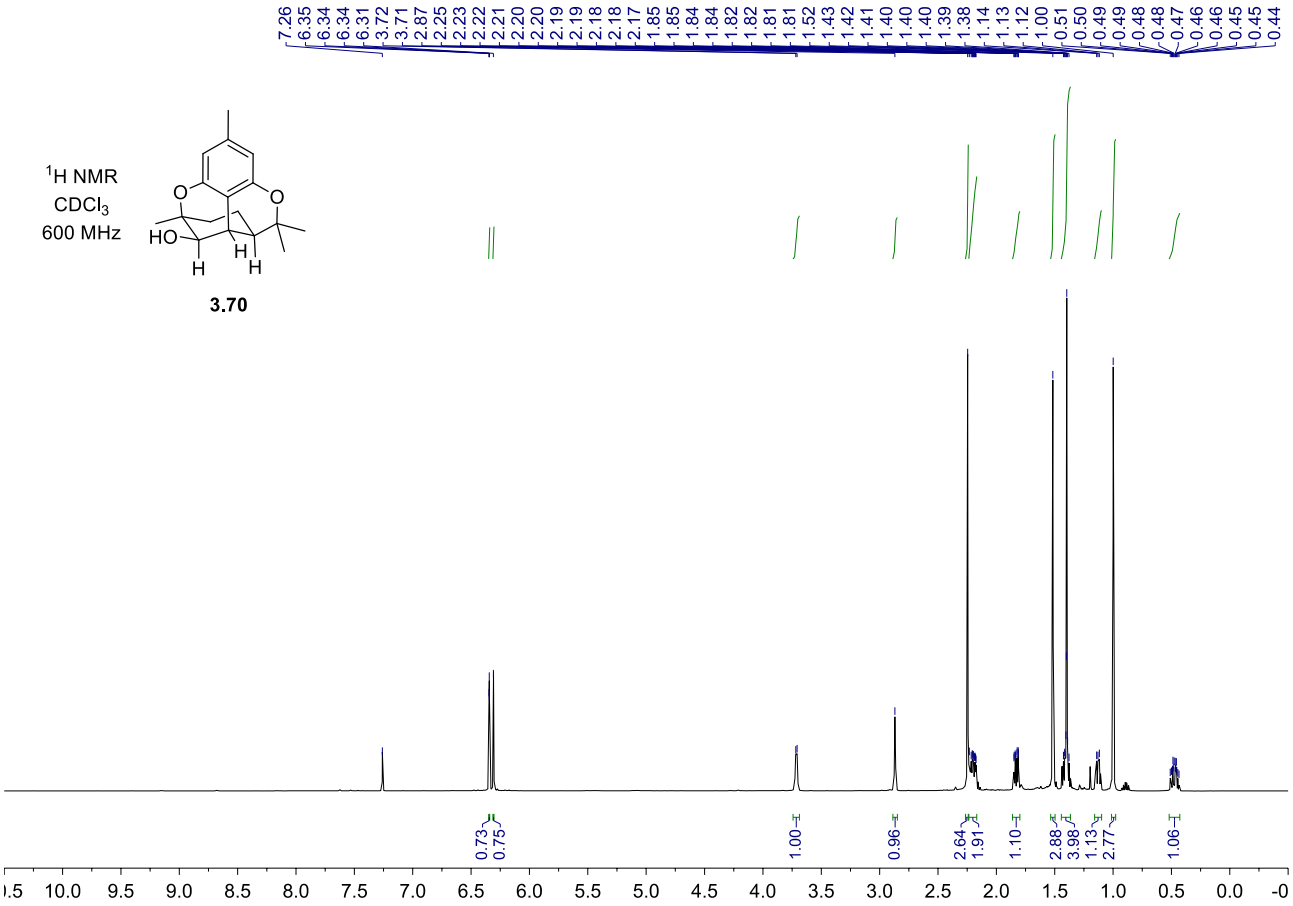

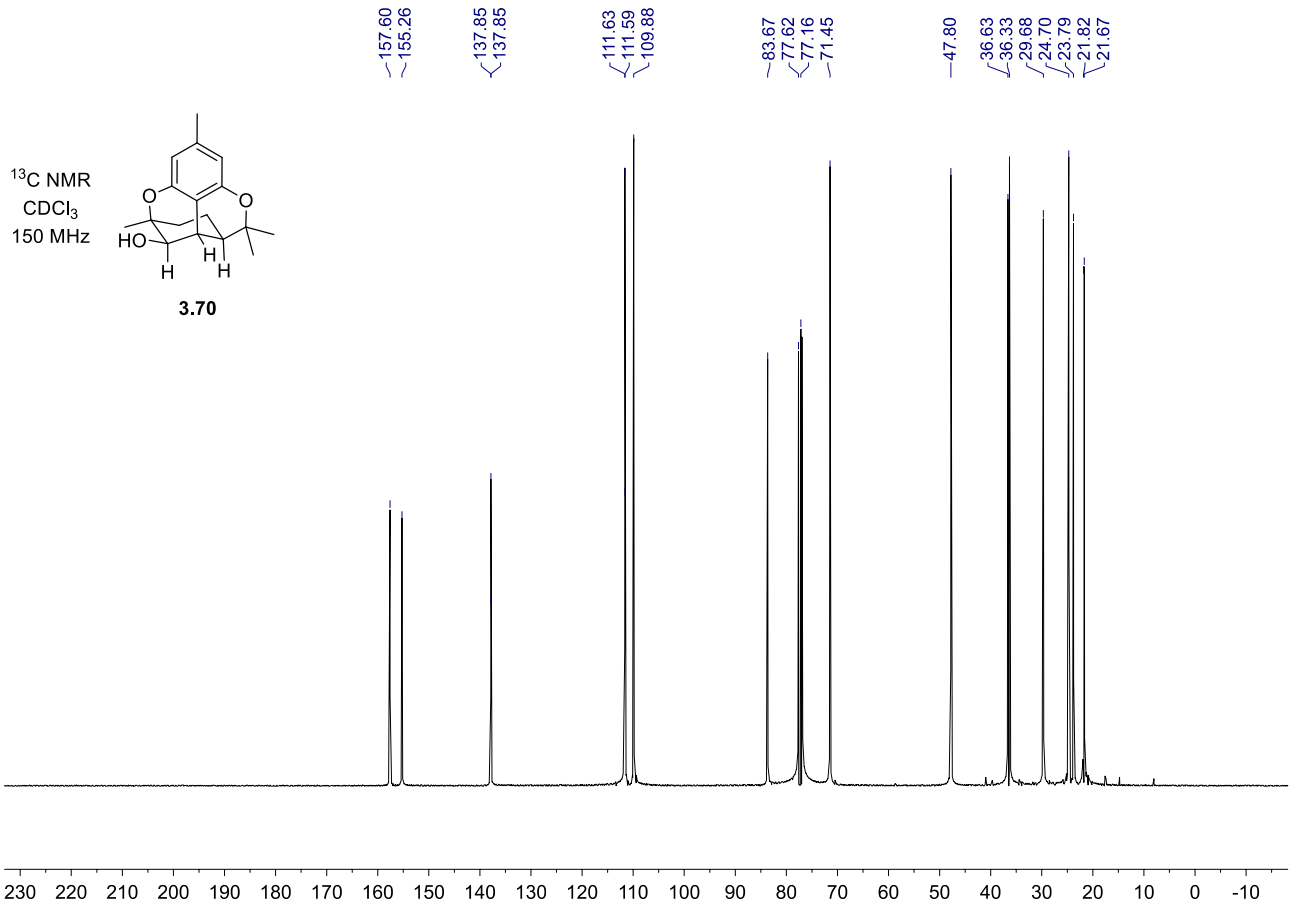

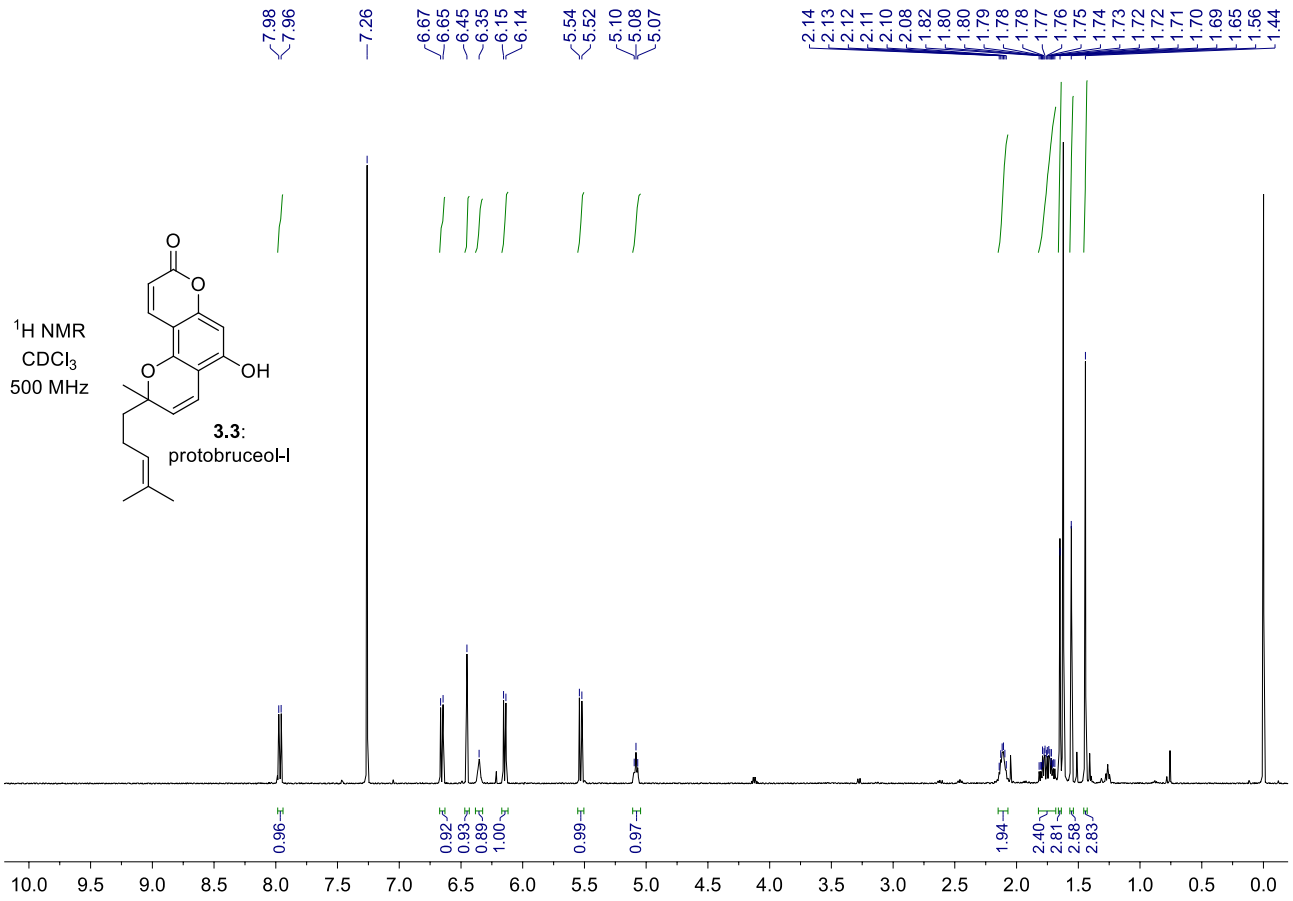
^{1}H NMR
$CDCl_3$
500 MHz
3.3:
protobruceol-I
OH
7.98
7.96
7.26
6.67
6.65
6.45
6.35
6.15
6.14
5.54
5.52
5.10
5.08
5.07
2.14
2.13
2.12
2.11
2.10
2.08
1.82
1.80
1.80
1.79
1.78
1.78
1.77
1.76
1.75
1.74
1.73
1.72
1.72
1.71
1.70
1.69
1.65
1.56
1.44
0.96
0.92
0.93
0.89
1.00
0.99
0.97
1.94
2.40
2.81
2.58
2.83
10.0
9.5
9.0
8.5
8.0
7.5
7.0
6.5
6.0
5.5
5.0
4.5
4.0
3.5
3.0
2.5
2.0
1.5
1.0
0.5
0.0

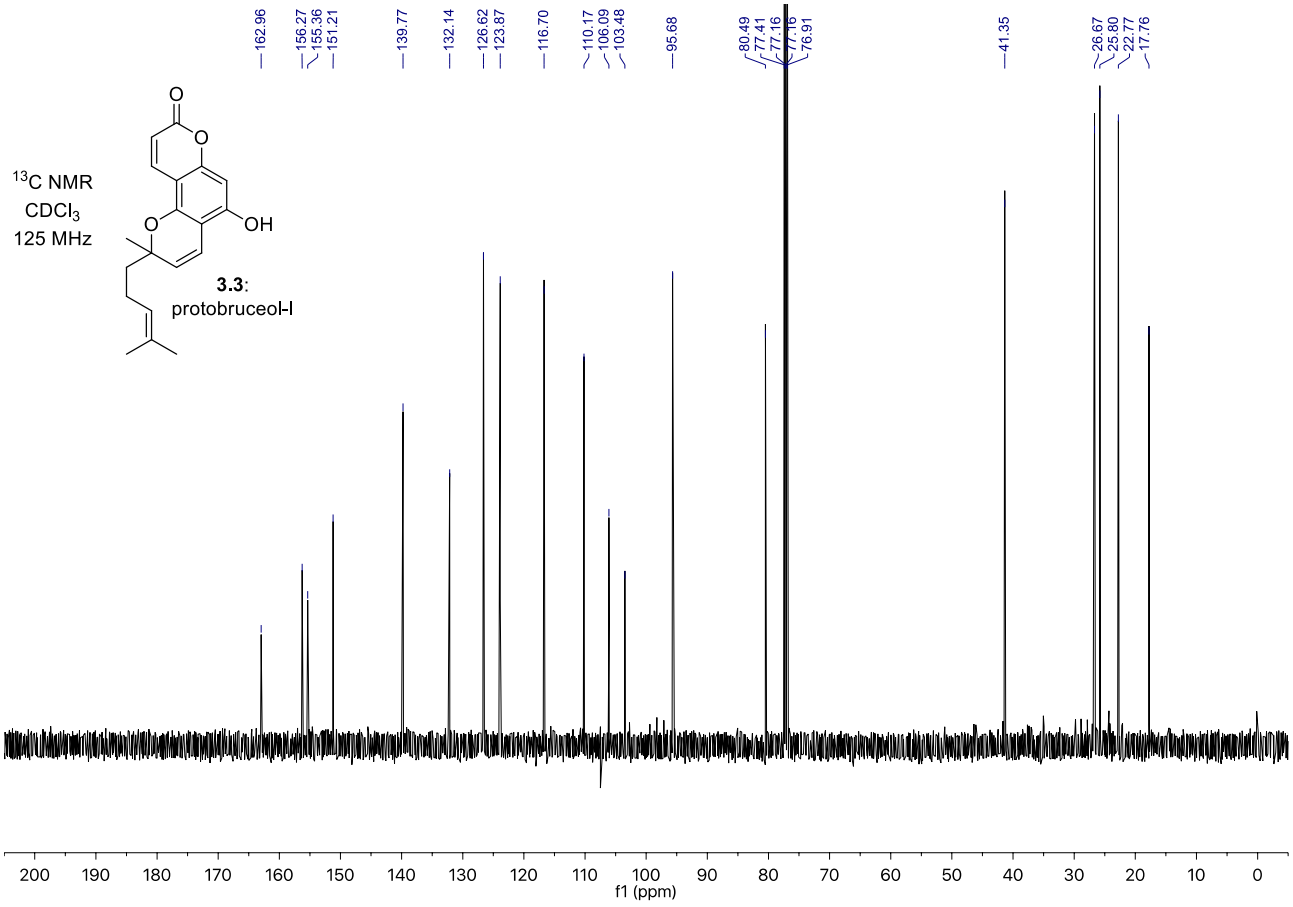
^{13}C NMR
$CDCl_3$
125 MHz
3.3:
protobruceol-I
OH
162.96
156.27
155.36
151.21
139.77
132.14
126.62
123.87
116.70
110.17
106.09
103.48
95.68
80.49
77.41
77.16
77.16
76.91
41.35
26.67
25.80
22.77
17.76
200
190
180
170
160
150
140
130
120
110
100
90
80
70
60
50
40
30
20
10
0
f1 (ppm)

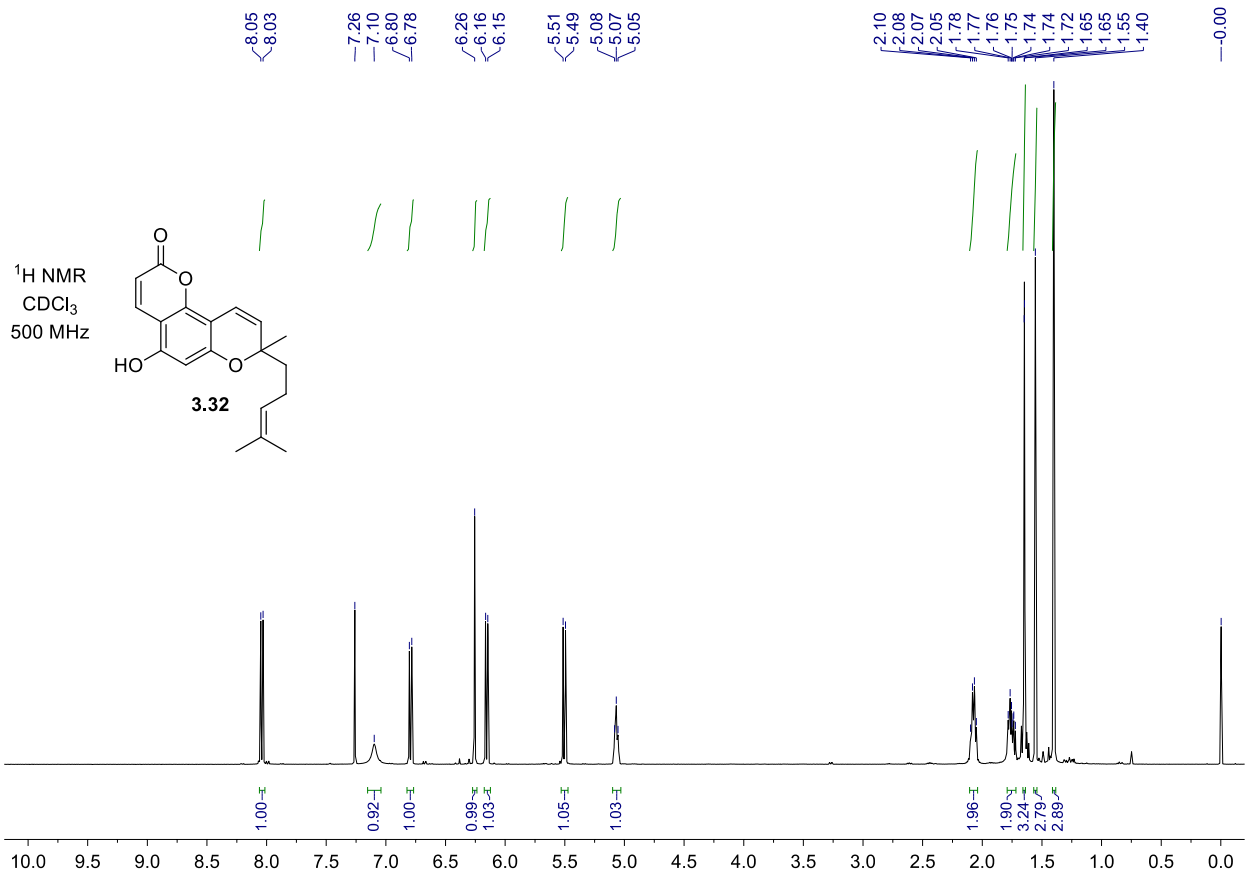
8.05
8.03
7.26
7.10
6.80
6.78
6.26
6.16
6.15
5.51
5.49
5.08
5.07
5.05
2.10
2.08
2.07
2.05
1.78
1.77
1.76
1.75
1.74
1.74
1.72
1.65
1.65
1.55
1.40
0.00
1H NMR
CDCl3
500 MHz
HO
O
3.32
1.00
0.92
1.00
0.99
1.03
1.05
1.03
1.96
1.90
3.24
2.79
2.89
10.0
9.5
9.0
8.5
8.0
7.5
7.0
6.5
6.0
5.5
5.0
4.5
4.0
3.5
3.0
2.5
2.0
1.5
1.0
0.5
0.0

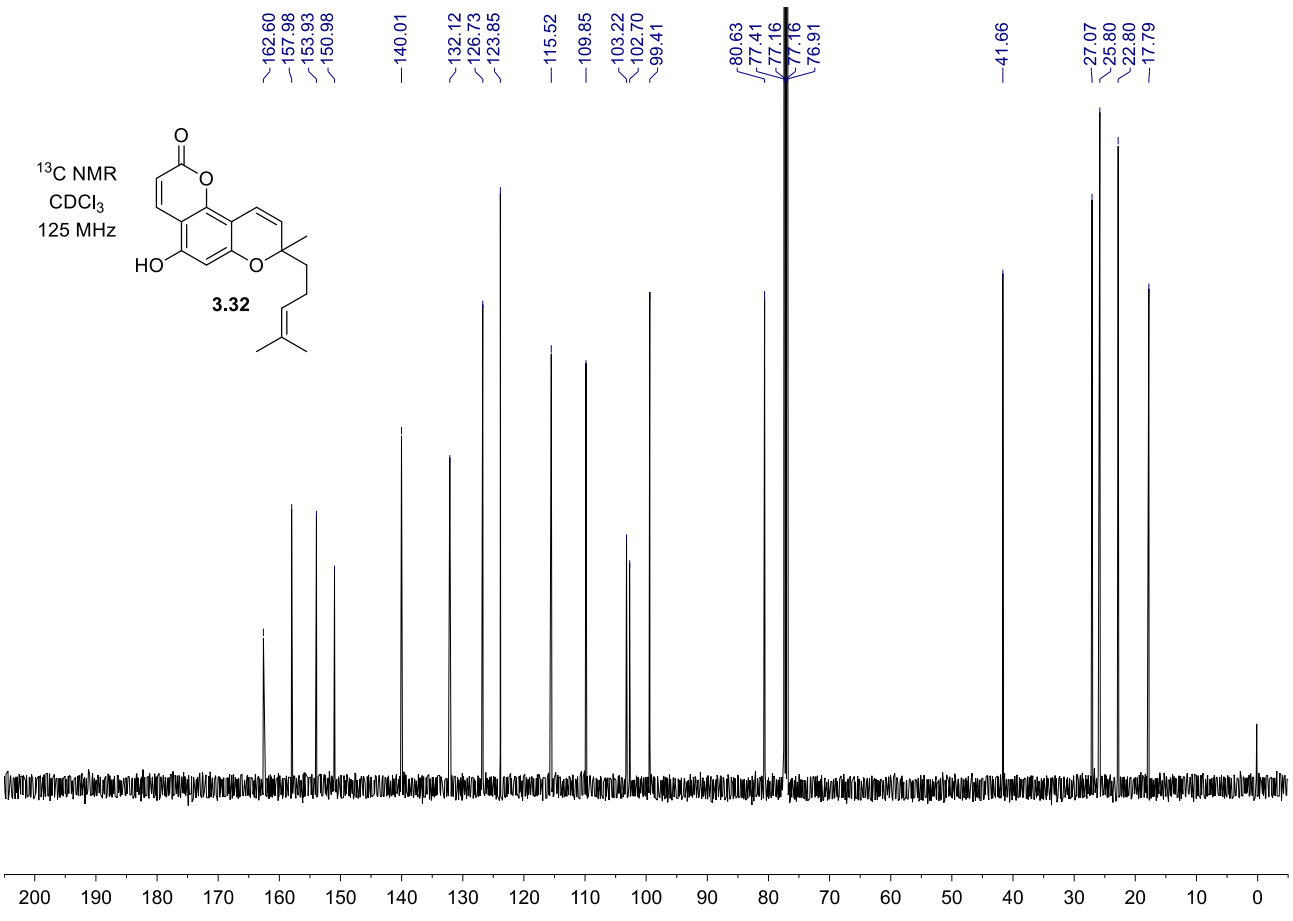
162.60
157.98
153.93
150.98
140.01
132.12
126.73
123.85
115.52
109.85
103.22
102.70
99.41
80.63
77.41
77.16
77.16
76.91
41.66
27.07
25.80
22.80
17.79
13C NMR
CDCl3
125 MHz
HO
O
3.32
200
190
180
170
160
150
140
130
120
110
100
90
80
70
60
50
40
30
20
10
0

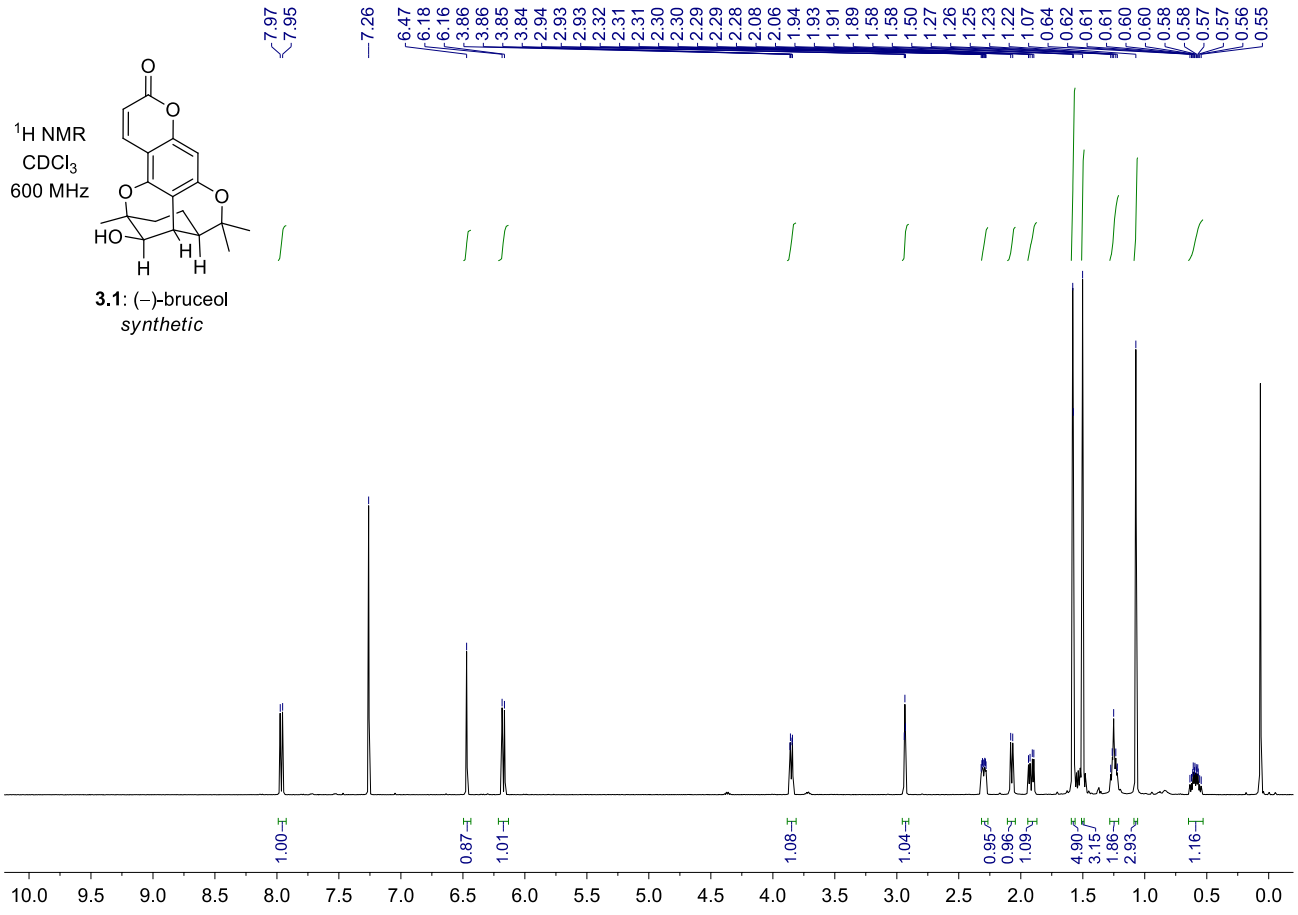
^{1}H NMR
$CDCl_3$
600 MHz
3.1: (–)-bruceol
synthetic

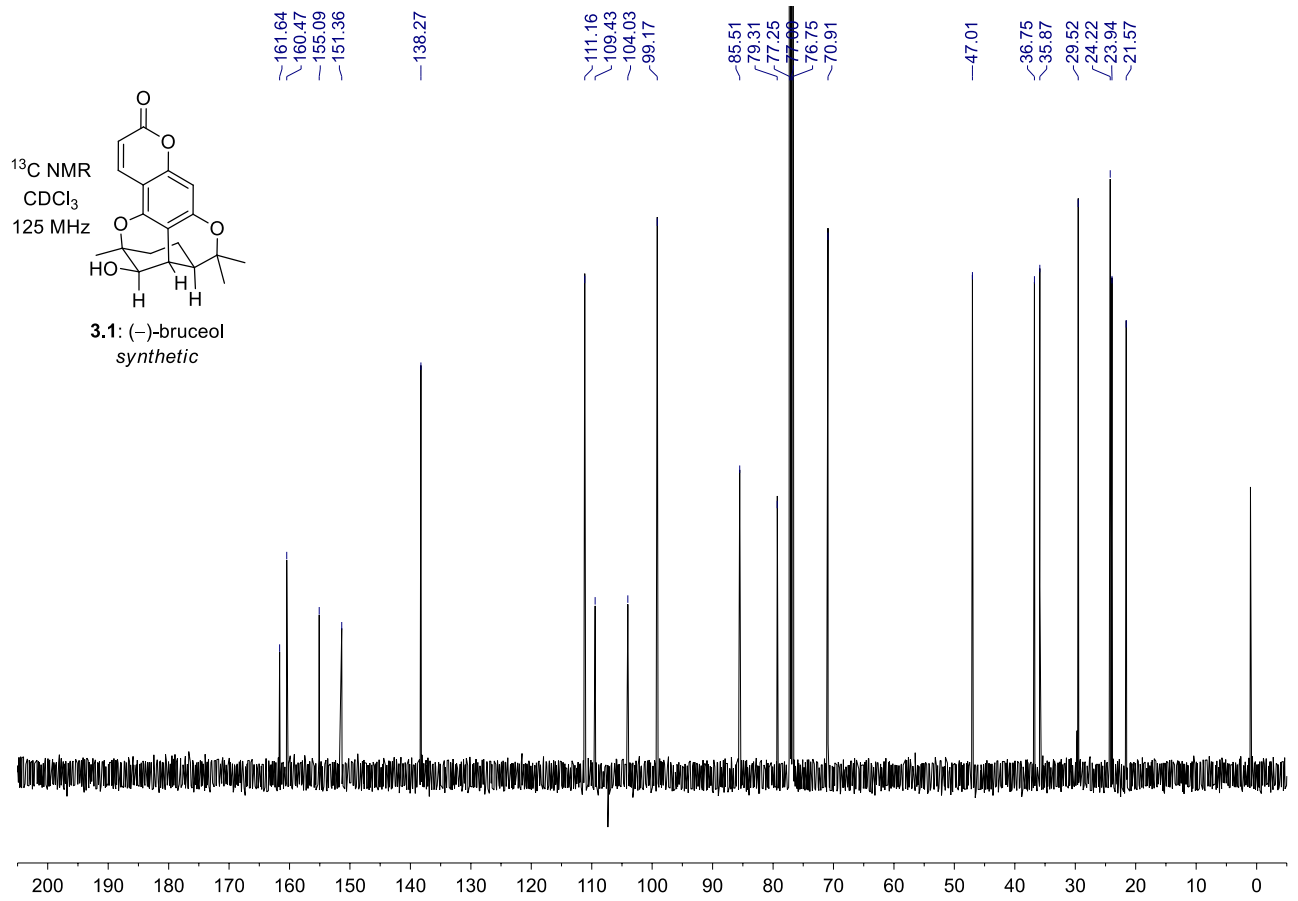
^{13}C NMR
$CDCl_3$
125 MHz
3.1: (–)-bruceol
synthetic

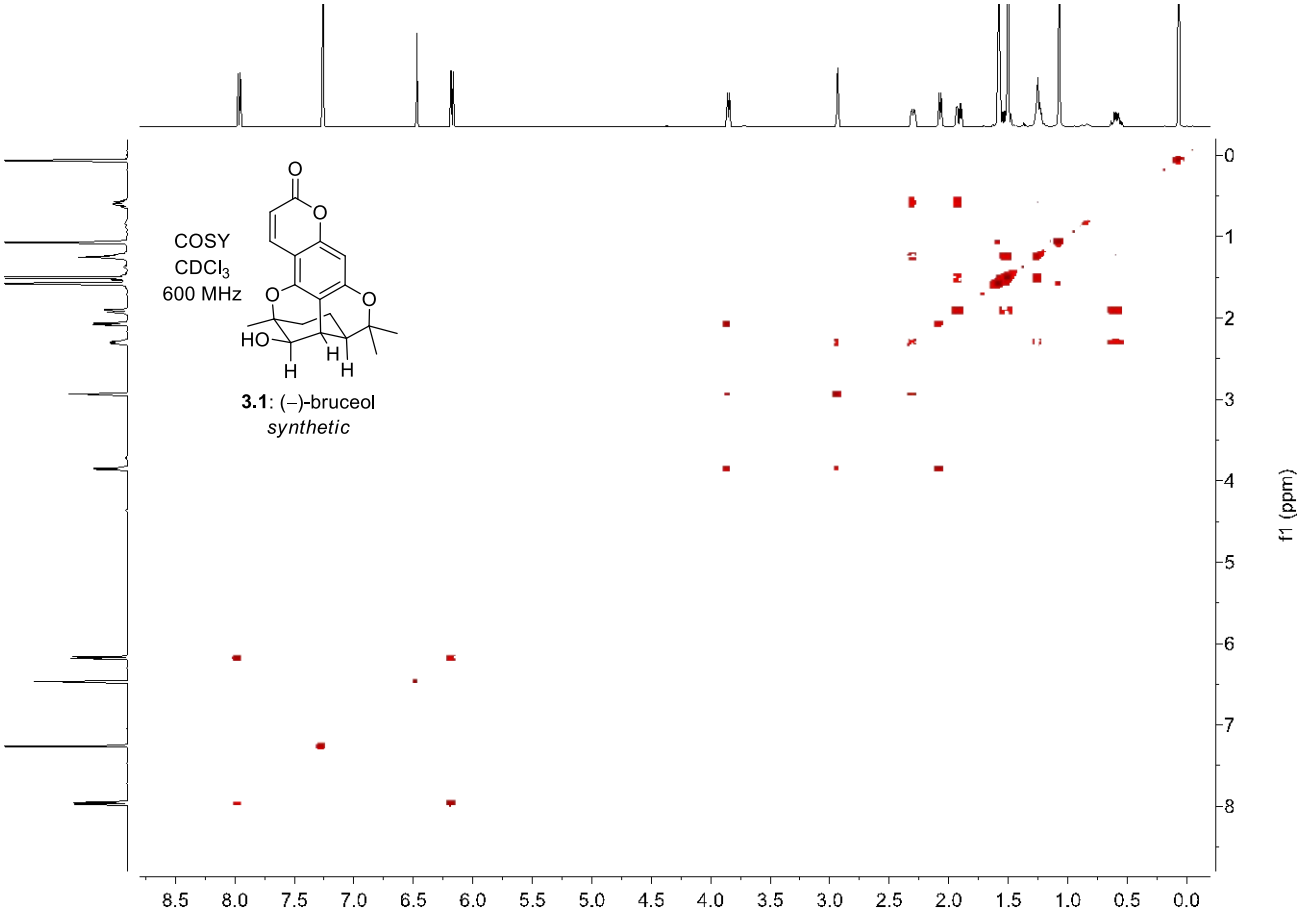
COSY
CDCl3
600 MHz
3.1: (–)-bruceol
synthetic
f1 (ppm)

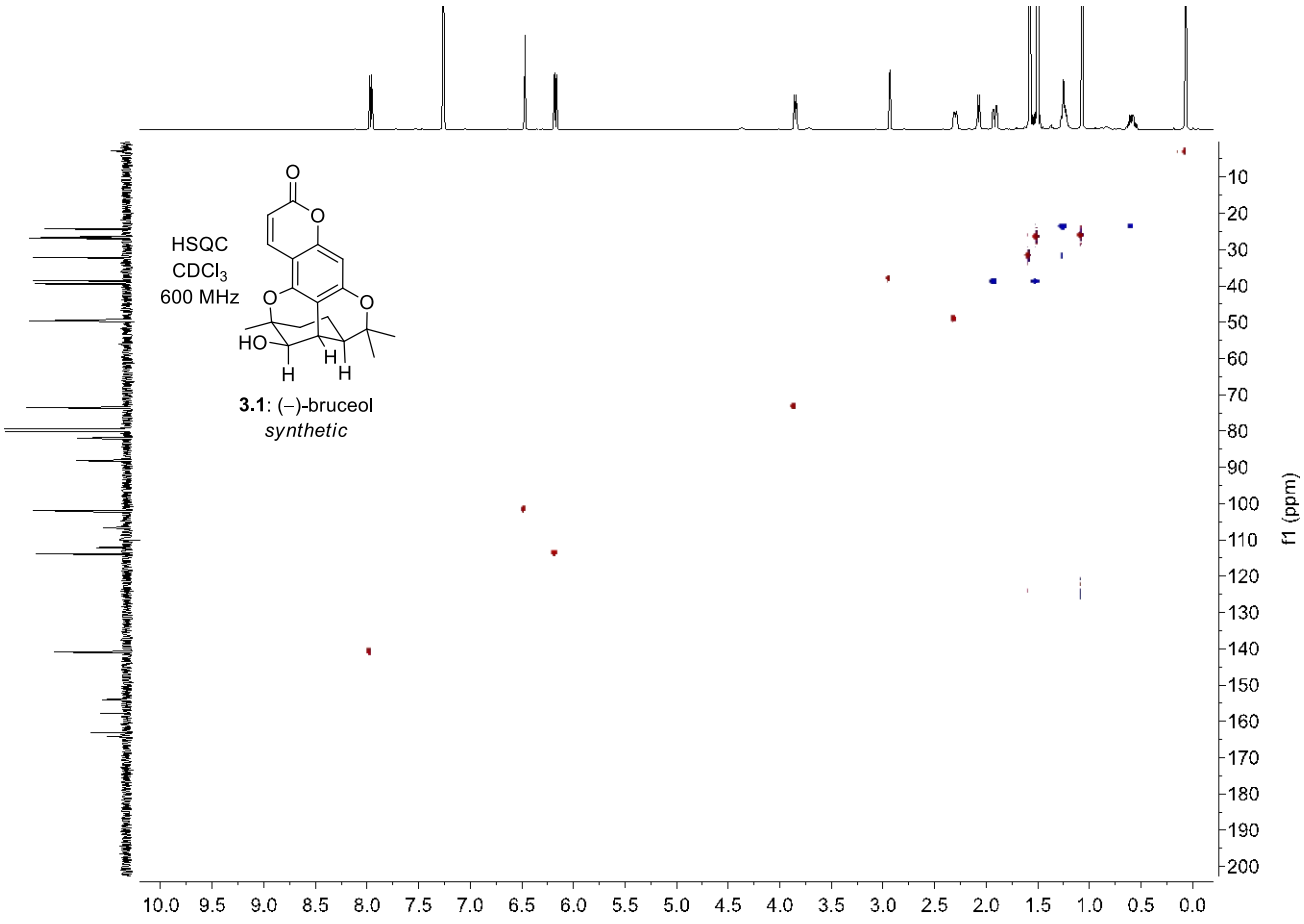
HSQC
CDCl3
600 MHz
3.1: (–)-bruceol
synthetic
f1 (ppm)

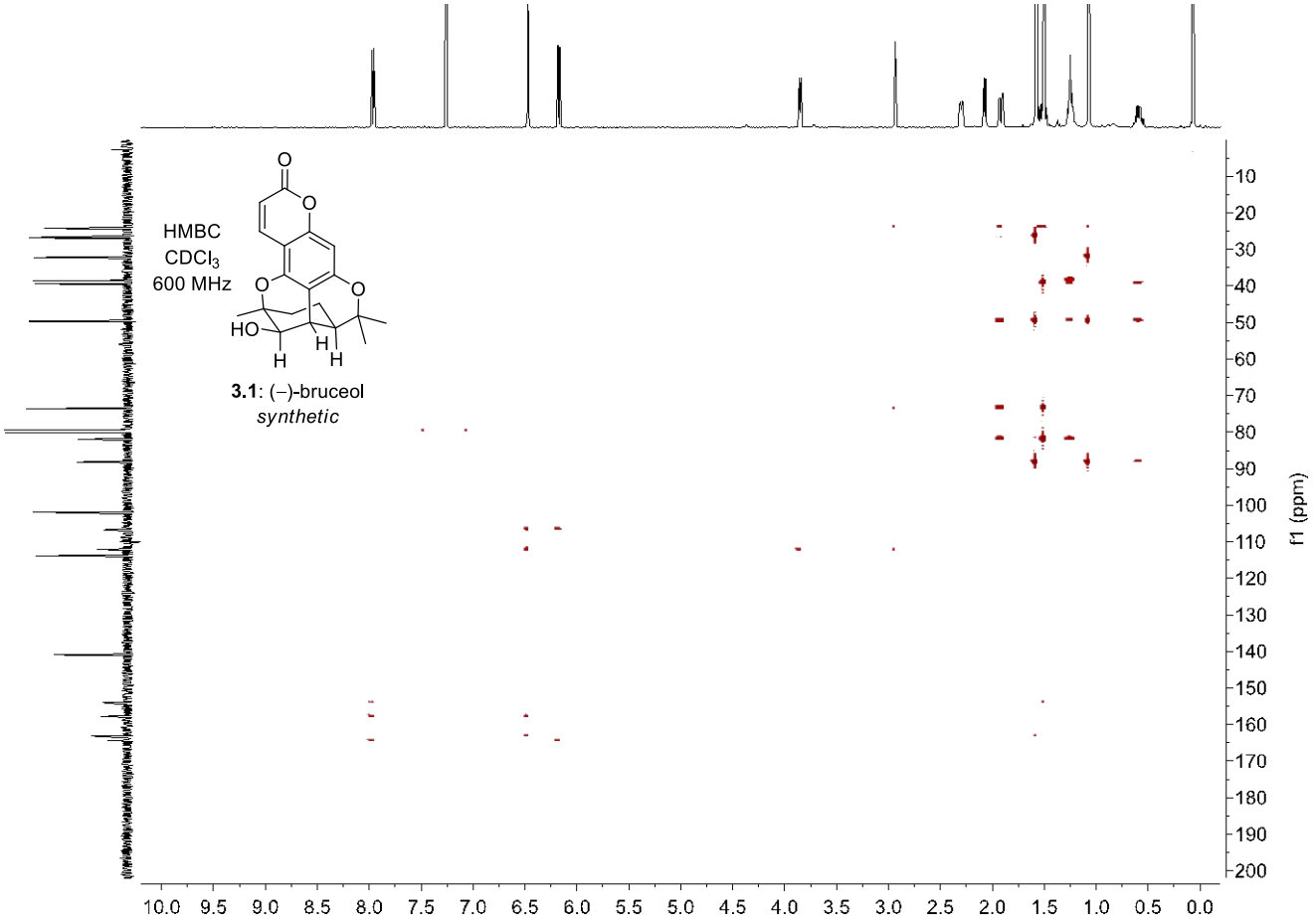
HMBC
CDCl3
600 MHz
3.1: (–)-bruceol
synthetic
f1 (ppm)

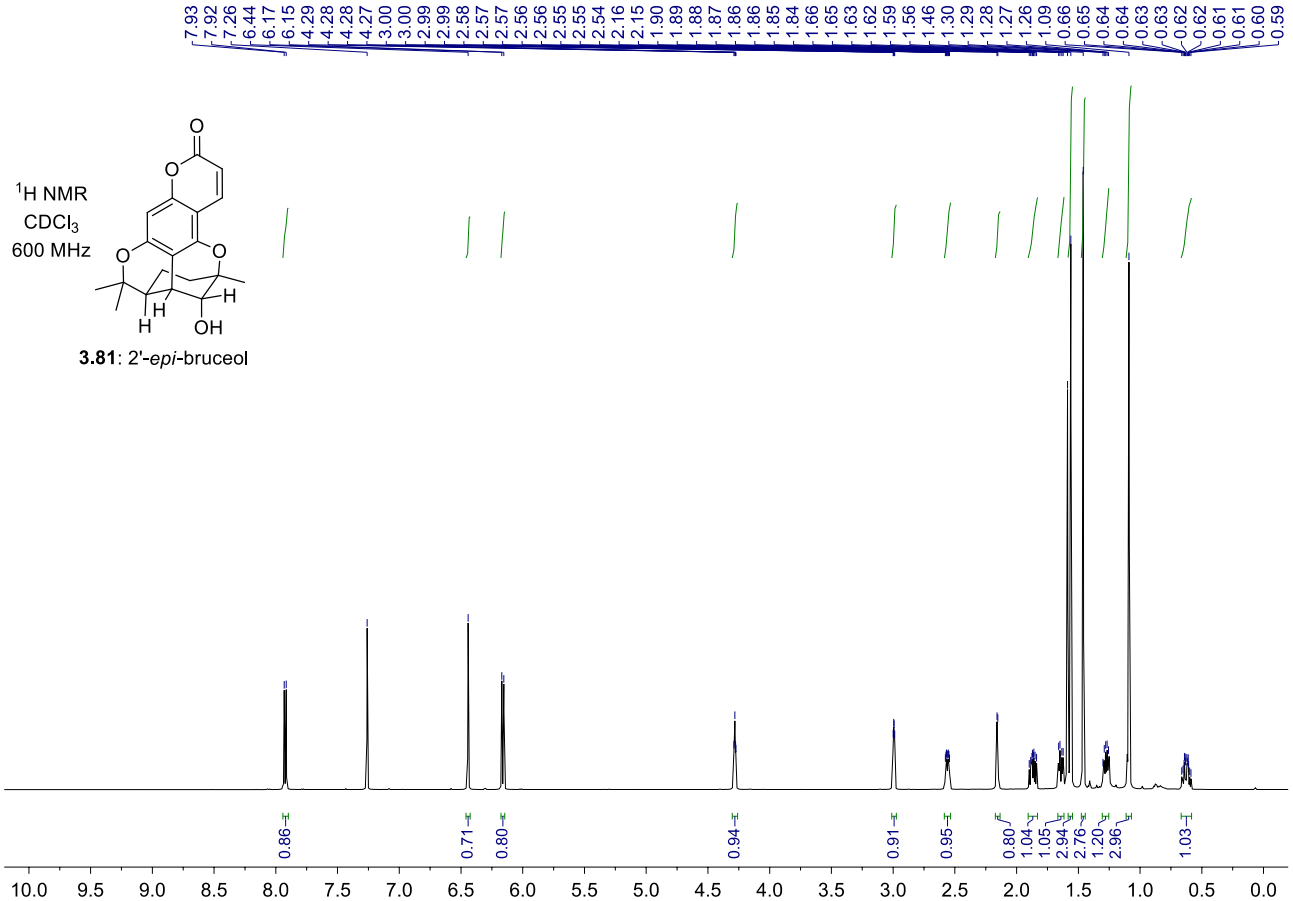
1H NMR
CDCl3
600 MHz
3.81: 2'-epi-bruceol

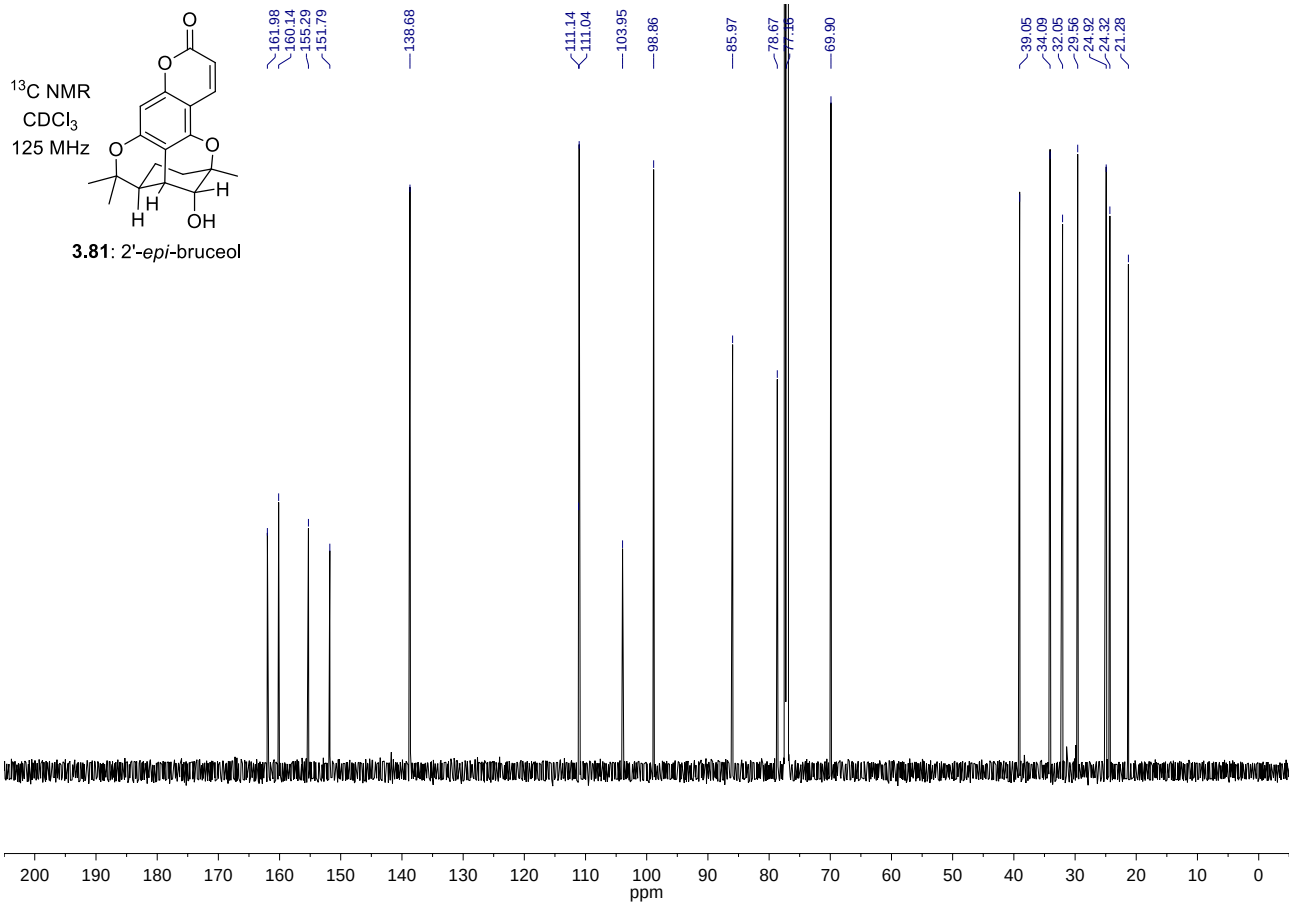
^{13}C NMR
$CDCl_3$
125 MHz
3.81: 2'-epi-bruceol
161.98
160.14
155.29
151.79
138.68
111.14
111.04
103.95
98.86
85.97
78.67
77.16
69.90
39.05
34.09
32.05
29.56
24.92
24.32
21.28
ppm

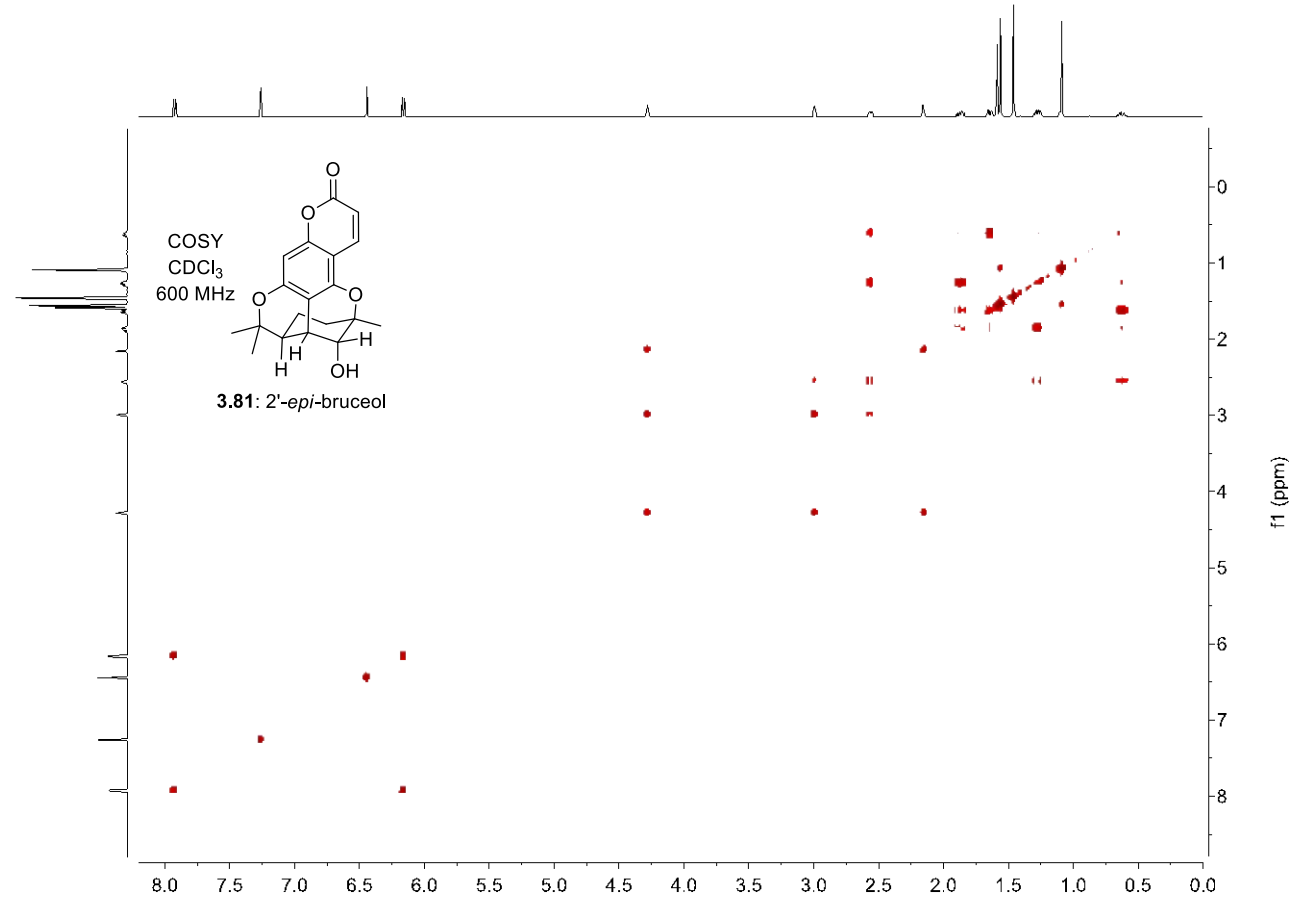
COSY
$CDCl_3$
600 MHz
3.81: 2'-epi-bruceol
f1 (ppm)

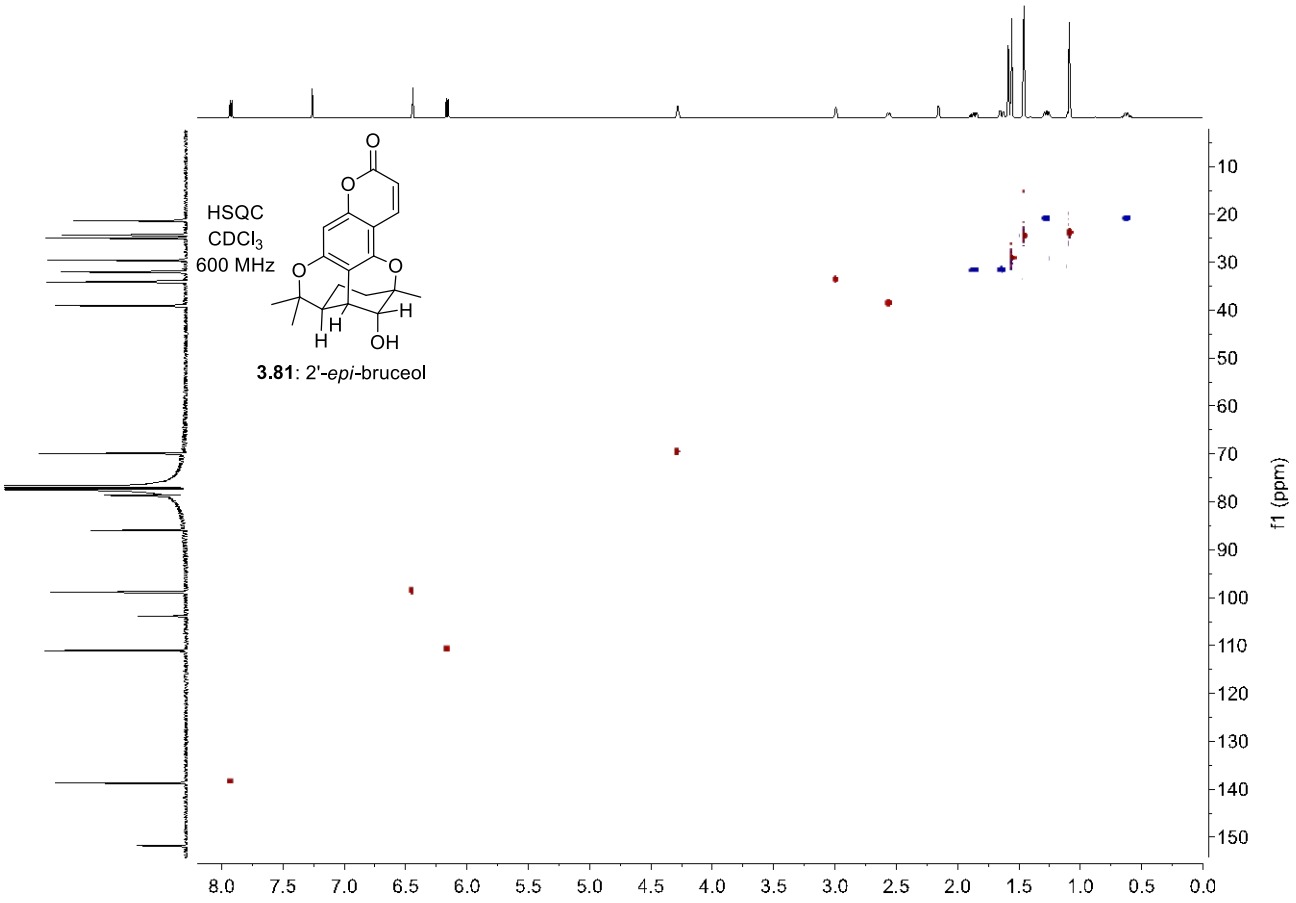
HSQC
CDCl3
600 MHz
3.81: 2'-epi-bruceol
f1 (ppm)

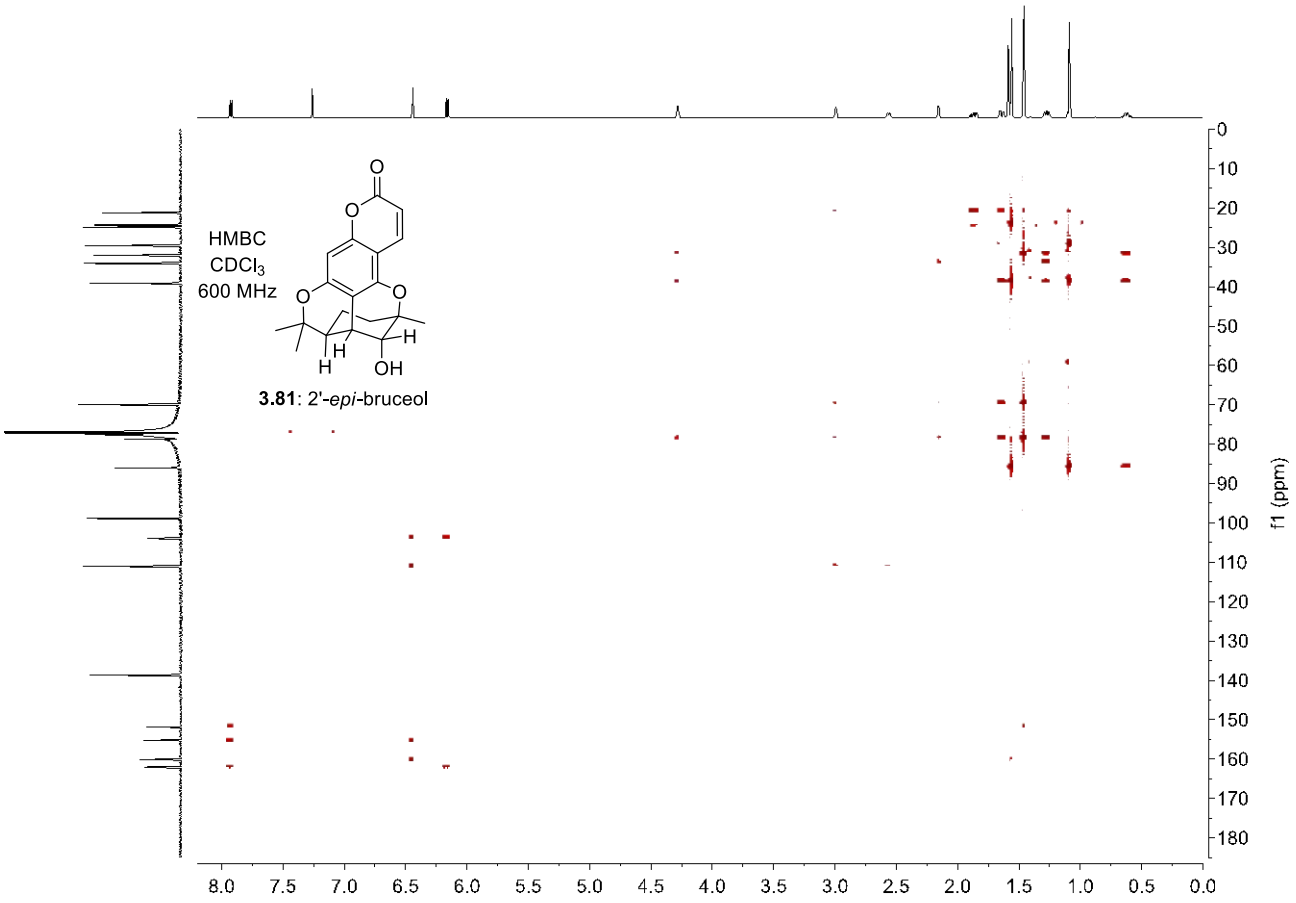
HMBC
CDCl3
600 MHz
3.81: 2'-epi-bruceol
f1 (ppm)

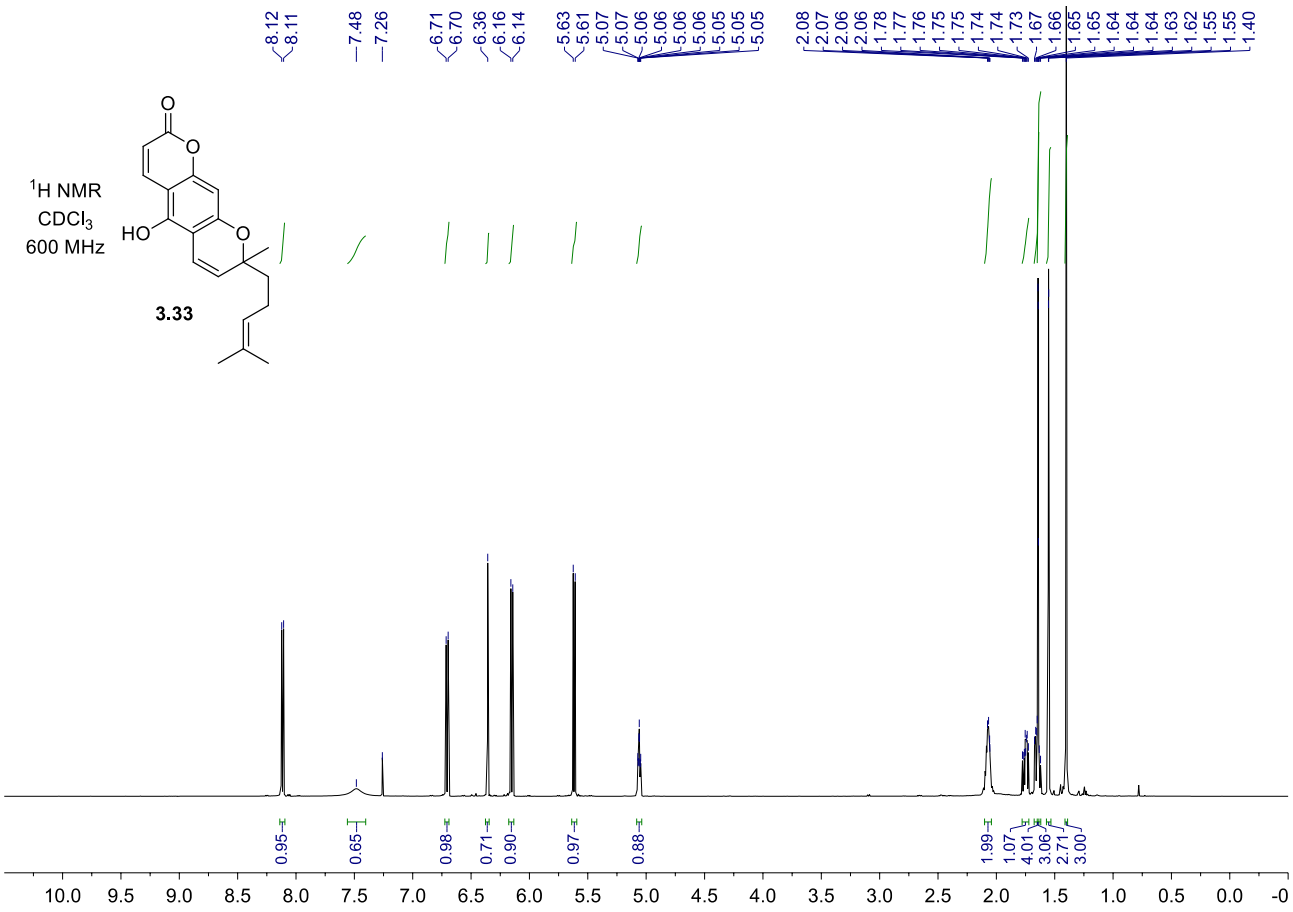
^{1}H NMR
$CDCl_3$
600 MHz
3.33
8.12
8.11
7.48
7.26
6.71
6.70
6.36
6.16
6.14
5.63
5.61
5.07
5.07
5.06
5.06
5.06
5.05
5.05
5.05
2.08
2.07
2.06
2.06
1.78
1.77
1.76
1.75
1.75
1.74
1.74
1.73
1.67
1.66
1.65
1.65
1.64
1.64
1.64
1.63
1.62
1.55
1.55
1.40
0.95
0.65
0.98
0.71
0.90
0.97
0.88
1.99
1.07
4.01
3.06
2.71
3.00
10.0 9.5 9.0 8.5 8.0 7.5 7.0 6.5 6.0 5.5 5.0 4.5 4.0 3.5 3.0 2.5 2.0 1.5 1.0 0.5 0.0 -0

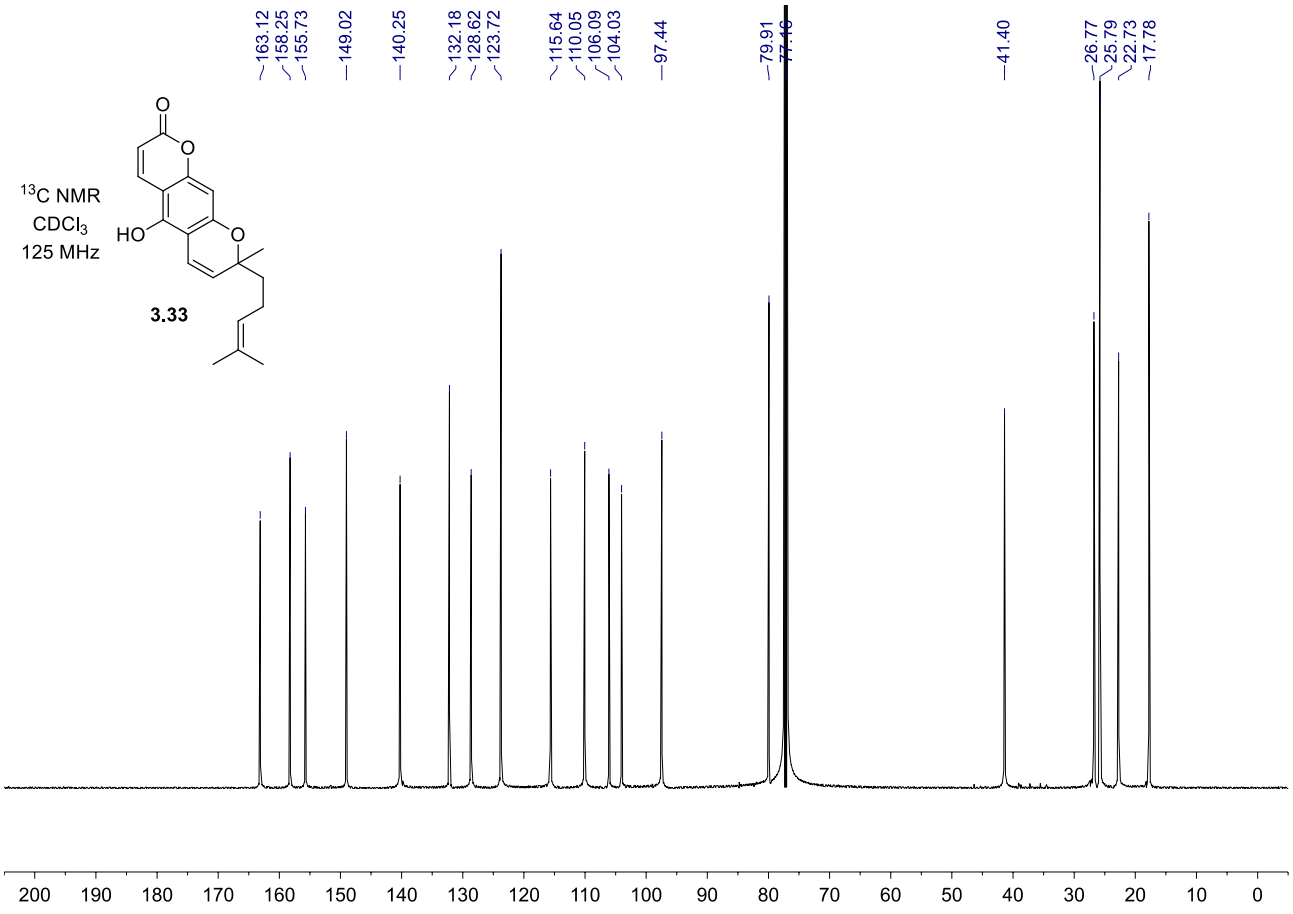
^{13}C NMR
$CDCl_3$
125 MHz
3.33
163.12
158.25
155.73
149.02
140.25
132.18
128.62
123.72
115.64
110.05
106.09
104.03
97.44
79.91
77.46
41.40
26.77
25.79
22.73
17.78
200 190 180 170 160 150 140 130 120 110 100 90 80 70 60 50 40 30 20 10 0

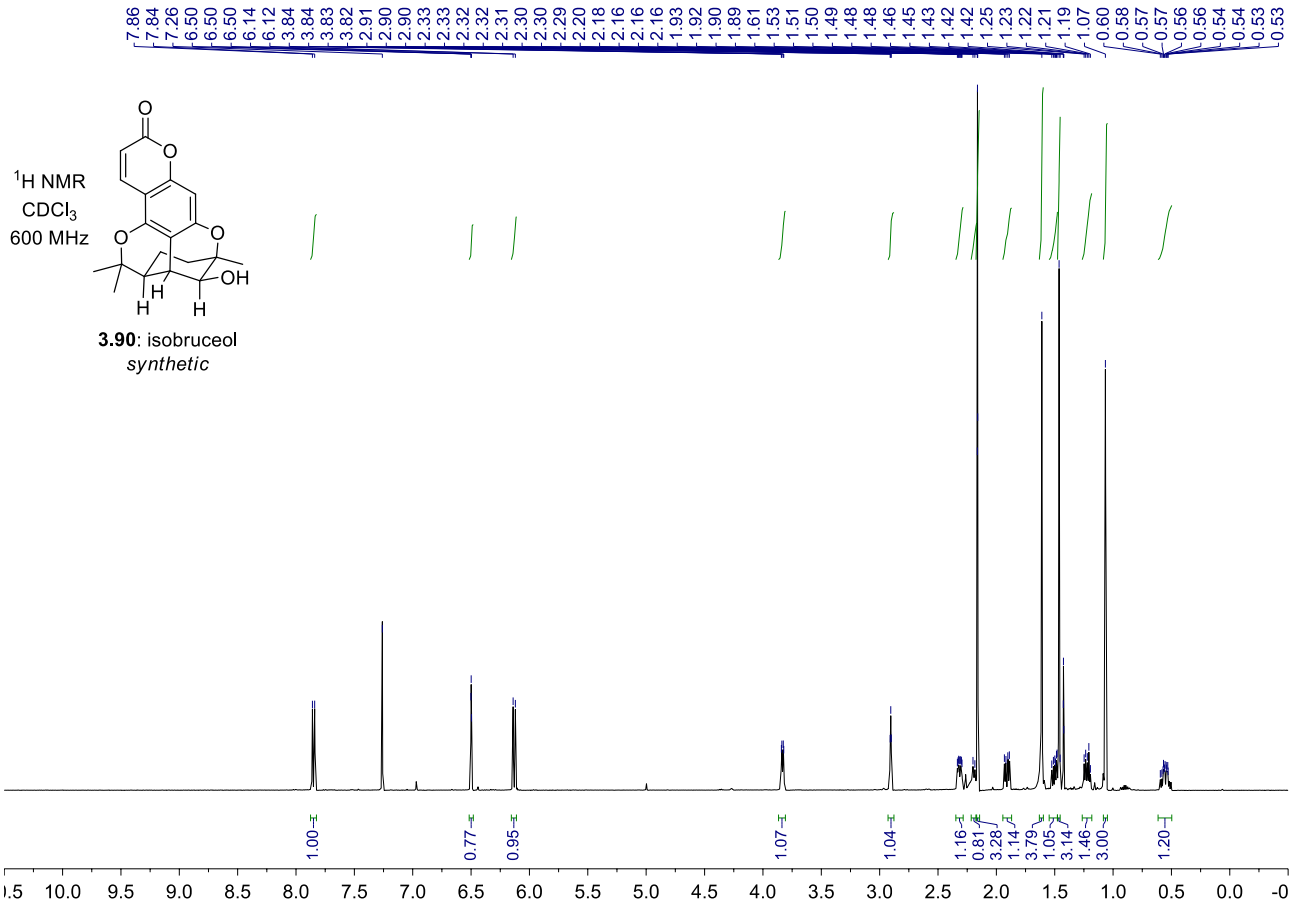
7.86 7.84 7.26 6.50 6.50 6.14 6.12 3.84 3.84 3.83 3.82 2.91 2.90 2.90 2.33 2.32 2.32 2.31 2.30 2.30 2.29 2.20 2.18 2.16 2.16 2.16 1.93 1.92 1.90 1.89 1.61 1.53 1.51 1.50 1.49 1.48 1.48 1.46 1.45 1.43 1.42 1.42 1.25 1.23 1.22 1.21 1.19 1.07 0.60 0.58 0.57 0.57 0.56 0.56 0.54 0.54 0.53 0.53
1H NMR
CDCl3
600 MHz
O
O
O
O
OH
H
H
H
3.90: isobruceol
synthetic
1.00 0.77 0.95 1.07 1.04 1.16 0.81 3.28 1.14 3.79 1.05 3.14 1.46 3.00 1.20
10.0 9.5 9.0 8.5 8.0 7.5 7.0 6.5 6.0 5.5 5.0 4.5 4.0 3.5 3.0 2.5 2.0 1.5 1.0 0.5 0.0

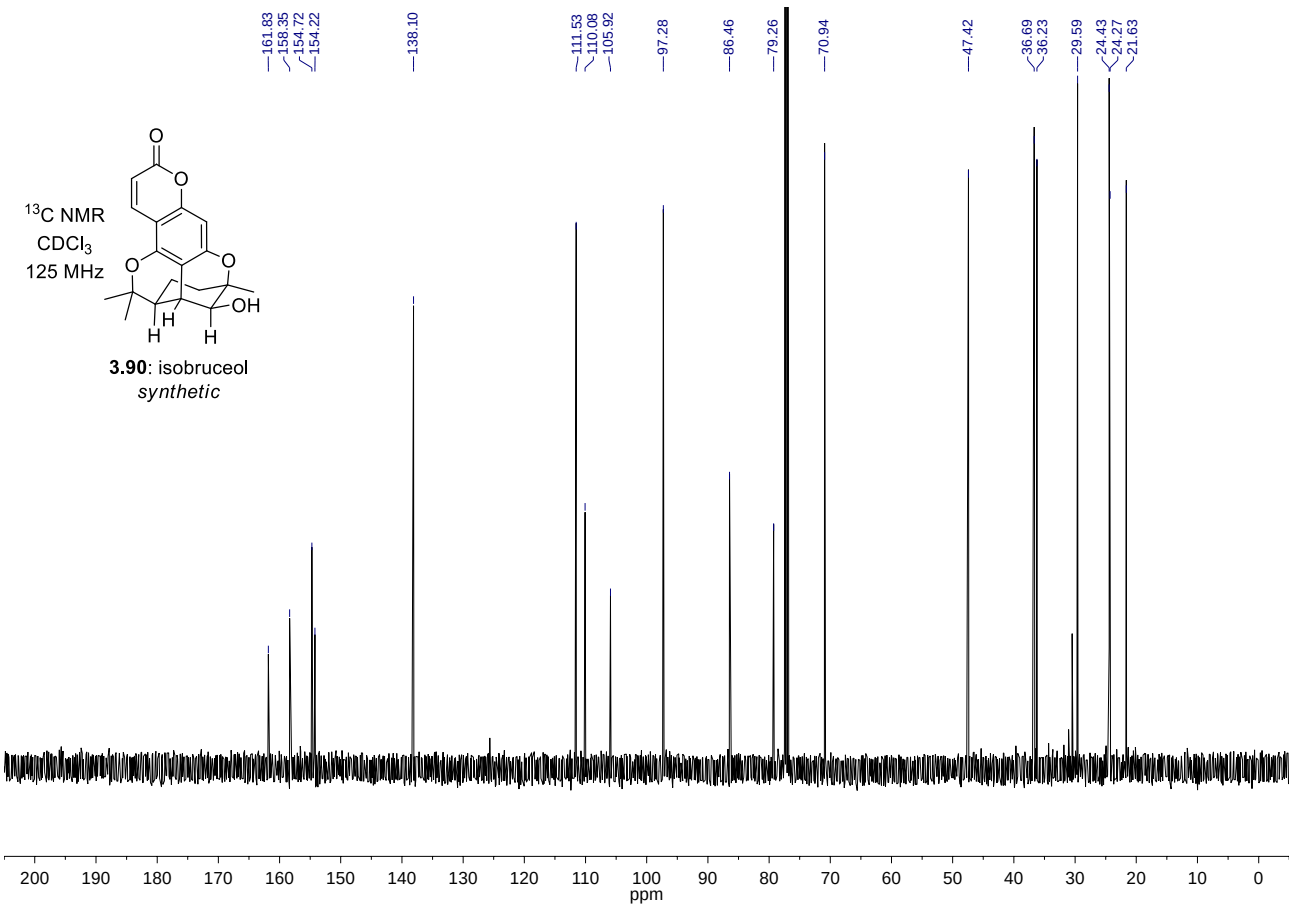
161.83 158.35 154.72 154.22 138.10 111.53 110.08 105.92 97.28 86.46 79.26 70.94 47.42 36.69 36.23 29.59 24.43 24.27 21.63
13C NMR
CDCl3
125 MHz
O
O
O
O
OH
H
H
H
3.90: isobruceol
synthetic
200 190 180 170 160 150 140 130 120 110 100 90 80 70 60 50 40 30 20 10 0
ppm

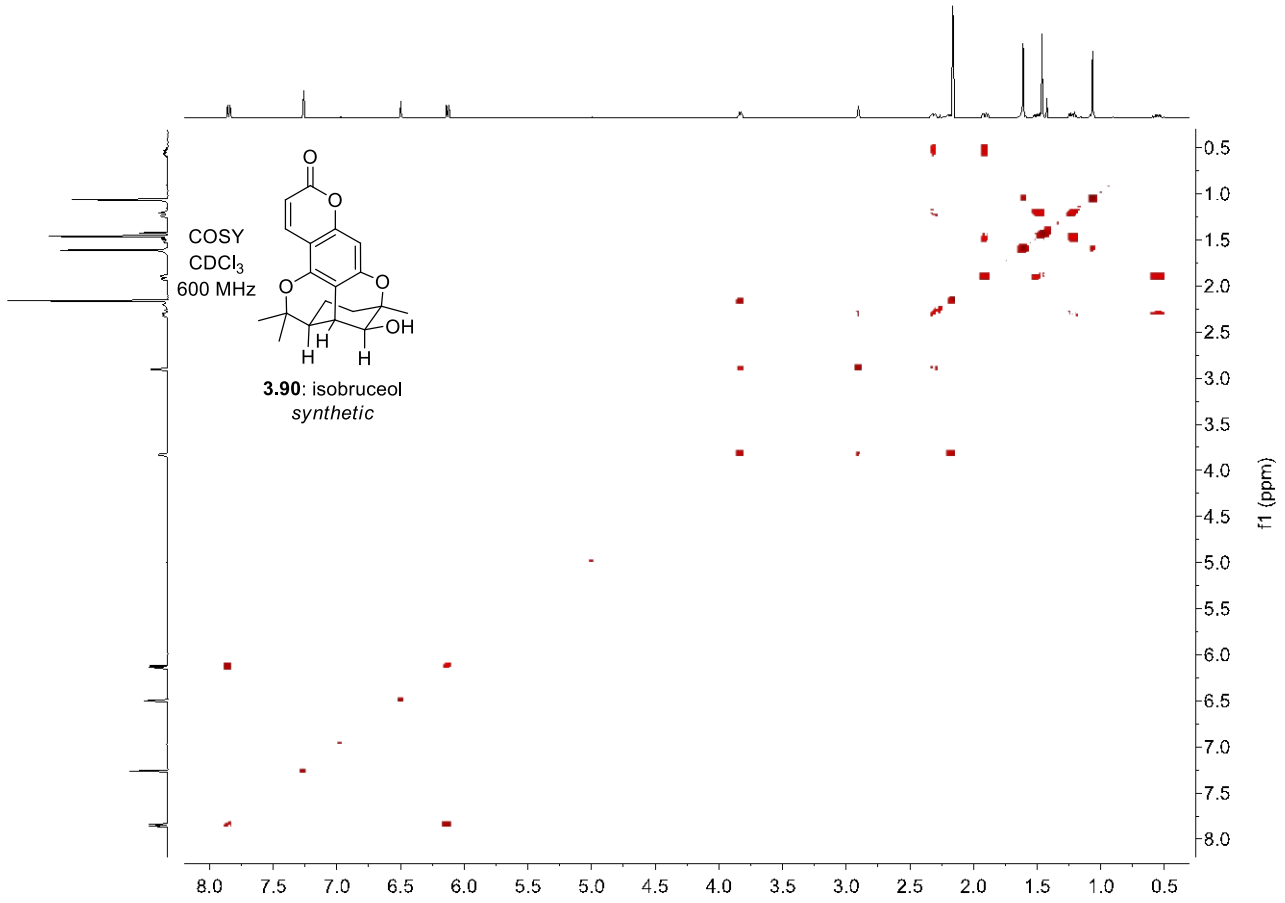
COSY
CDCl3
600 MHz
3.90: isobruceol
synthetic
f1 (ppm)

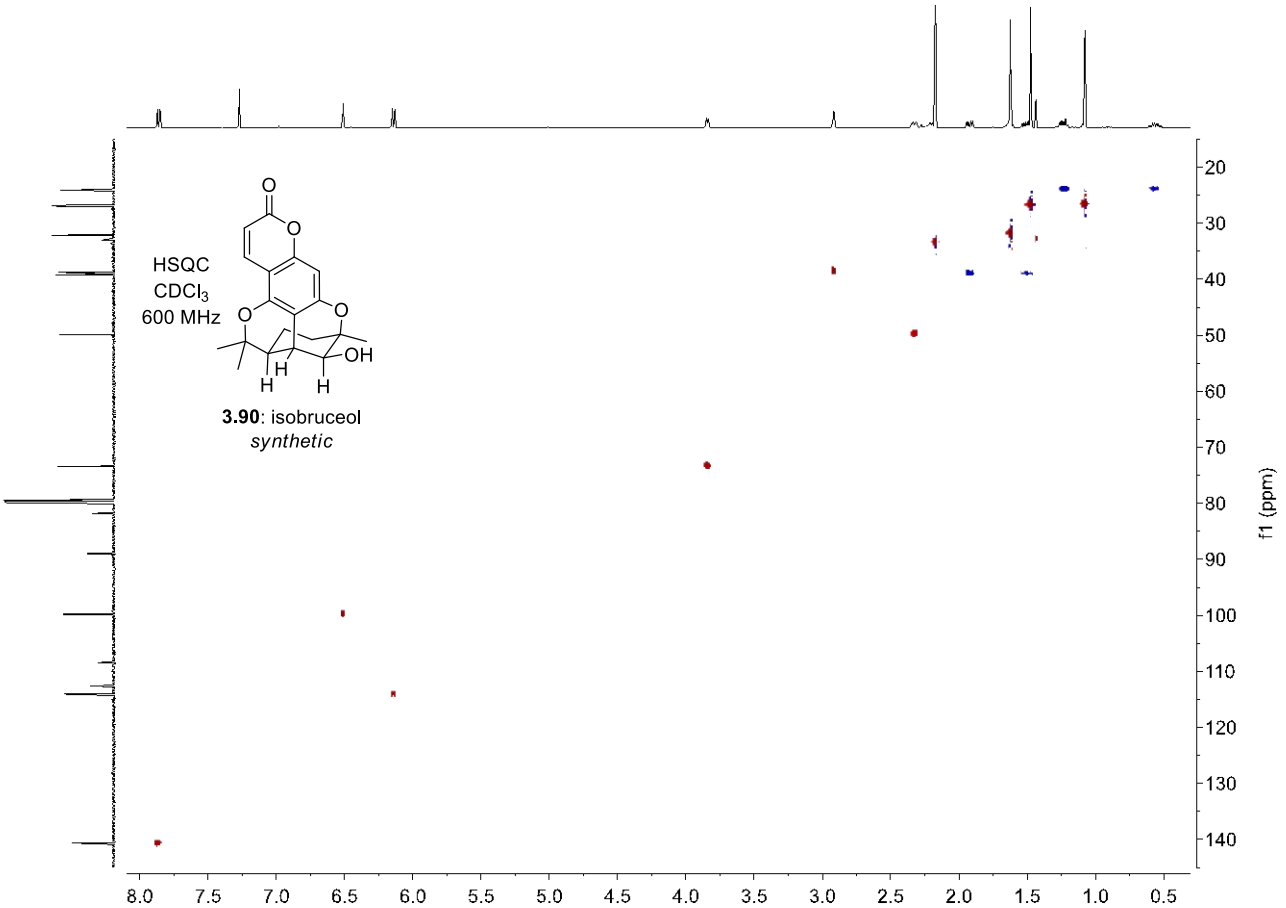
HSQC
CDCl3
600 MHz
3.90: isobruceol
synthetic
f1 (ppm)

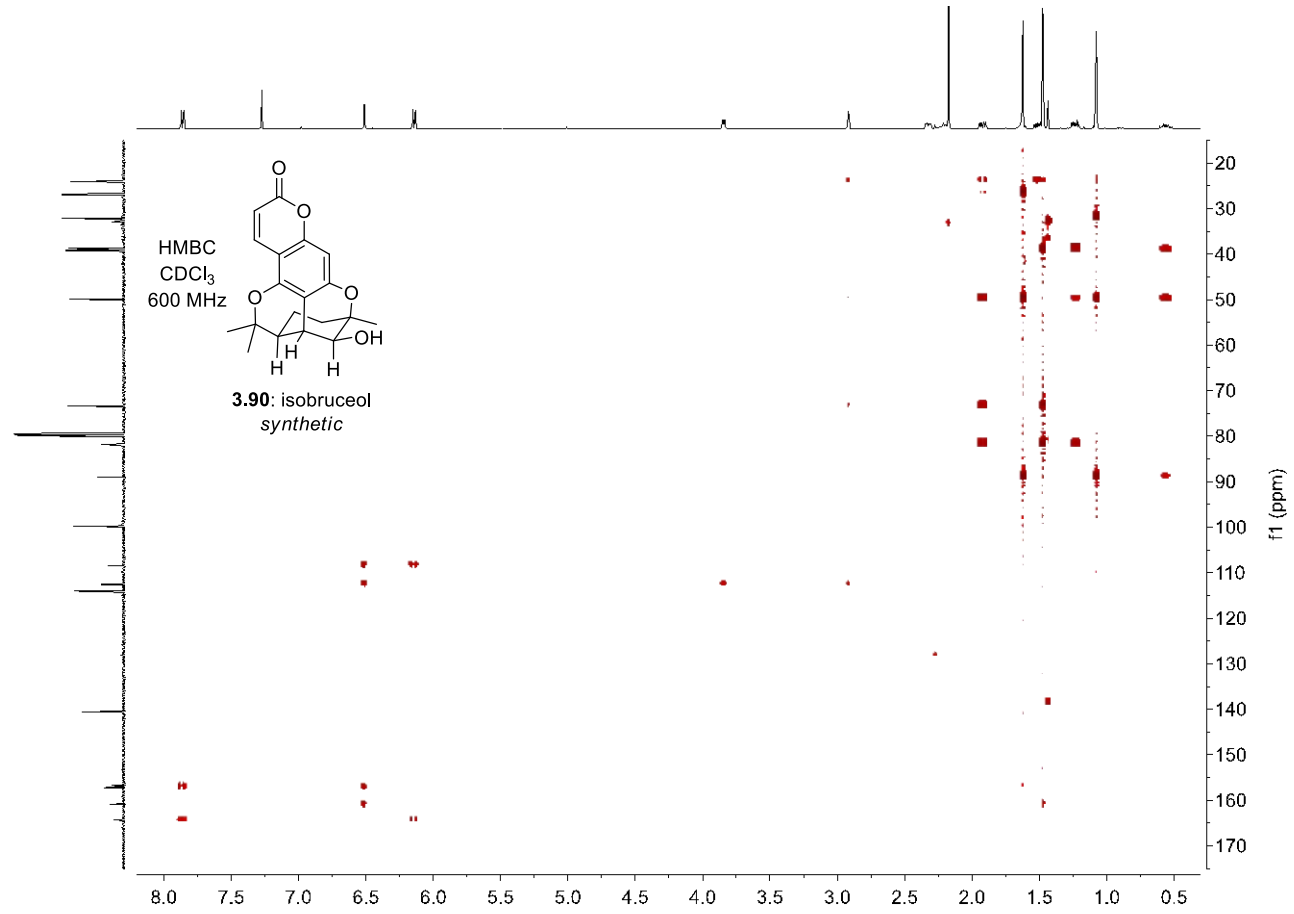
HMBC
CDCl3
600 MHz
3.90: isobruceol
synthetic
f1 (ppm)

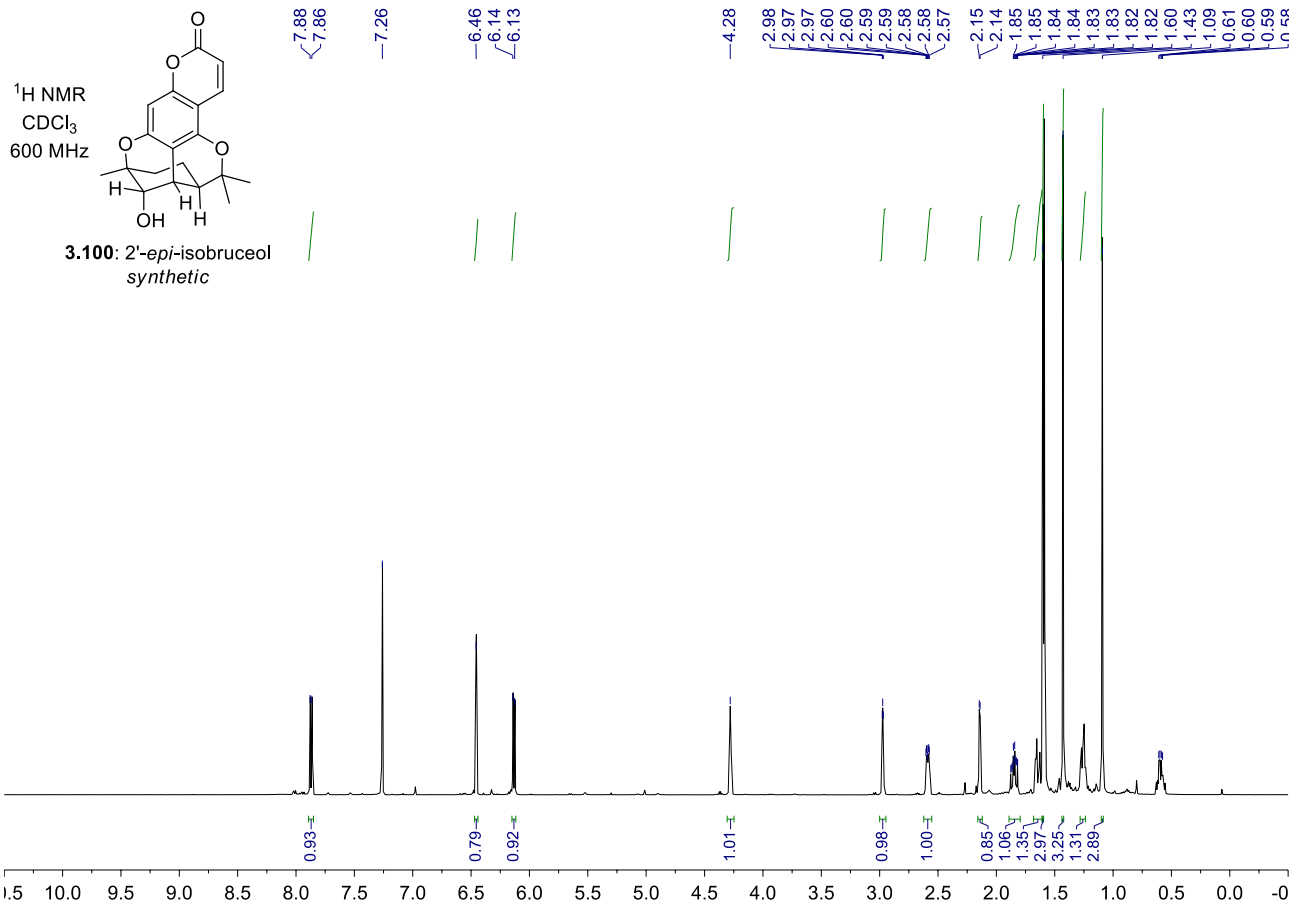
1H NMR
CDCl3
600 MHz
3.100: 2'-epi-isobruceol
synthetic

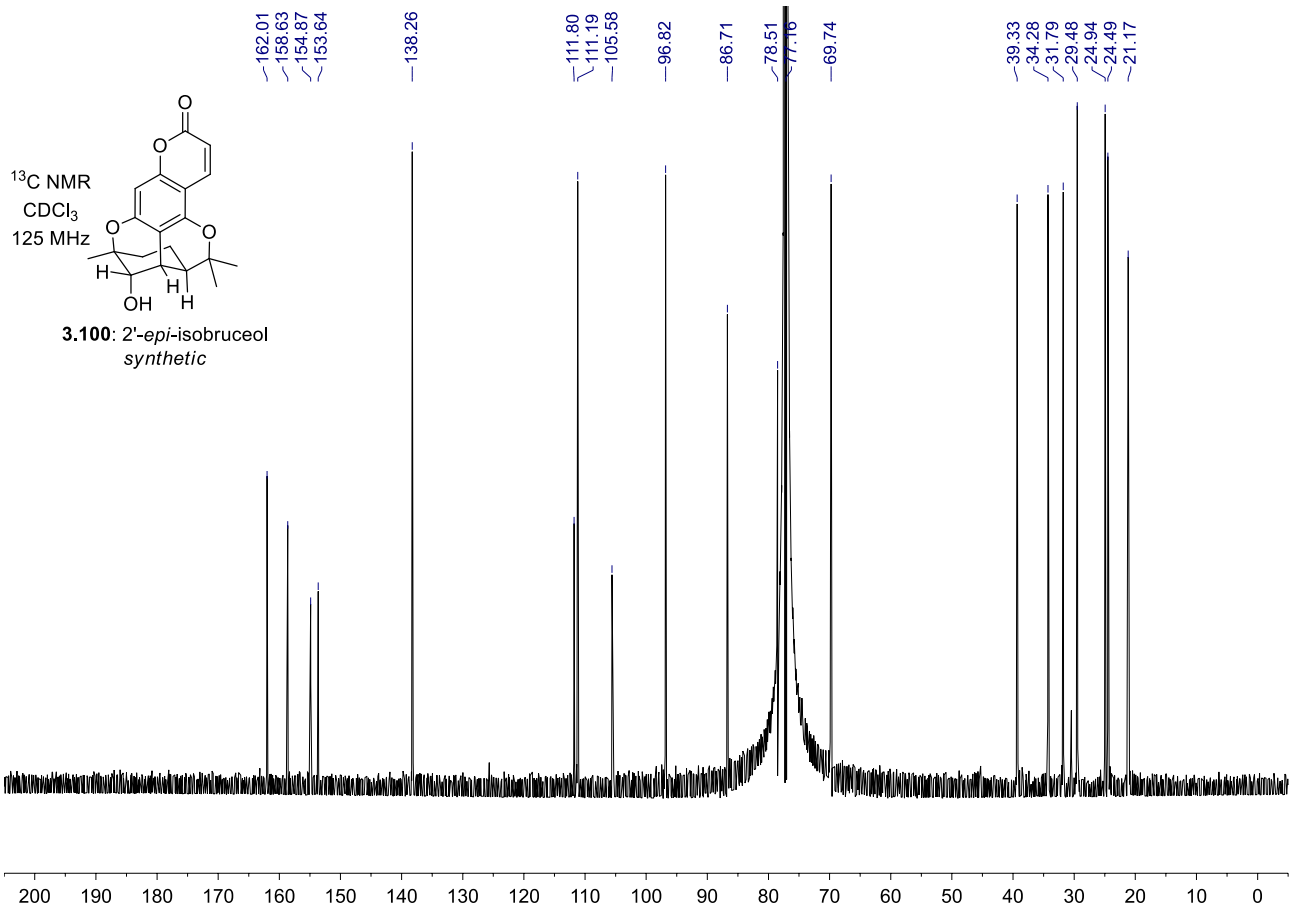

3.100: 2'-*epi*-isobruceol
synthetic

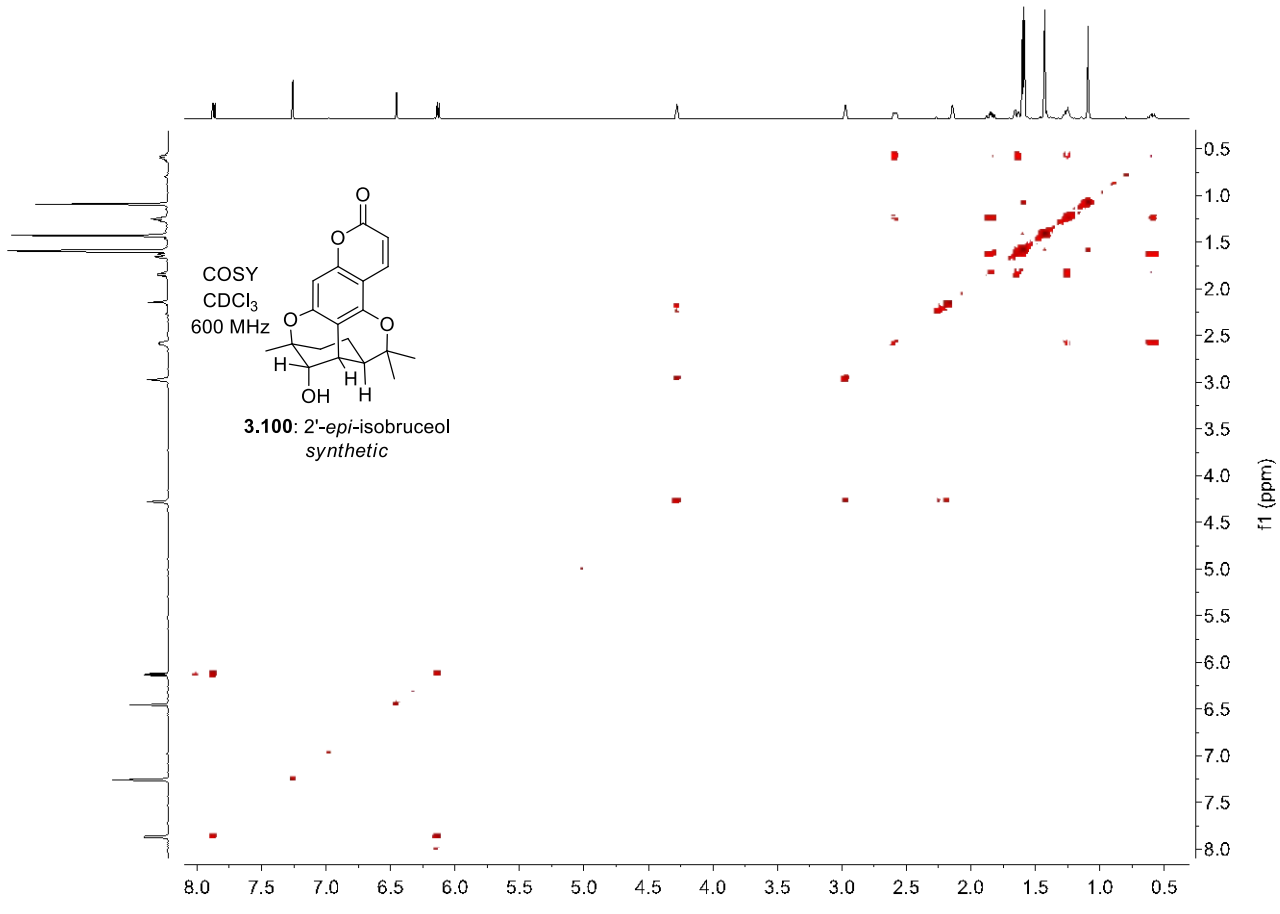

3.100: 2'-*epi*-isobruceol
synthetic

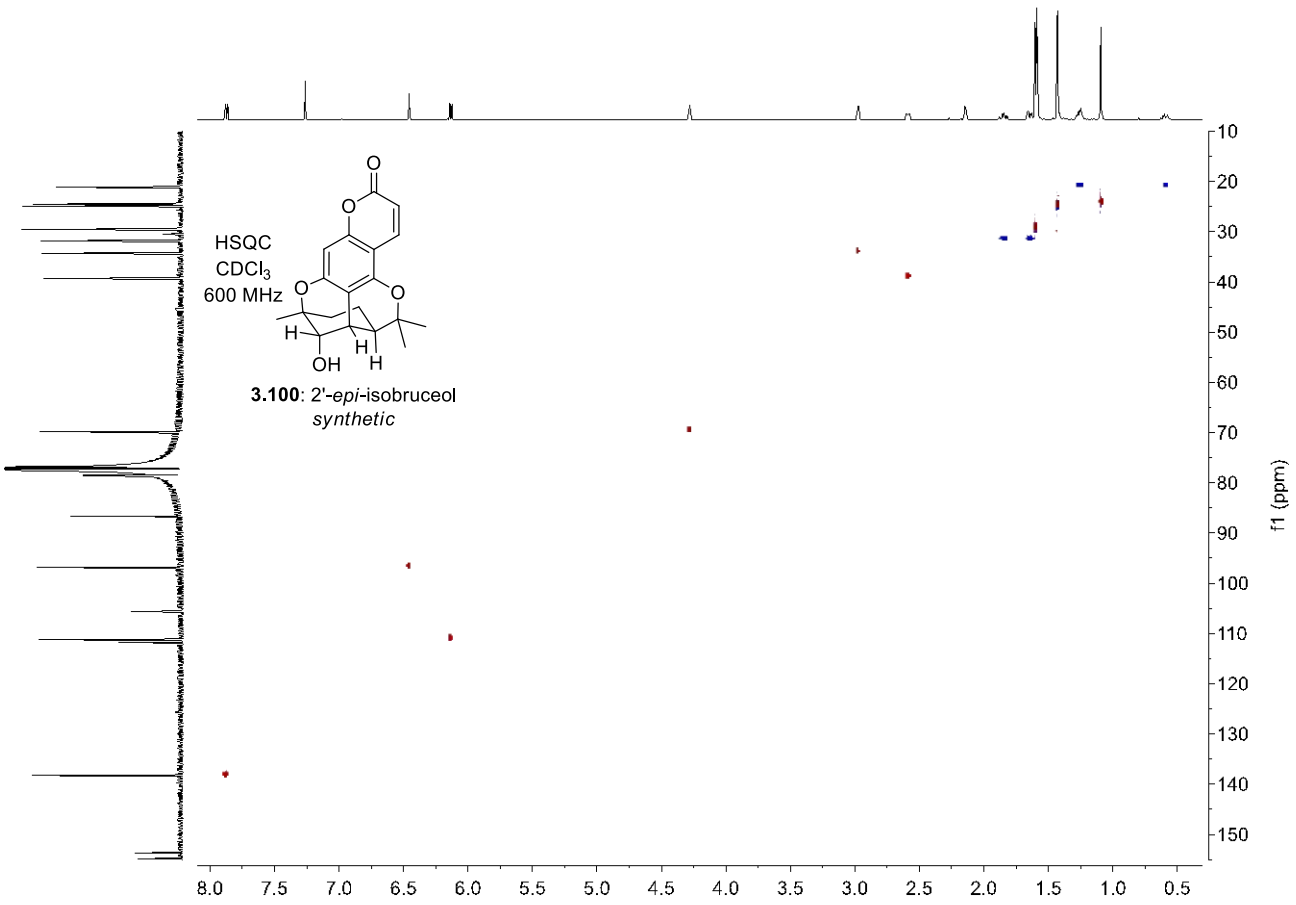
HSQC
CDCl3
600 MHz
3.100: 2'-epi-isobruceol
synthetic
f1 (ppm)

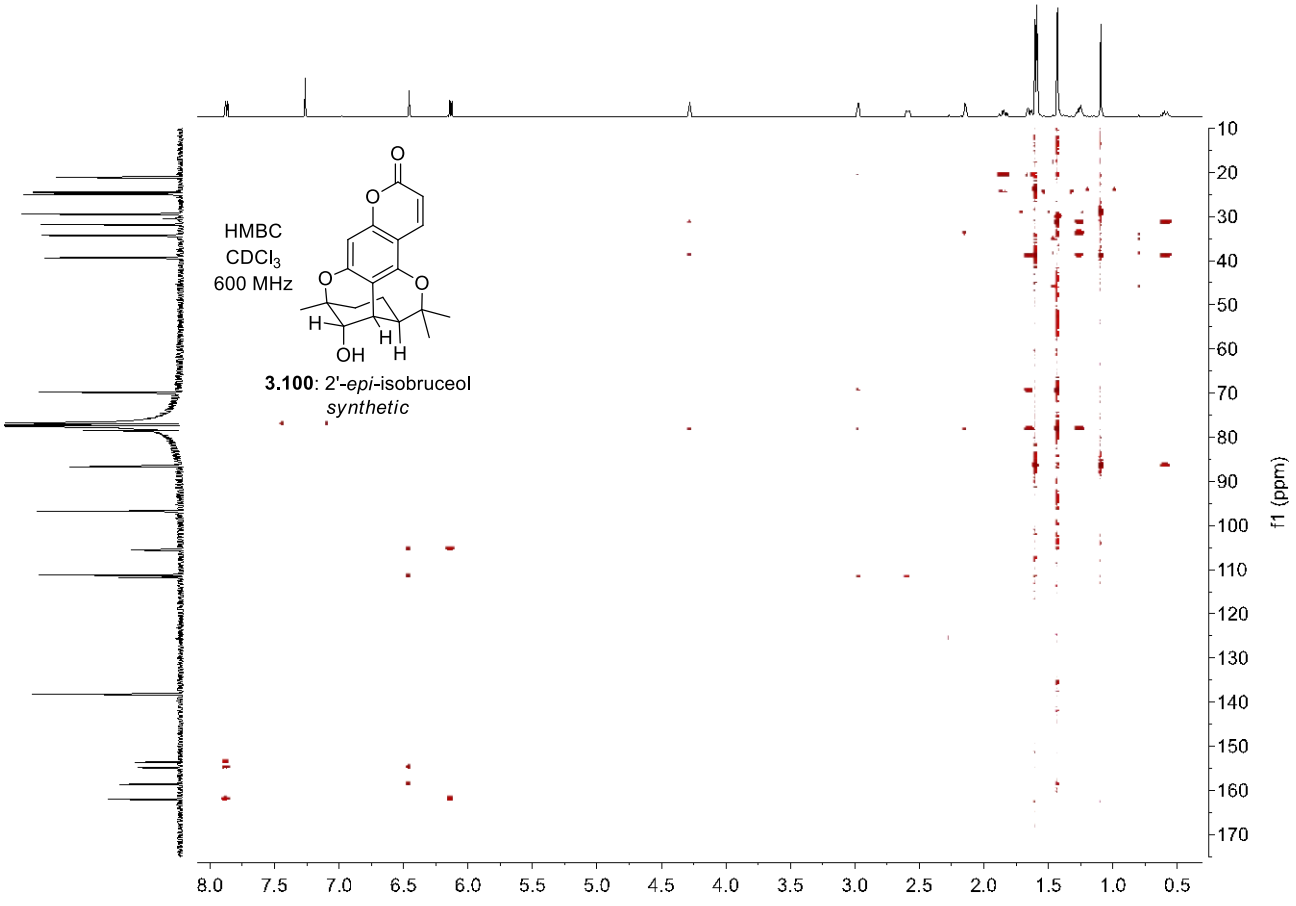
HMBC
CDCl3
600 MHz
3.100: 2'-epi-isobruceol
synthetic
f1 (ppm)

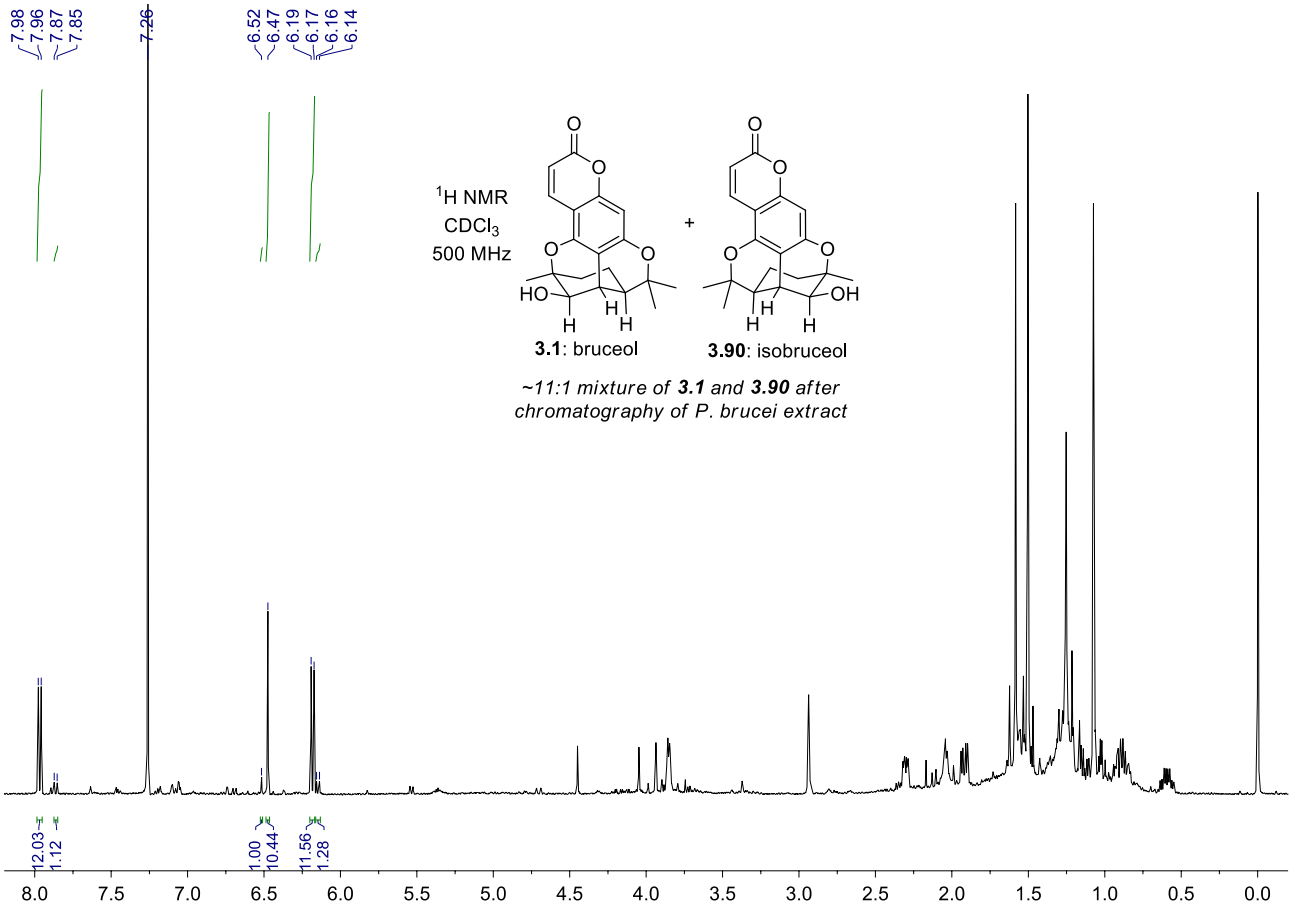

^{1}H NMR
$CDCl_3$
500 MHz

3.1: bruceol **3.90**: isobruceol

*~11:1 mixture of **3.1** and **3.90** after chromatography of P. brucei extract*

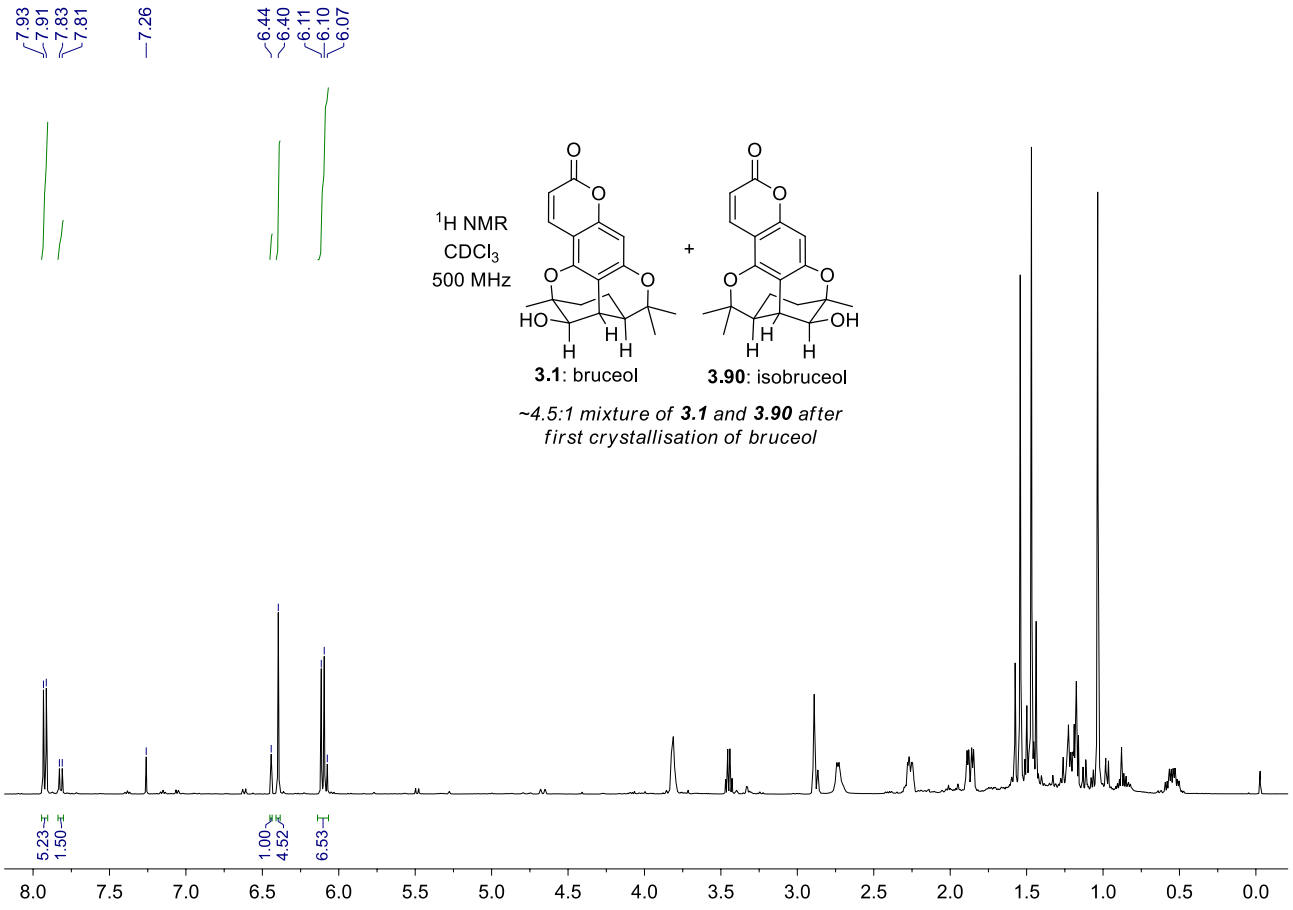

^{1}H NMR
$CDCl_3$
500 MHz

3.1: bruceol **3.90**: isobruceol

*~4.5:1 mixture of **3.1** and **3.90** after first crystallisation of bruceol*

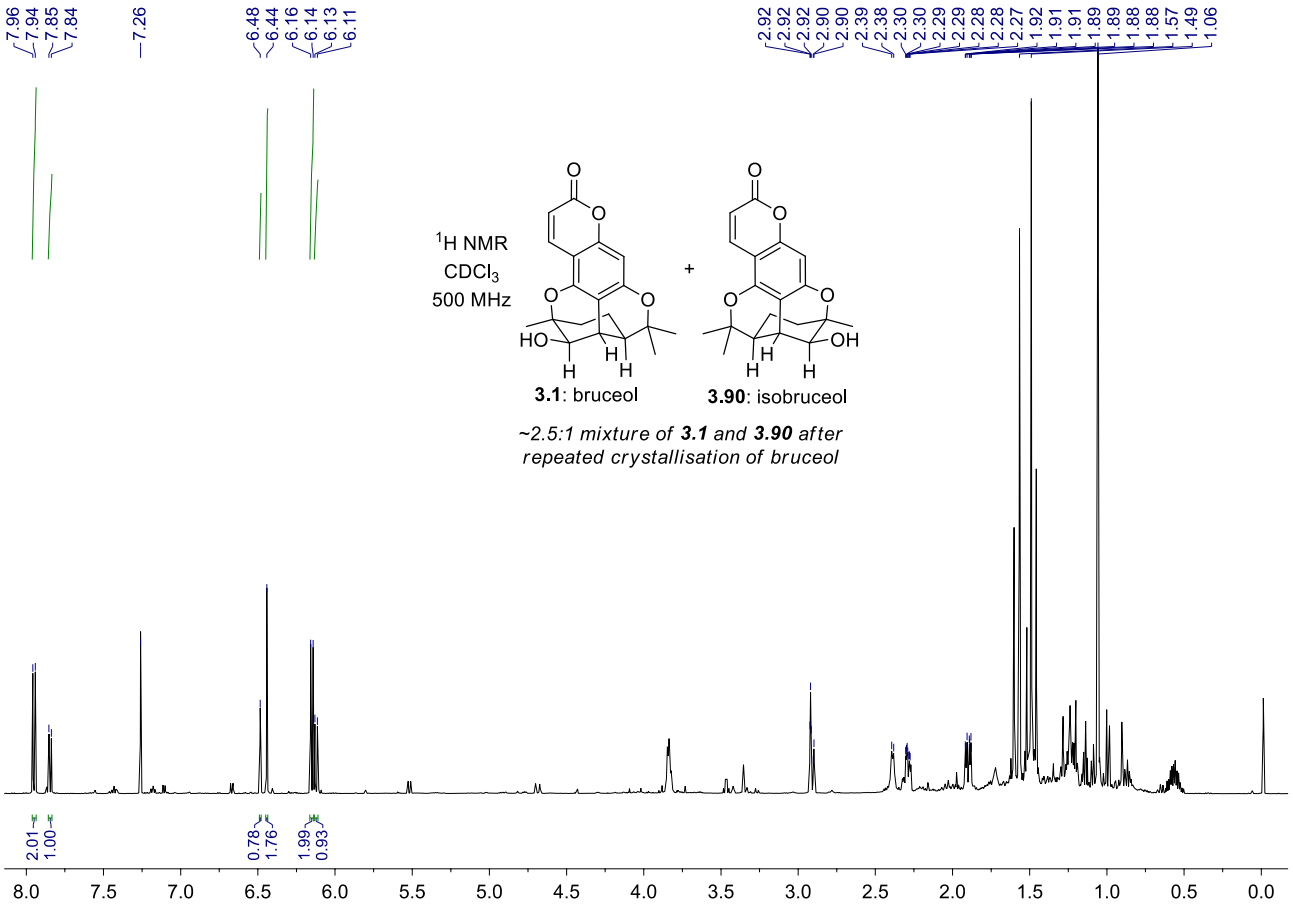
7.96
7.94
7.85
7.84
7.26
6.48
6.44
6.16
6.14
6.13
6.11
2.92
2.92
2.92
2.90
2.90
2.39
2.38
2.30
2.30
2.29
2.29
2.28
2.28
2.27
1.92
1.91
1.91
1.89
1.89
1.88
1.88
1.57
1.49
1.06
1H NMR
CDCl3
500 MHz
3.1: bruceol
3.90: isobruceol
~2.5:1 mixture of 3.1 and 3.90 after repeated crystallisation of bruceol
2.01
1.00
0.78
1.76
1.99
0.93
8.0
7.5
7.0
6.5
6.0
5.5
5.0
4.5
4.0
3.5
3.0
2.5
2.0
1.5
1.0
0.5
0.0

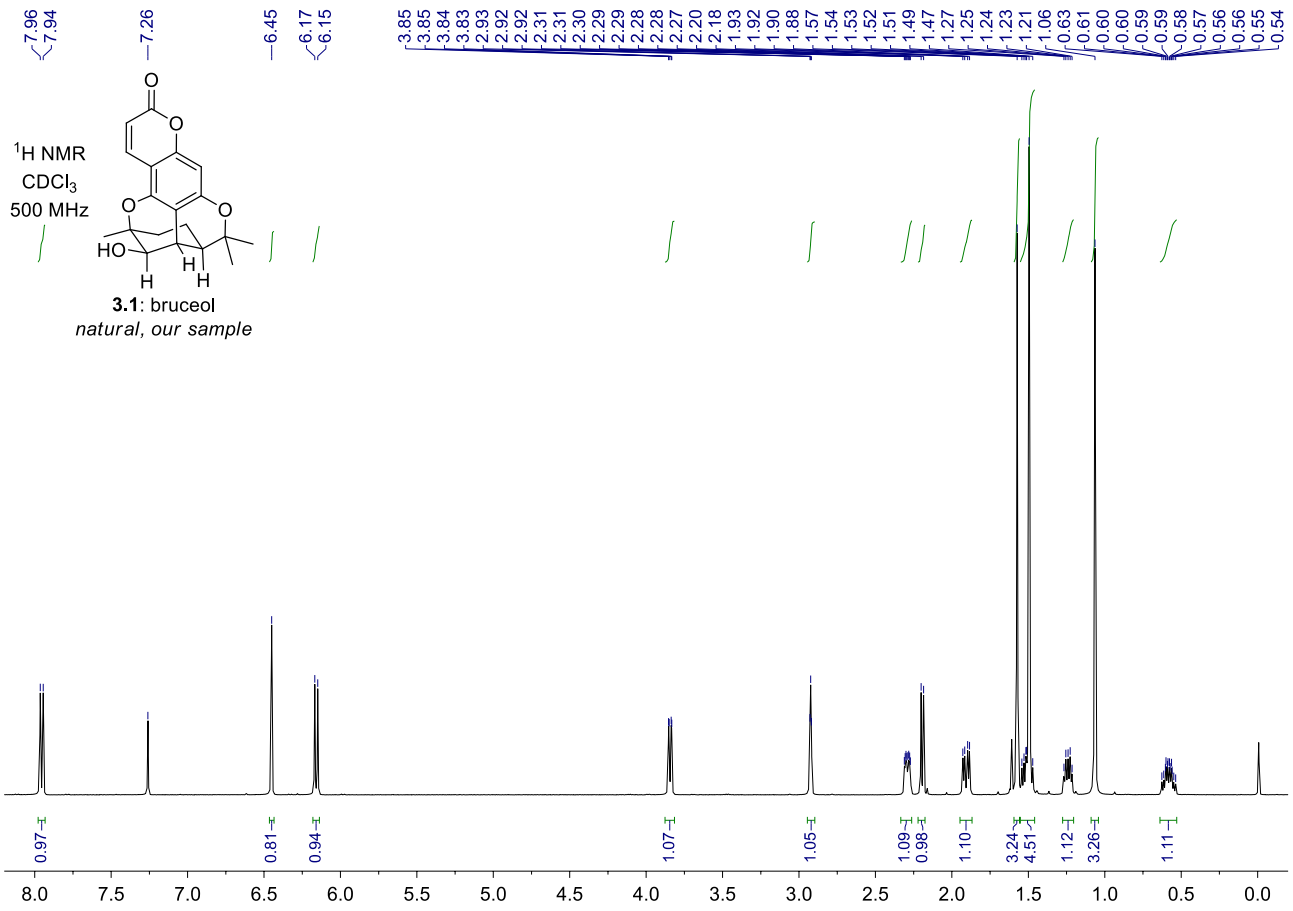
7.96
7.94
7.26
6.45
6.17
6.15
3.85
3.85
3.84
3.83
2.93
2.92
2.92
2.31
2.31
2.30
2.29
2.29
2.28
2.28
2.27
2.20
2.18
1.93
1.92
1.90
1.88
1.57
1.54
1.53
1.52
1.51
1.49
1.47
1.27
1.25
1.24
1.23
1.21
1.06
0.63
0.61
0.60
0.60
0.59
0.59
0.58
0.57
0.56
0.56
0.55
0.54
1H NMR
CDCl3
500 MHz
3.1: bruceol
natural, our sample
0.97
0.81
0.94
1.07
1.05
1.09
0.98
1.10
3.24
4.51
1.12
3.26
1.11
8.0
7.5
7.0
6.5
6.0
5.5
5.0
4.5
4.0
3.5
3.0
2.5
2.0
1.5
1.0
0.5
0.0

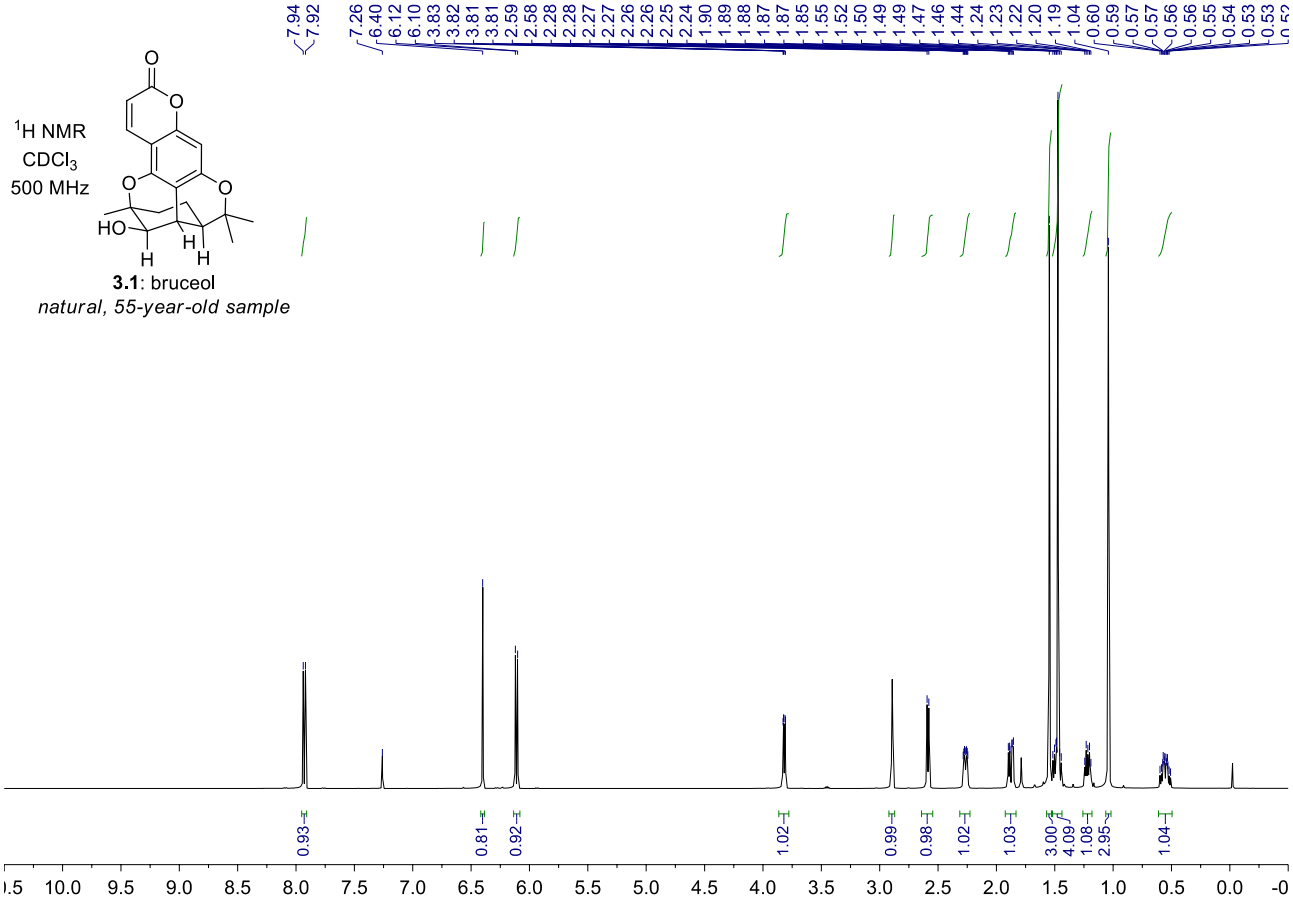
^{1}H NMR
$CDCl_3$
500 MHz
3.1: bruceol
natural, 55-year-old sample

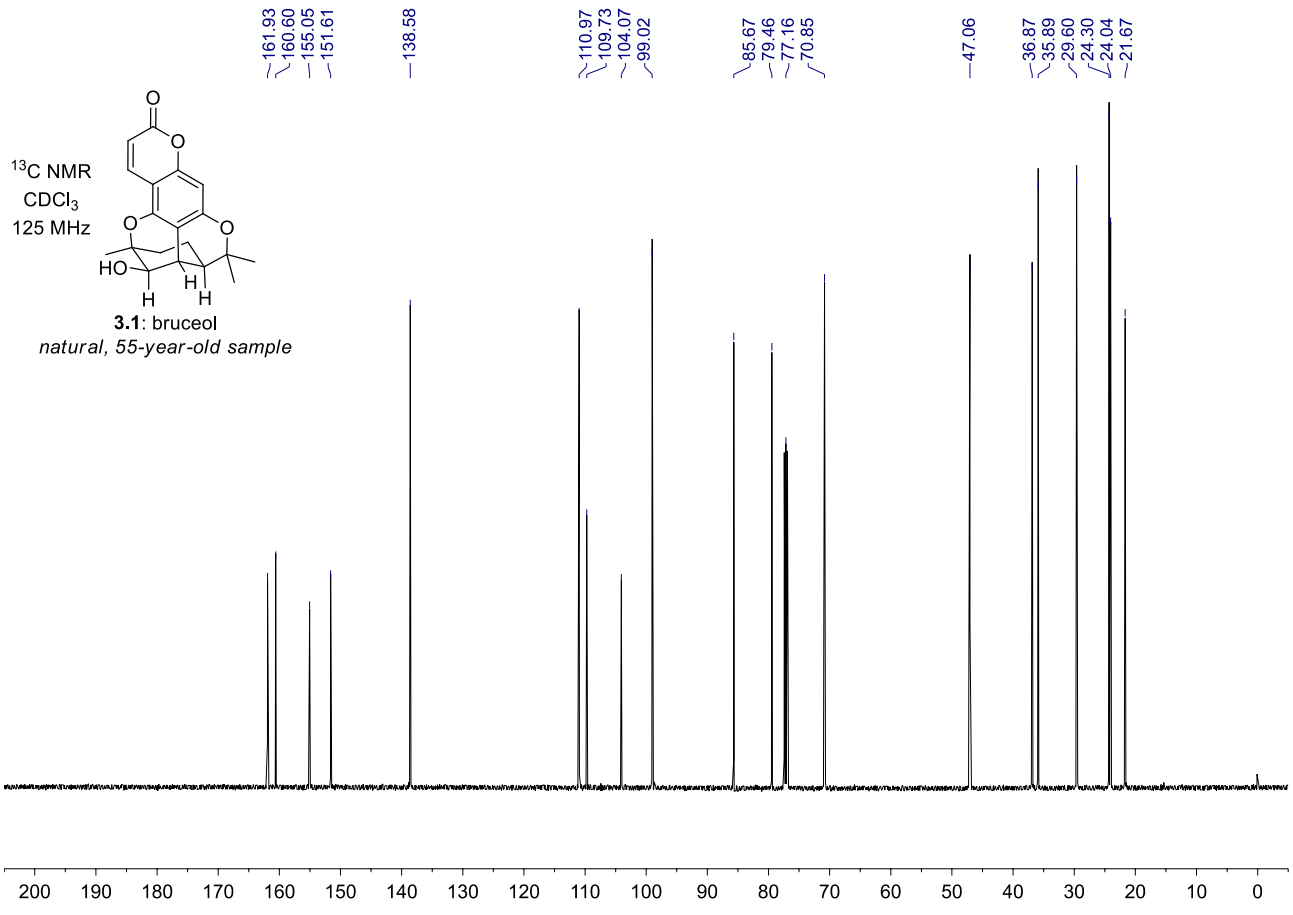
^{13}C NMR
$CDCl_3$
125 MHz
3.1: bruceol
natural, 55-year-old sample

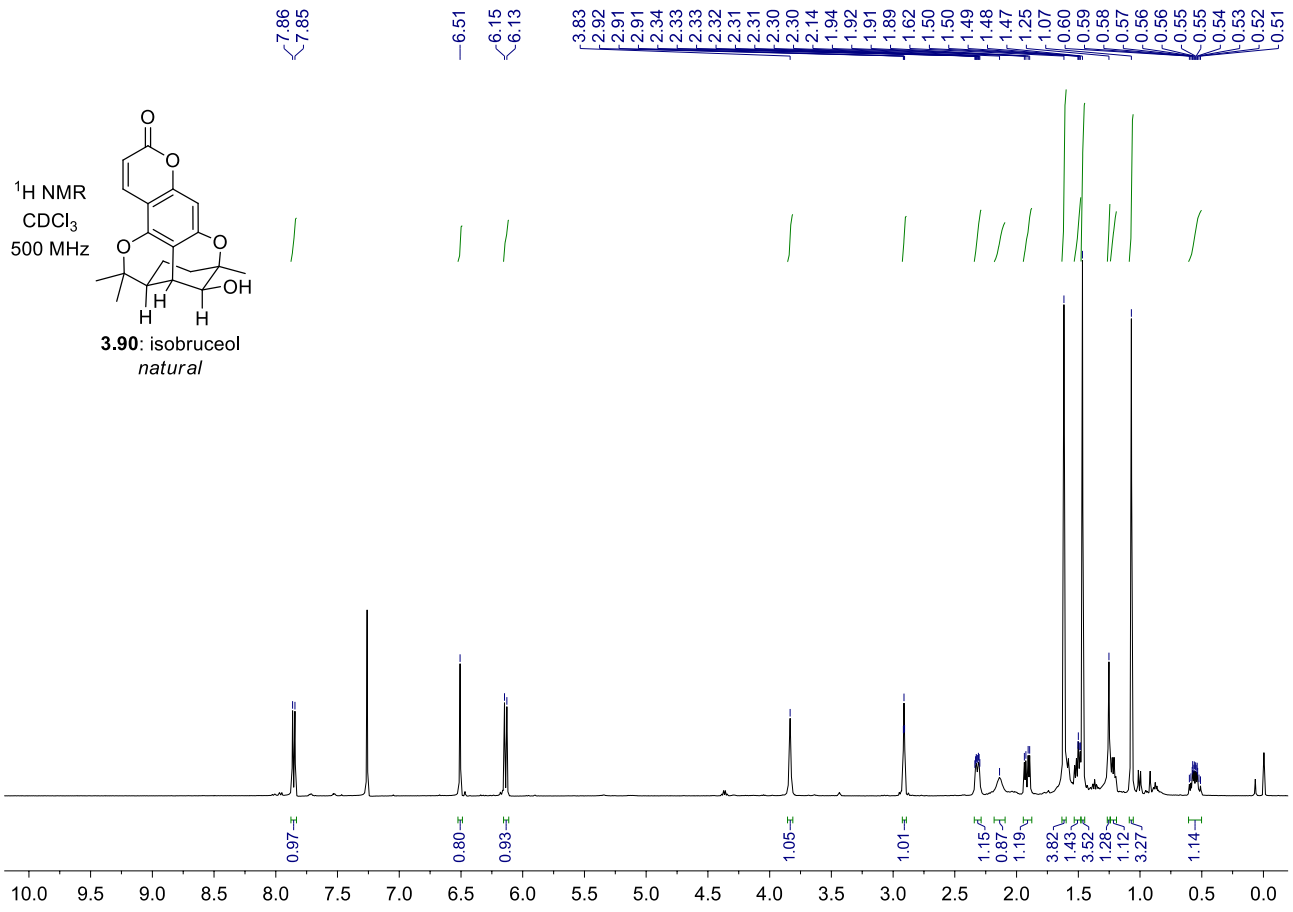
7.86
7.85
6.51
6.15
6.13
3.83
2.92
2.91
2.91
2.34
2.33
2.33
2.32
2.31
2.31
2.30
2.30
2.14
1.94
1.92
1.91
1.89
1.62
1.50
1.50
1.49
1.48
1.47
1.25
1.07
0.60
0.59
0.58
0.57
0.56
0.56
0.55
0.55
0.54
0.53
0.52
0.51
1H NMR
CDCl3
500 MHz
3.90: isobruceol
natural
0.97
0.80
0.93
1.05
1.01
1.15
0.87
1.19
3.82
1.43
3.52
1.28
1.12
3.27
1.14
10.0
9.5
9.0
8.5
8.0
7.5
7.0
6.5
6.0
5.5
5.0
4.5
4.0
3.5
3.0
2.5
2.0
1.5
1.0
0.5
0.0

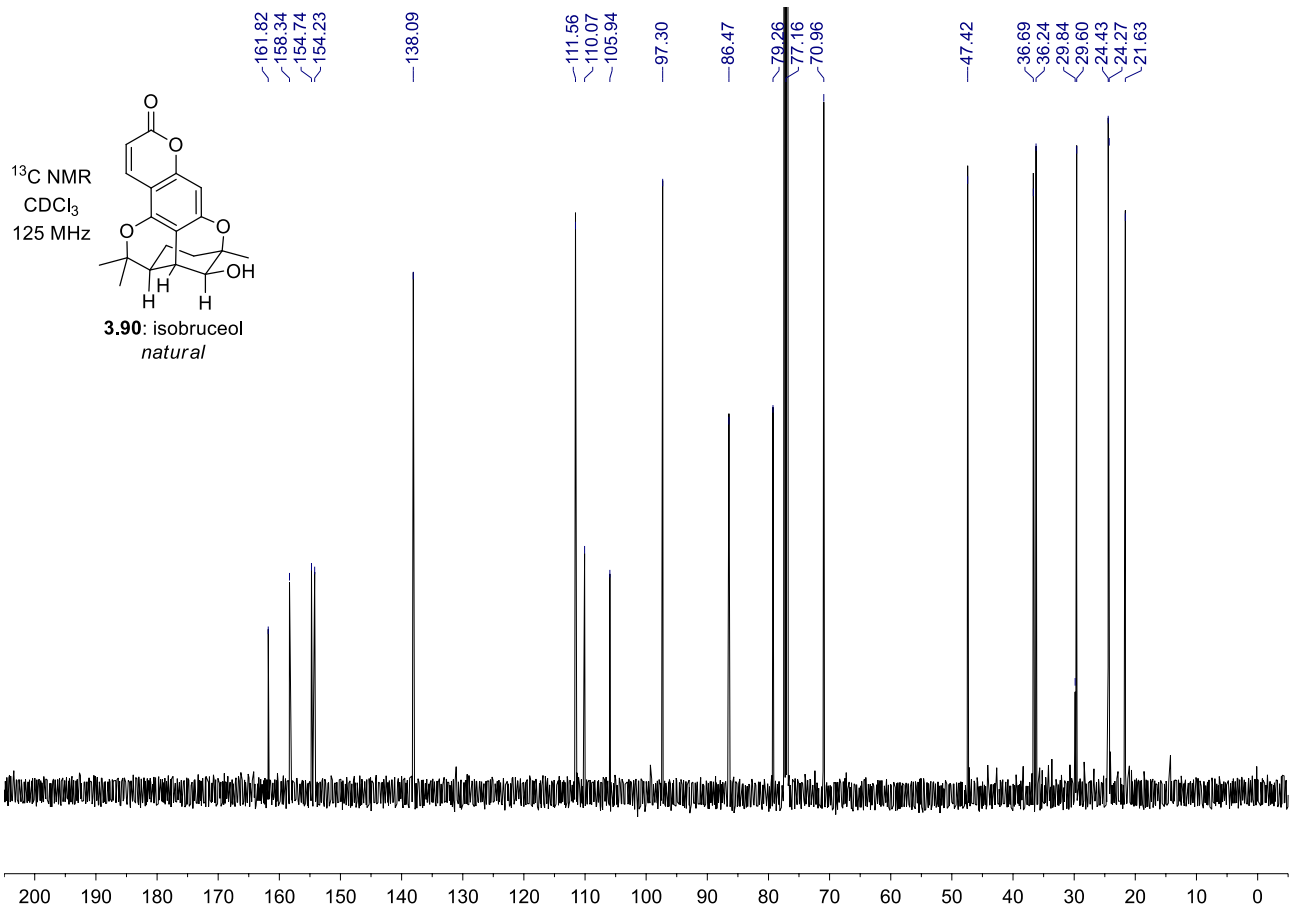
161.82
158.34
154.74
154.23
138.09
111.56
110.07
105.94
97.30
86.47
79.26
77.16
70.96
47.42
36.69
36.24
29.84
29.60
24.43
24.27
21.63
13C NMR
CDCl3
125 MHz
3.90: isobruceol
natural
200
190
180
170
160
150
140
130
120
110
100
90
80
70
60
50
40
30
20
10
0

3.4.7: ^{1}H and ^{13}C NMR Comparison Tables

Table 3.4: ^{13}C NMR comparison of bruceol (**3.1**)

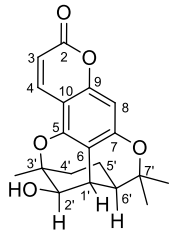

bruceol (**3.1**)

Position	Waterman's "bruceol" (1992) (100 MHz)	Natural bruceol **3.1** (2018) (125 MHz)	Synthetic bruceol **3.1** (2018) (125 MHz)
2	162.0	161.9	161.6
3	110.4	111.0	111.2
4	138.2	138.6	138.3
5	154.2	151.6	151.4
6	110.2	109.7	109.4
7	158.5	160.6	160.5
8	97.2	99.0	99.2
9	154.7	155.1	155.1
10	105.9	104.1	104.0
1'	36.2	35.9	35.9
2'	70.9	70.9	70.9
3'	79.3	79.5	79.3
3'-Me	24.5	24.3	24.2
4'	36.7	36.9	36.8
5'	21.7	21.7	21.6
6'	47.4	47.1	47.0
7'	86.5	85.7	85.5
7'-Me	29.6	29.6	29.5
7'-Me	24.3	24.1	23.9

Table 3.5: ^{1}H NMR comparison of isobruceol (**3.90**)

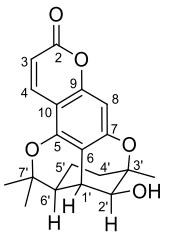

isobruceol (**3.90**)

Position	Waterman's "bruceol" (1992) (400 MHz)[4]	Natural isobruceol **3.90** (2018) (500 MHz)	Synthetic isobruceol **3.90** (2018) (500 MHz)
3	6.11 d (9.6)	6.14 d (9.5)	6.13 d (9.6)
4	7.84 dd (9.6, 0.6)	7.86 d (9.6)	7.85 d (9.5)
8	6.48 d (0.6)	6.51 br s	6.50 br s
1'	2.88 t (2.2)	2.91 t (2.4)	2.90 t (2.5)
2'	3.83 dd (7.1, 2.2)	3.83 br s	3.83 d (5.8)
2'-OH	2.38 d (7.2)	2.14 br s	2.17 d (8.0)
3'-Me	1.46 s	1.47 s	1.46 s
4'-ax.[##]	1.48 ddd (13.2, 11.5, 5.3)	1.50 ddd (15.0, 13.3, 7.2)	1.48 ddd (15.1, 13.3, 7.0)
4'-eq.	1.90 dd (13.2, 5.3)	1.92 dd (15.5, 6.2)	1.91 dd (15.5, 6.2)
5'-ax	0.54 dtd (13.4, 11.5, 5.3)	0.56 tdd (13.63, 11.68, 6.23)	0.55 tdd (13.5, 11.6, 6.3)
5'-eq.	1.20 dt (13.4, 5.3)	~1.2 mult (overlap)[#]	1.22 dt (13.3, 6.7)
6'	2.31 ddd (11.5, 5.3, 2.2)	2.32 (ddd) 11.7, 5.6, 2.7)	2.32 ddd (11.6, 5.5, 2.7)
7'-Me	1.59 s	1.61 s	1.61 s
7'-Me	1.09 s	1.07 s	1.07 s

Table 3.6: ^{13}C NMR comparison of isobruceol (**3.90**)

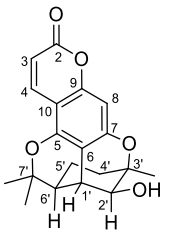

isobruceol (**3.90**)

Position	Waterman's "bruceol" (1992) (100 MHz)[4]	Natural isobruceol **3.90** (2018) (125 MHz)	Synthetic isobruceol **3.90** (2018) (125 MHz)
2	162.0	161.8	161.8
3	110.4	111.6	111.6
4	138.2	138.1	138.1
5	154.2	154.2	154.2
6	110.2	110.1	110.1
7	158.5	158.3	158.3
8	97.2	97.3	97.3
9	154.7	154.7	154.7
10	105.9	105.9	106.0
1'	36.2	36.2	36.3
2'	70.9	71.0	71.0
3'	79.3	79.3	79.3
3'-Me	24.5	24.3	24.3
4'	36.7	36.7	36.7
5'	21.7	21.6	21.6
6'	47.4	47.4	47.4
7'	86.5	86.5	86.5
7'-Me	29.6	29.6	29.6
7'-Me	24.3	24.4	24.4

3.4.8: Single Crystal X-ray Data

General experimental

Single crystals were mounted in paratone-N oil on a plastic loop. X-ray diffraction data were collected at 150(2) K on an Oxford X-Calibur single crystal diffractometer (λ = 0.71073 Å). Data sets were corrected for absorption using a multi-scan method, and structures were solved by direct methods using SHELXS-2014 [54] and refined by full-matrix least squares on F2 by SHELXL-2014,[55] interfaced through the program X-Seed.[56] In general, all non-hydrogen atoms were refined anisotropically and hydrogen atoms were included as invariants at geometrically estimated positions. Isobruceol, **3.90**, crystallises as small colourless rods (0.27 x 0.06 x 0.05 mm) in the monoclinic space group $P2_1$. As a consequence, the crystals were relatively weakly diffracting. Additionally, three molecules are present in the asymmetric unit with subtly different OH H atom torsion angles and hydrogen bonding interactions. The three molecules comprise part of a helical packing motif that extends along the *b-axis* of the unit cell. The structure was refined as a 2-component inversion twin.

Full details of the structure determinations have been deposited with the Cambridge Crystallographic Data Centre as CCDC 1865687-1865689 (CCDC 1865687 (bruceol, **3.1**); CCDC 1865688 (isobruceol, **3.90**); CCDC 1865689 (2'-*epi*-bruceol, **3.81**). Copies of this information may be obtained free of charge from The Director, CCDC, 12 Union Street, Cambridge CB2 1EZ, U.K. (fax, +44-1223-336-033; e-mail, deposit@ccdc.cam.ac.uk).

Absolute structure of hydroxyeriobrucinol (**3.91**)

The absolute structure of this hydroxyeriobrucinol (**3.91**) was determined by anomalous dispersion effects using Mo Kα radiation. When the reported enantiomer is chosen the Flack parameter is -0.2(2) for the refined structure and the Hooft parameter is -0.1(2). Further support for the absolute structure comes from analysing the Bijvoet pair data; the slope in a Bijvoet plot is positive (1.830) with P2(true) = 1.000 and P3(true) 0.993, suggesting the correct enantiomer has been assigned.[57] Two molecules, with the same absolute structure are present in the asymmetric unit but are involved in unique sets of hydrogen bonding interactions with the single water molecule and symmetry-related molecules of **3.91**.

Table 3.7: X-ray experimental data for **3.1**, **3.90**

Compound	bruceol (**3.1**)	isobruceol (**3.90**)
CCDC number	1865687	1865688
Empirical formula	$C_{19}H_{20}O_5$	$C_{57}H_{60}O_{15}$
Formula weight	328.35	985.05
Crystal system	Triclinic	Monoclinic
Space group	*P*-1	$P2_1$
a (Å)	7.3064(5)	15.1953(7)
b (Å)	8.2648(4)	9.8800(8)
c (Å)	14.1150(5)	16.2203(8)
α (°)	78.403(4)	
β (°)	85.652(4)	95.654(4)
γ (°)	68.875(5)	
Volume ($Å^3$)	778.83(8)	2423.3(3)
Z	2	2
Density (calc.) (Mg/m^3)	1.400	1.350
Absorption coefficient (mm^{-1})	0.101	0.097
F(000)	348	1044
Crystal size (mm3)	0.58×0.31×0.25	0.27×0.06×0.05
θ range for data collection (º)	3.32 to 29.43	3.26 to 29.41
Reflections total	3881	10818
Observed reflections [R(int)]	2959 [0.0453]	4527 [0.1304]
Goodness-of-fit on F2	1.070	0.939
R_1 [I>2σ(I)]	0.0492	0.0848
wR_2 (all data)	0.1329	0.1323
Largest diff. peak and hole ($e.Å^{-3}$)	0.344 and -0.229	0.299 and -0.299
Flack parameter	-	-

Table 3.8: X-ray experimental data for **3.81** and **3.91**.

Compound	2'-*epi*-bruceol (**3.81**)	hydroxyeriobrucinol (**3.91**)
CCDC number	1865689	1958707
Empirical formula	$C_{19}H_{20}O_5$	$C_{38}H_{42}O_{11}$
Formula weight	328.35	674.71
Crystal system	Triclinic	monoclinic
Space group	*P*-1	$P2_1$
a (Å)	7.6384(3)	6.33660(10)
b (Å)	9.8777(4)	15.3568(2)
c (Å)	11.2923(5)	16.6789(2)
α *(°)*	87.534(4)	90
β *(°)*	86.754(4)	99.6180(10)
γ *(°)*	67.644(4)	90
Volume ($Å^3$)	786.49(6)	1600.21(4)
Z	2	2
Density (calc.) (Mg/m^3)	1.387	1.400
Absorption coefficient (mm^{-1})	0.100	0.103
F(000)	348	716.0
Crystal size (mm3)	0.62×0.46×0.20	0.40 × 0.18 × 0.14
θ range for data collection (º)	3.47 to 29.31	3.521 – 29.357
Reflections total	3947	56739
Observed reflections [R(int)]	3340 [0.0374]	8066 [0.0391]
Goodness-of-fit on F2	1.029	1.032
R_1 [I>2σ(I)]	0.0406	0.0354
wR_2 (all data)	0.1112	0.0822
Largest diff. peak and hole ($e.Å^{-3}$)	0.357 and -0.218	0.27 and -0.25
Flack parameter	-	-0.2(2)

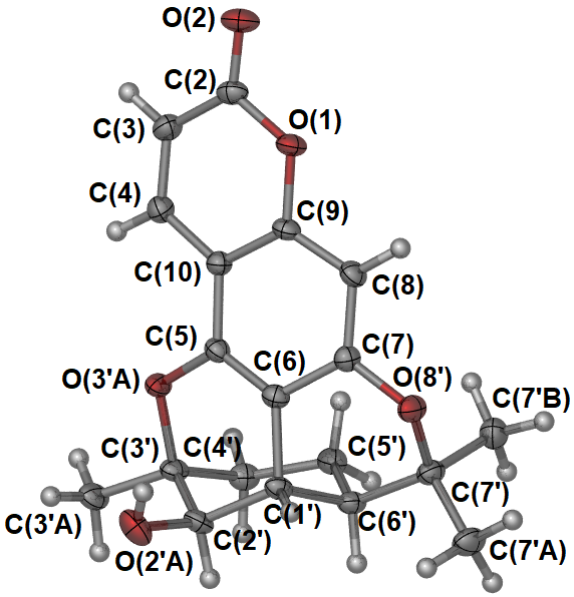

Figure 3.13: A representation of the structure of bruceol (**3.1**) with ellipsoids shown at the 50% probability level (carbon – grey; hydrogen – white; oxygen – red).

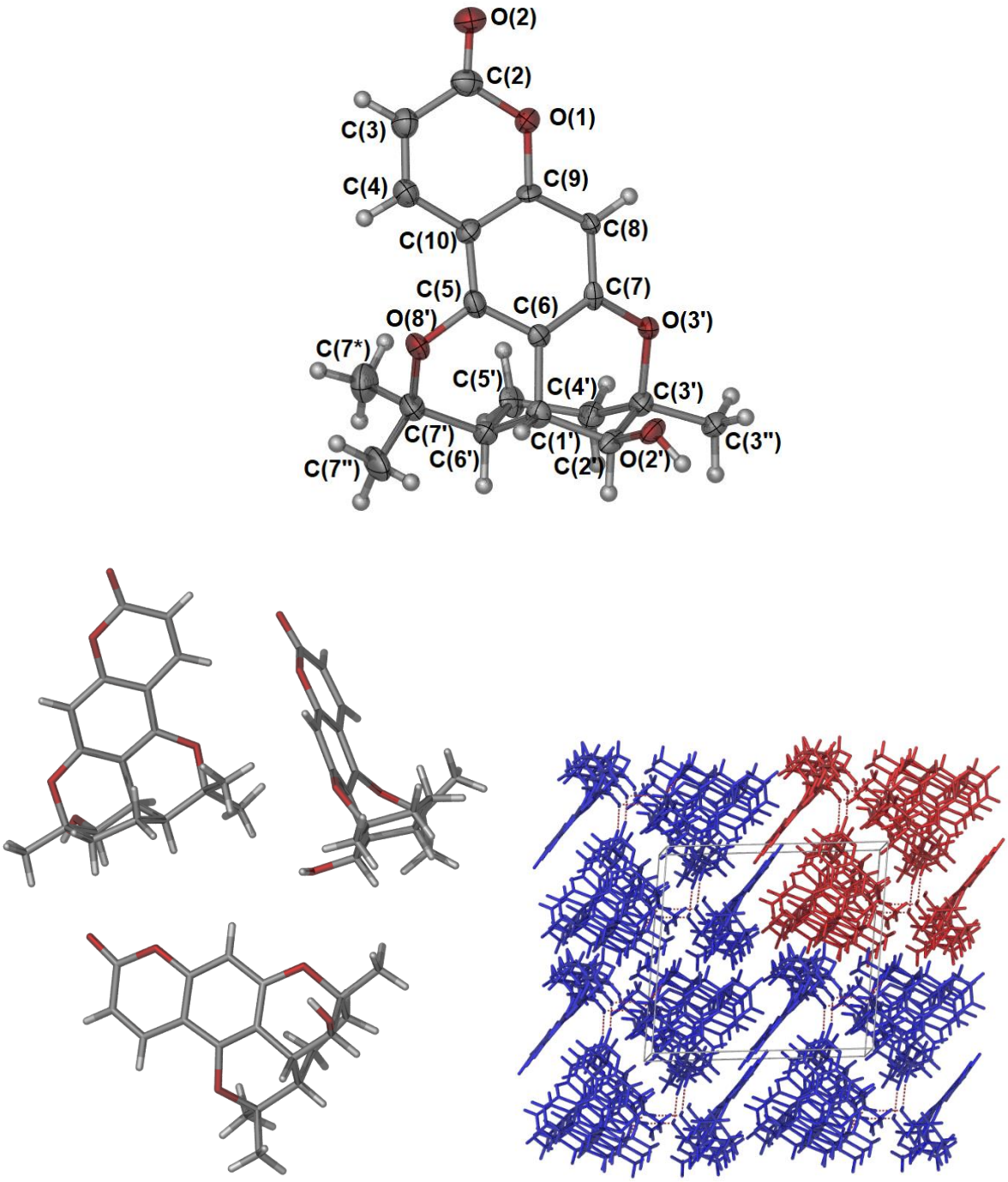

Figure 3.14: (a) A representation of one of the molecules of isobruceol (**3.90**) in the crystal with ellipsoids shown at the 50% probability level (carbon – grey; hydrogen – white; oxygen – red). The arrangement of (b) three molecules in the asymmetric unit and (c) the packing of the helical columns in the extended structure (one column shown in red, viewed almost down the *b*-axis).

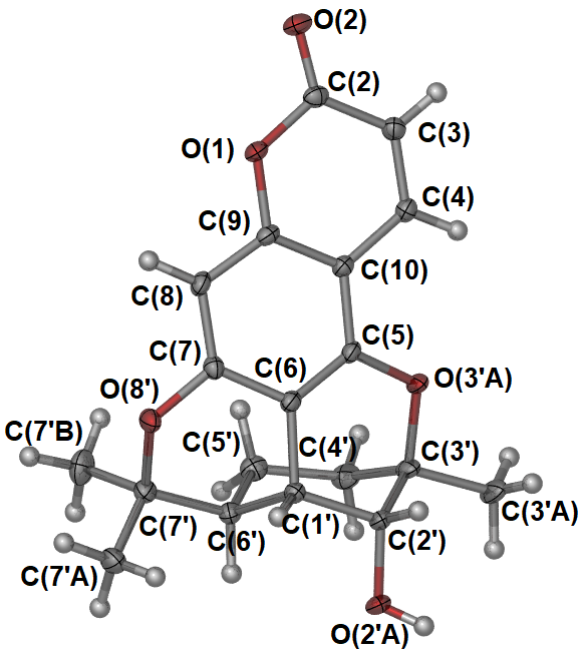

Figure 3.15: A representation of the structure of 2'-*epi*-bruceol (**3.81**) with ellipsoids shown at the 50% probability level (carbon – grey; hydrogen – white; oxygen – red).

3.5 References

[1] Duffield, A. M.; Jefferies, P. R.; Maslen, E. N.; Rae, A. I. M. *Tetrahefron*, **1963**, *19*, 593.

[2] Ghisalberti, E. L.; Jefferies, P. R.; Raston, C. L.; Skelton, B. W.; Stuart, A. D.; White, A. H. *J. Chem. Soc. Perkin Trans. 2* **1981**, 583.

[3] For a memoir detailing Crowfoot-Hodgkin's contributions to X-Ray crystallography: Dodson, G. *Biogr. Mems. Fell. R. Soc. Lond.* **2002**, *48*, 179.

[4] Woodward, R. B. *Perspectives in Organic Chemistry*; Interscience Publishers Inc.: New York, **1956**, 155.

[5] Roberts, J. D. *An Introduction to the Analysis of Spin-Spin Splitting in High-Resolution Nuclear Magnetic Resonance Spectra* **1961**, W. A. Benjamin Inc. (New York).

[6] Roberts' account of early NMR at Caltech is contained in his autobiography: Roberts, J. D. *The Right Place at the Right Time* **1990**, American Chemical Society (Washington, D.C.)

[7] Gray, A. I.; Rashid, M. A.; Waterman, P. G. *J. Nat. Prod.* **1992**, *55*, 691.

[8] Ghisalberti, E. L. *Phytochemistry* **1998**, *47*, 163.

[9] Beaudry, C. M.; Malerich, J. P.; Trauner, D. *Chem. Rev.* **2005**, *105*, 4757.

[10] Rahid. M. A.; Armstrong, J. A.; Gray, A. I.; Waterman. P. G. *Nat. Prod. Lett.* **1992**, *1*, 79.

[11] For a review on plant biosynthesis of coumarins: Bourgaud, F.; Hehn, A.; Larbat, R.; Doerper, S.; Gntier, E.; Kellner, S.; Matern, U. *Phytochem. Rev.* **2006**, *5*, 293.

[12] Camm, E. L.; Towers, G. H. N. *Phytochemistry*, **1973**, *12*, 961.

[13] For a review of coumarin natural products: a) Murray, R. D. H. *Nat. Prod. Rep.* **1989**, 591. For a review of coumarin natural products from *Rutacae*: Gray, A. J.; Waterman, P. G. *Phytochemistry*, **1978**, *17*, 845

[14] For a perspective on coumarin-meroterpenoid biosynthesis in *Philotheca* species: Sultana, N.; Sarker, S. D.; Armstrong, J. A.; Wilson, P. G.; Waterman, P. G. *Biochem. Syst. Ecol.* **2003**, *31*, 681.

[15] Verley, M. A. *Bull. Soc. Chim. France* **1899**, *21*, 414.

[16] Grünhagen, Ph.D. thesis, Heidelberg, **1898**.

[17] Kuhn, R. Hoffer, M. *Ber.* **1939**, *64*, 1243.

[18] a) Berkoff, C. E.; Crombie, L. *J. Chem. Soc.*, **1960**, 3734. b) Berkoff, C. E.; Crombie, L. *Proc. Chem. Soc.* **1959**, 400.

[19] Roberts, J. D. *J. Org. Chem.* **2009**, *74*, 4897.

[20] Crombie learned this from personal correspondence with Jefferies.

[21] a) Crombie, L.; Ponsford, R. *Chem. Commun. (London)* **1968**, 368. b) Crombie, L.; Ponsford, R. *J. Chem. Soc. C* **1971**, 788.

[22] Kaufman, K. D.; Kelly, R. C. *J. Heterocycl. Chem.* **1965**, *2*, 91.

[23] Begley, M. J.; Crombie, L.; Slack, D. A.; Whiting, D. A. *J. C. S. Chem. Comm.* **1976**, 140.

[24] Begley, M. J.; Crombie, L. Slack, D. A.; Whiting, D. A. *J. C. S. Perkin I* **1977**, 2402.

[25] a) Combes, G.; Vassort, P.; Winternitz, F. *Tetrahedron*, **1970**, *26*, 5981. b) de Alleluia, I. B.; Fo, R. B.; Gottlieb, O. R.; Magalhães, E. G.; Marques, R. *Phytochemistry*, **1978**, *17*, 517.

[26] Hua, S. -Z.; Wang, X. -B.; Luo, J. -G.; Wang, J. -S.; Kong, L. -Y. *Tetrahedron Lett.* **2008**, *49*, 5658.

[27] Kane, V. V.; Grayeck, T. L. *Tetrahedron Lett.* **1971**, *43*, 3994.

[28] Wang, X.; Lee, Y. R. *Tetrahedron*, **2009**, *65*, 10125.

[29] Lee, Y. R.; Kim, J. H. *Synlett* **2007**, *14*, 2232.

[30] Lee, Y. R.; Lee, W. K.; Noh, S. K.; Lyoo, W. S *Synthesis*, *5*, 853.

[31] Gruner, K. K.; Knölker, H. -J. *Org. Biomol. Chem.* **2008**, *6*, 3902.

[32] Melliou, E.; Magiatis, P.; Mitaku, D.; Skaltsounis, A. -L.; Chinou, E.; Chinou, I. *J. Nat. Prod.* **2005**, *68*, 78.

[33] Vander Velde, S. L.; Jacobsen, E. N. *J. Org. Chem.* **1995**, *60*, 5380.

[34] Kurti, L.; Czako, B. *Strategic Applications of Named Reactions in Organic Synthesis*, 1st Edition; Elsevier; **2005**, 222.

[35] Palucki, M.; McCormick, G. J.; Jacobsen, E. N. *Tetrahedron Lett.* **1995**, *36*, 5457.

[36] Wulff, H.; Rauer, H.; Düring, T.; Hanselmann, C.; Ruff, K.; Wrisch, A.; Grissmer, S.; Hänsel, W. *J. Med. Chem.* **1998**, *41*, 4542.

[37] Lee, N. H.; Muci, A. R.; Jacobsen, E. N. *Tetrahedron Lett.* **1991**, *32*, 5055.

[38] Braslau, R.; Naik, N.; Zipse, H. *J. Am. Chem. Soc.* **2000**, *122*, 8421.

[39] For a review of organocatalytic asymmetric epoxidation see: Ahu, Y.; Wang, Q.; Cornwall, R. G.; Shi, Y. *Chem. Rev.*, **2014**, *114*, 8199.

[40] Taber, D. F.; DeMatteo, P. W.; Hassan, R. A.; Wood, J. L.; Enquist, J. A. *Org. Synth.* **2013**, *90*, 350.

[41] Piggot, M. J. *Fitoterapia* **2018**, *126*, 1.

[42] Gavin Flematti, personal correspondence

[43] Teo, C. C.; Tan, S. N.; Yong, J,. W. H.; Hew, C. S.; Ong, E. S. *J. Chromatogr. A* **2010**, *1217*, 2484. . J. C.; Bell, S. G.; Wong, L. -L. *Chem. Soc. Rev.* **2012**, *41*, 1218.

[43] Seifert, A.; Vomund, S.; Grohmann, K.; Kriening, S.; Urlacher, V. B.; Lashat, S.; Pleiss, J. *ChemBioChem*, **2009**

[44] Deans, B. D.; Just, J.; Chhetri, J.; Burt, L. K.; Smith, J. N.; Kilah, N. L.; de Salas, M.; Gueven, N.; Bissember, A. C.; Smith, J. A. *Chem. Sel.* **2017**, *2*, 2439.

[45] Ghisalberti, E. L.; Jefferies; P. R. Raston, C. L.; Skelton, B. W.; White, A. H.; Worth, G. K. *J. Chem. Soc., Perkin Trans. 2* **1981**, 576.

[46] Yeom, H.-S.; Li, H.; Tang, Y.; Hsung, R. P. *Org. Lett.* **2013**, *15*, 3130.

[47] Murray, R. D. H.; Jorge, Z. D. *Tetrahedron*, **1984**, *40*, 3133.

[48] Munday, S. D.; Dezvarei, S.; Lau, I. C. -K.; Bell, S. G. *Chem. Cat. Chem.* **2017**, *9*, 2512.

[49] Whitehouse, C. J. C.; Bell, S. G.; Wong, L. -L. *Chem. Soc. Rev.* **2012**, *41*, 1218.

[50] Seifert, A.; Vomund, S.; Grohmann, K.; Kriening, S.; Urlacher, V. B.; Lashat, S.; Pleiss, J. *ChemBioChem*, **2009**, *10*, 853.

[51] Nazor, J.; Dannanmann, S.; Adjei, R. O.; Fordjour, Y. B.; Ghampson, I. T.; Blanusa, M.; Roccantano, D.; Schwaneberg, U. *Protein Eng. Des. Sel.* **2008**, *21*, 29.

[52] Whitehouse, C. J. C.; Bell, S. G.; Tufton, G. G.; Kenny, R. J. P.; Ogilvie, L. C. I.; Wong, L. -L. *Chem. Commun.* **2008**, 966.

[53] Coassini Lokar, L. R.; Delben, S. *Phytochemistry* **1988**, *27*, 1073.

[54] Sheldrick, G. M. *Acta Cryst.* **1990**, *A46*, 467.

[55] Sheldrick, G. M. *Acta Cryst.* **2015**, *C71*, 3.

[56] Barbour, L. J. *J. Supramol. Chem.* **2001**, *1*, 189.

[57] R. W. W. Hooft, L. H. Straver, and A. L. Spek, *J. Appl. Cryst*. **2008**, *41*, 96.

Chapter 4: Photochemical Reactions of Bruceol Related Compounds

The work presented in this chapter is a continuation of our investigations into *Philotheca* meroterpenoids, started in chapter 3. Here photochemical reactions of protobruceol-I and its isomers to synthesise the eriobrucinols and the protobruceols (II-IV) are presented.

4.1 Introduction

4.1.1: Chromenes of Interest

As discussed in the previous chapter, protobruceol-I (**4.1**) was the direct precursor to bruceol (**4.4**) in our biomimetic total synthesis, and **4.2** was the direct precursor to isobruceol (**4.5**) (Figure 4.1). The third isomeric coumarin-chromene **4.3** was used in the first preparation of **4.2** by an isomerisation reaction. As the preparation of **4.2** was not known before our work, experiments became available to us that were not previously possible. These chromenes can be used to make several other *Philotheca* natural products.

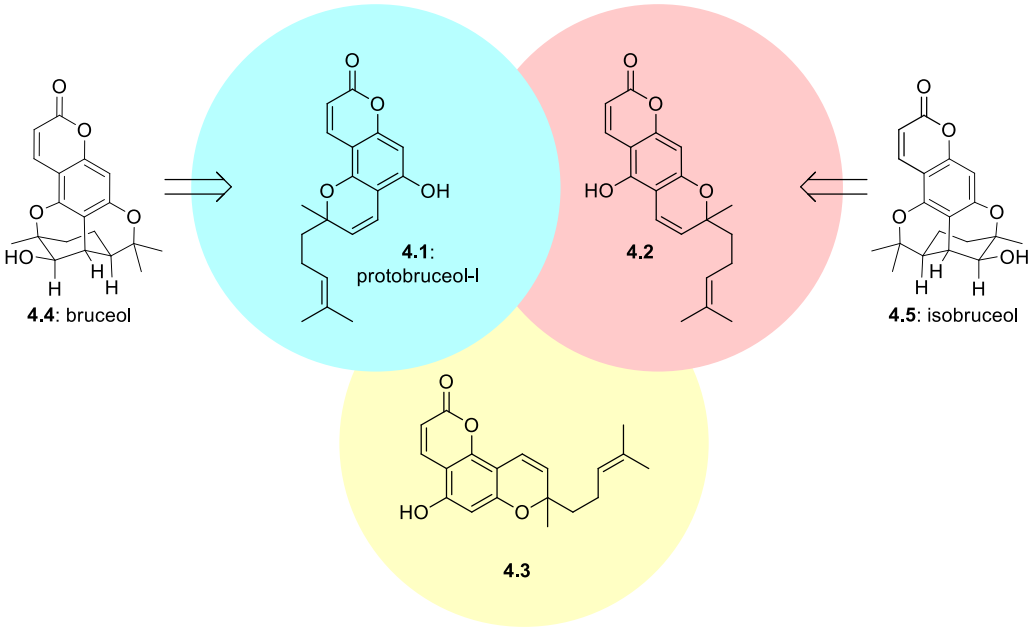

Figure 4.1: Coumarin chromenes protobruceol-I (**4.1**), **4.2**, and **4.3**.

4.1.2: Protobruceol Natural Products

Although its synthetic preparation was reported over 50 years ago by Crombie,[1] protobruceol-I (**4.1**) was first isolated in 1994 alongside several other oxygenated compounds collectively known as the protobruceols (**4.6** – **4.10**) (Figure 4.2).[2] Protobruceol-II (**4.6**) and protobruceol-III (**4.7**) have the same chromene-coumarin configuration as protobruceol-I (**4.1**) (blue box) and were isolated along with corresponding hydroperoides **4.8** and **4.9**. The oxidation pattern is consistent with the products of a singlet oxygen ene (Schenck ene) reaction – a reaction possible both in Nature and in the laboratory. Protobruceol-IV (**4.10**) was proposed to have the same linear configuration as **4.2** (pink box). This is a simple analogue of II (**4.6**) and similar analogues of **4.6** – **4.9** could potentially be undiscovered natural products.

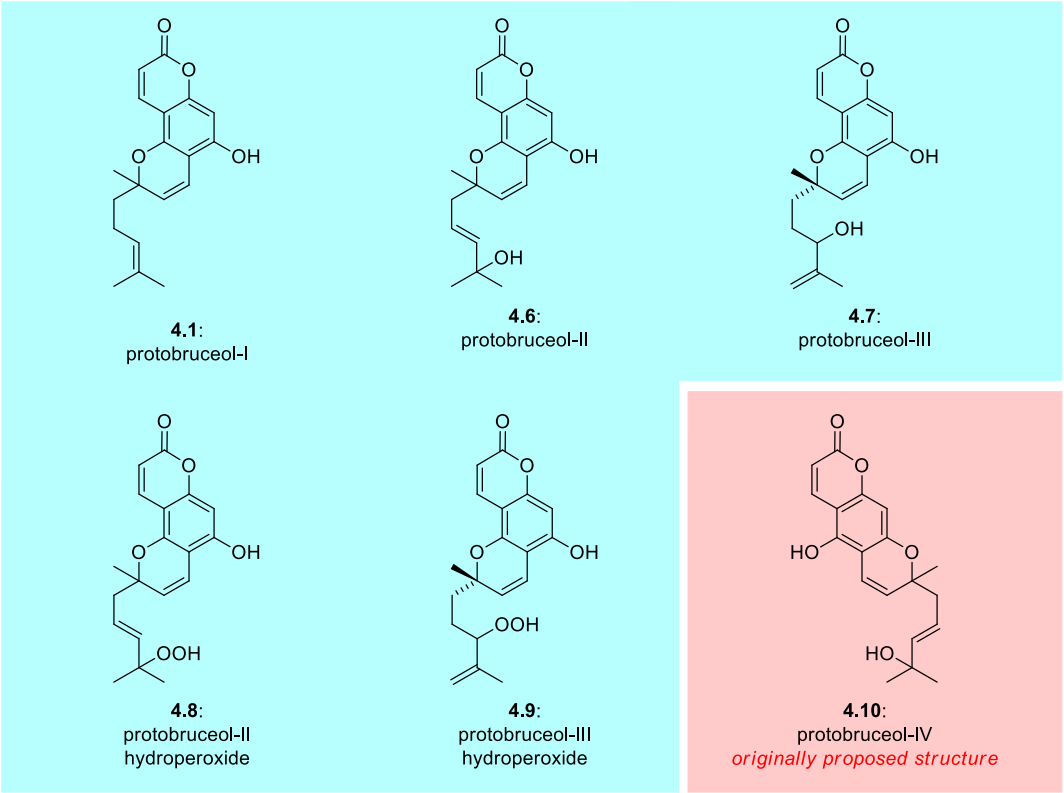

Figure 4.2: Protobruceols I-IV (**4.1**, **4.6** – **4.10**) from *P. brucei*. Waterman (1994)

4.1.3: Eriobrucinol Natural Products

Additionally, the three chromenes **4.1** – **4.3** have three corresponding cyclobutane "cyclol" natural products found in *P. brucei* (Figure 4.3). These are formed by photochemical [2+2] cycloaddition reactions in Nature.[3] The first discovered was eriobrucinol (**4.11**) which has the same orientation as isobruceol (**4.5**) and is derived from chromene (**4.2**).[4] Later, the isomeric isoeriobrucinol A (**4.12**) and B (**4.12**) were reported; these are derived from protobruceol-I (**4.1**) and **4.3** respectively.[5] Notably, isoeriobrucinol B (**4.12**) is the only known natural product of *Philotheca* bearing the angular configuration of **4.2** with a hydroxy group at C-5.[6]

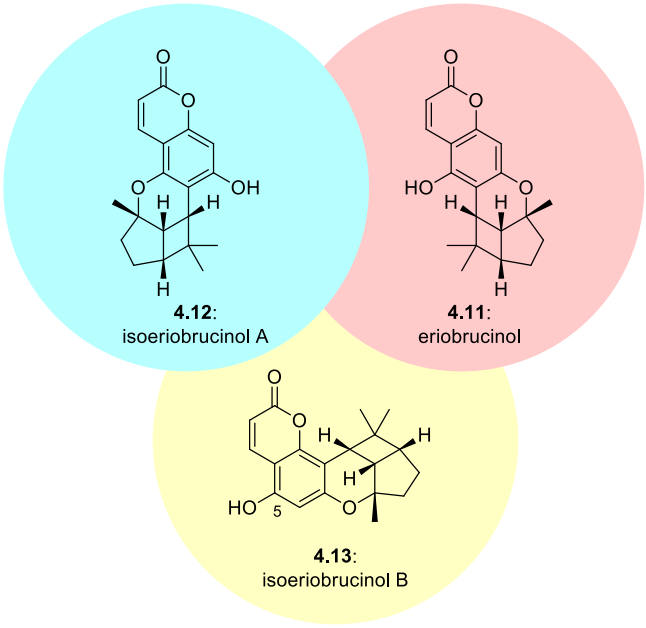

Figure 4.3: Eriobrucinols (**4.11** – **4.13**) from *P. brucei*.

The cyclol eriobrucinol (**4.11**) has two oxidised derivatives found in nature. 4'- and 5'-*β*-hydroxyeriobrucinol (**4.14** and **4.15**) (Figure 4.4). Oxidation presumably occurs through a P450 monoxygenase enzyme on the convex face of the puckered cyclol ring system.

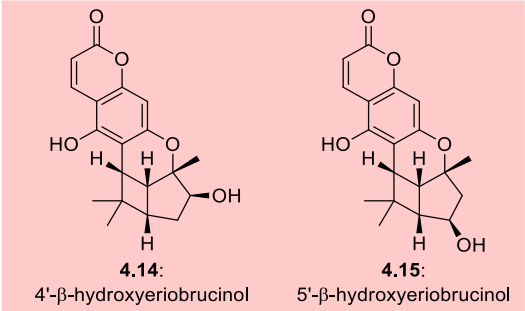

Figure 4.4: 4'-*β*-hydroxyeriobrucinol (**4.14**) and 5'-*β*-hydroxyeriobrucinol (**4.15**) from *P. brucei*. Waterman (1992).

4.2 Singlet Oxygen

4.2.1: Molecular Orbitals of Singlet Oxygen

Protobruceols-II and -III (**4.6** and **4.7**) are biosynthesised by oxidation with singlet oxygen. To understand the reactivity of singlet oxygen we will cover some basic molecular orbital theory.[7]

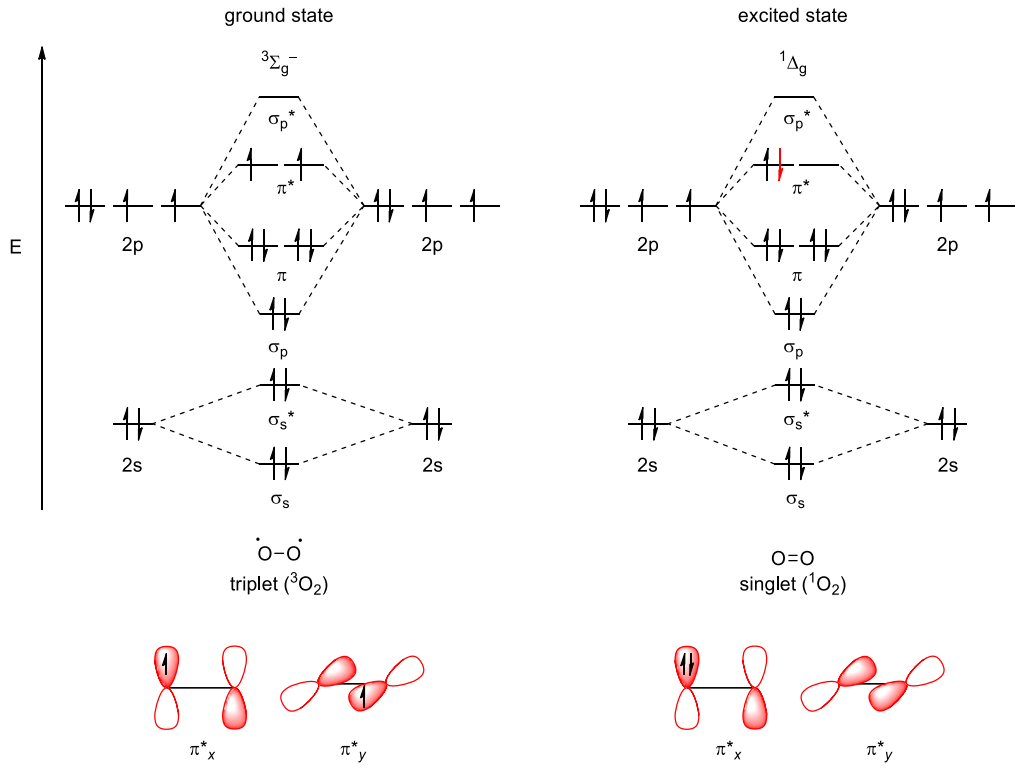

Figure 4.5: Molecular Orbital Diagram of Triplet and Singlet Oxygen.

Excited singlet Oxygen differs from the triplet ground state by the configuration of the highest occupied molecular orbital (HOMO), the π* (Figure 4.5). In the ground (triplet) state, unpaired electrons occupy both degenerate π* orbitals with parallel spin (following Hund's rule). It is a stable diradical. Singlet oxygen on the other hand has these electrons paired in the same π* orbital, leaving the other π* orbital empty as the lowest unoccupied molecular orbital (LUMO). In both cases the bond order of oxygen is 2, however triplet oxygen is drawn here with a single bond and with a radical positioned on either atom. This is somewhat misleading as the O-O bond of $^3O_2$ and $^1O_2$ are very similar (with $^3O_2$ slightly stronger), and each radical is distributed across the O_2 molecule (can be thought of two ½ bonds), even though it is drawn as a single bond in the Lewis representation. Resonance of this diradical has been connected to the stability of triplet oxygen.[8] The higher reactivity of singlet oxygen $^1O_2$ can be attributed to the lower energy LUMO, this low energy LUMO also makes it electrophilic.

Additionally, ground state $^3O_2$ typically reacts poorly with organic molecules, as these mostly do not have unpaired electrons (i.e., are not free-radicals), and have singlet ground states. This means the reaction of an organic molecule (singlet state) with triplet oxygen cannot form a new stable singlet state organic molecule via a concerted process as this would violate the conservation of quantum spin. Rather, a higher energy triplet adduct intermediate must form, which can subsequently relax to a new ground state. The result is a kinetically slow process, even if it is thermodynamically favourable. An example of this is the autoxidation of laboratory solvents such as Et_2O or THF which can take years to form dangerous amounts of organic peroxides. This restriction is lost when O_2 is excited to the singlet state.

Singlet oxygen is diamagnetic and therefore its reactivity with singlet state molecules is not restricted by the requirement for spin conservation. While this can be problematic for undesired autoxidation processes and as a biological reactive oxygen species (ROS), singlet oxygen finds niche use as a unique and selective chemical oxidant.

4.2.2: Generation of Singlet Oxygen

Relaxation to the triplet state is very fast (on the microsecond scale). It is also heavily solvent dependant as $^1O_2$ loses its energy to solvent vibrations (the transition directly to $^3O_2$ is spin forbidden). Solvents containing O-H (vibration ~3500 cm^{-1}) and C-H (~3000 cm^{-1}) break down $^1O_2$ the fastest.[9] In practice, singlet oxygen must be generated *in situ*, usually by excitation using a photosensitising dye (Figure 4.6). These strongly coloured dyes efficiently absorb visible light and transfer this energy to excite dissolved ground state O_2. In green leaves, oxygen can be sensitised by chlorophylls. The synthetic dyes shown share features of large, conjugated ring systems. This is what allows the absorption of visible light. The absorption spectra of these compounds are tuneable, as such hundreds of dyes are currently commercially available.

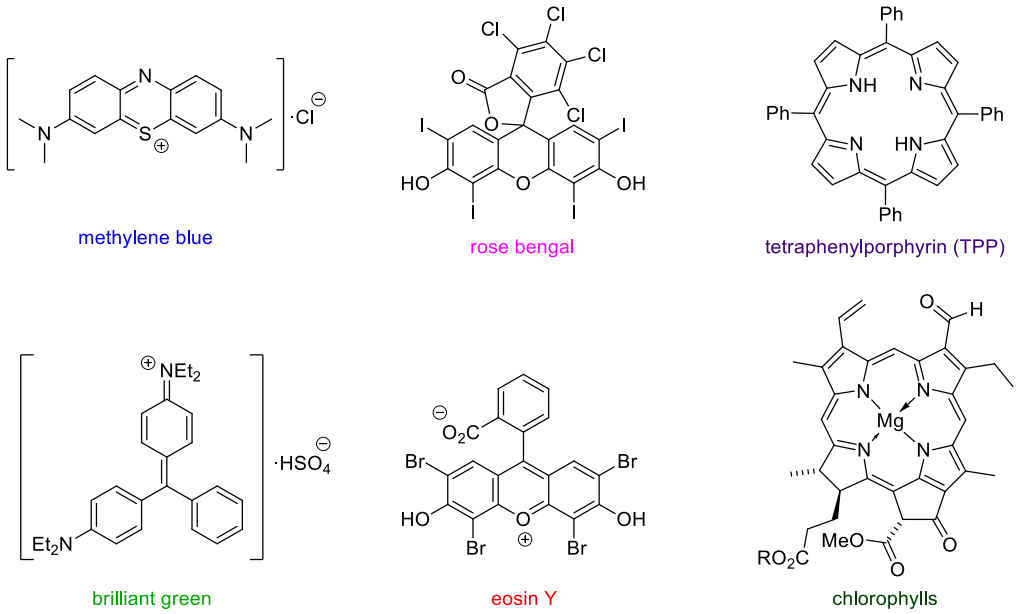

Figure 4.6: Several Photosensitiser Dyes.

4.2.3: Reactivity of Singlet Oxygen

Singlet oxygen reacts with organic molecules in two possible ways (Figure 4.7). Firstly, it can undergo cycloaddition reactions with dienes and alkenes to form endoperoxides. As previously stated, the empty π* orbital of $^1O_2$ means the molecule is electrophillic. As such, Diels-Alder reactions of this type work best with electron-rich dienes, such as furans – although products are typically unstable, difficult to isolate, and potentially explosive.[10] [2+2] cycloaddition reactions of $^1O_2$ are significantly less common. This transformation is symmetry forbidden, analogous to the more familiar all-carbon photochemical [2+2] cycloaddition. Reported reactions of this type usually include electron-rich olefins (most commonly enamines, or enol ethers) and the mechanism is not fully understood; however, it is unlikely it occurs through a concerted process. The dioxetane products formed are highly unstable and seldom isolatable.[11]

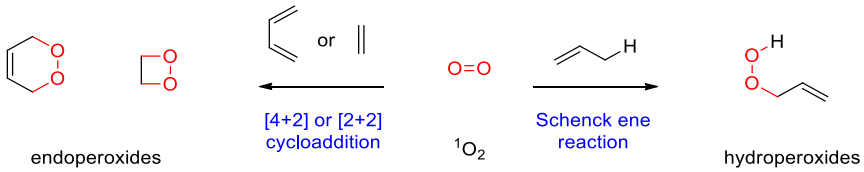

Figure 4.7: Known reactions involving singlet oxygen.

Lastly, singlet oxygen can undergo ene reactions. This is known as the Schenck ene reaction after German chemist and pioneer of singlet oxygen chemistry Gunther Otto Schenck.[12] Whilst the precise nature of the mechanism has been controversial, mainly due to conflicting results from computational and kinetic experiments, only the mechanism evoking a perepoxide intermediate will be considered here (Scheme 4.1). Cheletropic cycloaddition of the olefin to $^1O_2$ gives a key intermediate perepoxide. This unstable intermediate fragments by concerted abstraction of an allylic proton and opening of the oxirane ring, resulting in the observed hydroperoxide. A requirement for this fragmentation is for the allylic proton and C-O oxirane bond to be cleaved must overlap. This has consequences to selectivity in systems where multiple products are possible, particularly in strained cyclic molecules.

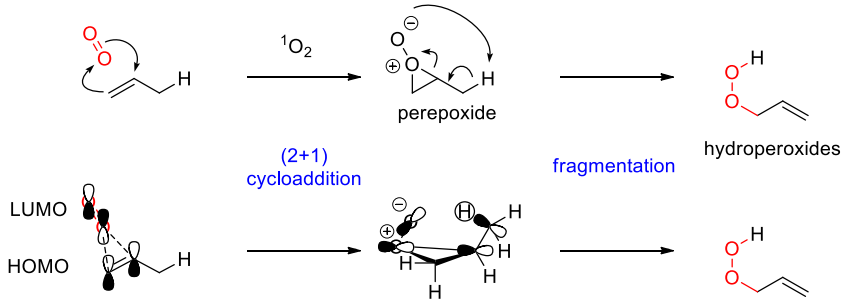

Scheme 4.1: Two-step mechanism for the Schenck ene reaction.

4.2.4: Selectivity of the Schenck Ene Reaction

The Schenck reaction has potential to be highly selective. Experiments by Laffer and co-workers on the oxidation of α-pinene (**4.16**) were shown to regio- and stereoselectively favour a single product (**4.19**) out of four possible isomers (Scheme 4.2).[13] The selectivity of this reaction is readily explained. Firstly, exo (the face of the alkene opposite the gem dimethyl group) addition is preferred on steric grounds. The dimethyl group physically blocks one side of the molecule. Secondly, the regiochemistry is explained by consideration of molecular orbitals. For the intermediate perepoxide to abstract the allylic proton good σ-π orbital overlap is needed. In this strained ring-system, the protons of C-4 are angled unfavourably orthogonal to the perepoxide. On the other hand, the exocyclic methyl group is free rotating and can much better facilitate the intramolecular rearrangement.

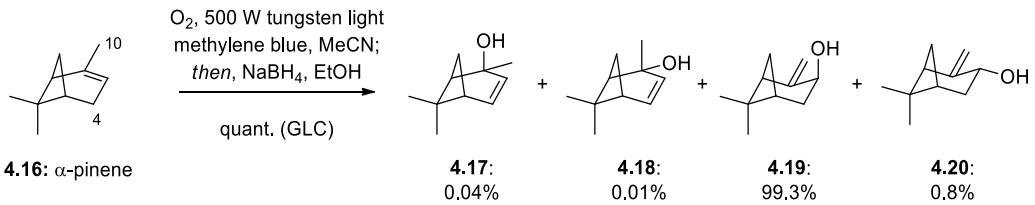

Scheme 4.2: Studies on the Schenck ene reaction of α-pinene (**4.16**). Laffer (1973)

Indeed, this rationalisation can be extended to many systems. For carbocycles, the orientation of the perepoxide intermediate relative to the available methine protons will dictate the favoured product. Conversely, in linear systems, such as in the protobruceols, it is quite a different story. Studies from

Orfanopoulos show a very clear trend in the oxygenation of dimethylpropene derivatives (Scheme 4.3).[14] Here, **4.21** reacts to give a mixture of internal alkene **4.22** and terminal alkene **4.23**. In the unsubstituted dimethylpropene (R = H) there is no selectivity, however, as R becomes large the internal alkene **4.22** becomes the major product. There are two points to be made here: firstly, the *trans* product is always observed. This is rationalised by the boat-like transition state preferring an *s*-trans orientation, with R opposing the quaternary carbon centre. Secondly, when R is large it is better able to stabilise the build-up of positive charge where the proton is abstracted. In the example where R = CPh_3 (trityl), selectivity is good. This study is particularly relevant to the protobruceols as it represents a good model the oxidation pattern for a prenyl group. For protobruceol-I (**4.1**) R = methylene (-CH_2-) connected to the rest of the molecule. This is smaller than *i*-Pr, so selectivity is expected to be low – somewhere between 50:50 and ~62:38.

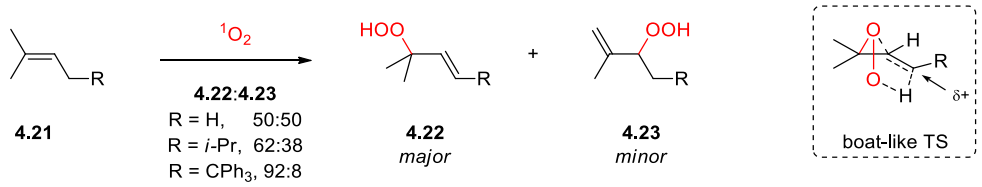

Scheme 4.3: Studies on the regioselectivity of the Scheck ene reaction. Orfanopoulos (1997)

The Schenck ene reaction is a highly substrate dependent reaction. However, during a biomimetic synthesis of kuwanons I and J (not shown) the Lei group were able to show the product distribution could be manipulated by solvent, and more strikingly the choice of sensitiser (Scheme 4.4).

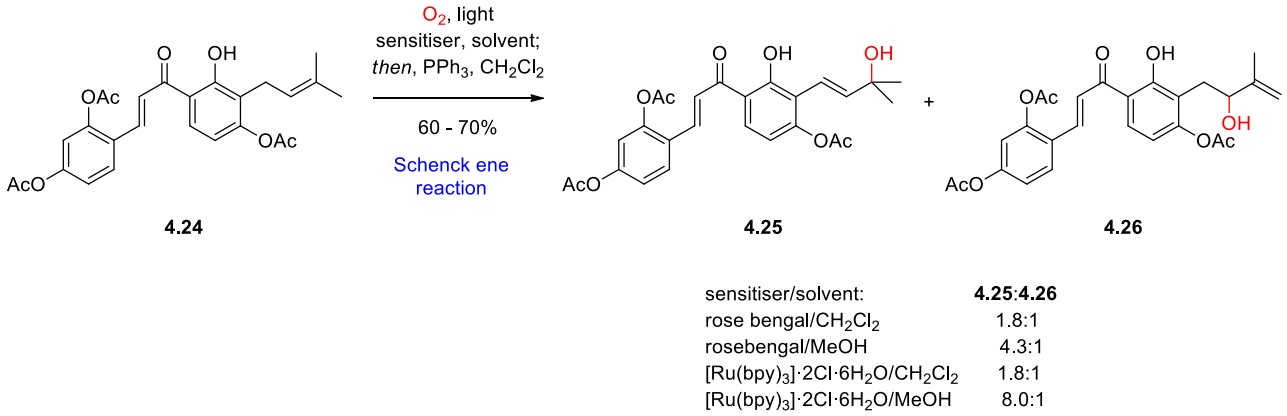

Scheme 4.4: Schenck ene reaction dependent on solvent and sensitiser. Lei (2014)

Four sensitisers were screened in both CH_2Cl_2 and MeOH for the oxygenation of **4.24**, all conditions gave similar yields of ~60–70%. TPP and methylene blue gave a ratio of ~2:1 **4.25**:**4.26**, consistent with what would be expected. However, when rose bengal was used, this ratio doubled in MeOH, and doubled again with $Ru(bpy)_3$ in MeOH.

Another example where reactivity was dependent on choice of sensitiser is in the photooxygenation of furylalkylamines to generate pyrrolizidines (Scheme 4.5).[15] Here, when rose bengal was used furylalkylamines **4.27** undergo $^1O_2$ Diels-Alder reaction and subsequent rearrangement to pyrrolidiidines **4.28**. Alternatively, when methylene blue was used the same cyclisation occurs, but additional oxidation by Schenck ene reaction of **4.28** to give **4.29**. Although the precise mechanism is not known, the differing reactivity is attributed to interaction of methylene blue with the substrate.

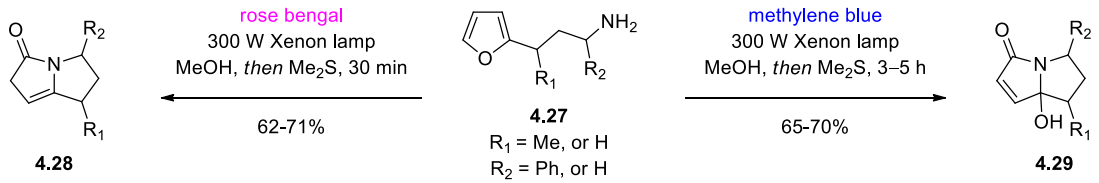

Scheme 4.5: Preparation of pyrrolizdines using $^1O_2$ methodology. Vassilikogiannakis (2016)

4.2.5: Singlet Oxygen in Organic Synthesis

While experimenting with the newly discovered naphthalene analogue, tetracene (**4.30**) Fritzsche discovered irradiating a solution of **4.30** with sunlight caused the solution to lose its colour and a precipitate formed.[16] Although he was unaware of what reaction had occurred, it was subsequently found the endoperoxide **4.31** was formed. This is the first known example of a singlet oxygen reaction. In this case, the tetracene (**4.30**) itself is acting as a photosensitiser, and O_2 is taken from the open air.

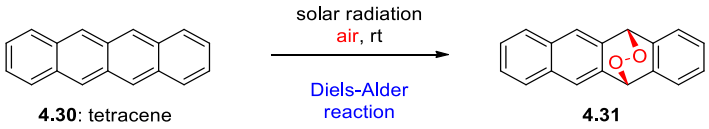

Scheme 3.6: First observed singlet oxygen reaction. Fritzsche (1867)

Singlet oxygen chemistry has made many advances in usage in the subsequent 150 years to present day.[17] The first reported synthesis of a natural product using singlet oxygen as a reagent was Schenck and Ziegler's classic biomimetic one-step synthesis of ascaridole (**4.33**) from α-terpinene (**4.32**) by Diels-Alder reaction (Scheme 4.7).[18] This reaction was of particular significance as ascaridole was used as a medicine for intestinal worms at the time. This borders on ideal synthesis, with 100% atom economy, step economy, and readily available and cheap reagents.

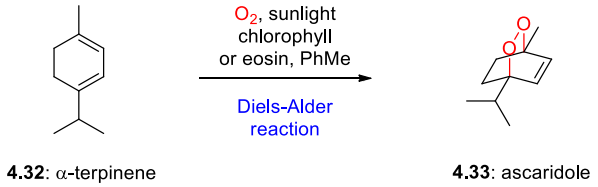

Scheme 4.7: Synthesis of ascaridole (**4.33**). Scheck (1944)

Similarly, in a diversity-oriented study of frondosin natural product analogues Mehta and Likhite used a $^1O_2$ Diels-Alder reaction to prepare **4.35** (Scheme 4.8).[19]

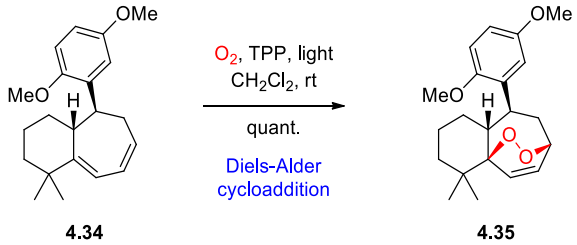

Scheme 4.8: Singlet oxygen Diels-Alder reaction of **4.34**. Mehta and Likhite (2009)

An example of this reaction from within our research group is the oxidation of capillobenzopyranol (**4.36**) (Scheme 4.9).[20] Following a successful synthesis of verrubenzospirolactone[21] (not shown) our group returned to explore how it could be prepared from capillobenzopyranol (**4.36**) in Nature. Diels-Alder reaction of **4.36** with singlet oxygen affords endoperoxide **4.37**, however this is quenched with solvent (MeOH) to give the peroxylactol **4.38** which was isolated. This in turn rearranged with classic Kornblum-DeLaMare conditions to give methoxylactone **4.39**. This was put forward as a viable route in biosynthesis, however in nature the endoperoxide **4.38** would need to be quenched with water. In practice the hydroxy analogue of hydroxybutenolide **4.39** was prepared by alternative methods and could be smoothly converted into the natural product.

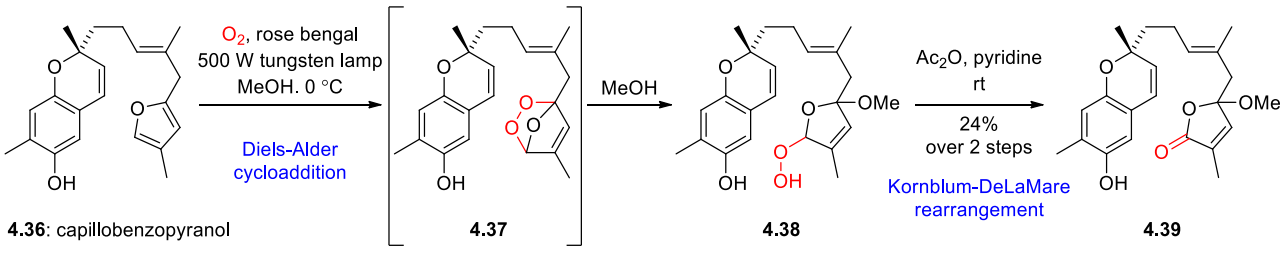

Scheme 4.9: Biomimetic oxidation of capillobenzopyranol (**4.36**). George (2017)

A great example of a selective Schenck ene reaction comes again from the Lei group in the final step of their biomimetic asymmetric synthesis of jungermatrobrunin A (**4.42**) (Scheme 4.10).[22] When **4.40**

is subjected to $^1O_2$ it preferentially attacks the convex face (top face as drawn). From here a perepoxide intermediate can select from two eligible methylene protons (explicitly drawn), abstraction from the highlighted proton to form **4.41** is strongly favoured and subsequent cyclisation gives the peroxylactol target jungermatrobrunin A (**4.42**) in 57% isolated yield (65% by NMR).

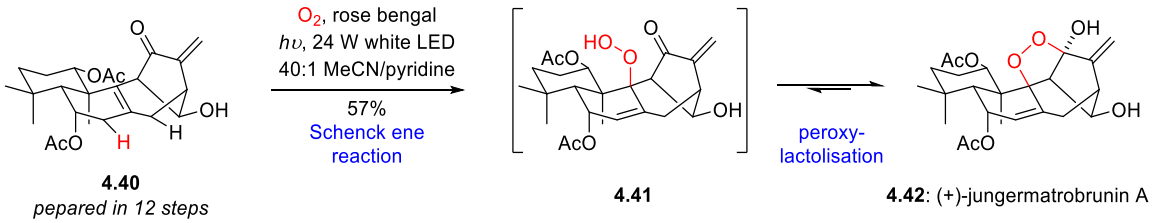

Scheme 4.10: Synthesis of jungermatrobrunin A. Lei (2019)

Perhaps a more socially relevant example comes from the semisynthesis of the antimalarial drug artemisinin (**4.50**). Seeberger and co-workers were able to convert a hitherto useless isolation by-product dihydroartemisinic acid (**4.43**) to the potent drug **4.50** in a cavalcade of oxygenation reactions and rearrangements.[23] **4.43** undergoes a modestly selective Schenck ene reaction to giving the trisubstituted olefin hydroperoxide **4.44** as well as other products. Hock fragmentation to the 7-membered lactol **4.45** and opening to enol **4.46** (at equilibrium with a lactone) facilitates further reaction with triplet oxygen to give the heavily oxygenated **4.47**. After a series of cyclisation steps such as those shown through **4.48** and **4.49** the final drug artemisinin (**4.50**) is formed. This reaction was developed as a continuous flow process and produced 10% yield of artemisinin (**4.50**) based on **4.43**.

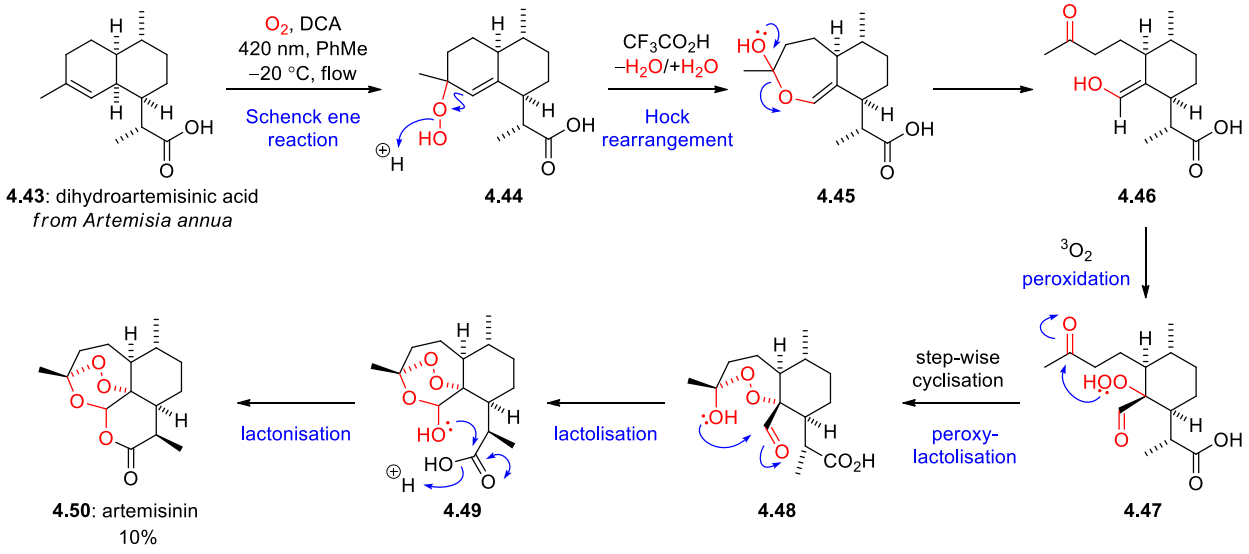

Scheme 4.11: Continuous flow synthesis of artemisinin (**4.50**). Seeberger (2013)

As encapsulated in the examples shown singlet oxygen, and the Schenck reaction are powerful tools to the organic chemist, as well as to Nature.

4.3 Previous Work on Eriobrucinol Natural Products

Returning to the cyclobutane "cyclol" natural products eriobrucinol (**4.11**) and isoeriobrucinol A and B (**4.12**, **4.13**), there have been two important syntheses that will be discussed herein.

The first synthesis of eriobrucinol (**4.11**) was reported by Leslie Crombie.[24] Continuing from his studies on deoxyisobruceol (discussed in Chapter 3), and with previous success in the [2+2] cycloaddition reaction of chromenes,[25] Crombie looked at preparing eriobrucinol (**4.11**) by photochemical means. Having chromenes **4.1** and **4.3** in hand from his previous work on *Philotheca* meroterpenoids the preparation of their respective cyclols was executed as a prophylactic measure against potential misassignment from the isolation chemists (Scheme 4.12a and 4.12b). Crombie had previously seen a misassignment regarding the chromene/coumarin orientation in his synthesis of deoxy(iso)bruceol. It was not until later that cyclols **4.12** and **4.13** were identified as separate natural products and named isoeriobrucinol A and B. Crombie had reported unsuccessfully attempting to

isomerise **4.12** to eriobrucinol (**4.11**) by heating or with base catalysis. The reaction Crombie would have liked to have done was the direct photochemical [2+2] cycloaddition of chromene **4.2** (Scheme 4.12c) but he did not have access to this material.

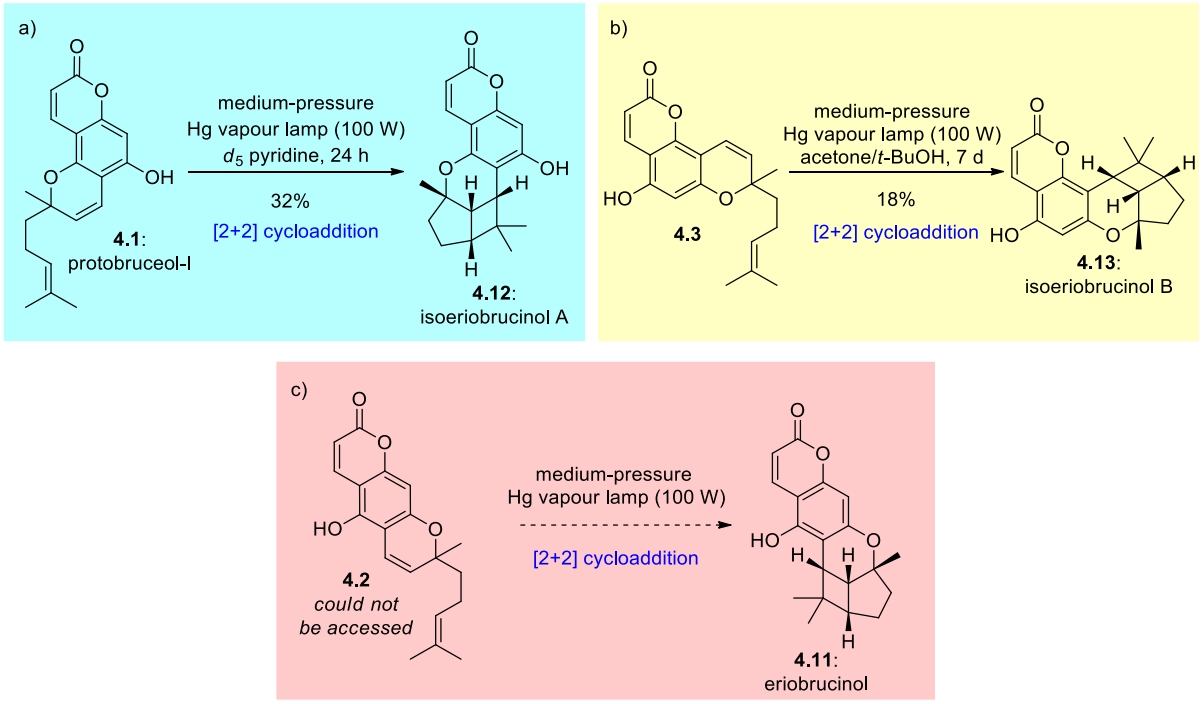

Scheme 4.12: a) Synthesis of isoeriobrucinol A (**4.12**). b) isoeriobrucinol B (**4.13**). c) theoretical reaction to form eriobrucinol (**4.11**). Crombie and Whiting (1979)

Without access to **4.2** Crombie needed to find a work-around (Scheme 4.13). Formylation of methyl phloroglucinol (**4.51**) to **4.52** and chromenylation with citral followed by actylation gave the functionalised chromene **4.54**. This was a good substrate for photochemical [2+2] reaction and gave the cyclobutane **4.55** in good yield, whereas the previous unprotected phenol **4.53** was completely unreactive. With the cyclobutane moiety in place all that was left was the introduction of the coumarin. Demethylation of **4.55** was enacted using MgI_2, affording **4.56**. The coumarin was formed via a Perkin reaction, which is a subset type of Dieckmann condensation reaction. After acetylation of the free phenol in **4.56** the condensation reaction has no preference between the two acetyl groups and an equal mixture of **4.57** and the isoeriobrucinol B type isomer (not shown) is formed. Final acid catalysed diacylation afforded eriobrucinol (**4.11**) which matched the natural product.

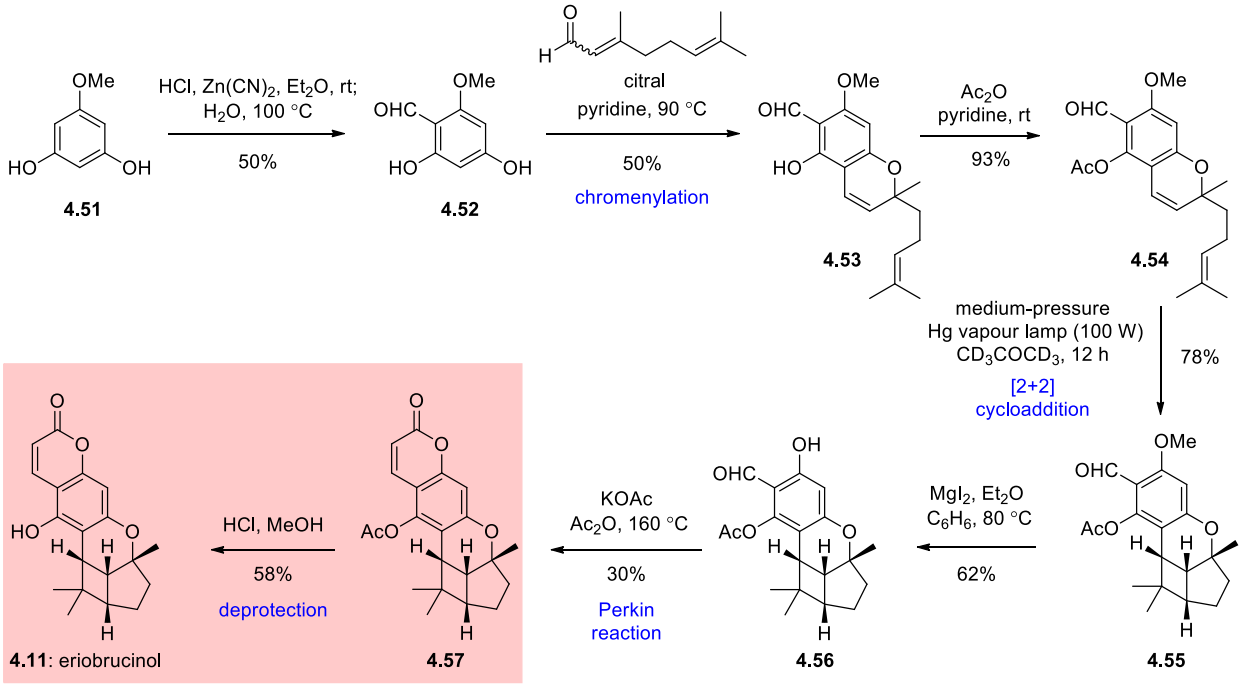

Scheme 4.13: Synthesis of eriobrucinol (**4.11**). Crombie and Whiting (1979).

More recently, the synthesis of eriobrucinol (**4.11**) was completed by Hsung and co-workers (Scheme 4.14). Hsung's synthesis contrasts Crombie's, primarily in the complete lack of protective groups, but also the use of an acid mediated [2+2] cycloaddition rather than photochemical [2+2]. Both approaches leave the formation of the coumarin until last and do not intercept the putative biosynthetic precursor chromene **4.2**. After a high yielding chromenylation of phloroglucinol (**4.58**), chromene **4.59** undergoes a facile acid catalysed cationic [2+2] reaction to give the cyclobutane **4.60**. UV irradiation of chromene **4.59** did not facilitate a photochemical [2+2] reaction, and lead only to decomposition. Friedel-Crafts acylation of **4.60** with ethyl propiolate gave a mixture of all three possible products, with eriobrucinol (**4.11**) being the major product when $ZnCl_2$ is used as a Lewis acid.

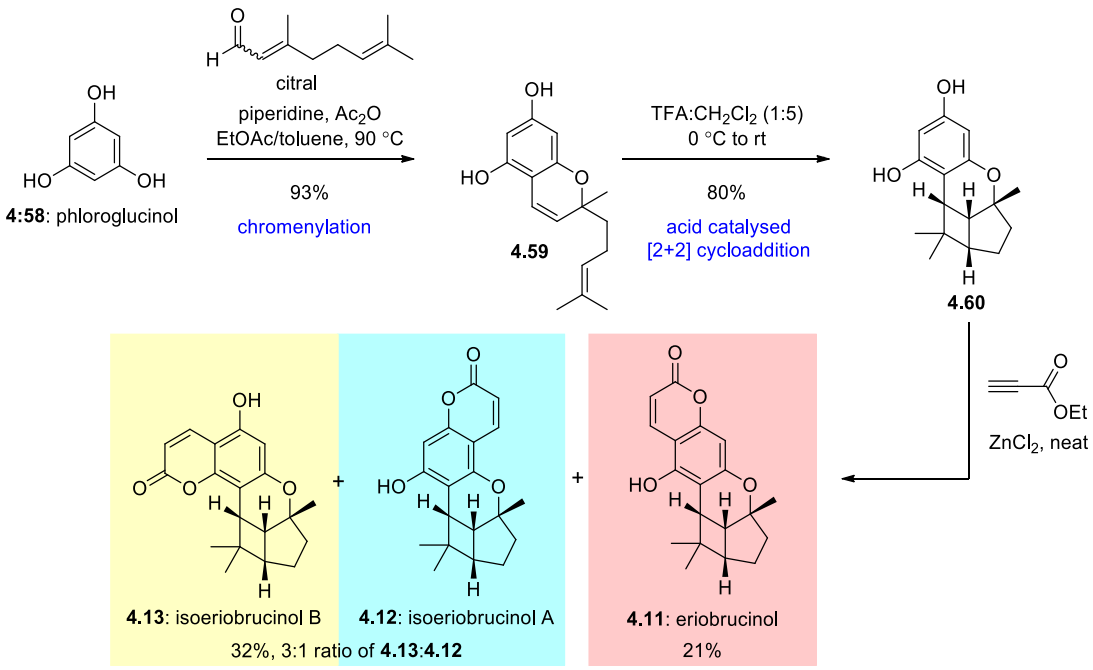

Scheme 4.14: Divergent synthesis of eriobrucinol (**4.11**), isoeriobrucinol A (**4.12**), and isoeriobrucinol B (**4.13**). Hsung (2013)

4.4 Results and Discussion

4.4.1: Photochemical [2+2] Reactions

The previously elusive chromene (**4.2**) (from the synthesis of isobruceol, Chapter 3, Scheme 3.32) was subjected to UV radiation (Scheme 4.15). Initially quite forcing conditions were employed. Irradiation using a high-pressure mercury vapour lamp in acetone gave rapid conversion but resulted in an underwhelming 30% isolated yield. The loss of yield was caused by photochemical degradation, to this end milder conditions were explored. Pleasingly, conversion was smooth using a low-power household UVA LED (λ_{max} = 355 nm), with no need for an added sensitiser or sensitising solvent mixture. The chromene **4.2** acts as a great chromophore, and harsh irradiation such as with a strong mercury vapour lamp is unnecessary.

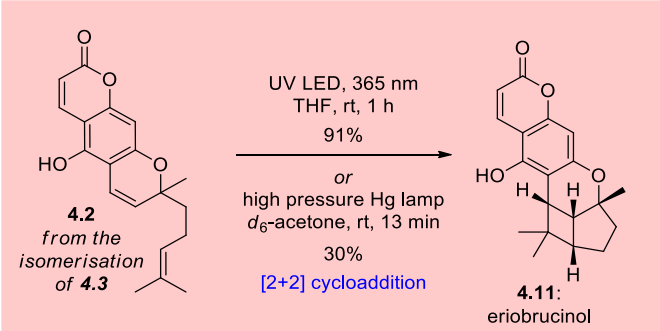

Scheme 4.15: Photochemical [2+2] cycloaddition to form eriobrucinol (**4.11**).

To bring our synthesis a step closer in line with biologically relevant conditions, the reaction was repeated using natural sunlight (Scheme 4.16). THF was kept as the solvent because both **4.2** and eriobrucinol (**4.11**) dissolved well and our previous results showed a sensitising solvent would not be necessary (for example: acetone). Additionally, Crombie's reactions to form isoeriobrucinol A and B (**4.12** and **4.13**) were repeated, and would give a good comparison for the reactivity of these chromenes. For these reactions, deuterated chloroform was used so the reaction could be more easily monitored by NMR.

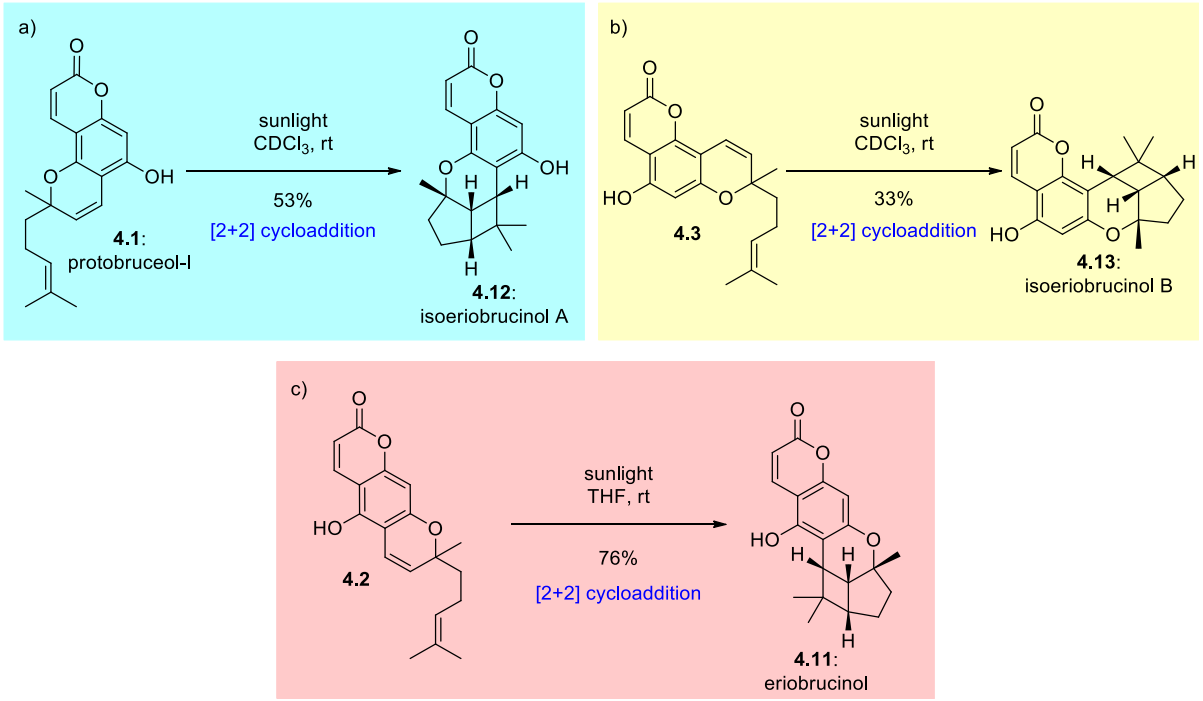

Scheme 4.16: Solar photochemical [2+2] reactions of a) protobruceol-I (**4.1**), b) **4.3**, and c) **4.2**.

A draw back to using the sun as a light source is inconsistency. When doing these experiments it was difficult to gauge which is the best substrate for the [2+2] cyclization. However, when the reactions were performed in parallel and monitored periodically by NMR the relative reactivity was qualitatively determined (Figure 4.8). **4.2** reacted the fastest, protobruceol-I (**4.1**) was slightly slower, and chromene **4.3** was significantly slower. This difference in reaction rate may explain the difference in the natural abundance of the eriobrucinols. It could also explain why **4.2** has not been found in nature, it is the most susceptible to UV.

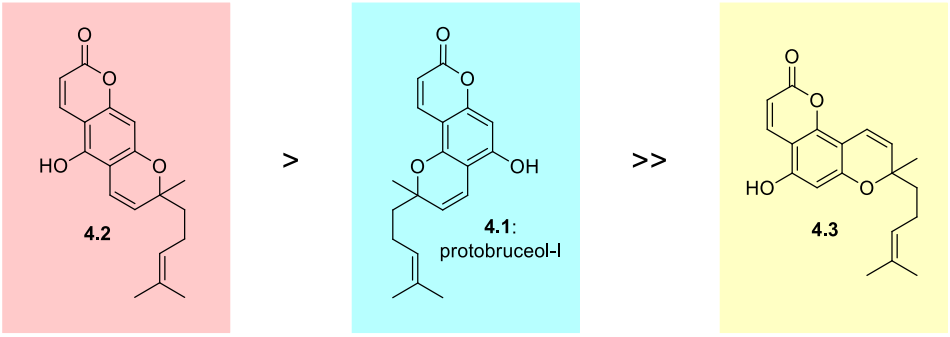

Figure 4.8: Reactivity series for [2+2] cycloaddition in $CDCl_3$ with sunlight.

We hoped some insight[26] could be gained by analysing the UV-Vis spectra (Table 4.1). The spectra of the three chromenes had similar shape, having two separate broad peaks. Each of the chromenes were excellent chromophores, and as such to properly record the spectra sample were heavily diluted (0.01 mg/mL). There is a trend relating wavelength (λ_{max}) to the rate of reaction. **4.2** reacts mildly faster than the slightly red-shifted **4.1**, and much faster than the more red-shifted **4.3**. **4.3** also has a noticeably poorer extinction coefficient (ε), meaning it absorbs light less efficiently.

Table 4.1: UV-Vis absorption spectra of chromenes **4.1**, **4.2**, and **4.3**. Spectra were recorded in $CHCl_3$ (c = 0.01 $mg.mL^{-1}$, or 0.000032 $mol.L^{-1}$) at room temperature

Chromene	Peak	λ_{max} (nm)	Abs	ε ($L.mol^{-1}.cm^{-1}$)
4.1	Major	284	0.606	18,938
	Minor	330	0.473	14,781
4.2	Major	280	0.604	18,844
	Minor	330	0.341	10,625
4.3	Major	294	0.421	13,125
	Minor	327	0.280	8,750

This interpretation of the UV-vis is somewhat speculative, but it is consistent with the results we observe.

4.4.2: Synthesis of Deoxyisobruceol (**4.62**)

While studying Crombie's previous work with our new chromene **4.2** in mind, we decided to revisit his synthesis of deoxyisobruceol (**4.62**) (discussed in detail in Chapter 3.1.3). In Crombie's synthesis, protobruceol-I (**4.1**) undergoes thermal isomerisation to **4.2** which is more reactive, and goes to form deoxyisobruceol (**4.62**) faster than deoxybruceol (**4.51**) (Scheme 4.17). As this reaction relies on a quite forcing thermal isomerisation to **4.2**, and this material was in hand, it would be too simple to subject this chromene directly to these reaction conditions.

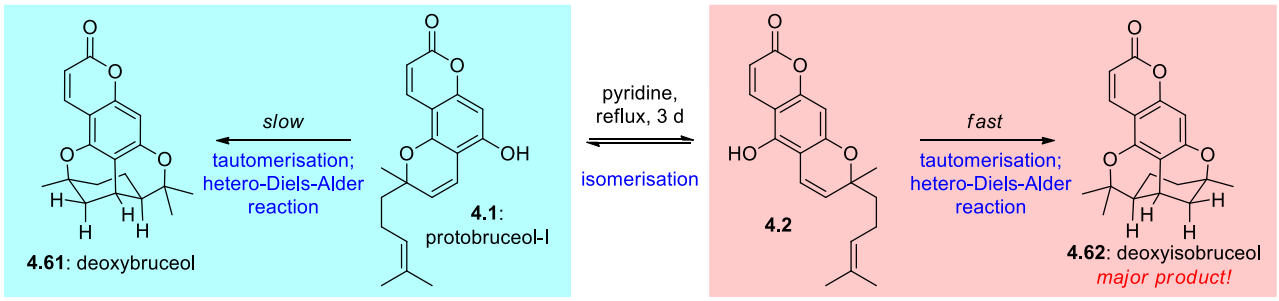

4.17: Synthesis of deoxyisobruceol (**4.62**). Crombie (1976)

Heating **4.2** in pyridine to 150 °C (using a microwave reactor) gave deoxyisobruceol (**4.62**) in good yield (Scheme 4.18). Conversion was complete in only 30 min, showing this is very efficient reaction, and suggests the lower yield of Crombie's reaction is partly due to the isomerisation step. A small amount of protobruceol-I (**4.1**) was also observed, showing the equilibrium between **4.1** and **4.2** is truly reversable.

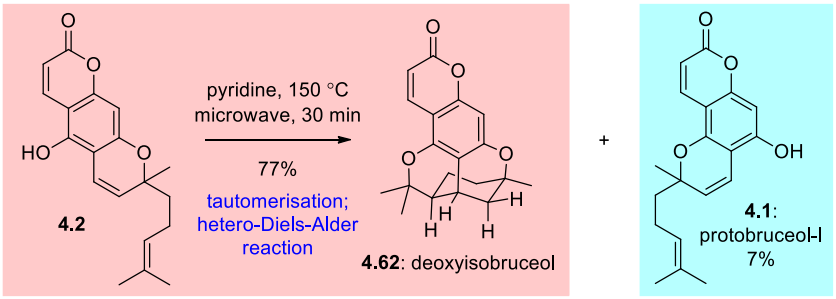

Scheme 4.18: Synthesis of deoxyisobruceol (**4.62**) from chromene (**4.2**).

4.4.3: Synthesis of Protobruceols II – IV (**4.6** – **4.10**)

Returning to photochemical reactions of the bruceol chromenes, we aimed to synthesise the allylic alcohols and allylic hydroperoxides that make up the remaining protobruceols II-IV (**4.6** – **4.10**) as well as isomers of **4.6** – **4.10** that could be undiscovered natural products.

As summarised in Figure 4.2, protobruceols II-III (**4.6** -**4.7**) are derivatives of protobruceol-I (**4.1**) and protobruceol-IV (**4.10**) is a derivative of **4.2**. All of these compounds should be accessible using singlet oxygen chemistry. Subjecting **4.1** to singlet oxygen generated with visible light and methylene blue produced a mixture of hydroperoxides **4.8** and **4.9** (Scheme 4.19). The ratio of isolated yields of the two hydorperoxides deviated each time the reaction was performed because the chromatographic separation of **4.8** and **4.9** was difficult.

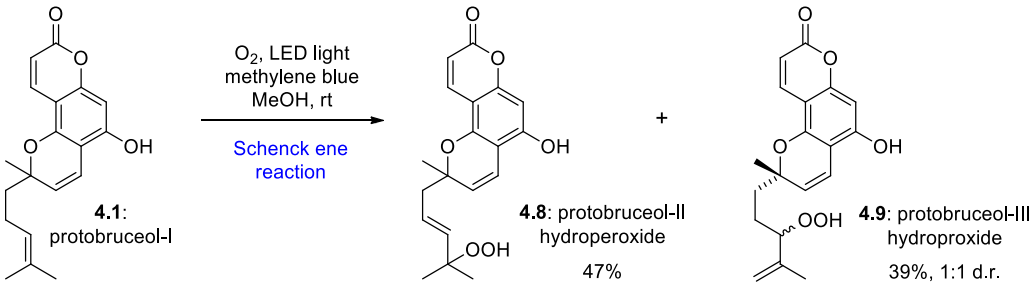

Scheme 4.19: Singlet oxygen reaction of protobruceol-I (**4.1**).

The next step was to reduce the hydroperoxides to their respective allylic alcohols. TLC-scale tests showed PPh_3 and Me_2S reacted very slowly, whereas $NaBH_4$ reduced hydroperoxides instantly, which was seen as preferable. As the separation of the hydroperoxides was difficult, it was easier to reduce the mixture of hydroperoxides together, directly after the $^1O_2$ reaction takes place (Scheme 4.20). Here the use of methylene blue in MeOH was advantageous as $NaBH_4$ could be added directly to the reaction mixture. Separation of protobruceol-II (**4.6**) and -III (**4.7**) was cleaner, and the isolated yields better reflect the selectivity of this reaction, which is about 50:50.

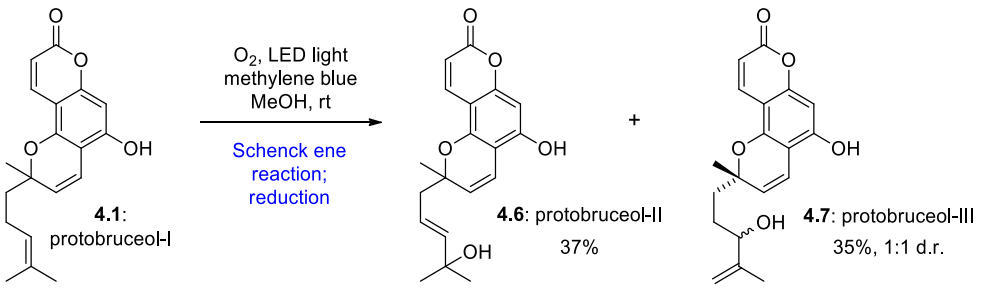

Scheme 4.20: Synthesis of protobruceol-II (**4.6**) and protobruceol-III (**4.7**).

Spectral data for protobruceol-II (**4.6**), protobruceol-III (**4.7**), and their respective hydroperoxides (**4.8** and **4.9**) matched what was reported in the literature perfectly. The last remaining member of the family was protobruceol-IV (**4.10**), which was reported to bear the configuration of **4.2**.

Using rose bengal, a near equal mixture of allylic hydroperoxides **4.63** and **4.64** was formed (Scheme 4.21). The choice of sensitiser was thought of as superficial, and TPP, rose begal, and methylene blue were used interchangeably throughout the optimisation stages of the project. The biggest considerations when it came to the choice of dye was how easy it was to remove, and how would it affect purification of the product. As CH_2Cl_2 was used as the chromatography solvent to separate the hydoperoxides (the usual petrol/EtOAc failed), it easily doubled as a reaction solvent. MeOH was best avoided as any residual solvent could flush the chromatography column. Methylene blue is not soluble in CH_2Cl_2.

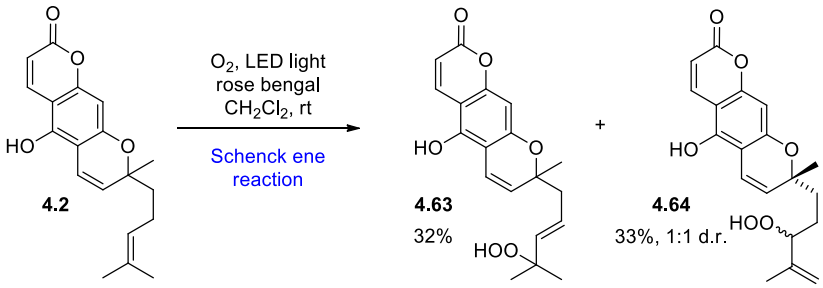

Scheme 4.21: Schenck ene reaction of **4.2**.

The one-pot, or telescoped reduction procedure used for the protobruceol-II and -III gave very poor and inconsistent yields for the **4.2** orientation hydroperoxides. This strange subtle difference in the systems was best overcome by simply reducing the purified hydroperoxides **4.63** and **4.64** separately. This was found to be a surprisingly sensitive reaction; best results came from careful addition of only a slight excess of $NaBH_4$ until full conversion has occurred. The reduction of **4.63** gave the allylic alcohol **4.10** which was the proposed structure of Waterman's protobruceol-IV (Scheme 4.22a). However, the ^1H NMR spectra of our synthetic **4.10** did not match what was reported (Table 4.2).

For the sake of completion **4.64** was also reduced to allylic alcohol **4.65**) (Scheme 4.22b). As these molecules are believed to arise from non-selective $^1O_2$ autoxidation, all of these compounds may be present in Nature as undiscovered natural products.

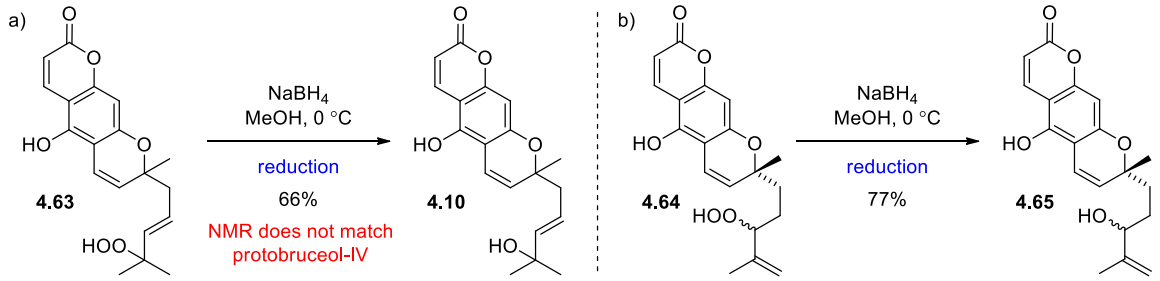

Scheme 4.22: Reduction of hydroperoxides a) **4.63** and b) **4.64**; synthesis of protobruceol-IV (**4.10**).

Clear differences of the spectra of our synthetic **4.10** and Waterman's protobruceol-IV laid in the coupling constants of the oxidised prenyl chain. Immediately obvious is the splitting of the protons of C-4'. In Waterman's spectra C-4' methylene gives a 2H doublet ($^3J_{H\text{-}H}$ = 5.6 Hz), whereas our synthetic material gave two 1H signals with a similar $^3J_{H\text{-}H}$ but with additional geminal coupling ($^2J_{H\text{-}H}$ = 13.3 Hz). Furthermore, the H-5' and H-6' signals are heavily overlapped in our spectra, but well separated in Wateman's. Finally, chemical shifts of the aromatic protons sporadically differ, showing these cannot be the same compound. Unfortunately, the ^{13}C NMR spectra of protobruceol-IV was not reported.

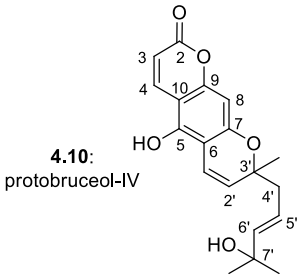

4.10:
protobruceol-IV

Table 4.2: ^{1}H NMR comparison of protobrcueol-IV and synthetic **4.10**. (*J* in Hz)

	Waterman 1992 250 MHz ($CDCl_3$) protobruceol-IV	George 2019 500 MHz ($CDCl_3$) (**4.10**)
3	6.15 d	6.08 d (9.7)
4	7.97 bd	8.03 d (9.7)
8	6.56 bs	6.29 s
1’	6.58 bd	6.68 d (10.1)
2’	5.63 d	5.54 d (10.1)
3’-Me	1.45 s	1.40 s
4’-α	2.38 d (5.6)	2.41 dd (13.3, 5.1)
4’-β	-	2.33 dd (13.4, 4.9)
5’	5.63 dt (15.0, 5.6)	5.66 – 5.61 m (overlapped)
6’	5.68 d (15.0)	5.66 – 5.61 m (overlapped)
7’-Me	1.20 s	1.20 s
7’-Me	1.26 s	1.25 s

In lieu of any printed specta of natural protobruceol-IV, the difference in *J* coupling of reported and synthetic **4.10** can be visualised by comparing with protobruceol-II (**4.6**) (Figure 4.9) as coupling constants reported for **4.10** closely match that of **4.6**. The difference between the two is dramatic. It is not always easy to predict but the methylene CH_2 on C-4’ are sometimes magnetically equivalent and sometimes not. This is very useful for characterisation purposes as both chemical shift and *J* can be used to identify products. H-5’ and H-6’ suffer from severe “tenting” making the multiplets difficult to interpret, however as seen in **4.6** they should be rational / first order, and this is what the

isolated protobruceol-IV was identified with. In our synthetic **4.10** these signals were completely overlapped.

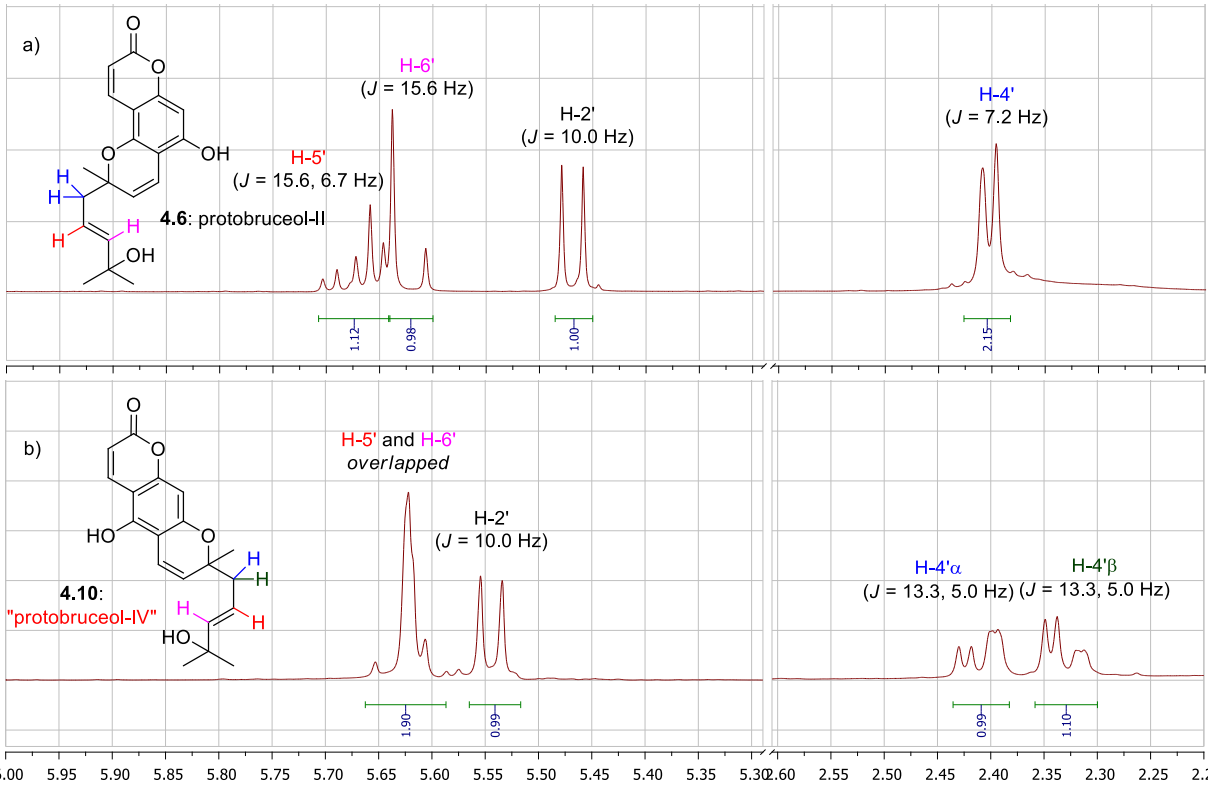

Figure 4.9: ^{1}H NMR comparison of a) protobruceol-II (**4.6**) and b) protobruceol-IV structure **4.10**.

As the spectra of synthetic **4.10** did not match what was reported as protobruceol-IV, and was obviously different to the spectra of protobruceol-II (**4.6**), it seemed possible to have been misassigned and actually had the orientation of **4.3**. To this end, Schenck ene reaction and reduction of **4.3** was performed to give the last possible isomer protobruceol-IV could be **4.69** (Scheme 4.23). Disappointingly, the spectra of **4.69** also did not match the reported spectral data of protobruceol-IV.

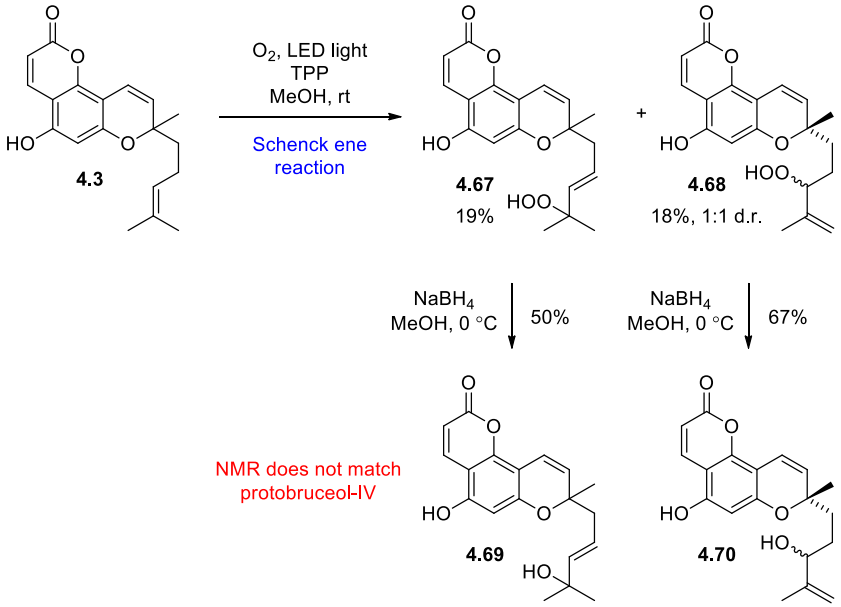

Scheme 4.23: Synthesis of possible protobruceol-IV isomer **4.69**.

With allylic alcohols of all three coumaric chromenes synthesised and none matching Waterman's protobruceol-IV there was nothing left to make. With no clear direction to take this project it was resigned that we may never be sure what Waterman had isolated.

4.4.4: Attempted Synthesis of 5'-*β*-Hydroxyeriobrucinol (**4.15**) via a Schenck Rearrangement

While in the mind-set of the unique Schenck oxidation pattern, ideas began to arise on how this could be better utilised as a synthetic tool. As the major draw-back of the Schenck ene reaction is it typically gives mixtures of products, the benefit of *selectivity* would have to overcome inefficiency.

Our imagination was captured by a potential sequence involving Schenck ene reaction followed by allylic transposition (Scheme 4.24). Formally what is occurring is the C-H activation of the internal allylic position, which is not directly possible by conventional means. This could be applied in a synthesis of 5'-*β*-hydroxyeriobrucinol (**4.15**).

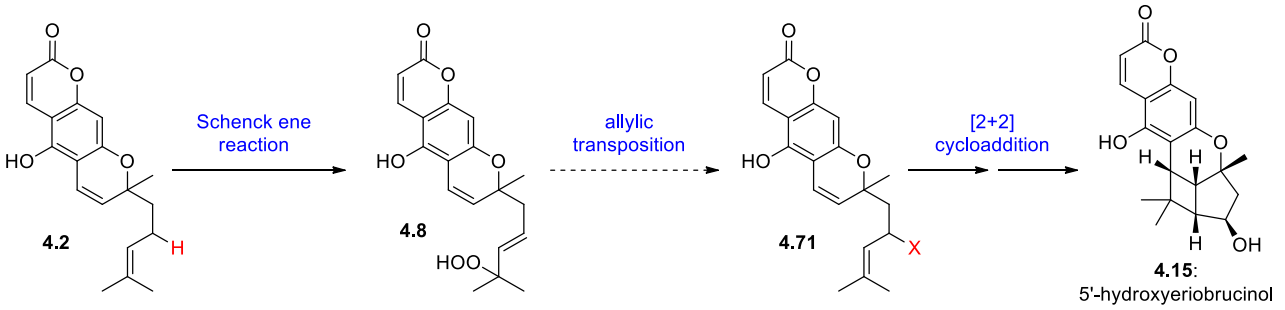

Scheme 4.24: Schecnk ene / allylic transposition sequence *en route* to 5'-hydroxyeriobrucinol (**4.15**).

To better illustrate the difficulty of this transformation, this manipulation was recently done by Hsung in his synthesis of rhodonoid B (**4.73**) (Scheme 4.25, described also in Chapter 2.1.4).[27] 9 steps were required to oxygenate at this allylic position! Using the Schenck ene reaction 5 steps were bypassed in a formal synthesis of **4.73** from our group.[28]

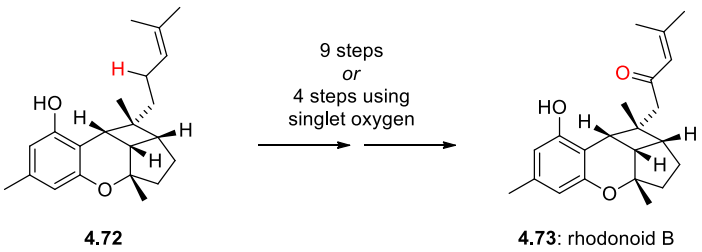

Scheme 4.25: Syntheses of rhodonoid B (**4.73**). Hsung (2017), George (2020)

The transposition used in the synthesis of rhodonoid B (**4.73**) was the Babler-Daubin oxidation reaction (Scheme 4.26). A tertiary allylic alcohol forms an adduct with CrO_3 (or equivalent, e.g., PCC), oxidation is impossible at this position as the alcohol is fully substituted. After a (2,3) sigmatropic rearrangement there is now an oxymethine proton available to be abstracted, carbon is formally oxidised to give an α,β-unsaturated ketone and Cr(VI) is reduced to Cr(IV).

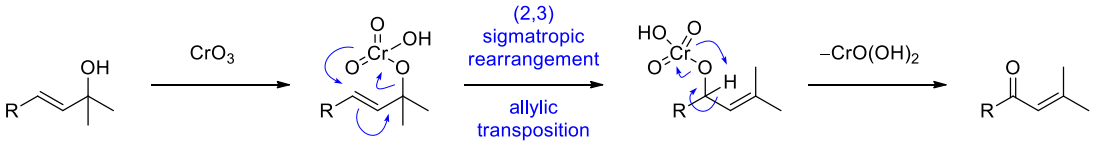

Scheme 4.26: Mechanism for the Babler-Daubin Oxidation.

Although the Babler-Daubin oxidation completes the allylic transposition prescribed, when sequenced with the Schenck oxidation it comes at a cost. The hydroperoxide product of the Schenck ene reaction would have to be reduced to an allylic alcohol, only to be oxidised again during the transposition. If the allylic alcohol product is desired, it would need to be reduced yet again! This is a non-synergistic and poor redox economy process with four alternating oxidation/reduction steps.

However, the allylic transposition of hydroperoxides has been seen in the Schenck rearrangement (not to be confused with the Schenck reaction) and this lends itself to synthetic investigation.

The Schenck rearrangement is a spontaneous radical process. The putative mechanism involves fragmentation and recombination of an allylic peroxy radical (Scheme 4.27). This reaction has not been used in total synthesis and is rather an undesired reaction which occurs during storage. For example, dilute solutions of pure allylic hydroperoxide **4.74** *or* the isomeric **4.75** were found to isomerise to a 50:50 equilibrium mixtures when left at 40 °C for several days.[29]

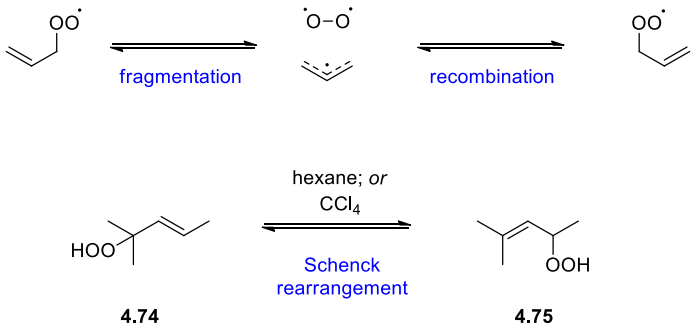

Scheme 4.27: a) mechanism for the Schenck rearrangement. b) example of Schenck rearrangement on a prenyl chain. Brill (1965)

Taking the allylic hydroperoxide **4.63** several reaction conditions were screened from simply leaving in NMR solvent for two weeks to refluxing in PhMe in the presence of AIBN. Unfortunately, there was never any sign of constructive reaction forming **4.76** observed, and material would slowly degrade (Scheme 4.28). This was disappointing but should not have been surprising. **4.76** contains a

phenol which should presumably act as a good radical inhibitor. The structure of **4.76** can be compared with Nature's radical inhibitor vitamin E (**4.77**) or butylated hydroxytoluene (BHT, **4.78**). The Schenck rearrangement pathway is known to be completely closed in the presence of radical inhibitors.

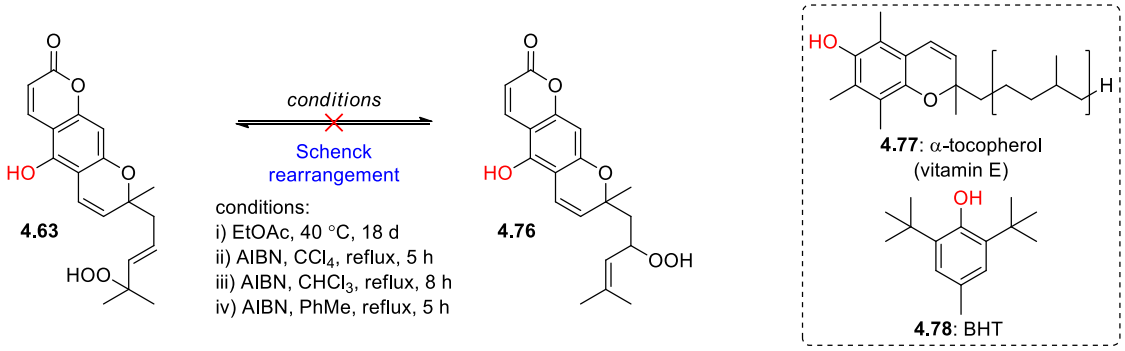

Scheme 4.28: Attempted Schenck rearrangement of **4.63**.

The obvious response to this negative result was to protect this problematic phenol (Scheme 4.29). Chromene **4.2** was treated with TBSOTf and the resultant **4.79** underwent the Schenck ene reaction again, this time to give TBS protected allylic hydroperoxide **4.80**, as well as the terminal olefin **4.81**.

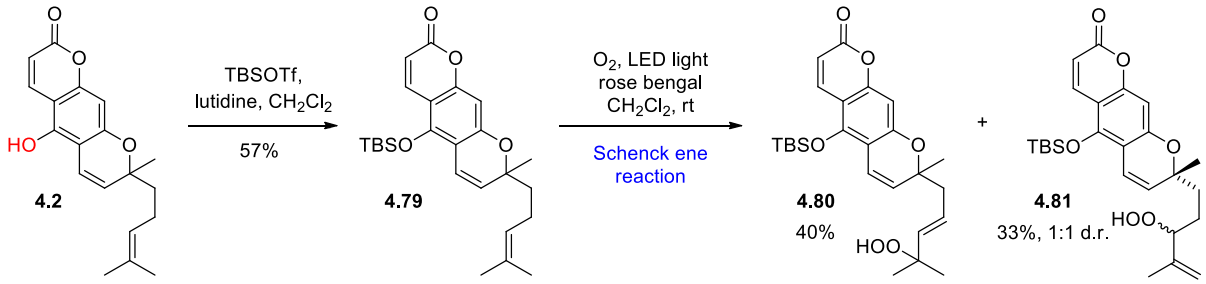

Scheme 4.29: Preparation of TBS protected hydroperoxide **4.80**.

Only a few conditions were tried for the Schenck rearrangement of **4.80** (Table 4.3). The compound was stable as a dilute NMR solution after 1 week (entry 1), so heating in $CHCl_3$ was tried (entry 2). AIBN was added to the solution in the hopes of initiating the radical reaction. Nothing happened, which may have been because the reflux temperature of $CHCl_3$ (~60 °C) is lower than the activation

temperature of AIBN (65 – 85 °C). Swapping to toluene and heating to 75 °C gave a promising result, with conversion after 1.5 h (entry 3). This was repeated at a slightly milder 65 °C using the remainder of the material (entry 4).

Table 4.3: Conditions screened for the Schenck rearrangement of **4.80**

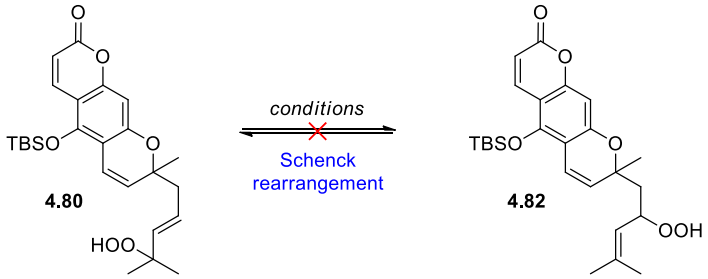

Entry	Additive	Solvent	Temp.	Time	Result
1	-	$CDCl_3$	rt	7 d	no reaction
2	AIBN	$CHCl_3$	reflux	6 h	no reaction
3	AIBN	PhMe	75 °C	1.5 h	4 products
4	AIBN	PhMe	65 °C	2.5 h	4 products

Unfortunately, the products formed under thermal radical conditions could not be identified. There was one promising compound the NMR suggested what looked like a cyclisation product which was a mixture of isomers. Optimistically this could have been the [2+2] cycloaddition product of **4.82**, however insufficient material and purity for good quality spectra prevented thorough and convincing structure determination.

While the results of the Schenck rearrangement were ambiguous, it was clear it would require a lot of time to properly explore, with no guarantee of success. It was decided at this point to not pursue this side-project any further. Preparation of **4.80** was tedious. Despite being prepared in only 5 steps from phloroglucinol, 3 steps gave mixed products with ~50:50 isomer selectivity (chromenylation, isomerisation, and Schenck ene reaction), meaning the process was low-yielding and required difficult chromatographic purification at most steps. Also, there were other projects in the bruceol saga the key chromene **4.2** could be used on.

4.5 Summary and Conclusion

In conclusion the reactions involving the chromenes **4.1**, **4.2**, and **4.3** were explored including the photochemical [2+2] cycloaddition to form eriobrucinol (**4.11**), isoeriobrucinol A (**4.12**) and isoeriobrucinol B (**4.13**). These chromenes were also subjected to singlet oxygen, allowing the first synthesis of protobruceols II-IV (**4.6** – **4.10**) via the Schenck ene reaction. These results suggested protobruceol-IV (**4.10**) was most likely misassigned. Lastly, the classic synthesis of deoxyisobruceol (**4.62**) was revisited, this time using the correctly oriented chromene **4.2**.

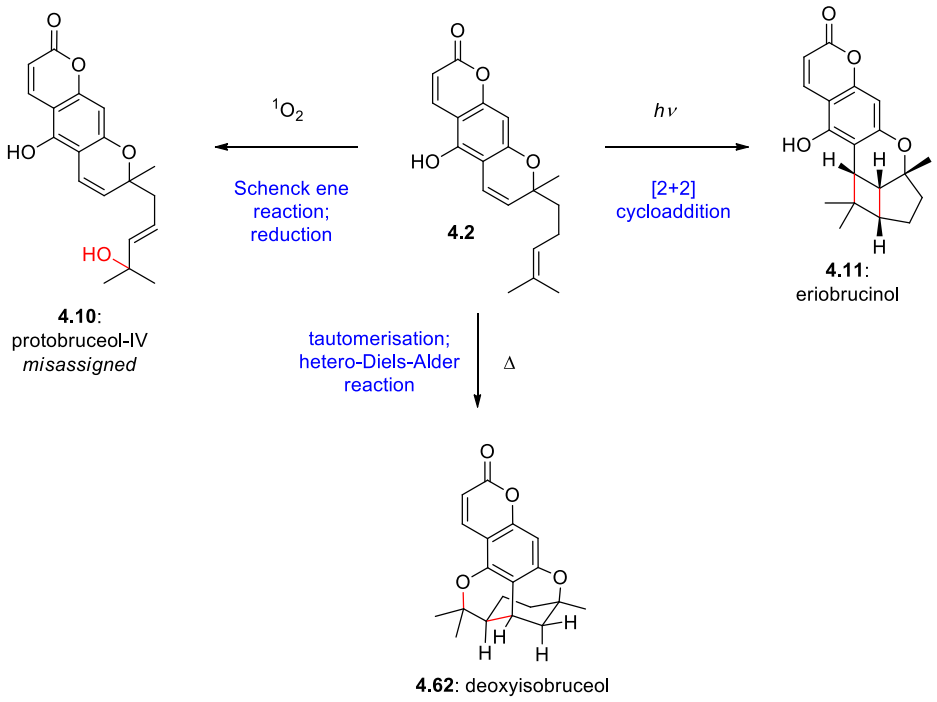

Scheme 4.30: Divergent synthesis of natural products from **4.2**.

4.6 Experimental

4.6.1: General Methods

All chemicals were purchased from commercial suppliers and used as received. All reactions were performed under an inert atmosphere of N_2. All organic extracts were dried over anhydrous magnesium sulfate. Thin layer chromatography was performed using aluminium sheets coated with silica gel F_{254}. Visualization was aided by viewing under a UV lamp and staining with ceric ammonium molybdate stain followed by heating. All R_f values were measured to the nearest 0.05. Flash column chromatography was performed using 40-63 micron grade silica gel. Melting points were recorded on a digital melting point apparatus and are uncorrected. Infrared spectra were recorded using an FT-IR spectrometer as the neat compounds. High field NMR spectra were recorded using either a 500 MHz spectrometer (^{1}H at 500 MHz, ^{13}C at 125 MHz) or 600 MHz spectrometer (^{1}H at 600 MHz, ^{13}C at 150 MHz). The solvent used for NMR spectra was $CDCl_3$ unless otherwise specified. ^{1}H chemical shifts are reported in ppm on the δ-scale relative to TMS (δ 0.00) or $CDCl_3$ (δ 7.26) and ^{13}C NMR chemical shifts are reported in ppm relative to $CDCl_3$ (δ 77.16). Multiplicities are reported as (br) broad, (s) singlet, (d) doublet, (t) triplet, (q) quartet, (quin) quintet, (sext) sextet, (hept) heptet and (m) multiplet. All *J*-values were rounded to the nearest 0.1 Hz. ESI high resolution mass spectra were recorded on an ESI-TOF mass spectrometer.

4.6.2: Synthetic Procedures

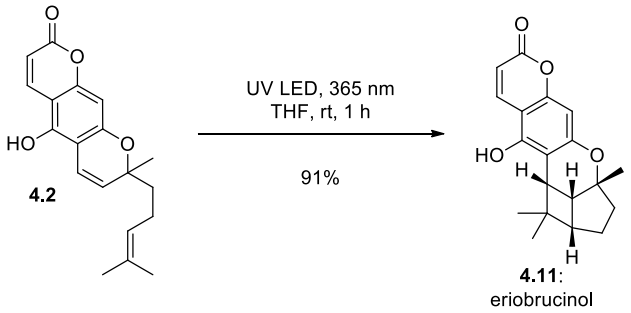

A solution of **4.2** (45.4 mg, 0.145 mmol) in THF (2.5 mL) was irradiated with a LED UV lamp (λ = 365 nm) for 1 h. The solvent was then removed, and the residue was purified by flash column chromatography on SiO_2 (2:1 petrol/EtOAc) to afford eriobrucinol **4.11** as a white foam.

Data for eriobrucinol (**4.11**):

^{1}H NMR (500 MHz, $CDCl_3$) δ 7.98 (d, *J* = 9.7 Hz, 1H), 6.46 (s, 1H), 6.15 (d, *J* = 9.6 Hz, 1H), 5.40 (s, 1H), 3.08 (d, *J* = 9.7 Hz, 1H), 2.66 (dd, *J* = 9.7, 7.6 Hz, 1H), 2.48 (t, *J* = 7.5 Hz, 1H), 1.96 – 1.87 (m, 1H), 1.75 – 1.67 (m, 1H, overlapped), 1.75 – 1.61 (m, 2H, overlapped), 1.45 (s, 3H), 1.41 (s, 3H), 0.79 (s, 3H)

^{13}C NMR (150 MHz, $CDCl_3$) δ 162.1, 157.8, 154.6, 151.3, 138.9, 111.0, 107.1, 103.2, 99.0, 84.7, 46.4, 39.1, 38.7, 37.3, 35.6, 34.6, 27.4, 25.7, 18.2

IR (neat) 3225, 2949, 1690, 1615, 1445, 1205, 1355, 1278, 1137, 1109, 1082

R_f 0.25 (2:1 petrol/EtOAc)

mp 163 – 165 °C (from toluene) (*lit.*[10] = 185 °C)

HRMS (ESI) calculated for $C_{19}H_{21}O_4$ 313.1434 $[M+H]^+$, found: 313.1438.

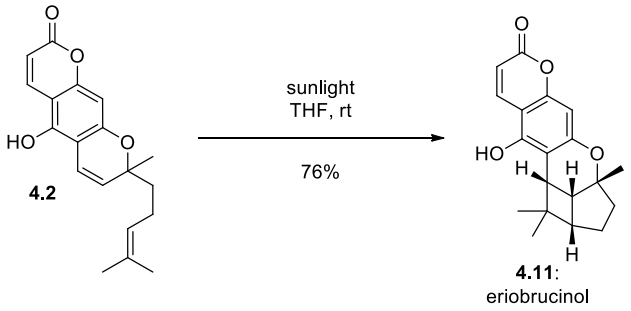

A solution of **4.2** (25 mg, 0.80 mmol) in THF (2 mL) was placed in direct sunlight for 6 h. The solvent was removed and the residue was purified by flash column chromatography on SiO_2 (2:1 petrol/EtOAc) to afford eriobrucinol (**4.11**) as a yellow oil (18.9 mg, 76%). Data for eriobrucinol (**4.11**) matched what was previously reported.

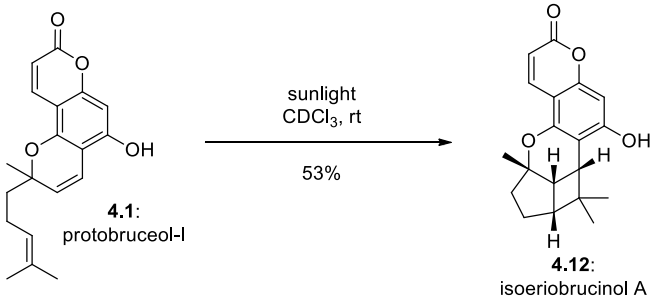

A solution of protobruceol-I (**4.1**) (80.0 mg, 0.256 mmol) in $CHCl_3$ (2 mL) was placed in direct sunlight for 5 h. The solvent was removed and the residue was purified by flash column chromatography on SiO_2 (2:1 petrol/EtOAc) to afford isoeriobrucinol A (**4.12**) as a white solid (42.5 mg, 53%).

Data for isoeriobrucinol A (**4.12**):

^{1}H NMR (500 MHz, d_5-pyridine) δ 8.09 (d, *J* = 9.6 Hz, 1H), 6.61 (s, 1H), 6.27 (d, *J* = 9.6 Hz, 1H), 4.92 (br s, 1H), 3.34 (d, *J* = 9.6 Hz, 1H), 2.56 (dd, *J* = 9.6, 7.5 Hz, 1H), 2.35 (t, *J* = 7.5 Hz, 1H), 2.04 (td, *J* = 12.6, 7.5 Hz, 1H), 1.72 – 1.64 (m, overlapped, 2H), 1.57 (ddd, *J* = 13.7, 12.3, 7.6 Hz, 1H), 1.49 (s, 3H), 1.47 (s, 3H), 0.98 (s, 3H)
^{13}C NMR (125 MHz, d_5-pyridine) δ 162.2, 162.1, 156.1, 151.7, 140.0, 110.2, 109.2, 104.2, 95.6, 85.4, 47.1, 39.9, 39.2, 38.5, 37.0, 34.3, 27.9, 26.4, 18.5
IR (neat) 3212, 2959, 1679, 1595, 1572, 1440, 1397, 1366, 1258, 1229, 1137, 1084
R_f 0.30 (neat Et_2O)
HRMS (ESI) calculated for $C_{19}H_{20}O_4Na$ 335.1254 $[M+Na]^+$, found: 335.1261.

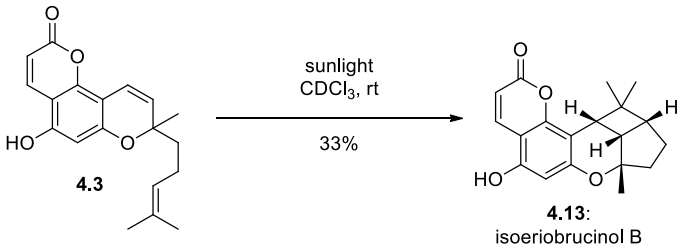

A suspension of **4.3** (60.0 mg, 0.192 mmol) in $CHCl_3$ (2 mL) was placed in direct sunlight for a total of 40 h over the course of 5 days. The mixture was diluted with $CHCl_3$ (3 mL) and filtered to afford isoeriobrucinol B (**4.13**) as a pale yellow solid (19.9 mg, 33%).

Data for isoeriobrucinol B (**4.13**):

^{1}H NMR (500 MHz, d_5-pyridine) δ 8.31 (d, *J* = 9.5 Hz, 1H), 6.63 (s, 1H), 6.29 (d, *J* = 9.5 Hz, 1H), 3.30 (d, *J* = 9.6 Hz, 1H), 2.50 (dd, *J* = 9.7, 7.3 Hz, 1H), 2.31 (t, *J* =7.4 Hz, 1H), 2.02 (td, *J* = 12.8, 7.8 Hz, 1H), 1.64 – 1.57 (m, 1H), 1.56 (s, 3H), 1.53 – 1.45 (m, 1H), 1.37 (s, 3H), 0.87 (s, 3H)
^{13}C NMR (125 MHz, d_5-pyridine) δ 161.8, 158.4, 155.9, 155.5, 140.5, 110.4, 104.8, 103.7, 100.7, 85.3, 47.2, 39.6, 39.0, 37.9, 36.2, 34.2, 28.0, 26.2, 18.6
IR (neat) 3331, 2938, 1686, 1606, 1498, 1455, 1356, 1263, 1135, 1108
R_f 0.30 (neat Et_2O)
HRMS (ESI) calculated for $C_{19}H_{21}O_4$ 313.1434 $[M+H]^+$, found: 313.1435.

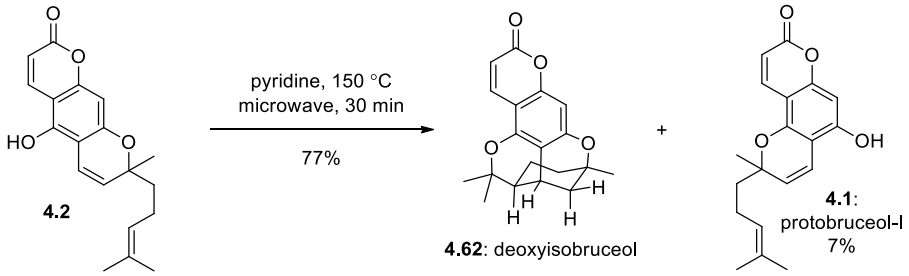

A solution of **4.2** (43.3 mg, 0.139 mmol) in pyridine (1 mL) was heated to 150 °C by microwave for 30 min. The solvent was removed *in vacuo* and the residue was purified by flash column chromatography on SiO_2 (3:1 petrol/EtOAc) to afford deoxyisobruceol (**4.62**) as a colourless oil (33.5 mg, 77%). Further elution afforded protobruceol-I as a pale solid **4.1** (3.0 mg, 7%). Data for **4.1** matched what as previously been reported.

Data for deoxyisobruceol (**4.62**):

^{1}H NMR (500 MHz, $CDCl_3$) δ 7.86 (d, *J* = 9.5 Hz, 1H), 6.44 (s, 1H), 6.11 (d, *J* = 9.5 Hz, 1H), 2.90 – 2.84 (m, 1H), 2.24 (ddd, *J* = 13.4, 4.7, 3.2 Hz, 1H), 2.13 (ddd, *J* = 11.6, 5.4, 2.8 Hz, 1H), 1.91 (dd, *J* = 13.4, 1.7 Hz, 1H), 1.81 (ddd, *J* = 14.9, 5.6, 3.4 Hz, 1H), 1.60 (s, 3H), 1.47 (ddd, *J* = 15.1, 13.1, 6.8 Hz, 1H), 1.42 (s, 3H), 1.30 (dt, *J* = 12.8, 6.0 Hz, 1H), 1.07 (s, 3H), 0.64 (tdd, *J* = 13.4, 11.6, 6.1 Hz, 1H)

^{13}C NMR (125 MHz, $CDCl_3$) δ 162.0, 159.8, 154.6, 153.6, 138.3, 112.4, 110.7, 105.1, 96.9, 86.5, 76.4, 46.2, 37.3, 34.8, 29.6, 28.8, 28.0, 24.2, 22.0

IR (neat) 2975, 2933, 1728, 1616, 1568, 1445, 1355, 1258, 1138, 1125, 1071

R_f 0.35 (2:1 petrol/EtOAc)

HRMS (ESI) calculated for $C_{19}H_{20}O_4Na$ 335.1254 $[M+Na]^+$, found: 335.1259.

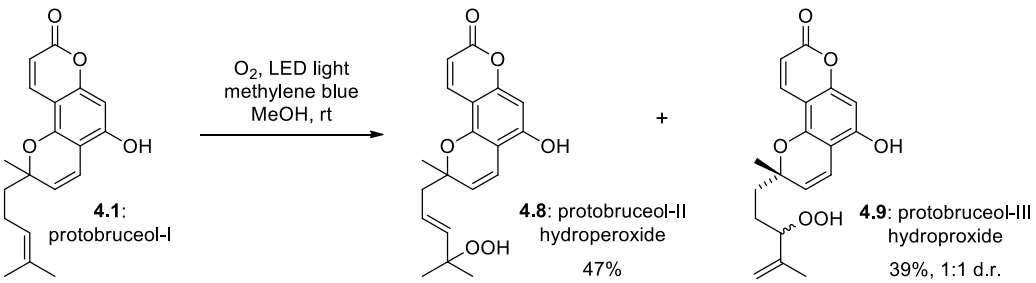

To a solution of protobruceol-I (**4.1**) (80.0 mg, 0.256 mmol) in MeOH (10 mL) was added methylene blue (0.9 mg, 0.003 mmol). O_2 was bubbled through the resultant solution while it was irradiated with LED light for 15 h. The solvent was removed *in vacuo* and the residue was purified by flash column chromatography on SiO_2 (8:1 → 7:1 CH_2Cl_2/EtOAc) to afford protobruceol-III hydroperoxide (**4.9**)

as a pale yellow oil (34.6 mg, 39%, d.r. 1:1). Further elution afforded protobruceol-II hydroperoxide (**4.8**) as a pale yellow oil (41.8 mg, 47%).

Data for protobruceol-III hydroperoxide (**4.9**):

^{1}H NMR (500 MHz, $CDCl_3$) δ 8.14 (br s, 1H), 8.05 (br s, 1H), 7.97 (dd, *J* = 9.6, 1.4 Hz, 1H), 6.70 (dd, *J* = 10.1, 1.3 Hz, 1H), 6.62 (s, 1H), 6.13 (dd, *J* = 9.6, 1.2 Hz, 1H), 5.47 (dd, *J* = 10.1, 1.2 Hz, 1H), 5.02 (q, *J* = 1.6 Hz, 1H), 5.00 (s, 1H), 4.30 (td, *J* = 6.4, 2.8 Hz, 1H), 1.90 – 1.76 (m, 2H), 1.76 – 1.60 (m, overlapped, 2H) 1.70 (dd, *J* = 5.0, 1.3 Hz, 3H), 1.42 (s, 3H)
^{13}C NMR (125 MHz, $CDCl_3$) δ 163.1, 156.5, 155.4, 150.97, 150.94, 143.3, 143.2, 139.7, 126.1, 126.1, 117.2, 114.9, 114.8, 110.2, 106.0, 103.40, 103.39, 95.8, 89.5, 80.2, 80.1, 37.31, 37.2, 26.8, 26.6, 25.5, 25.3, 17.38, 17.36 (Note: more than 19 ^{13}C signals are observed as **4.9** is a 1:1 mixture of diastereoisomers)
IR (neat) 3263, 2973, 1691, 1638, 1615, 1594, 1442, 1364, 1263, 1208, 1187, 1141, 1086
R_f 0.20 (6:1 CH_2Cl_2/EtOAc)
HRMS (ESI) calculated for $C_{19}H_{21}O_6$ 345.1333 $[M+H]^+$, found: 345.1334.

Data for protobruceol-II hydroperoxide (**4.8**):

^{1}H NMR (500 MHz, $CDCl_3$) δ 8.16 (brs, 1H), 7.98 (d, *J* = 9.6 Hz, 1H), 6.70 (d, *J* = 10.0 Hz, 1H), 6.60 (s, 1H), 6.13 (d, *J* = 9.6, 1H), 5.71 (dt, *J* = 15.9, 7.2 Hz, 1H), 5.59 (d, *J* = 15.8 Hz, 1H), 5.50 (d, *J* = 10.1 Hz, 1H), 2.46 (d, *J* = 7.2 Hz, 2H), 1.47 (s, 3H), 1.24 (s, 3H), 1.22 (s, 3H)
^{13}C NMR (125 MHz, $CDCl_3$) δ 163.0, 156.5, 155.4, 151.1, 139.7, 137.9, 126.0, 125.2, 117.2, 110.2, 106.3, 103.2, 95.8, 82.3, 79.9, 44.4, 26.8, 24.5, 24.3
IR (neat) 3267, 2978, 2933, 1692. 1638, 1615, 1594, 1443, 1363, 1259, 1141, 1095
R_f 0.15 (6:1 CH_2Cl_2/EtOAc)
HRMS (ESI) calculated for $C_{19}H_{21}O_6$ 345.1333 $[M+H]^+$, found: 345.1333.

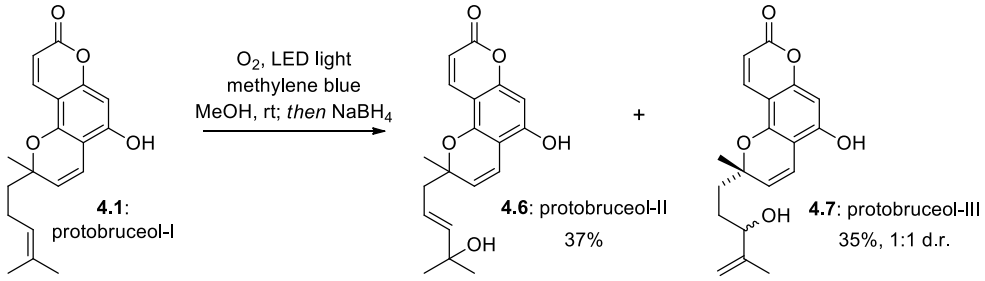

To a solution of protobruceol-I (**4.1**) (66.8 mg, 0.214 mmol) in MeOH (15 mL) was added methylene blue (3.1 mg, 0.0097 mmol). O_2 was bubbled through the resultant solution while it was irradiated with LED light for 26 h. $NaBH_4$ (150 mg, 3.96 mmol) was added and the mixture was stirred for a further 1.5 h. The reaction was quenched by addition of 1 M HCl solution (10 mL) and diluted with brine (10 mL). The resultant mixture was then extracted with Et_2O (5 × 5 mL), and the combined organic extracts were washed with brine (10 mL), dried over $MgSO_4$, filtered, and concentrated *in vacuo*. The residue was purified by flash column chromatography on SiO_2 (3:2 → 1:1 petrol/EtOAc) to afford protobruceol-III (**4.7**) as a clear colourless oil (24.5 mg, 35%). Further elution gave protobruceol-II (**4.6**) as a clear colourless oil (25.8 mg, 37%).

Data for protobruceol-III (**4.7**):

^{1}H NMR (500 MHz, $CDCl_3$) δ 8.92 (br s, 1H), 7.94 (d, *J* = 9.5 Hz, 1H), 6.67 (dd, *J* = 10.1, 1.3 Hz, 1H), 6.58 (s, 1H), 6.08 (dd, *J* = 9.5, 1.5 Hz, 1H), 5.47 (d, *J* = 10.1 Hz, 1H), 4.95 (s, 1H), 4.86 (q, *J* = 1.7 Hz, 1H), 4.12 (ddd, *J* = 15.5, 8.1, 5.1 Hz, 1H), 1.86 (td, *J* = 9.8, 9.0, 3.6 Hz, 1H), 1.71 (d, *J* = 5.2 Hz, 3H), 1.42 (s, 3H)

^{13}C NMR (125 MHz, $CDCl_3$) δ 163.3, 156.94, 156.92, 155.3, 150.9, 146.8, 146.7, 139.9, 126.2, 126.1, 117.1, 117.0, 112.0, 111.9, 109.7, 106.11, 106.10, 103.1, 95.6, 80.24, 80.22, 76.09, 76.07, 37.3, 37.1, 29.04, 28.97, 26.7, 17.72, 17.68 (Note: more than 19 ^{13}C signals are observed as **4.7** is a 1:1 mixture of diastereoisomers)

IR (neat) 3246, 3005, 2971, 1708, 1638, 1615, 1595, 1443, 1365, 1299, 1262, 1141, 1085

R_f 0.17 (6:1 CH_2Cl_2/EtOAc)

HRMS (ESI) calculated for $C_{19}H_{21}O_5$ 329.1384 $[M+H]^+$, found: 329.1383.

Data for protobruceol-II (**4.6**):

^{1}H NMR (500 MHz, $CDCl_3$) δ 8.88 (br s, 1H), 7.96 (d, *J* = 9.6 Hz, 1H), 6.68 (d, *J* = 10.1 Hz, 1H), 6.55 (s, 1H), 6.09 (d, *J* = 9.5 Hz, 1H), 5.72 – 5.64 (m, 1H), 5.63 (d, *J* = 15.6 Hz, 1H), 5.48 (d, *J* = 10.1 Hz, 1H), 2.42 (d, *J* = 7.1 Hz, 1H), 1.45 (s, 3H), 1.25 (s, 3H), 1.22 (s, 3H)

^{13}C NMR (125 MHz, $CDCl_3$) δ 163.2, 156.9, 155.3, 151.1, 141.9, 139.9, 125.9, 121.0, 117.3, 109.7, 106.4, 103.0, 95.6, 79.9, 71.5, 44.0, 29.7, 29.6, 26.6

IR (neat) 3211, 2974, 2930, 1708, 1615, 1444, 1365, 1299, 1259, 1208, 1181, 1141, 1096

R_f 0.13 (6:1 CH_2Cl_2/EtOAc)

HRMS (ESI) calculated for $C_{19}H_{21}O_5$ 329.1384 $[M+H]^+$, found: 329.1385.

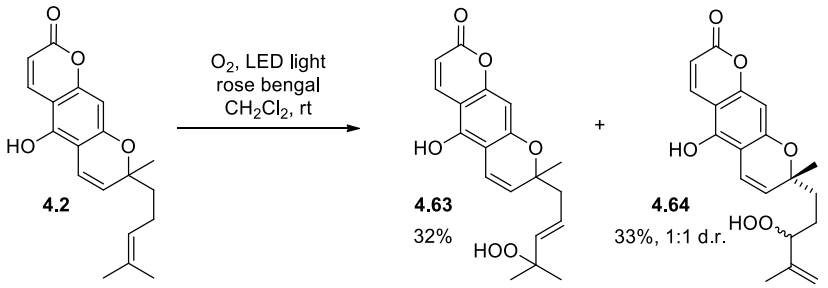

To a solution of **4.2** (500 mg, 1.60 mmol) in MeOH (45 mL) was added rose bengal (15.0 mg, 0.0160 mmol). O_2 was bubbled through the resultant solution while it was irradiated with LED light for 18 h. The solvent was removed *in vacuo* and the residue was purified by flash column chromatography on SiO_2 (6:1 → 4:1 CH_2Cl_2/EtOAc, gradient elution) to afford **4.64** as a pale yellow oil (181 mg, 33%, d.r. 1:1). Further elution afforded **4.63** as a pale yellow oil (178 mg, 32%).

Data for **4.64**:

^{1}H NMR (500 MHz, $CDCl_3$) δ 8.03 (d, *J* = 9.7 Hz, 1H), 6.65 (d, *J* = 10.1 Hz, 1H), 6.34 (s, 1H), 6.13 (dd, *J* = 9.6, 1.1 Hz, 1H), 5.57 (d, *J* = 10.1 Hz, 1H), 5.29 (s, 2H), 5.04 – 5.00 (m, 1H), 4.99 (s, 1H), 4.29 (t, *J* = 6.6 Hz, 1H), 1.83 – 1.51 (m, overlapped, 4H) 1.70 (s, 3H), 1.39 (s, 3H

^{13}C NMR (125 MHz, $CDCl_3$) δ 162.52, 157.83, 157.76, 155.9, 148.79, 148.78, 139.6, 128.3, 128.2, 115.94, 115.91, 114.8, 114.8, 110.6, 105.9, 105.8, 104.1, 104.0, 97.6, 97.6, 89.5, 89.4, 79.7, 79.5, 37.4, 37.1, 27.0, 26.7, 25.5, 25.2, 17.4 (Note: more than 19 ^{13}C signals are observed as **4.64** is a 1:1 mixture of diastereoisomers)

IR (neat) 3319, 2973, 1767, 1686, 1615, 1567, 1453, 1405, 1354, 1303, 1196, 1139, 1081

R_f 0.25 (5:1 CH_2Cl_2/EtOAc)

HRMS (ESI) calculated for $C_{19}H_{21}O_6$ 345.1333 $[M+H]^+$, found: 345.1334.

Data for **4.63**

^{1}H NMR (500 MHz, $CDCl_3$) δ 8.05 (d, *J* = 9.6 Hz, 1H), 7.58 (s, 1H), 6.69 (d, *J* = 10.1 Hz, 1H), 6.34 (s, 1H), 6.13 (dd, *J* = 9.6, 1.3 Hz, 1H), 5.67 (dt, *J* = 15.9, 7.0 Hz, 1H), 5.63 – 5.56 (m, 2H), 2.46 (dd, *J* = 14.0, 7.1 Hz, 1H), 2.39 (dd, *J* = 14.0, 6.9 Hz, 1H), 1.43 (s, 3H), 1.24 (s, 3H), 1.23 (s, 3H)
^{13}C NMR (125 MHz, $CDCl_3$) δ 162.4, 157.9, 155.9, 148.8, 139.6, 137.9, 128.0, 125.2, 116.1, 110.7, 106.2, 104.1, 97.5, 82.4, 79.4, 44.5, 26.8, 24.5, 24.2
IR (neat) 3316, 2979, 1692, 1616, 1567, 1454, 1406, 1355, 1196, 1140, 1084, 975
R_f 0.20 (5:1 CH_2Cl_2/EtOAc)
HRMS (ESI) calculated for $C_{19}H_{21}O_6$ 345.1333 $[M+H]^+$, found: 345.1333.

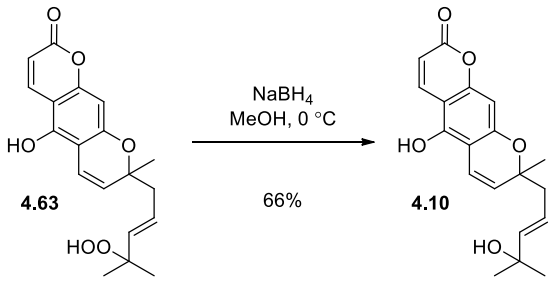

To a solution of **4.63** (44.6 mg, 0.130 mmol) in MeOH (5 mL) was added $NaBH_4$ (7.3 mg, 0.17 mmol) in one portion, and the reaction mixture was stirred at 0 °C for 5 min. Further $NaBH_4$ (7.3 mg, 0.168 mmol) was added, then the reaction was quenched with 1 M HCl solution (0.5 mL) at 0 °C and diluted with brine (10 mL). The mixture was extracted with EtOAc (3 × 15 mL). The combined organic extracts were washed with brine (10 mL), dried over $MgSO_4$, filtered, and concentrated *in vacuo*. The residue was purified by flash column chromatography on SiO_2 (neat Et_2O) to afford protobruceol-IV structure (**4.10**) as a pale yellow oil (27.9 mg, 66%).

Data for protobruceol-IV structure (**4.10**):

^{1}H NMR (500 MHz, $CDCl_3$) δ 8.03 (d, *J* = 9.7 Hz, 1H), 6.68 (d, *J* = 10.1 Hz, 1H), 6.29 (s, 1H), 6.08 (d, *J* = 9.7 Hz, 1H), 5.63 – 5.60 (m, 2H), 5.54 (d, *J* = 10.1 Hz, 1H), 2.41 (dd, *J* = 13.3, 5.1 Hz, 1H), 2.33 (dd, *J* = 13.4, 4.9 Hz, 1H), 1.40 (s, 3H), 1.25 (s, 3H), 1.20 (s, 3H)
^{13}C NMR (125 MHz, $CDCl_3$) δ 162.7, 158.1, 155.8, 149.2, 142.0, 140.0, 127.6, 121.0, 116.5, 110.2, 106.7, 104.3, 97.3, 79.4, 71.4, 44.2, 29.8, 29.5, 26.7
IR (neat) 3331, 2974, 1699, 1615, 1567, 1452, 1355, 1138
R_f 0.25 (neat Et_2O), 0.05 (2:1 petrol/EtOAc)
HRMS (ESI) calculated for $C_{19}H_{21}O_5$ 329.1384 $[M+H]^+$, found: 329.1383.

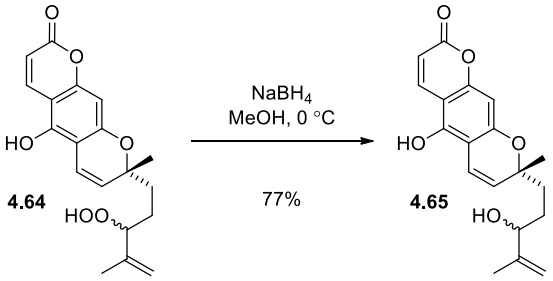

To a solution of **4.64** (96.5 mg, 0.280 mmol) in MeOH (5 mL) at 0 °C was added $NaBH_4$ (19.0 mg, 0.504 mmol). The reaction was stirred at 0 °C for 5 minutes, then was diluted with brine (5 mL) and quenched with 1 M HCl (0.8 mL). The mixture was extracted with EtOAc (3 × 10 mL), and the combined organic extracts were washed with brine (10 mL), dried over $MgSO_4$, filtered, and concentrated *in vacuo*. The residue was purified by flash column chromatography on SiO_2 (neat Et_2O) to afford **4.65** as a yellow oil (70.4 mg, 77%, d.r. 1:1).

Data for **4.65**:

^{1}H NMR (500 MHz, $CDCl_3$) δ 8.02 (d, *J* = 9.6, 1H), 6.66 (d, *J* = 10.1 Hz, 1H), 6.28 (s, 1H), 6.09 (d, *J* = 9.4 Hz, 1H), 5.54 (d, *J* = 10.2 Hz, 1H), 4.93 (s, 1H), 4.84 (br d, *J* = 5.2 Hz, 1H), 4.10 – 4.05 (m, 1H), 1.84 – 1.57 (m, overlapped, 4H), 1.69 (s, 3H), 1.38 (s, 3H).

^{13}C NMR (125 MHz, $CDCl_3$) δ 162.7, 157.92, 157.91, 155.8, 149.1, 146.9, 146.7, 139.9, 128.1, 116.1, 112.0, 111.8, 110.3, 106.1, 106.0, 104.2, 97.3, 79.7, 76.11, 76.09, 37.4, 37.1, 29.1, 29.0, 27.0, 26.8, 17.73, 17.69 (Note: more than 19 ^{13}C signals are observed as **4.65** is a 1:1 mixture of diastereoisomers)

IR (neat) 3307, 2972, 1691, 1615, 1567, 1453, 1354, 1235, 1139, 1080, 1081

R_f 0.30 (neat Et_2O)

HRMS (ESI) calculated for $C_{19}H_{21}O_5$ 329.1384 $[M+H]^+$, found: 329.1385.

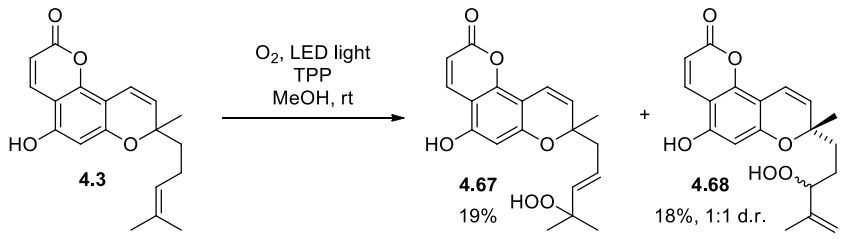

To a solution of **4.3** (156 mg, 0.498 mmol) in CH_2Cl_2 (45 mL) was added TPP (6.1 mg, 0.01 mmol). O_2 was bubbled through the resultant solution and it was irradiated with LED light for 3 h. The solvent was removed *in vacuo* and the residue was purified by flash column chromatography on SiO_2 (10:1

→ 5:1 CH_2Cl_2/EtOAc) to afford **4.68** as a bright yellow gum (31.4 mg, 18%, d.r. 1:1). Further elution afforded **4.67** as a bright yellow gum (32.2 mg, 19%).

Data for **4.68**:

^{1}H NMR (600 MHz, *d*$_6$-acetone) δ 10.49 (br s, 1H), 9.76 (br s, 1H), 8.02 (d, *J* = 9.7, 1H), 6.75 (d, *J* = 10.1, 1H), 6.27 (d, 1H), 6.09 (d, *J* = 9.7 Hz, 1H), 5.66 (d, *J* = 10.1, 1H), 4.93 – 4.86 (m, 2H), 4.24 (td, *J* = 6.6, 2.4 Hz, 1H), 1.85 – 1.67 (m, 3H), 1.67 (s, 1H), 1.64 – 1.57 (m, 1H), 1.41 (s, 3H).
^{13}C NMR (150 MHz, *d*$_6$-acetone) δ 170.5, 168.02, 167.99, 161.7, 155.1, 155.0, 149.5, 136.94, 136.92, 125.80, 125.78, 123.6, 123.5, 120.43, 113.37, 112.1, 112.0, 108.94, 108.92, 99.03, 98.98, 90.5, 90.4, 47.8, 47.7, 36.74, 36.68, 35.8, 35.7, 26.9, 26.8. N.B. Greater than 19 ^{13}C signals are observed as **4.68** is a 1:1 mixture of diastereoisomers.
IR (neat) 3252, 2971, 1692, 1621, 1599, 1354, 1264, 1149, 1078, 824.
R$_f$ 0.35 (5:1 CH_2Cl_2/EtOAc).
HRMS (ESI) calculated for $C_{19}H_{21}O_6$ 345.1333 $[M+H]^+$, found: 345.1334.

Data for **4.67**:

^{1}H NMR (600 MHz, *d*$_6$-acetone) δ 9.96 (s, 1H), 9.73 (s, 1H), 8.02 (d, *J* = 9.6 Hz, 1H), 6.74 (d, *J* = 10.1 Hz, 1H), 6.27 (s, 1H), 6.08 (d, *J* = 9.6 Hz, 1H), 5.71 – 5.63 (m, overlapped, 3H), 3.08 (s, 1H), 2.44 (d, *J* = 5.8 2H), 1.43 (s, 3H), 1.19 (s, 3H), 1.17 (s, 3H).
^{13}C NMR (150 MHz, *d*$_6$-acetone) δ 160.9, 158.4, 156.0, 152.0, 139.82, 139.81, 127.2, 124.2, 116.1, 110.7, 103.7, 102.7, 99.3, 89.3, 81.5, 80.6, 44.9, 26.8, 24.8.
IR (neat) 3244, 2979, 1687, 1622, 1596, 1464, 1375, 1354, 1259, 1144, 1077, 1001.
R$_f$ 0.30 (5:1 CH_2Cl_2/EtOAc).
HRMS (ESI) calculated for $C_{19}H_{21}O_6$ 345.1333 $[M+H]^+$, found: 345.1337.

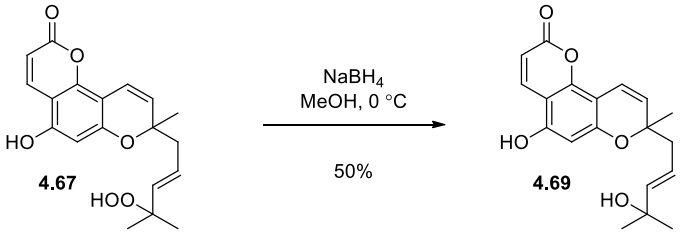

To a solution of **4.67** (31.7 mg, 0.0921 mmol) in MeOH (5 mL) at 0 °C was added $NaBH_4$ (17.4 mg, 0.460 mmol) in one portion. The resultant mixture was stirred at 0 °C for 30 min, then quenched with 1 M HCl (1 mL). Brine (10 mL) was added and the mixture was extracted with EtOAc (10 mL × 3). The combined organic extracts were then washed with brine (20 mL), dried over $MgSO_4$, filtered and concentrated *in vacuo*. The residue was purified by flash column chromatography on SiO_2 (1:1 petrol/EtOAc) to afford **4.69** as a cream coloured solid (15.0 mg, 50%).

Data for **4.69**:

^{1}H NMR (600 MHz, $CDCl_3$) δ 7.96 (d, *J* = 9.6 Hz, 1H), 6.80 (d, *J* = 10.0 Hz, 1H), 6.19 (s, 1H), 6.12 (d, *J* = 9.5 Hz, 1H), 5.67 – 5.61 (m, overlapped, 2H), 5.49 (d, *J* = 10.1 Hz, 1H), 2.41 – 2.33 (m, 2H), 1.42 (s, 3H), 1.26 (s, 3H), 1.21 (s, 3H).
^{13}C NMR (150 MHz, $CDCl_3$) δ 161.9, 157.6, 154.1, 151.0, 142.1, 139.5, 126.4, 121.0, 116.0, 110.31, 103.30, 102.9, 99.2, 80.0, 71.4, 44.0, 29.6, 29.6, 26.6.
IR (neat) 3199, 1693, 1622, 1597, 1464, 1354, 1263, 1147, 1077.
R_f 0.15 (1:1 petrol/EtOAc)
HRMS (ESI) calculated for $C_{19}H_{20}O_5Na$ 355.1203 $[M+Na]^+$, found: 355.1207.

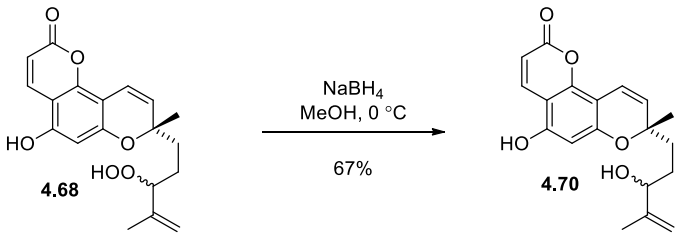

To a solution of **4.68** (36.0 mg, 0.110 mmol) in MeOH (5 mL) at 0 °C was added $NaBH_4$ (19.8 mg, 0.523 mmol) in one portion. The resultant mixture was stirred at 0 °C for 10 min, the quenched with 1 M HCl (1 mL). Brine (10 mL) was added and the mixture was extracted with EtOAc (10 mL × 3). The combined organic extracts were then washed with brine (20 mL), dried over $MgSO_4$, filtered and

concentrated *in vacuo*. The residue was purified by flash column chromatography on SiO_2 (1:1 petrol/EtOAc) to afford **4.70** as a cream colured solid (23.1 mg, 67%, d.r. 1:1).

Data for **4.70**:

^{1}H NMR (600 MHz, $CDCl_3$) δ 7.96 (d, *J* = 9.6 Hz, 1H), 6.78 (d, *J* = 10.1 Hz, 1H), 6.17 (s, 1H), 6.11 (d, *J* = 9.5 Hz, 1H), 5.45 (d, *J* = 10.2 Hz, 1H), 4.92 (br s, 1H), 4.84 (br s, 1H), 4.08 (t, *J* = 6.4 Hz, 1H), 1.85 – 1.78 (m, 1H), 1.73 – 1.66 (m, overlapped, 1H), 1.68 (s, 3H), 1.62 – 1.49 (m, 2H), 1.38 (s, 3H), 1.20 (s, 3H).
^{13}C NMR (150 MHz, $CDCl_3$) δ 164.7, 160.1, 156.7, 153.5, 149.4, 149.3, 142.3, 128.7, 118.4, 114.5, 112.5, 105.8, 104.8, 101.7, 82.9, 82.8, 78.7, 43.5, 40.0, 39.8, 36.5, 31.6, 31.1, 29.7, 26.5, 23.4, 20.1, 17.3. N.B. Greater than 19 ^{13}C NMR signals are observed as **4.70** is a 1:1 mixture of diastereoisomers
IR (neat) 3253, 2971, 1696, 1622, 1599, 1355, 1263, 1161, 1078, 1003.
R_f 0.20 (1:1 petrol/EtOAc).
HRMS (ESI) calculated for $C_{19}H_{21}O_5$ 329.1384 $[M+Na]^+$, found: 329.1386.

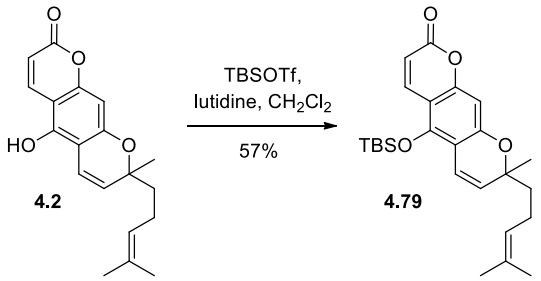

To a solution of **4.2** (663 mg, 2.12 mmol) in dry CH_2Cl_2 (30 mL) was added 2,6-lutidine (0.47 mL, 4.25 mmol) and the mixture was cooled to 0 °C. TBSOTf (0.45 mL, 2.34 mmol) was then added dropwise and the reaction mixture was stirred at 0 °C for 30 min. The reaction was quenched by addition of saturated $NaHCO_3$ solution (10 mL) and the layers were separated. The aqueous phase was extracted with CH_2Cl_2 (10 mL) and the combined organic phases were dried over $MgSO_4$, filtered, and concentrated *in vacuo*. The residue was purified by flash column chromatography on phosphate buffered SiO_2 (pH 7) (4:1 petrol/EtOAc) to afford **4.79** as a clear colourless oil. (622 mg, 69%).

Data for **4.79**:

^{1}H NMR (500 MHz, $CDCl_3$) δ 7.75 (d, *J* = 9.7 Hz, 1H), 6.54 (d, *J* = 10.1 Hz, 1H), 6.11 (d, *J* = 9.8 Hz, 1H), 5.56 (d, *J* = 10.2 Hz, 1H), 5.06 (t, *J* = 6.9 Hz, 1H), 2.10 – 2.04 (m, 2H), 1.75 (ddd, *J* = 13.7,

10.0, 6.6 Hz, 1H), 1.67 – 1.60 (m, overlapped, 1H), 1.64 (s, 3H), 1.55 (s, 3H), 1.40 (s, 3H), 1.07 (s, 9H), 0.14 (s, 6H).

^{13}C NMR (125 MHz, $CDCl_3$) δ 161.3, 158.0, 156.0, 148.2, 139.3, 132.0, 127.9, 123.7, 117.7, 111.0, 110.3, 106.9, 98.8, 79.6, 41.3, 26.6, 25.9, 25.7, 22.7, 18.6, 17.7, -3.72, -3.75.

R_f 0.60 (2:1 petrol/EtOAc)

HRMS (ESI) calculated for $C_{25}H_{35}O_4Si$ 427.2299 $[M+H]^+$, found: 427.2297

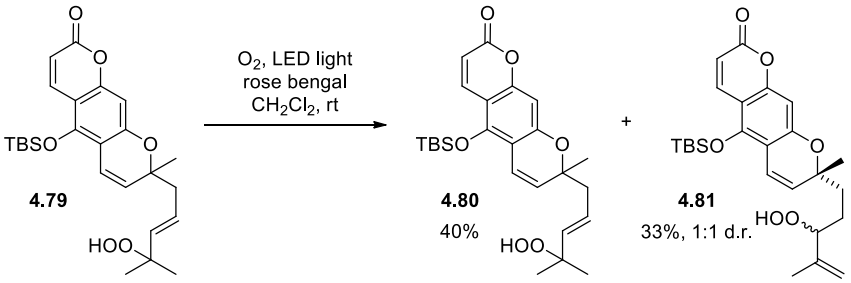

To a solution of **4.79** (263 mg, 0.616 mmol) in MeOH (20 mL) was added rose Bengal (5.8 mg, 6.16 μmol). The resultant solution was bubbled with O_2 and irradiated with LED light for 15 h. The solvent was removed *in vacuo* and the residue was purified by flash column chromatography on SiO_2 (1:0 → 20:1 CH_2Cl_2) to afford **4.81** as a clear colourless oil (93.6 mg, 33%), further elution afforded **4.80** as a clear and colourless oil (114 mg, 40%).

Data for **4.81**:

^{1}H NMR (500 MHz, $CDCl_3$) δ 7.77 (d, *J* = 9.8 Hz, 1H), 6.57 (d, *J* = 10.1 Hz, 1H), 6.44 (d, *J* = 1.6 Hz, 1H), 6.14 (dt, *J* = 9.7, 1.4 Hz, 1H), 5.54 (dd, *J* = 10.1, 3.8 Hz, 1H), 5.04 – 4.97 (m, 2H), 4.34 – 4.27 (m, 1H), 1.87 – 1.73 (m, 1H), 1.71 (s, 3H), 1.71 – 1.59 (m, 1H), 1.40 (d, *J* = 1.4 Hz, 3H), 1.09 (s, 9H), 0.15 (s, 6H).

^{13}C NMR (125 MHz, $CDCl_3$) δ 161.4, 157.8, 157.7, 156.0, 148.4, 143.4, 143.3, 139.4, 127.6, 127.4, 118.2, 114.8, 114.7, 111.2, 110.2, 110.0, 107.10, 107.08, 89.5, 89.4, 79.5, 79.2, 37.5, 37.1, 27.0, 26.6, 25.9, 25.6, 25.2, 18.6, 17.44, 17.39, -3.6, -3.7. N.B. Greater than 19 ^{13}C signals are observed as **4.81** is a 1:1 mixture of diastereoisomers

R_f 0.30 (20:1 CH_2Cl_2/EtOAc)

HRMS (ESI) calculated for $C_{25}H_{35}O_6Si$ 459.2197 [M+H] found: 459.2196

Data for **4.80**:

^{1}H NMR (600 MHz, $CDCl_3$) δ 7.76 (d, *J* = 9.7 Hz, 1H), 7.20 (s, 1H), 6.57 (d, *J* = 10.1 Hz, 1H), 6.45 (s, 1H), 6.14 (d, *J* = 9.6 Hz, 1H), 5.72 (dt, *J* = 15.9, 7.2 Hz, 1H), 5.62 (dt, *J* = 15.8, 1.2 Hz, 1H), 5.57 (d, *J* = 10.1 Hz, 1H), 2.51 – 2.40 (m, 2H), 1.43 (s, 3H), 1.28 (s, 3H), 1.27 (s, 3H), 1.09 (s, 9H), 0.16 (d, *J* = 6.2 Hz, 6H).

^{13}C NMR (150 MHz, $CDCl_3$) δ 161.3, 157.7, 156.1, 148.4, 139.4, 138.0, 127.5, 125.4, 118.1, 111.3, 110.3, 107.1, 99.0, 82.2, 79.1, 44.2, 26.5, 25.9, 24.4, 24.3, 18.6, 0.2, -3.6, -3.7.

IR (neat) 3387, 2955, 2931, 1897, 2860, 1736, 1719, 1611, 1597, 1566, 1472, 1441, 1389, 1350, 1257.

R_f 0.25 (20:1 CH_2Cl_2/EtOAc)

HRMS (ESI) calculated for $C_{25}H_{35}O_6Si$ 459.2197 [M+H] found: 459.2197

4.6.3: NMR Spectra

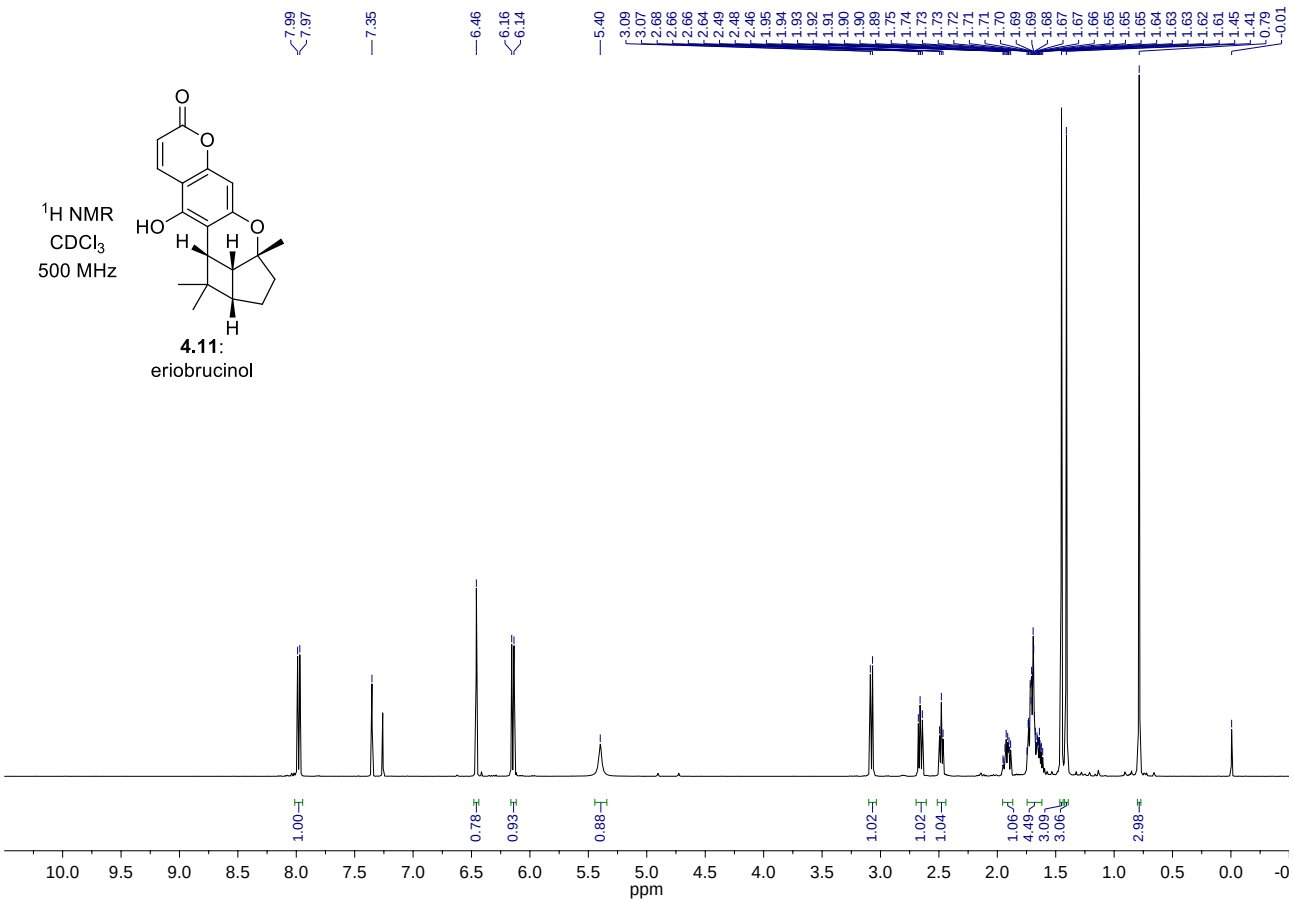

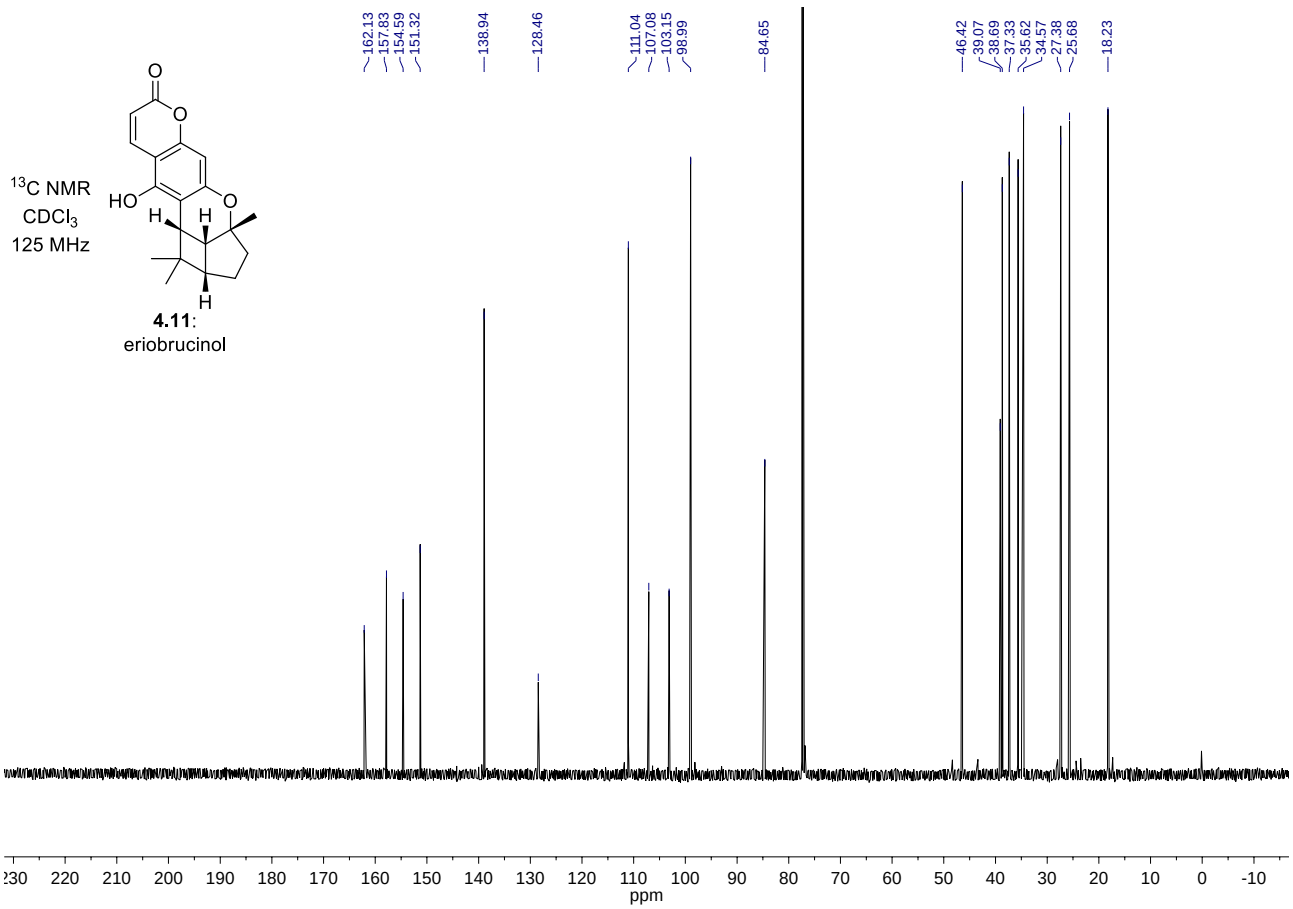

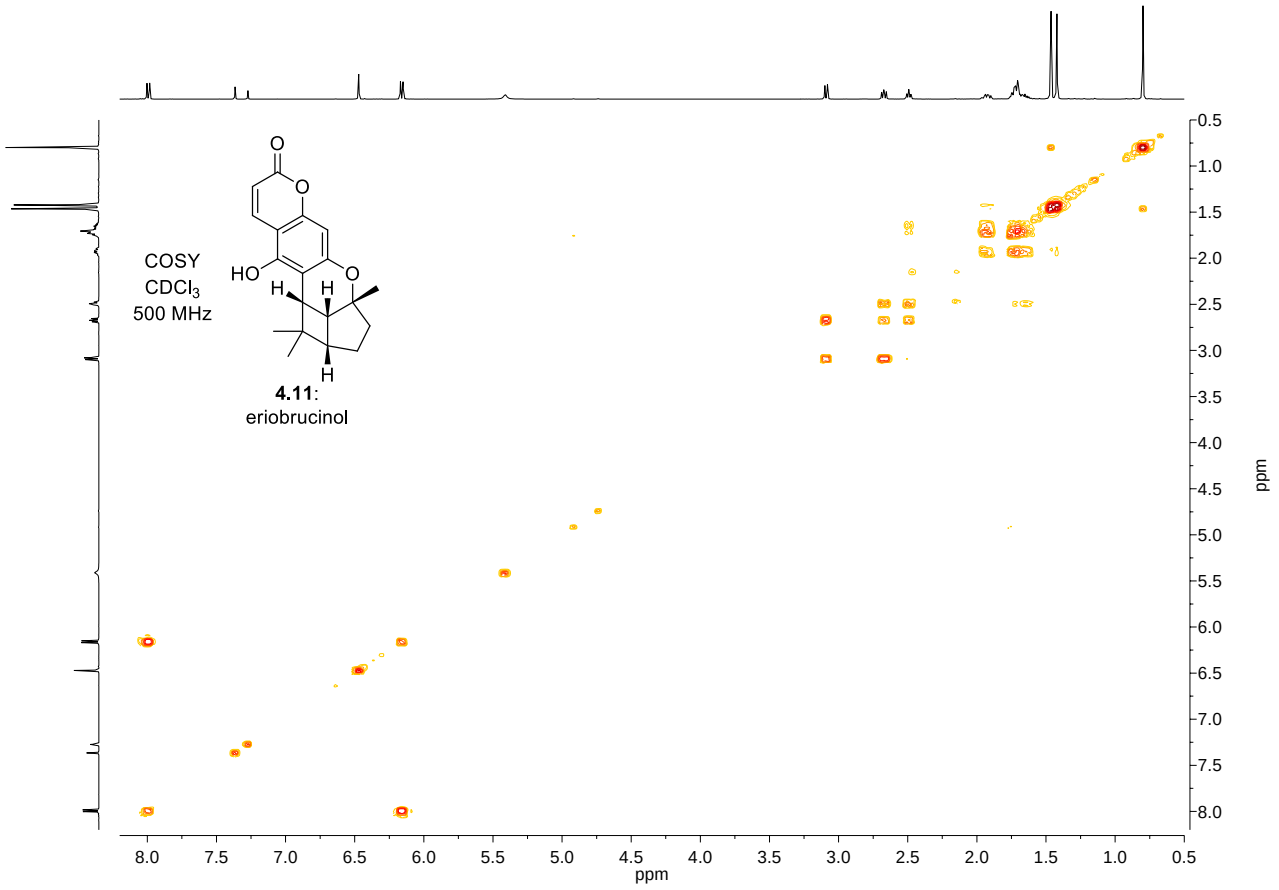
COSY
CDCl3
500 MHz
4.11:
eriobrucinol
ppm
ppm

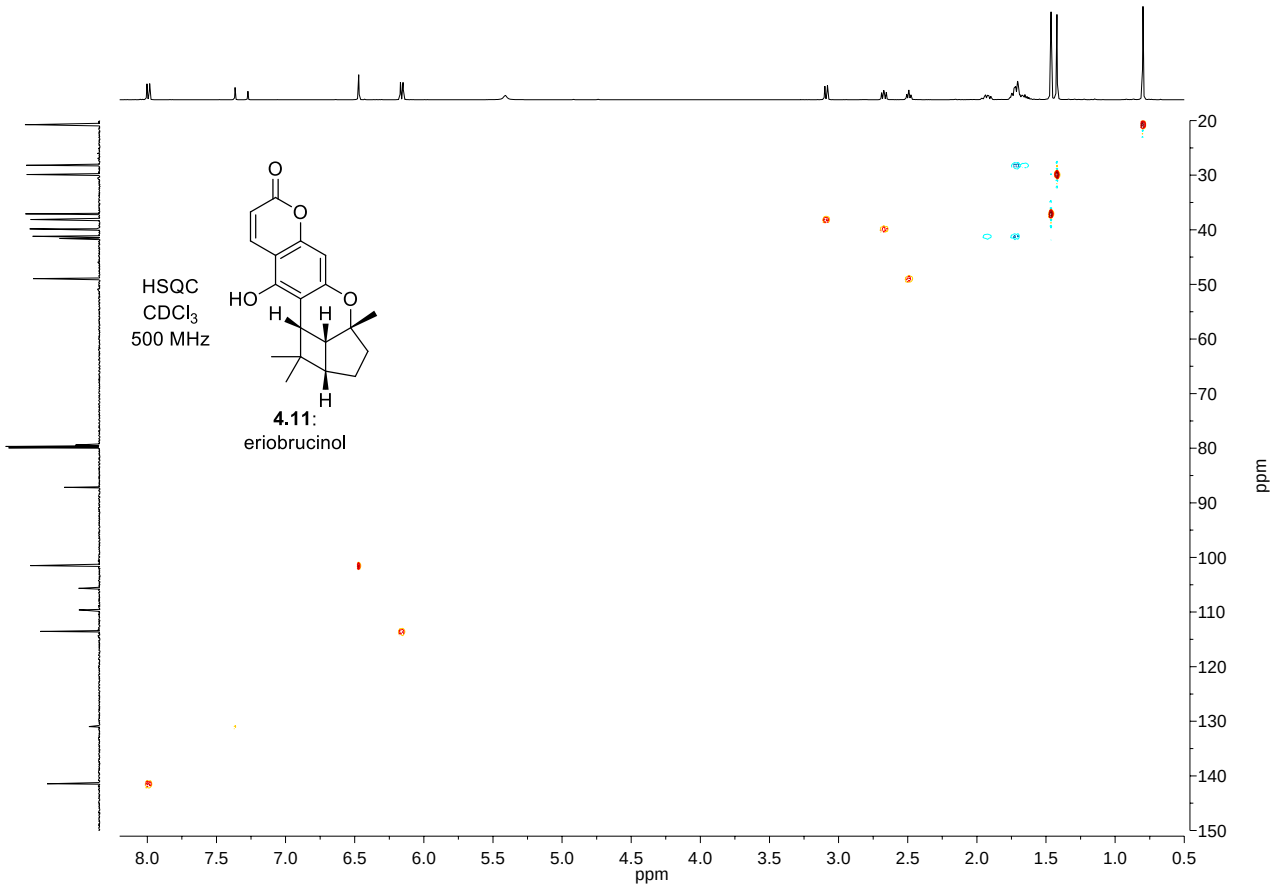
HSQC
CDCl3
500 MHz
4.11:
eriobrucinol
ppm
ppm

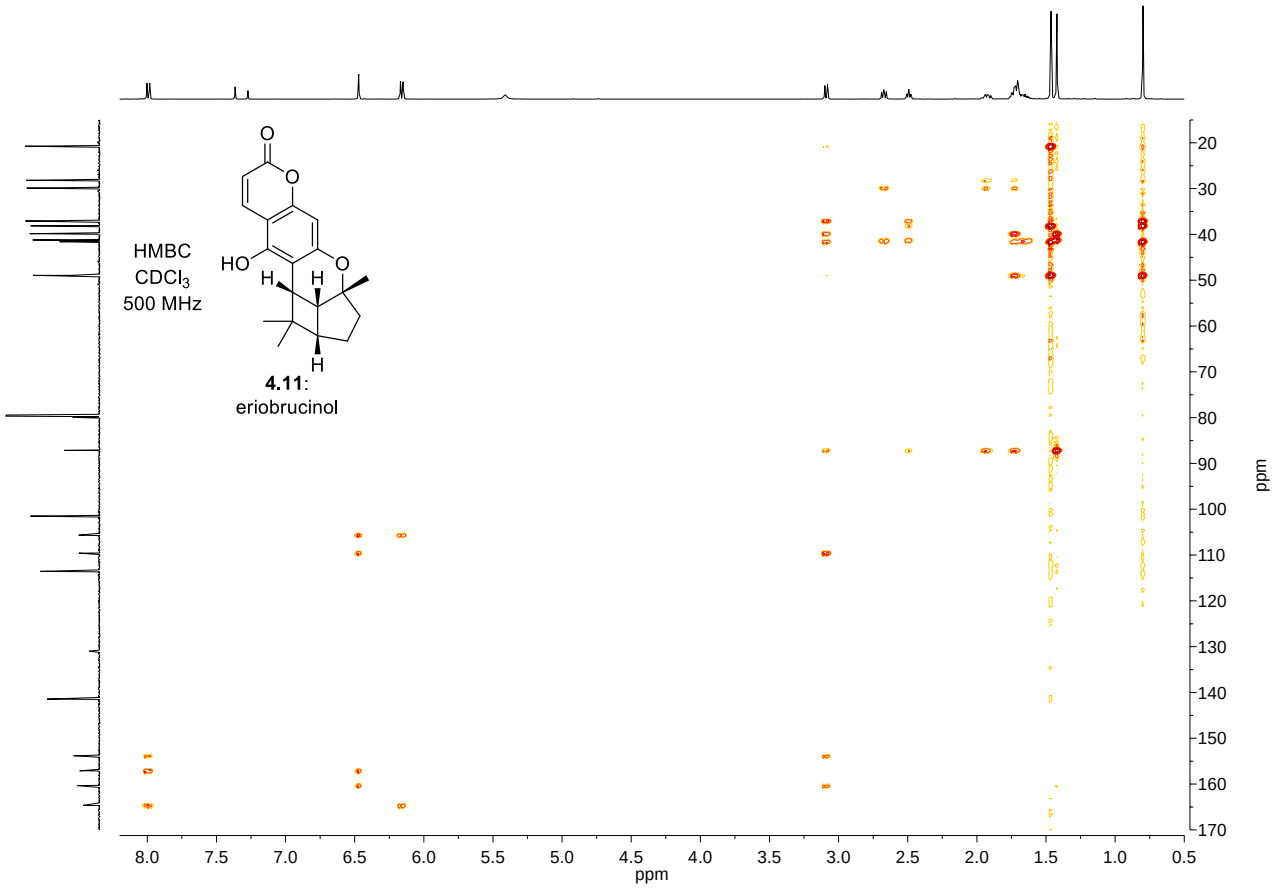
HMBC
CDCl3
500 MHz
4.11:
eriobrucinol
ppm

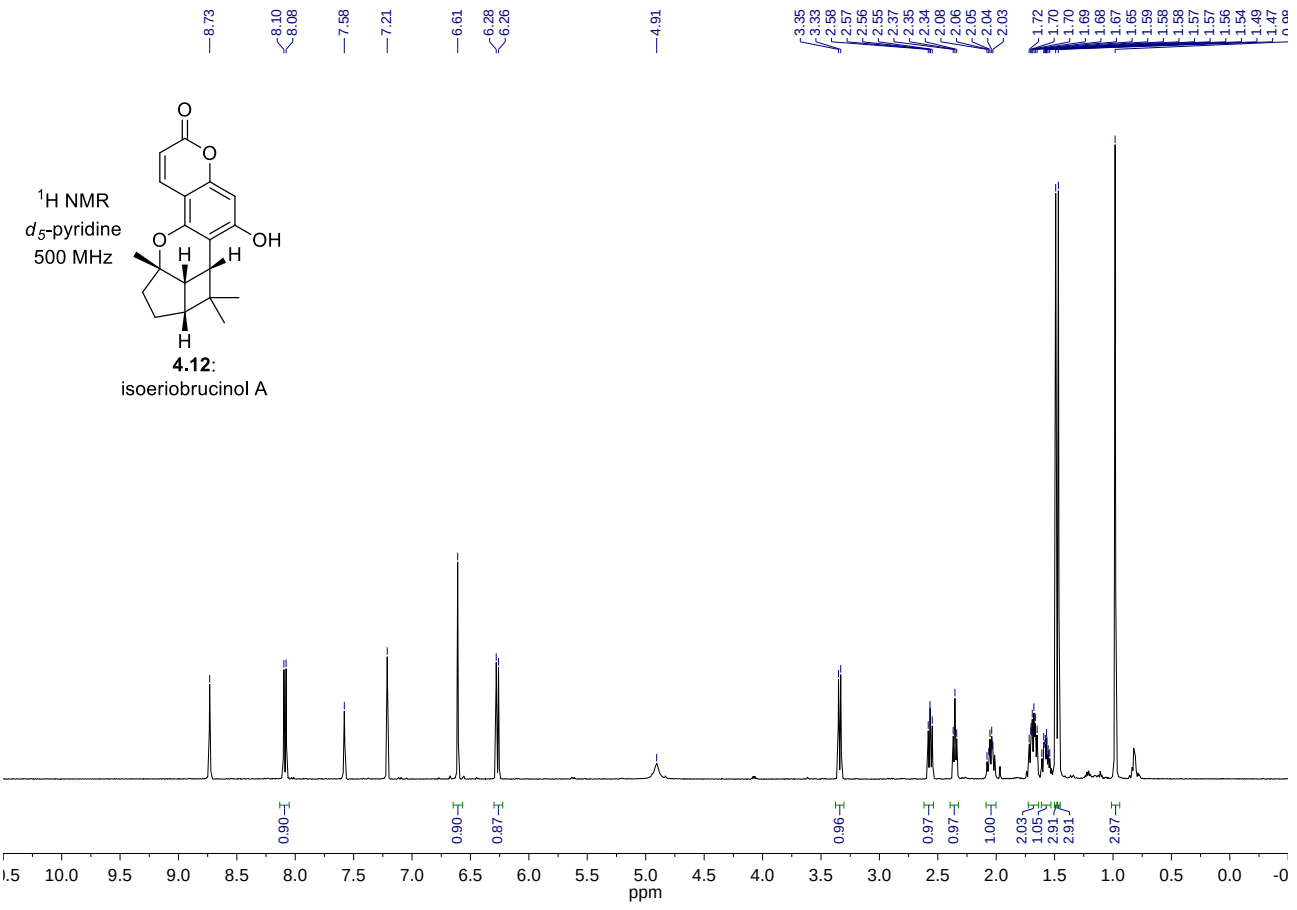
1H NMR
d5-pyridine
500 MHz
4.12:
isoeriobrucinol A
ppm

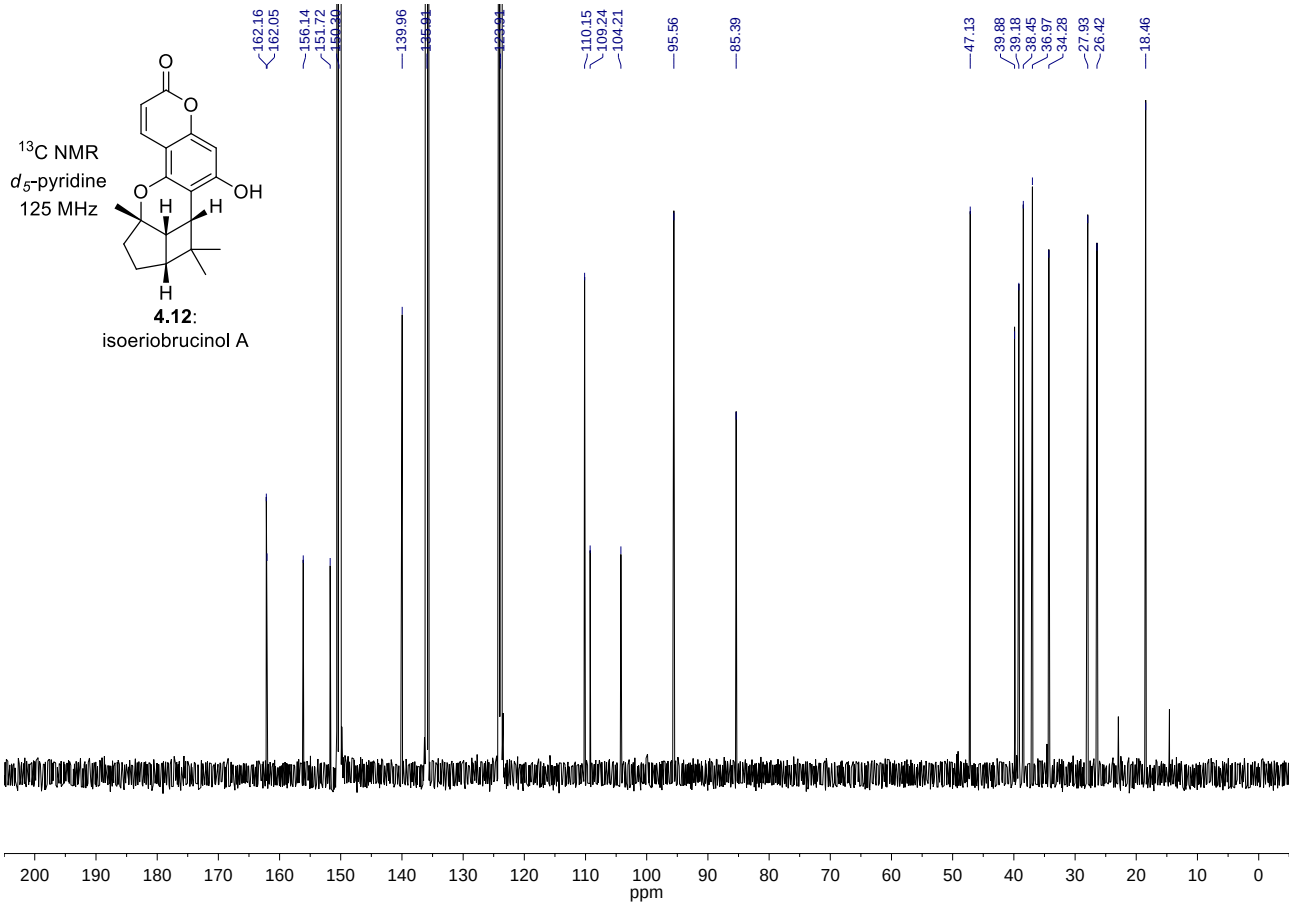
162.16
162.05
156.14
151.72
150.30
139.96
135.91
129.91
110.15
109.24
104.21
95.56
85.39
47.13
39.88
39.18
38.45
36.97
34.28
27.93
26.42
18.46
^{13}C NMR
d_5-pyridine
125 MHz
4.12:
isoeriobrucinol A
200 190 180 170 160 150 140 130 120 110 100 90 80 70 60 50 40 30 20 10 0
ppm

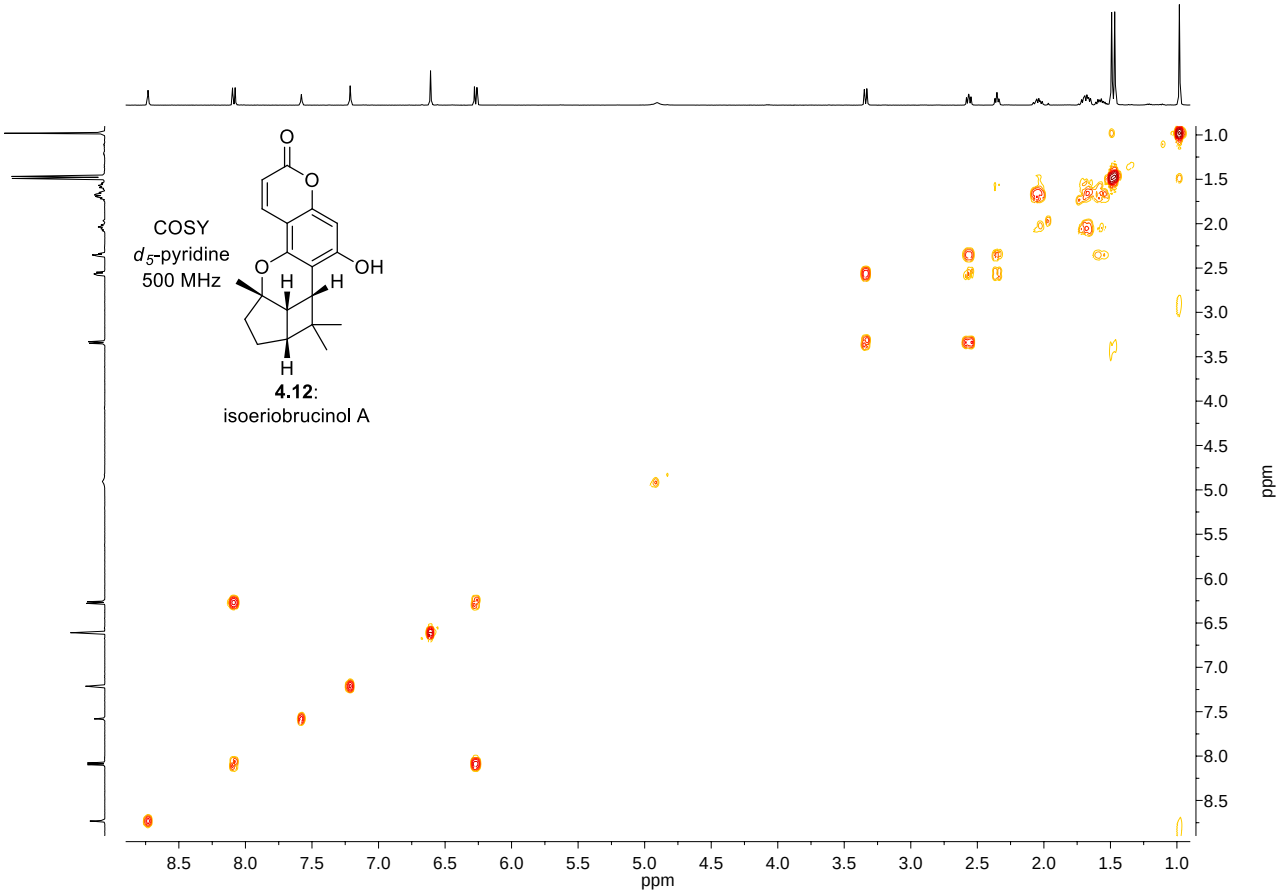
COSY
d_5-pyridine
500 MHz
4.12:
isoeriobrucinol A
8.5 8.0 7.5 7.0 6.5 6.0 5.5 5.0 4.5 4.0 3.5 3.0 2.5 2.0 1.5 1.0
ppm
1.0 1.5 2.0 2.5 3.0 3.5 4.0 4.5 5.0 5.5 6.0 6.5 7.0 7.5 8.0 8.5
ppm

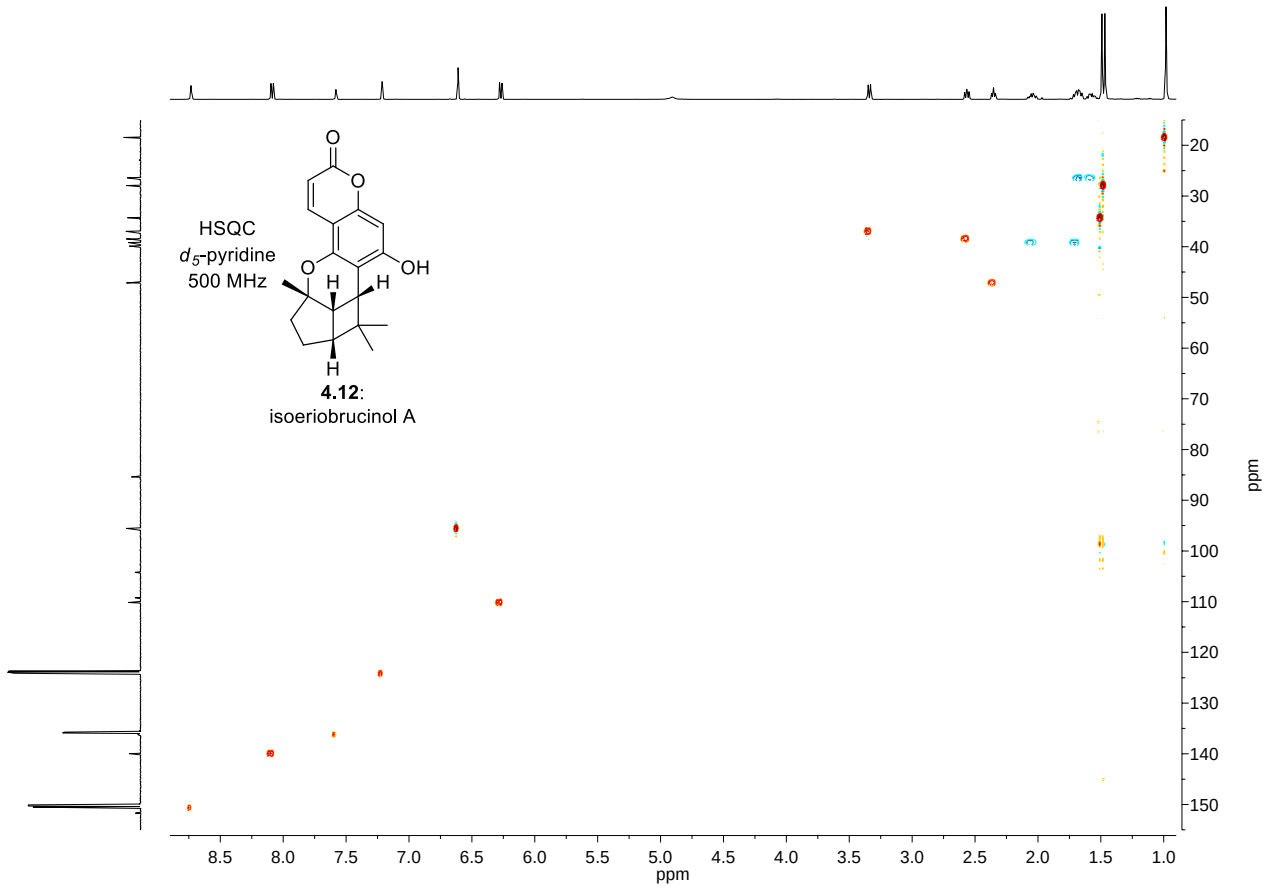
HSQC
d_5-pyridine
500 MHz
O
O
O
OH
H
H
H
4.12:
isoeriobrucinol A
8.5 8.0 7.5 7.0 6.5 6.0 5.5 5.0 4.5 4.0 3.5 3.0 2.5 2.0 1.5 1.0
ppm
20 30 40 50 60 70 80 90 100 110 120 130 140 150
ppm

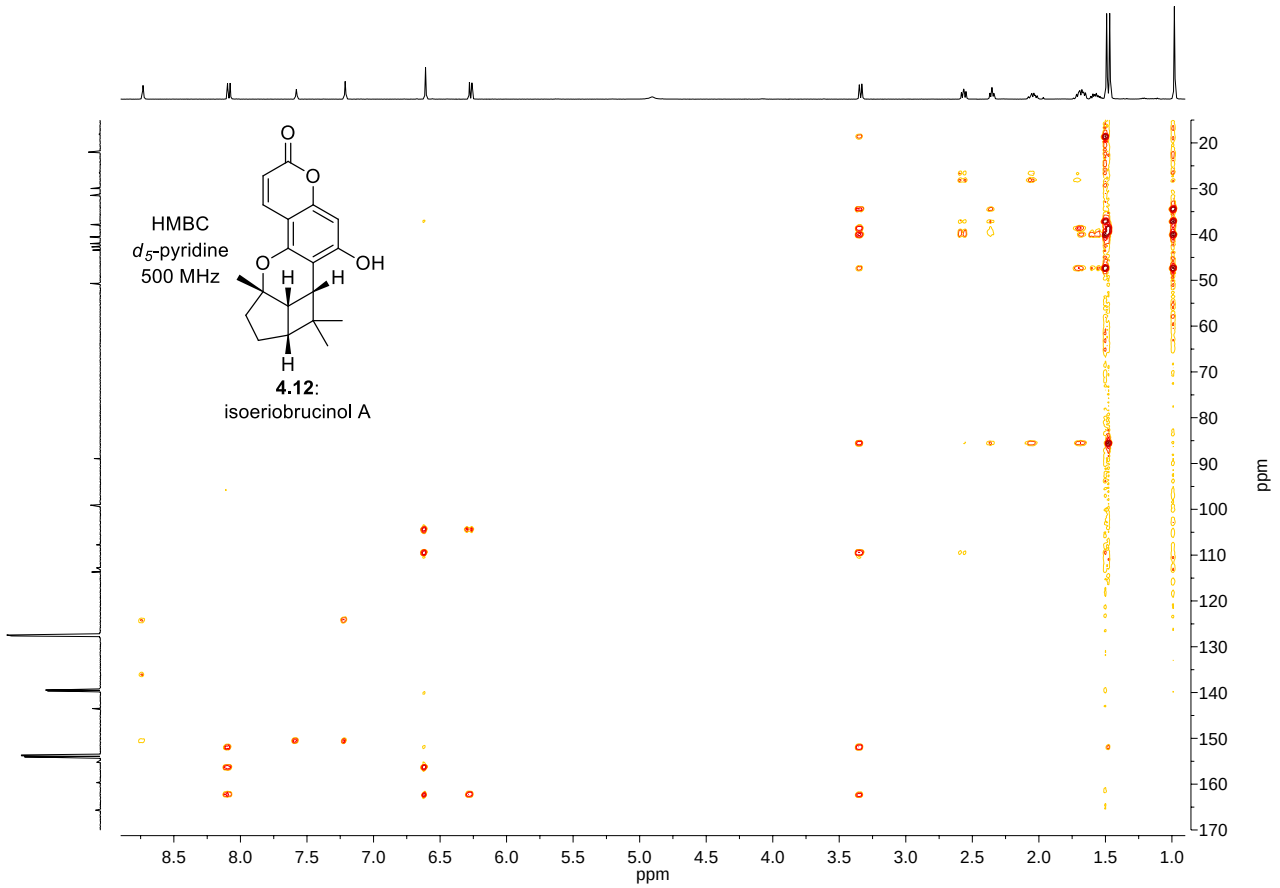
HMBC
d_5-pyridine
500 MHz
O
O
O
OH
H
H
H
4.12:
isoeriobrucinol A
8.5 8.0 7.5 7.0 6.5 6.0 5.5 5.0 4.5 4.0 3.5 3.0 2.5 2.0 1.5 1.0
ppm
20 30 40 50 60 70 80 90 100 110 120 130 140 150 160 170
ppm

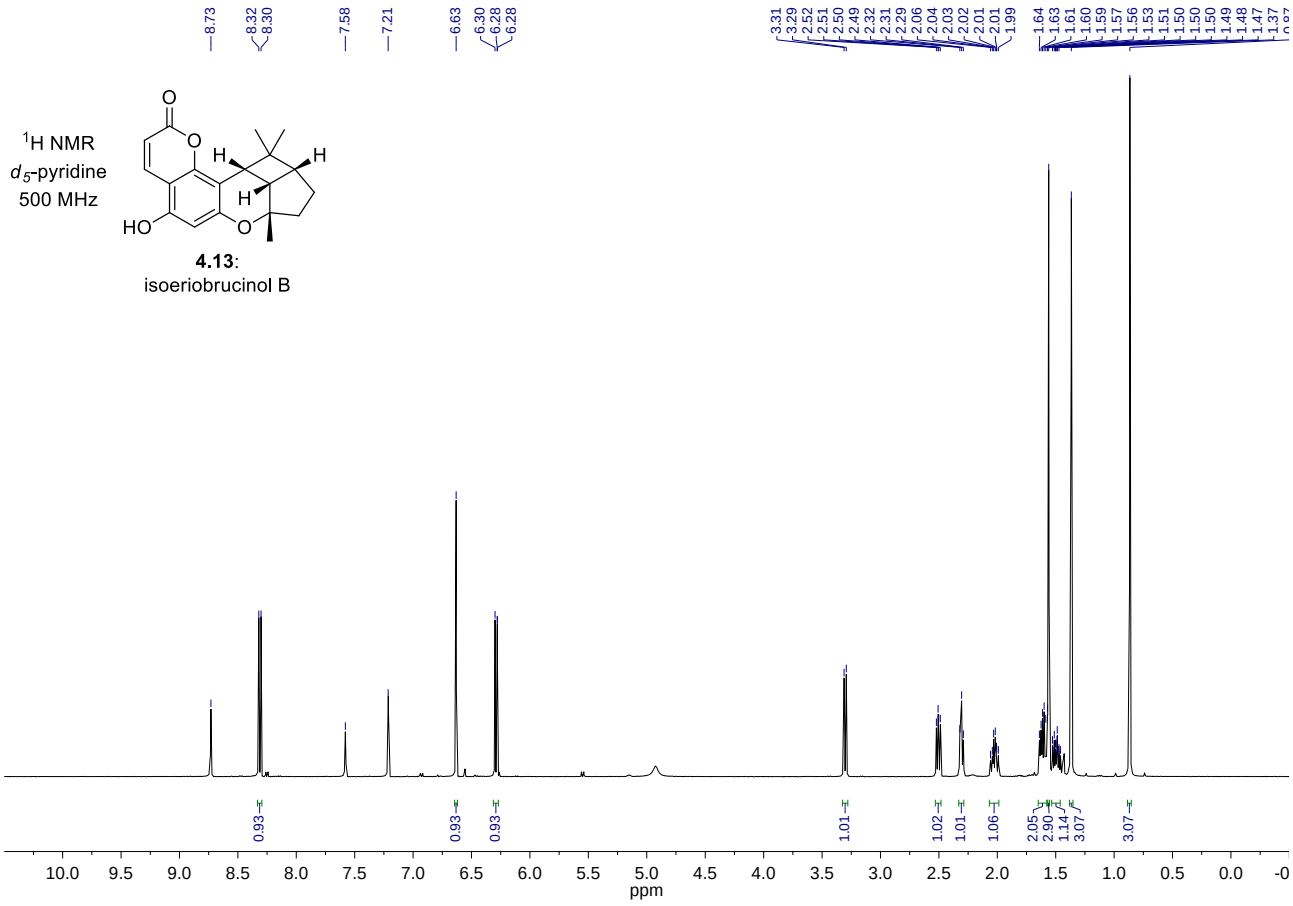
^{1}H NMR
d_5-pyridine
500 MHz
4.13:
isoeriobrucinol B
ppm

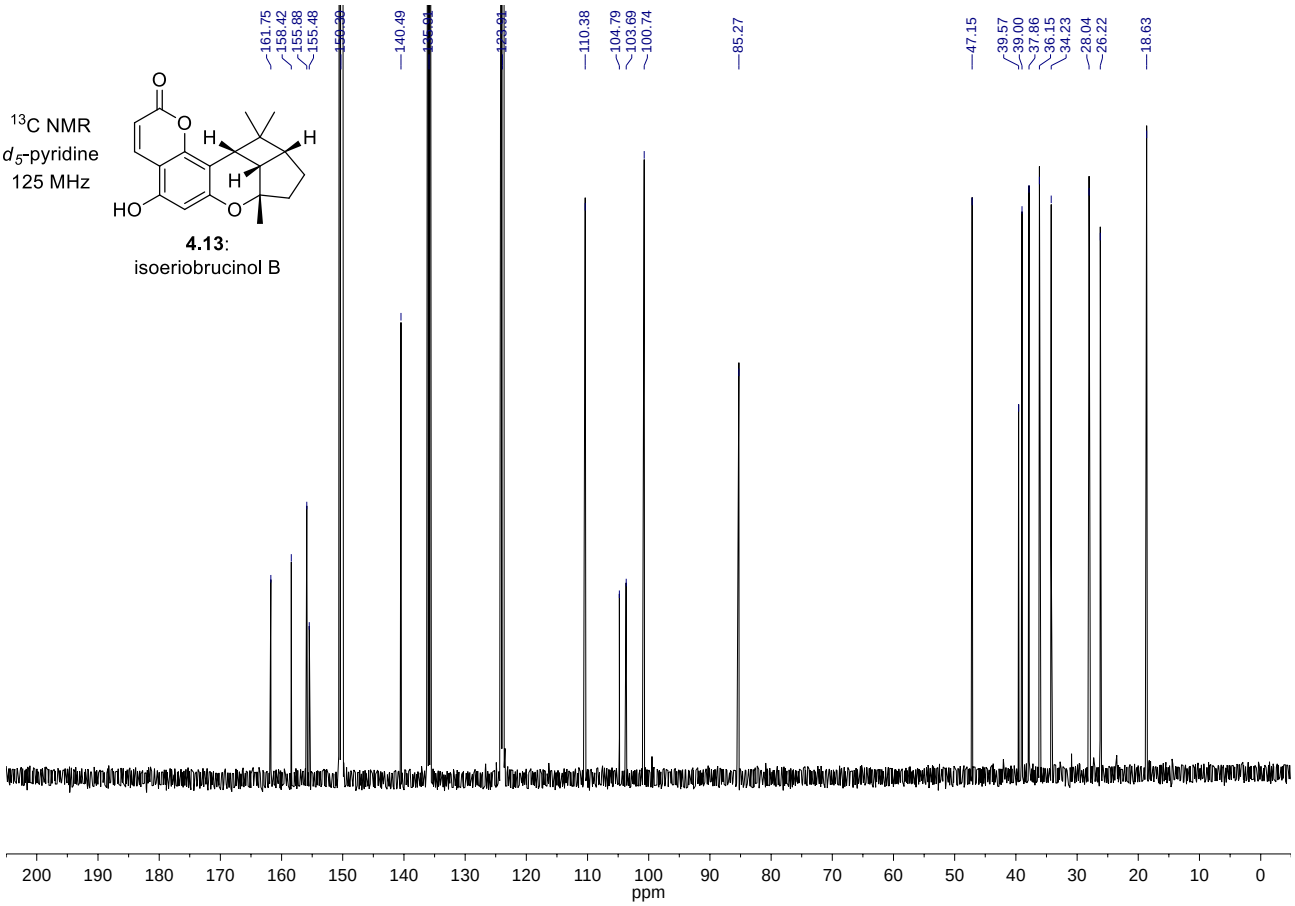
^{13}C NMR
d_5-pyridine
125 MHz
4.13:
isoeriobrucinol B
ppm

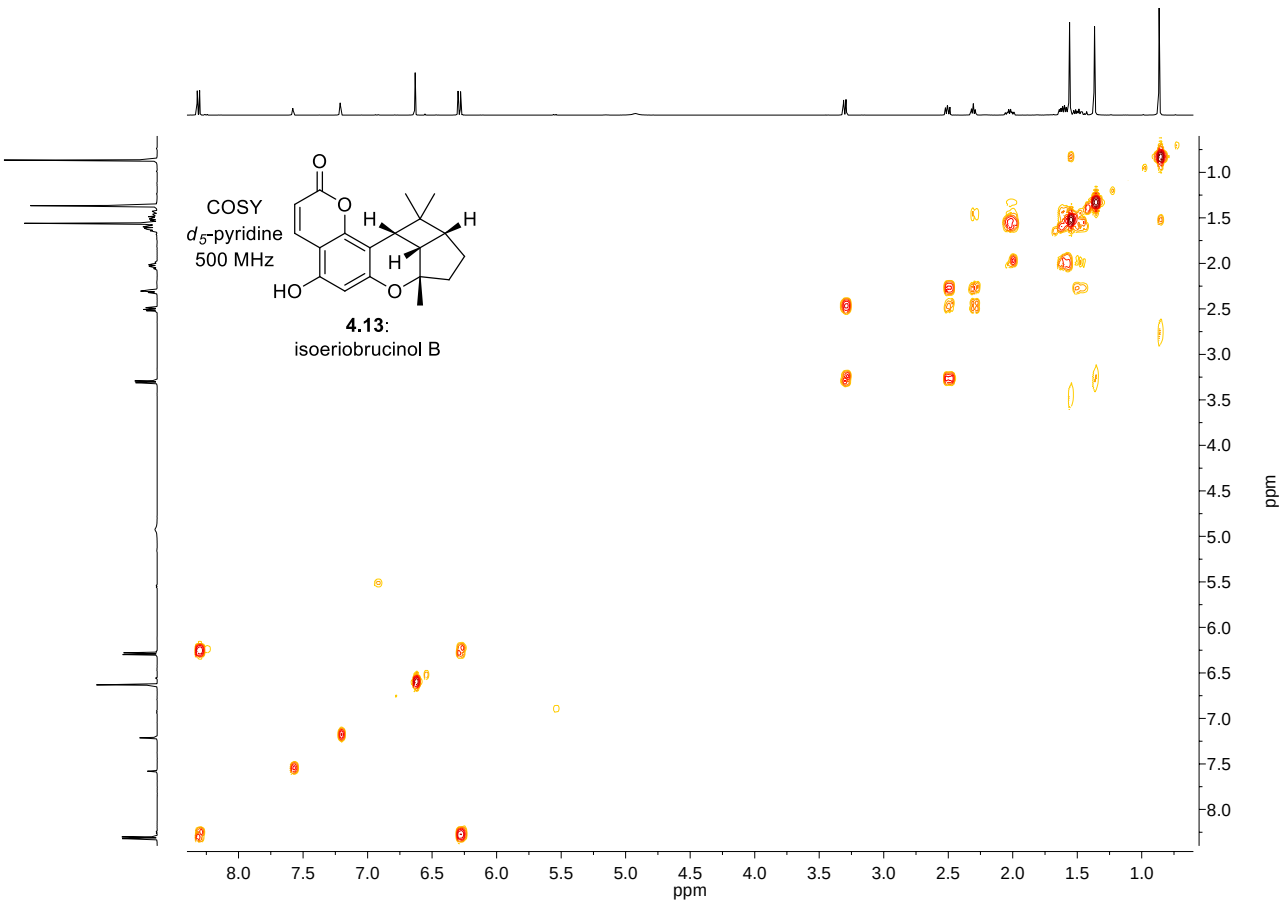
COSY
d_5-pyridine
500 MHz
4.13:
isoeriobrucinol B
ppm
ppm

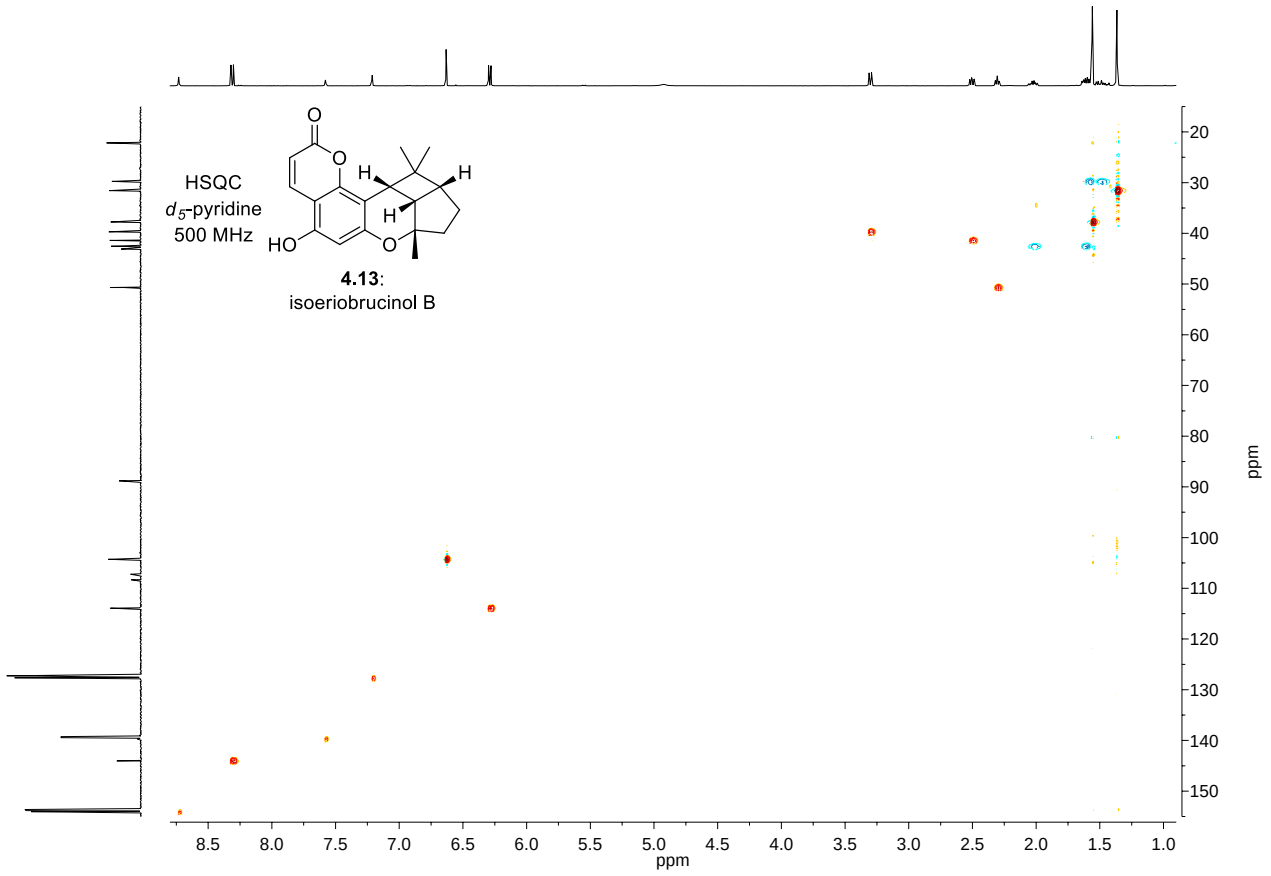
HSQC
d_5-pyridine
500 MHz
4.13:
isoeriobrucinol B
ppm
ppm

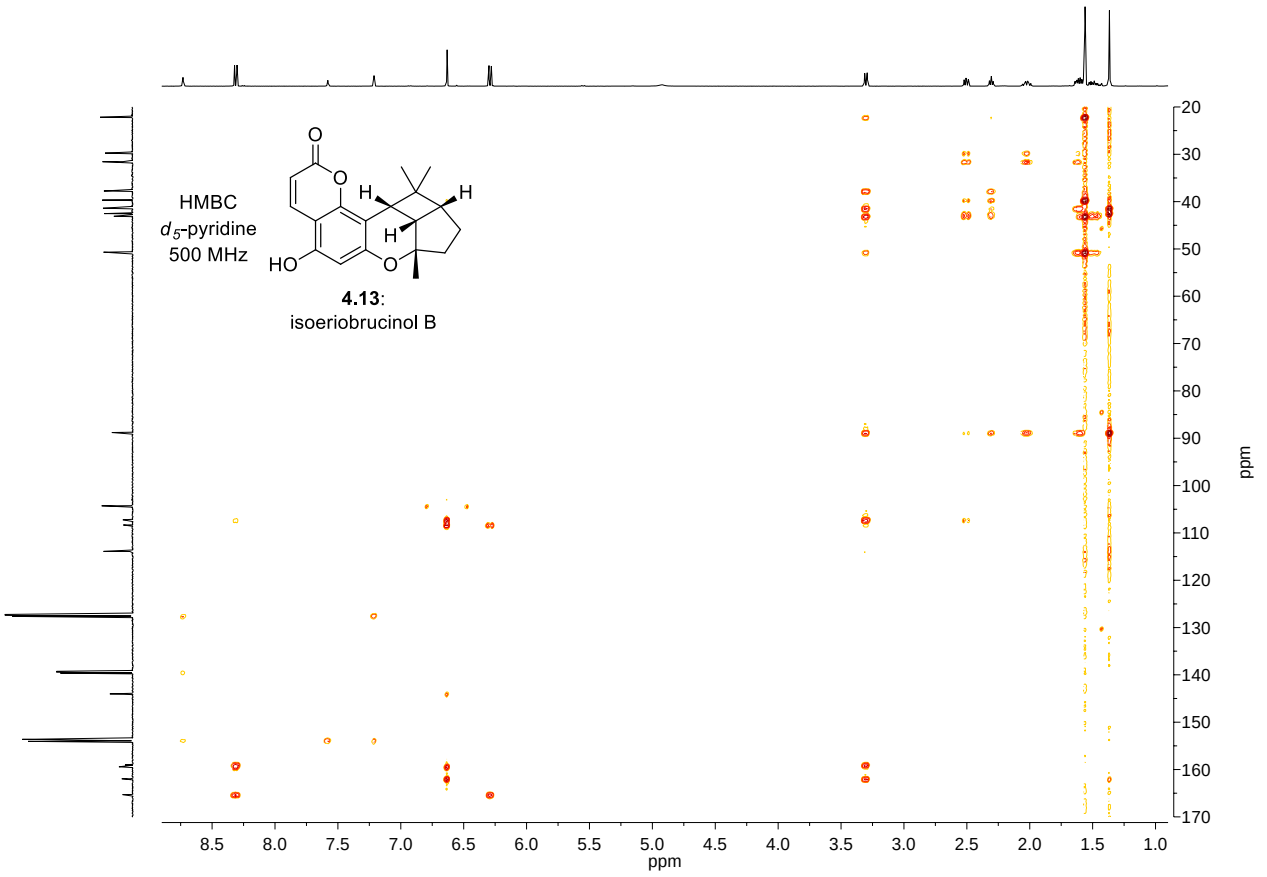
HMBC
d_5-pyridine
500 MHz
HO
O
H
H
H
O
O
4.13:
isoeriobrucinol B
ppm
ppm

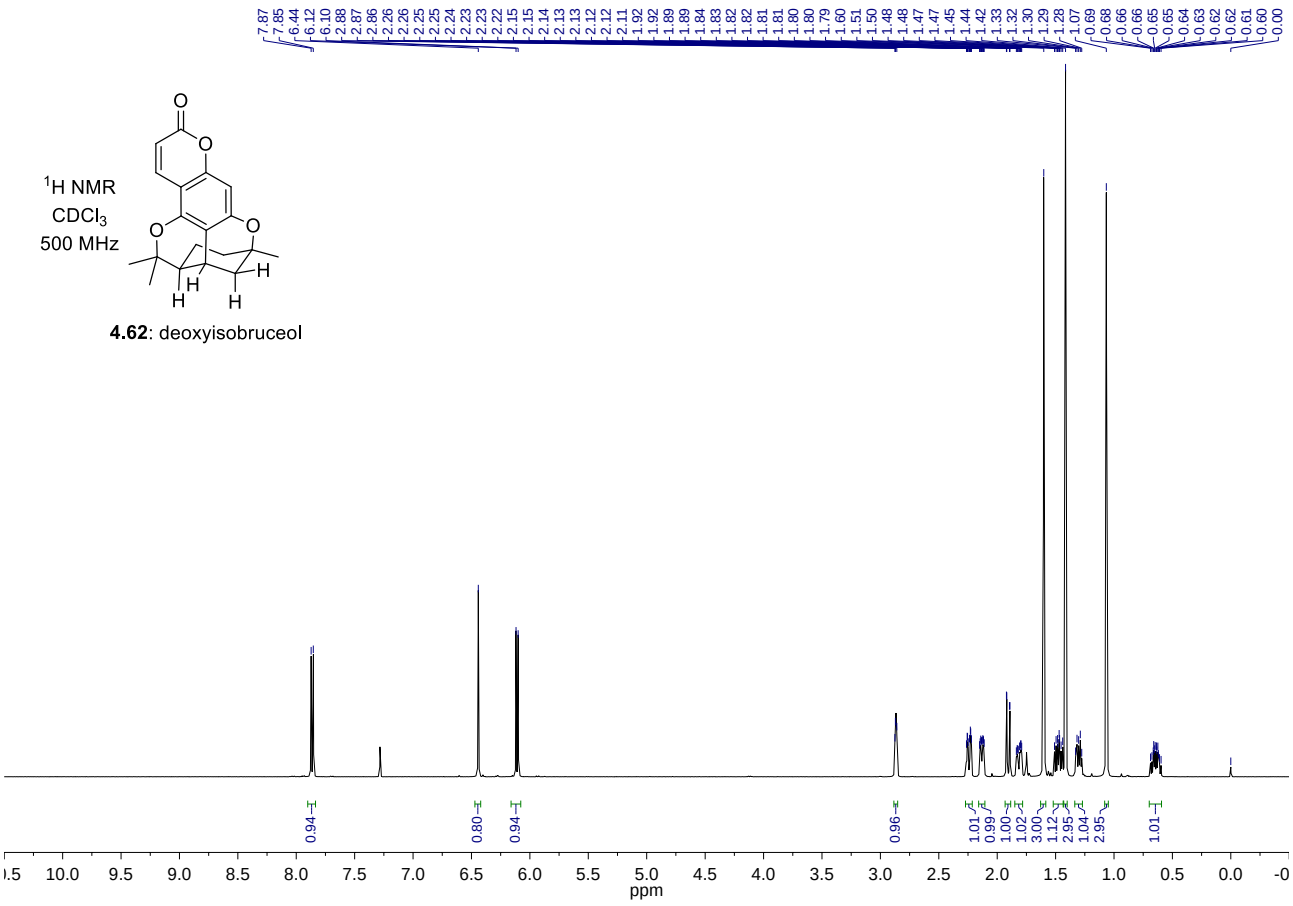
^{1}H NMR
$CDCl_3$
500 MHz
O
O
O
O
H
H
H
4.62: deoxyisobruceol
ppm

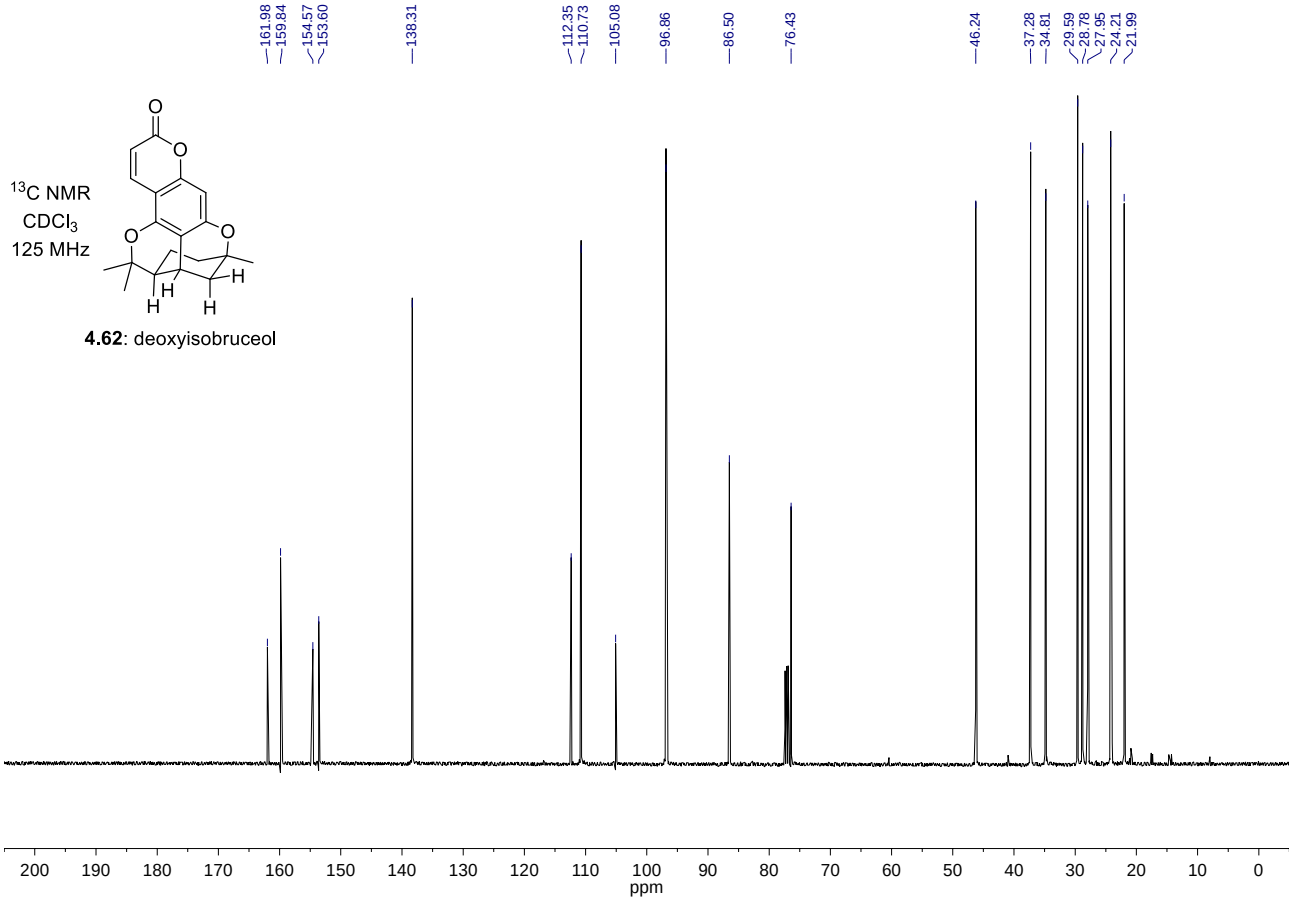
161.98
159.84
154.57
153.60
138.31
112.35
110.73
105.08
96.86
86.50
76.43
46.24
37.28
34.81
29.59
28.78
27.95
24.21
21.99
13C NMR
CDCl3
125 MHz
4.62: deoxyisobruceol
ppm

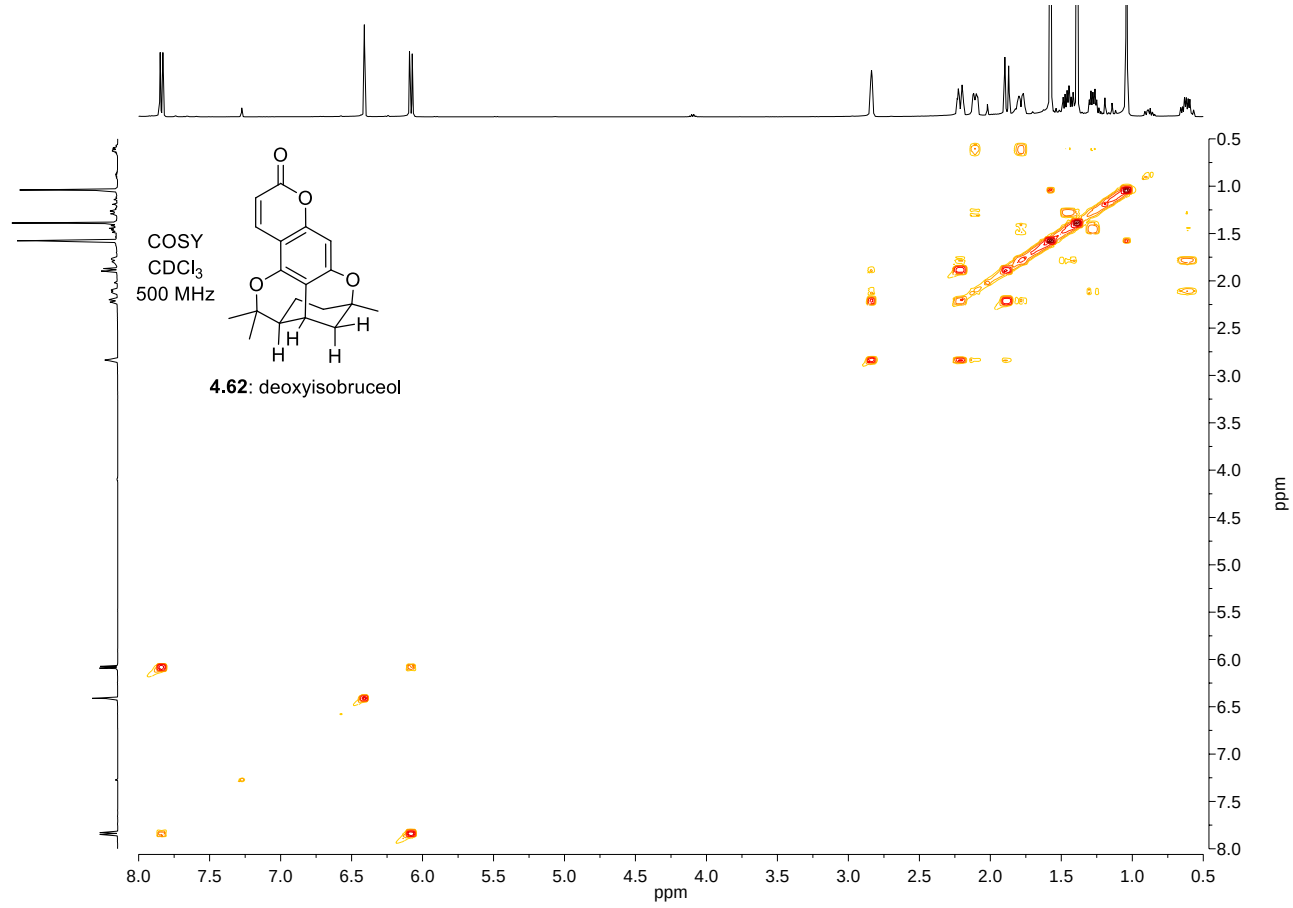
COSY
CDCl3
500 MHz
4.62: deoxyisobruceol
ppm
ppm

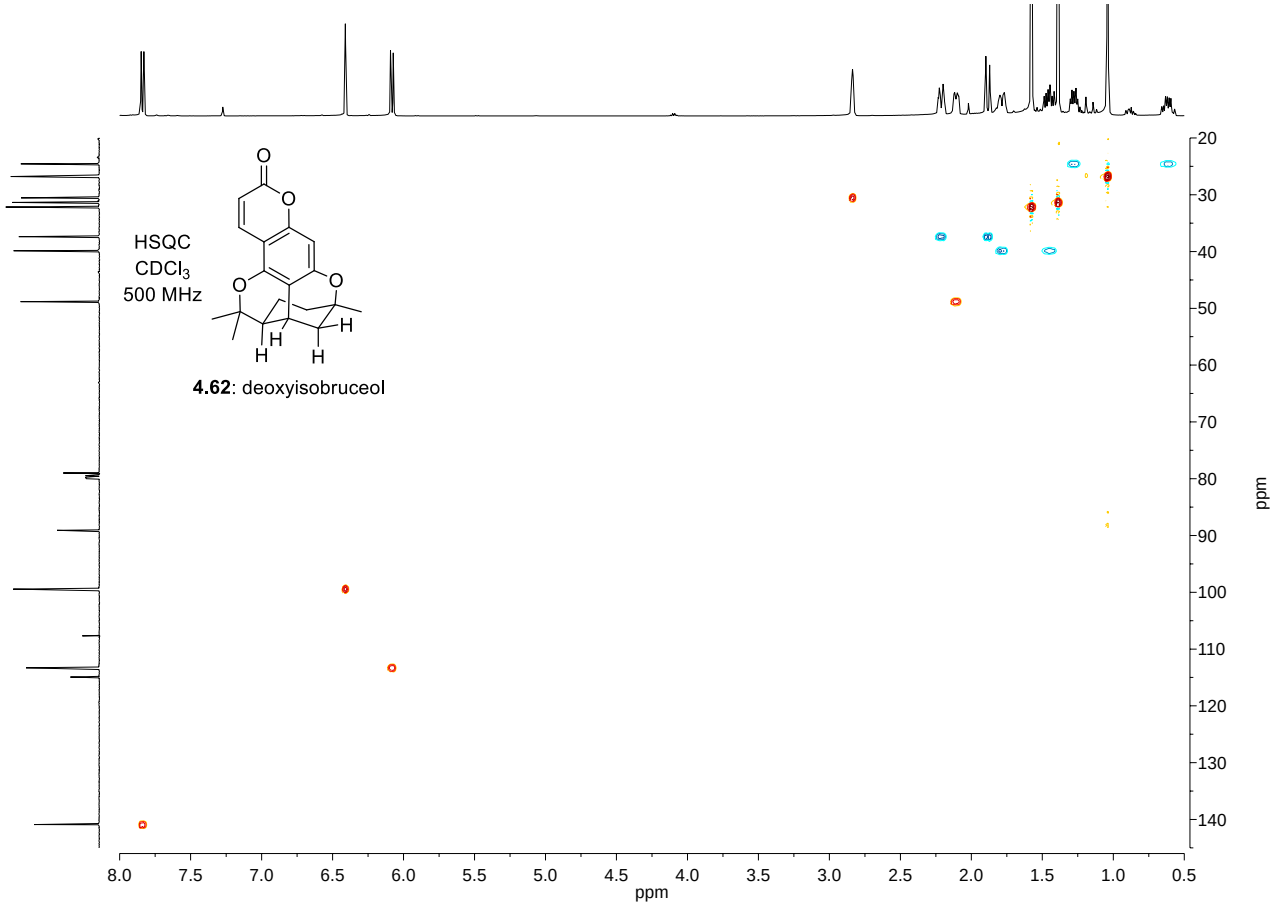
HSQC
CDCl3
500 MHz
4.62: deoxyisobruceol
ppm
ppm

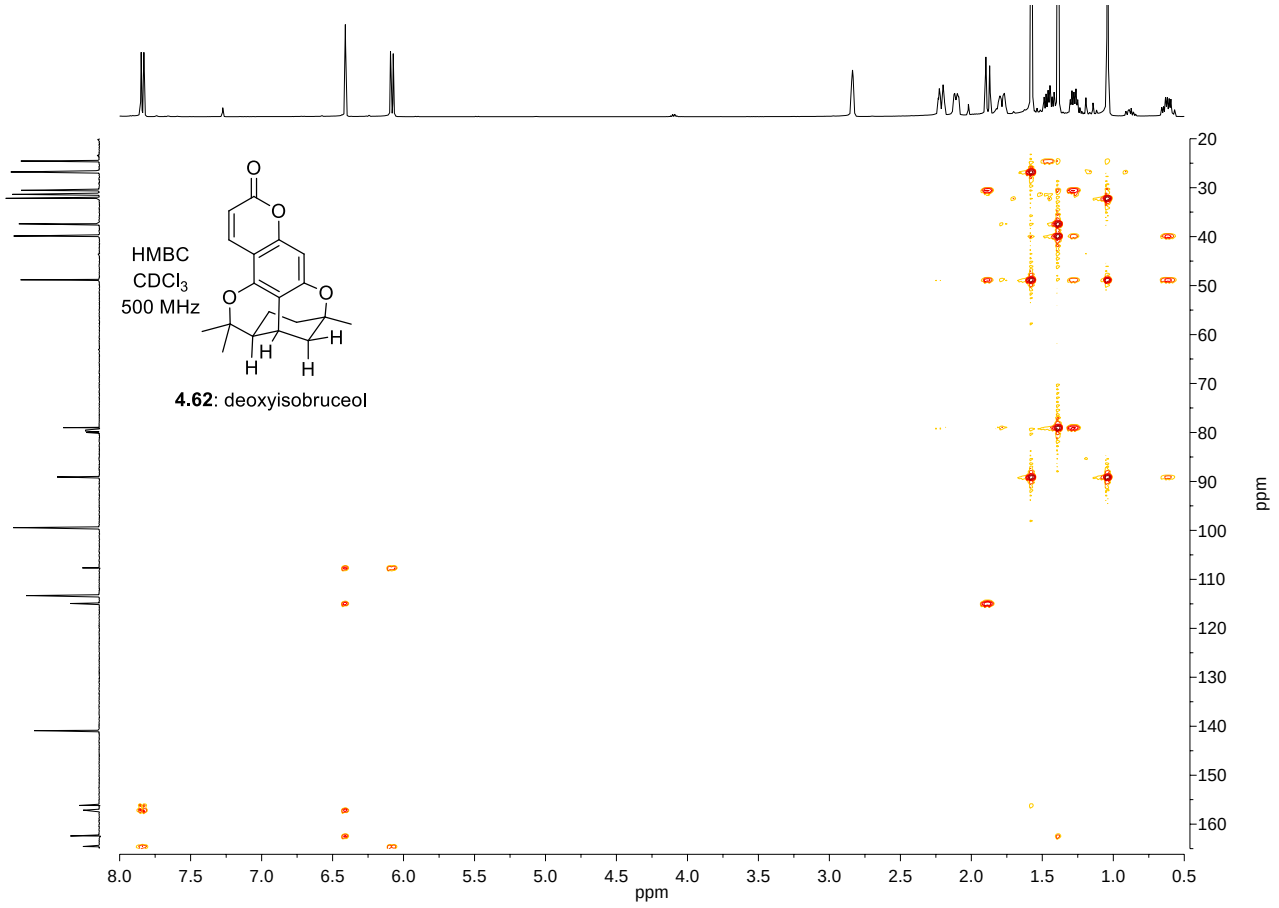
HMBC
CDCl3
500 MHz
4.62: deoxyisobruceol
ppm
ppm

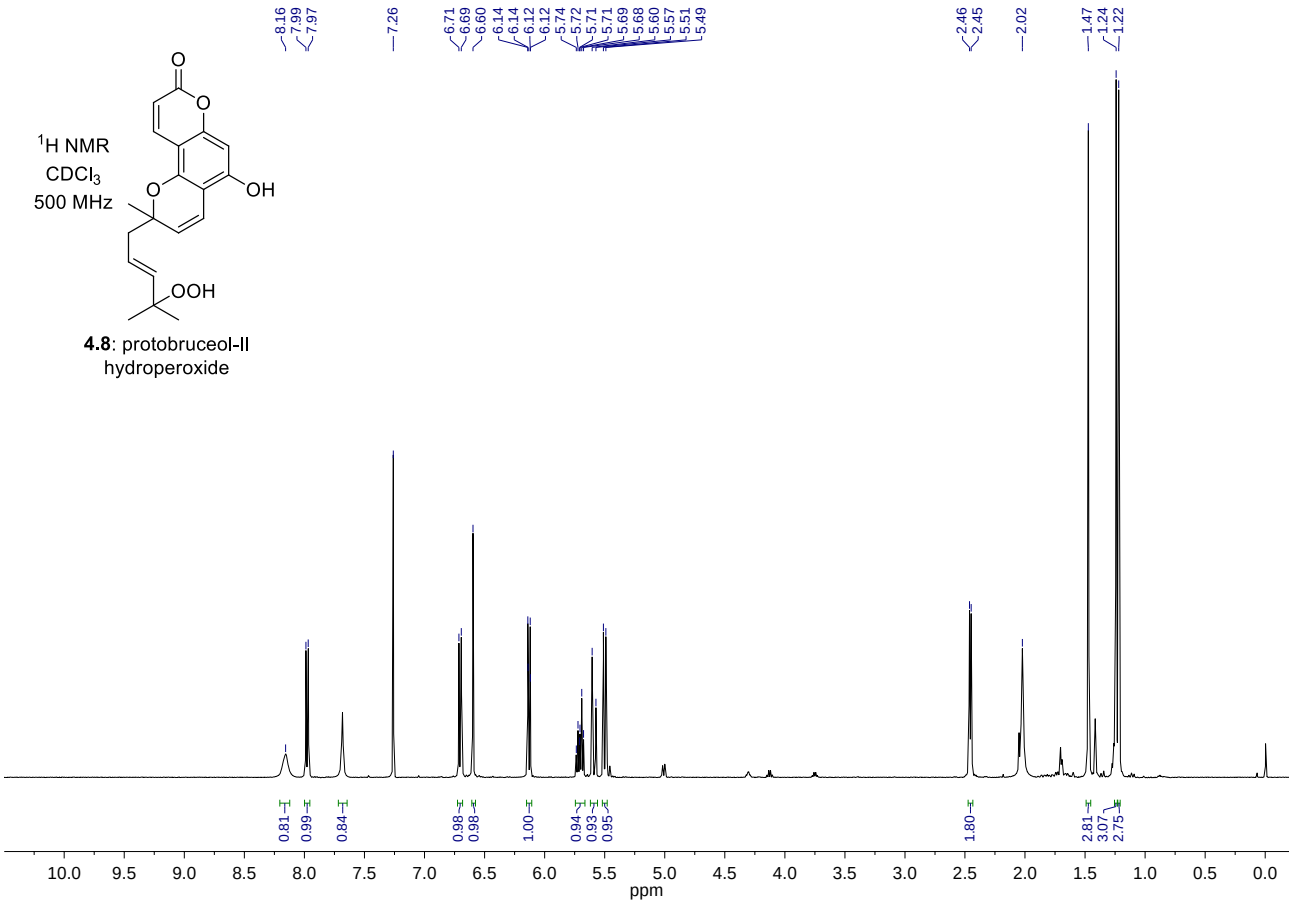

4.8: protobruceol-II hydroperoxide

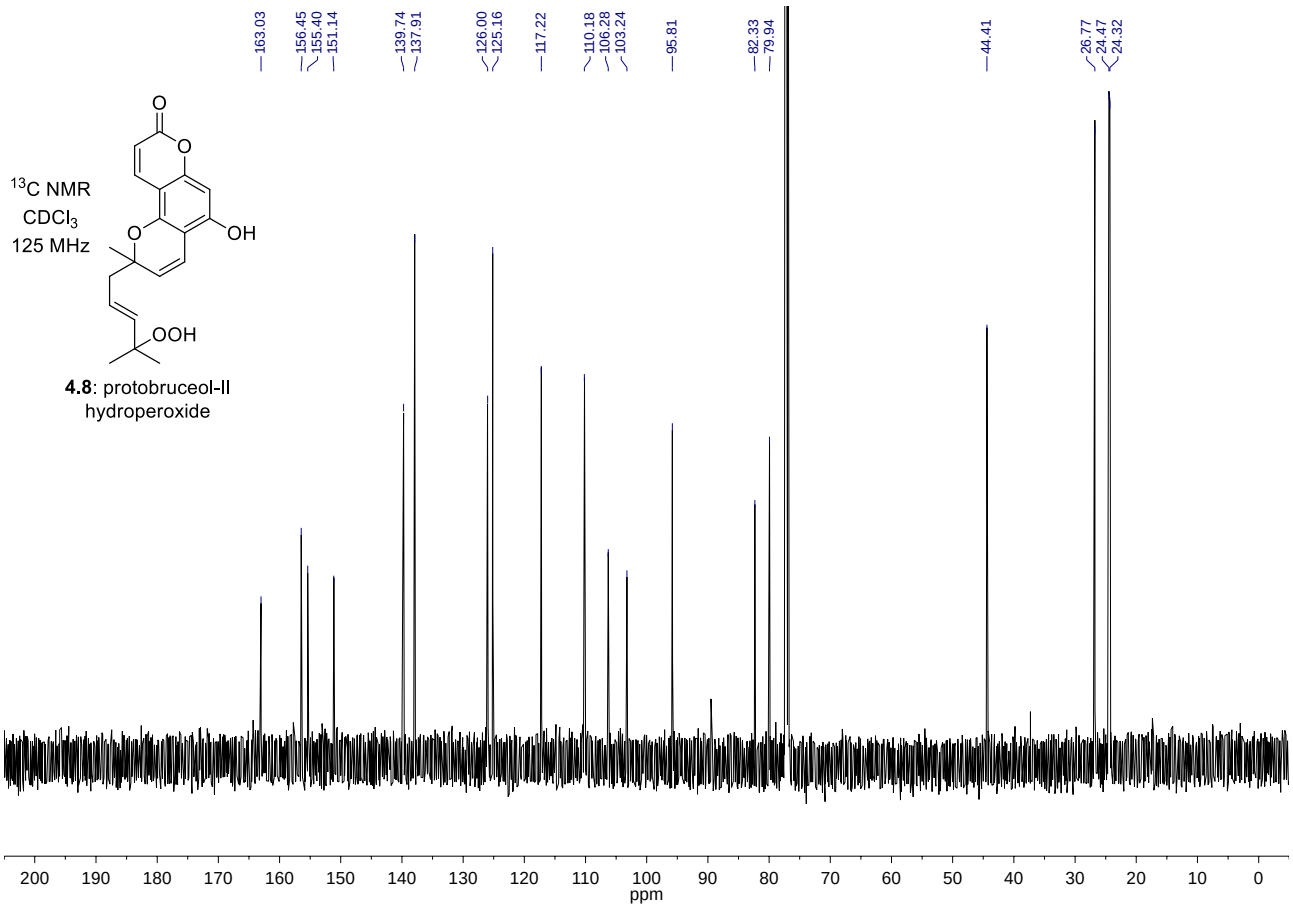

4.8: protobruceol-II hydroperoxide

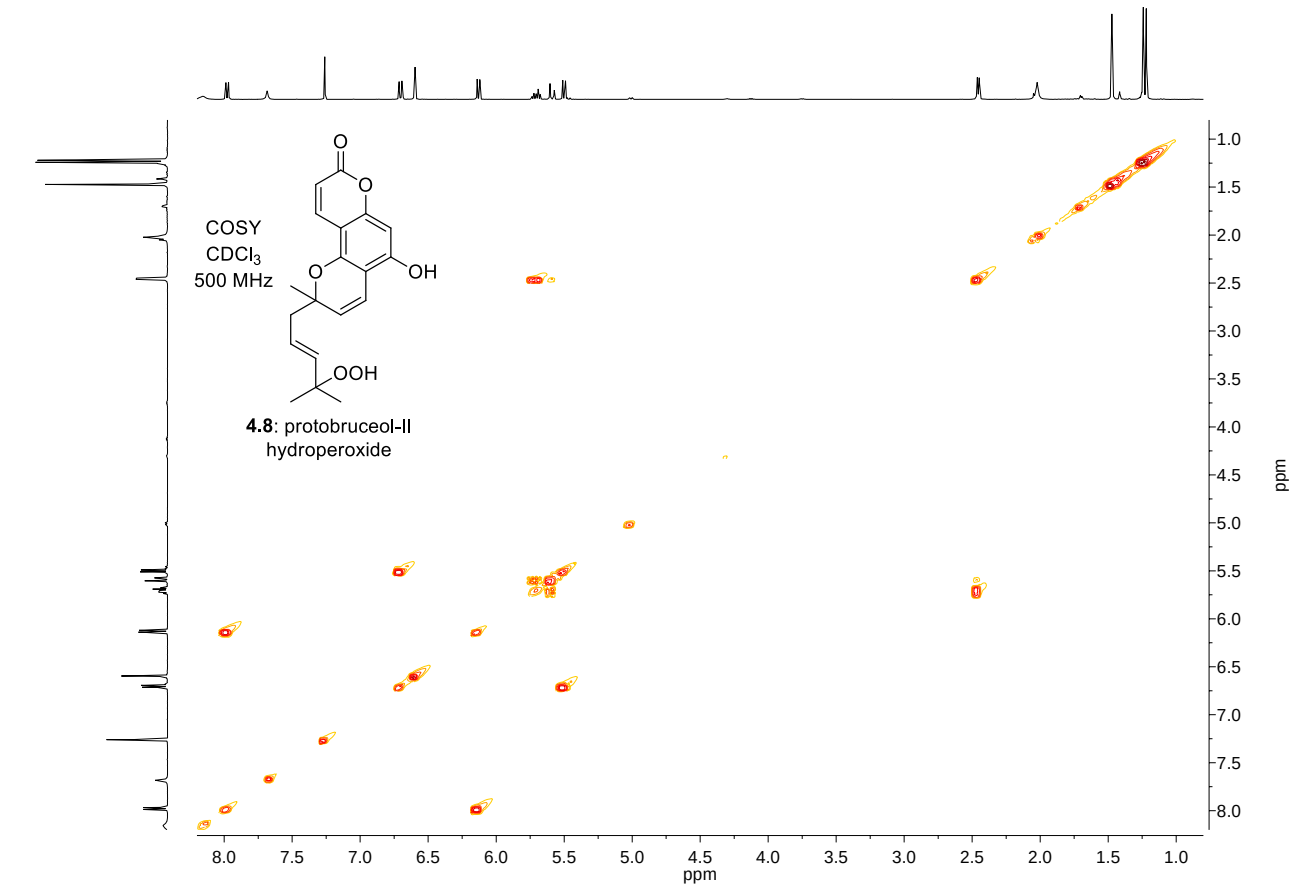
COSY
CDCl3
500 MHz
OH
OOH
4.8: protobruceol-II
hydroperoxide
ppm
ppm

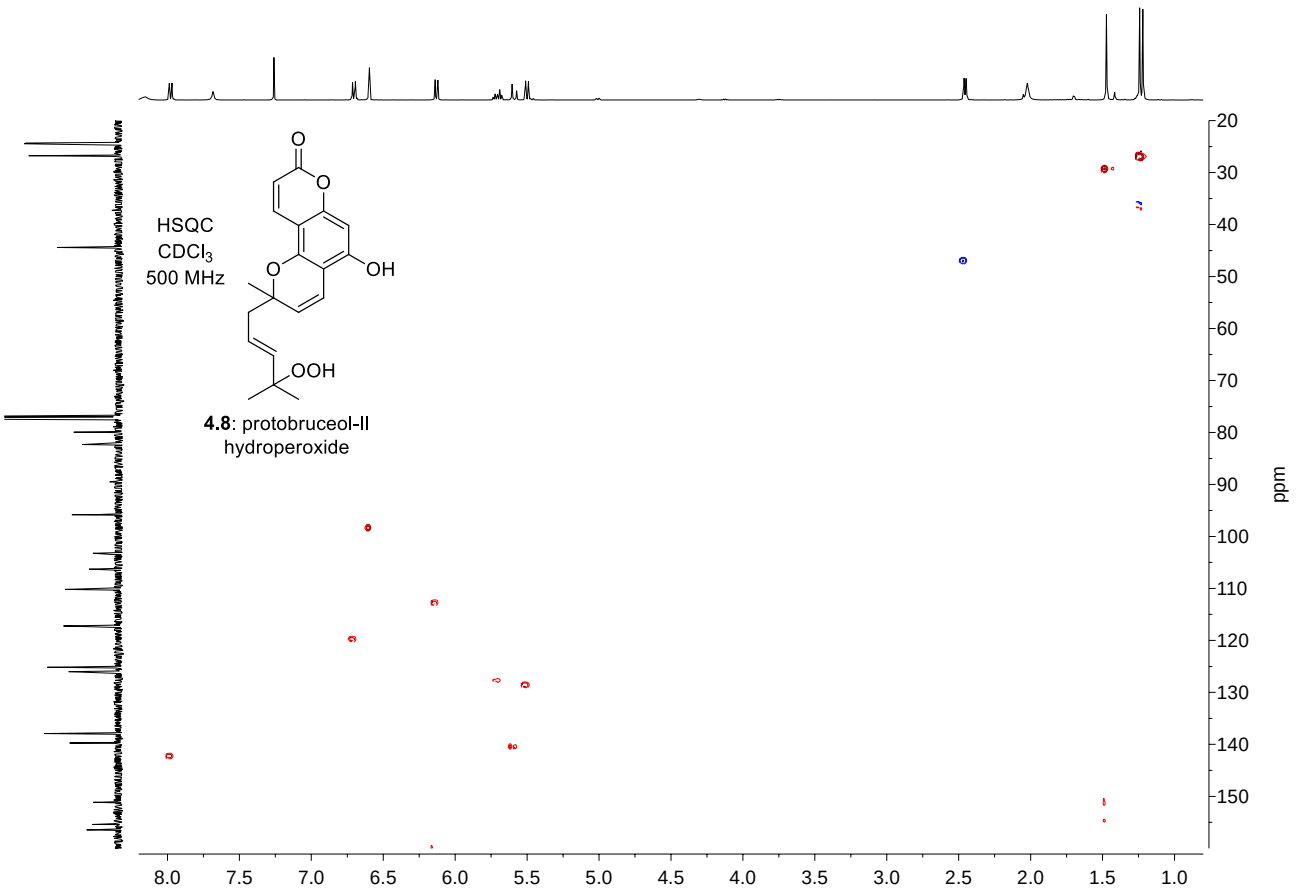
HSQC
CDCl3
500 MHz
OH
OOH
4.8: protobruceol-II
hydroperoxide
ppm
ppm

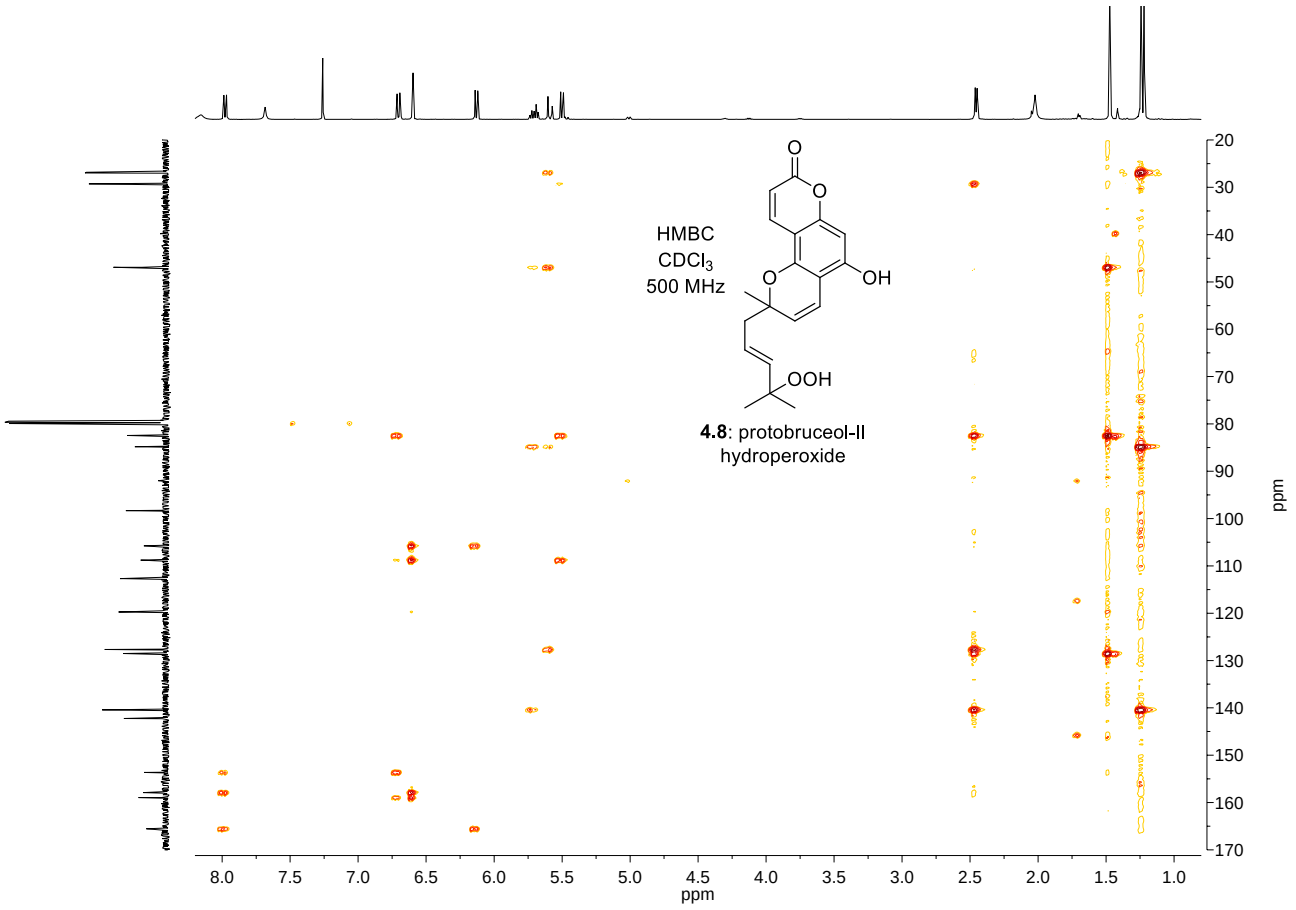

4.8: protobruceol-II hydroperoxide

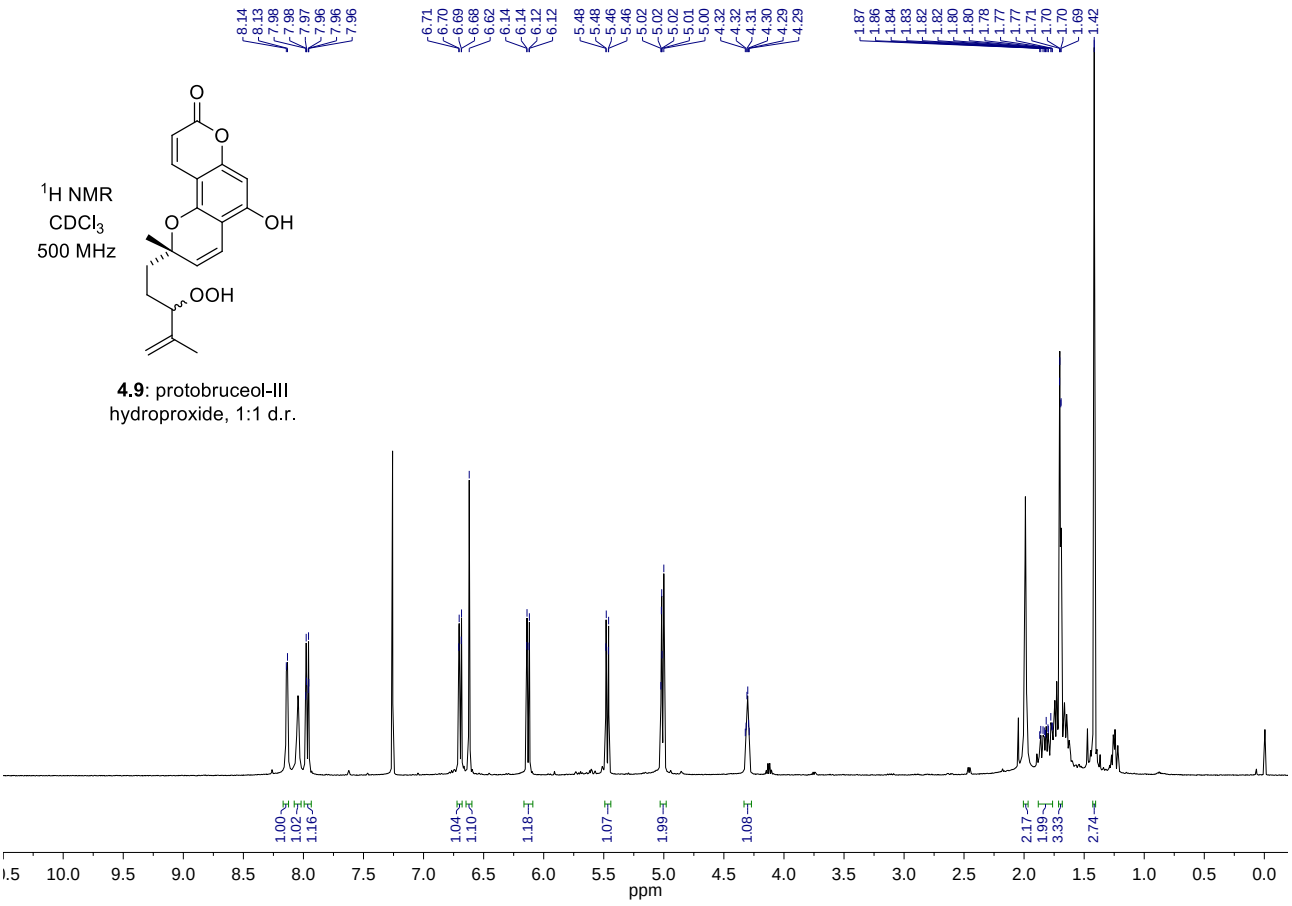

4.9: protobruceol-III hydroproxide, 1:1 d.r.

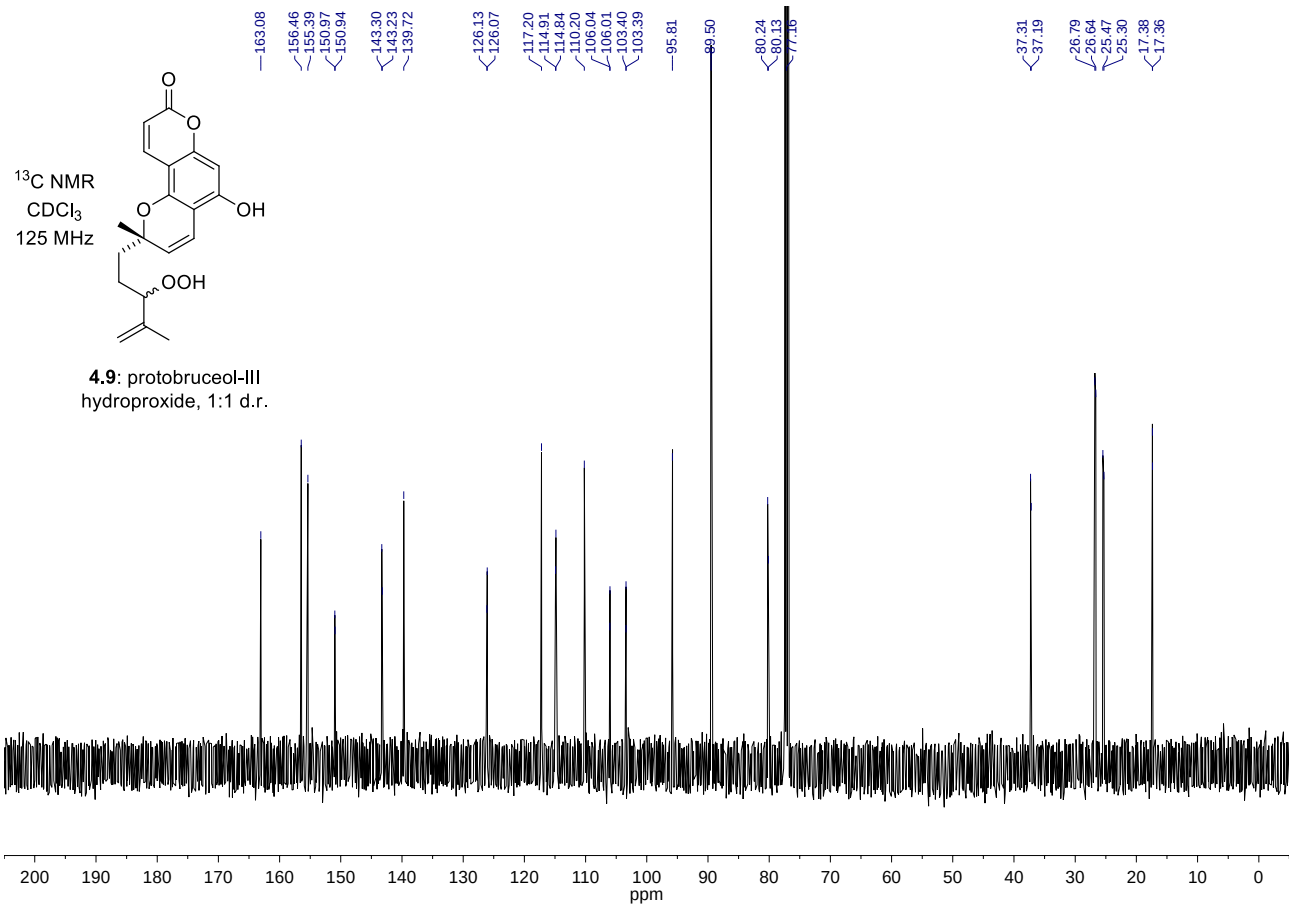
163.08
156.46
155.39
150.97
150.94
143.30
143.23
139.72
126.13
126.07
117.20
114.91
114.84
110.20
106.04
106.01
103.40
103.39
95.81
89.50
80.24
80.13
77.16
37.31
37.19
26.79
26.64
25.47
25.30
17.38
17.36
13C NMR
CDCl3
125 MHz
OH
OOH
4.9: protobruceol-III
hydroproxide, 1:1 d.r.
200 190 180 170 160 150 140 130 120 110 100 90 80 70 60 50 40 30 20 10 0
ppm

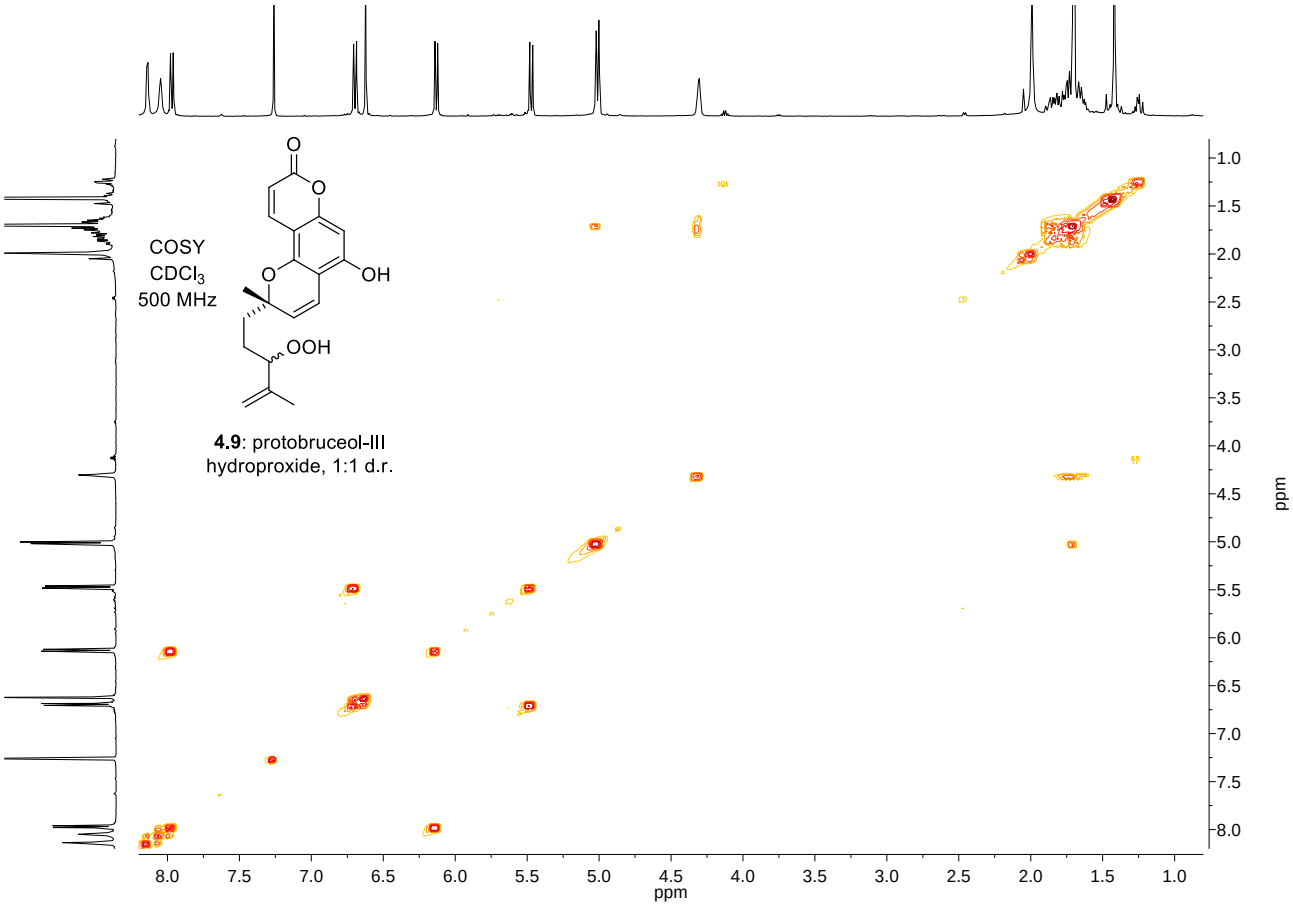
COSY
CDCl3
500 MHz
OH
OOH
4.9: protobruceol-III
hydroproxide, 1:1 d.r.
8.0 7.5 7.0 6.5 6.0 5.5 5.0 4.5 4.0 3.5 3.0 2.5 2.0 1.5 1.0
ppm
1.0 1.5 2.0 2.5 3.0 3.5 4.0 4.5 5.0 5.5 6.0 6.5 7.0 7.5 8.0
ppm

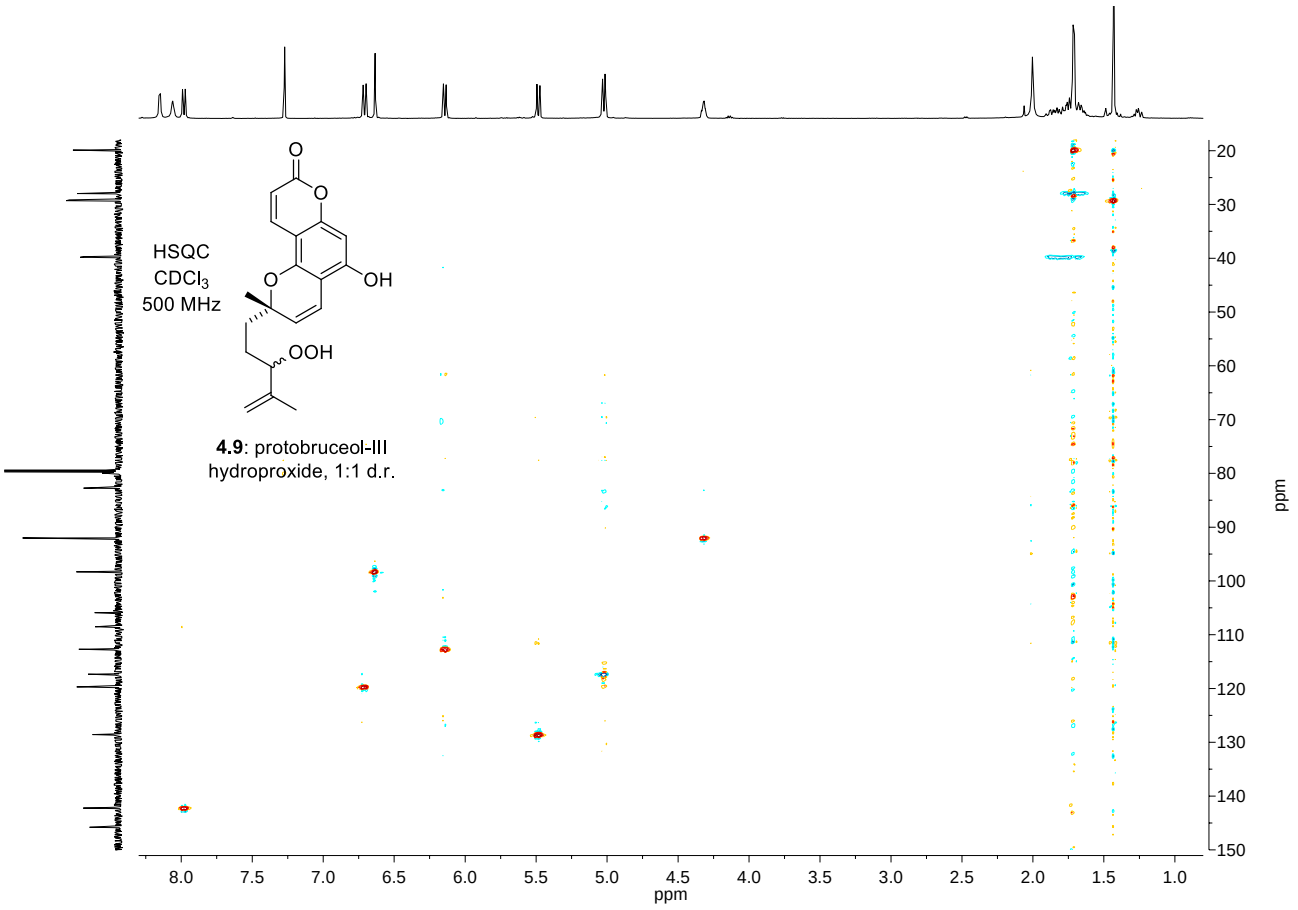
HSQC
CDCl3
500 MHz
OH
OOH
4.9: protobruceol-III
hydroproxide, 1:1 d.r.
ppm
ppm

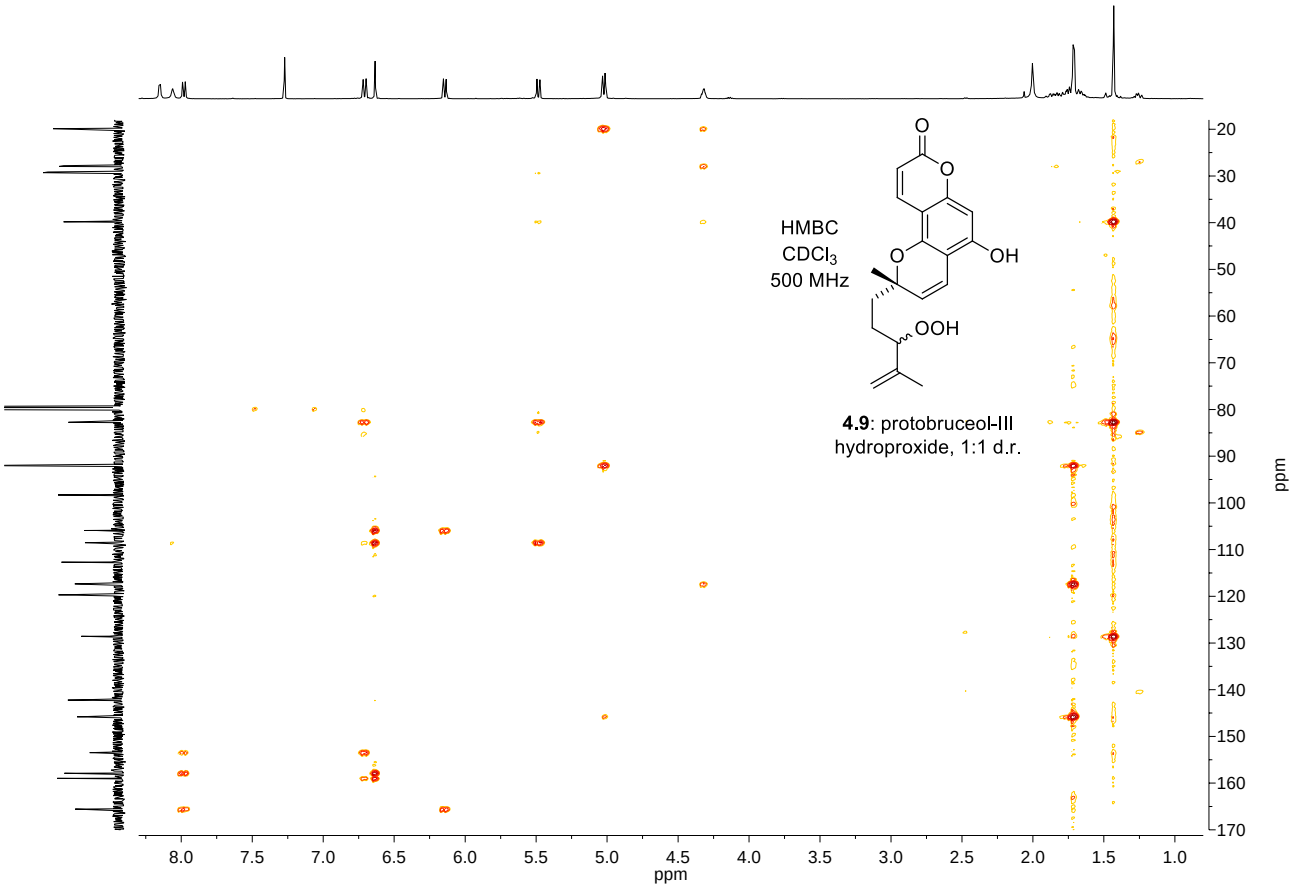
HMBC
CDCl3
500 MHz
OH
OOH
4.9: protobruceol-III
hydroproxide, 1:1 d.r.
ppm
ppm

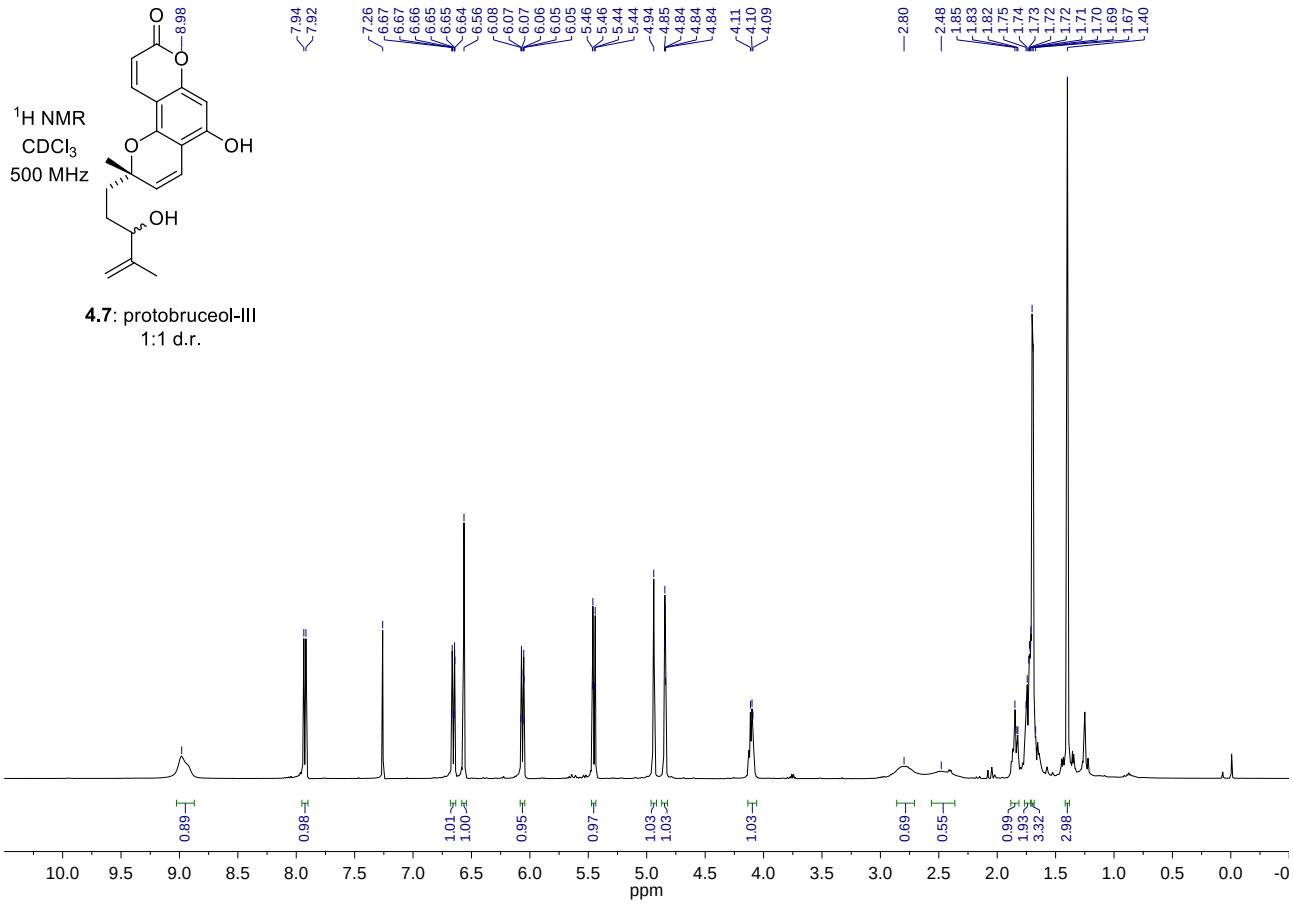
^{1}H NMR
$CDCl_3$
500 MHz
4.7: protobruceol-III
1:1 d.r.
ppm

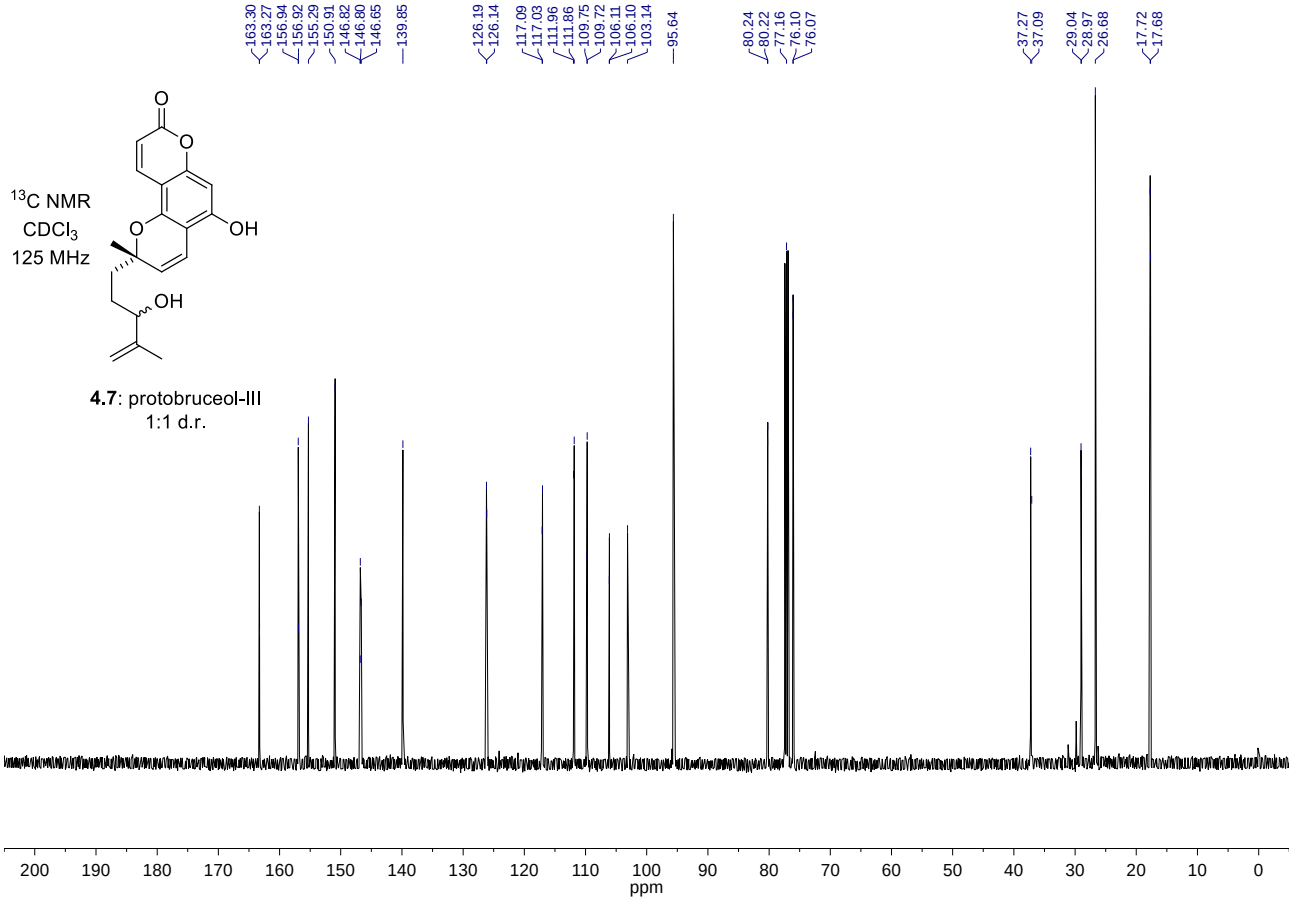
^{13}C NMR
$CDCl_3$
125 MHz
4.7: protobruceol-III
1:1 d.r.
ppm

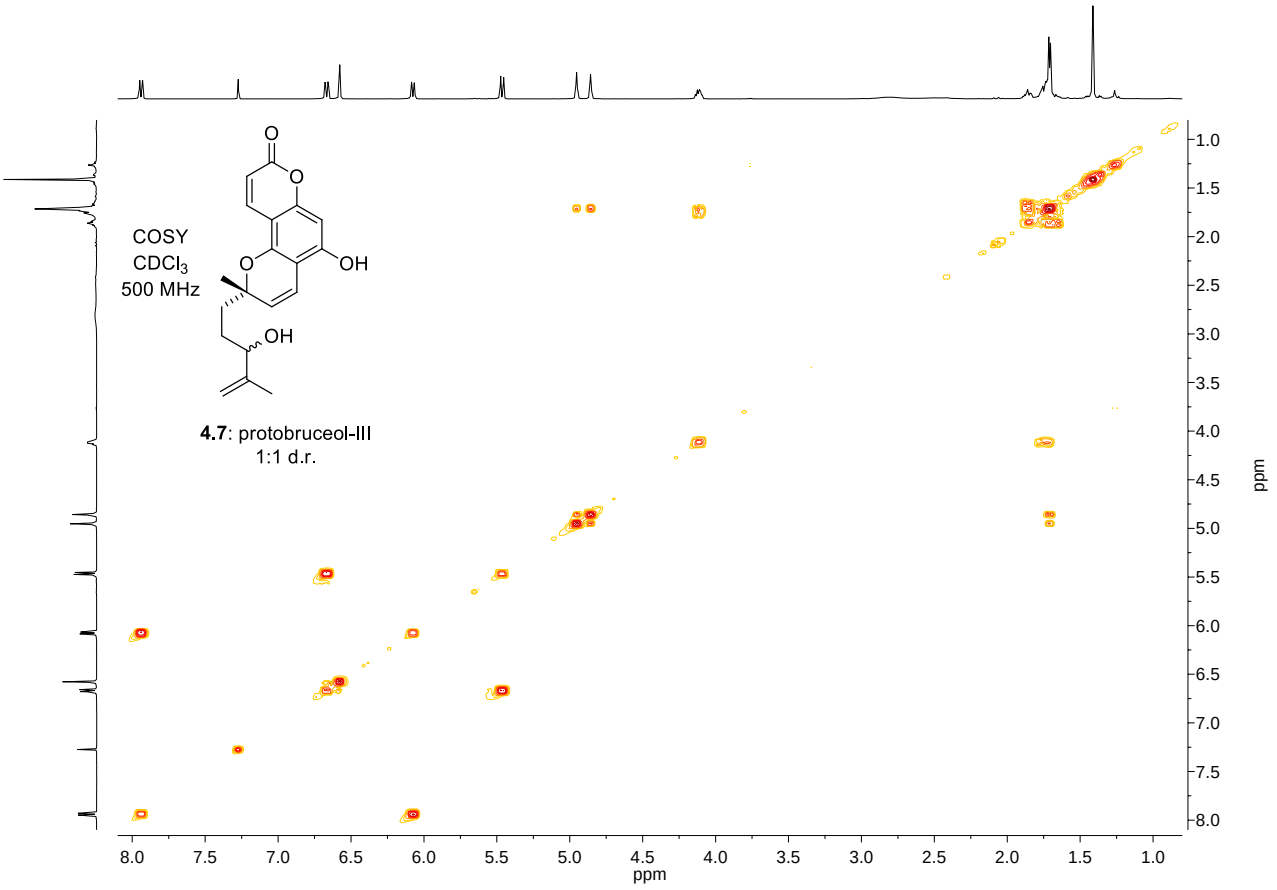
COSY
CDCl3
500 MHz
4.7: protobruceol-III
1:1 d.r.
OH
OH
ppm
ppm

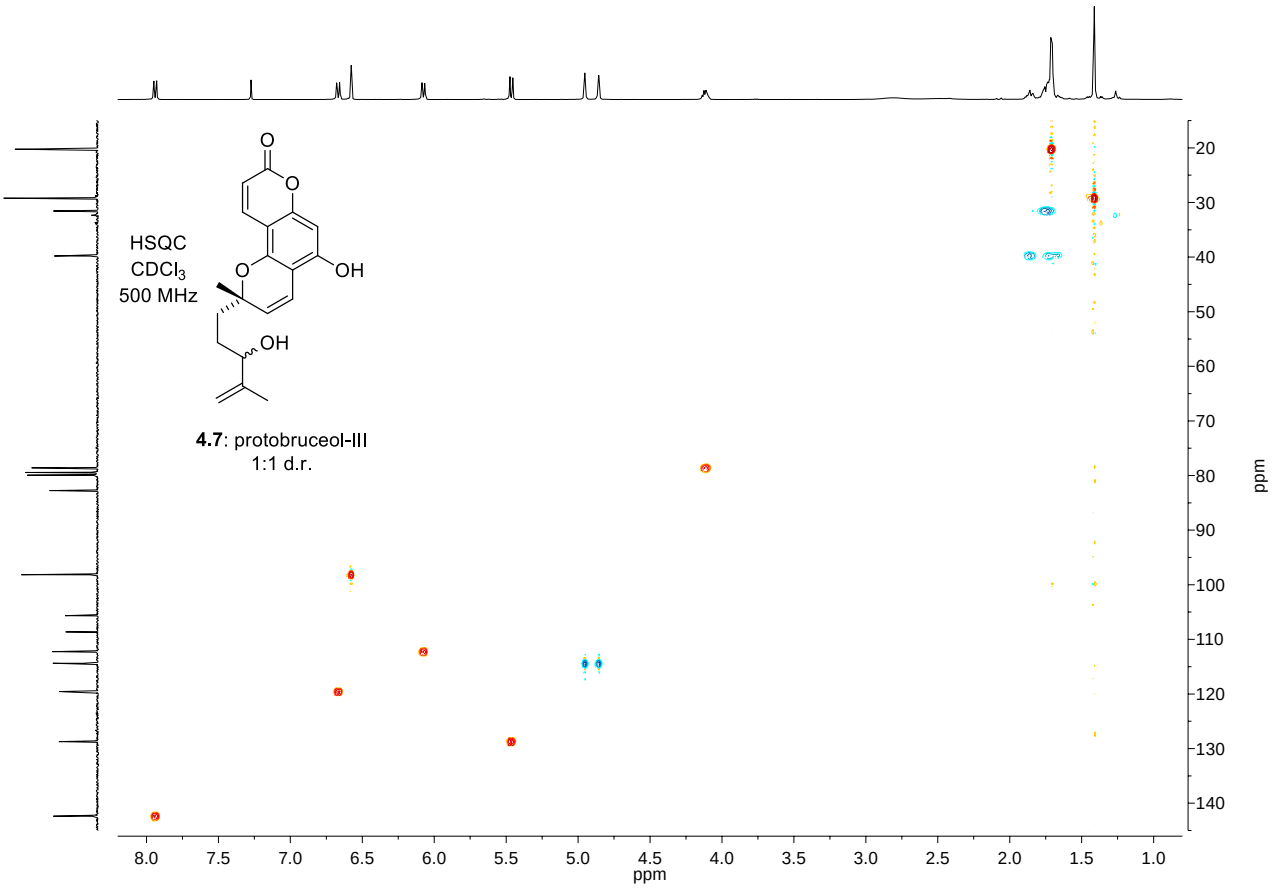
HSQC
CDCl3
500 MHz
4.7: protobruceol-III
1:1 d.r.
OH
OH
ppm
ppm

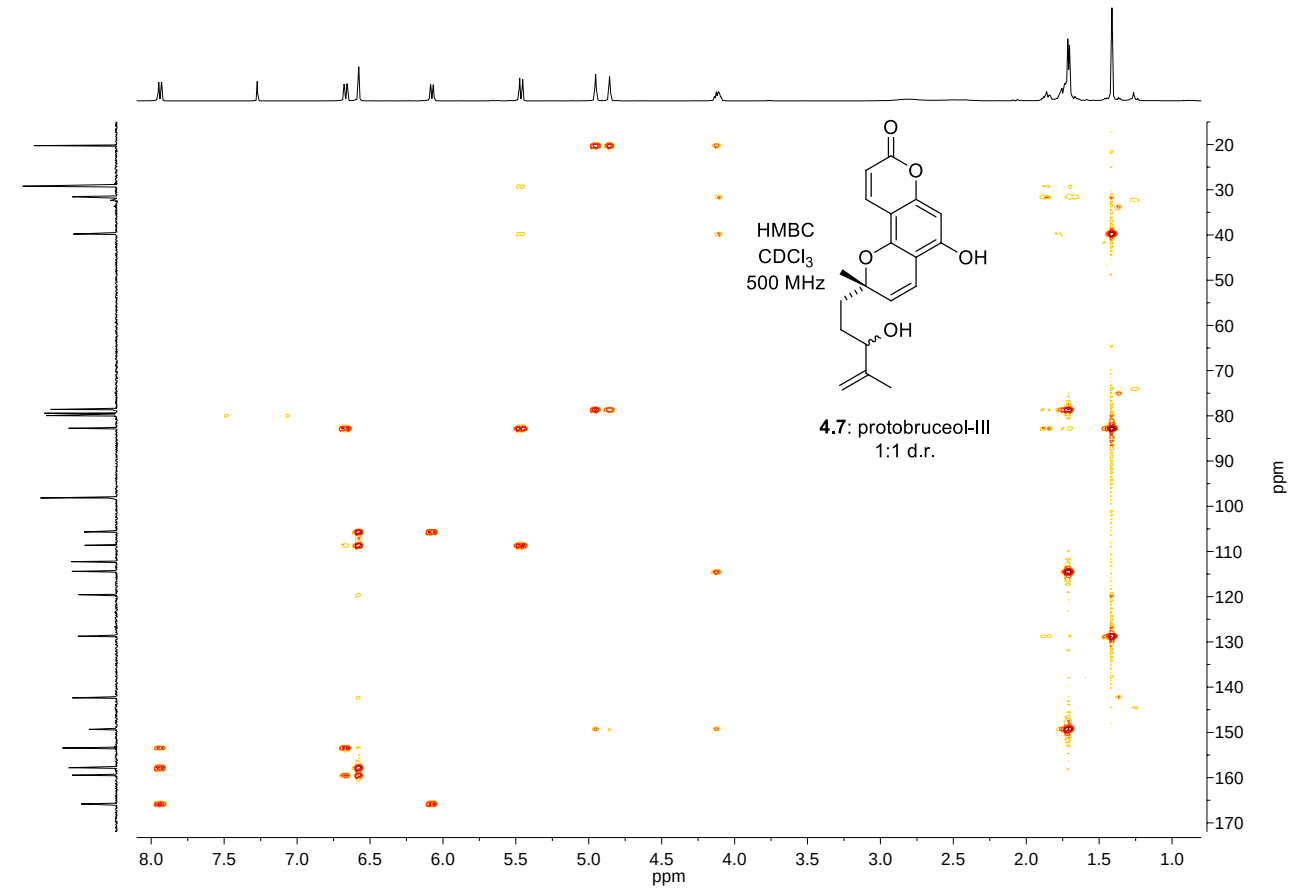
HMBC
CDCl3
500 MHz
OH
OH
4.7: protobruceol-III
1:1 d.r.
ppm
ppm

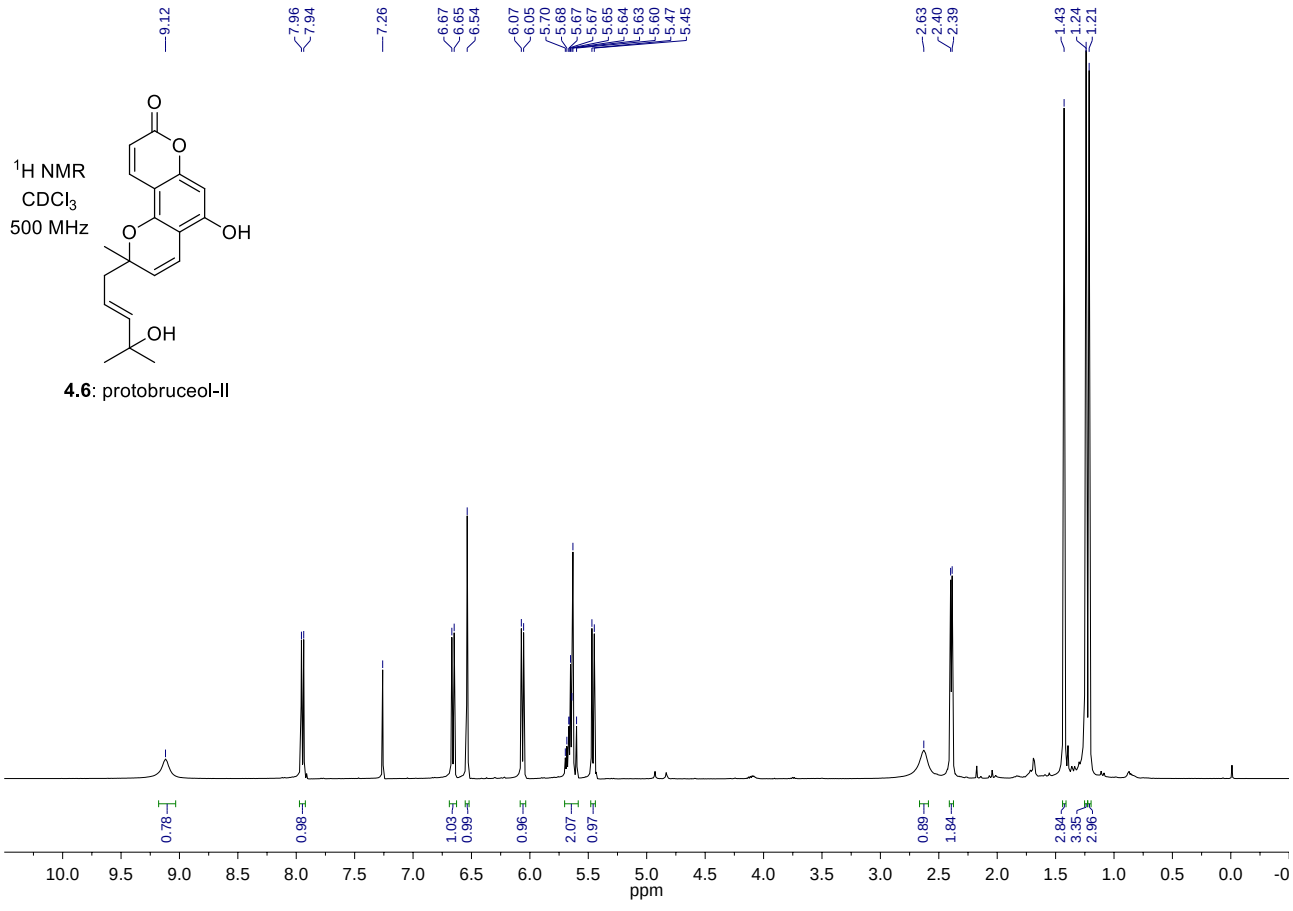
9.12
7.96
7.94
7.26
6.67
6.65
6.54
6.07
6.05
5.70
5.68
5.67
5.67
5.65
5.64
5.63
5.60
5.47
5.45
2.63
2.40
2.39
1.43
1.24
1.21
1H NMR
CDCl3
500 MHz
OH
OH
4.6: protobruceol-II
0.78
0.98
1.03
0.99
0.96
2.07
0.97
0.89
1.84
2.84
3.35
2.96
ppm

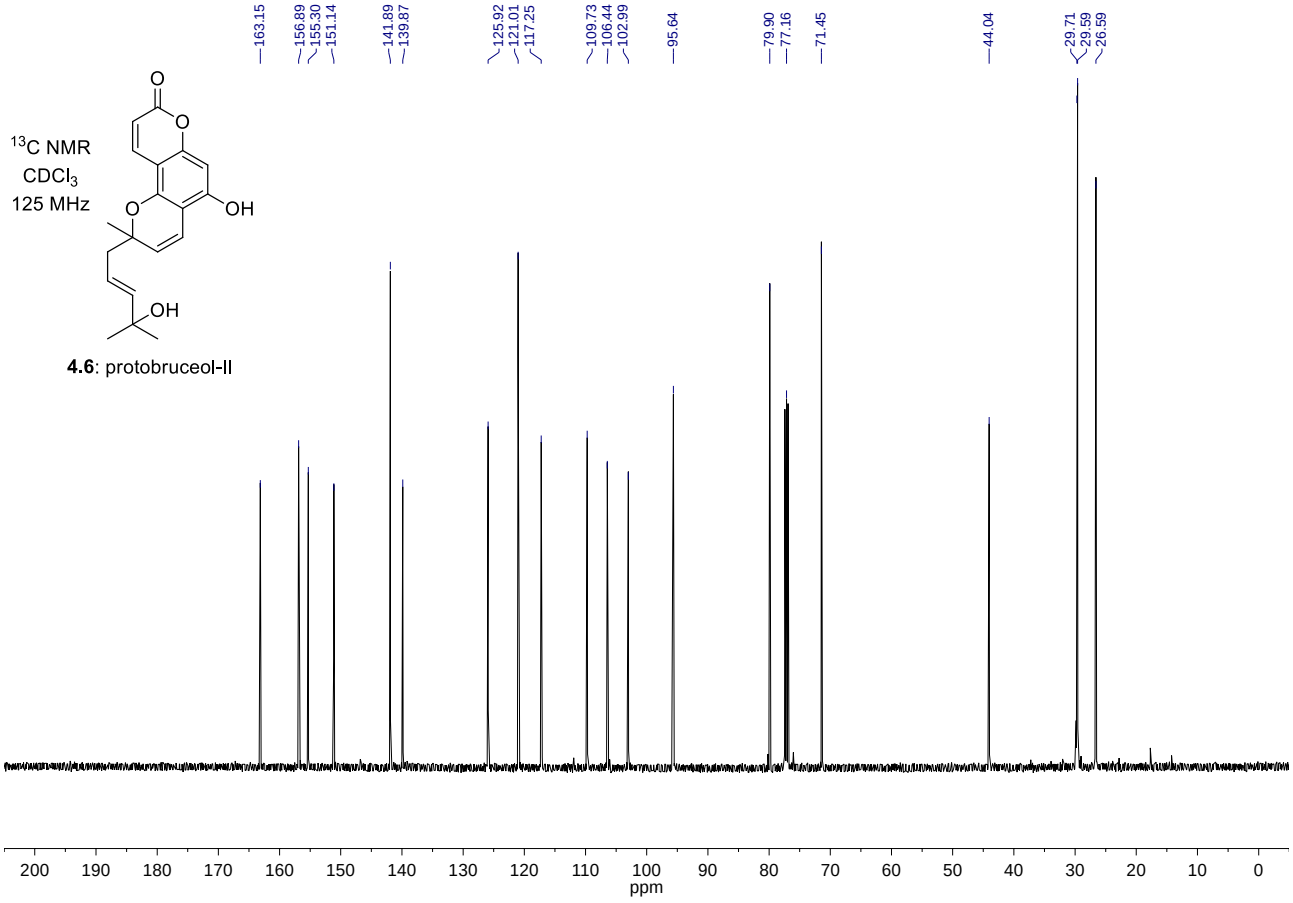
163.15
156.89
155.30
151.14
141.89
139.87
125.92
121.01
117.25
109.73
106.44
102.99
95.64
79.90
77.16
71.45
44.04
29.71
29.59
26.59
13C NMR
CDCl3
125 MHz
OH
OH
4.6: protobruceol-II
200 190 180 170 160 150 140 130 120 110 100 90 80 70 60 50 40 30 20 10 0
ppm

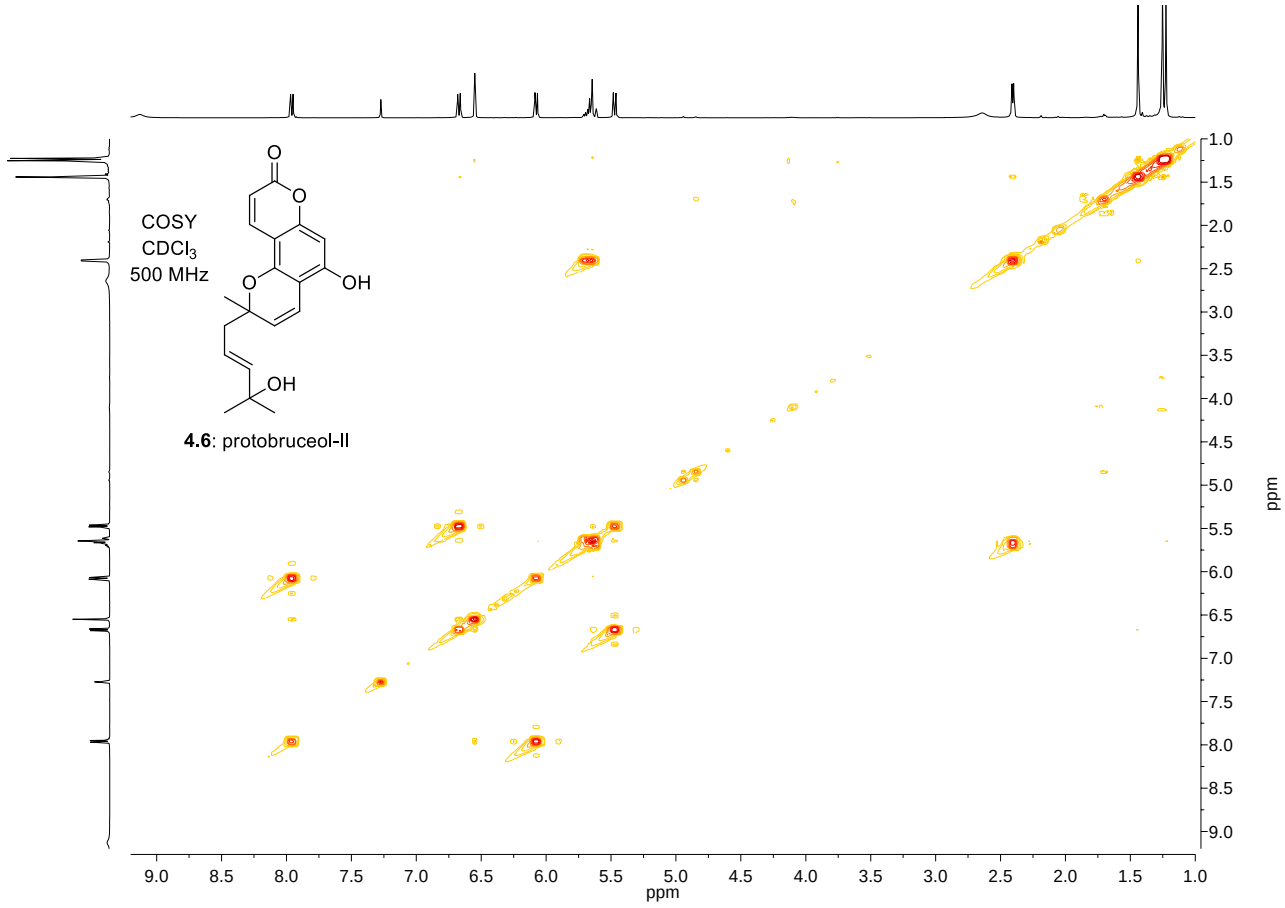
COSY
CDCl3
500 MHz
OH
OH
4.6: protobruceol-II
9.0 8.5 8.0 7.5 7.0 6.5 6.0 5.5 5.0 4.5 4.0 3.5 3.0 2.5 2.0 1.5 1.0
ppm
1.0 1.5 2.0 2.5 3.0 3.5 4.0 4.5 5.0 5.5 6.0 6.5 7.0 7.5 8.0 8.5 9.0
ppm

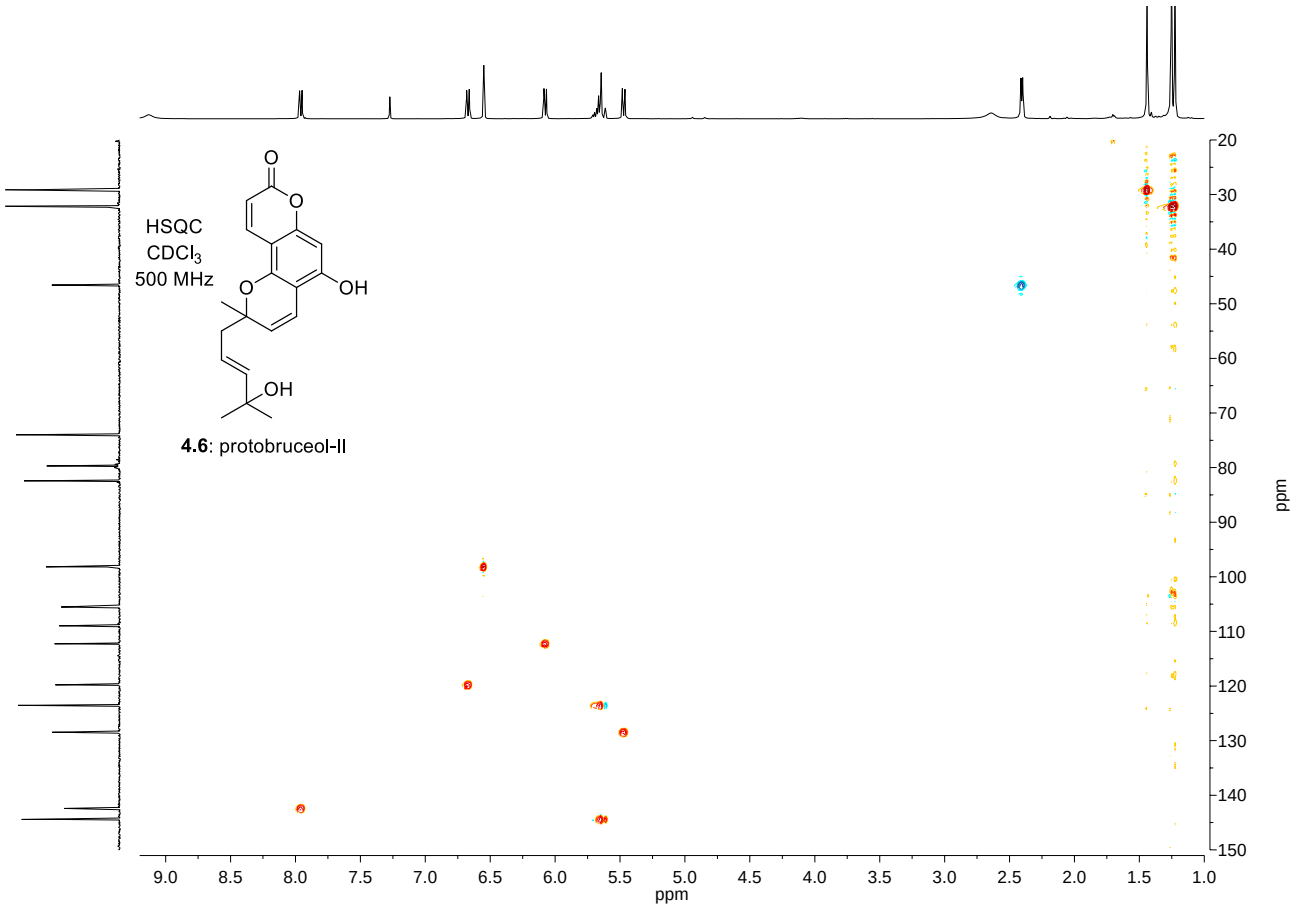
HSQC
CDCl3
500 MHz
OH
OH
4.6: protobruceol-II
ppm
ppm

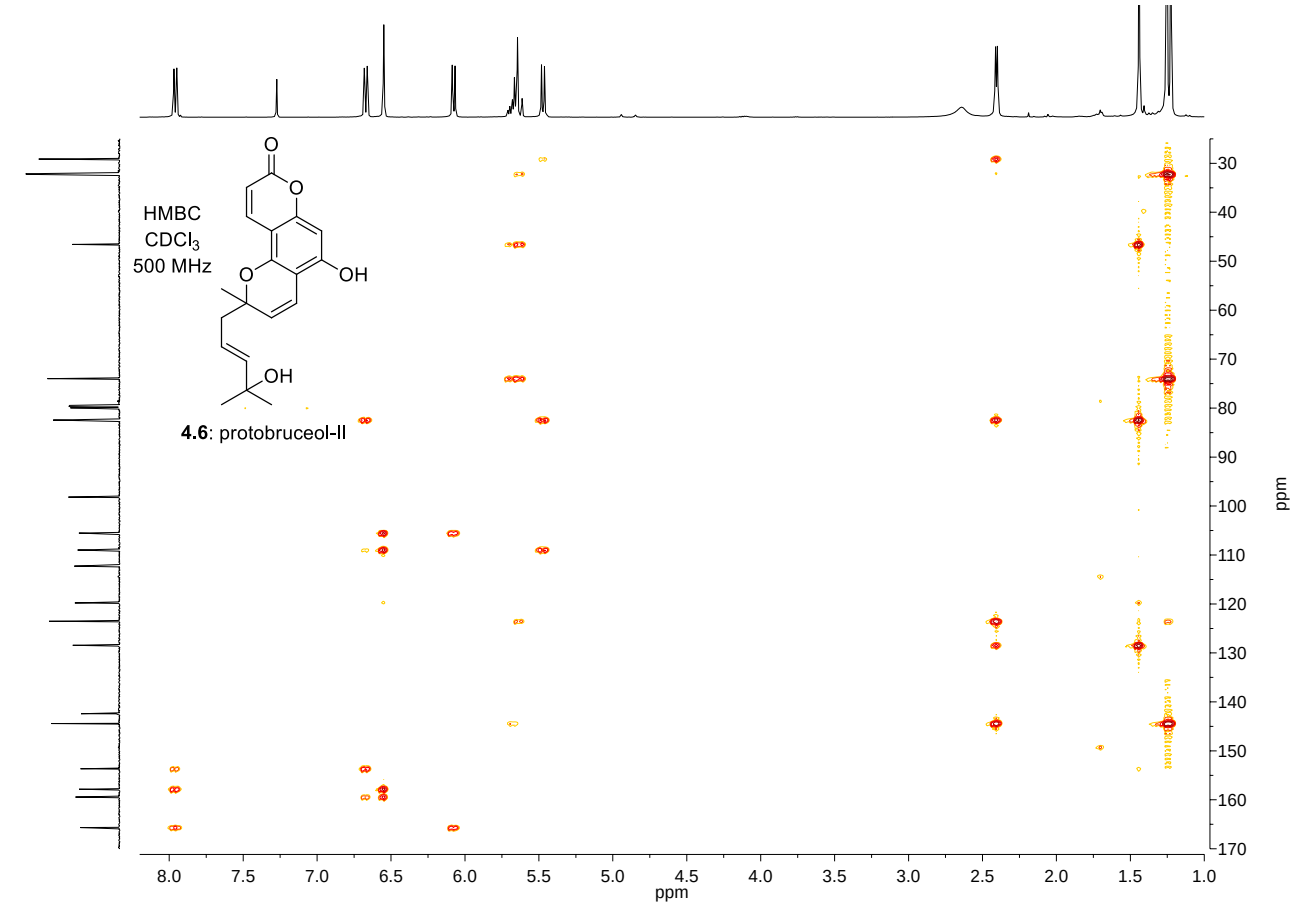
HMBC
CDCl3
500 MHz
OH
OH
4.6: protobruceol-II
ppm
ppm

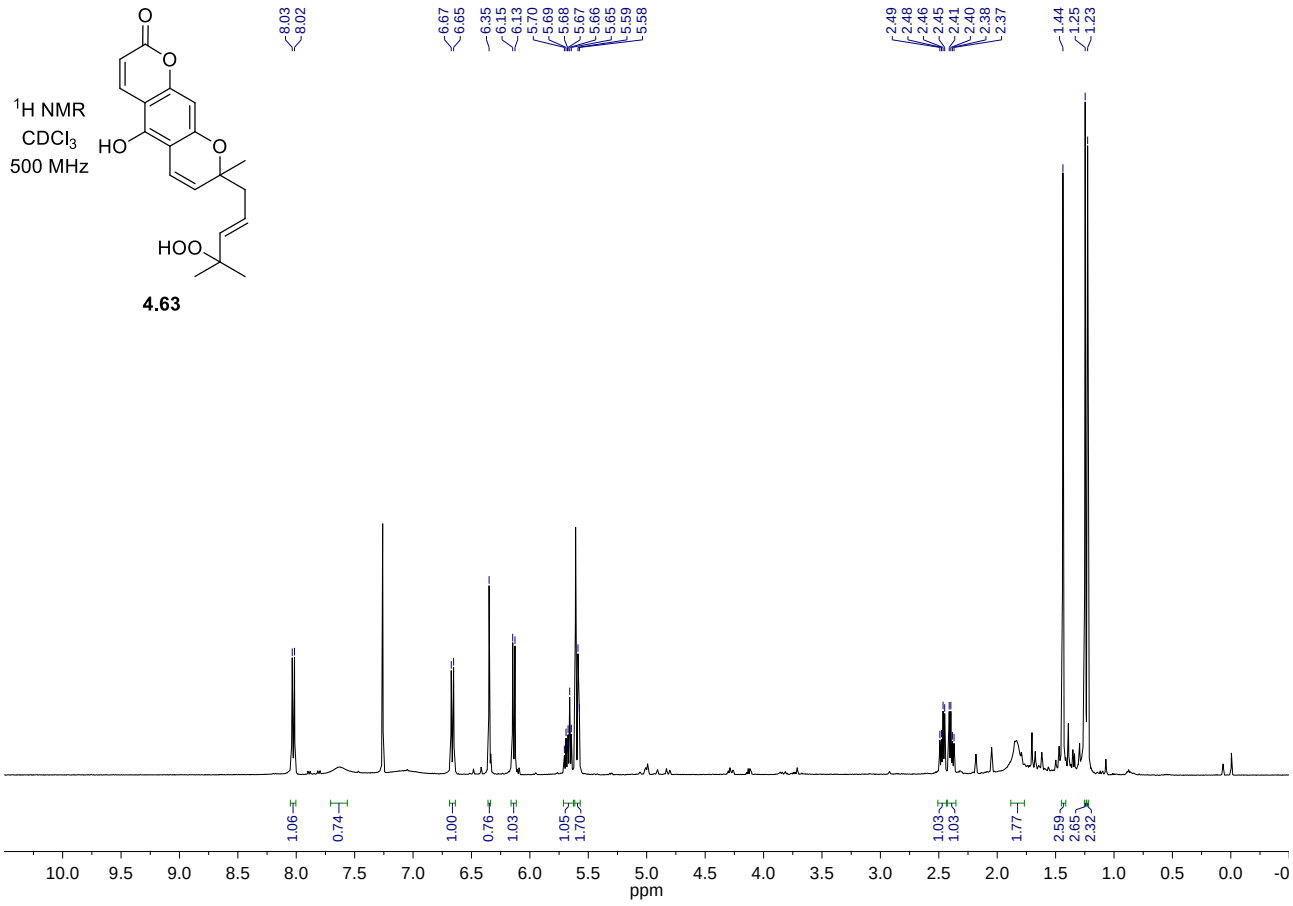
^{1}H NMR
$CDCl_3$
500 MHz
HO
O
HOO
4.63
8.03
8.02
6.67
6.65
6.35
6.15
6.13
5.70
5.69
5.68
5.67
5.66
5.65
5.59
5.58
2.49
2.48
2.46
2.45
2.41
2.40
2.38
2.37
1.44
1.25
1.23
1.06
0.74
1.00
0.76
1.03
1.05
1.70
1.03
1.03
1.77
2.59
2.65
2.32
ppm

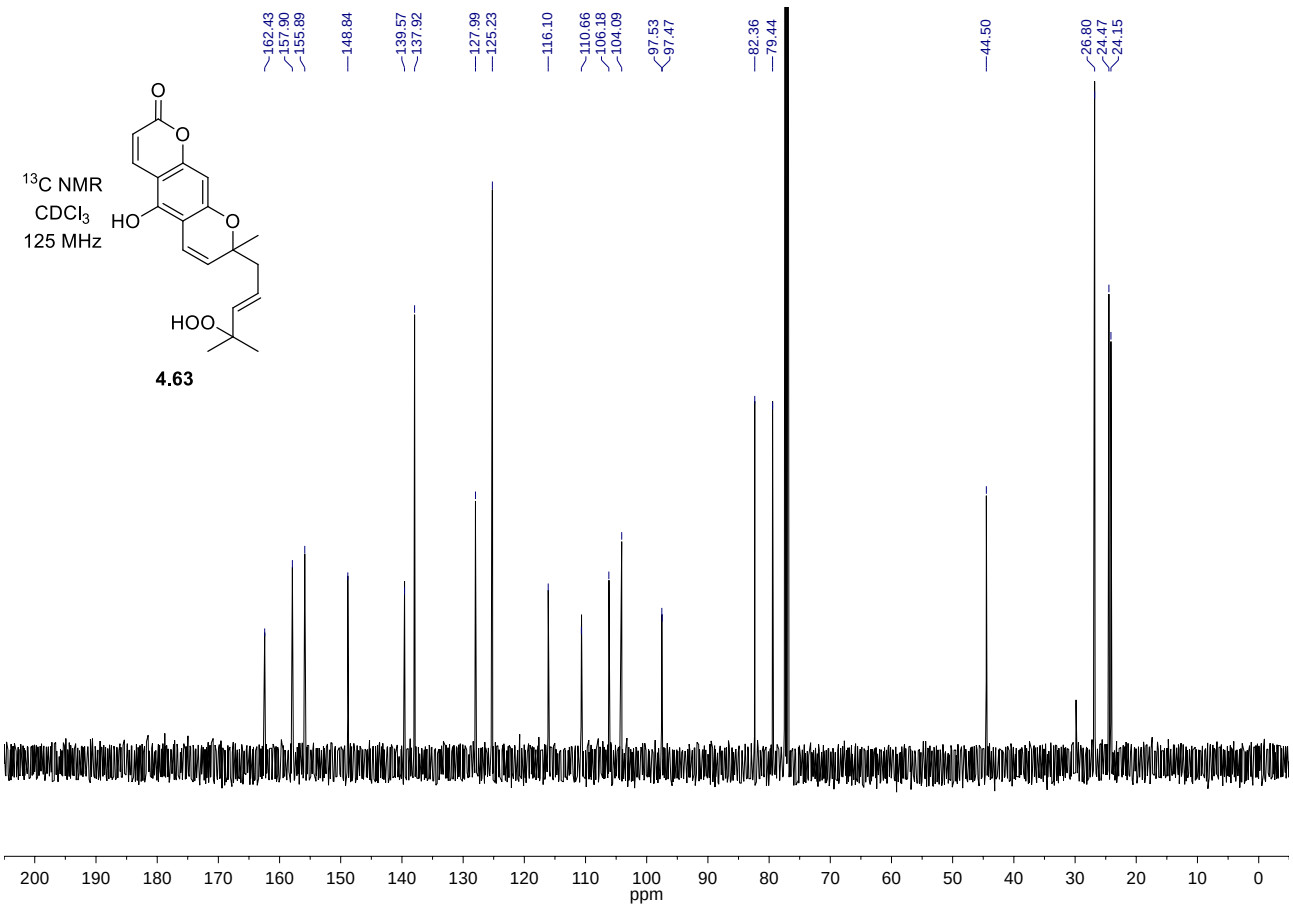
^{13}C NMR
$CDCl_3$
125 MHz
HO
O
HOO
4.63
162.43
157.90
155.89
148.84
139.57
137.92
127.99
125.23
116.10
110.66
106.18
104.09
97.53
97.47
82.36
79.44
44.50
26.80
24.47
24.15
ppm

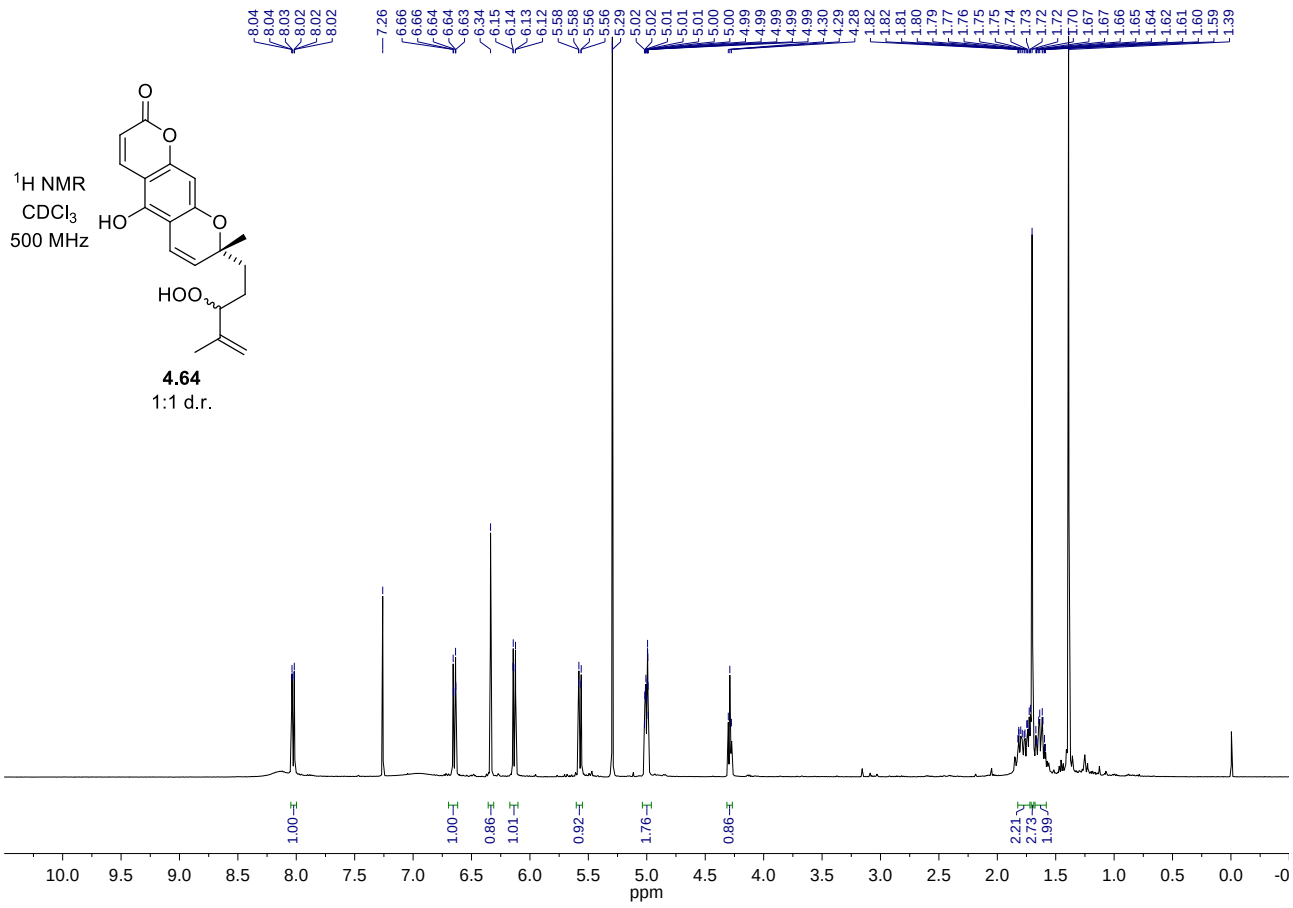
^{1}H NMR
$CDCl_3$
500 MHz
HO
O
HOO
4.64
1:1 d.r.
ppm

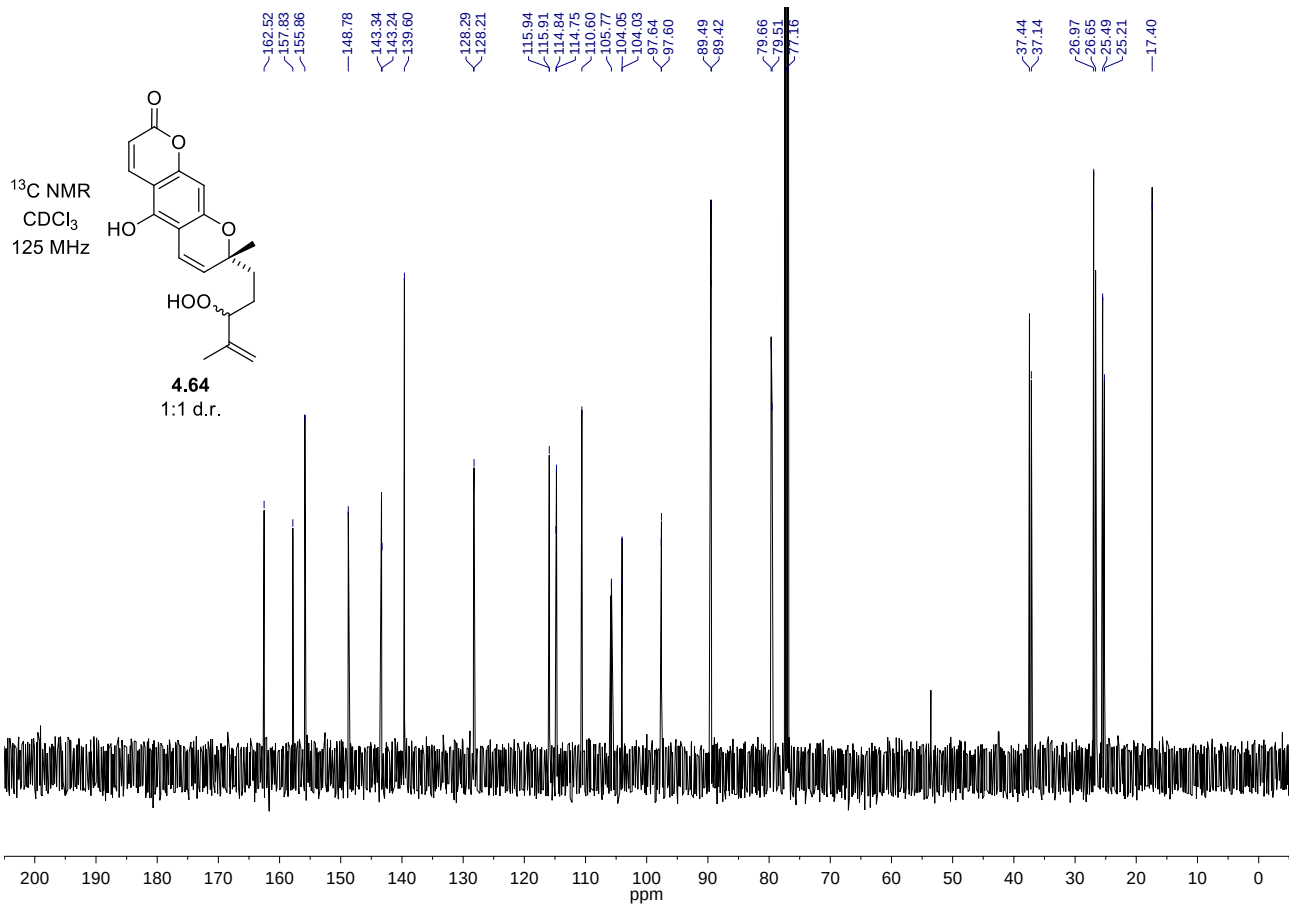
^{13}C NMR
$CDCl_3$
125 MHz
HO
O
HOO
4.64
1:1 d.r.
ppm

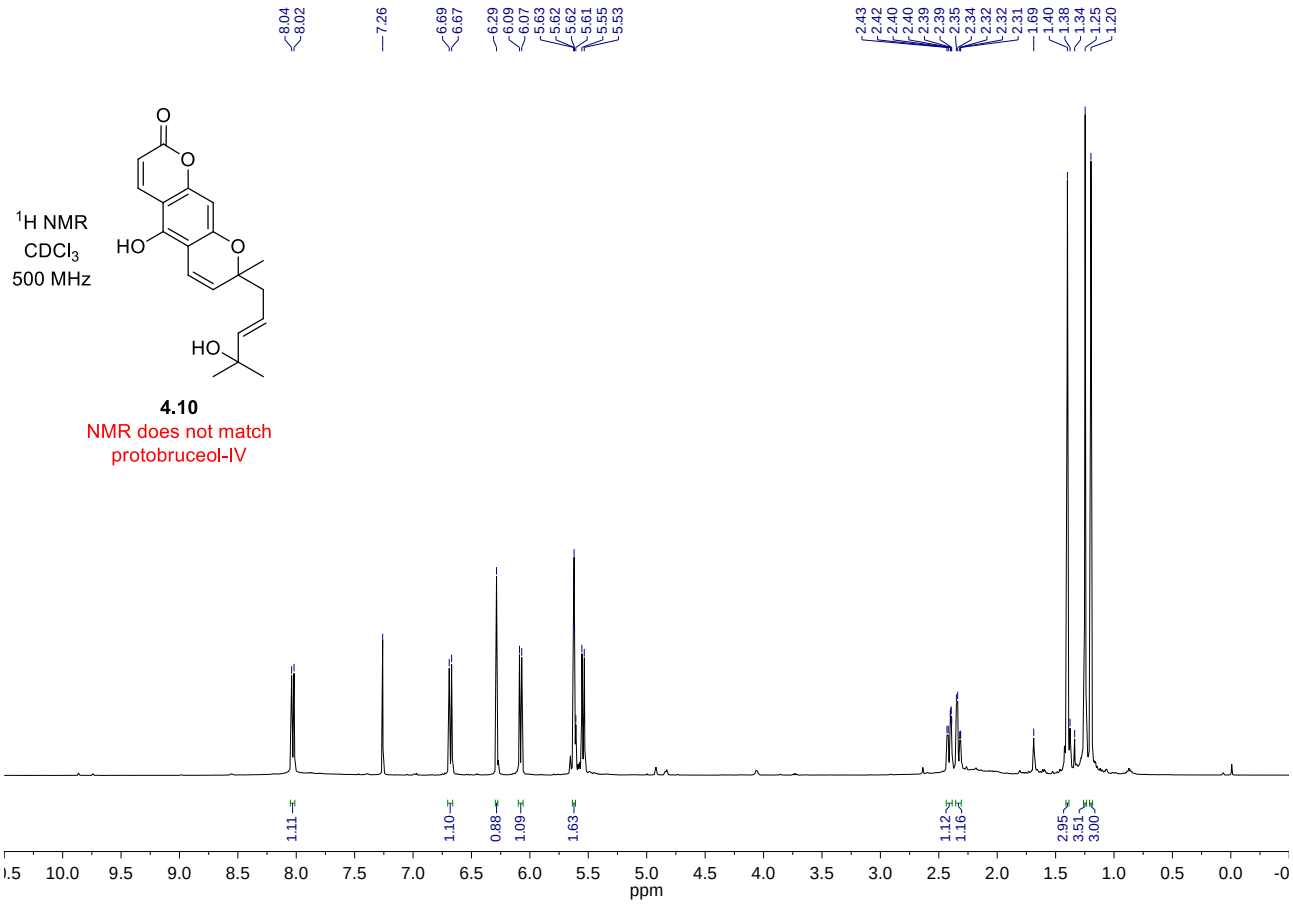
8.04
8.02
7.26
6.69
6.67
6.29
6.09
6.07
5.63
5.62
5.62
5.61
5.55
5.53
2.43
2.42
2.40
2.40
2.39
2.39
2.35
2.34
2.32
2.32
2.31
1.69
1.40
1.38
1.34
1.25
1.20
1H NMR
CDCl3
500 MHz
HO
HO
4.10
NMR does not match
protobruceol-IV
1.11
1.10
0.88
1.09
1.63
1.12
1.16
2.95
3.51
3.00
ppm

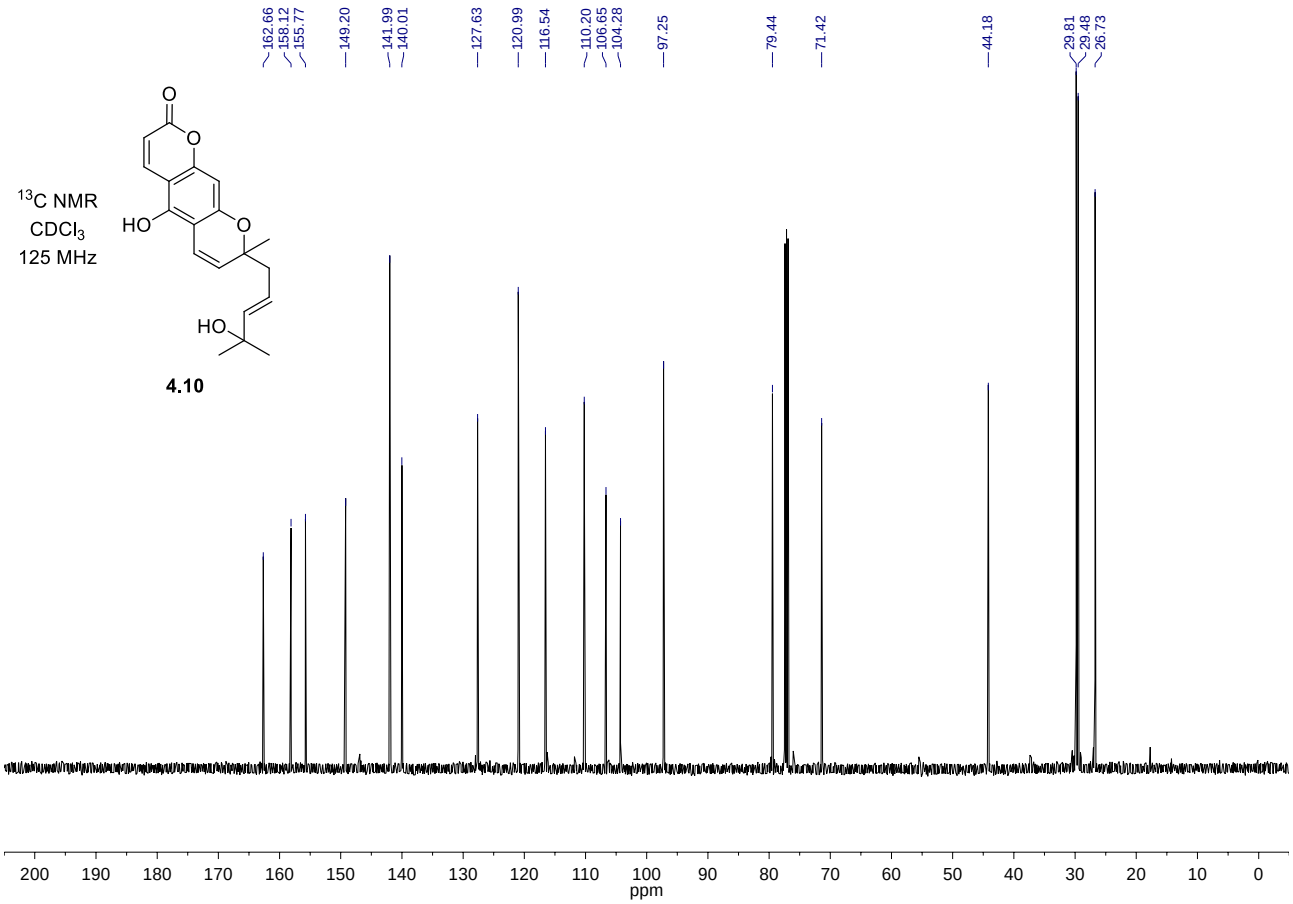
162.66
158.12
155.77
149.20
141.99
140.01
127.63
120.99
116.54
110.20
106.65
104.28
97.25
79.44
71.42
44.18
29.81
29.48
26.73
13C NMR
CDCl3
125 MHz
HO
HO
4.10
ppm

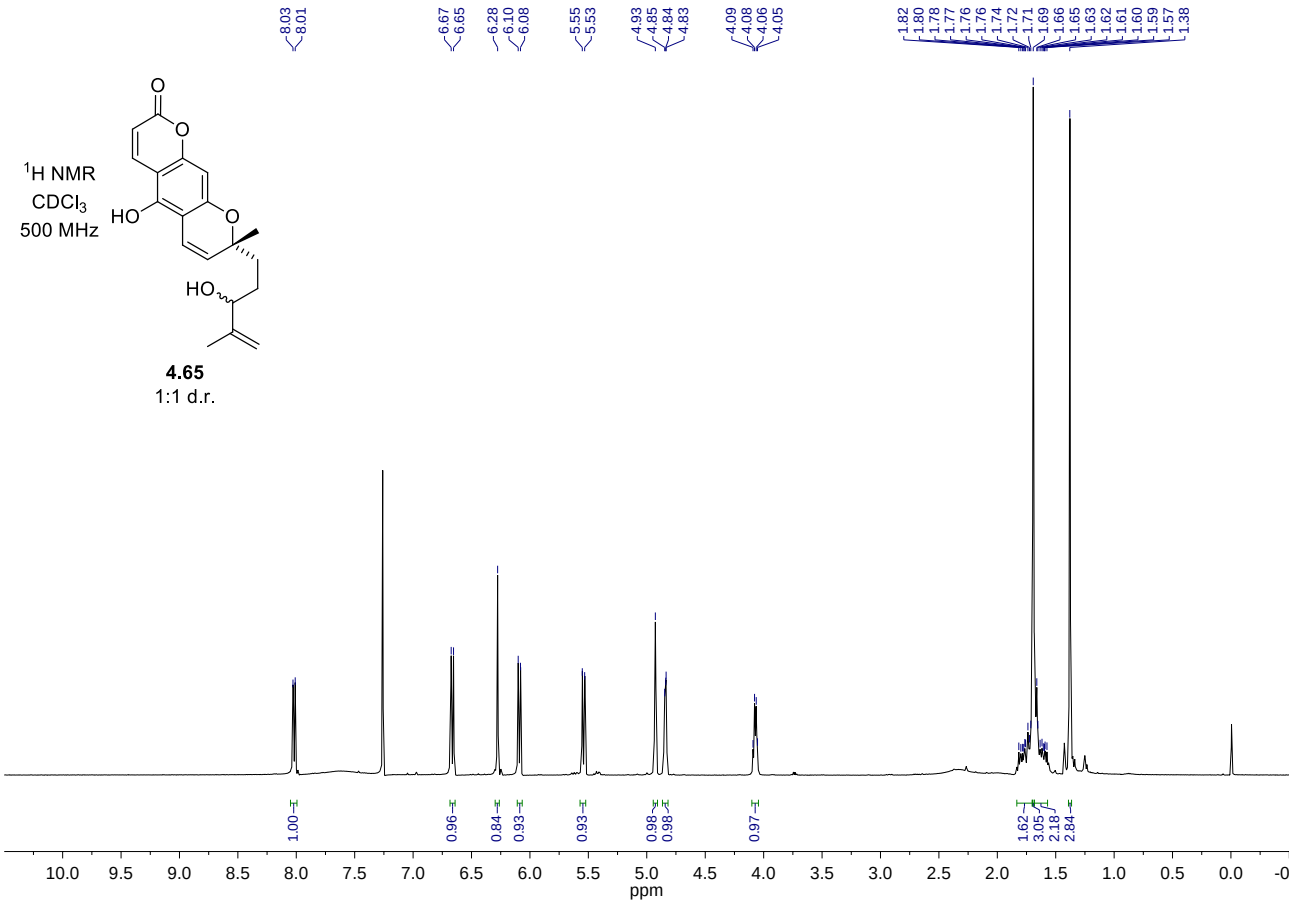
8.03
8.01
6.67
6.65
6.28
6.10
6.08
5.55
5.53
4.93
4.85
4.84
4.83
4.09
4.08
4.06
4.05
1.82
1.80
1.78
1.77
1.76
1.76
1.74
1.72
1.71
1.69
1.66
1.65
1.63
1.62
1.61
1.60
1.59
1.57
1.38
1H NMR
CDCl3
500 MHz
HO
O
HO
4.65
1:1 d.r.
1.00
0.96
0.84
0.93
0.93
0.98
0.98
0.97
1.62
3.05
2.18
2.84
10.0 9.5 9.0 8.5 8.0 7.5 7.0 6.5 6.0 5.5 5.0 4.5 4.0 3.5 3.0 2.5 2.0 1.5 1.0 0.5 0.0 -0
ppm

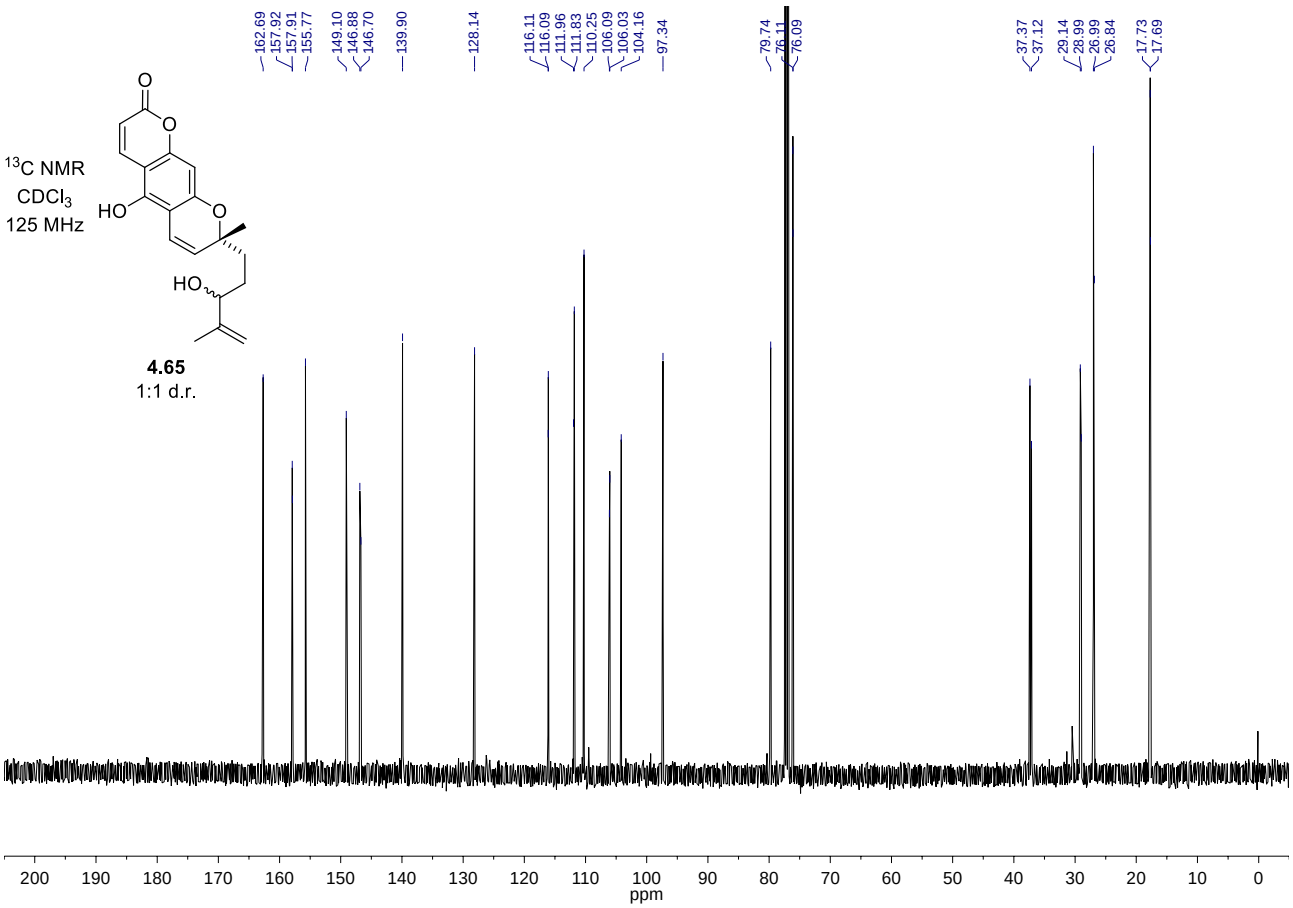
162.69
157.92
157.91
155.77
149.10
146.88
146.70
139.90
128.14
116.11
116.09
111.96
111.83
110.25
106.09
106.03
104.16
97.34
79.74
76.11
76.09
37.37
37.12
29.14
28.99
26.99
26.84
17.73
17.69
13C NMR
CDCl3
125 MHz
HO
O
HO
4.65
1:1 d.r.
200 190 180 170 160 150 140 130 120 110 100 90 80 70 60 50 40 30 20 10 0
ppm

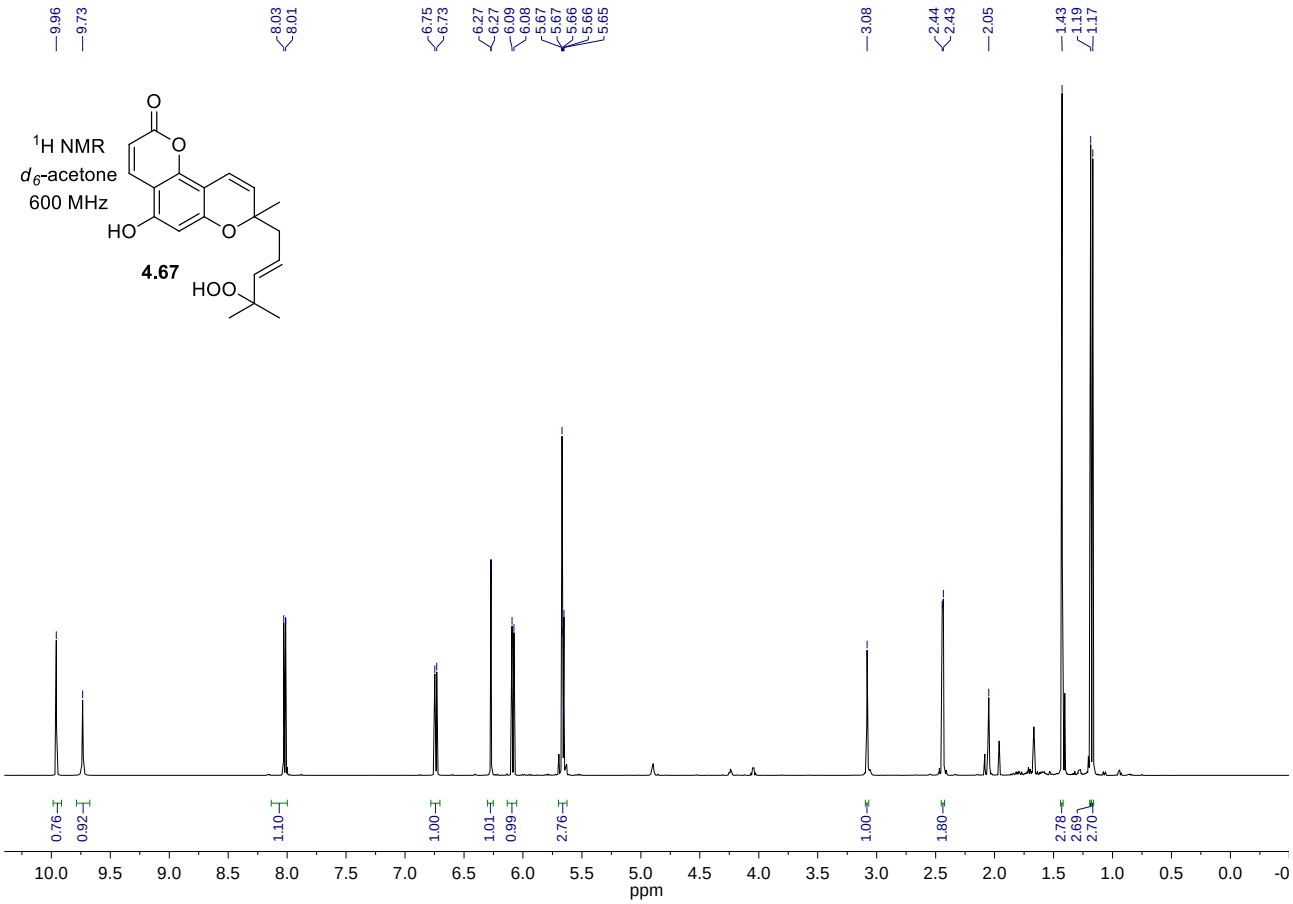
9.96
9.73
8.03
8.01
6.75
6.73
6.27
6.27
6.09
6.08
5.67
5.67
5.66
5.66
5.65
3.08
2.44
2.43
2.05
1.43
1.19
1.17
^{1}H NMR
d_6-acetone
600 MHz
HO
O
HOO
4.67
0.76
0.92
1.10
1.00
1.01
0.99
2.76
1.00
1.80
2.78
2.69
2.70
ppm

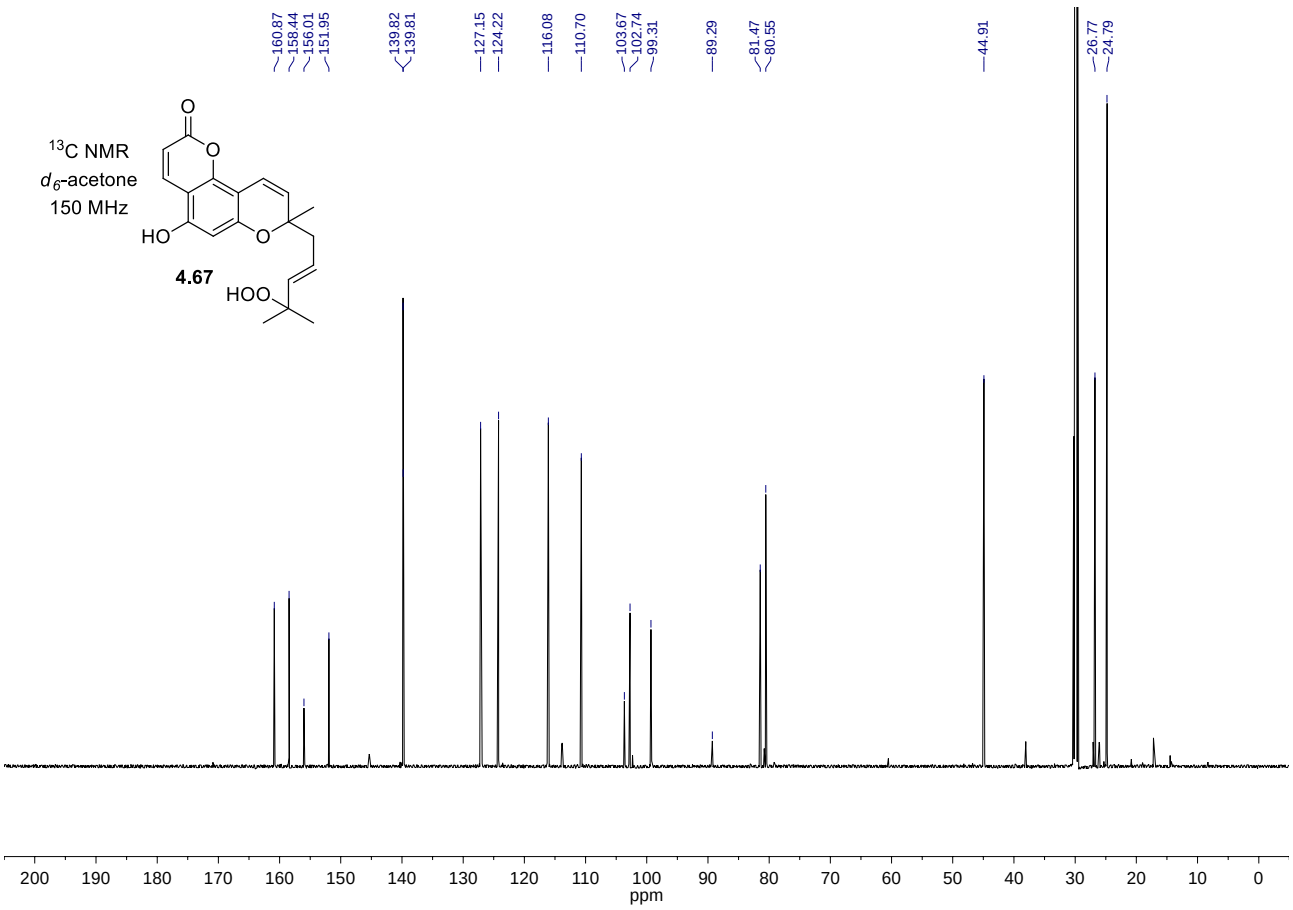
160.87
158.44
156.01
151.95
139.82
139.81
127.15
124.22
116.08
110.70
103.67
102.74
99.31
89.29
81.47
80.55
44.91
26.77
24.79
^{13}C NMR
d_6-acetone
150 MHz
HO
O
HOO
4.67
ppm

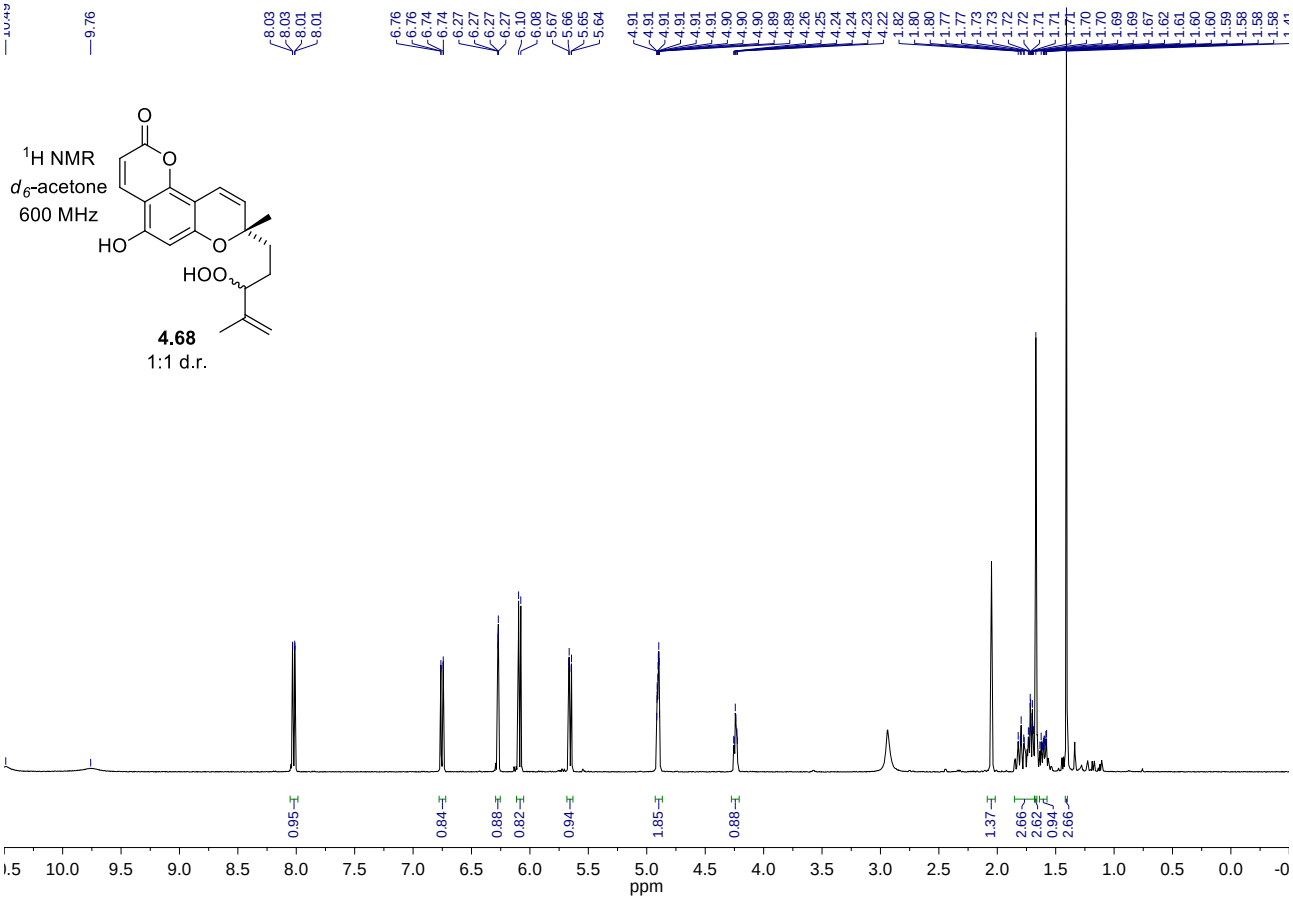
^{1}H NMR
d_6-acetone
600 MHz
HO
O
HOO
4.68
1:1 d.r.
ppm

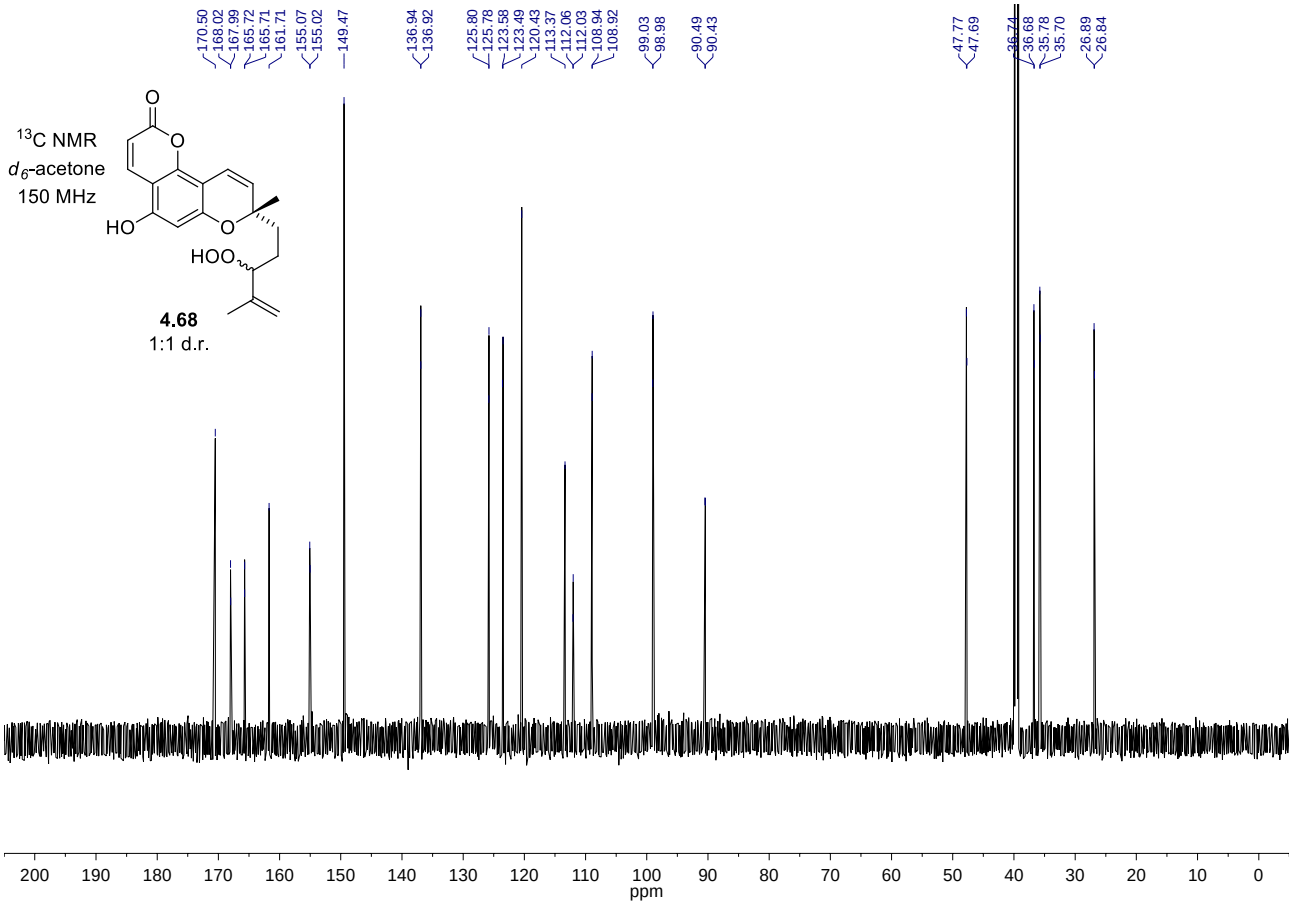
^{13}C NMR
d_6-acetone
150 MHz
HO
O
HOO
4.68
1:1 d.r.
ppm

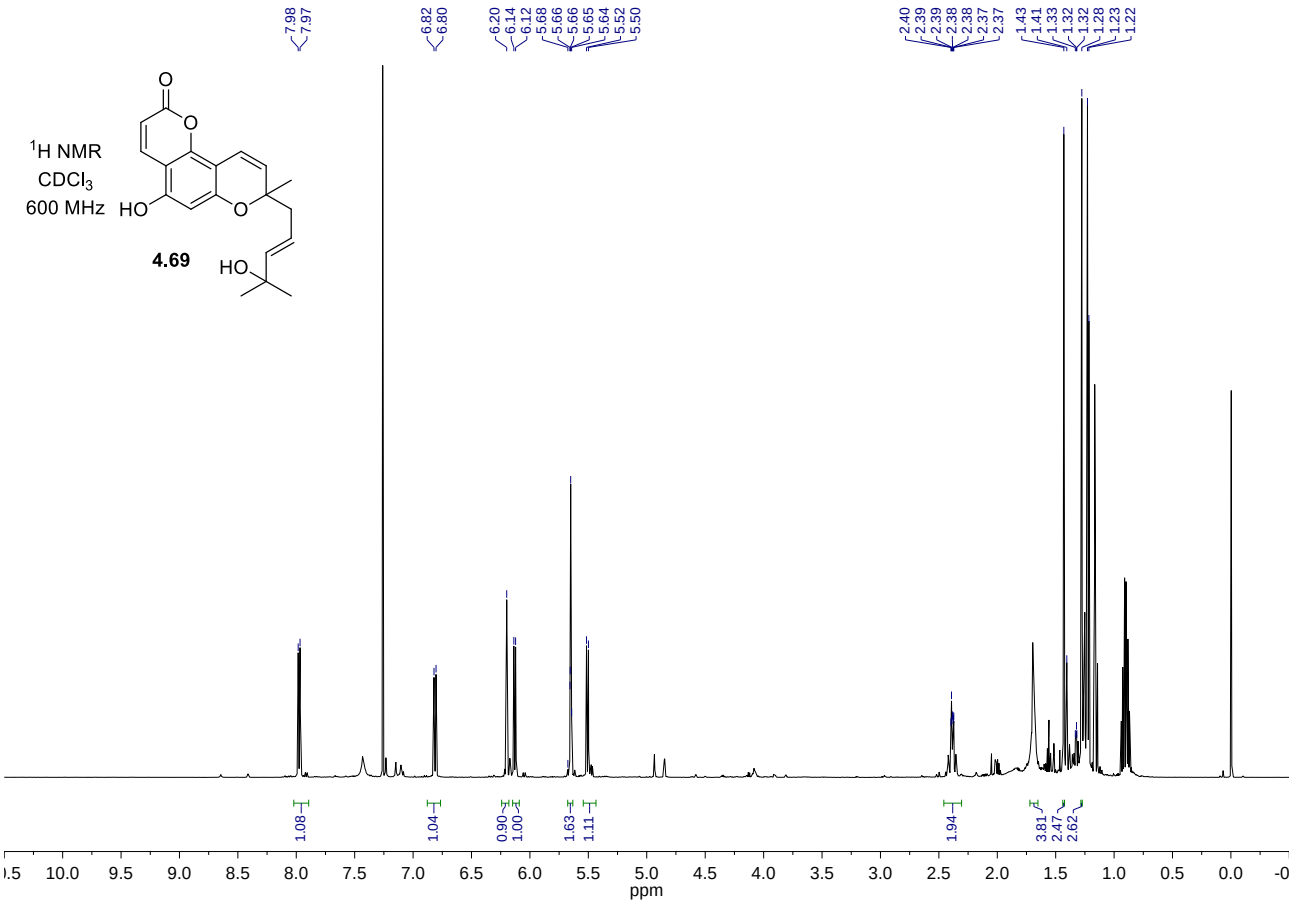
7.98
7.97
6.82
6.80
6.20
6.14
6.12
5.68
5.66
5.66
5.65
5.64
5.52
5.50
2.40
2.39
2.39
2.38
2.38
2.37
2.37
1.43
1.41
1.33
1.32
1.32
1.28
1.23
1.22
1H NMR
CDCl3
600 MHz
HO
O
O
HO
4.69
1.08
1.04
0.90
1.00
1.63
1.11
1.94
3.81
2.47
2.62
ppm

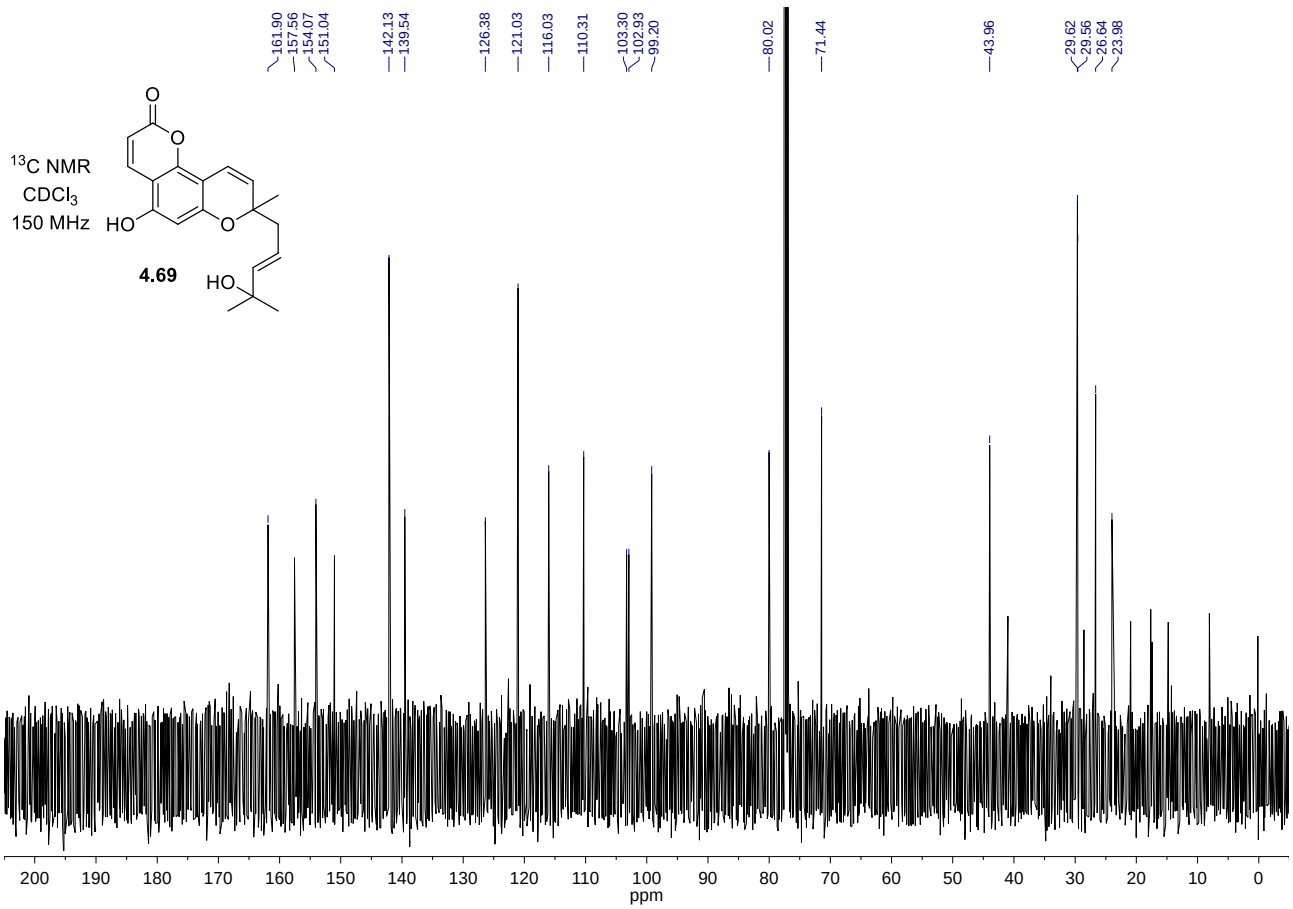
161.90
157.56
154.07
151.04
142.13
139.54
126.38
121.03
116.03
110.31
103.30
102.93
99.20
80.02
71.44
43.96
29.62
29.56
26.64
23.98
13C NMR
CDCl3
150 MHz
HO
O
O
HO
4.69
ppm

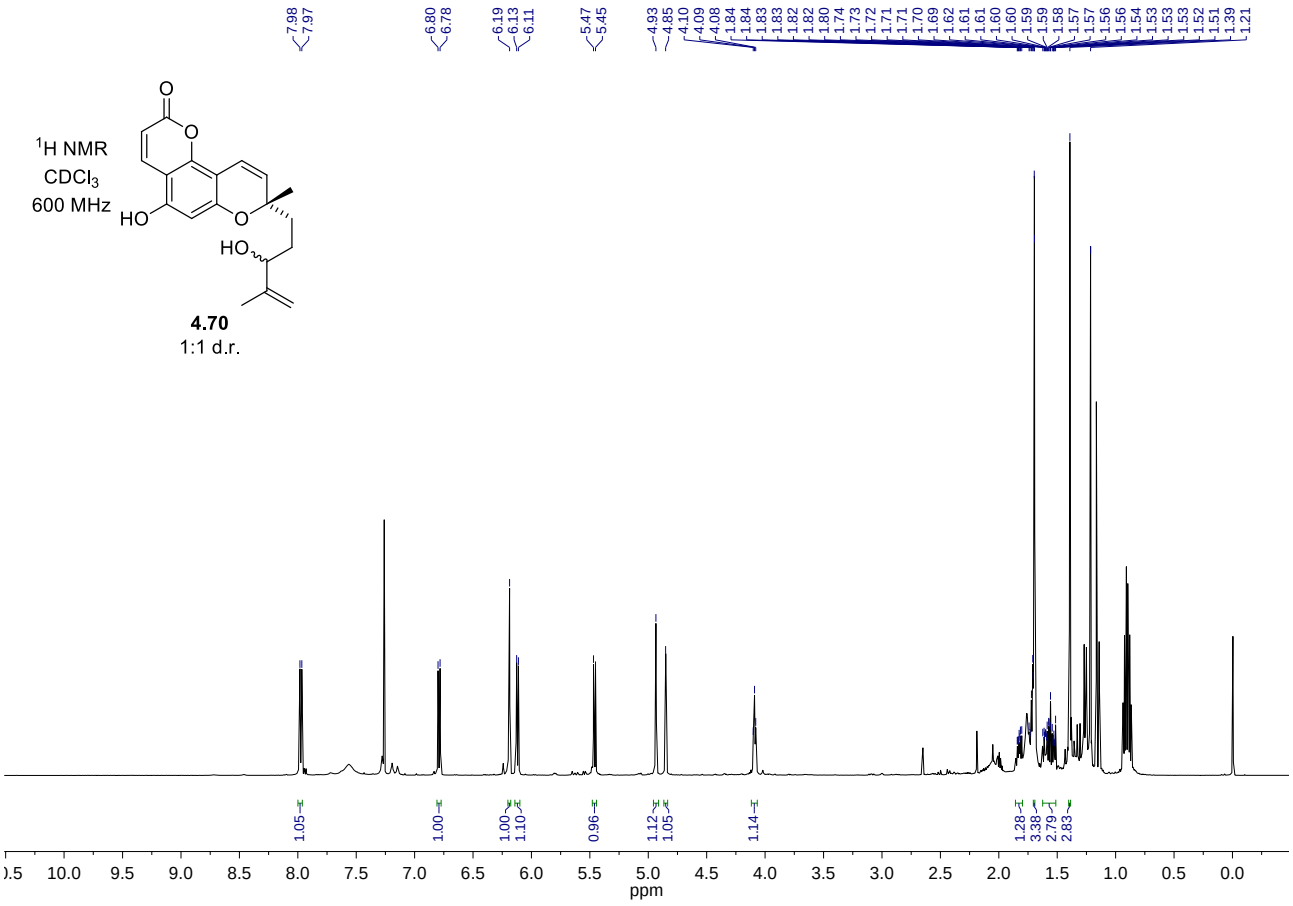
7.98
7.97
6.80
6.78
6.19
6.13
6.11
5.47
5.45
4.93
4.85
4.10
4.09
4.08
1.84
1.84
1.83
1.83
1.82
1.82
1.80
1.74
1.73
1.72
1.71
1.71
1.70
1.69
1.62
1.61
1.61
1.60
1.60
1.59
1.59
1.58
1.57
1.57
1.56
1.56
1.54
1.53
1.53
1.52
1.51
1.39
1.21
^{1}H NMR
$CDCl_3$
600 MHz
HO
O
HO
4.70
1:1 d.r.
1.05
1.00
1.00
1.10
0.96
1.12
1.05
1.14
1.28
3.38
2.79
2.83
ppm

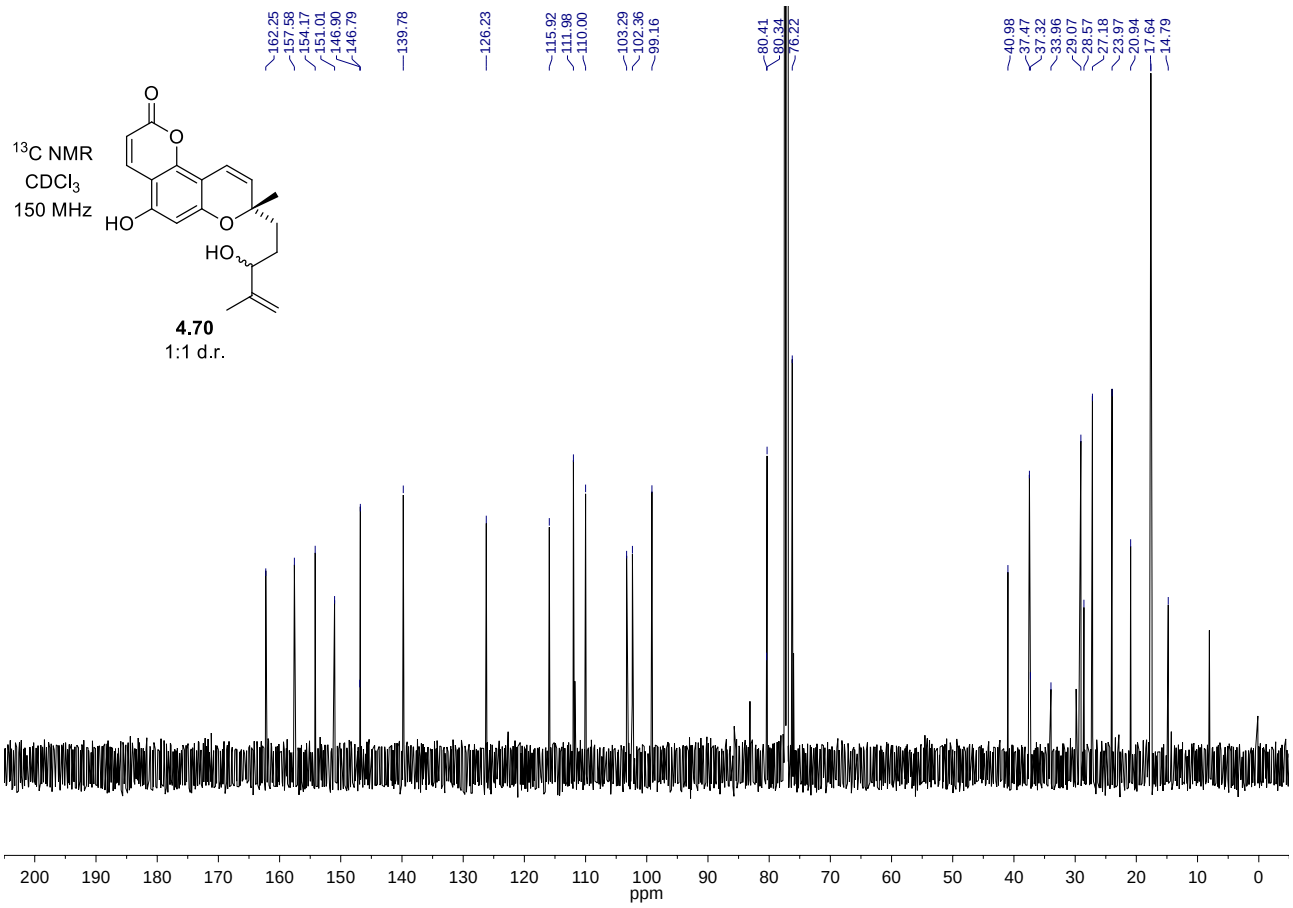
162.25
157.58
154.17
151.01
146.90
146.79
139.78
126.23
115.92
111.98
110.00
103.29
102.36
99.16
80.41
80.34
76.22
40.98
37.47
37.32
33.96
29.07
28.57
27.18
23.97
20.94
17.64
14.79
^{13}C NMR
$CDCl_3$
150 MHz
HO
O
HO
4.70
1:1 d.r.
ppm

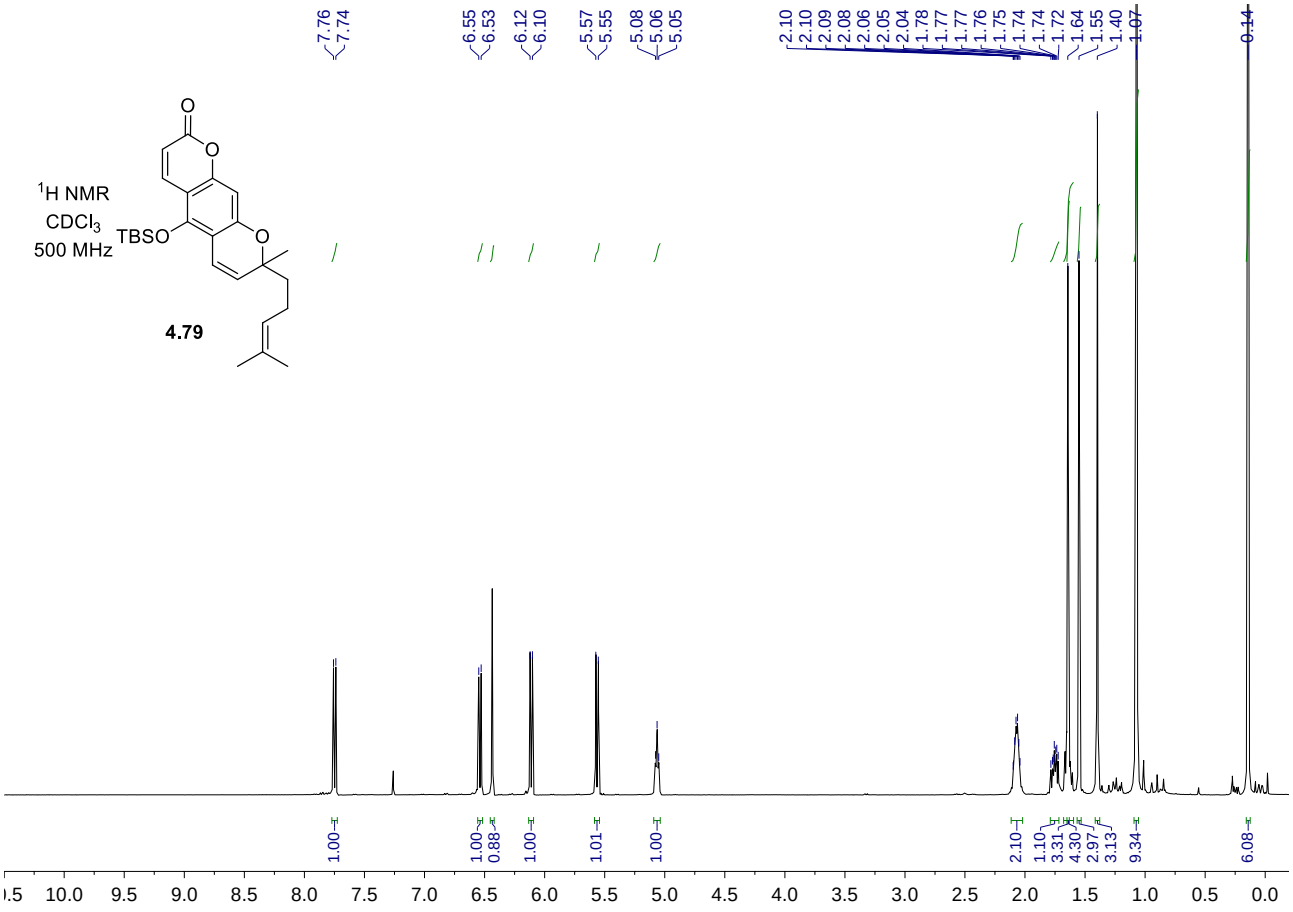
7.76
7.74
6.55
6.53
6.12
6.10
5.57
5.55
5.08
5.06
5.05
2.10
2.10
2.09
2.08
2.06
2.05
2.04
1.78
1.77
1.77
1.76
1.75
1.74
1.74
1.72
1.64
1.55
1.40
1.07
0.14
1.00
1.00
0.88
1.00
1.01
1.00
2.10
1.10
3.31
4.30
2.97
3.13
9.34
6.08
10.0
9.5
9.0
8.5
8.0
7.5
7.0
6.5
6.0
5.5
5.0
4.5
4.0
3.5
3.0
2.5
2.0
1.5
1.0
0.5
0.0
^{1}H NMR
$CDCl_3$
500 MHz
TBSO
O
O
O
4.79

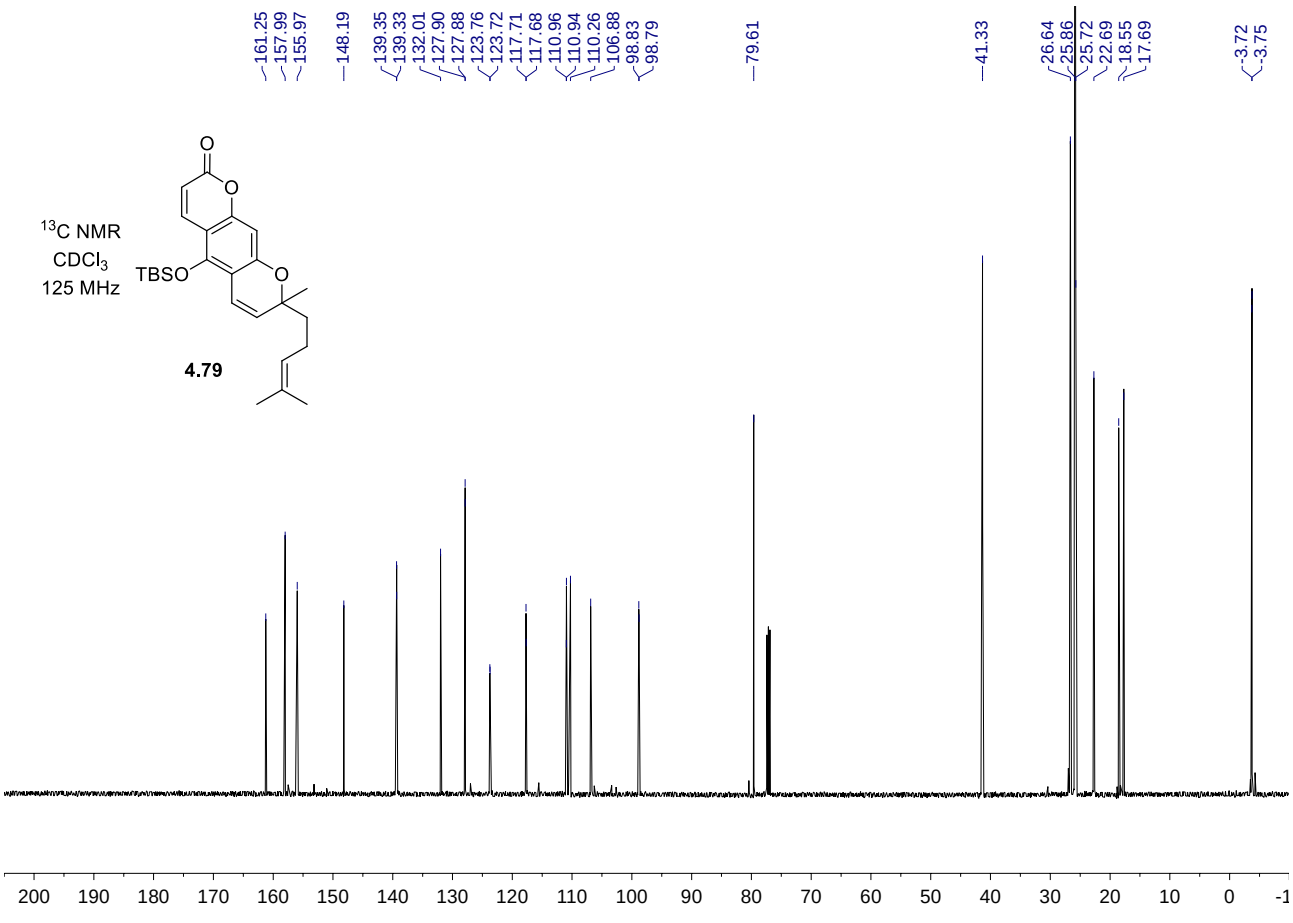
161.25
157.99
155.97
148.19
139.35
139.33
132.01
127.90
127.88
123.76
123.72
117.71
117.68
110.96
110.94
110.26
106.88
98.83
98.79
79.61
41.33
26.64
25.86
25.72
22.69
18.55
17.69
-3.72
-3.75
200
190
180
170
160
150
140
130
120
110
100
90
80
70
60
50
40
30
20
10
0
-1
^{13}C NMR
$CDCl_3$
125 MHz
TBSO
O
O
O
4.79

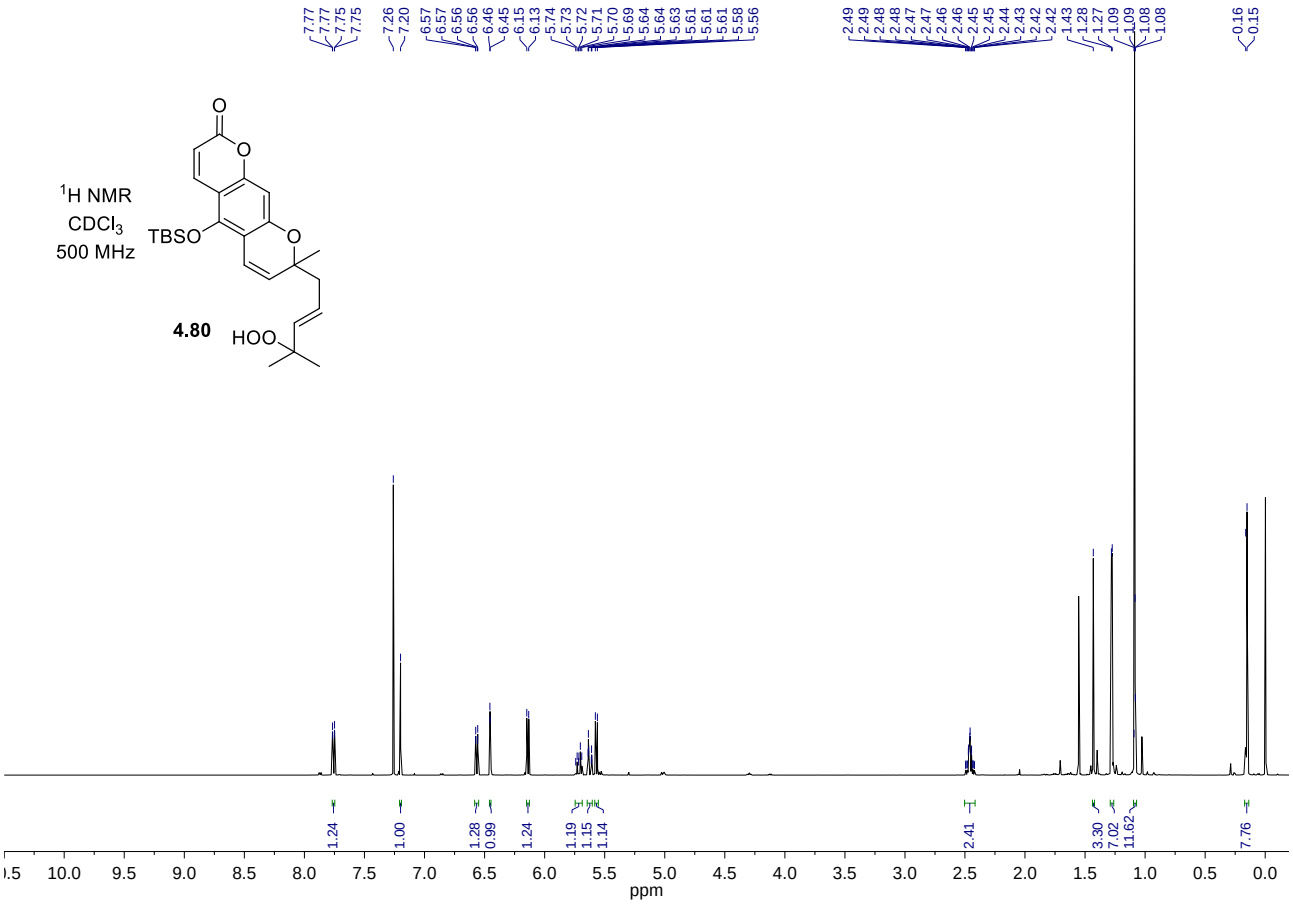
^{1}H NMR
$CDCl_3$
500 MHz
TBSO
O
HOO
4.80
ppm

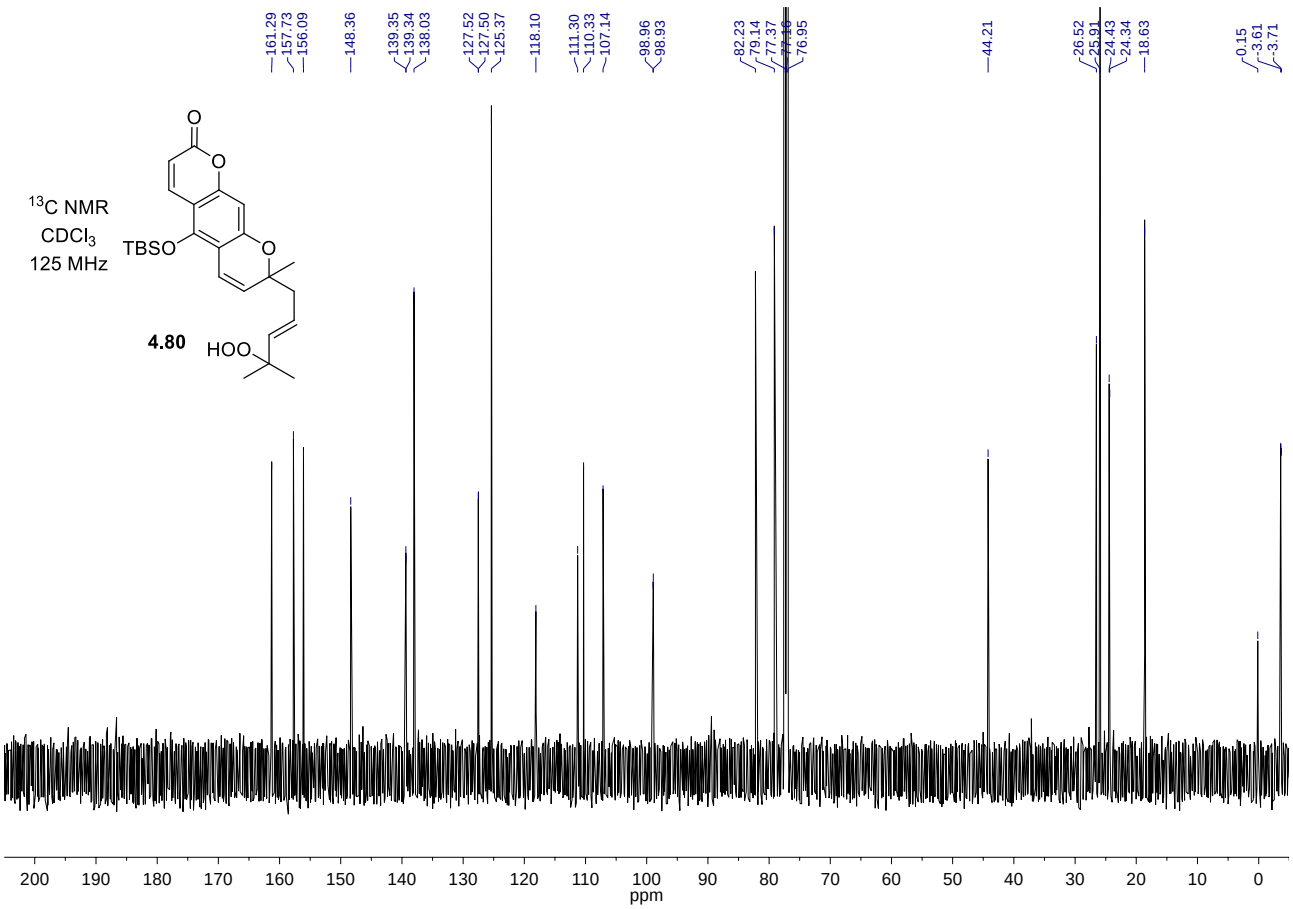
^{13}C NMR
$CDCl_3$
125 MHz
TBSO
O
HOO
4.80
ppm

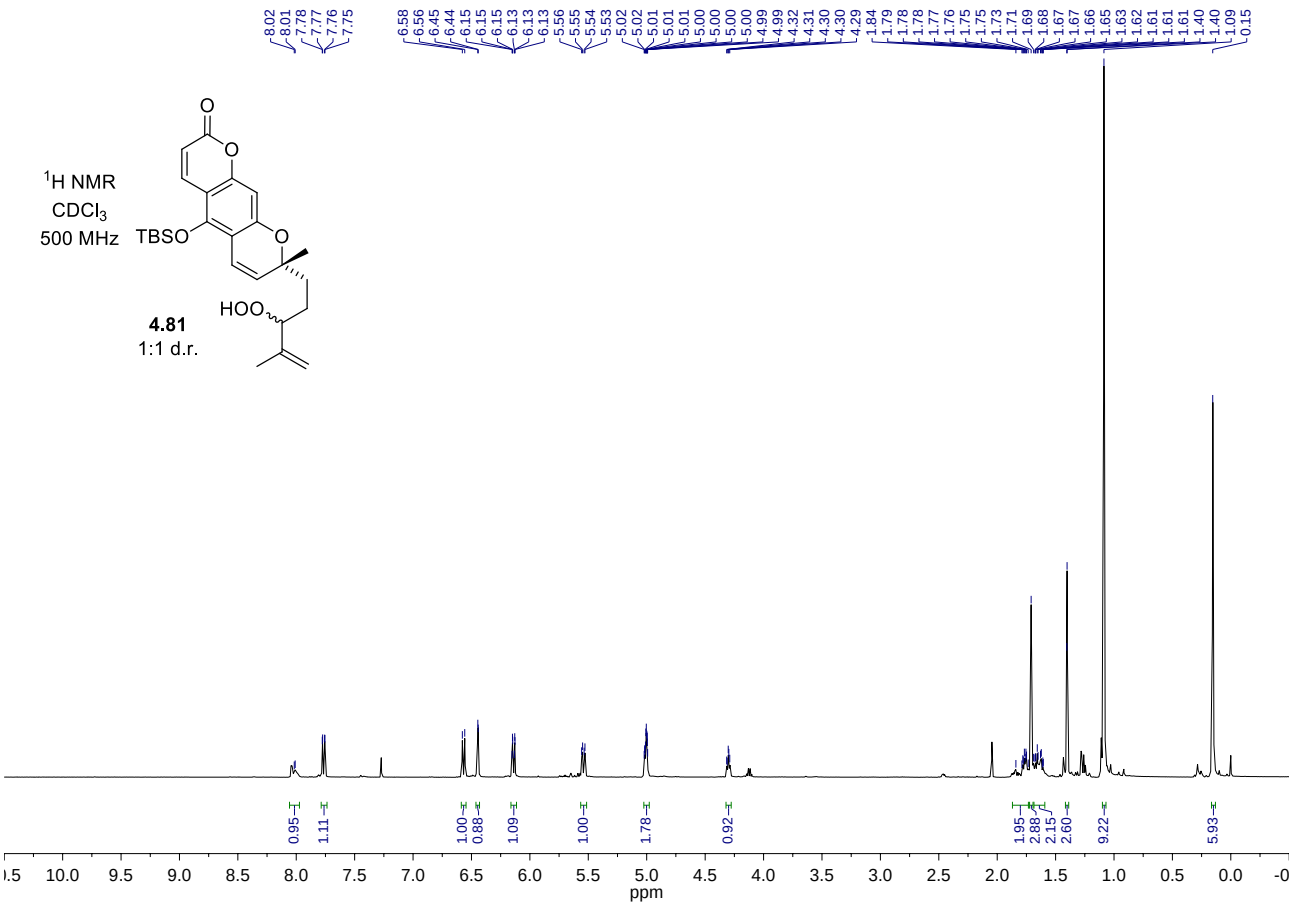
^{1}H NMR
$CDCl_3$
500 MHz
TBSO
HOO
4.81
1:1 d.r.
ppm

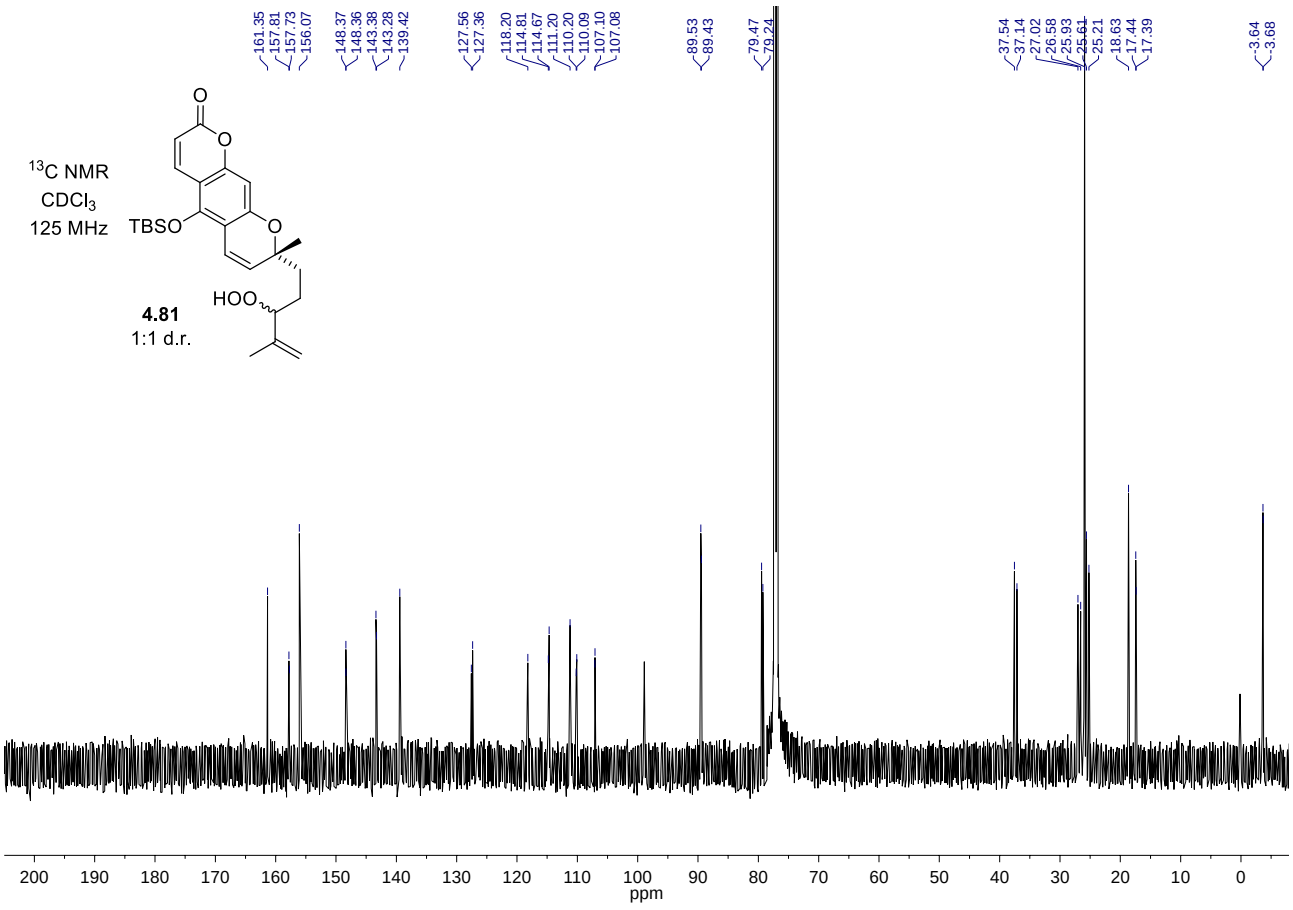
^{13}C NMR
$CDCl_3$
125 MHz
TBSO
HOO
4.81
1:1 d.r.
ppm

4.6.4: ^{1}H and ^{13}C NMR Comparison Tables

Table 4.4: Eriobrucinol (**4.12**) ^{1}H NMR comparison

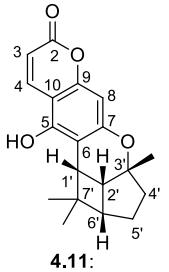

4.11:
eriobrucinol

	Jefferies 1973 90 MHz (d_5-pyridine)	Waterman 1992 400 MHz ($CDCl_3$)	Hsung 2013 400 MHz ($CDCl_3$)	George 2019 500 MHz ($CDCl_3$)
3	6.18 d (10)	6.16 d (9.6)	6.15 (9.5)	6.14 d (9.6)
4	8.33 d (10)	8.01 dd (9.6, 0.6)	7.97 d (9.5)	8.02 d (9.6)
8	6.46 s	6.47 d (0.6)	6.47 s	6.44 s
1’	3.4 m (10)	3.09 d (9.7)	3.06 d (9.7)	3.10 d (9.7)
2’	2.54, t (~8.5)	2.67 dd (12.0, 6.8)	2.66 dd (9.5, 7.5)	2.64 dd (9.7, 7.6)
3’-Me	1.39 s	1.42 s	1.41 s	1.40 s
4’-α	n.r.	1.74 m	1.56-1.80 m	1.7 m (2H)
4’-β	n.r.	1.71 m	1.56-1.80 m	1.7 m (2H)
5’-α	n.r.	1.92 dt (12.0, 6.8)	1.84 – 1.98 m	1.9 m
5’-β	n.r.	1.65 m	1.56-1.80 m	1.63 td (8.0, 6.9, 4.4)
6’	n.r.	2.49 t (7.4)	2.48 t (7.5)	2.46 t (7.6)
7’-Me	0.86 s	0.80 s	0.79 s	0.77 s
7’-Me	1.48 s	1.46 s	1.45 s	1.44 s

Table 4.5: Eriobrucinol (**4.12**) ^{13}C NMR comparison

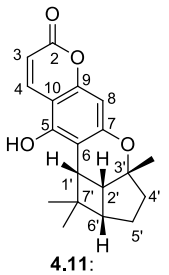

4.11:
eriobrucinol

	Waterman 1992 100 MHz ($CDCl_3$)	Hsung 2013 100 MHz ($CDCl_3$)	George 2019 125 MHz ($CDCl_3$)
2	162.3	162.0	162.1
3	111.1	111.1	111.0
4	139.1	139.0	138.9
5	151.5	151.2	151.3
6	107.2	106.8	107.1
7	157.9	157.7	157.8
8	99.1	99.0	99.0
9	154.7	154.6	154.6
10	103.2	103.1	103.2
1’	35.7	35.6	35.6
2’	37.4	37.2	37.3
3’	84.7	84.6	84.7
3’-Me	27.4	27.4	27.4
4’	38.8	38.6	38.7
5’	25.7	25.7	25.7
6’	46.5	46.4	46.4
7’	39.1	39.0	39.1
7’-Me	18.3	18.2	18.2
7’-Me	34.6	34.6	34.6

Table 4.6: Isoeriobrucinol A (**4.12**) ^{1}H NMR comparison

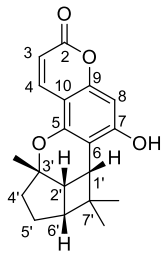

4.12:
isoeriobrucinol A

	Crombie 1983 (d_5-pyridine)	Waterman 1992 250 MHz (d_5-pyridine)	Hsung 2013 600 MHz (d_5-pyridine)	George 2019 500 MHz (d_5-pyridine)
3	6.24 d (10)	6.25 d (9.6)	6.26 d (9.6)	6.27 d (9.6)
4	8.08 d (10)	8.06 dd (9.6, 0.6)	8.04 d (9.6)	8.09 d (9.6)
8	6.59 s	6.60 d (0.6)	6.60 s	6.61 s
1’	3.34 d (10)	3.31 d (9.5)	3.32 d (9.6)	3.34 d (9.6)
2’	n.r.	2.56 dd (9.5, 7.6)	2.55 dd (9.0, 7.8)	2.56 dd (9.6, 7.5)
3’-Me	1.45 s	1.44 s	1.45 s	1.47 s
4’-α	n.r.	1.55 dt (11.8, 7.6)	1.56 dt (12.6, 7.8)	1.57 ddd (13.7, 12.3, 7.6)
4’-β	n.r.	1.62 m	1.70 – 1.64 m	1.72-1.65 (overlapped)
5’-α	n.r.	2.12 m	2.11 – 2.00 m	2.04 td (12.6, 7.5)
5’-β	n.r.	1.68 dt (13.9, 7.6)	1.70 – 1.64 m	1.74-1.68 (overlapped)
6’	n.r.	2.31 t (7.6)	2.34 t (7.8)	2.35 t (7.5)
7’-Me	0.96 s	0.96 s	0.97 s	0.98 s
7’-Me	1.48 s	1.46 s	1.48 s	1.47 s

Table 4.7: Isoeriobrucinol A (**4.12**) ^{13}C NMR comparison

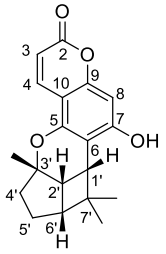

4.12:
isoeriobrucinol A

	Hsung 2013 150 MHz (d_5-pyridine)	George 2019 125 MHz (d_5-pyridine)
2	161.7	162.2
3	109.7	110.2
4	139.5	140.0
5	151.3	151.7
6	108.8	109.2
7	161.6	162.1
8	95.1	95.6
9	155.7	156.1
10	103.7	104.2
1’	36.5	37.0
2’	38.0	38.5
3’	84.9	85.4
3’-Me	27.4	27.9
4’	38.7	39.2
5’	25.9	26.4
6’	46.6	47.1
7’	39.4	39.9
7’-Me	18.0	18.5
7’-Me	33.8	34.3

Note. The residual pyridine ^{13}C NMR peak at 135.91 was used as a reference (our chemical shift values for **4.12** are ~0.4 – 0.5 ppm higher than for Hsungs’ synthetic **4.12**).

^{13}C NMR data for **4.12** was not reported by Waterman and co-workers.

Table 4.8: Isoeriobrucinol B (**4.13**) ^{1}H NMR comparison table

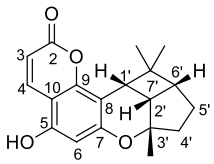

4.13:
isoeriobrucinol B

	Crombie 1983 (d_5-pyridine)	Waterman 1992 250 MHz ($CDCl_3$)	Hsung 2013 600 MHz (d_5-pyridine)	George 2019 500 MHz (d_5-pyridine)
3	6.25 d (10)	6.16 d (9.7)	6.28 d (9.6)	6.29 d (9.5
4	8.30 d (10)	7.98 d (9.7)	8.30 d (9.6)	8.31 d (9.5)
6	6.60 s	6.21 s	6.63 s	6.63 s
1’	3.29 d (10)	3.26 d (9.4)	3.29 d (9.6)	3.30 d (9.6)
2’	2.30 – 1.7 m	2.60 dd (9.4, 7.4)	2.49 dd (7.2, 8.1)	2.50 dd (9.7, 7.3)
3’-Me	1.34 s	1.42 s	1.35 s	1.37 s
4’-α	2.30 – 1.7 m	1.75 – 1.50	1.62 – 1.57 m	1.61 – 1.55 overlapped
4’-β	2.30 – 1.7 m	1.75 – 1.50	1.62 – 1.57 m	1.53 – 1.44 m
5’-α	2.30 – 1.7 m	1.90 m	2.04 – 1.98 m	2.02 td (12.8, 7.8)
5’-β	2.30 – 1.7 m	1.75 – 1.50	1.62 – 1.57 m	1.64 – 1.47 overlapped
6’	2.30 – 1.7 m	2.46 t (7.4)	2.29 t (7.2)	2.31 t (7.4)
7’-Me	0.84	0.77 s	0.85 s	0.87 s
7’-Me	1.34	1.52 s	1.55 s	1.56 s

Table 4.9: Isoeriobrucinol B (**4.13**) ^{13}C NMR comparison table

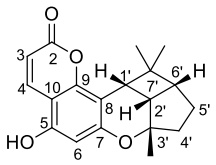

4.13:
isoeriobrucinol B

	Hsung 2013 125 MHz (d_5-pyridine)	George 2019 500 MHz (d_5-pyridine)
2	161.3	161.8
3	109.9	110.4
4	140.1	140.5
5	155.4	155.9
6	100.3	100.7
7	-*	158.4
8	-	103.7
9	155.1	155.5
10	-	104.8
1’	35.7	36.2
2’	37.4	37.9
3’	84.8	85.3
3’-Me	27.6	28.0
4’	25.8	26.2
5’	38.5	39.0
6’	46.7	47.2
7’	39.1	39.6
7’-Me	18.2	18.6
7’-Me	33.8	34.2

Note: The residual pyridine ^{13}C NMR peak at 135.91 was used as a reference (our chemical shift values for **4.13** are ~0.4 – 0.6 ppm higher than for Hsung’s synthetic **4.13**).

Note: *Only 18 ^{13}C peaks were reported. Signals were reported at 79.7 and 79.5 are possibly misassigned residual chloroform.

^{13}C NMR data for **4.13** was not reported by Waterman and co-workers.

Table 4.10: Deoxyisobruceol (**4.62**) ^{1}H NMR comparison

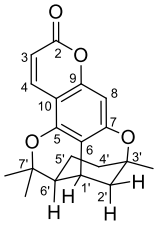

deoxyisobruceol (**4.62**)
previously known as deoxybruceol

	Crombie 1971 100 MHz ($CDCl_3$)	Waterman 1992 400 MHz ($CDCl_3$)	George 2019 500 MHz ($CDCl_3$)
3	6.11 d (10)	6.11 d (9.7)	6.11 d (9.5)
4	7.87 d (10)	7.86 dd (9.7, 0.6)	7.86 d (9.5)
8	6.44 s	6.44 d (0.6)	6.44 s
1’	2.82 s	2.86 ddd (4.6, 2.8, 1.7)	2.90-2.84 m
2’-ax.	n.r.	1.90 dd (13.4, 1.7)	1.91 dd (13.4, 1.7)
2’-eq.	n.r.	2.24 ddd (13.1, 4.6, 3.2)	2.24 ddd (13.4, 4.7, 3.2)
3’-Me	1.42 s	1.41 s	1.42 s
4’-ax.	n.r.	1.48 ddd (14.9, 11.6, 5.4)	1.47 ddd (15.1, 13.1, 6.8)
4’-eq.	n.r.	1.81 ddd (14.9, 6.4, 2.8)	1.81 ddd (14.9, 5.6, 3.4)
5’-ax.	n.r.	0.64 dtd (14.0, 11.6, 6.4)	0.64 tdd (13.4, 11.6, 6.1)
5’-eq.	n.r.	1.31 dt (1.40, 5.4)	1.30 dt (12.8, 6.0)
6’	n.r.	2.13 ddd (11.6, 5.4, 2.8)	2.13 ddd (11.6, 5.4, 2.8)
7’-Me	1.60 s	1.60 s	1.60 s
7’-Me	1.09 s	1.06 s	1.07 s

Table 4.11: Deoxyisobruceol (**4.62**) ^{13}C NMR comparison

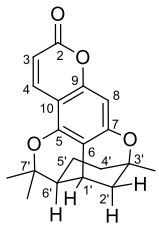

deoxyisobruceol (**4.62**)
previously known as deoxybruceol

	Waterman 1992 100 MHz ($CDCl_3$)	George 2019 500 MHz ($CDCl_3$)
2	162.1	162.0
3	110.9	110.7
4	138.4	138.3
5	153.7	153.6
6	112.5	112.4
7	160.0	159.8
8	97.1	96.9
9	154.7	154.6
10	105.2	105.1
1’	28.1	28.0
2’	35.0	34.8
3’	76.5	76.4
3’-Me	28.9	28.8
4’	37.4	37.3
5’	22.1	22.0
6’	46.4	46.2
7’	86.6	86.5
7’-Me	24.3	24.4
7’-Me	29.7	29.6

Table 4.12: Protobruceol-II and (**4.6**) -II hydroperoxide (**4.8**) ^{1}H NMR comparison

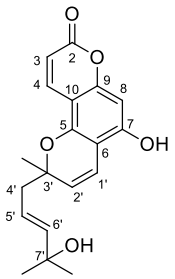

4.6: protobruceol-II

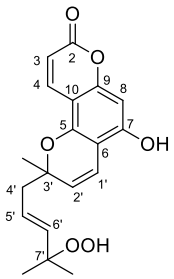

4.8: protobruceol-II hydroperoxide

	Waterman 1992 400 MHz ($CDCl_3$) **4.6**	George 2019 500 MHz ($CDCl_3$) **4.6**	Waterman 1992 400 MHz ($CDCl_3$) **4.8**	George 2019 500 MHz ($CDCl_3$) **4.8**
3	6.10 d (7.6)	6.09 d (9.5)	6.14 (7.6)	6.13 d (9.6)
4	7.97 br d (7.6)	7.96 d (9.6)	7.98 bd (7.6)	7.98 d (9.6)
8	6.50 br s	6.55 s	6.54 br s	6.60 s
1’	6.69 d (10.0)	6.68 d (10.1)	6.61 d (10.0)	6.70 d (10.0)
2’	5.49 d (10.0)	5.48 d (10.1)	5.53 d (10.0)	5.50 d (10.1)
3’-Me	1.47 s	1.45 s	1.49 s	1.47
4’-α/ β	2.43 br d (6.7)	2.42 d (7.1)	2.47 br d (6.9)	2.46 d (7.2)
5’	5.69 dt (15.4, 6.7)	5.72-5.64 m (overlapped)	5.70 dt (15.8, 6.9)	5.71 dt (15.9, 7.2)
6’	5.63 d (15.4)	5.63 d (15.6)	5.59 d (15.8)	5.59 d (15.8)
7’-Me	1.21 s	1.22 s	1.23 s	1.22 s
7’-Me	1.23 s	1.25 s	1.25 s	1.24 s

Table 4.13: Protobruceol II and (**4.6**) II hydroperoxide (**4.8**) ^{13}C NMR comparison

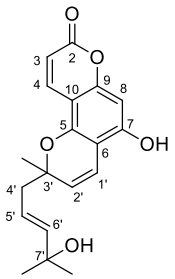

4.6: protobruceol-II

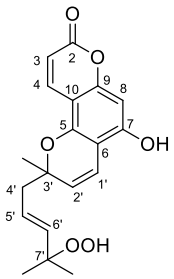

4.8: protobruceol-II hydroperoxide

	Waterman 1992 400 MHz ($CDCl_3$) **4.6**	George 2019 500 MHz ($CDCl_3$) **4.6**	Waterman 1992 400 MHz ($CDCl_3$) (as C7 methyl ether of **4.8**)[8]	George 2019 500 MHz ($CDCl_3$) **4.8**
2	162.8	163.2	161.6	163.0
3	110.2	109.7	111.5	110.2
4	139.6	139.9	138.6	139.7
5	151.3	151.1	150.6	151.1
6	106.3	106.4	106.6	106.3
7	156.4	156.9	158.5	155.4
8	95.7	95.6	91.8	95.8
9	155.4	155.3	156.2	156.5
10	103.2	103.0	103.6	103.2
1’	117.2	117.3	117.2	117.2
2’	126.0	125.9	126.2	126.0
3’	80.0	79.9	79.9	79.9
3’-Me	26.8	26.6	26.8	26.8
4’	44.2	44.0	44.4	44.4
5’	121.0	121.0	125.2	125.2
6’	142.1	141.9	138.4	137.9
7’	71.4	71.5	82.3	82.3
7’-Me	29.7	29.6	24.4	24.5
7’-Me	29.9	29.7	24.4	24.3

Table 4.14: Protobruceol-III (**4.7**) and -III hydroperoxide (**4.9**) ^{1}H NMR comparison

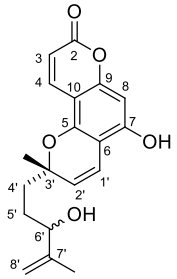

4.7: protobruceol-III

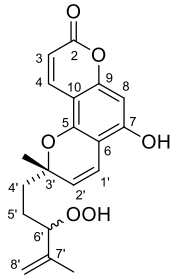

4.9: protobruceol-III hydroproxide

	Waterman 1992 400 MHz ($CDCl_3$) **4.7**	George 2019 500 MHz ($CDCl_3$) **4.7**	Waterman 1992 400 MHz ($CDCl_3$) **4.9**	George 2019 500 MHz ($CDCl_3$) **4.9**
3	6.11 d (9.6)	6.08 d (9.5)	6.15 d (9.6)	6.13 d (9.6)
4	7.96 br d (9.6)	7.94 d (9.5)	7.95 br d (9.6)	7.97 d (9.6)
8	6.54 br s	6.58 s	6.44 br s	6.62 s
1’	6.67 d (10.0)	6.67 d (10.1)	6.68 d(10.0)	6.70 d (10.1)
2’	5.49 d (10.0)	5.47 d (10.1)	5.50 d (10.0)	5.47 d (10.1)
3’-Me	1.43 s	1.42 s	1.44 s	1.42 s
4’-α/β	2.00 – 1.60 m	1.90 – 1.60 m	2.00 – 1.50 m	1.92 – 1.63 m
5’-α/β	2.00 – 1.60 m	1.79 – 1.70 m	2.00 – 1.50 m	1.80 – 1.63 m
6’	4.10 br s	4.12 m	4.30 br t	4.30 t (6.4)
7’-Me	1.71 t*	1.71 d (5.2)	1.71 br s	1.70 d (5.0)
8’	4.87 br s	4.86 br s	5.02 br s	5.00 br s
8’	4.97 br s	4.95 br s	5.04 br s	5.02 br s

^{13}C NMR was not reported for protobruceol-III (**4.7**) or hydroperoxide (**4.9**)

*coupling constant was not specified

4.7 References

[1] a) Crombie, L.; Ponsford, R. *Chem. Commun. (London)* **1968**, 368. b) Crombie, L.; Ponsford, R. *J. Chem. Soc. C* **1971**, 788.

[2] Rashid, M. A.; Armstrong, J. A.; Gray, A. I.; Waterman, P. G. *Nat. Prod. Lett.* **1992**, *1*, 79.

[3] Kärkäs, M. D.; Proco, J. A.; Stephenson, C. R. *Chem. Rev.* **2016**, *116*, 9683.

[4] Jefferies, P. R.; Worth, G. K. *Tetrahedron* **1973**, *29*, 903.

[5] Rashid, M. A.; Armstrong, J. A.; Gray, A. I.; Waterman, P. H.; *Phytochemistry* **1992**, *31*, 3583.

[6] Ghisalberti, E. L. *Phytochemistry* **1998**, *47*, 163.

[7] Foote, C. S.; Valentine, J. S.; Greenberg, A.; Liebman, J. F. *Active Oxygen in Chemistry* **1996**, Blackie Academic & Professional (Glasgow).

[8] Borden, W. T.; Hoffman, R.; Stuyver, T.; Chen B. *J. Am. Chem. Soc.* **2017**, *139*, 9010.

[9] Gorman, A. A.; Rogers, M. A. J. *CRC Handbook of Organic Photochemistry, Vol II* **1989**, CRC Press (Boca Raton, Florida, USA).

[10] Graziano, M. L; Iesce, M. R.; Cinotti, A.; Scarpati, R. *J. Chem. Perkin Trans. 1* **1987**, 1833.

[11] For an example of [2+2] singlet oxygen reaction: Celaje, J. A.; Zhang, D.; Guerrero, A. M.; Selke, M. *Org. Lett.* **2011**, *13*, 4846.

[12] For a memoir of G. O. Schenck: Schaffner, K. *Angew. Chem. Int. Ed.* **2003**, *42*, 2932.

[13] Jefford, C. W.; Boschung, A. F.; Moriarty, R. M.; Rimbault, C. G.; Laffer, M. H. *Helv. Chim. Acta* **1973**, *56*, 2649.

[14] Stratakis, M.; Orfanopoulos, M. *Tetrahedron Lett.* **1997**, *38*, 1067.

[15] Kalaitzakis, D.; Triantafyllakis, M.; Sofiadis, M.; Noutsias, D.; Vassilikogiannakis, G. *Angew. Chem. Int. Ed.* **2016**, *55*, 4605.

[16] Fitzsche, M. *C. R. Acad. Sci.* **1867**, 1035.

[17] For a review on the use of singlet oxygen for the synthesis of natural products: Ghogare, A. A; Greer, A. *Chem. Rev.* **2016**, *116*, 9994.

[18] Schenck, G. O.; Ziegler, K. *Naturwissenschaften* **1944**, *32*, 157.

[19] Mehta, G.; Likhite, N. S. *Tetrahedron Lett.* **2009**, *50*, 5263.

[20] Pepper, H. P.; Lam, H. C.; George, J. H. *Org. Biomol. Chem.* **2017**, *15*, 4811.

[21] Lam, H. C.; Pepper, H. P.; Sumby, C. J.; George, J. H. *Angew. Chem. Int. Ed.* **2017**, *56*, 8532.

[22] Wu, J.; Kadonaga, Y.; Hong, B.; Wang, J.; Lei, X. *Angew. Chem. Int. Ed.* **2019**, *58*, 10879.

[23] a) Kopetzki, D.; Lévesque, F.; Seeberger, P. H. *Chem. Eur. J.* **2013**, *19*, 5450. b) Lévesque, F.; Seeberger, P. H. *Angew. Chem. Int. Ed.* **2012**, *51*, 1706.

[24] a) Crombie, L.; Redshaw, S. D.; Slack, D. A.; Whiting, D. A. *J. C. S. Chem. Comm.* **1979**, 628. b) Crombie, L.; Redshaw, S. D.; Slack, D. A.; Whiting, D. A. *J. Chem. Soc. Perkin Trans. I* **1983**, 1411.

[25] Crombiee, L.; Ponsford, R. *Tetrahedron Lett.* **1968**, *55*, 5771.

[26] This was inspired by the interpretation of UV-vis spectra from the Porco group around this time: Wen, S.; Boyce, J. H.; Kandappa, S. K.; Sivaguru, J.; Porco, J. A. *J. Am. Chem. Soc.* **2019**, *141*, 11315.

[27] Wu, H.; Hsung, R. P.; Tang, Y. *Org. Lett.* **2017**, *82*, 1545.

[28] Burchill. L.; George, J. H. *J. Org. Chem.* **2020**, *85*, 2260.

[29] Brill, W. F. *J. Am. Chem. Soc.* **1965**, *87*, 3286.

Chapter 5: Synthetic Studies, Isolation, and Biomimetic Oxidation of Prenylbruceol A

The work presented in this chapter is a continuation of our studies on *Philotheca* meroterpenoids presented in Chapter 3 and revisits the Schenck ene reaction discussed in Chapter 4. Some of the work presented in this chapter was completed with assistance from Dr. Henry Pepper and Joong Phan who are credited where relevant.

5.1 Introduction

5.1.1: Prenylbruceol Natural Products

In 1994, seven citran containing coumarins (**5.2** – **5.8**) were isolated from the aerial parts of *Philotheca myoporoides* (formerly *Eriostemon myoporoides*) (Figure 5.1).[1] These all contain the "bruceol" structure, differing by substitution of the C-2' hydroxyl group with differently oxidised prenyl groups. These prenylated bruceol analogues presumably share the common biosynthetic precursor **5.1**. Being close structural analogues of bruceol, these compounds naturally commanded our attention.

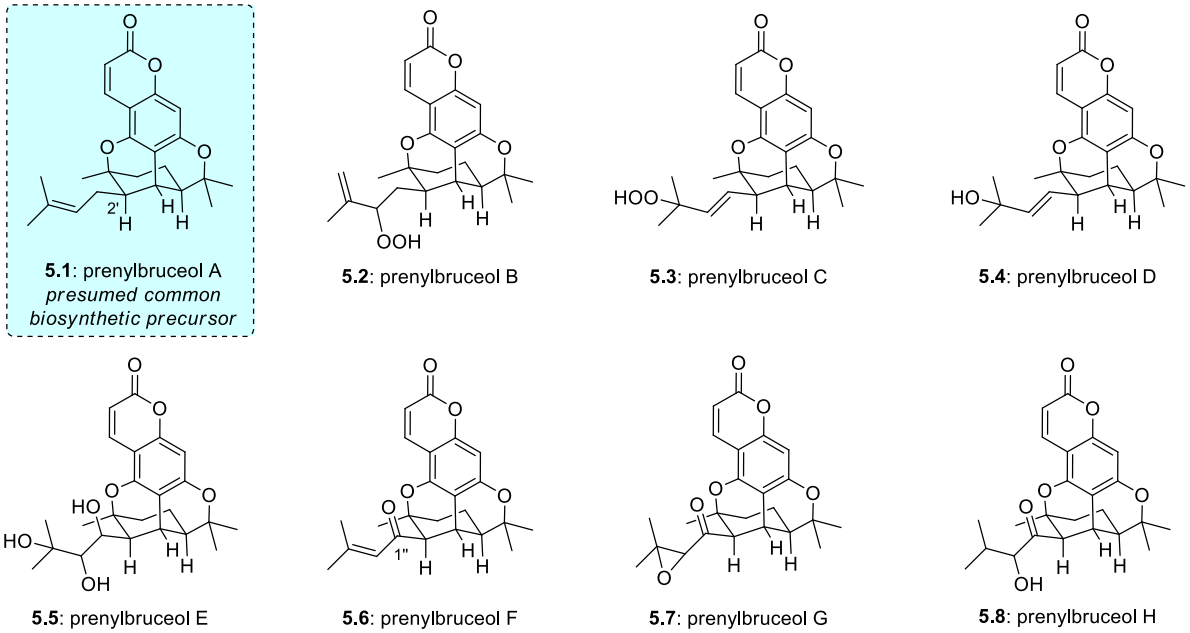

Figure 5.1: Prenylbruceol A-H (**5.1** – **5.8**) from *P. myoporoides*. Waterman (1994)

The isolation chemists did not give **5.2** – **5.8** trivial names, instead referring to them by semi-systematic names based on bruceol (for example, **5.2** was called 2'-{(*E*)-3-hydroperoxy-3-methylbut-1-enyl}-2'-deoxybruceol). These names are cumbersome, and we felt they detracted their significance as unique natural products, separate from bruceol. For this reason, we renamed the family the "prenylbruceols" and assigned alpha numerals A-H. **5.1** was given the name "prenylbruceol A" as we strongly believe this is the parent molecule. The remaining prenylbruceols were arranged in an arbitrary, but logical order. Prenylbruceol B – D (**5.2** – **5.4**) are products of a Schenck ene reaction (see Chapter 4), prenylbruceol E (**5.5**) is **5.4** that has been dihydroxylated. And lastly, prenylbruceol F-G (**5.6** – **5.8**) all contain oxidised C-1'' carbonyls.

5.1.2: Biosynthesis of the Prenylbruceols

Our interest in the prenylbruceols mainly stemmed from their unusual biosynthesis. The biosynthetic pathway was previously speculated by Ghisalberti in a review on the phytochemistry of Australian *Rutacae* (Scheme 5.2).[2] Here Ghisalberti proposed that protobruceol-I (**5.9**) could be prenylated at C-2' to give the *ortho*-quinone methide (*o*-QM) **5.10** which is primed to undergo intramolecular hetero-Diels-Alder reaction to prenylbruceol A (**5.1**). This pathway is analogous to the biosynthesis of bruceol (Chapter 3), where C-2' is oxidised with a monooxygenase enzyme. However, for this pathway to work a strange prenyltransferase enzyme would be required which can alkylate at C-2'.

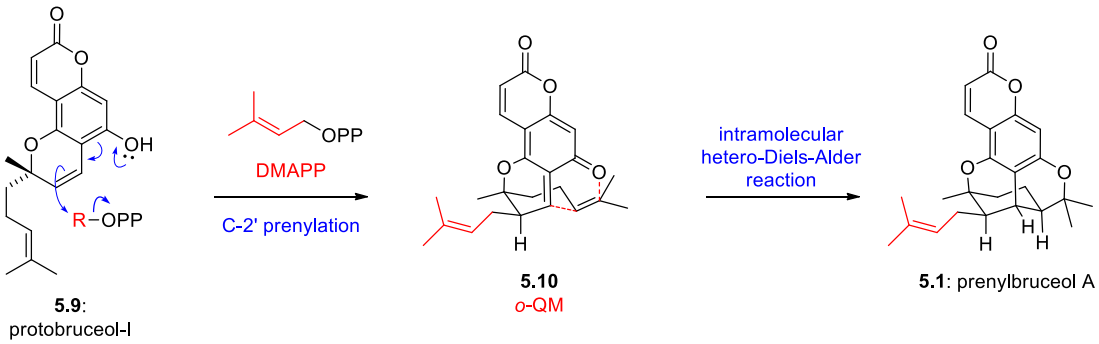

Scheme 5.1: Proposed biosynthesis of prenylbruceol A (**5.1**) via C-2' prenylation. Ghisalberti (1998)

We put forth an alternative biosynthetic hypothesis (Scheme 5.2). Protobruceol-I (**5.9**) can undergo a more conventional *O*-prenylation, which is very common in these plant families, to give the prenyl ether **5.11**. This could now undergo an aromatic Claisen rearrangement to **5.12**, followed by Cope rearrangement to give the same *o*-QM intermediate **5.10** from Scheme 5.1, which should readily give prenylbruceol A (**5.1**) by the same intramolecular hetero-Diels-Alder reaction.

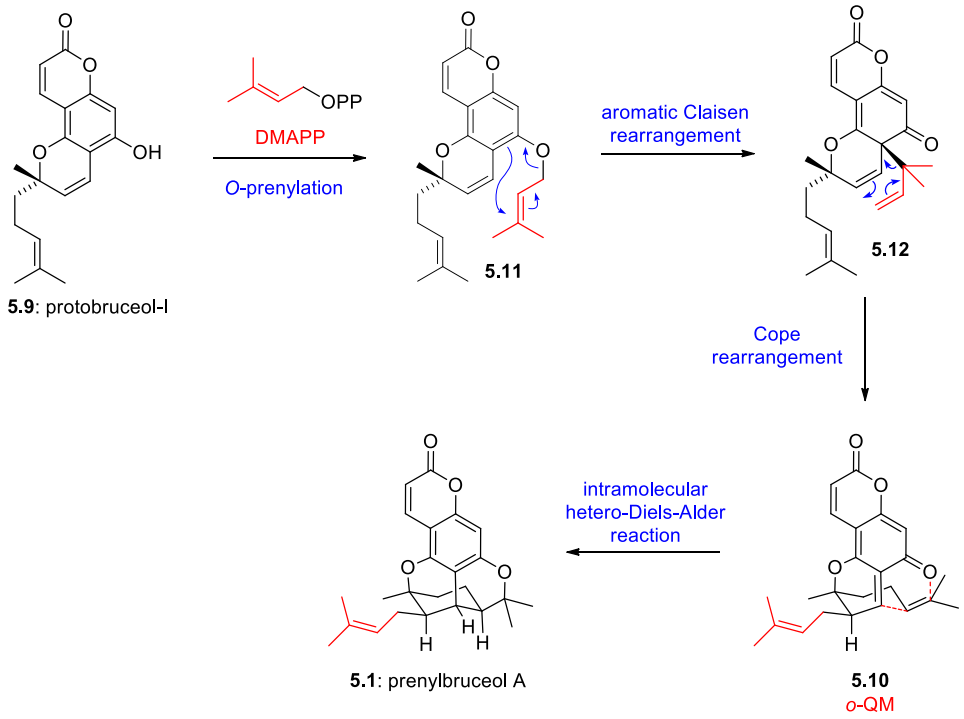

Scheme 5.2: Our proposed biosynthesis of prenylbruceol A (**5.1**) by Claisen-Cope rearrangements.

5.1.3: Artifacts of Natural Product Isolation

A necessary evil of natural products chemistry is the assault of the chemical source of interest (plant, fungi, bacteria culture, etc.) with a barrage of chemical (solvents, air, acid, or base) and physical (heat, or light) stresses during the extraction process. These stresses can alter the natural products within so that when the isolation is eventually complete, the new "natural products" isolated are in fact artifacts of what actually exists inside the natural source.[3] An ongoing challenge in natural products chemistry is being able to tell the difference between artifacts and true natural products. Generally, it

is best if the natural product can be detected as early as possible, with the fewest manipulation steps (ideally by analysis of crude extracts with NMR or GC-MS) or to isolate the same compound using different, milder extraction techniques.

Coumarins have previously been shown to be vulnerable to artifact formation under thermal conditions.[4] For example, angelical (**5.14**) was isolated from *Angelica pubescens* by saponification followed by high vacuum sublimation; however, when the extraction of *A. pubescens* was revisited by Hata and Koawa, this time instead by maceration in Et_2O followed by SiO_2 gel chromatography, no **5.14** was found but a new compound angelol (**5.13**) was found instead. Further, when pure angelol (**5.13**) was resubjected to the sublimation conditions the fragmented angelical (**5.14**) was collected in the receiver (Scheme 5.3a).[5] Similarly, Fukushima and co-workers showed that alloisoimperatorin (**5.16**) is probably an artifact of the related furanocoumarin isoimperatorin (**5.15**) by successive Claisen and Cope rearrangements during the dry vacuum sublimation of the petroleum ether extract of *Angelica dahurica* at 150 °C (Scheme 5.3b).[6]

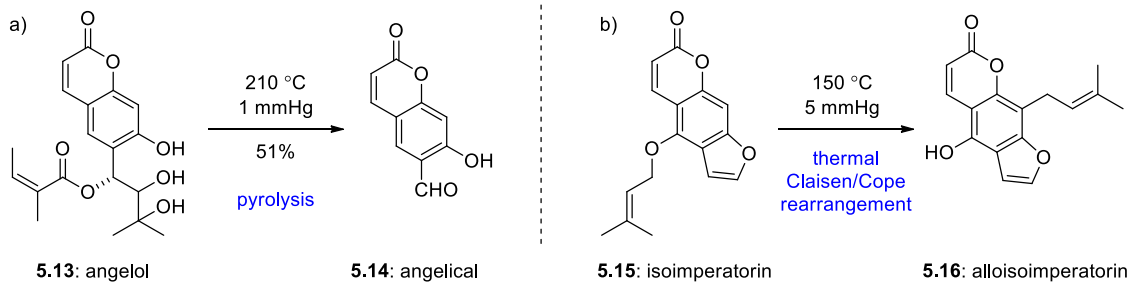

Scheme 5.3: Coumarin natural products believed to be isolation artifacts: a) angelical (**5.14**). Hata and Koawa (1967); and b) alloisoimperatorin (**5.16**). Fukushima (1971)

An example where biosynthetic speculation has been used to gain insight into natural products which may be artifacts of their isolation comes from our group. Our group has long been interested in the marine sponge meroterpenoid liphagal (not shown), and was able to demonstrate that its likely biosynthetic precursor is siphonodictyal B (**5.17**) by a biomimetic total synthesis.[7] It was during this

investigation that attention was brought to the related diastereomeric spirocycles corralidictyals A and B (**5.19** and **5.20**).[8] The fact that these are found as a mixture of epimers led us to believe the spiro-stereogenic centre was not formed under enzymatic control. The mechanism proposed was the electron rich aromatic ring is easily oxidised to a quinone (*para* or *ortho*, **5.18**) which could subsequently undergo a facile intramolecular cyclisation to give the corallidictyal natural products. In the laboratory, this transformation could occur by simply leaving siphonodictyal B (**5.17**) in an oxygen rich solution of MeOH for several days, resulting in a mixture of corallidictyal A (**5.19**) and corallidictyal B (**5.20**) of a similar ratio as what was isolated in Nature (Scheme 5.4).[9] Speculating on these results, it is plausible that **5.19** and **5.20** may be isolation artefacts, and formed after the marine sponge was removed from the relatively oxygen poor ocean.

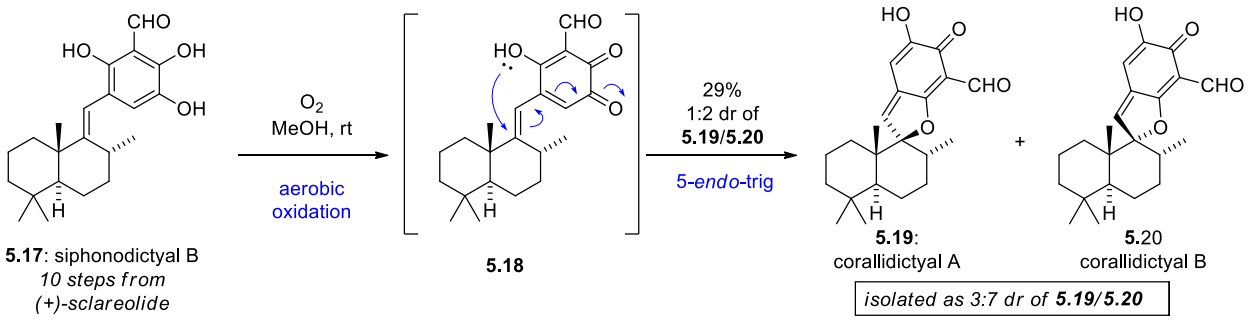

Scheme 5.4: Synthesis of corallidictyal A (**5.19**) and B (**5.20**) by aerobic oxidation. George (2015)

Returning to this current project: for the original extraction of *P. myoporoides*, the plant material was reported as being collected in New South Wales in 1991, whereas Waterman's group was based at the University of Strathclyde in Glasgow, Scotland, and the communication of **5.2** – **5.8** was published in 1994. Presumably, a long time had passed between collection and extraction. Further, the technique used by Waterman was Soxhlet extraction of the dried powdered material with petroleum ether for an unspecified time. It is for these two reasons we were suspicious of at least some of prenylbruceol B – H (**5.2** – **5.8**) being in fact artifacts of their isolation.

5.1.4: Aromatic Claisen and Cope Rearrangements

As mentioned previously, we proposed it is possible that the prenylbruceol family are biosynthesised through an aromatic Claisen/Cope/hetero-Diels-Alder cascade (*vide infra*). The Claisen rearrangement and the Cope rearrangement are classes of sigmatropic rearrangement reactions, and in this case, we are interested in those which occur in aromatic systems. The aromatic Claisen rearrangement (Scheme 5.5a) of the prenyl ether **5.21** for example will give the dearomatised intermediate **5.22**. This is the rate determining step and fast tautomerisation will give the *ortho*-reverse prenylated **5.23** (reverse prenyl = *α*,*α*-dimethylallyl) . The aromatic Cope rearrangement (Scheme 5.5b) must dearomatise before the sigmatropic rearrangement occurs. For example, the prenylated phenol **5.24** could tautomerise to the keto form **5.25** which is no longer aromatic. Following [3,3] sigmatropic rearrangement **5.26** can tautomerise to give the *para*-reverse prenylated **5.27**. In this case the Cope rearrangement would presumably give a mixture of **5.24** and **5.27** whereas the Claisen reaction always favours the carbonyl (or phenol).

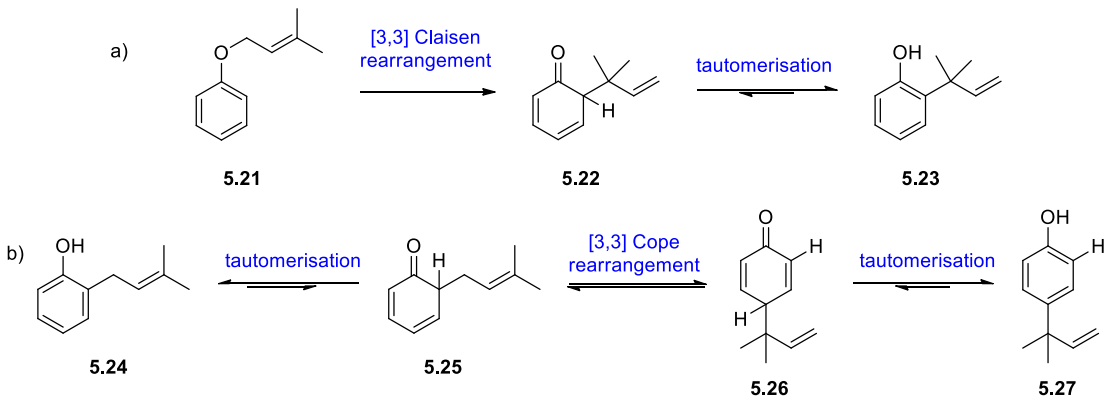

Scheme 5.5: Mechanism for: a) aromatic Claisen rearrangement; and b) Cope rearrangement.

The aromatic Claisen reaction has been utilised in biomimetic cascade reactions. Nicolaou and Lee developed a tandem double Claisen rearrangement and intramolecular Diels-Alder sequence in their synthesis of 1-*O*-methylforbesione (**5.31**) (Scheme 5.6). The tri-reverse prenylated (*α*,*α*-dimethylallyl) xanthone **5.28** was heated in DMF causing the thermal rearrangement to **5.29** as the

major pathway. Intramolecular Diels-Alder reaction affords the caged molecule **5.30**, which after a second Claisen rearrangement gives the natural product **5.31**. This reaction also gives rise to several isomers **5.32** – **5.34** from alternative Claisen rearrangement. The major by-product **5.33** is derived from an alternative initial Claisen reaction of the other reverse prenyl group.

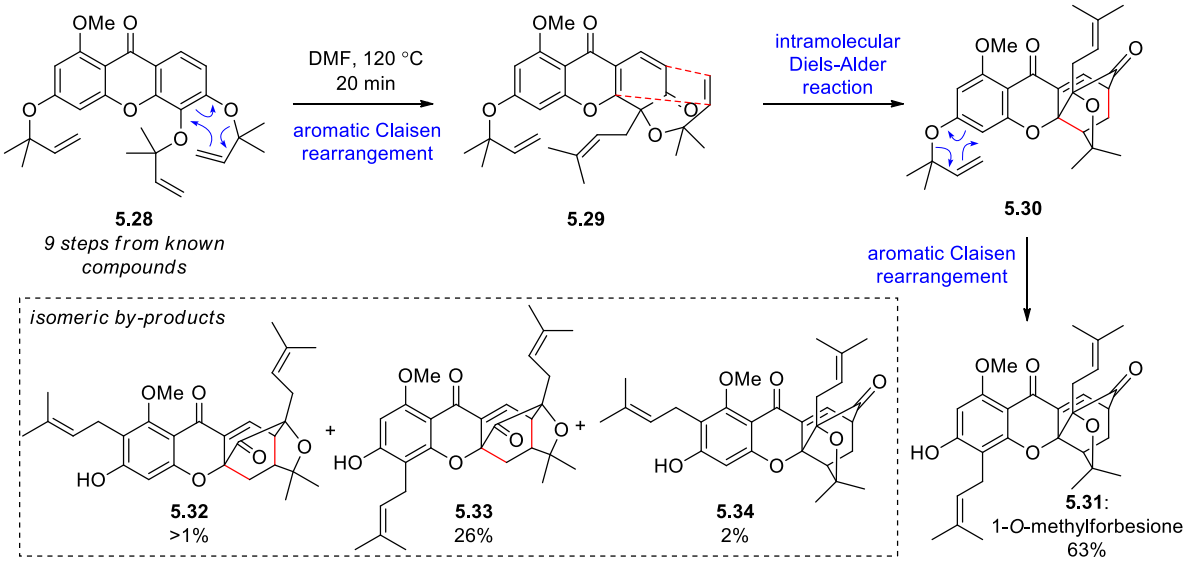

Scheme 5.6: Synthesis of 1-*O*-methylforbesione (**5.31**). Nicolaou and Lee (2001)

When paired, aromatic Claisen and Cope rearrangement reactions can be exploited to move a prenyl group to the *para* position of a phenol. Zhang and co-workers used this sequence in their synthesis of icaritin (**5.38**) (Scheme 5.7).[10] Here the functionalised chromone **5.35** was heated in the presence of the lanthanide catalyst $Eu(fod)_3$ in PhCl to promote the sigmatropic rearrangements. Aromatic Claisen rearrangement gives the reverse prenylated intermediate **5.36**, which undergoes further rearrangement to give **5.37** in good yield. The reaction favours the normal prenylated **5.37** as the quaternary centre in the reverse prenylated **5.36** is in a crowded position. Removal of the MOM and Bn protecting groups completed the synthesis of icaritin (**5.38**).

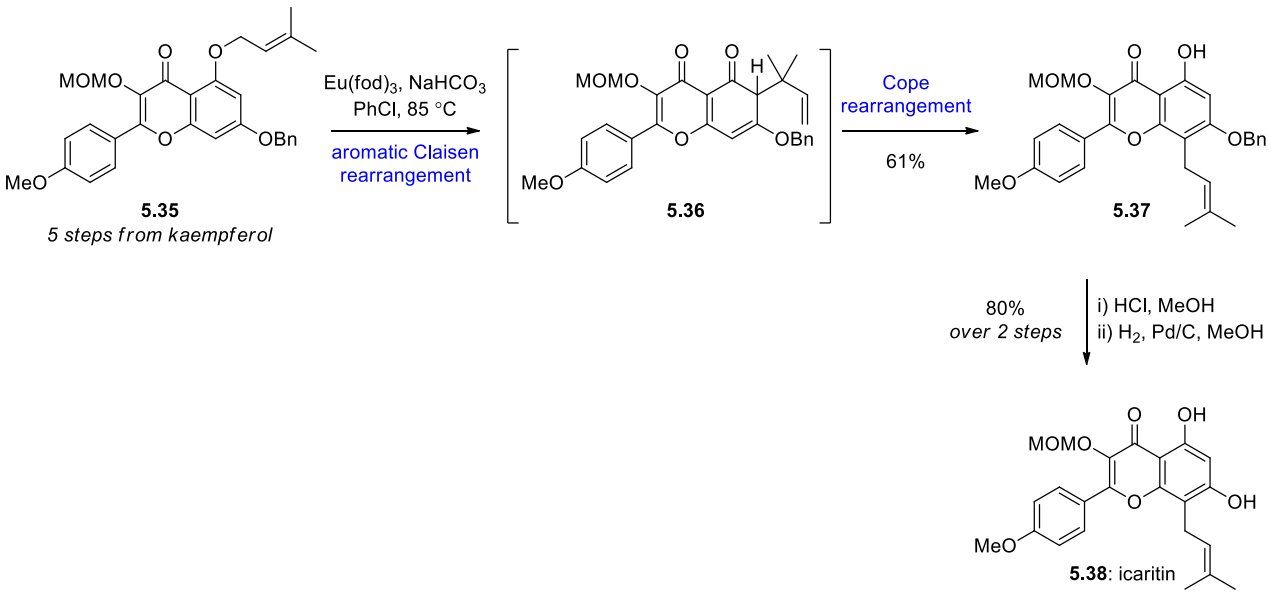

Scheme 5.7: Synthesis of icaritin (**5.38**) via Claisen-Cope rearrangements. Zhang (2015)

An example of coumarin meroterpenoid synthesis where successive Claisen and Cope rearrangements were used is in Harwood's synthesis of gravelliferone (Scheme 5.8).[11] Starting from 7-methoxycoumarin (**5.39**), methanolysis and alkene isomersation to phenol ester **5.40** followed by *O*-prenylation gives the substrate **5.41**. Heating **5.41** in dimethylaniline gave suberosin (**5.44**) in good yield by a Claisen rearrangement to either **5.42** or **5.43** and subsequent Cope rearrangement. Demethylation with boron trichloride to **5.45** and a second *O*-prenylation with prenylbromide and K_2CO_3 gave **5.46**. Heating this material in dimethylaniline facilitated Claisen rearrangement to intermediate **5.47** which can undergo two successive Cope rearrangements, to **5.48**, then to the natural product gravellifereone (**5.50**). Alternatively, the Claisen product **5.47** can intermediately cyclise and give the benzofuran **5.49**.

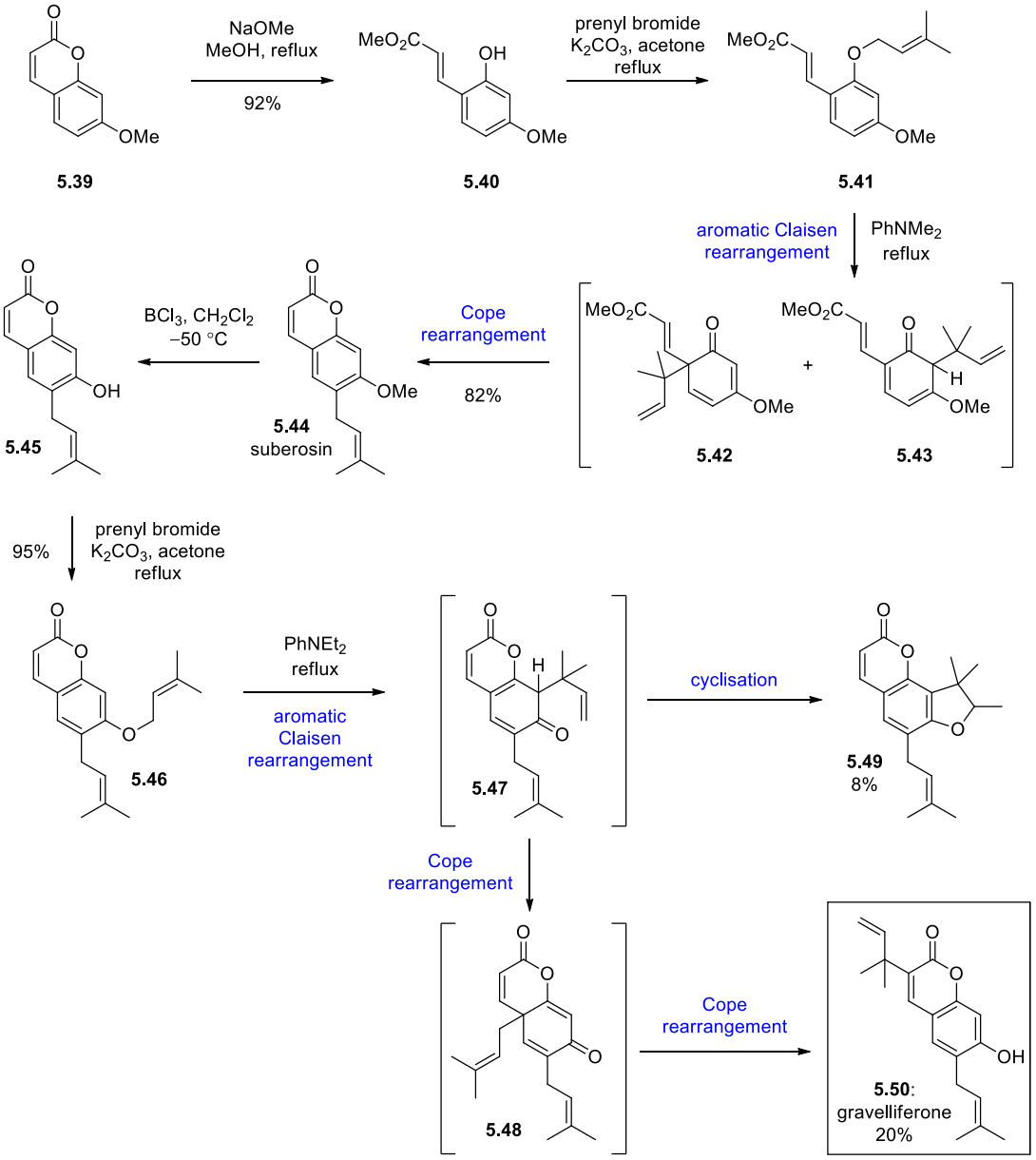

Scheme 5.8: Synthesis of gravelliferone (**5.50**) via Claisen-Cope rearrangements. Harwood (1987)

Similarly, Claisen-Cope rearrangements were used in Murray and Jorge's synthesis of the chromene-coumarin trachyphyllin (**5.54**) (Scheme 5.9).[12] Here prenyl ether **5.51** is heated in acetic anhydride, where after the initial Claisen and Cope rearrangements, the newly exposed phenol **5.52** is swiftly masked as the acetate **5.53**. This is a very clever trick as phenol **5.52** has the potential to tautomerise and undergo further Cope rearrangements, or other unwanted degradation pathways. Using acetic anhydride, the phenol is sequestered as it is formed. Deprotection to the natural product trachyphyllin (**5.54**) is easy and was achieved quantitatively by reaction with activated zinc powder in methanol.

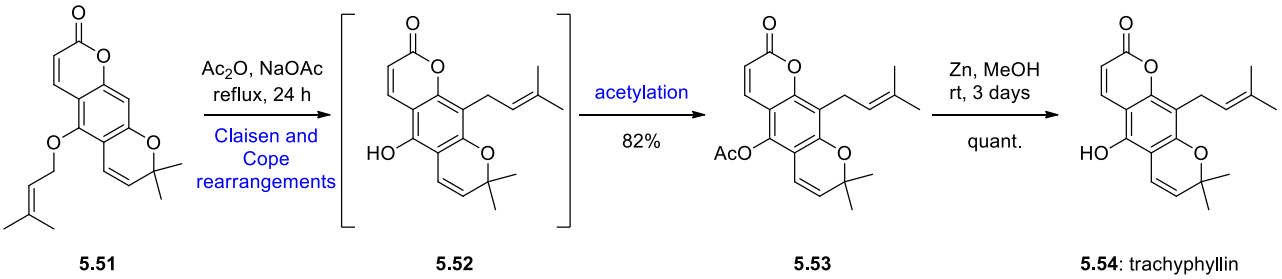

Scheme 5.9: Synthesis of trachyphyllin. Murray and Jorge (1984).

5.2 Results and Discussion

5.2.1: Attempted Synthesis of Prenylbruceol A (**5.1**) via Claisen-Cope Rearrangement

The first approach to the synthesis of prenylbruceol A (**5.1**) was the simplest, and most closely mirrored our biosynthetic proposal (Scheme 5.10). Prenylation of protobruceol-I (**5.9**) was smooth and readily gave the prenyl ether **5.11**. This reaction was checked carefully for the formation of any prenylbruceol A (**5.1**) by direct C-2' addition, but none was ever observed, including when alternative base and solvents (e.g. NaH, THF) were used, or with Tsuji-Trost conditions. For the rearrangement, heating in $PhNMe_2$, pyridine, $CHCl_3$ (with catalytic $Eu(fod)_3$), and PhCl (with catalytic $Eu(fod)_3$) were screened (Table 5.1). The thermal reactions all formed complex mixtures, but unfortunately prenylbruceol A (**5.1**) was never observed. The cleanest reaction came from heating **5.11** in pyridine to 150 °C in a microwave reactor (entry 1). Two major products were observed, **5.57** and **5.58**, which both arise from Claisen reaction to the less sterically hindered C-8 position to give **5.55**. From here, *O*-cyclisation gives the lesser product **5.57** as a 1:1 mixture of diastereoisomers (similar to the byproduct **5.49** observed by Harwood, Scheme 5.8). Alternatively, isomerisation of intermediate **5.55** to the linear chromene **5.56** by retro-6π- and 6π-electrocylisations afforded the deoxyisobruceol analogue **5.58** via a hetero-Diels-Alder cycloaddition. When **5.11** was refluxed in $PhNMe_2$ (entry 2), similar results were obtained, but the reaction was much messier. **5.57** and **5.58** were observed again, but the citran **5.58** was isolated as a mixture, presumably of the "bruceol orientation" citran **5.59** (though this could not be separated.

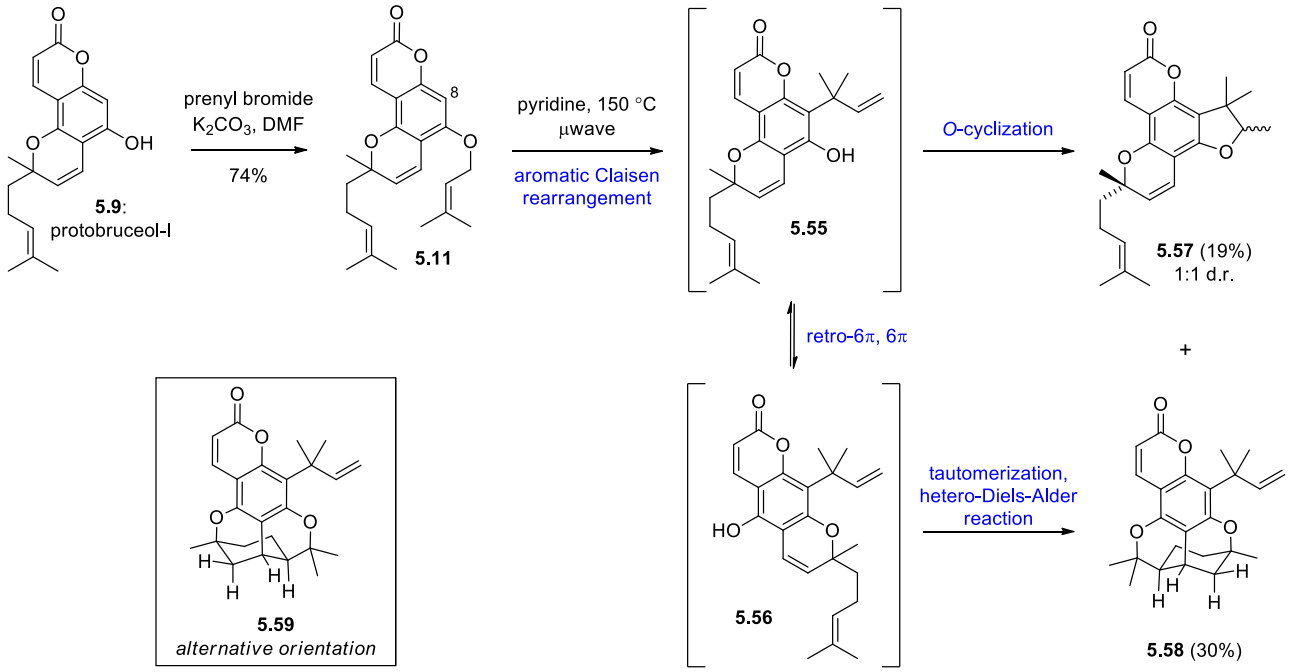

Scheme 5.10: Claisen rearrangement of **5.11**.

Table 5.1: Conditions screened for the rearrangement cascade of **5.11**.

Entry	Solvent/ additive	Temperature/ time	Result
1	pyridine	150 °C (μwave) 1 h 15 min	**5.57** (19%), **5.58** (30%)
2	$PhNMe_2$	reflux (194 °C), 2 h	**5.57** (17%), **5.58**/**5.59** (13% mixture) recovered **5.11** (5%),
3	$CHCl_3$, $Eu(fod)_3$ (10%)	60 °C, 14 d	No reaction
4	PhCl $Eu(fod)_3$ (10%)	85 °C, 7 d	Slow degradation

An important consideration was the orientation of the citran in **5.58**. With beautiful 1D and 2D NMR spectra this assignment was relatively straight forward. The most critical clue to the configuration comes from the HMBC spectrum. The C-5, C-7, and C-9 ^{13}C NMR signals are first assigned independently, for example, H-1' has $^{3}J_{H\text{-}C}$ with C-5 and C-7, but not with C-9 ($^{5}J_{H\text{-}C}$ is not observed). Additional HMBC correlations from H-1''-Me and H-4 are used to unambiguously assign the coumarin core. The key signals come from the $^{4}J_{H\text{-}C}$ correlation between H-3'-Me and H-7'-Me with C-7 and C-5 respectively (Figure 5.2). This correlation is only possible in the configuration shown in

5.58. Further, these HMBC signals are consistent with what was observed with isobruceol and *reversed* to what was observed with bruceol.

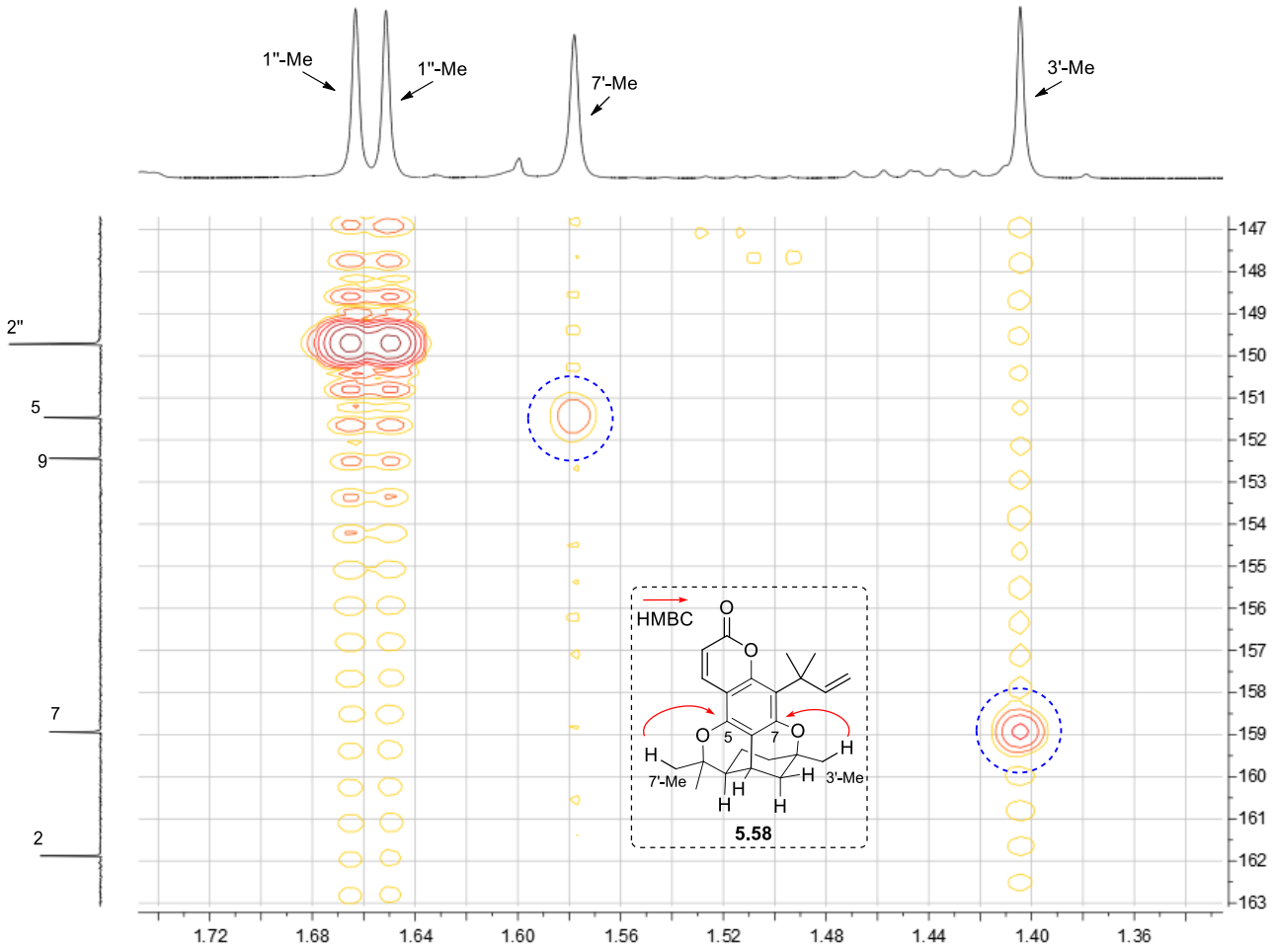

Figure 5.2: Determination of citran orientation using HMBC experiments.

While looking at the ^{1}H NMR spectra of bruceol, isobruceol, and related citrans that had been made up to this point a convenient observation was made. The chemical shifts of the coumarin ^{1}H signals (H-3 and H-4) remain fairly constant regardless of the substitution at C-2' (Figure 5.3). Of the citrans characterised, all which bare the coumarin/citran configuration of bruceol (10 compounds to date) had H-4 chemical shift within the 8.00 – 7.90 ppm, whereas those which have the isobruceol configuration (5 compounds to date) have lower H-4 chemical shifts between 7.90 – 7.80 ppm. With this trend, new compounds such as **5.58** can be tentatively assigned based on its proton spectrum. While the H-3 chemical shift is also quite consistent, it is not as distinct between the regioisomers.

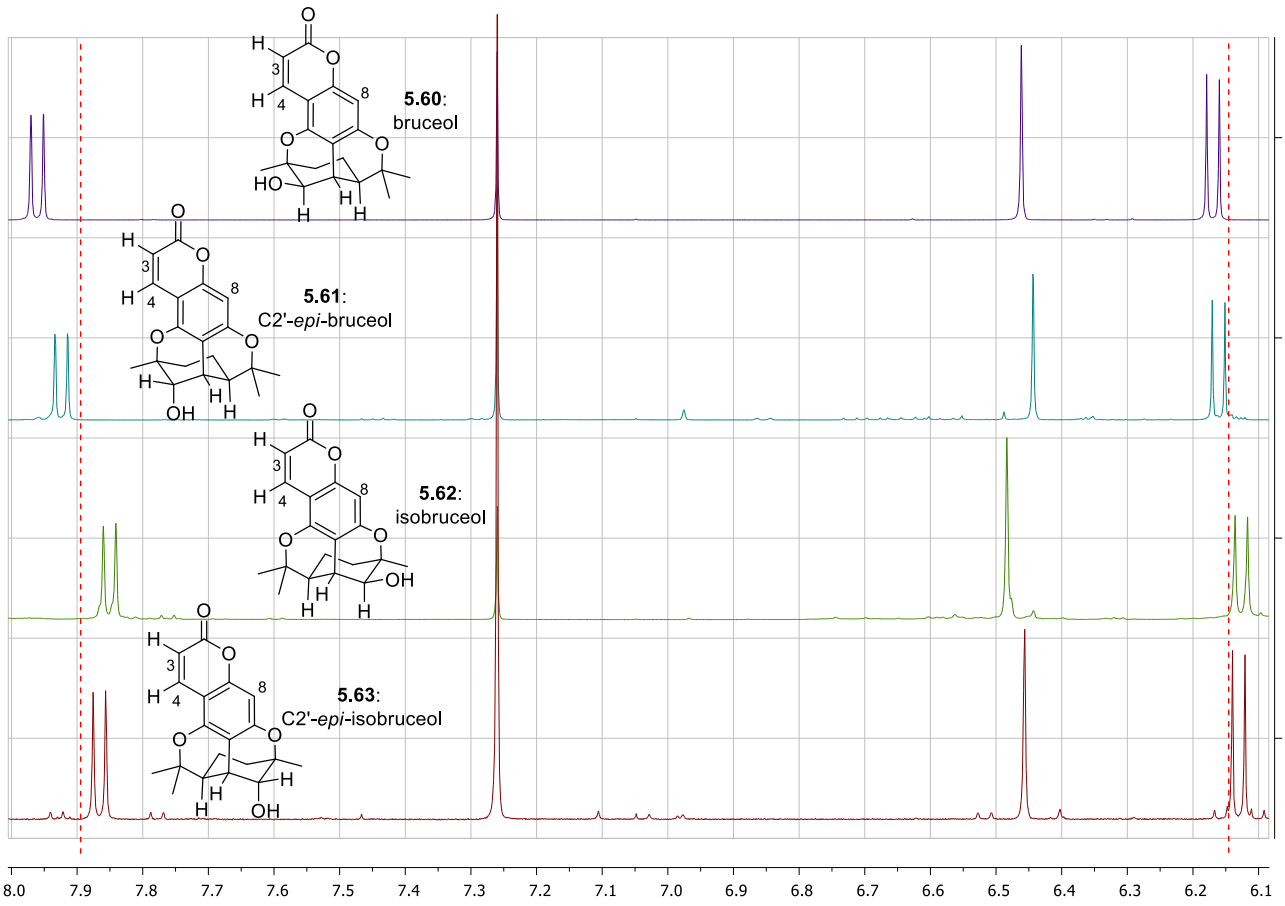

Figure 5.3: ^{1}H NMR comparison of a) bruceol (**5.60**); b) **5.61**; c) isobruceol (**5.62**); and d) **5.63**.

The problem with the proposed cascade was that the initial Claisen rearrangement would strongly favour migration to the prenyl group to the vacant C-8 position over C-6. Furthermore, the formation of by-products like **5.57** or **5.58** would destroy any chance of funnelling toward prenylbruceol A (**5.1**) by further rearrangements. To this end, we envisioned a similar cyclisation could be possible using the prenyl ether of the isobruceol precursor chromene **5.64** (Scheme 5.11). In this system, the prenyl ether is flanked by the substituted C-8 and C-10 carbons. We had hoped this would increase the chance of migration to C-6, and from here rearrangement to C-2' would be possible. A downside of this approach would be that the product would be **5.64**, not the natural product prenylbruceol A (**5.1**). Nonetheless, it would still be a beautiful cascade reaction, inspired by biosynthetic speculation.

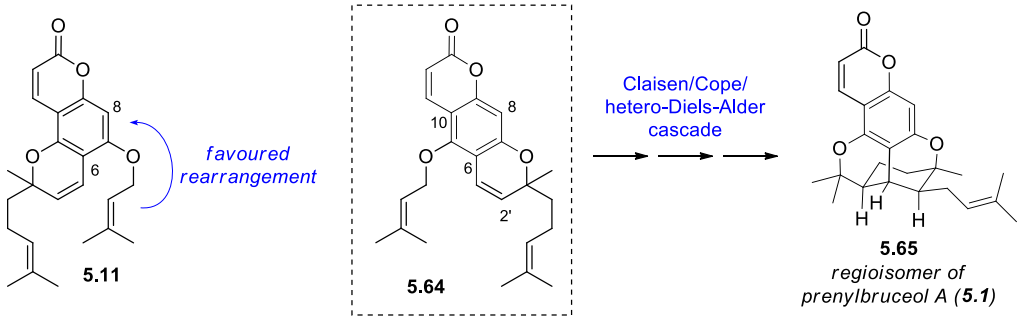

Scheme 5.11: Idea for an alternative cascade reaction using the new substrate **5.64**.

To execute this idea chromene **5.66** was prenylated to give the new substrate **5.64** (Scheme 5.12) and then heated to 150 °C in pyridine by microwave reactor. Unfortunately, this afforded the C-8 prenylated citran **5.71**. A possible mechaninsm for this reaction involves the prenyl ether **5.64** undergoing a Claisen rearrangement to C-10 **5.67** and Cope rearrangement to C-8 **5.68**, tautomerising to the chromene **5.69**. From here a reaction analogous to the deoxyisobruceol synthesis (Chapter 4.4.2) is possible: tautomerisation to *o*-QM **5.70** and intramolecular hetero-Diels-Alder reaction gives the observed product **5.71**. Interestingly, when the reaction was done in PhMe at the same temperature the observed product was instead the cyclobutane containing **5.72**, an analogue of eriobrucinol.

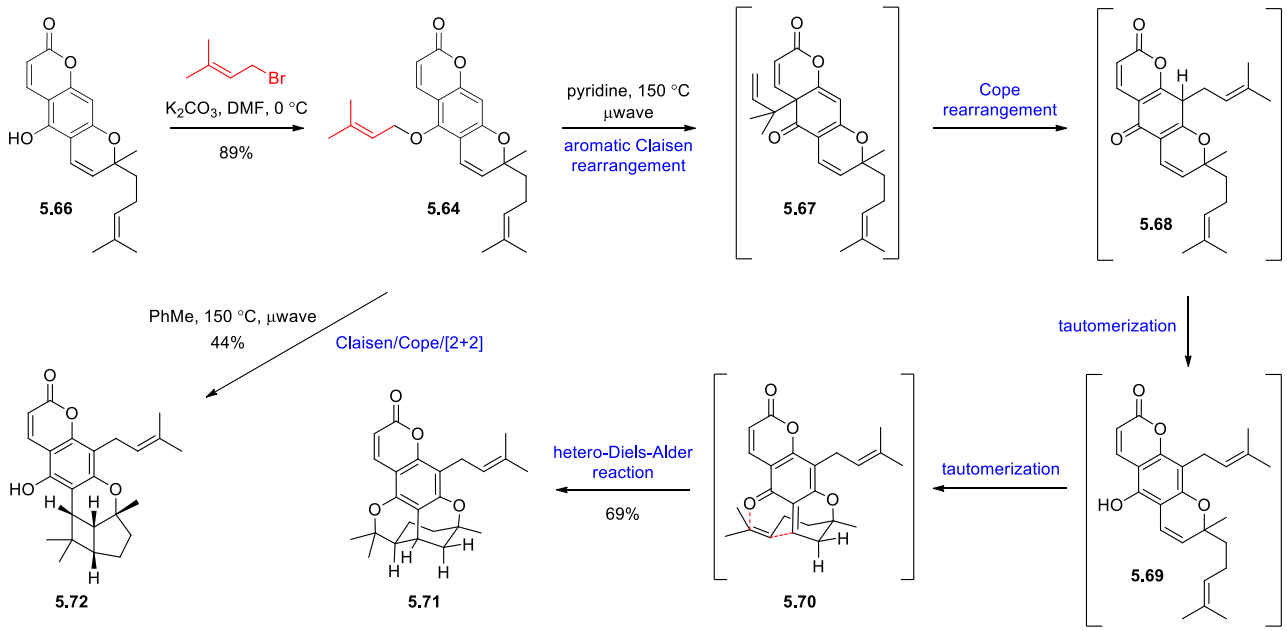

Scheme 5.12: Thermal rearrangements of the isomeric prenyl ether **5.64**.

After this approach did not work, we tried to think of alternative ways to prevent the vagabond prenyl group from rearranging to C-8. This work was completed alongside Joong Phan, an undergraduate placement student. One solution would be to "block" C-8 with a bulky group, forcing the rearrangement to favour the desired C-6 position. This could be done by using our existing thermal rearrangement chemistry but stopping after just the Claisen reaction. Inspired by the work of Murray[12] (*vide infra*), heating the *O*-prenylated protobruceol-I (**5.11**) in acetic anhydride gave the *O*-protected rearrangement product **5.73** in a very modest yield (Scheme 5.13). This low yield was due to various other competing reactions of the C_{10} chromene not possible in Murray's synthesis. Following this, ester hydrolysis to **5.74** and re-*O*-prenylation gave the prenyl ether **5.75** which contained a bulky quaternary centre blocking C-8.

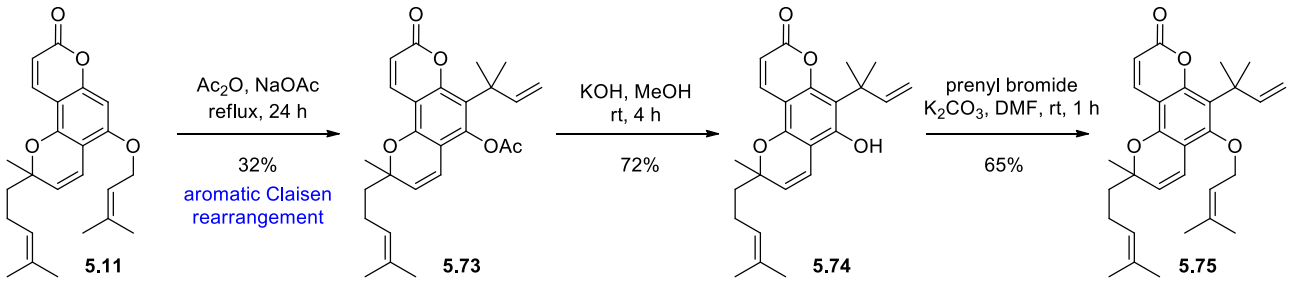

Scheme 5.13: Preparation of Claisen-Cope substrate **5.75** containing "blocking group" at C-8. This work was completed by Joong Phan under my supervision.

With the new substrate **5.75** in hand, it was subjected to the standard conditions of 150 °C in pyridine (Scheme 5.14). Again, none of the desired C-2' prenylated product (**5.78**) was formed. Instead, the major product was again **5.76** resulting from some kind of dealkylation, and also observed was the C-3 reverse prenylated **5.77**.

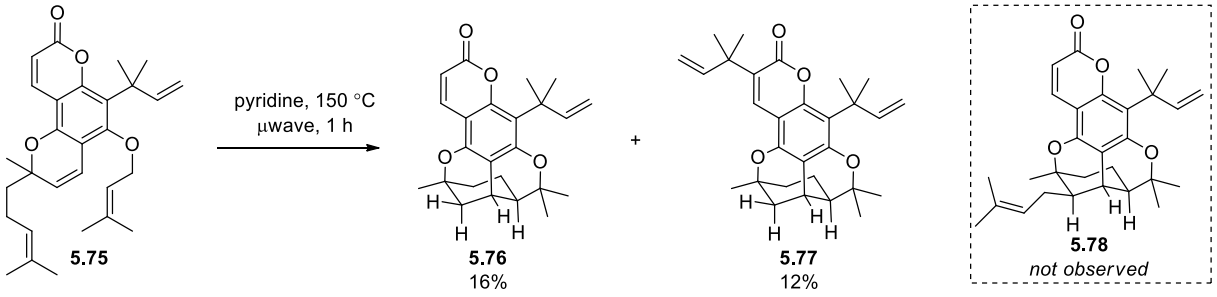

Scheme 5.14: Attempted thermal Claisen-Cope cascade of **5.75**. This work was completed by Joong Phan under my supervision.

With only negative results coming from the Claisen-Cope strategy it was time to consider other approaches to the synthesis of prenylbruceol A (**5.1**)

5.2.2: Attempted Synthesis of Prenylbruceol A (**5.1**) via [2+2], Retro-Diels-Alder, Diels-Alder Cascade

A key point of our strategy was to intercept the *o*-QM intermediate **5.10**. As an alternative to the initial Claisen-Cope cascade, an idea using a [2+2] cycloaddition / fragmentation sequence was envisioned (Scheme 5.15). Here the reverse prenyl ether of protobruceol-I (**5.79**) could undergo an intramolecular [2+2] cycloaddition to give the cyclobutane **5.80**. The rigid cyclobutane can open by a strain-release retro-Diels-Alder reaction revealing the desired *o*-QM (**5.10**) which can give the natural product prenylbruceol A through a hetero-Diels-Alder reaction. A potential downside of this approach is that the [2+2] cycloaddition to form the cyclol **5.81** might be faster than **5.80**. However, we thought this reaction might to be reversible using photo-redox conditions.

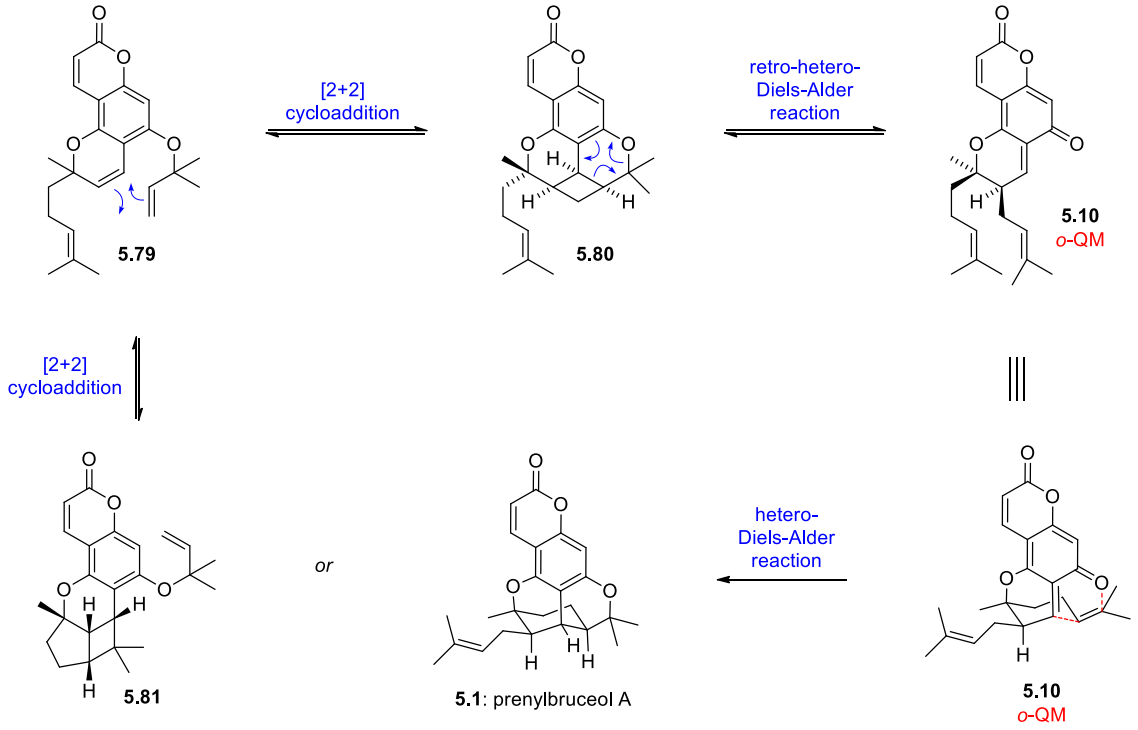

Scheme 5.15: Proposed mechanism for the synthesis of prenylbruceol A (**5.1**) involving a [2+2], fragmentation, hetero-Diels-Alder cascade.

Within our group, work on the nyingchinoid family of natural products had a similar reversible reaction. Subjecting chromene **5.82** to the photocatalyst 4-MeO-TPT with blue light gave fast conversion to the cyclol **5.83** which after deprotection became nyingchinoid D. However, if the reaction was left under the same conditions the endoperoxide **5.84** would slowly form as the dominant product. This work was completed by Jacob Hart. We hoped a similar reversible [2+2] would be possible with the reverse prenyl ether **5.79**.

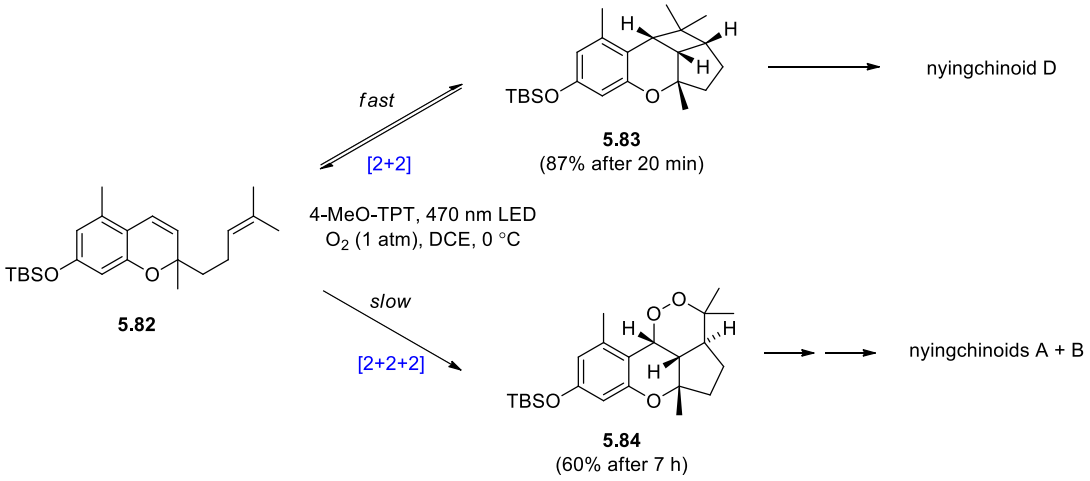

Scheme 5.16: Reversible photo-redox [2+2] and [2+2+2] in the synthesis of nyigchinoids A, B, and D. George (2019). This work was completed by honours student Jacob Hart under my supervision.

It was also apparent that the cyclobutane intermediate **5.80** could equally come from the linoloyl ether **5.85** (Scheme 5.17). This could be advantageous as there would not be a competing [2+2] reaction. Intramolecular [2+2] cycloaddition to **5.80** followed by retro-hetero-Diels-Alder reaction gives the *o*-QM **5.10** which can subsequently cyclise to give the natural product **5.1**.

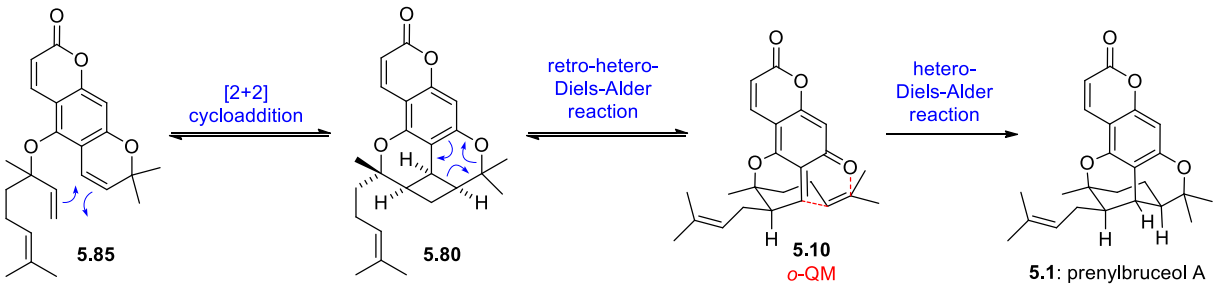

Scheme 5.17: Synthesis of prenylbruceol A (**5.1**) using alternative linaloyl ether **5.85**.

In order to have a more thorough investigation we planned to also try the cascade on the chromene ethers **5.86** and **5.87** (Figure 5.4, pink box). These would react to give the isomer of prenylbruceol A **5.65**.

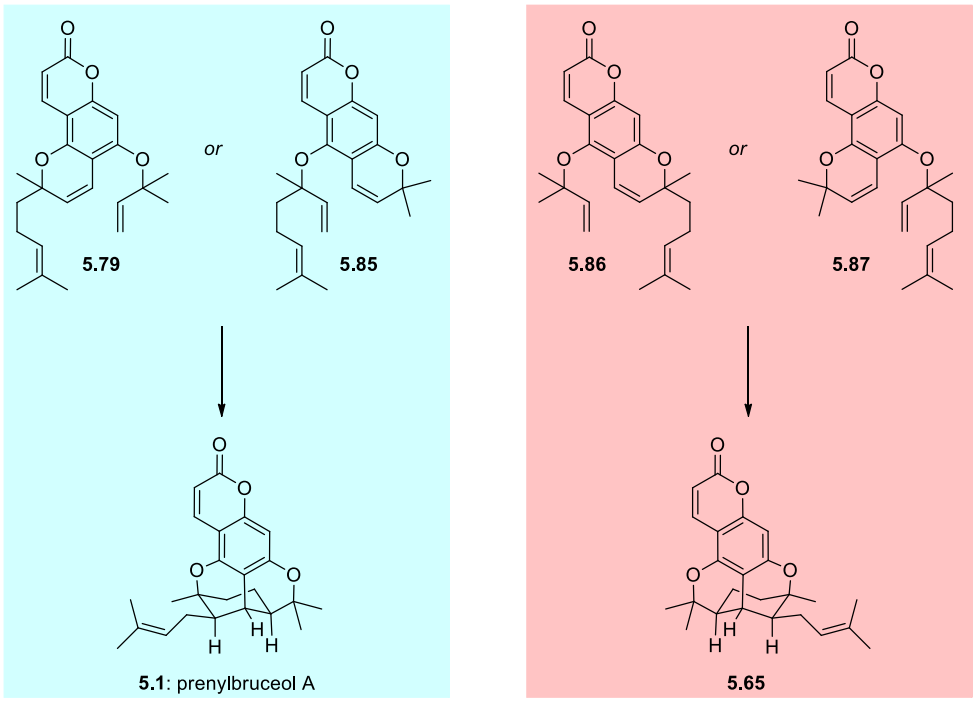

Figure 5.4: Four reverse prenyl substrates to try the cascade reaction on.

To make the substrates **5.85** and **5.87** the C_5 chromenes 7-hydroxyalloxanthyletin (**5.90**) and 5-hydroxyxanthyletin (**5.92**) were synthesised by analogous methods to the preparation of protobruceol-I (**5.9**) and its isomer (Scheme 5.18). Chromenylation of 5,7-dihydroxycoumarin gave a mixtrure of **5.90** and **5.91**. The purification of this reaction mixture was more difficult than the analogous mixture from the chromenylation of **5.89** with citral. The products were significantly less soluble and tended to precipitate within the chromatography column. Isomerisation of **5.91** gave the linear chromene **5.92**.

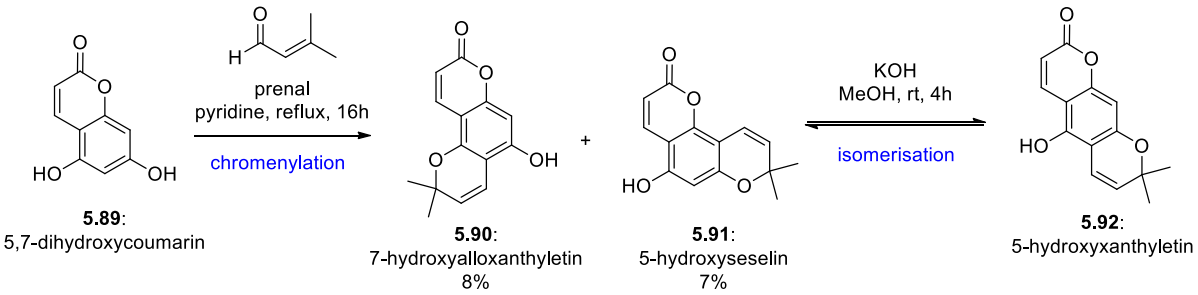

Scheme 5.18: Preparation of chromenes **5.90** and **5.92**.

The first [2+2] substrate **5.79** was prepared easily via a Tsuji-Trost allylation of protobruceol-I (**5.9**) (Scheme 5.19).

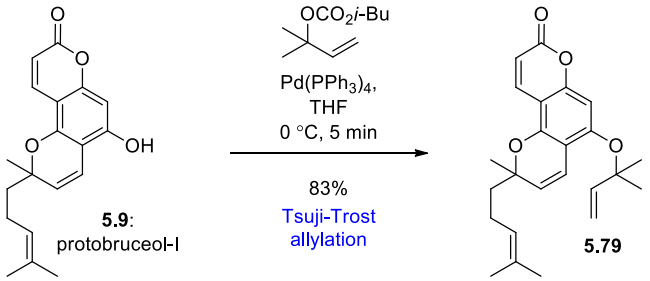

Scheme 5.19: Preparation of **5.79** by Tsuji-Trost allylation.

Tsuji-Trost allylation of 7-hydroxyalloxanthyletin (**5.90**) with linoloyl isobutyl carbonate gave the ether **5.87** in modest unoptimised yield (Scheme 5.20).

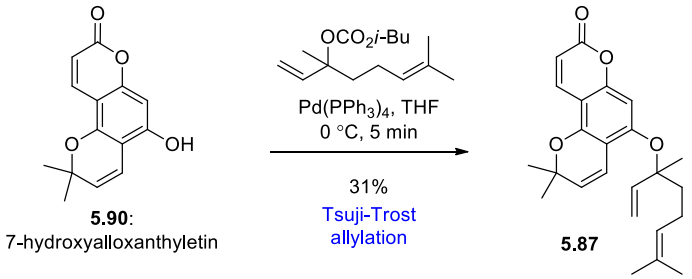

Scheme 5.20: Preparation of **5.87** by Tsuji-Trost allylation.

Tsuji-Trost allylation of the linear chromene **5.66** was not as straightforward (Table 5.2). Using the same isobutyl carbonate as for protobruceol-I (**5.9**) gave inconsistent results with the major product being the isobutyl ether **5.93** (entries 1 – 7), only once was the desired reverse prenyated product **5.86** observed as the major product over the normal prenylated **5.64**, this was on the first attempt and could not be reproduced (entry 1). Still, the ethers **5.86** and **5.64** (as well as **5.93**) could not be separated by chromatography, so more conditions were screened to try and fix this.

Table 5.2: Conditions for the Tsuji-Trost allylation of **5.66**. [a] **5.66** added to reaction mixture. [b] addition via syringe pump. [c] ratio from crude ^{1}H NMR.

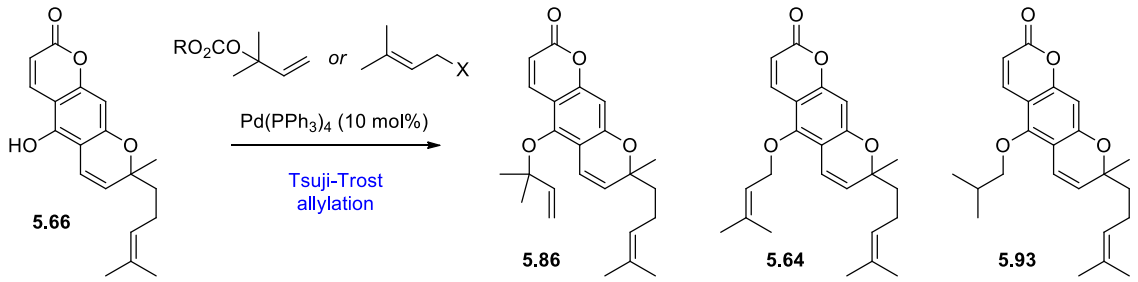

Entry	Electrophile	Solvent	Temp/time	Base	Result (Yield/ratio)
1	*i*-Bu carbonate (5.0)	THF	rt, 1 h	-	2.7:1:5.7 **5.86**/**5.64**/**5.93** (~55%)
2	*i*-Bu carbonate (5.0)	THF	0 °C, 20 min	-	**5.93** (20%)
3	*i*-Bu carbonate (5.0)	THF	0 °C, 20 min	-	**5.93** (24%)
4	*i*-Bu carbonate (5.0)	THF	40 °C, 4.5 h	-	**5.93** (20%), RSM (64%)
5	*i*-Bu carbonate (5.0)	PhMe	60 °C, 3 h	-	**5.93** (27%) RSM (60%)
6	*i*-Bu carbonate (5.0)	THF	5 °C → rt, 2 h	Cs_2CO_3 (2.0)	**5.93** (23%), No RSM
7	*i*-Bu carbonate (10.0)[a]	THF	rt, 1 h 40 min[b], +15 min, rt	-	1:1.8:2.7 **5.86**/**5.64**/**5.93** (~34%), RSM (54%)
8	methyl carbonate (5.0)	THF	0 °C, 3 h	-	No rxn
9	*t*-Bu carbonate (5.0) *10 mol% Pd_2dba_2	THF	0 °C, 3 h,	-	1:1.7[c] **5.64**/dba ligand
10	*t*-Bu carbonate (5.0)) *1 mol% $Pd(PPh_3)_4$	THF	0 °C → rt	-	1:5.2 **5.86**/**5.64** (20%) RSM (74%)
11	prenyl Br (5.0)[a]	THF	0 °C → rt, ~2 h[b]	Cs_2CO_3 (2.0)	2:1 **5.86**/**5.64** (69%)
12	prenyl Br (5.0)[a]	THF	0 °C, 2 h[b] +15 min	NaH (2.0)	1:2.1 **5.86**/**5.64** (18%) RSM (54%)
13	prenyl Br (5.0)[a]	THF	rt, 2 h[b], +15 min	NaH (2.0)	1:2.2:5.7[c] **5.86**/**5.64**/RSM
14	prenyl Cl (5.0)[a]	THF	−10 °C, 1 h[b] → rt, 1h	Cs_2CO_3 (2.0)	1:7:0 **5.86**/**5.64** (23%)
15	prenyl Cl (5.0)[a]	THF	0 °C, 1 h[b]	NaH (2.0)	2.2:1 **5.86**/**5.64**(15%)

As the unwanted transfer of the isobutyl group was observed, the methyl carbonate was used instead but resulted in no reaction (entry 8). Similarly, the *t*-butyl carbonate was made, this was reactive but showed poor selectivity toward the desired **5.86** over **5.64** (entries 9 and 10). From here the more old-fashioned use of allyl halides with base additive was considered. To combat the obviously problematic direct reaction of **5.66** with the prenyl halide the order of addition was reversed (i.e. a solution of **5.66** was added to a mixture of the electrophile, base, and catalyst). The first attempt of this type of reaction was very promising using prenyl bromide and $CsCO_3$ giving **5.86** as the major isomer and in good yield (entry 11) but was not so successful with NaH (entries 12 and 13). Prenyl chloride was tried, the hope being that as a poorer electrophile it might be less susceptible to direct reaction with **5.66**. Unfortunately, yields were much poorer, and selectivity was not good (entries 14 and 15).

A reason why the reaction was not very successful for the chromene **5.66** might be because the phenol is sterically hidden, flanked by two rings, and has trouble adding to a bulky π-allyl palladium complex. Formation of mixtures of **5.86** and **5.64** was not useful, and combined with the poor overall yields there was not much reason continue pursuing this approach. The same would be true of the C_5 chromene 5-hydroxyxanthyletin (**5.92**) so the reaction substrates **5.86** and **5.87** could not be accessed.

Taking the substrate **5.79** the optimised photoredox conditions from the nyngchinoids project was employed (Scheme 5.21). Although O_2 is not incorporated into the product it is still necessary for the reaction to progress, acting as a "shuttle" for electrons. The reaction quickly formed the cyclol **5.81** with complete conversion after only a few minutes. To prevent potential oxidation, anthracene was used as an additive so the reaction could be done under an inert Nitrogen atmosphere. After 3 hours the reaction was quenched and no prenylbruceol A (**5.1**) was observed whatsoever. This suggested that the [2+2] reaction was not reversible and this strategy would not be viable.

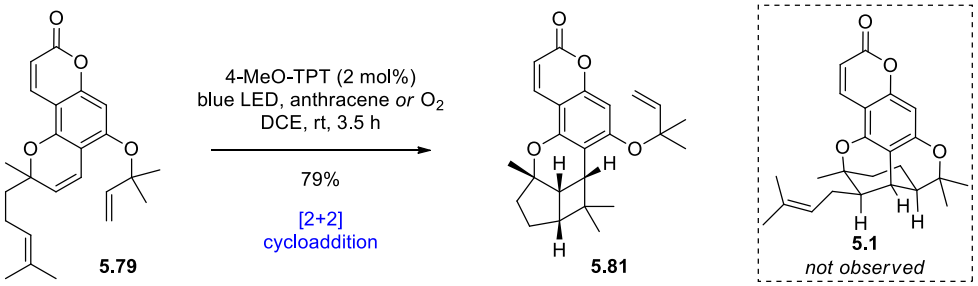

Scheme 5.21: Subjecting substrate **5.79** to photoredox conditions.

With the linoloyl substrate **5.87** the same conditions were employed (Scheme 5.22). This time undesired [2+2] reaction is not possible. Disappointingly, no reaction occurred at all.

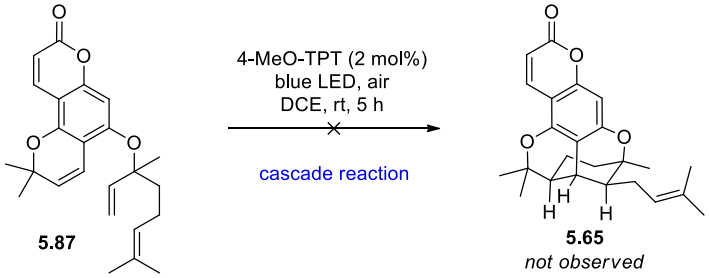

Scheme 5.22: Subjecting substrate **5.87** to photoredox conditions.

5.2.3: Synthesis of Halogenated Bruceol Analogues

Searching for an alternative to a cascade reaction a more conservative cross-coupling approach was envisioned (Scheme 5.23). An activated analogue of bruceol **5.94** could react with prenyl nucleophile via a palladium catalysed cross coupling reaction. This work was done with the help of Dr Henry Pepper.

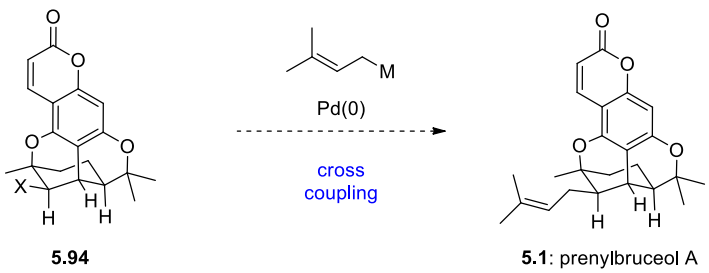

Scheme 5.23: Proposed synthesis of prenylbruceol A (**5.1**) from halogenated bruceol analogue **5.94**.

From the outset, a problem with cross coupling reactions with a dimethyl allyl substrate is the poor selectivity for the α product compared to γ product (Scheme 5.24). It is for this reason the reversed prenylated product is observed in the Tsuji-Trost reaction (*vide infra*).

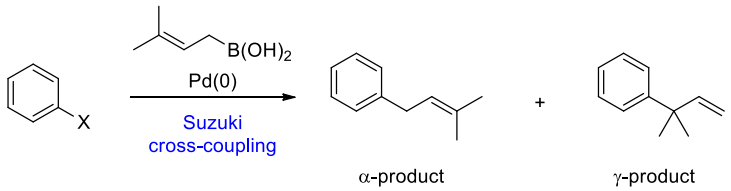

Scheme 5.24: Selectivity problem with cross-coupling reactions of allylic boronic acids/esters.

This has been overcome through the development of specialised palladium catalysts. Organ and co-workers were able to prenylate the model substrate **5.95** with excellent (97:3 **5.96**/**5.97**) α selectivity using the somewhat exotic air-stable Pd-PEPPSI-IPent catalyst developed within their group (Scheme 5.25).[13] When using the more common $Pd(PPh_3)_4$ the selectivity was reversed (5:95, **5.96**/**5.97**).

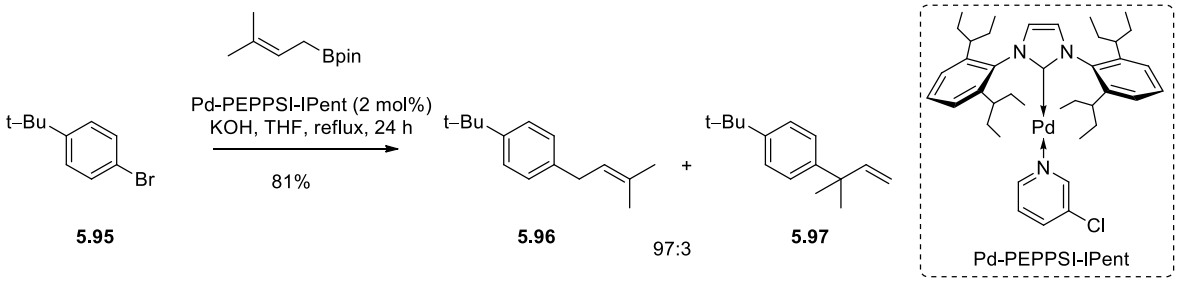

Scheme 5.25: Selective Suzuki cross-coupling using Pd-PEPPSI-IPent catalyst. Organ (2012)

As for the substrates for cross coupling reaction to form **5.1**, we imagined that the cascade reaction to make bruceol could also be done using an electrophilic halogen source. To this end, protobruceol-I (**5.9**) was treated with 3 equivalents of NBS (Scheme 5.26). The fastest reaction is the bromination at C-8, each product isolated contained bromine at this position. Bromination at C-3 is slower and

occurs only to some degree, bromination at C-2 gives **5.98** with only slight facial selectivity. This opens to *o*-QM **5.99** which cyclises to give the mixture of products **5.100a/b** and **5.101a/b**. Initially, reactions done in THF gave similar results; however, the bruceol analogues were contaminated with an unusual brominated THF side product. To simplify the reaction mixture a large excess of NBS was used. This had little to no effect on the ratio of products. Presumably, all of the bromination at C-3 occurs before cyclisation, and after cyclisation C-3 is no longer nucleophilic. To try to make just the mono-brominated product a handful of brominating reagents were screened, using just a single equivalent. This was not fruitful. What was observed in every case was a mixture of mostly C-8 brominated chromene, as well as the four citran products **5.100a/b** and **5.101a/b** and starting material. The brominating reagents screened were: NBS, Br_2, tetrabromocyclohexadieneone, and the exotic $Et_2SBr{\cdot}SbCl_5Br$ (Snyder's reagent) which has been used to initiate polyene cyclisation cascade reactions.[14] The halogenation work was completed alongside Dr. Henry Pepper.

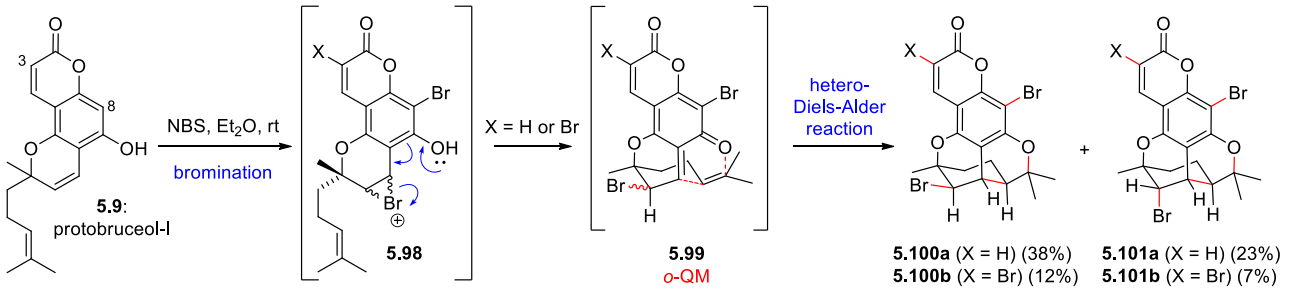

Scheme 5.26: Bromination of **5.9**. This work was completed with help from Dr. Henry Pepper.

The halogenation reaction was also induced using NIS (Scheme 5.27). This worked similarly well to the bromination reaction, giving mixture of **5.102a/b** and **5.1023/b**.

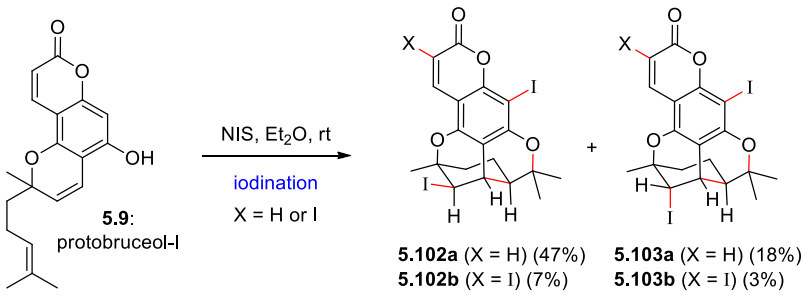

Scheme 5.27: Iodination of **5.9**.

Lastly, the cascade was attempted using chlorination reagents (Scheme 5.28). This did not work at all. The reaction gave a complex mixture of products, the only one which was identified was the product of chlorination at C-8. No trace of citran products was observed.

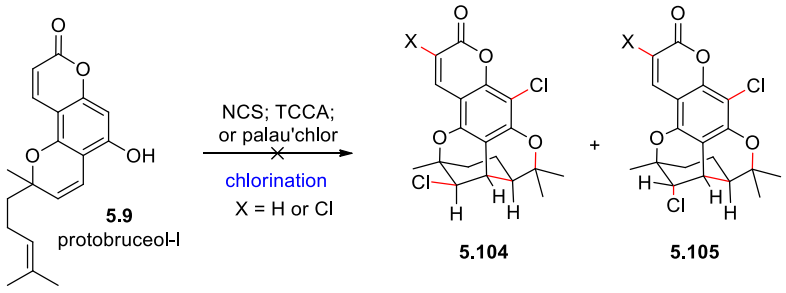

Scheme 5.28: Attempted chlorination of **5.9**.

With these halogenated products in hand, we focused on trying to convert the dibrominated **5.100a** into the monobrominated **5.106** which would be suitable for cross coupling (Table 5.3). The aromatic bromide could be removed using *n*-BuLi (entry 1) but was very low yielding with mostly decomposition. Using *t*-BuLi gave complete decomposition, with no product observed (entry 2). Next, catalytic palladium was used, but resulted in no reaction (entry 3). Finally, radical debromination with tributyltinhydride lead to decomposition. This was disappointing and meant there would not be much **5.106** to try cross coupling reactions with.

Table 5.3: Conditions screened for the monodebromination of **5.100a**. This work was completed by Dr Henry Pepper

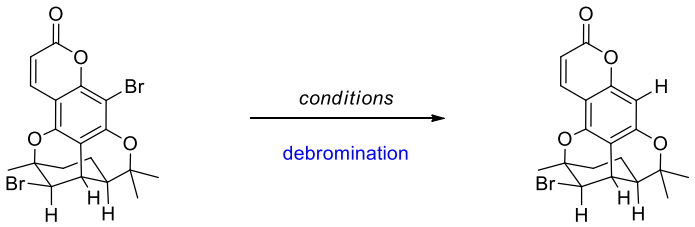

5.100a **5.106**

entry	reagents (equiv)	conditions	result
1	*n*-BuLi (1.2)	THF, −78 °C	**5.106** 16%
2	*t*-BuLi (1.2)	THF, −78 °C	Decomposition
3	$Pd(OAc)_2$ (0.05), PPh_3 (0.2), K_2CO_3 (2.0)	*n*-BuOH, 100 °C	No reaction
4	$HSnBu_3$ (10), AIBN (cat.)	PhH, reflux	decomposition

Some attempts at a Stille cross-coupling reaction with allyltributylstannane as a proof of concept for this reaction were performed on both **5.106** and the dibromide **5.100a**, however only decomposition was observed. A more thorough investigation may have been warranted, but this was where the project was left off. An exhaustive screen could have been done if I made significant amounts of **5.106**, a library of exotic palladium catalysts (such as the Pd-PEPPSI-IPent catalyst), and several prenyl electrophiles (prenylB(OH_2), prenylBpin, prenylBcat etc.); but this would have taken a long time. This would also be truly outside the biomimetic ideology of the research group so it was not pursued any further.

5.2.4: Isolation of Prenylbruceol A (**5.1**)

In the wake of three failed synthetic expeditions into the prenylbruceol family of natural products a new way forward was needed to progress further in this venture. Having a taste for natural product

isolation from our discovery of isobruceol in *Philotheca brucei* (Chapter 3.2.4) we saw extraction as something to explore.

The natural source of prenylbruceols B – H *Philotheca myoporoides* is often used as an ornamental native plant and is commonly sold at gardening stores. I was able to purchase two small plants (Figure 5.5) for ~$26 AUD from Bunnings Warehouse, a chain hardware store.

Figure 5.5: left: *P. myorporoides* plant purchased from Bunning's Warehouse. right: the same plant 12 months later.

After having the plants for only 1-2 weeks we were able to find a large *P. myoporoides* plant in Dernancourt, in the northern suburbs of Adelaide (Figure 5.6). The plant was easily 10 times the size of the sapling purchased from Bunnings and the owner agreed to donate the clippings from their annual pruning, after the plant finished flowering. The clippings were taken, and the leaves were carefully removed from the twigs and branches. Only about 300 – 400 g of fresh leaves were harvested, most of the bulk of the clippings was in the sticks; however, this was more than adequate for our investigations, and meant that the saplings could be saved.

Figure 5.6: left) Large *P. myporoides* plant form a suburban Adelaide garden; centre) fresh plant clippings as received; right) plant material separated into twigs, leaves, and flowers.

Our hypothesis was that the true precursor to prenylbruceols B – H (**5.2** – **5.8**) was prenylbruceol A (**5.1**) so the main goal was to isolate **5.1** and prove that it is a natural product. For this, special care was taken to avoid the formation of artifacts during the handling and extraction of the plant material. The separated leaves were kept out of direct sunlight and used shortly after the harvest. For the extraction, the pressurised hot water extraction (PHWE) method was used. This was chosen as it has been shown to minimise formation of artifacts and works well on smaller scale extractions. This method was also used in the isolation of bruceol and isobruceol (Chapter 3.2.4).

Using 35% aqueous ethanol solution, the fresh chopped leaves of *P. myoporoides* was extracted using a conventional unmodified espresso machine (Scheme 5.29). The characteristic ^{1}H NMR signal s of the citran ring system allowed prenylbruceol A (**5.1**) to be quickly identified out of the extract. Four other major products were observed in the mixture which had not been observed in *P. myoporoides* previously. These were: protobruceol-I (**5.9**) which was the most abundant product, ostruthin (**5.107**), the natural precursor to **5.9**, and dipetalolactone (**5.109**). Lastly, there was the dihydrocoumarin **5.108**, which had never been reported as a natural product.

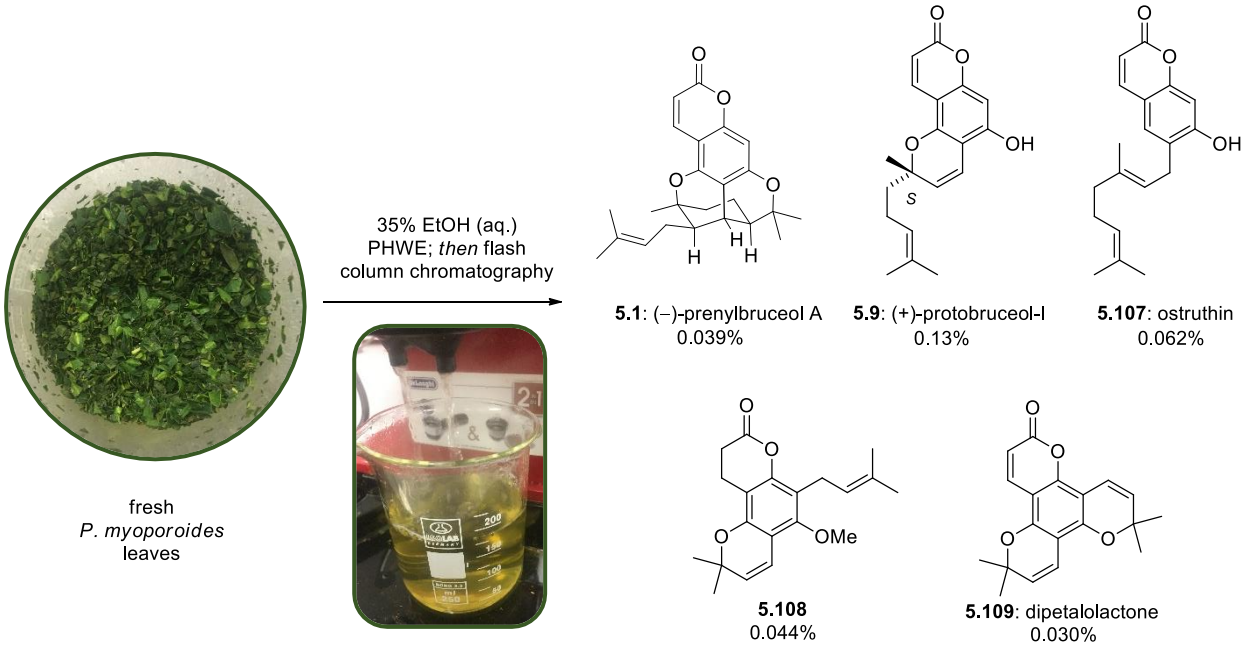

Scheme 5.29: Isolated products from the PHWE extraction of *Philotheca myoporoides*.

The structure of prenylbruceol A (**5.1**) was proven by NMR analysis. Assignment of the ^{1}H and ^{13}C NMR spectra was greatly assisted by comparison with the multitude of published spectra of similar molecules such as bruceol (**5.60**) and prenylbruceols B – H (**5.2** – **5.8**). However, special care was taken to ensure the relative orientation of the citran and coumarin rings was correct, as mistakes have been made regarding this in the past. This regiochemical problem could be addressed in the same way the synthetic compound **5.58** was determined (Figure 5.2, *vide infra*). Firstly, the ^{13}C signals for C-5, C-7, and C-9 of the coumarin core were independently assigned using $^{3}J_{C\text{-}H}$ and $^{2}J_{C\text{-}H}$ HMBC correlations from H-4 and H-1', and H-8 respectively (Figure 5.7a). From here, the relative citran/coumarin orientation is determined by $^{4}J_{C\text{-}H}$ correlations from H-Me-3' and H-Me-7' (Figure 5.7b).

Lastly, the orientation of the prenyl group at C-2' was determined. The H-2' signal appears as a broad singlet, with $^{3}J_{H\text{-}H}$ coupling constant close to 0 Hz; this was rationalised by the rigid caged framework keeping H-1' and H-3' with an approximately 90° dihedral angle. Furthermore, a clear co-axial NOE correlation is observed between H-2' and H-6' (Figure 5.7c). The absolute configuration is

presumably the same as that of natural (−)-bruceol (i.e. as drawn) as it has similar optical rotation of the same sign, and was co-isolated with (+)-protobruceol-I (**5.9**) which is known to have the *S* configuration at C-3'.

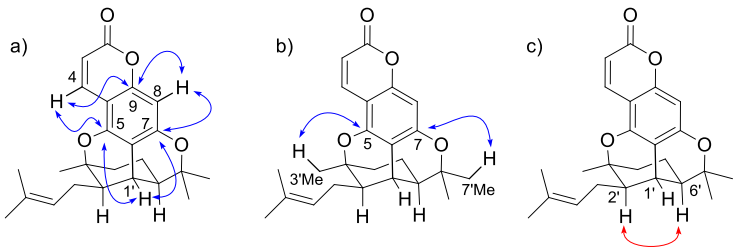

Figure 5.7: Key HMBC (blue) and NOESY (red) correlations for the structural assignment of prenylbruceol A (**5.1**).

This extraction was repeated several times. Each time the extract was carefully examined for the presence of prenylbruceols B – H (**5.2** – **5.8**), however, none of these products were ever found. This supported our suspicion that these natural products may be artifacts. It must be noted that other factors (age of the plant, season, health) can affect what natural products are present, so denouncing the status of the other members of the prenylbruceols is still somewhat speculative.

5.2.5: Biomimetic Oxidation of Prenylbruceol A (**5.1**)

Overall, about 100 – 150 mg of prenylbruceol A (**5.1**) was isolated using all of the *P. myoporoides* leaves available to us. Rather than leaving this on the shelf, the material was taken on to use in a semi-synthesis of the remaining prenylbruceols.

Prenylbruceol A (**5.1**) was subjected to singlet oxygen giving a mixture of prenylbruceol B (**5.2**) and prenylbruceol C (**5.3**) (Scheme 5.30). The formation of **5.3** as the major product is consistent with the observations of Orfanopolous (See Chapter 4.2.4).[15] Interestingly, the minor product prenylbruceol B (**5.2**) was formed as a single isomer, evidence of high facial selectivity of the approach of singlet

oxygen. The configuration of C-2'' was not assigned in the initial isolation of **5.2**. Attempts to form crystals of **5.2** for X-ray diffraction were unsuccessful. Derivatisation, for example, reduction of the hydroperoxide and esterification with (+)- and (−)-Mosher's acid could potentially be used to determine the absolute stereochemistry of C-2'.[16] Based on the assumption of the absolute stereochemistry of prenylbruceol A (**5.1**), the relative configuration of **5.2** would be known.

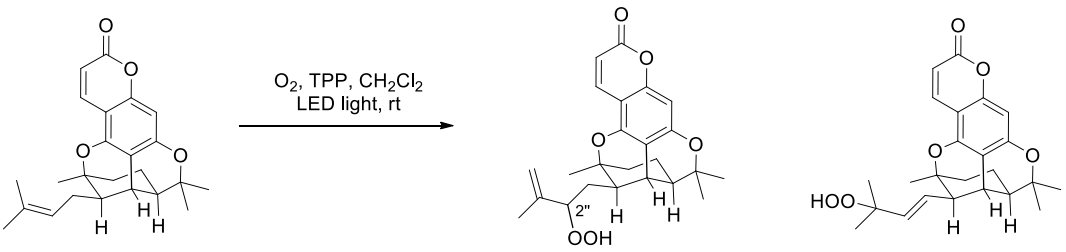

5.1: prenylbruceol A

5.2: prenylbruceol B
16%

5.3: prenylbruceol C
46%

Scheme 5.30: Singlet oxygen reaction of prenylbruceol A (**5.1**).

Both hydroperoxides **5.2** and **5.3** were reduced using $NaBH_4$ but unfortunately, the recovery of these reductions was poor. Only a few milligrams of **5.110**, from the reduction of prenylbruceol B (**5.2**) was obtained (Scheme 5.31a). Attempted crystallisation of this material was not successful, and there was not enough material for Mosher ester analysis. Reduction of the more predominant prenylbruceol C (**5.3**) gave prenylbruceol D (**5.4**) (Scheme 5.31b). A milder reducing agent such as PPh_3 may have given better yields, but there was insufficient material to optimise this reaction.

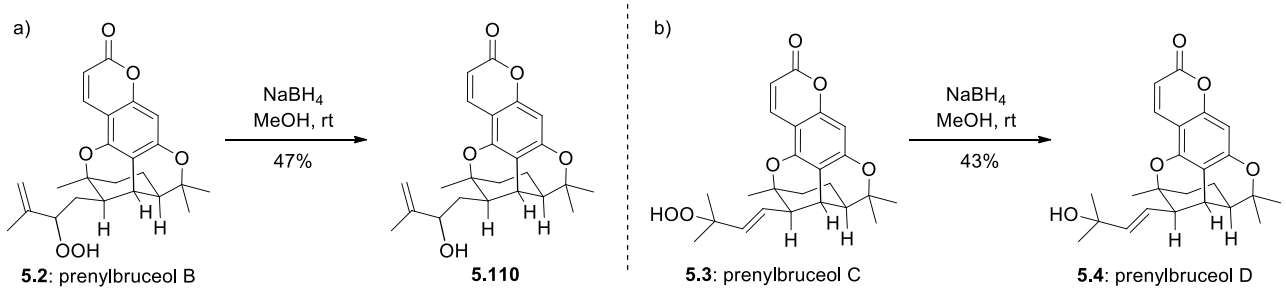

5.2: prenylbruceol B

5.110

5.3: prenylbruceol C

5.4: prenylbruceol D

Scheme 5.31: Hydroperoxide reduction of a) prenylbruceol B (**5.2**); and b) prenylbruceol C (**5.3**).

With 20 – 30 mg of prenylbruceol D (**5.4**) in hand attention was turned to the synthesis of the remaining prenylbruceols. There was two obvious ways to use **5.4**: dihydroxylation would give prenylbruceol E (**5.5**), and oxidative allylic transposition would give prenylbruceol F (**5.6**). A potential pitfall of dihydroxylation is diastereoselectivity (Scheme 5.32). Prenylbruceol E (**5.5**) has 2 undefined stereocentres, and thus has 4 potential structures. Dihydroxylation of **5.4** with either syn selectivity (e.g. Upjohn dihydroxylation) or anti selectivity (e.g. epoxidation and hydrolysis) would give the complementary isomer pairs. While this is an interesting problem, there would be no guarantee the correct isomer would be made, and a mixture of isomers would be undesirable considering there is not much material to work with. On the other hand, oxidative transposition would not lead to stereochemical problems, and has the added bonus that it could potentially lead to synthesis of prenylbruceol G (**5.7**) and prenylbruceol H (**5.8**).

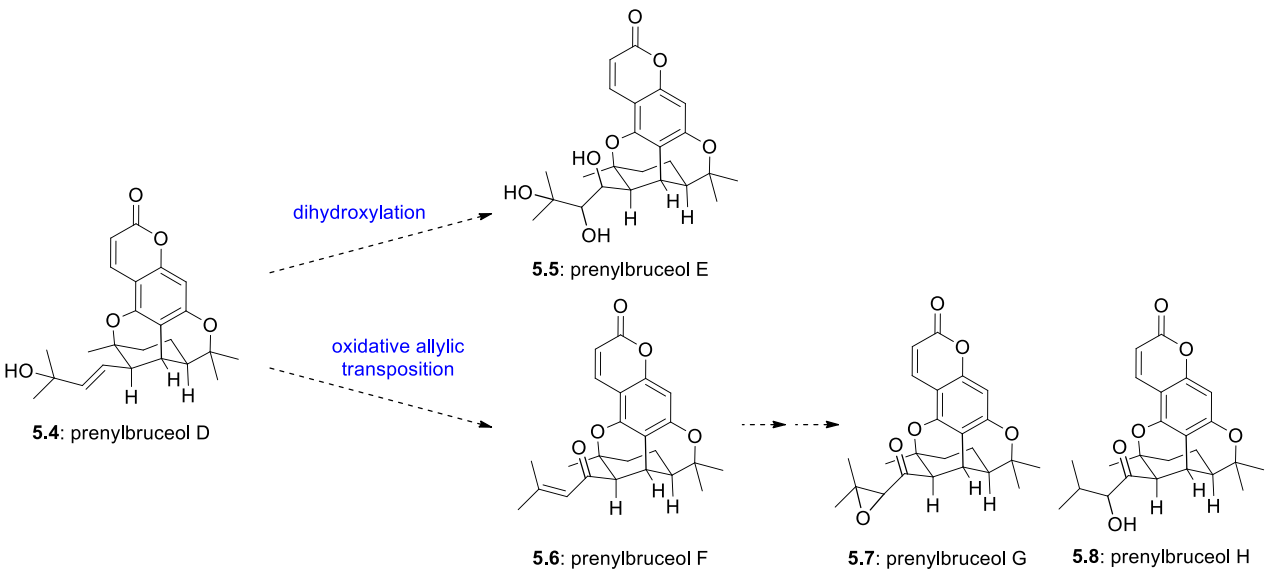

Scheme 5.32: Possible uses of prenylbruceol D (**5.**) in semi-synthesis of the prenylbruceols.

As there was only a small amount of material, milder conditions were employed first. There had been some precedent for the Babler-Daubin oxidation of cyclic allylic alcohols using IBX in DMSO for Iwabuchi and co-workers.[17] Finney and More had shown oxidations of alcohols to carbonyls using IBX in refluxing EtOAc.[18] As IBX is poorly soluble in EtOAc at ambient temperatures and *slightly* soluble in EtOAc at reflux, purification is as simple as filtering the cooled reaction. This was tried using freshly recrystallised IBX, but no reaction was observed (entry 1). From here Iwabuchi's exact

conditions were followed, but again no reaction occurred (entry 2). At this point only a few milligrams of **5.4** remained (the material was repurified after each reaction with IBX by chromatography). The final conditions tried were classic Babler-Daubin conditions using PCC which resulted in no initial reaction, but slowly degraded as it was left overnight (entry 3).

Table 5.4: Conditions for Babler-Daubin oxidation of prenylbruceol D (**5.4**).

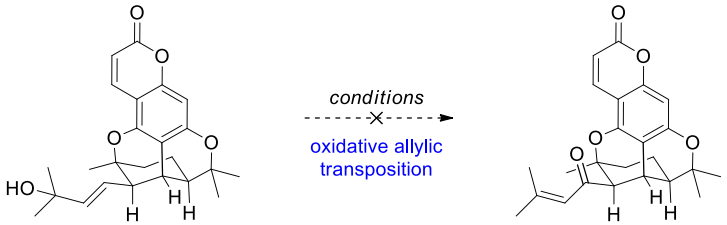

5.4: prenylbruceol D

5.6: prenylbruceol F

entry	oxidant (equiv.)	conditions	result
1	IBX (1.5)	EtOAc, reflux, 5 h	no reaction
2	IBX (2.0)	DMSO, 60 °C, 16 h	no reaction
3	PCC (2.0)	CH_2Cl_2, rt, 18 h	slow degradation

With no material left, and no *P. myoporoides* remaining, the project had reached its natural conclusion. While synthesis of the remaining prenylbruceols E – H (**5.5** – **5.8**) had not been achieved, the main goal of isolating prenylbruceol A (**5.1**) which biosynthetic speculation suggests *should* exist was a success. Using **5.1** in the semi-synthesis of prenylbruceols B – D (**5.2** – **5.4**) highlighted the relationship of the prenybruceols through autoxidation pathways.

5.3 Summary and Conclusion

In conclusion, biosynthetic considerations of the meroterpenoids of *P. myoporoides* led us to believe prenylbruceol A (**5.1**) was an undiscovered natural product. Three unique approaches were explored for the synthesis of **5.1** which required the development of cascade reactions involving pericyclic mechanisms. None of these approaches were successful in synthesising prenylbruceol A (**5.1**). Instead, prenylbruceol A (**5.1**) was isolated from *P. myoporoides* using fresh plant material and the mild PHWE method alongside four coumarin natural products not previously reported within the species. The natural prenylbruceol A (**5.1**) then used in a semi-synthesis of prenylbruceol B – D (**5.2** – **5.4**) by a biomimetic Schenck ene reaction.

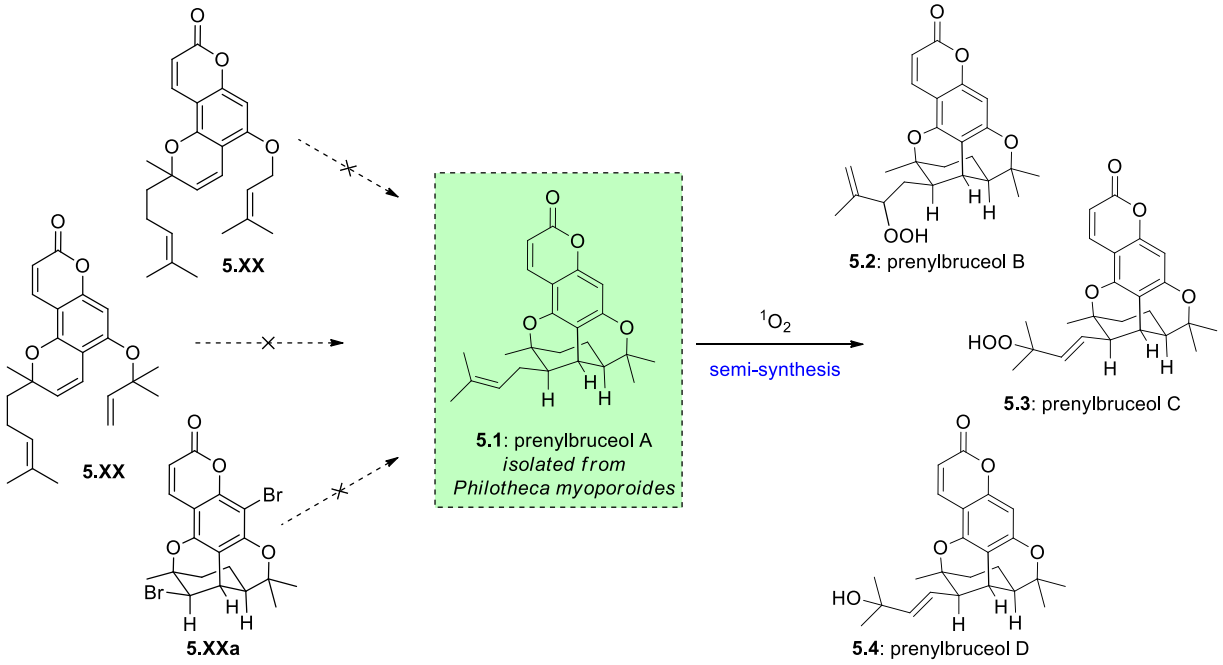

Scheme 5.33: Summary of the prenylbruceol project.

This work shows the importance of using biosynthetic speculation to rationalise and predict natural products which should exist. It also emphasises the symbiotic relationship between natural products chemistry and synthetic organic chemistry.

5.4 Experimental

5.4.1: General Methods

All chemicals were purchased from commercial suppliers and used as received. All reactions were performed under an inert atmosphere of N_2. All organic extracts were dried over anhydrous magnesium sulfate. Thin layer chromatography was performed using aluminium sheets coated with silica gel F_{254}. Visualisation was aided by viewing under a UV lamp and staining with ceric ammonium molybdate stain followed by heating. All R_f values were measured to the nearest 0.05. Flash column chromatography was performed using 40-63 micron grade silica gel. Melting points were recorded on a digital melting point apparatus and are uncorrected. Infrared spectra were recorded using an FT-IR spectrometer as the neat compounds. High field NMR spectra were recorded using either a 500 MHz spectrometer (^{1}H at 500 MHz, ^{13}C at 125 MHz) or 600 MHz spectrometer (^{1}H at 600 MHz, ^{13}C at 150 MHz). The solvent used for NMR spectra was $CDCl_3$ unless otherwise specified. ^{1}H chemical shifts are reported in ppm on the δ-scale relative to TMS (δ 0.00) or $CDCl_3$ (δ 7.26) and ^{13}C NMR chemical shifts are reported in ppm relative to $CDCl_3$ (δ 77.16). Multiplicities are reported as (br) broad, (s) singlet, (d) doublet, (t) triplet, (q) quartet, (quin) quintet, (sext) sextet, (hept) heptet and (m) multiplet. All *J*-values were rounded to the nearest 0.1 Hz. ESI high resolution mass spectra were recorded on an ESI-TOF mass spectrometer. Optical rotations were recorded on an Anton Paar Modular Circular Polirimeter at 20 °C.

5.4.2: Synthetic Procedures

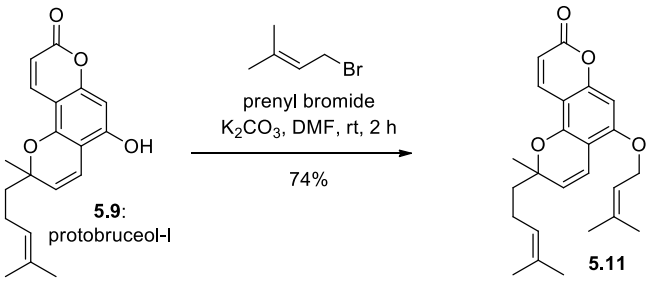

To a solution of protobruceol-I (**5.9**) (999 mg, 3.20 mmol) in DMF (40 mL) at 0 °C was added K_2CO_3 (1.33 g, 9.59 mmol), followed by prenyl bromide (0.41 mL, 3.5 mmol). The reaction was stirred at 0 °C for 5 min, then warmed to room temperature and stirred for a further 2 h. The mixture was diluted with brine (50 mL) and extracted with EtOAc (5 × 50 mL). The combined organic extracts were washed with brine (5 × 50 mL), dried over $MgSO_4$, filtered, and concentrated *in vacuo*. The residue

was purified by flash column chromatography on SiO_2 (8:1 petrol/EtOAc) to afford **5.11** as a pale, yellow oil (900 mg, 74%).

Data for **5.11**

^{1}H NMR (500 MHz, $CDCl_3$) δ 7.94 (d, *J* = 9.6 Hz, 1H), 6.67 (d, *J* = 10.1 Hz, 1H), 6.14 (d, *J* = 9.6 Hz, 1H), 5.48 (d, *J* = 10.2 Hz, 1H), 5.45 (t, *J* = 6.6, 1H), 5.08 (t, *J* = 7.3 Hz, 1H), 4.57 (d, *J* = 6.6 Hz, 2H), 2.15 – 2.07 (m, 2H), 1.80 (s, 3H), 1.80 – 1.67 (m, overlapped, 2H), 1.76 (s, 3H), 1.65 (s, 3H), 1.55 (s, 3H), 1.42 (s, 3H)

^{13}CNMR (125 MHz, $CDCl_3$) δ 161.8, 157.7, 155.9, 150.6, 138.83, 138.75, 132.1, 126.5, 123.9, 119.0, 116.9, 111.1, 106.7, 103.6, 92.6, 80.3, 65.9, 41.3, 26.6, 26.0, 25.8, 22.8, 18.5, 17.8

IR (neat) $\bar{\nu}$ 2791, 2915, 1733, 1614, 1597, 1437, 1377, 1137, 1107 cm^{-1}

R_f 0.45 (5:1 petrol/EtOAc)

HRMS (ESI) calculated for $C_{24}H_{29}O_4$ 381.2060 $[M+H]^+$, found 381.2062

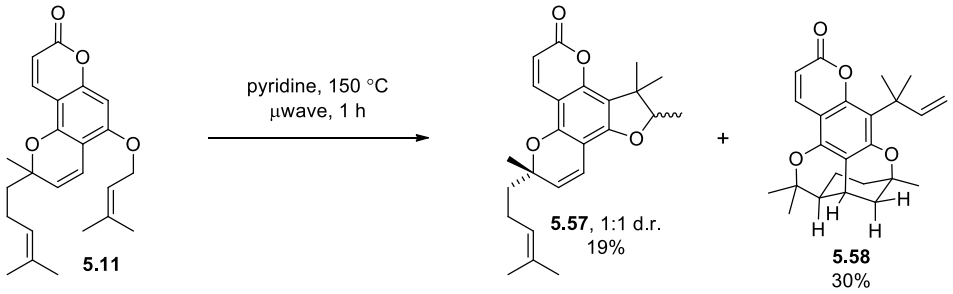

A solution of **5.11** (44.6 mg, 0.117 mmol) in pyridine (5 mL) was heated to 150 °C in a microwave reactor for 1 h. The solvent was removed *in vacuo* and the residue was purified by flash column chromatography on SiO_2 (8:1 → 3:1 petrol/EtOAc, gradient elution) to afford chromene **5.57** as a clear and colourless oil (8.3 mg, 19%, 1:1 d.r.). Further elution gave citran **5.58** as a light yellow solid (13.5 mg, 30%).

Data for **5.57**

^{1}H NMR (600 MHz, $CDCl_3$) δ 7.92 (d, *J* = 9.6 Hz, 1H), 6.48 (d, *J* = 10.0 Hz, 1H), 6.07 (d, *J* = 9.7 Hz, 1H), 5.50 (d, *J* = 10.0 Hz, 1H), 5.08 (t, *J* = 7.2 Hz, 1H), 4.48 (qd, *J* = 6.6, 1.8 Hz, 1H), 2.10 (tt, *J* = 11.3, 6.5 Hz, 2H), 1.82 – 1.67 (m, 2H), 1.65 (s, 3H), 1.56 (s, 3H), 1.52 (d, *J* = 1.5 Hz, 3H), 1.42 (s, 3H), 1.39 (d, *J* = 6.6 Hz, 3H), 1.25 (d, *J* = 2.6 Hz, 3H)

^{13}C NMR (150 MHz, $CDCl_3$) δ 161.42, 161.41, 158.22, 158.21, 151.2, 150.58, 150.56, 139.4, 132.1, 127.0, 126.9, 123.89, 123.88, 116.47, 116.46, 114.24, 114.23, 109.9, 103.60, 103.59, 101.79, 101.77, 91.17, 91.16, 80.5, 44.1, 41.4, 41.3, 26.68, 26.65, 25.8, 25.7, 25.6, 22.81, 22.78, 21.4, 21.3, 17.8, 14.40, 14.37 (Note: more than 24 ^{13}C signals are observed as **5.57** is a 1:1 mixture of diastereoisomers)

IR (neat) $\bar{\nu}$ 2968, 2926, 1733, 1623, 1603, 1584, 1435, 1380, 1345, 1313, 1136, 1093, 1093 cm^{-1}

R_f 0.40 (5:1 petrol/EtOAc)

HRMS (ESI) calculated for $C_{24}H_{29}O_4$ 381.2060 $[M+H]^+$, found 381.2062

Data for **5.58**

^{1}H NMR (600 MHz, $CDCl_3$) δ 7.87 (d, *J* = 9.5 Hz, 1H), 6.31 (dd, *J* = 17.4, 10.6 Hz, 1H), 6.08 (d, *J* = 9.5 Hz, 1H), 4.90 (dd, *J* = 17.4, 1.2 Hz, 1H), 4.86 (dd, *J* = 10.6, 1.3 Hz, 1H), 2.88 – 2.84 (m, 1H), 2.18 (ddd, *J* = 13.2, 4.8, 3.1 Hz, 1H), 2.08 (ddd, *J* = 11.7, 5.4, 2.7 Hz, 1H), 1.85 (dd, *J* = 13.2, 1.6 Hz, 1H), 1.76 (ddd, *J* = 15.2, 5.1, 2.9 Hz, 1H), 1.66 (s, 3H), 1.65 (s, 4H), 1.58 (s, 3H), 1.47 – 1.41 (m, overlapped, 1H), 1.40 (s, 3H), 1.29 (dt, *J* = 12.8, 5.9 Hz, 1H), 1.06 (s, 3H), 0.64 (tdd, *J* = 13.5, 11.7, 6.2 Hz, 1H)

^{13}CNMR (150 MHz, $CDCl_3$) δ 161.9, 158.9, 152.4, 151.5, 149.7, 138.8, 115.3, 112.2, 110.1, 108.3, 105.1, 85.6, 76.2, 46.7, 41.1, 37.4, 34.9, 29.7, 29.6, 29.4, 28.9, 28.5, 24.2, 22.2

IR (neat) $\bar{\nu}$ 2975, 2931, 1707, 1638, 1596, 1561, 1458, 1428, 1335, 1310, 1273, 1166, 1136 cm^{-1}

R_f 0.25 (5:1 petrol/EtOAc)

m.p. 170.9 – 172.3 °C (prisms from EtOAc)

HRMS (ESI) calculated for $C_{24}H_{29}O_4$ 381.2060 $[M+H]^+$, found 381.2063

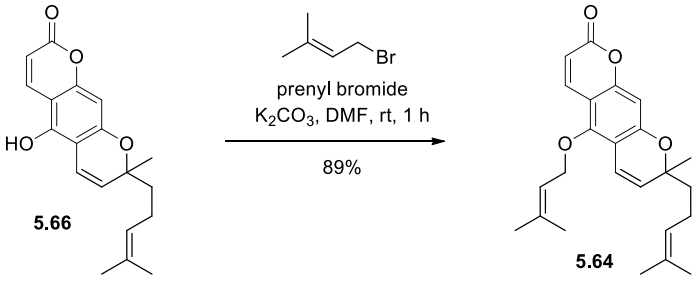

To a solution of **5.66** (151 mg, 0.484 mmol) in DMF (10 mL) at 0 °C was added K_2CO_3 (201 mg, 1.45 mmol), followed by prenyl bromide (0.06 mL, 0.53 mmol). The reaction mixture was stirred at 0 °C for 5 min, then warmed to room temperature and stirred for a further 1 h. The reaction was quenched with 1 M HCl (2 mL) and diluted with water (10 mL). The mixture was extracted with Et_2O (3 × 15 mL) and the combined organic extracts were washed with brine (5 × 15 mL), dried over $MgSO_4$, filtered, and concentrated *in vacuo*. The residue was purified by flash column chromatography on SiO_2 (8:1 petrol/EtOAc) to afford **5.64** as a pale yellow oil (165 mg, 89%).

Data for **5.64**:

^{1}H NMR (600 MHz, $CDCl_3$) δ 7.84 (d, *J* = 9.6 Hz, 1H), 6.62 (d, *J* = 10.1 Hz, 1H), 6.53 (s, 1H), 6.17 (d, *J* = 9.6 Hz, 1H), 5.64 (d, *J* = 10.1 Hz, 1H), 5.51 (t, *J* = 7.5 Hz, 1H), 5.07 (t, *J* = 6.7 Hz, 1H), 4.46 (d, *J* = 7.4 Hz, 2H), 2.14 – 2.03 (m, 2H), 1.80 – 1.74 (m, overlapped, 1H), 1.76 (s, 3H), 1.68 – 1.62 (m, overlapped, 1H), 1.65 (s, 3H), 1.60 (s, 3H), 1.56 (s, 3H), 1.42 (s, 3H)
^{13}C NMR (150 MHz, $CDCl_3$) δ 161.4, 158.0, 155.7, 151.9, 140.2, 139.3, 132.2, 129.4, 123.7, 119.2, 116.9, 112.0, 111.9, 108.1, 100.6, 80.0, 73.0, 41.6, 26.9, 26.0, 25.8, 22.8, 18.2, 17.8
IR (neat) $\bar{\nu}$ 2973, 1736, 1615, 1599, 1564, 1449, 1380, 1367, 1316, 1196, 1136, 1079 cm^{-1}
R_f 0.35 (5:1 petrol/EtOAc)
HRMS (ESI) calculated for $C_{24}H_{29}O_4$ 381.2060 $[M+H]^+$, found 381.2061

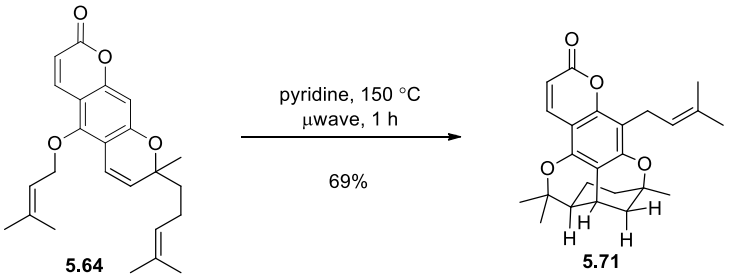

A solution of **5.64** (23.5 mg, 0.0617 mmol) in pyridine (5 mL) was heated to 150 °C in a microwave reactor for 30 min. The solvent was removed *in vacuo*, and the residue was purified by flash column chromatography on SiO_2 (5:1 petrol/EtOAc) to afford **5.71** as a pale yellow oil (16.3 mg, 69%).

Data for **5.71**:

^{1}H NMR (600 MHz, $CDCl_3$) δ 7.86 (d, *J* = 9.5 Hz, 1H), 6.10 (d, *J* = 9.4 Hz, 1H), 5.27 (t, *J* = 7.7 Hz, 1H), 3.43 (d, *J* = 7.5 Hz, 2H), 2.86 (br s, 1H), 2.24 (ddd, *J* = 13.3, 4.8, 3.2 Hz, 1H), 2.09 (ddd, *J* = 11.7, 5.5, 2.8 Hz, 1H), 1.88 (dd, *J* = 13.3, 1.6 Hz, 1H), 1.82 (s, 3H), 1.74 (ddd, *J* = 14.9, 5.5, 2.7 Hz, 1H), 1.67 (s, 3H), 1.58 (s, 3H), 1.46 (ddd, *J* = 13.2, 8.7, 6.7 Hz, 1H), 1.43 (s, 3H), 1.29 – 1.24 (m, 1H), 1.03 (s, 3H), 0.59 (tdd, *J* = 13.5, 11.7, 6.2 Hz, 1H)
^{13}C NMR (125 MHz, $CDCl_3$) δ 162.3, 157.6, 151.7, 151.3, 138.6, 131.8, 122.2, 112.1, 110.5, 110.0, 105.1, 86.0, 76.1, 46.6, 37.5, 34.9, 29.7, 29.0, 28.3, 26.0, 24.2, 22.2, 21.4, 18.1
IR (neat) $\bar{\nu}$ 2975, 1724, 1606, 1573, 1442, 1338, 1270, 1239, 1214, 1187, 1166, 1142, 1124 cm^{-1}
R_f 0.20 (5:1 petrol/EtOAc)
HRMS (ESI) calculated for $C_{24}H_{29}O_4$ 381.2060 $[M+H]^+$, found 381.2062

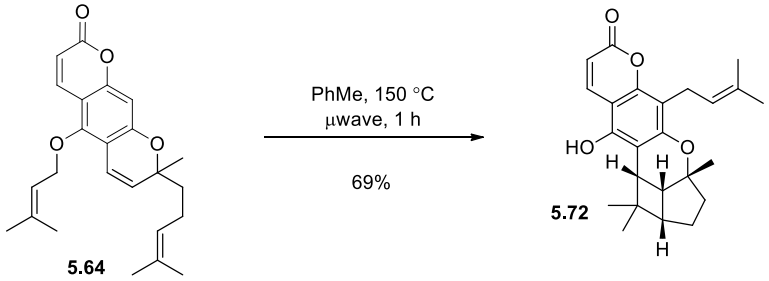

A solution of **5.64** (28.7 mg, 0.0754 mmol) in toluene (10 mL) was heated to 150 °C in a microwave reactor for 1.5 h. The solvent was removed *in vacuo* and the residue was purified by flash column chromatography on SiO_2 (5:1→ 3:1 petrol/EtOAc) to afford **5.72** as a yellow solid (12.7 mg, 44%).

Data for **5.72**:

^{1}H NMR (600 MHz, $CDCl_3$) δ 7.94 (d, *J* = 9.6 Hz, 1H), 6.16 (d, *J* = 9.6 Hz, 1H), 5.22 (t, *J* = 7.5 Hz, 1H), 4.64 (br s, 1H), 3.45 (d, *J* = 7.4 Hz, 2H), 3.03 (d, *J* = 9.7 Hz, 1H), 2.67 (t, *J* = 8.5 Hz, 1H), 2.47 (t, *J* = 7.2 Hz, 1H), 1.91 – 1.86 (m, 1H), 1.83 (s, 3H), 1.73 – 1.64 (m, overlapped, 3H), 1.66 (s, 3H), 1.45 (s, 3H), 1.44 (s, 3H), 0.77 (s, 3H)
^{13}C NMR (150 MHz, $CDCl_3$) δ 162.0, 155.1, 152.0, 148.8, 138.8, 131.7, 122.1, 111.5, 111.1, 106.3, 102.8, 84.5, 46.3, 39.0, 38.5, 37.2, 35.9, 34.7, 27.5, 26.0, 25.7, 21.8, 18.3, 18.2
R_f 0.10 (5:1 petrol/EtOAc)
HRMS (ESI) calculated for $C_{24}H_{29}O_4$ 381.2060 $[M+H]^+$, found 381.2059.

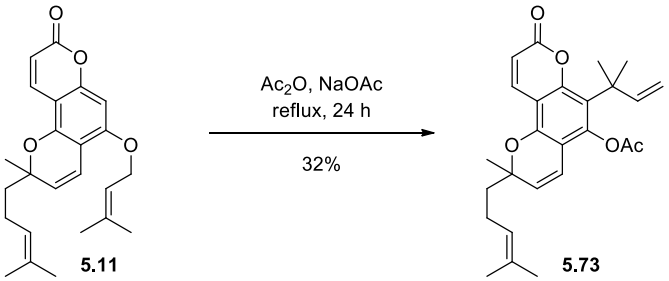

To a solution of **5.11** (240 mg, 0.629 mmol) in Ac_2O (8.2 mL) was added NaOAc (207 mg, 2.52 mmol) and the resultant mixture was heated to 140 °C for 24 h. The reaction was then cooled to room temperature, filtered and the solvent was removed *in vacuo*. The residue was purified by flash column chromatography (10:1→5:1 petrol/EtOAc) to afford **5.73** as a pale yellow oil (89.0 mg, 33%)

Data for **5.73**

^{1}H NMR (600 MHz, $CDCl_3$) δ 8.03 (d, *J* = 9.7 Hz, 1H), 6.28 (d, *J* = 9.7 Hz, 1H), 6.27 (dd, *J* = 17.2, 10.9 Hz, overlapped, 1H) 6.16 (d, *J* = 10.1 Hz, 1H), 5.58 (d, *J* = 10.2 Hz, 1H), 5.07 (br m, 1H), 4.96 (d, *J* = 17.5 Hz, 1H), 4.89 (d, *J* = 10.7 Hz, 1H), 2.24 (s, 3H), 2.13 – 2.05 (m, 2H), 1.81 – 1.68 (m, 2H), 1.65 (s, 3H), 1.61 (s, 6H), 1.55 (s, 3H)
^{13}C NMR (150 MHz, $CDCl_3$) 169.1, 160.4, 153.5, 149.0, 149.0, 147.4, 138.5, 132.3, 129.2, 123.7, 120.3, 116.8, 113.6, 110.8, 108.2, 107.4, 80.4, 41.2, 29.9, 26.7, 25.8, 21.3, 17.8
IR (neat) $\bar{\nu}$ 2969, 2928, 1769, 1736, 1622, 1585, 1448, 1363, 1191, 1131, 1086 cm^{-1}
R_f 0.20 (4:1 petrol/EtOAc).

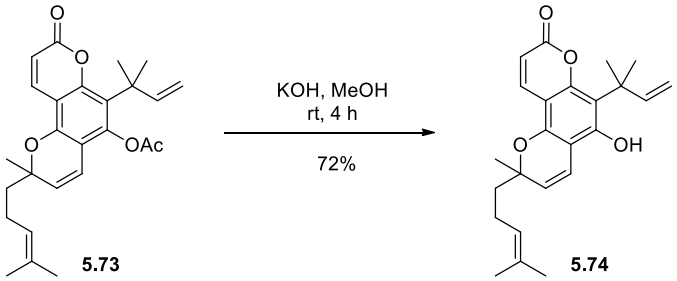

To a solution of **5.73** (76.3 mg, 0.181 mmol) in MeOH (5 mL) was added KOH (35 mg, 0.625 mmol) in MeOH (5 mL). The resultant mixture was stirred at room temperature for 3 h, then quenched with 1 M HCl (1 mL). The mixture was diluted with water (10 mL) and extracted with EtOAc (15 mL × 3). The combined organic extracts were washed with brine (15 mL × 3), dried over $MgSO_4$, filtered, and concentrate *in vacuo*. The residue was purified by flash column chromatography on SiO_2 (10:1 petrol/EtOAc) to afford **5.74** as a pale oil (60.0 mg, 87%)

^{1}H NMR (600 MHz, $CDCl_3$) δ 7.99 (d, *J* = 9.6 Hz, 1H), 7.33 (s, 1H), 6.64 (d, *J* = 10.1 Hz, 1H), 6.46 (dd, *J* = 10.5, 17.9 Hz, 1H), 6.12 (d, *J* = 9.6 Hz, 1H), 5.52 – 5.47 (m, overlapped, 2H), 5.40 (d, *J* = 10.5 Hz, 1H), 5.08 (t, *J* = 6.6 Hz, 1H), 2.14 – 2.05 (m, 2H), 1.79 – 1.70 (m, 2H), 1.69 (s, 6H), 1.65 (s, 3H), 1.56 (s, 3H), 1.41 (s, 3H).
^{13}C NMR (150 MHz, $CDCl_3$) δ 161.3, 154.4, 154.0, 149.5, 149.4, 139.2, 132.1, 126.8, 123.9, 117.1, 113.9, 111.0, 110.2, 106.4, 103.9, 80.1, 41.4, 41.2, 27.8, 27.7, 26.7, 25.8, 22.8, 17.8
IR (neat) 3404, 2968, 2928, 1730, 1616, 1588, 1450, 1377, 1341, 1180, 1132, 1105.
R_f 0.40 (4:1 petrol/EtOAc)

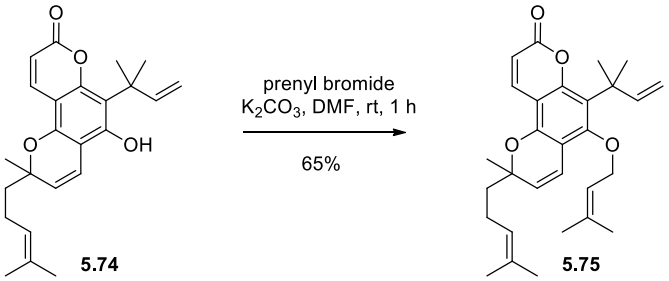

To a solution of **5.74** (172 mg, 0.452 mmol) in DMF (20 mL) was added K_2CO_3 (188 mg, 1.36 mmol), followed by prenyl bromide (74 mg, 0.497 mmol). The reaction was stirred at room temperature for 2 h, then quenched by the addition of aqueous 1 M HCl solution (10 mL). Brine (50 mL) was added and the mixture was extracted with Et_2O (25 mL × 5). The combined organic extracts were washed with brine (50 mL × 5), dried over $MgSO_4$, filtered, and concentrated *in vacuo*. The residue was purified by flash column chromatography to afford prenyl ether **5.75** as a yellow oil (132 mg, 65%).

^{1}H NMR (600 MHz, $CDCl_3$) δ 8.00 (d, *J* = 9.7 Hz, 1H), 6.55 (d, *J* = 10.1 Hz, 1H), 6.41 (dd, *J* = 10.6, 17.4 Hz, 1H), 6.21 (d, *J* = 9.7 Hz, 1H), 5.56 (d, *J* = 10.1 Hz, 1H), 5.48 (t, *J* = 6.2 Hz, 1H), 5.08 (t, *J* = 6.4 Hz, 1H), 4.95 (d, *J* = 17.4 Hz, 1H), 4.86 (d, *J* = 10.6 Hz, 1H), 4.20 (d, *J* = 6.9 Hz, 2H), 2.14 – 2.04 (m, 2H), 1.78 (s, 3H), 1.76 – 1.65 (m, 2H), 1.66 (s, 3H), 1.65 (m, overlapped, 9H), 1.55 (s, 3H), 1.43 (s, 3H)

IR (neat) $\bar{\nu}$ 2969, 2929, 1733, 1618, 1582, 1563, 1447, 1358, 1314, 1130, 1099, 1000, 827 cm^{-1}

R_f 0.50 (5:1 petrol/EtOAc)

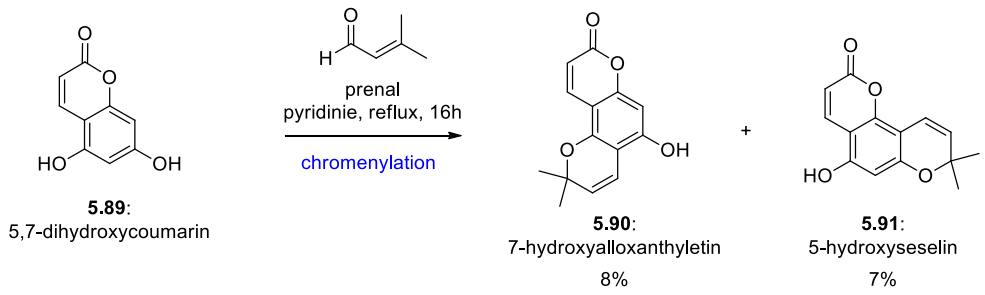

5,7-dihydroxycoumarin (**5.89**) (10.0 g, 56.1 mmol), prenal (5.67 g, 67.4 mmol), and pyridine were combined and heated to reflux for 16 h. The solvent was removed *in vacuo* (60 °C bath temperature) and the residue was adsorbed on to Celite (~20 g) using THF, then purified by flash column chromatography on SiO_2 (20:1→15:1 CH_2Cl_2/EtOAc) to give a mixture of chromenes **5.90** and **5.91** (~4.0 g) but with poor separation. The mixture was resubjected to flash column chromatography on SiO_2 (20:1→15:1 CH_2Cl_2/EtOAc) to afford **5.91** as a white solid (1.16 g, 7%), and **5.90** as a tan solid (1.34 g, 8%), as well as further unseparated mixture (2.6:1 **5.91**/**5.90**, 1.02 g, 6%)

Data for **5.90**

^{1}H NMR (500 MHz, d_6-acetone) δ 8.03 (d, *J* = 9.7 Hz, 1H), 6.69 (d, *J* = 10.0 Hz, 1H), 6.27 (s, 1H), 6.09 (d, *J* = 9.7 Hz, 1H), 5.69 (d, *J* = 10.0 Hz, 1H), 1.43 (s, 6H)
IR (neat) $\bar{\nu}$ 3180. 1676, 1601, 1355, 1266, 1152, 1079, 814 cm^{-1}
R_f 0.25 (15:1 CH_2Cl_2/EtOAc)

Data for **5.91**

^{1}H NMR (500 MHz, d_6-acetone) δ 7.98 (d, *J* = 9.7 Hz, 1H), 6.66 (d, *J* = 10.0 Hz, 1H), 6.33 (s, 1H), 6.08 (d, *J* = 9.6 Hz, 1H), 5.68 (d, *J* = 10.0 Hz, 1H), 1.48 (s, 6H).
IR (neat) $\bar{\nu}$ 3208, 1693, 1589, 1442, 1363, 1264, 1145, 1084, 827 cm^{-1}
R_f 0.15 (5:1 petrol/EtOAc)

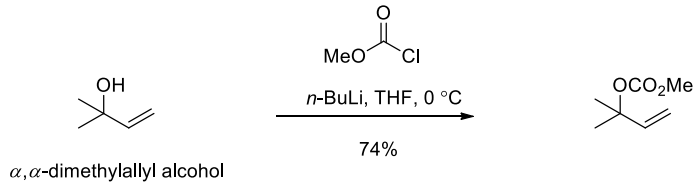

To a solution of 2-methyl-3-buten-2-ol (3.0 mL, 28.7 mmol) in THF (50 mL) cooled to 0 °C was slowly added *n*-BuLi (2.5 M in *n*-hexane, 12.6 mL, 31.6 mmol) and stirred at 0 °C for 15 min. Methyl chloroformate (3.3 mL, 43.0 mmol) was then added dropwise and the mixture was stirred for 2 h at room temperature. The reaction was quenched with 1 M HCl (50 mL). The layers were separated, and the organic phase was washed with brine (20 mL × 2), dried over $MgSO_4$, filtered, and concentrated *in vacuo* to afford the methyl carbonate (3.04 g, 74%).

Data for methyl carbonate:

^{1}H NMR (600 MHz, $CDCl_3$) δ 6.08 (dd, *J* = 10.9, 17.5 Hz, 1H), 5.21 (d, *J* = 17.5 Hz, 1H), 5.12 (d, *J* = 10.9 Hz, 1H), 3.70 (s, 3H), 1.54 (s, 6H)
IR (neat) $\bar{\nu}$ 2985, 2958, 1745, 1441, 1367, 1263, 1232, 1128, 1098
HRMS (ESI) calculated for $C_7H_{12}O_3Na$ 167.0679 $[M+Na]^+$, found 167.0680

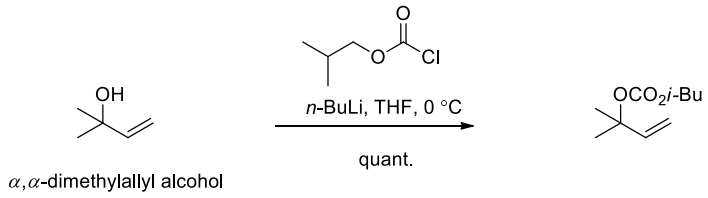

To a solution of 2-methyl-3-buten-2-ol (5.0 mL, 47.8 mmol) in THF (30 mL) at 0 °C was slowly added *n*-BuLi (2.5 M in *n*-hexane, 21 mL, 52.6 mmol) and stirred at 0 °C for 30 min. *iso*-Butyl chloroformate (9.4 mL, 71.7 mmol) was then added dropwise at 0 °C and the resulting mixture was warmed to room temperature and stirred for 1 h. The reaction was quenched by addition of 1 M HCl (50 mL) and brine (20 mL) was added. The layers were separated and the aqueous phase was extracted with Et_2O (20 mL × 3). The combined organic extracts were washed with brine (30 mL), dried over $MgSO_4$, filtered, and carefully concentrated *in vacuo*. The remaining yellow oil was purified by distillation under reduced pressure (b.p. 82 °C/25 mmHg) to afford the isobutyl carbonate as a clear and colourless oil (7.00 g, quant.)

Data for *i*-butyl carbonate:

^{1}H NMR (600 MHz, $CDCl_3$) δ 6.09 (dd, *J* = 17.5, 10.9 Hz, 1H), 5.21 (d, *J* = 17.5 Hz, 1H), 5.12 (d, *J* = 11.0 Hz, 1H), 3.84 (d, *J* = 6.8 Hz, 2H), 1.94 (hept, *J* = 6.7 Hz, 1H), 1.54 (s, 6H), 0.92 (d, *J* = 6.8 Hz, 6H).
IR (neat) $\bar{\nu}$ 2964, 2877, 1741, 1471, 1380, 1254, 1132, 1092 cm^{-1}

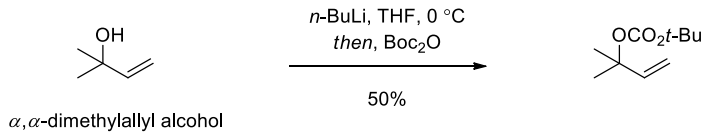

Following the procedure of Carreira.[19] To a solution of 2-methyl-3-buten-2-ol (5.2 mL, 50.0 mmol) in THF (90 mL) at 0 °C was slowly added *n*-BuLi (2.5 M in *n*-hexane, 22 mL, 55.0 mmol) and stirred at 0 °C for 20 min. di-*tert*-butyl dicarbonate (11.0 g, 50.0 mmol) was then added as a solid in one portion at 0 °C and the resulting mixture was warmed to room temperature and stirred for 4 h. The reaction was quenched by addition of saturated aqueous $NaHCO_3$ solution (200 mL). The layers were separated and the organic phase was washed with brine (150 mL), dried over $MgSO_4$, filtered, and carefully concentrated *in vacuo*. The remaining yellow oil was purified by distillation under reduced pressure (b.p. 83 °C/41 mmHg) to afford the tertbutyl carbonate as a clear and colourless oil (4.48 g, 50%).

Data for *t*-butyl carbonate:

^{1}H NMR (600 MHz, $CDCl_3$) δ 6.10 (dd, *J* = 17.5, 10.9 Hz, 1H), 5.18 (d, *J* = 17.5 Hz, 1H), 5.10 (d, *J* = 10.9 Hz, 1H), 1.52 (s, 6H), 1.45 (s, 9H)
^{13}C NMR (150 MHz, $CDCl_3$) δ 152.0, 142.4, 113.1, 81.6, 81.5, 28.03, 27.99, 26.6
IR (neat) $\bar{\nu}$ 2981, 1737, 1367, 1282, 1143, 1121, 920, 844 cm^{-1}
HRMS (ESI) calculated for $C_{10}H_{18}O_3Na$ 209.1148 $[M+Na]^+$, found 209.1154

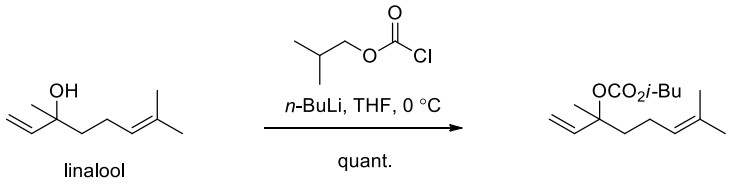

To a solution of linalool (3.5 mL, 19.5 mmol) in dry THF (50 mL) was added *n*-BuLi (2.0 M in cyclohexane, 10.7 mL, 21.5 mmol) and stirred at 0 °C for 30 min. *iso*-Butyl chloroformate (3.8 mL, 29.3 mmol) was then added dropwise at 0 °C and warmed to room temperature and stirred for a further 30 min. The reaction was quenched with 1 M HCl (50 mL) and the layers were separated. The aqueous phase was extracted with Et_2O (30 mL × 2). The combined organic extracts were washed with water (50 mL), then brine (50 mL), dried over $MgSO_4$, filtered and concentrated *in vacuo* to afford the linaloyl isobutyl carbonate (5.71 g, quant.).

Data for linaloyl isobutyl carbonate:

^{1}H NMR (600 MHz, $CDCl_3$) δ 6.01 (dd, *J* = 17.5, 11.0 Hz, 1H), 5.20 (dd, *J* = 17.6, 0.8 Hz, 1H), 5.17 (dd, *J* = 11.0, 0.8 Hz, 1H), 5.08 (ddt, *J* = 7.2, 5.7, 1.5 Hz, 1H), 3.85 (d, *J* = 6.8 Hz, 2H), 1.99 – 1.93 (m, 2H), 1.67 (s, 3H), 1.59 (s, 3H), 1.56 (s, 3H), 1.55 (s, 3H), 0.94 (d, *J* = 6.7 Hz, 6H).
IR (neat) $\bar{\nu}$ 2965, 1876, 1742, 1470, 1377, 1247, 1171, 1078 cm^{-1}
HRMS (ESI) calculated for $C_{15}H_{26}O_3Na$ 277.1774 $[M+Na]^+$, found 277.1769.

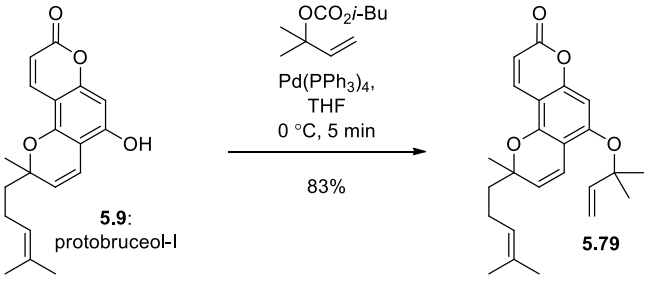

To a solution of protobruceol-I (**5.9**) (244 mg, 0.781 mmol) in THF (6 mL) at 0 °C was added α,*α*-dimethylallyl isobutyl carobonate (782 mg, 3.91 mmol), then $Pd(PPh_3)_4$ (90.2 mg, 0.0781 mmol). The reaction was stirred at 0 °C for 5 min, then the solvent was removed *in vacuo*. The residue was purified by flash column chromatography on SiO_2 (15:1 → 10:1 petrol/EtOAc) to afford **5.79** as a pale yellow oil (245 mg, 83%).

Data for **5.79**:

^{1}H NMR (500 MHz, $CDCl_3$) δ 7.93 (dd, *J* = 9.6, 0.6 Hz, 1H), 6.66 (d, *J* = 10.1 Hz, 1H), 6.58 (d, *J* = 0.6 Hz, 1H), 6.13 (d, *J* = 9.5 Hz, 1H), 6.10 (dd, *J* = 17.6, 10.8 Hz, 1H), 5.49 (d, *J* = 10.1 Hz, 1H), 5.26 (dd, *J* = 17.6, 0.7 Hz, 1H), 5.22 (dd, *J* = 10.9, 0.7 Hz, 1H), 5.09 (tt, *J* = 7.0, 1.3 Hz, 1H), 2.16 – 2.05 (m, 2H), 1.82 – 1.68 (m, 2H), 1.65 (s, 3H), 1.56 (s, 3H), 1.54 (s, 6H), 1.42 (s, 3H)
^{13}C NMR (150 MHz, $CDCl_3$) δ 161.7, 155.4, 154.9, 150.5, 143.4, 138.6, 132.0, 126.6, 123.8, 117.4, 114.5, 111.2, 108.9, 103.8, 98.2, 81.4, 80.1, 41.2, 27.2, 27.1, 26.5, 25.7, 22.7, 17.7
IR (neat) $\bar{\nu}$ 1956, 1927, 1732, 1637, 11613, 1595, 1435, 1375, 1350, 1124, 1102, 1088 cm^{-1}
R_f 0.40 (5:1 petrol/EtOAc)
HRMS (ESI) calculated for $C_{24}H_{29}O_4$ 381.2060 $[M+H]^+$, found 381.2066

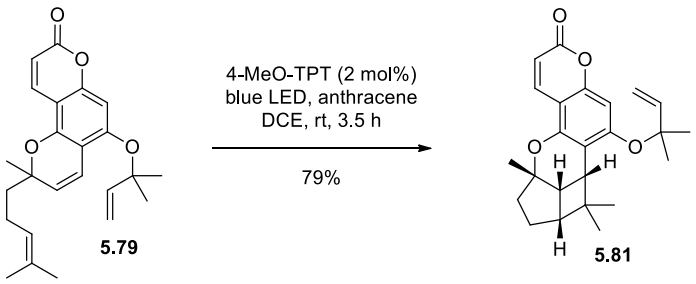

To a solution of **5.79** (13.4 mg, 0.0352 mmol) in DCE (0.4 mL, 0.1 M) was added 4-MeO-TPT (0.3 mg, 0.0007 mmol) and anthracene (1.9 mg, 0.011 mmol). The mixture was purged with N_2 and irradiated with blue LED light for 3.5 h. The solvent was removed *in vacuo* and the residue was purified by flash column chromatography on SiO_2 (4:1 petrol/EtOAc) to afford cyclol **5.81** (10.6 mg, 79%).

Data for **5.81**:

^{1}H NMR (500 MHz, $CDCl_3$) δ 8.00 (d, *J* = 9.6 Hz, 1H), 6.61 (s, 1H), 6.10 (d, *J* = 9.6 Hz, 1H), 6.08 (dd, overlapped, 1H), 5.24 (d, *J* = 14.8 Hz, 1H), 5.22 (d, 8.1 Hz, 1H), 3.10 (d, 9.6 Hz, 1H), 2.59 (dd, *J* = 7.5, 9.5 Hz, 1H), 2.40 (t, *J* = 7.3 Hz, 1H), 2.27 (d, *J* = 1.3 Hz, 1H), 1.95 – 1.88 (m, 1H), 1.78 – 1.63 (m, 3H), 1.60 (s, 3H), 1.54 (s, 3H), 1.42 (s, 3H), 1.39 (s, 3H), 0.77 (s, 3H)
IR (neat) $\bar{\nu}$ 2947, 1732, 1608, 1436, 1362, 1131, 1111, 1088, 1008,821 cm^{-1}
R_f 0.35 (5:1 petrol/EtOAc)

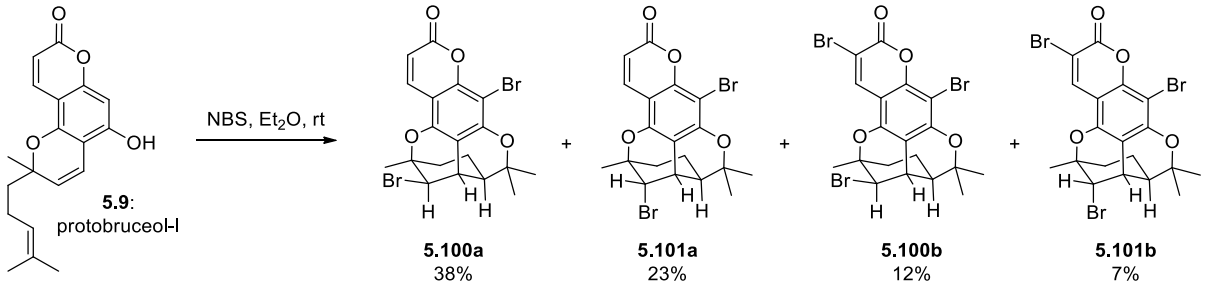

To a solution of protobruceol-I (**5.9**) (195 mg, 0.624 mmol) in Et_2O (10 mL) was added NBS (333 mg, 1.87 mmol) at room temperature for 10 min. The reaction mixture was quenched with $Na_2S_2O_3$, filtered through Celite, flushed with Et_2O (20 mL) and concentrated *in vacuo*, and the residue was purified by flash chromatography on SiO_2 (8:1 → 3:1 petrol/EtOAc, gradient elution) to afford **101b** (23 mg, 7%), **101a** (68 mg, 23%), **100b** (41 mg, 12%) and **100a** (111 mg, 38%).

Data for **101b**:

^{1}H NMR (500 MHz, $CDCl_3$) δ 8.20 (s, 1H), 4.71 (dd, *J* = 4.4, 2.0 Hz, 1H), 3.11 (dd, *J* = 4.4, 2.7 Hz, 1H), 2.75 (ddd, *J* = 11.7, 5.5, 2.7 Hz, 1H), 2.10 (ddd, *J* = 15.7, 13.0, 7.1 Hz, 1H), 1.74 (dd, *J* = 15.6, 6.5 Hz, 1H), 1.63 (s, 3H), 1.61 (s, 3H), 1.35 (dt, *J* = 13.2, 6.3 Hz, 1H), 1.13 (s, 3H), 0.63 (ddt, 1H)
^{13}C NMR (125 MHz, $CDCl_3$) δ 159.4, 159.1, 153.5, 152.5, 141.6, 115.4, 109.5, 108.0, 94.3, 91.1, 82.2, 55.5, 44.1, 38.7, 34.4, 31.8, 30.1, 27.1, 23.8
IR (neat) 2979, 2939, 1739, 1611, 1554, 1454, 1433, 1372, 1433, 1372, 1348, 1295, 1240, 1117 cm^{-1}
R_f 0.45 (2:1 petrol/EtOAc)
m.p. 206 – 208 °C (white needles from petrol/EtOAc)
HRMS (ESI) calculated for $C_{19}H_{18}Br_3O_4$ 546.8750 $[M+H]^+$, found: 546.8746.

Data for **101a**:

^{1}H NMR (500 MHz, $CDCl_3$) δ 7.87 (d, *J* = 9.7 Hz, 1H), 6.21 (d, *J* = 9.6 Hz, 1H), 4.72 (dd, *J* = 4.5, 2.1 Hz, 1H), 3.11 (dd, *J* = 4.5, 2.7 Hz, 1H), 2.75 (ddd, *J* = 11.8, 5.5, 2.6 Hz, 1H), 2.10 (ddd, *J* = 15.6, 13.0, 7.1 Hz, 1H), 1.73 (dd, J = 15.6, 6.5 Hz, 1H), 1.64 (s, 3H), 1.59 (s, 3H), 1.35 (dt, *J* = 13.3, 6.3 Hz, 1H), 1.14 (s, 3H), 0.67 (tdd, *J* = 14.0, 12.4, 6.4 Hz, 1H)
^{13}C NMR (125 MHz, $CDCl_3$) δ 160.6, 156.3, 151.8, 150.7, 137.9, 112.4, 112.1, 105.1, 92.1, 88.3, 79.3, 53.4, 41.7, 36.3, 31.9, 29.3, 27.7, 24.5, 21.3
IR (neat) 2980, 1736, 1612, 1560, 1461, 1431, 1390, 1356, 1240, 1185, 1126 1080 cm^{-1}
R_f 0.35 (2:1 petrol/EtOAc)

m.p. 210 – 212 °C (white needles from petrol/EtOAc)

HRMS (ESI) calculated for $C_{19}H_{19}Br_2O_4$ 468.9645 $[M+H]^+$ found: 468.9645.

Data for **100b**:

^{1}H NMR (500 MHz, $CDCl_3$) δ 8.33 (s, 1H), 4.42 (d, *J* = 1.9 Hz, 1H), 3.28 (t, *J* = 2.2 Hz, 1H), 2.42 (ddd, *J* = 11.8, 5.4, 2.7 Hz, 1H), 2.12 (dd, *J* = 15.6, 6.0 Hz, 1H), 1.66 (m, overlapped, 1H), 1.65 (s, 3H), 1.56 (s, 3H), 1.39 (dt, *J* = 13.1, 6.0 Hz, 1H), 1.10 (s, 3H), 0.70 (tdd, *J* = 13.7, 11.7, 6.1 Hz, 1H)

^{13}C NMR (125 MHz, $CDCl_3$) δ 157.2, 157.0, 150.9, 149.6, 139.3, 110.9, 107.0, 105.7, 92.0, 88.1, 78.4, 53.7, 49.0, 39.3, 37.9, 29.6, 27.8, 24.5, 22.1

IR (neat) $\bar{\nu}$ 1737, 1611, 1431, 1367, 1241, 1138, 1012 cm^{-1}

R_f 0.25 (2:1 petrol/EtOAc)

m.p. 185 – 187 °C (petrol/EtOAc)

HRMS (ESI) calculated for $C_{19}H_{18}Br_3O_4$ 546.8750 $[M+H]^+$, found: 546.8742.

Data for **100a**:

^{1}H NMR (500 MHz, $CDCl_3$) δ 7.98 (d, *J* = 9.6 Hz, 1H), 6.23 (d, *J* = 9.6 Hz, 1H), 4.42 (d, *J* = 1.8 Hz, 1H), 3.28 (t, *J* = 2.3 Hz, 1H), 2.40 (ddd, *J* = 11.7, 5.4, 2.8 Hz, 1H), 2.11 (ddd, *J* = 15.6, 6.1, 1.4 Hz, 1H), 1.69 – 1.61 (m, overlapped, 1H), 1.64 (s, 3H), 1.54 (s, 3H), 1.38 (dt, *J* = 12.6, 5.5 Hz, 1H), 1.10 (s, 3H), 0.72 (tdd, *J* = 13.6, 11.6, 6.1 Hz, 1H)

^{13}C NMR (125 MHz, $CDCl_3$) δ 160.7, 151.7, 150.4, 138.2, 112.0, 110.5, 105.3, 92.1, 87.8, 78.0, 54.0, 49.1, 39.3, 37.9, 29.6, 27.9, 24.4, 22.1

IR (neat) $\bar{\nu}$ 2980, 1731, 1612, 1561, 1460, 1429, 1394, 1366, 1317, 1283, 1260, 1194, 1127 cm^{-1}

R_f 0.20 (2:1 petrol/EtOAc)

m.p. 175 – 177 °C (white needles from petrol/EtOAc)

HRMS (ESI) calculated for $C_{19}H_{19}Br_2O_4$ 468.9645 $[M+H]^+$, found: 468.9644.

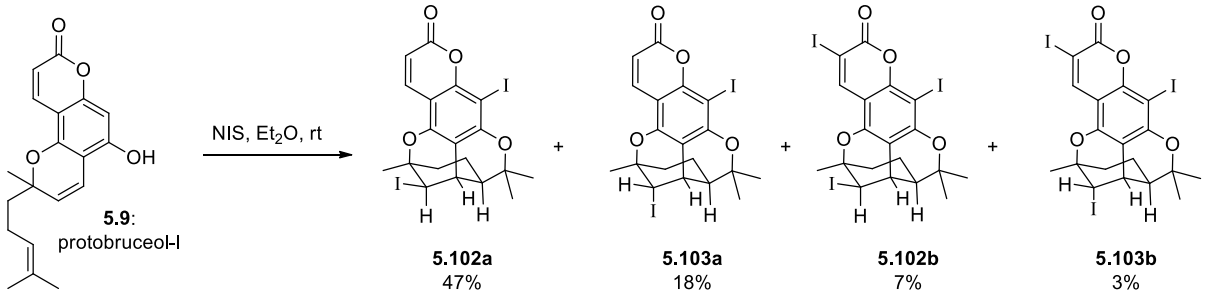

To a solution of protobruceol-1 (**5.9**) (200 mg, 0.640 mmol) in THF (15 mL) at 0 °C was added NIS (360 mg, 1.60 mmol) in one portion. The mixture was stirred at 0 °C for 10 min then quenched with $Na_2S_2O_3$ (~1 g) and filtered through a pad of Celite, flushed with CH_2Cl_2 (20 mL) The solvent was removed *in vacuo* and the residue was purified by flash column chromatography on SiO_2 (8:1 → 2:1 petrol/EtOAc, gradient elution) to afford **5.103b** as an off white solid (13.8 mg, 3%), **5.103a** as a white solid (63.8 mg, 18%), **5.102b** as a light brown solid (28.9 mg, 7%), and **5.102a** as a pale orange solid (171 mg, 47%).

Data for **5.103b**:

^{1}H NMR (500 MHz, $CDCl_3$) δ 8.40 (s, 1H), 4.88 (dd, *J* = 4.3, 2.3 Hz, 1H), 3.06 – 3.03 (m, 1H), 2.70 (ddd, *J* = 11.7, 5.5, 2.7 Hz, 1H), 2.20 (ddd, *J* = 15.7, 13.0, 7.1 Hz, 1H), 1.78 (dd, *J* = 15.9, 6.6 Hz, 1H), 1.67 (s, 3H), 1.64 (s, 3H), 1.34 (dt, *J* = 12.9, 6.2 Hz, 1H), 1.15 (s, 3H), 0.73 – 0.62 (m, 1H)
^{13}C NMR (125 MHz, $CDCl_3$) δ 159.4, 157.6, 154.4, 151.5, 146.5, 112.2, 106.7, 89.0, 80.1, 79.4, 65.0, 44.5, 37.7, 33.5, 32.4, 30.2, 29.3, 24.8, 21.5
IR (neat) $\bar{\nu}$ 2925, 2853, 1728, 1608, 1424, 1343, 1293, 1139, 1119 cm^{-1}
R_f 0.55 (2:1 petrol/EtOAc)
m.p. 163 – 171 °C (decomposition)
HRMS (ESI) calculated for $C_{19}H_{17}I_3O_4$ 690.8334 $[M+H]^+$, found: 690.8332.

Data for **5.103a**:

^{1}H NMR (500 MHz, $CDCl_3$) δ 7.82 (d, *J* = 9.5 Hz, 1H), 6.18 (d, *J* = 9.7 Hz, 1H), 4.90 (dd, *J* = 4.2, 2.4 Hz, 1H), 3.04 (dd, *J* = 4.2, 2.6 Hz, 1H), 2.69 (ddd, *J* = 11.7, 5.5, 2.6 Hz, 1H), 2.18 (ddd, *J* = 15.5, 13.0, 7.1 Hz, 1H), 1.76 (ddd, *J* = 15.9, 13.0, 6.1 Hz, 1H), 1.65 (s, 4H), 1.63 (s, 3H), 1.33 (dt, *J* = 13.2, 6.3 Hz, 1H), 1.14 (s, 3H), 0.68 (tdd, *J* = 13.6, 11.7, 6.3 Hz, 1H)
^{13}C NMR (125 MHz, $CDCl_3$) δ 160.9, 158.9, 154.3, 152.5, 137.8, 112.1, 105.1, 88.6, 79.0, 65.3, 44.5, 37.7, 33.91, 33.86, 32.4, 30.3, 29.3, 24.7, 21.5

IR (neat) $\bar{\nu}$ 2976, 2933, 1730, 1606, 1556, 1457, 1384, 1355, 1271,1239, 1200, 1185, 1117 cm^{-1}

R_f 0.45 (2:1 petrol/EtOAc)

m.p. 143 – 153 °C (decomposition)

HRMS (ESI) calculated for $C_{19}H_{18}I_2O_4$ 564.9367 $[M+H]^+$, found: 564.9365.

Data for **5.102b**:

^{1}H NMR (500 MHz, $CDCl_3$) δ 8.51 (s, 1H), 4.57 (d, *J* = 1.7 Hz, 1H), 3.39 (t, *J* = 2.2 Hz, 2H), 2.39 (ddd, *J* = 11.7, 5.5, 2.8 Hz, 1H), 2.16 (dd, *J* = 15.5, 6.0 Hz, 1H), 1.71 (ddd, *J* = 15.4, 13.2, 6.7 Hz, 1H), 1.64 (s, 3H), 1.53 (s, 3H), 1.47 (dt, *J* = 14.9, 6.1 Hz, 1H), 1.10 (s, 3H), 0.73 (tdd, *J* = 13.6, 11.7, 6.1 Hz, 1H)

^{13}C NMR (125 MHz, $CDCl_3$) δ 160.3, 157.6, 154.4, 150.6, 146.7, 112.2, 110.9, 106.9, 78.4, 65.6, 49.6, 41.7, 36.4, 33.9, 31.2, 29.7, 24.7, 22.3, 14.3

IR (neat) $\bar{\nu}$ 2925, 1729, 1542, 1448, 1424, 1344, 1293, 1237, 1134, 1119, 1086 cm^{-1}

R_f 0.25 (2:1 petrol/EtOAc)

m.p. 140 – 145 °C (decomposition)

HRMS (ESI) calculated for $C_{19}H_{17}I_3O_4$ 690.8334 $[M+H]^+$, found: 690.8328.

Data for **5.101a**:

^{1}H NMR (500 MHz, $CDCl_3$) δ 7.94 (d, *J* = 9.6 Hz, 1H), 6.21 (d, *J* = 9.6 Hz, 1H), 4.58 (d, *J* = 1.7 Hz, 1H), 3.38 (t, *J* = 2.2 Hz, 1H), 2.39 (ddd, *J* = 11.7, 5.4, 2.8 Hz, 1H), 2.13 (ddd, *J* = 15.4, 6.2, 1.3 Hz, 1H), 1.70 (ddd, *J* = 15.4, 13.2, 6.9 Hz, 1H), 1.62 (s, 3H), 1.50 (s, 3H), 1.46 (dt, *J* = 13.0, 6.1 Hz, 1H), 1.09 (s, 3H), 0.73 (tdd, *J* = 13.5, 11.6, 6.1 Hz, 1H)

^{13}C NMR (125 MHz, $CDCl_3$) δ 161.0, 159.8, 154.3, 151.6, 138.2, 112.1, 110.7, 105.3, 88.0, 78.1, 65.9, 49.6, 41.7, 36.4, 34.3, 31.2, 29.7, 24.6, 22.3

IR (neat) $\bar{\nu}$ 2978, 2935, 1724, 1606, 1557, 1455, 1422, 1387, 1357, 1131 cm^{-1}

R_f 0.20 (2:1 petrol/EtOAc)

m.p. 123 – 130 °C (decomposition)

HRMS (ESI) calculated for $C_{19}H_{18}I_2O_4$ 564.9367 $[M+H]^+$, found: 564.9369.

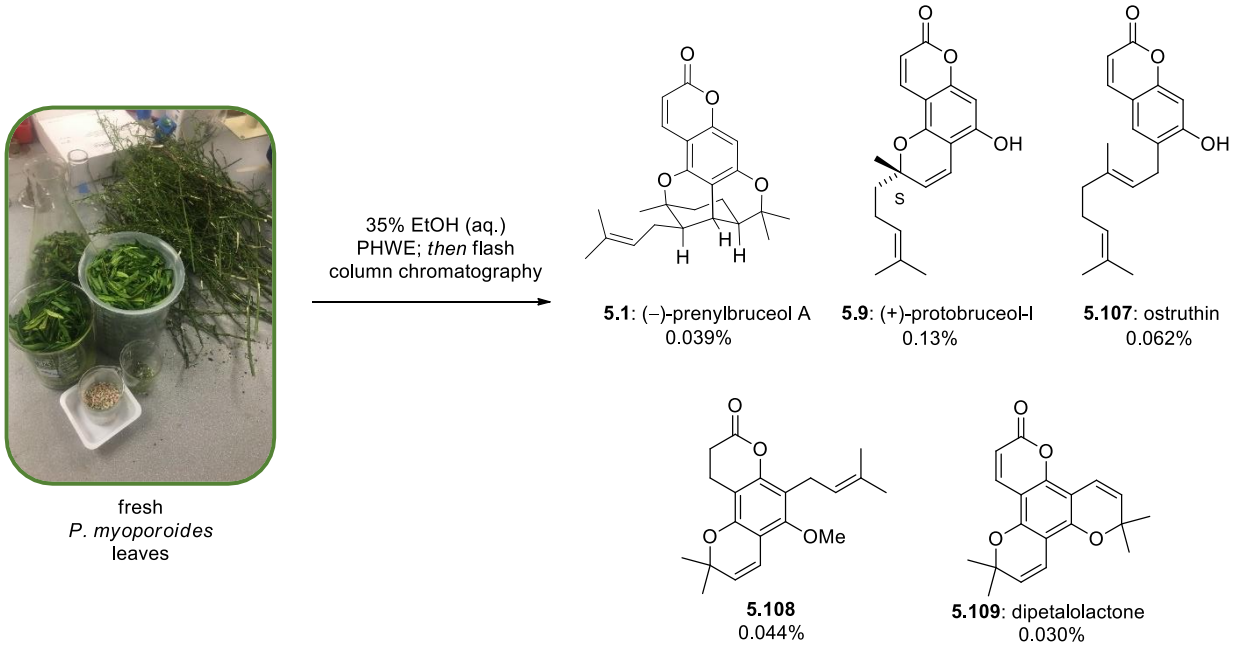

Branches of *Philotheca myoporoides* were collected from a suburban garden in Dernancourt, Adelaide, South Australia. The leaves were separated and carefully dried to minimise exposure to air and sunlight. A voucher specimen of *P. myoporoides* was deposited at the State Herbarium of South Australia in Adelaide (AD283914).

Dry, finely chopped leaves of *P. myoporoides* (~10 g) were combined with sand (~2 g) and extracted with 35% aqueous ethanol (200 mL) using a conventional, unmodified espresso machine. This process was repeated a further six times on a total 70 g of plant material. The combined aqueous extracts (~1.4 L) were concentrated to approximately 100 mL *in vacuo*, diluted with water (500 mL), and extracted with EtOAc (500 mL × 3). The combined organic extracts were then washed with water (500 mL) and brine (500 mL × 2), dried over $MgSO_4$, filtered, and concentrated *in vacuo* to give a crude green residue (1.5 g). This residue was subjected to flash column chromatography on SiO_2 (8:1 → 2:1 petrol/EtOAc, gradient elution) giving in order of increasing polarity: dipetalolactone (**5.109**) as a yellow oil (21.0 mg, 0.030%), **5.108** as a pale off-white solid (31.0 mg, 0.044%), crude prenylbruceol A (**5.1**) as a yellow oil (~40 mg), a crude mixture containing mostly ostruthin (**5.107**) and protobruceol-I (**5.9**) as a deep yellow oil (~300 mg). Crude prenylbruceol (**5.1**) was purified by flash column chromatography on SiO_2 (30:1 CH_2Cl_2/EtOAc) to give a clear colourless oil (27.6 mg, 0.039%). The crude mixture of **5.107** and **5.9** was separated via flash column chromatography on SiO_2 (15:1 CH_2Cl_2/EtOAc) affording ostruthin (**5.107**) as a white solid (43.9 mg, 0.062%), then protobruceol-I (**5.9**) as a pale yellow oil (98.0 mg, 0.13%).

Data for dihydrocoumarin **5.108**:

^{1}H NMR (600 MHz, $CDCl_3$) δ 6.53 (d, *J* = 10.0 Hz, 1H), 5.57 (d, *J* = 10.0 Hz, 1H), 5.17 (t, *J* = 7.1 Hz, 1H), 3.73 (s, 3H), 3.31 (d, *J* = 6.6 Hz, 2H), 2.89 (dd, *J* = 8.2, 6.4 Hz, 2H), 2.70 (dd, *J* = 8.2, 6.5 Hz, 2H), 1.79 (s, 3H), 1.67 (s, 3H), 1.42 (s, 6H)
^{13}C NMR (150 MHz, $CDCl_3$) δ 168.7, 153.7, 150.6, 148.6, 131.8, 129.1, 122.8, 117.3, 115.4, 111.1, 107.1, 76.5, 62.6, 28.9, 28.1, 25.9, 22.6, 18.0, 17.5.
IR (neat) $\bar{\nu}$ 2975, 2924, 1773, 1601, 1437, 1271, 1171, 1126, 1105 cm^{-1}
R_f 0.85 (15:1 CH_2Cl_2/EtOAc), 0.55 (1:1 petrol/Et_2O)
HRMS (ESI) calculated for $C_{20}H_{25}O_4$ $[M+H]^+$ 329.1747; found 329.1740

Data for dipetatolactone (**5.109**):

^{1}H NMR (600 MHz, $CDCl_3$) δ 7.93 (d, *J* = 9.6 Hz, 1H), 6.77 (d, *J* = 10.0 Hz, 1H), 6.61 (d, *J* = 10.0 Hz, 1H), 6.10 (d, *J* = 9.6 Hz, 1H), 5.57 (d, *J* = 10.1 Hz, 1H), 5.54 (d, *J* = 10.0 Hz, 1H), 1.45 (s, 6H), 1.44 (s, 6H)
^{13}C NMR (150 MHz, $CDCl_3$) δ 161.4, 152.0, 150.19, 150.16, 138.9, 127.8, 127.6, 116.0, 115.3, 110.7, 106.1, 103.3, 102.4, 78.1, 78.1, 28.3, 28.1
IR (neat) $\bar{\nu}$ 2976, 1729, 1639, 1613, 1591, 1441, 1364, 1181, 1131, 1018
R_f 0.55 (2:1 petrol/EtOAc), 0.15 (10:1 petrol/EtOAc)
HRMS (ESI) calculated for $C_{19}H_{19}O_4$ $[M+H]^+$ 311.1278; found 311.1280.

Data for prenylbruceol A (**5.1**):

^{1}H NMR (600 MHz, $CDCl_3$) δ 7.96 (dd, *J* = 9.5, 0.7 Hz, 1H), 6.42 (d, *J* = 0.6 Hz, 1H), 6.15 (d, *J* = 9.6 Hz, 1H), 5.16 (t, *J* = 7.3 Hz, 1H), 2.77 (br s, 1H), 2.43 – 2.36 (m, 1H), 2.10 (ddd, *J* = 11.6, 5.4, 2.8 Hz, 1H), 1.99 (ddd, *J* = 14.8, 10.3, 8.4 Hz, 1H), 1.82 (dd, *J* = 15.2, 6.1 Hz, 1H), 1.72 (dd, overlapped, 1H), 1.71 (s, 3H), 1.54 (s, 3H), 1.52 – 1.49 (m, overlapped, 1H), 1.48 (s, 3H), 1.42 (s, 3H), 1.28 (dt, *J* = 13.0, 6.2 Hz, 1H), 1.05 (s, 3H), 1.05 (s, 3H), 0.65 (tdd, *J* = 13.5, 11.5, 6.3 Hz, 1H)
^{13}C NMR (150 MHz, $CDCl_3$) δ 162.1, 160.8, 155.0, 152.4, 138.8, 134.2, 122.1, 110.9, 110.7, 104.0, 98.5, 85.8, 79.1, 47.3, 43.0, 39.2, 31.5, 29.8, 26.5, 26.0, 25.9, 24.0, 22.4, 18.0
IR (neat) $\bar{\nu}$ 2974, 2931, 1727, 1616, 1568, 1445, 1357, 1242, 1189, 1119, 1104, 1075, 964, 909 cm^{-1}
R_f 0.65 (15:1 CH_2Cl_2/EtOAc), 0.40 (1:1 petrol/Et_2O)

$[\alpha]^{25}_D$ = –292.3 ($CHCl_3$, c = 0.91)

HRMS (ESI) calculated for $C_{24}H_{28}O_4Na$ $[M+H]^+$ 403.1885; found 402.1880.

Data for ostruthin (**5.107**):

^{1}H NMR (600 MHz, $CDCl_3$) δ 7.65 (d, *J* = 9.4 Hz, 1H), 7.20 (s, 1H), 7.06 (s, 1H), 6.23 (d, *J* = 9.4 Hz, 1H), 5.33 (t, *J* = 7.4 Hz, 1H), 5.09 (t, *J* = 6.6 Hz, 1H), 3.39 (d, *J* = 7.3 Hz, 2H), 2.15 – 2.06 (m, 4H), 1.73 (s, 3H), 1.68 (s, 3H), 1.60 (s, 3H)

^{13}C NMR (150 MHz, $CDCl_3$) δ 162.8, 158.9, 154.2, 144.6, 138.6, 131.9, 128.3, 126.1, 124.1, 121.1, 112.3, 112.1, 103.3, 39.8, 28.3, 26.6, 25.9, 17.9, 16.3

IR (neat) $\bar{\nu}$ 3242, 2967, 2915, 1688, 1618, 1570, 1442, 1392, 1273, 1257, 1236, 1130, 821 cm^{-1}

R_f 0.35 (CH_2Cl_2/EtOAc), 0.35 (petrol/EtOAc).

m.p. 114 – 116 °C (white needles from cyclohexane)

HRMS (ESI) calculated for $C_{19}H_{23}O_3$ $[M+H]^+$ 299.1642; found 299.1643.

Data for (+)-protobruceol-I (**5.9**):

^{1}H NMR (600 MHz, $CDCl_3$) δ 7.99 (dd, *J* = 9.6, 0.7 Hz, 1H), 7.19 (br s, 1H), 6.68 (d, *J* = 10.1 Hz, 1H), 6.57 (d, *J* = 0.8 Hz, 1H), 6.14 (d, *J* = 9.5 Hz, 1H), 5.52 (d, *J* = 10.0 Hz, 1H), 5.08 (t, *J* = 7.2 Hz, 1H), 2.15 – 2.08 (m, 2H), 1.81 – 1.69 (m, 2H), 1.65 (s, 3H), 1.56 (s, 3H), 1.44 (s, 3H)

^{13}C NMR (150 MHz, $CDCl_3$) δ 162.6, 155.9, 155.4, 151.2, 139.5, 132.2, 126.7, 123.8, 116.6, 110.4, 106.0, 103.6, 95.6, 80.5, 41.4, 26.7, 25.8, 22.8, 17.8

IR (neat) $\bar{\nu}$ 3242, 2926, 2970, 1694, 1638, 1615, 1595, 1443, 1365, 1258, 1206, 1141, 1090 cm^{-1}

R_f 0.30 (CH_2Cl_2/EtOAc), 0.35 (petrol/EtOAc)

m.p. 114.5-115.5 °C (white needles from cyclohexane)

$[\alpha]^{25}_D$ = +119.0 ° ($CHCl_3$, c = 1.0)

HRMS (ESI) calculated for $C_{19}H_{21}O_4$ $[M+H]^+$ 313.1434; found 313.1435.

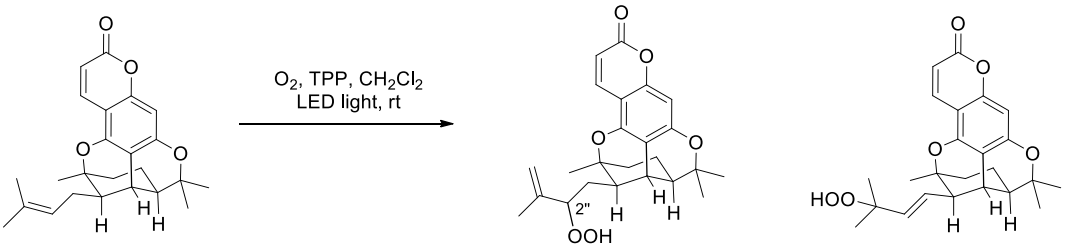

5.1: prenylbruceol A

5.2: prenylbruceol B
16%

5.3: prenylbruceol C
46%

To a solution of prenylbruceol (**1**) (45.4 mg, 0.199 mmol) in CH_2Cl_2 (20 mL) was added TPP (1.5 mg, 0.002 mmol). O_2 was bubbled through as the resultant mixture was irradiated with LED light for 1.5 h. The solvent was removed *in vacuo* and the residue was purified by flash column chromatography on SiO_2 (15:1 CH_2Cl_2/EtOAc) to afford **2** as a single diastereoisomer (8.0 mg, 16%), further elution afforded **3** (22.8 mg, 46%).

Data for prenylbruceol B (**5.2**):

^{1}H NMR (600 MHz, $CDCl_3$) δ 7.96 (s, 1H), 7.93 (dd, *J* = 9.5, 0.7 Hz, 1H), 6.44 (d, *J* = 0.6 Hz, 1H), 6.15 (d, *J* = 9.6 Hz, 1H), 5.07 – 5.06 (m, 1H), 5.04 – 5.02 (m, 1H), 4.48 (dd, *J* = 10.3, 3.5 Hz, 1H), 2.84 (br s, 1H), 2.21 (ddd, *J* = 11.7, 5.4, 2.8 Hz, 1H), 2.04 – 2.02 (m, overlapped, 1H), 2.04 – 1.99 (m, overlapped, 1H), 1.83 (dd, *J* = 15.2, 5.0, 1H), 1.73 (s, 3H), 1.59 (s, 3H), 1.41 (s, 3H), 1.33 – 1.28 (m, 1H), 1.07 (s, 3H), 0.65 (tdd, *J* = 13.5, 11.5, 6.3 Hz, 1H)
^{13}C NMR (150 MHz, $CDCl_3$) δ 162.0, 160.9, 155.1, 152.4, 143.8, 138.7, 114.2, 111.0, 110.4, 104.2, 98.8, 86.9, 86.0, 79.0, 47.0, 39.1, 38.6, 32.3, 30.1, 29.8, 25.9, 24.0, 22.3, 18.0
IR (neat) $\bar{\nu}$ 3360, 2977, 2937, 1711, 1616, 1567, 1445, 1358, 1242, 1125, 1123, 1076 cm^{-1}
R_f 0.35 (10:1 CH_2Cl_2/EtOAc)
HRMS (ESI) calculated for $C_{24}H_{29}O_6$ $[M+H]^+$ 413.1959; found 413.1955.

Data for prenylbruceol C (**5.3**):

^{1}H NMR (600 MHz, $CDCl_3$) δ 7.96 (d, *J* = 9.6 Hz, 1H), 7.50 (s, 1H), 6.45 (s, 1H), 6.17 (d, *J* = 9.6 Hz, 1H), 5.81 (d, *J* = 15.8 Hz, 1H), 5.66 (dd, *J* = 15.9, 9.3 Hz, 1H), 2.71 (br s, 1H), 2.45 (dd, *J* = 9.3, 1.4 Hz, 1H), 2.20 (ddd, *J* = 11.7, 5.4, 2.8 Hz, 1H), 1.87 (dd, *J* = 15.0, 5.7 Hz, 1H), 1.57 (s, 3H), 1.51 (ddd, *J* = 15.2, 13.1, 6.9 Hz, 1H), 1.34 – 1.29 (m, overlapped, 1H), 1.34 (s, 3H), 1.33 (s, 3H), 1.32 (s, 3H), 1.06 (s, 3H), 0.65 (tdd, *J* = 13.5, 11.6, 6.2 Hz, 1H)

^{13}C NMR (150 MHz, $CDCl_3$) δ 162.0, 160.5, 155.1, 152.3, 138.8, 137.5, 128.6, 111.0, 110.7, 104.2, 98.9, 85.6, 82.3, 78.4, 47.0, 46.8, 38.5, 34.1, 29.7, 26.8, 24.5, 24.5 (overlapped), 24.0, 22.3

IR (neat) $\bar{\nu}$ 3378, 2978, 2935, 1725, 1617, 1567, 1446, 1358, 1243, 1122, 1108, 1077 cm^{-1}

R_f 0.25 (10:1 CH_2Cl_2/EtOAc)

HRMS (ESI) calculated for $C_{24}H_{29}O_6$ $[M+H]^+$ 413.1959; found 413.1957.

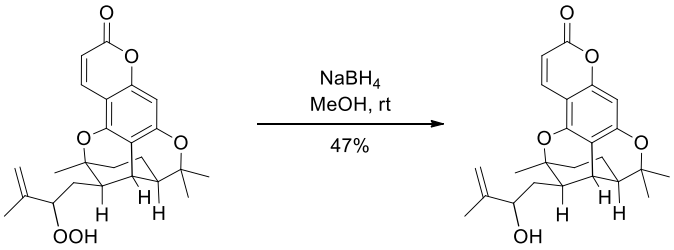

5.2: prenylbruceol B **5.110**

To a solution of **5.2** (14.7 mg, 0.0357 mmol) in MeOH (1 mL) was added $NaBH_4$ (2.7 mg, 2 mmol) in one portion. The reaction was stirred for 10 min, and the solvent was then removed *in vacuo* without heating. The crude was purified by flash column chromatography on SiO_2 (10:1 CH_2Cl_2/EtOAc). To afford allylic alcohol 5.**110** as a clear oil (6.6 mg, 47%).

Data for **5.110**

^{1}H NMR (600 MHz, $CDCl_3$) δ 7.94 (d, *J* = 9.7 Hz, 1H), 6.44 (s, 1H), 6.15 (d, *J* = 9.6 Hz, 1H), 5.00 (s, 1H), 4.85 (s, 1H), 4.21 (dd, *J* = 9.9, 3.2 Hz, 1H), 2.89 (br s, 1H), 2.19 (ddd, *J* = 11.6, 5.5, 2.8 Hz, 1H), 2.09 (ddd, *J* = 10.4, 2.7, 1.4 Hz, 1H), 1.92 (ddd, *J* = 14.4, 9.8, 2.7 Hz, 1H), 1.83 (ddd, *J* = 15.3, 6.3, 1.3 Hz, 1H), 1.70 (s, 3H), 1.58 (s, 3H), 1.57 – 1.52 (m, overlapped, 1H), 1.47 (ddd, *J* = 14.1, 10.4, 3.4 Hz, 1H), 1.42 (s, 3H), 1.33 – 1.27 (m, 1H), 1.06 (s, 3H), 0.65 (tdd, *J* = 13.5, 11.6, 6.3 Hz, 1H)

^{13}C NMR (150 MHz, $CDCl_3$) δ 162.0, 160.9, 155.0, 152.5, 148.2, 138.7, 110.9, 110.8, 110.7, 104.2, 98.6, 86.0, 79.3, 73.1, 47.1, 39.2, 38.5, 33.3, 31.8, 29.8, 26.0, 24.1, 22.3, 18.3

IR (neat) $\bar{\nu}$ 3443, 2976, 2936, 1719, 1616, 1567, 1446, 1358, 1242, 1121, 1076 cm^{-1}

HRMS (ESI) $C_{24}H_{29}O_5$ $[M+H]^+$ 379.1915; found 379.1905

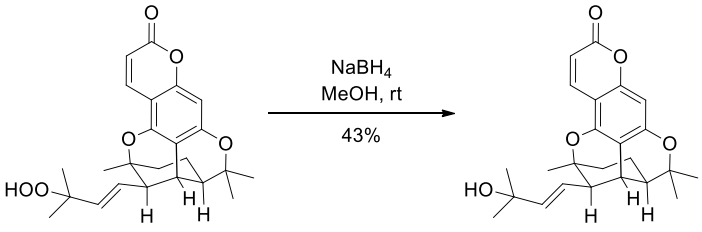

5.3: prenylbruceol C **5.4**: prenylbruceol D

To a solution of **5.3** (31.6 mg, 0.0767 mmol) in MeOH (2 mL) was added $NaBH_4$ (5.8 mg, 0.153 mmol) in one portion. The reaction mixture was stirred at room temperature for 5 min then quenched with 1 M HCl (1 drop), and the solvent was removed *in vacuo*. The residue was dissolved in Et_2O (15 mL) and washed with water (10 mL × 2) and brine (10 mL). The organic extract was dried over $MgSO_4$, filtered and concentrated *in vacuo*. The residue was purified by flash column chromatography to afford **5.4** as a white foam (13.0 mg, 43%).

Data for prenylbruceol D (**5.4**):

^{1}H NMR (600 MHz, $CDCl_3$) δ 7.94 (dd, *J* = 9.4, 0.6 Hz, 1H), 6.43 (s, 1H), 6.15 (d, *J* = 9.6 Hz, 1H), 5.84 (d, *J* = 15.7 Hz, 1H), 5.66 (dd, *J* = 15.6, 9.2 Hz, 1H), 2.70 (br s, 1H), 2.41 (dd, *J* = 9.2, 1.4 Hz, 1H), 2.19 (ddd, *J* = 11.5, 5.4, 2.8 Hz, 1H), 1.87 (dd, *J* = 15.3, 5.0 Hz, 1H), 1.57 (s, 3H), 1.55 – 1.48 (m, 1H), 1.34 (s, 3H), 1.32 – 1.27 (m, overlapped, 1H) 1.32 (s, 3H), 1.31 (s, 3H), 1.06 (s, 3H), 0.67 (tdd, *J* = 13.4, 11.5, 6.3 Hz, 1H)

^{13}C NMR (150 MHz, $CDCl_3$) δ 161.8, 160.6, 155.3, 152.4, 142.0, 138.6, 124.6, 111.0, 110.7, 104.2, 98.8, 85.5, 78.5, 70.9, 47.2, 46.6, 38.6, 34.4, 30.2, 30.0, 29.8, 26.7, 24.0, 22.4

IR (neat) $\bar{\nu}$ 3454, 2975, 1721, 1616, 1567, 1445, 1357, 1121, 1107 cm^{-1}

R_f 0.15 (10:1 CH_2Cl_2/EtOAc)

HRMS (ESI) calculated for $C_{24}H_{29}O_5$ $[M+H]^+$ 379.1915; found 379.1905.

5.4.3: NMR Spectra

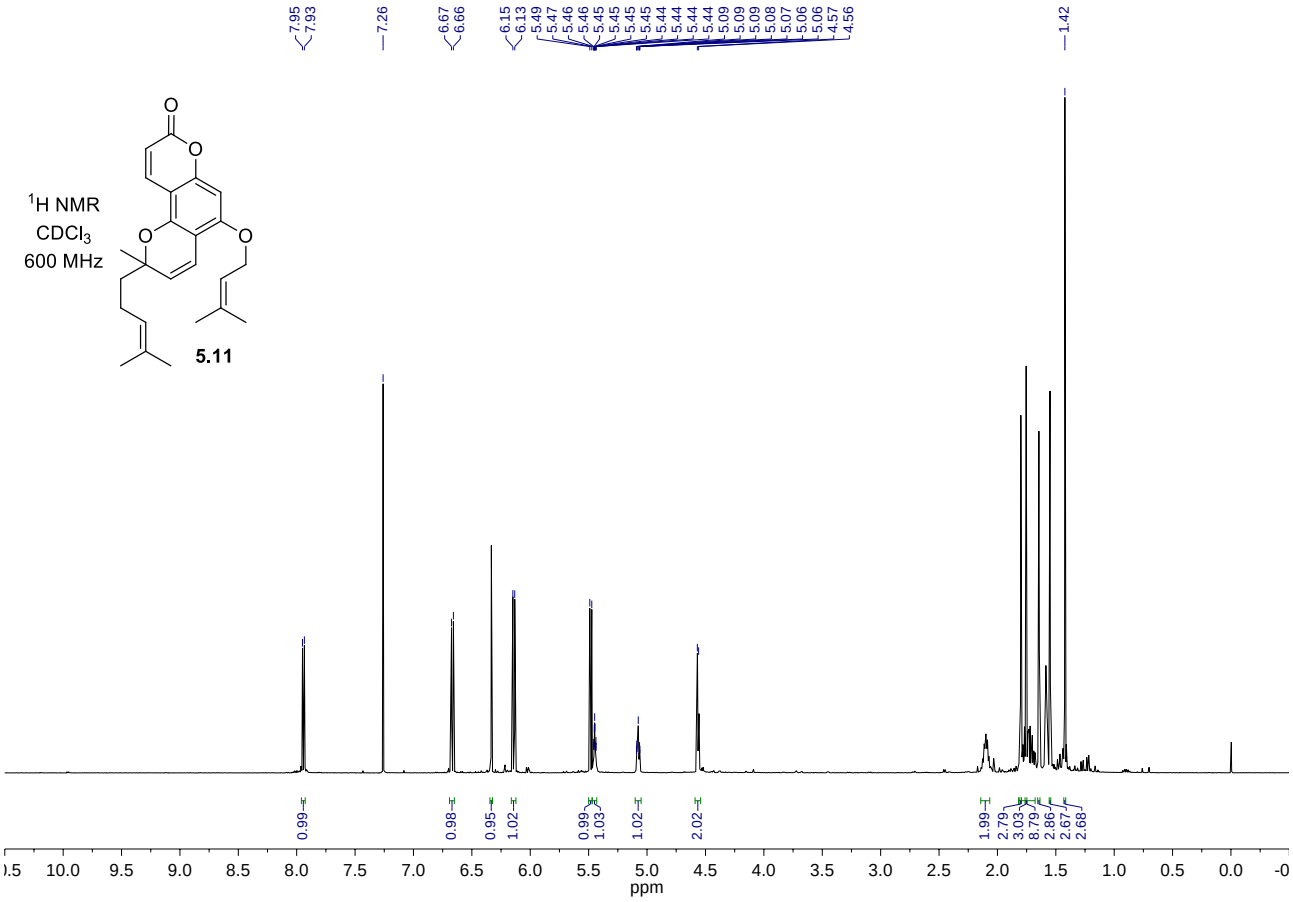

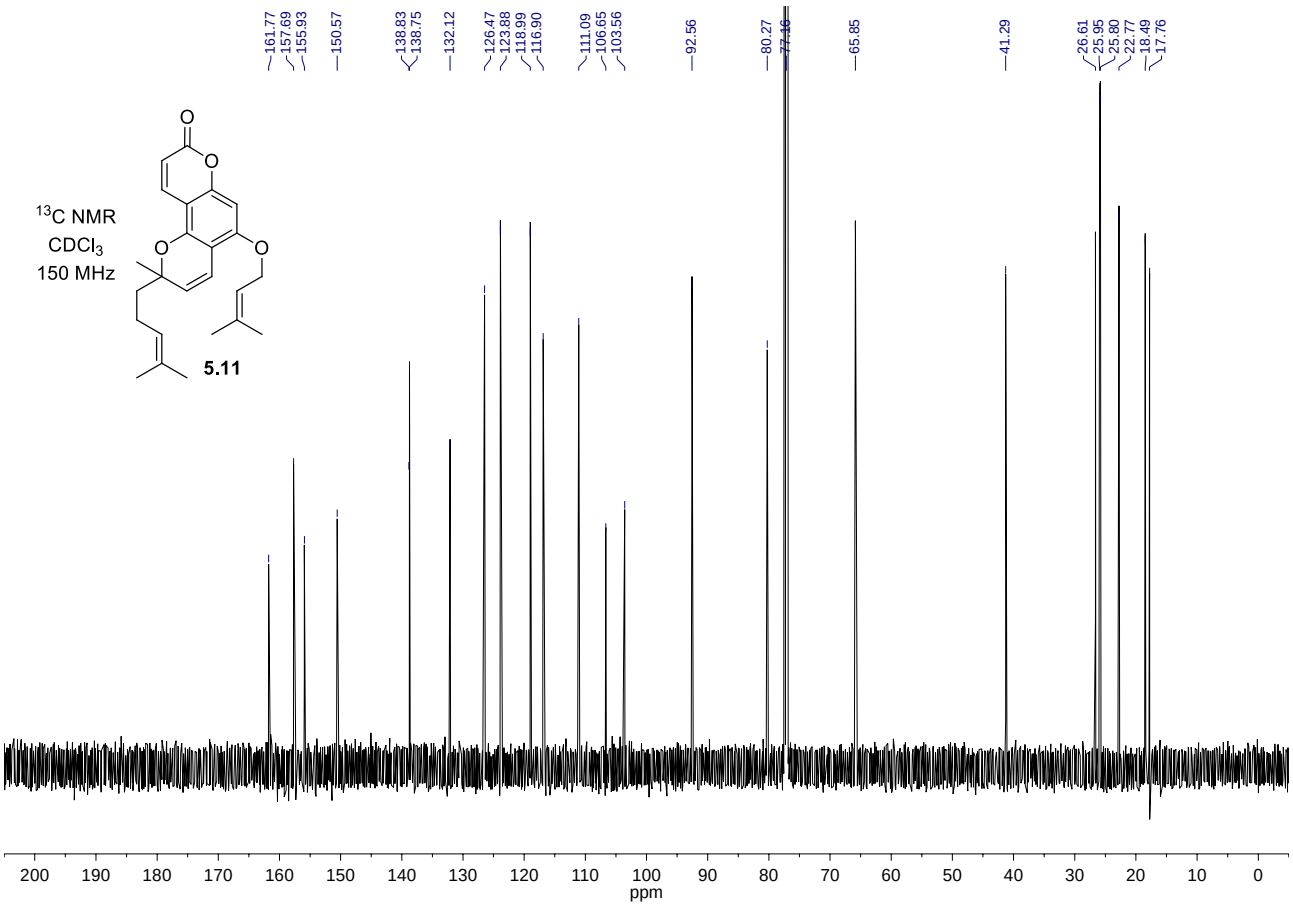

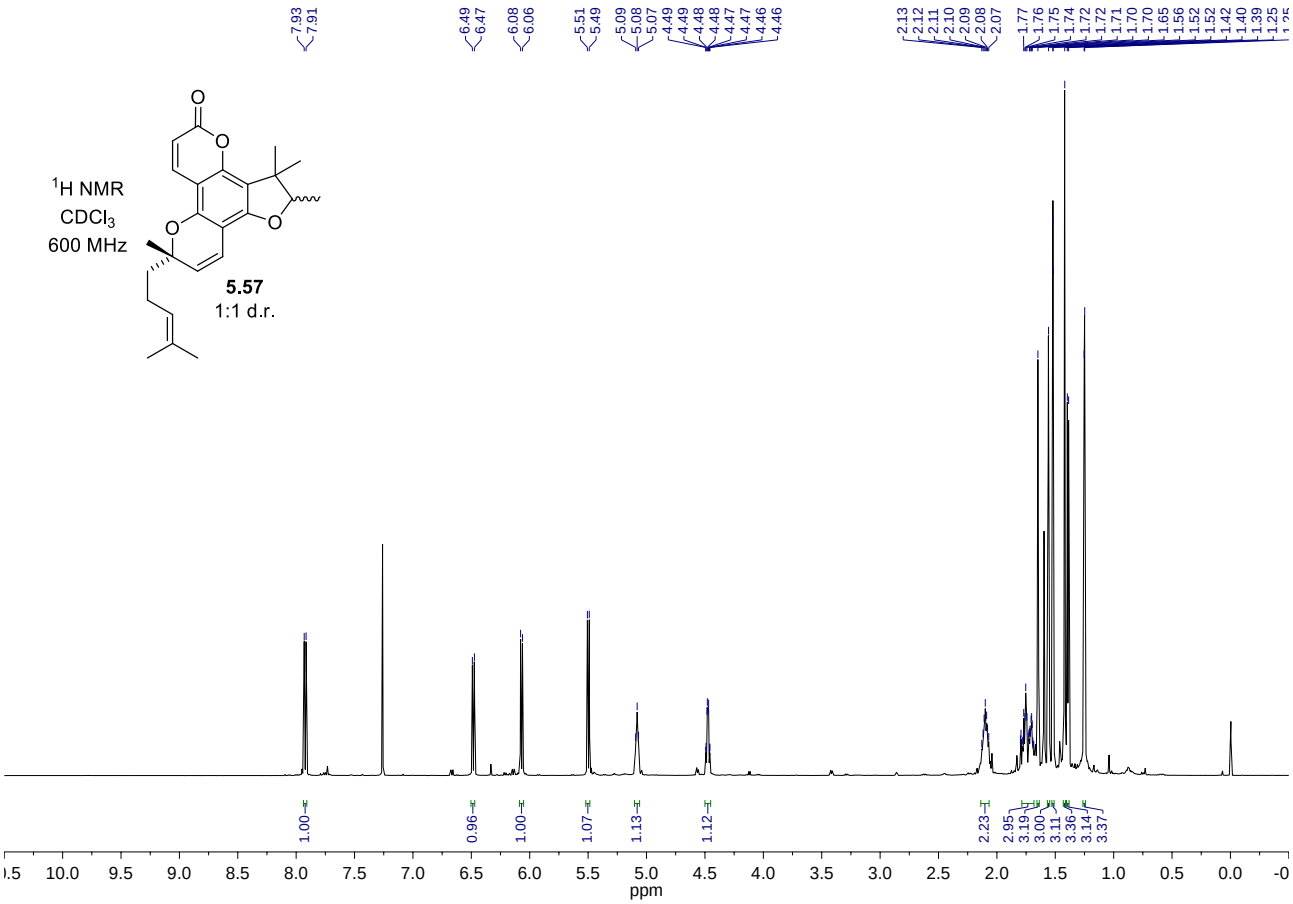
^{1}H NMR
$CDCl_3$
600 MHz
5.57
1:1 d.r.
ppm

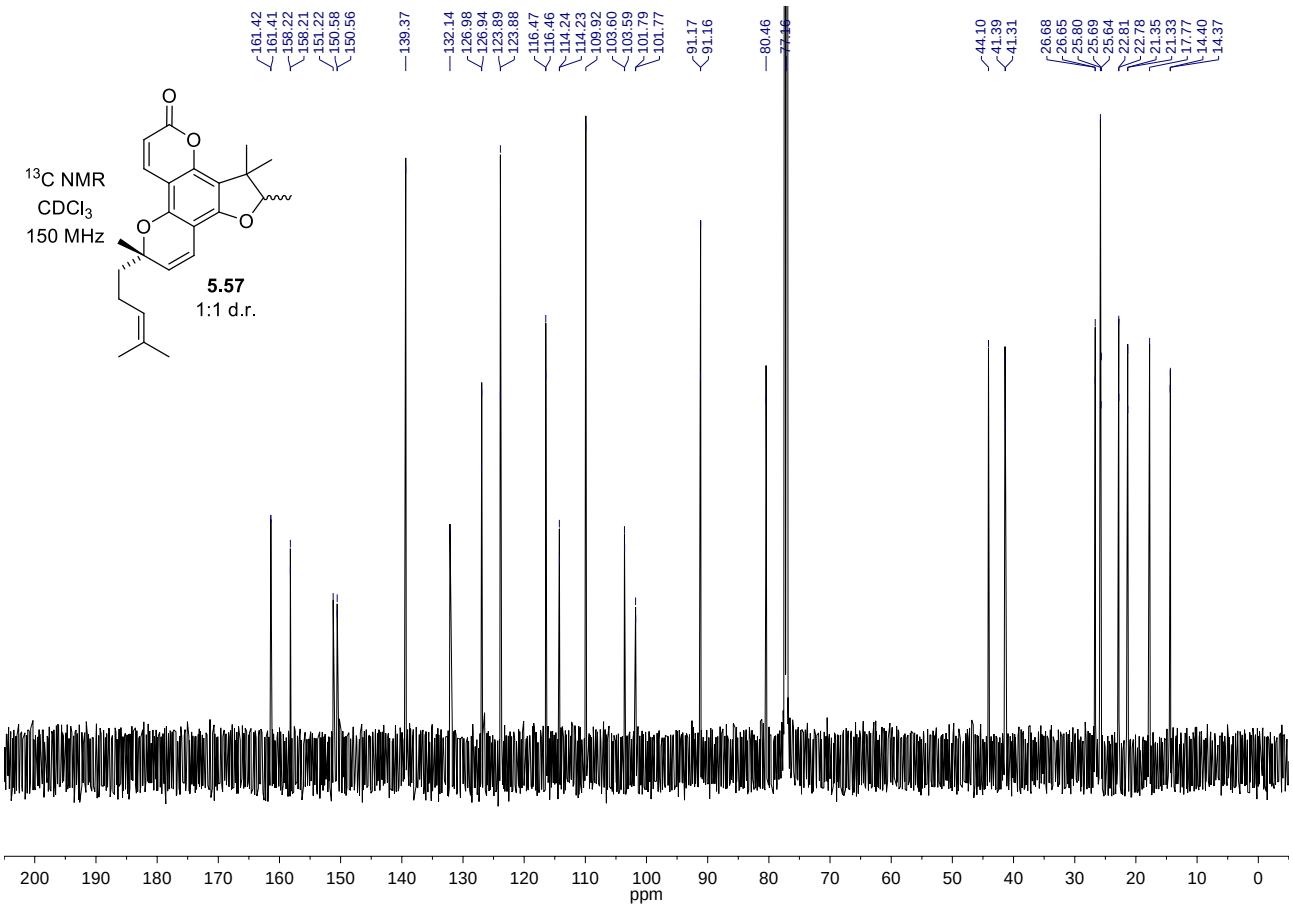
^{13}C NMR
$CDCl_3$
150 MHz
5.57
1:1 d.r.
ppm

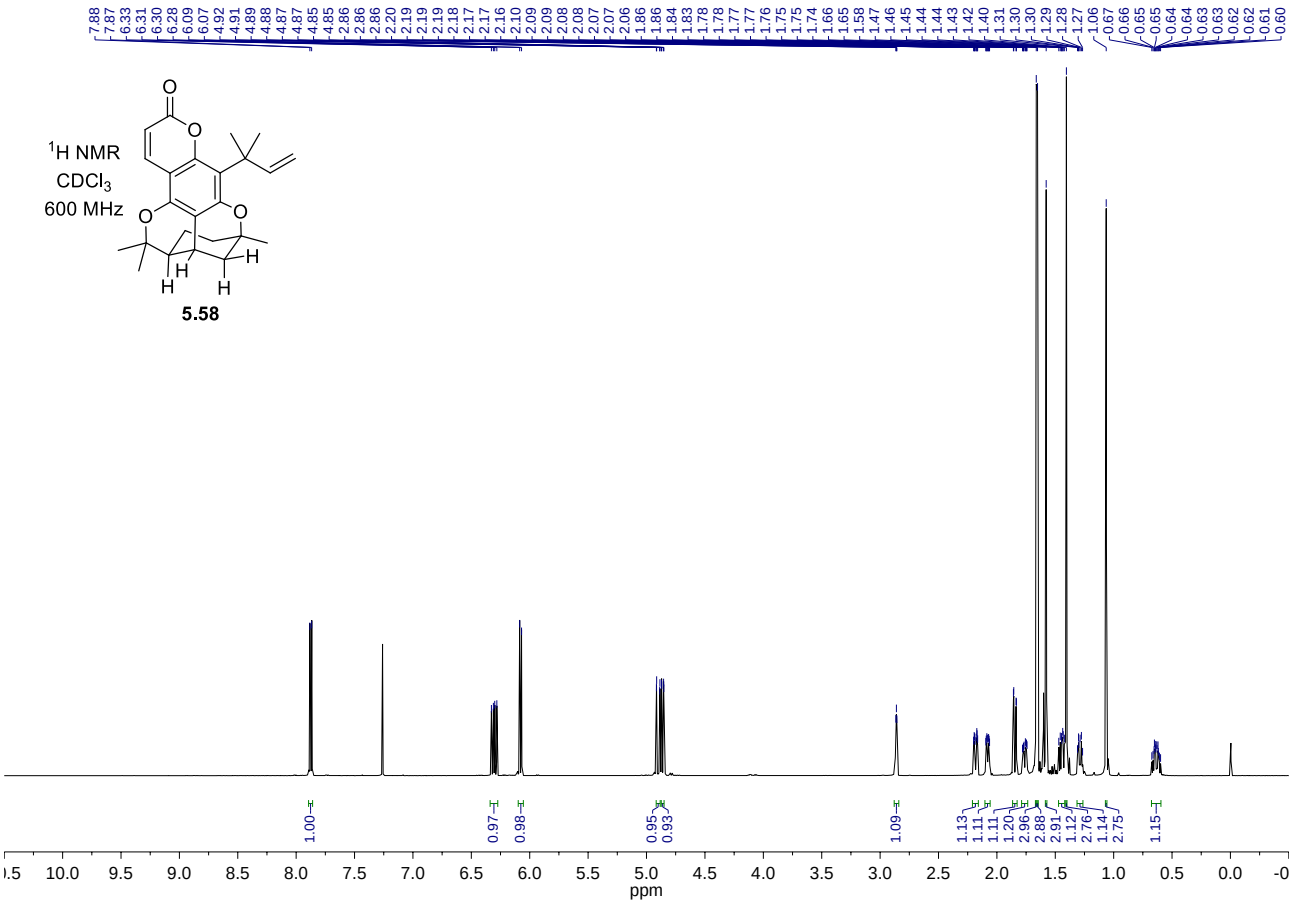
^{1}H NMR
$CDCl_3$
600 MHz
5.58
ppm

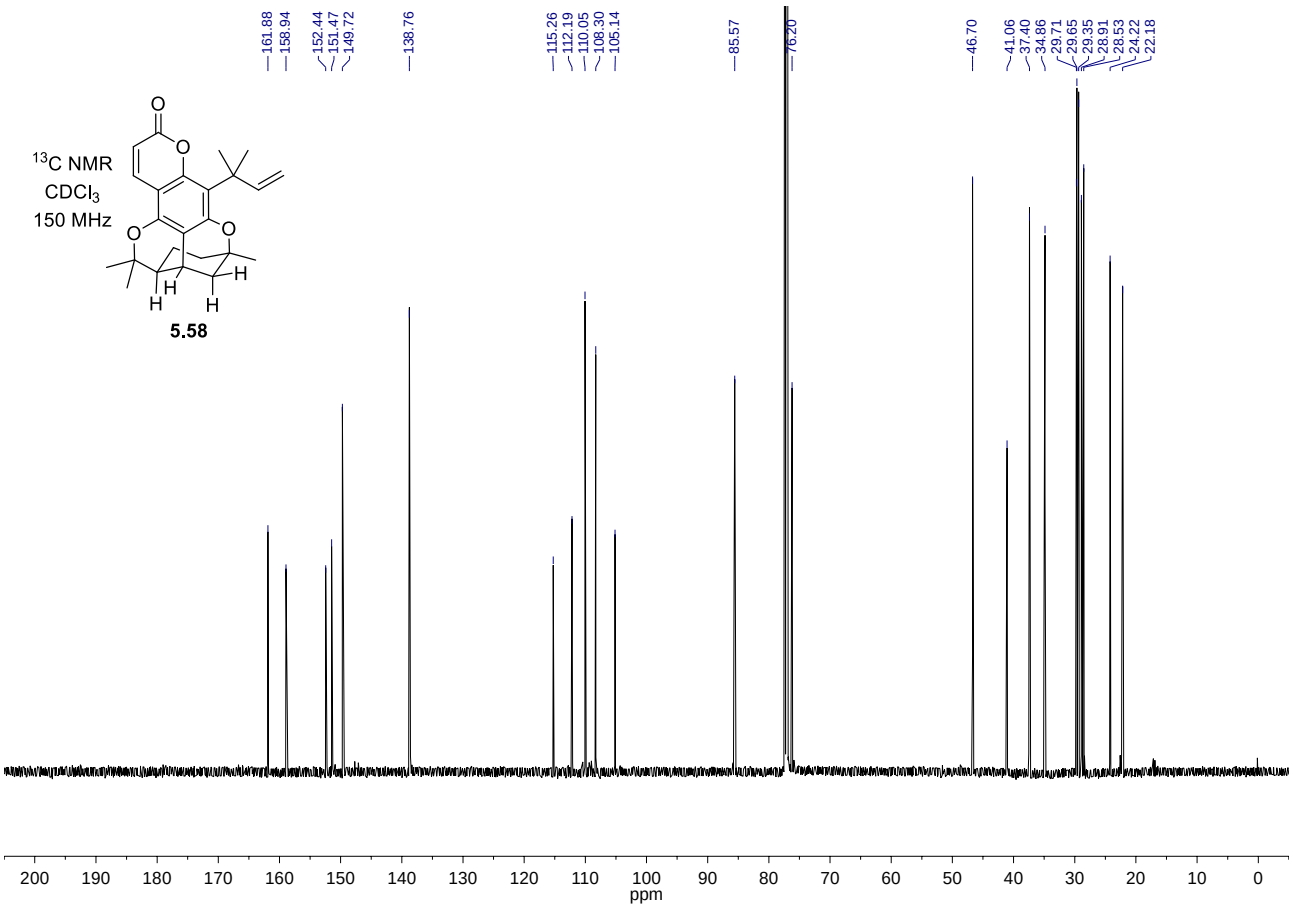
^{13}C NMR
$CDCl_3$
150 MHz
5.58
ppm

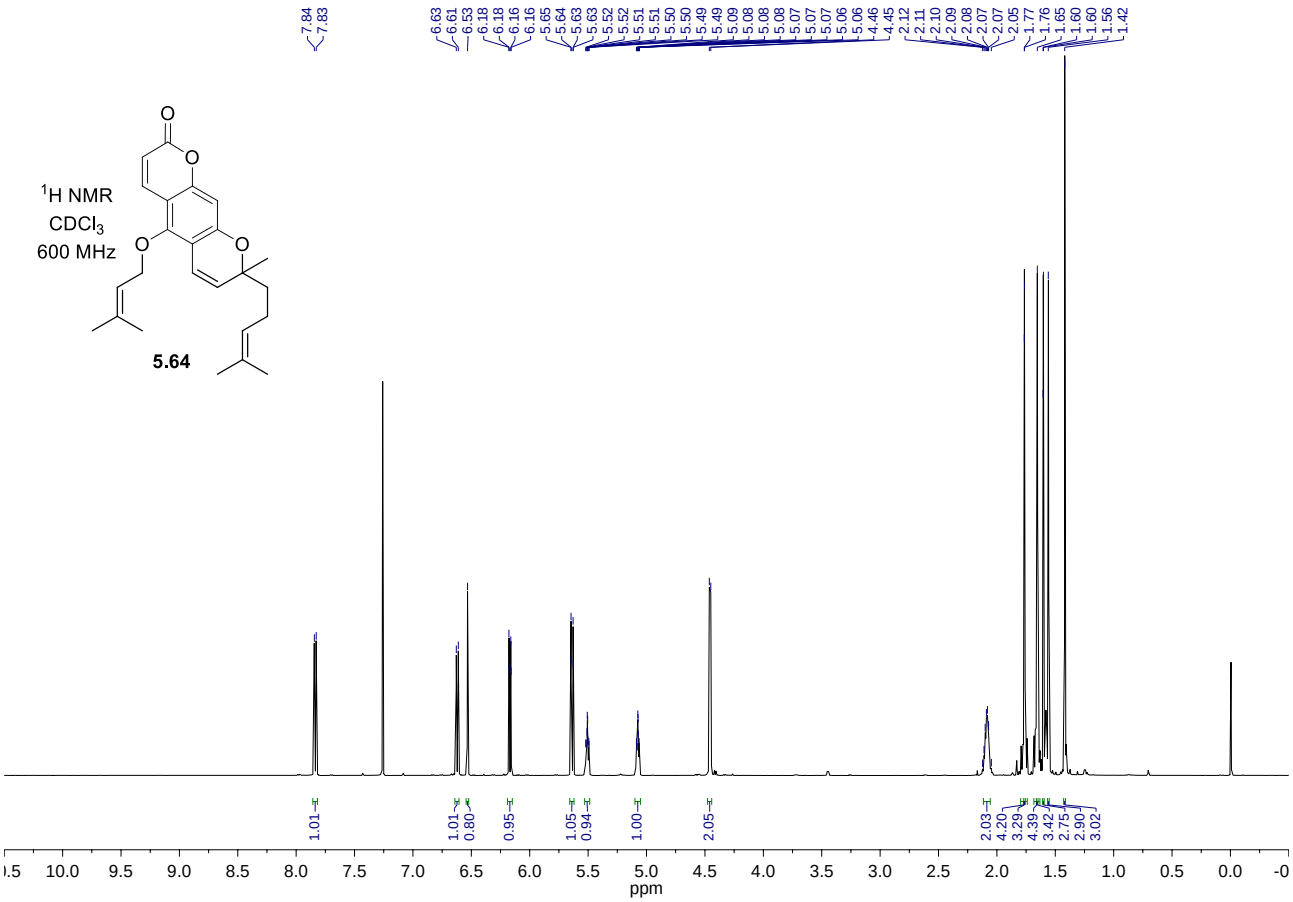
^{1}H NMR
$CDCl_3$
600 MHz
5.64
ppm

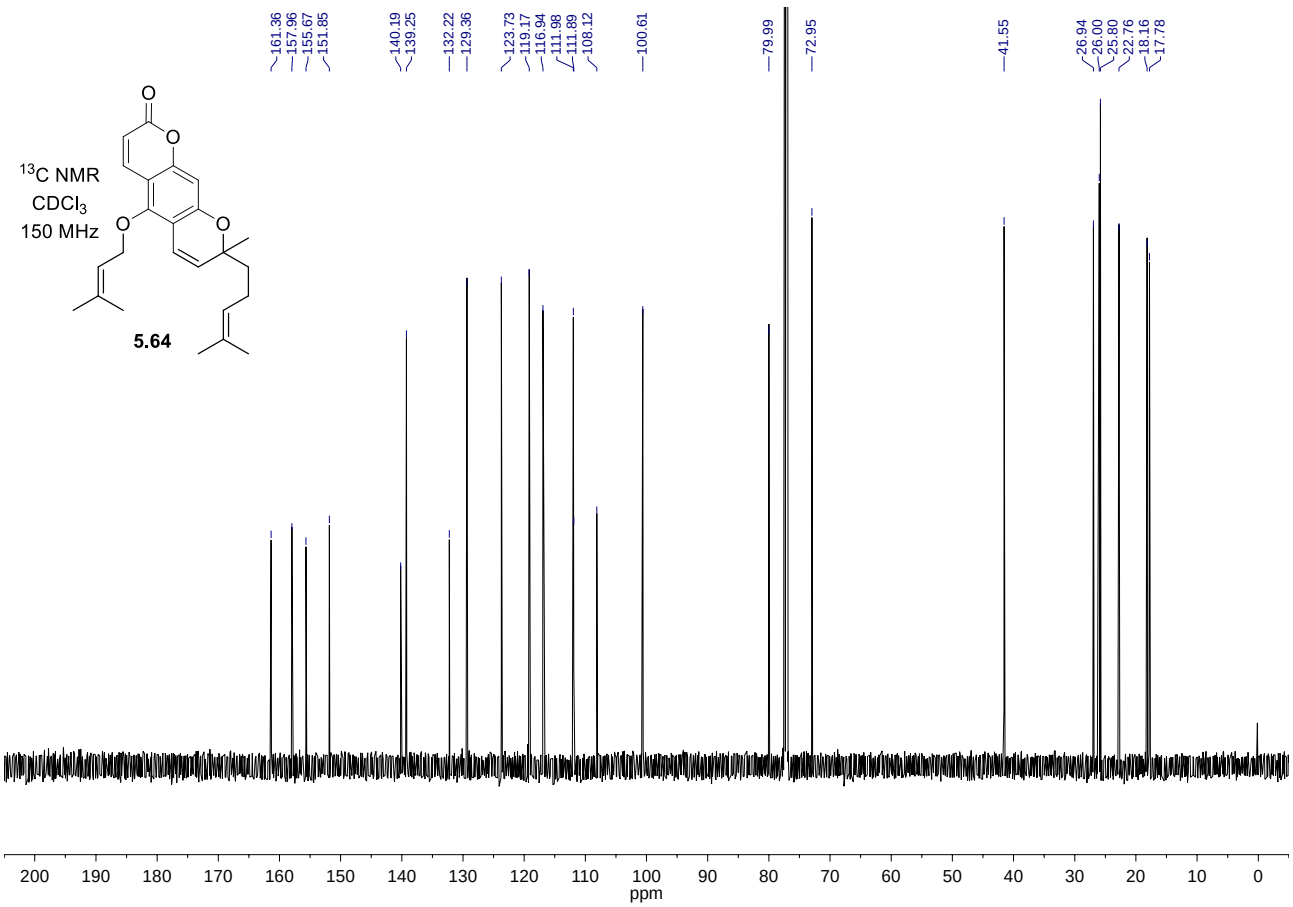
^{13}C NMR
$CDCl_3$
150 MHz
5.64
ppm

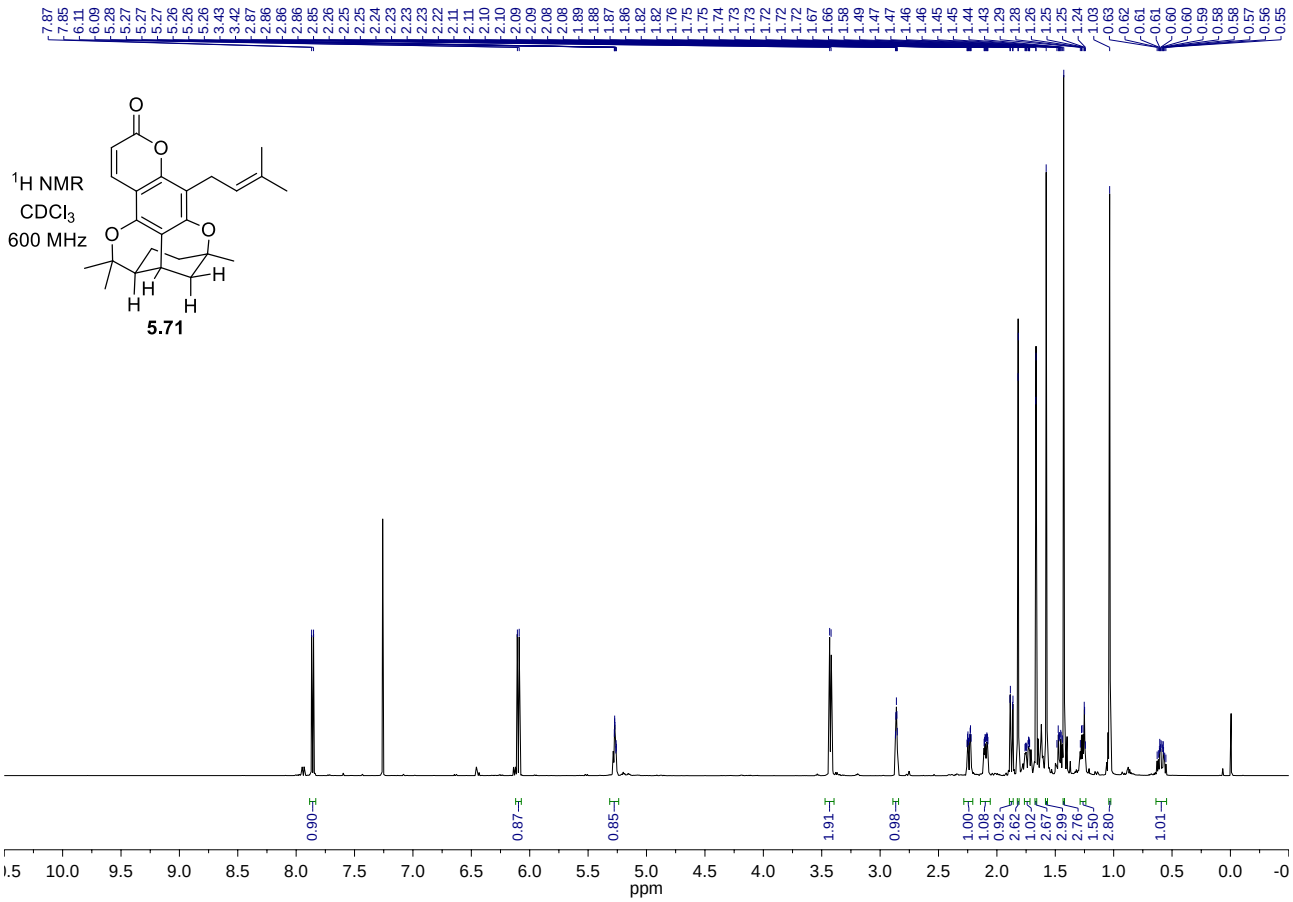
^{1}H NMR
$CDCl_3$
600 MHz
5.71
ppm

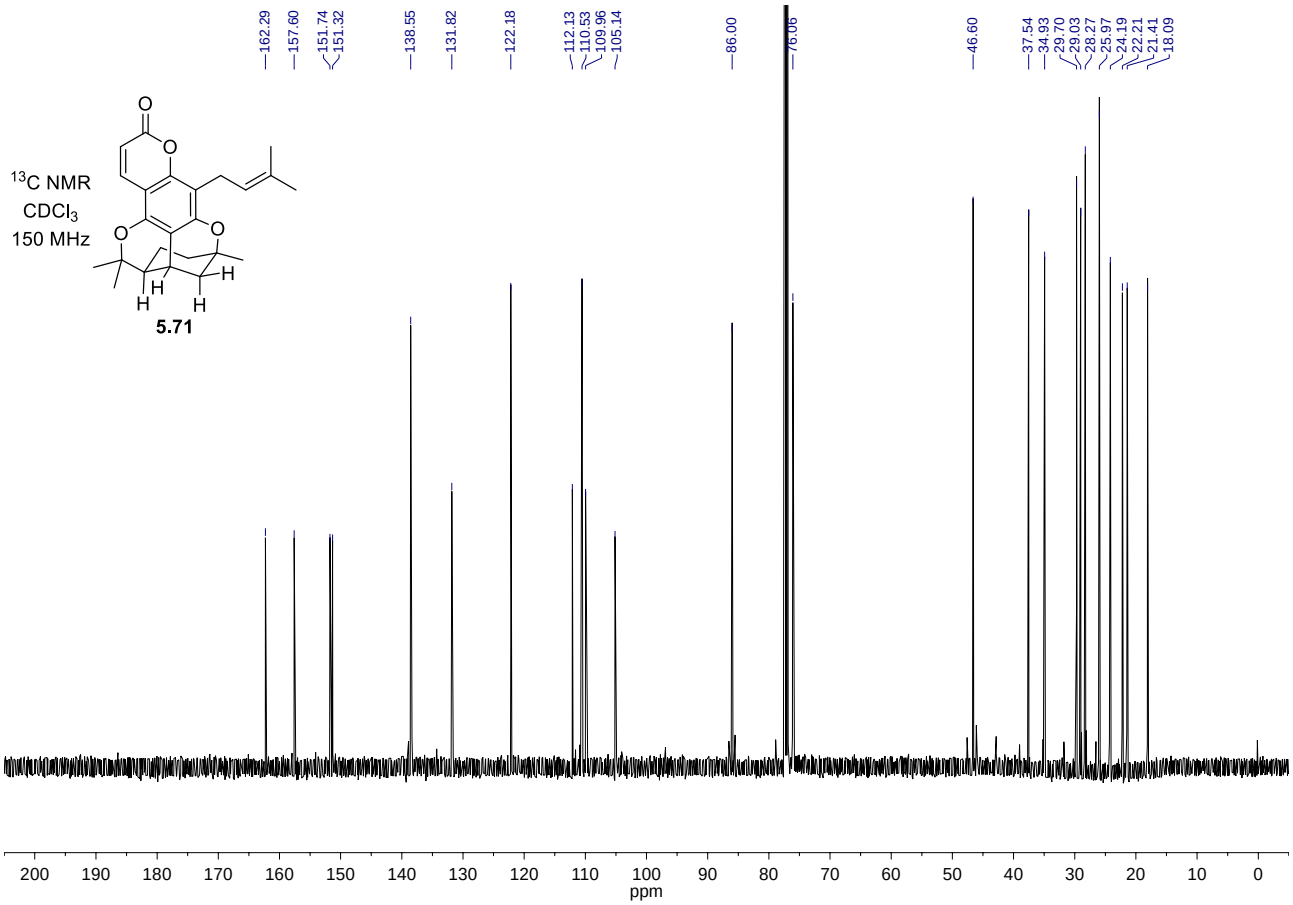
^{13}C NMR
$CDCl_3$
150 MHz
5.71
ppm

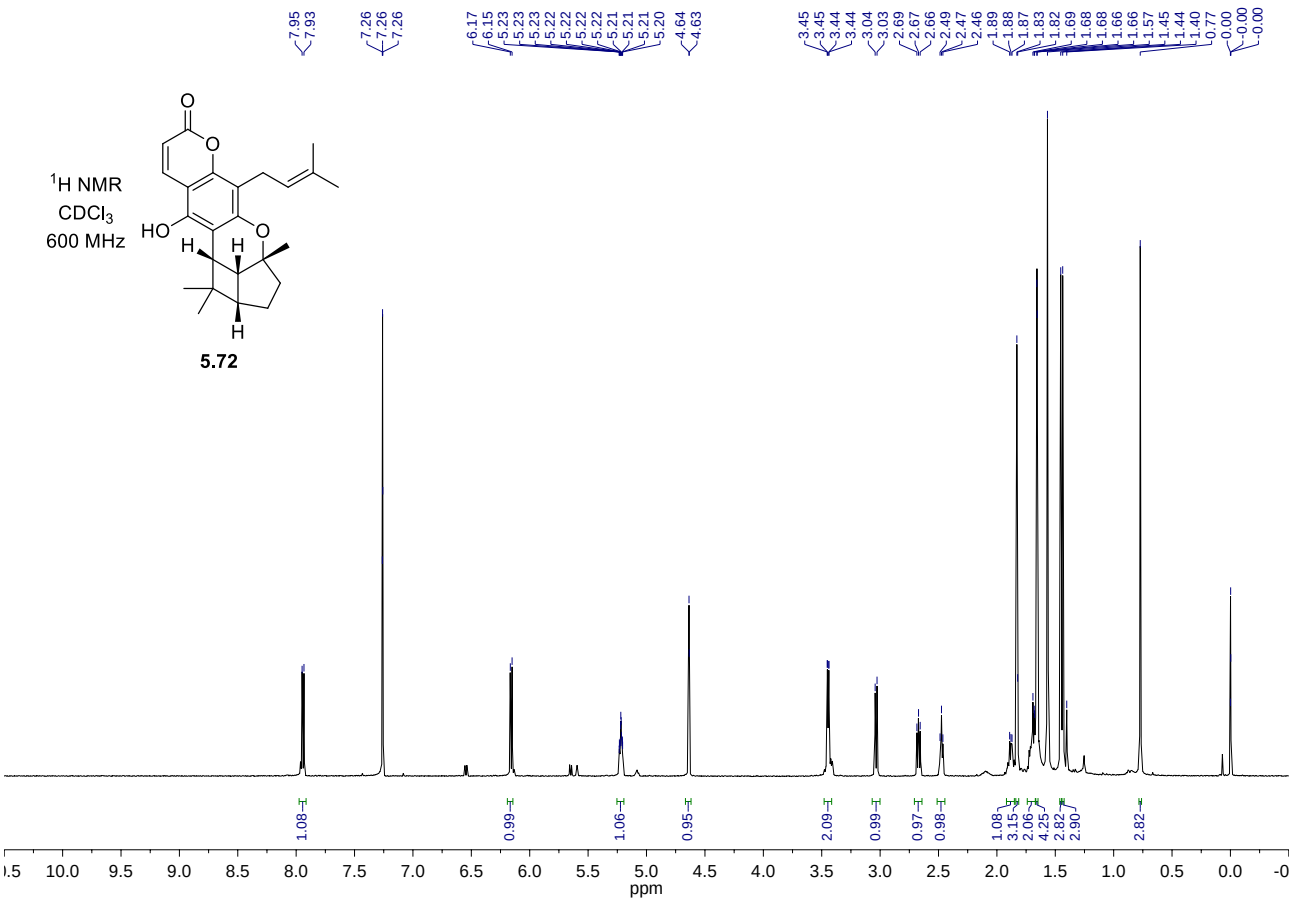
^{1}H NMR
$CDCl_3$
600 MHz
HO
O
H
H
H
5.72
ppm

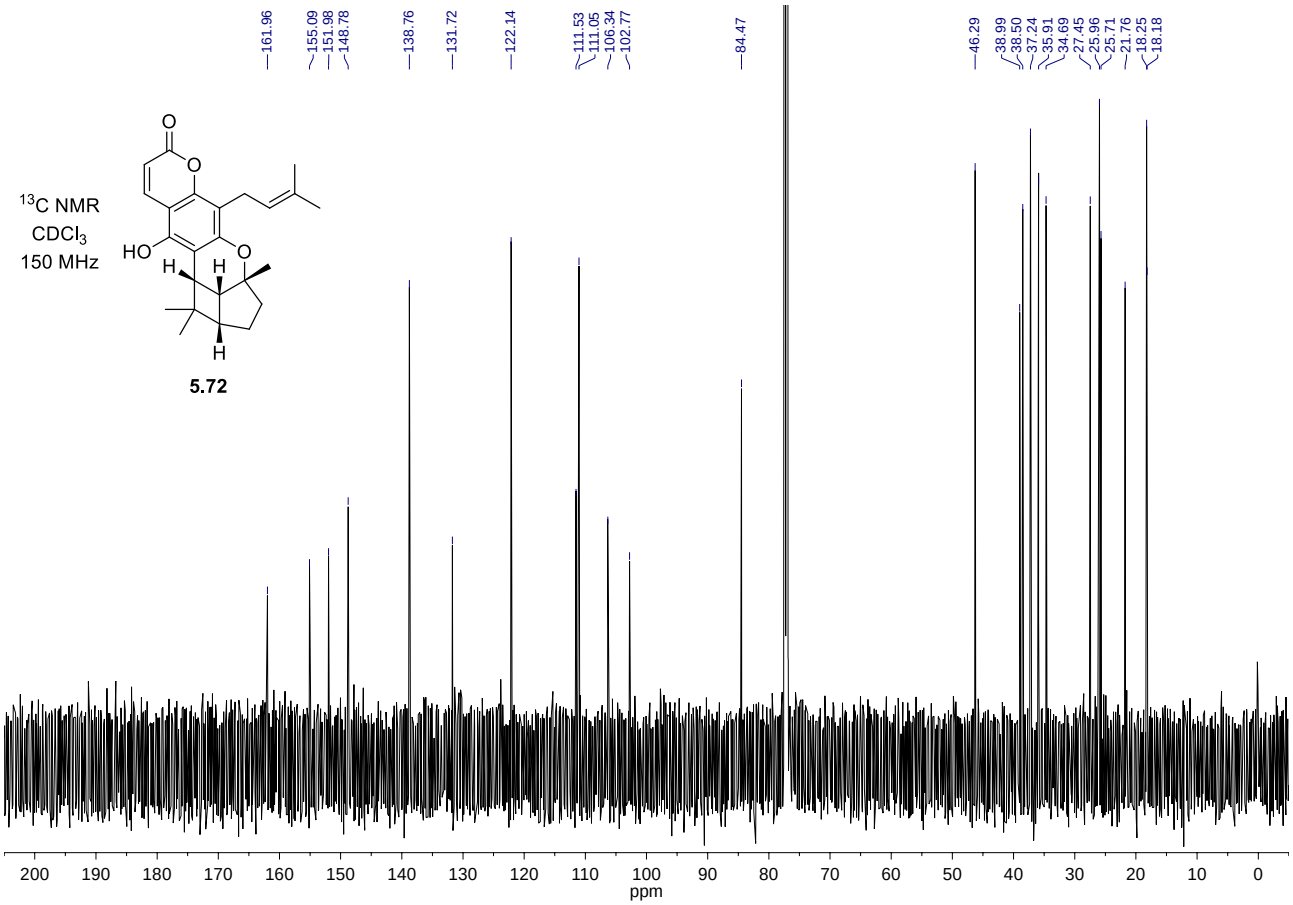
^{13}C NMR
$CDCl_3$
150 MHz
HO
O
H
H
H
5.72
ppm

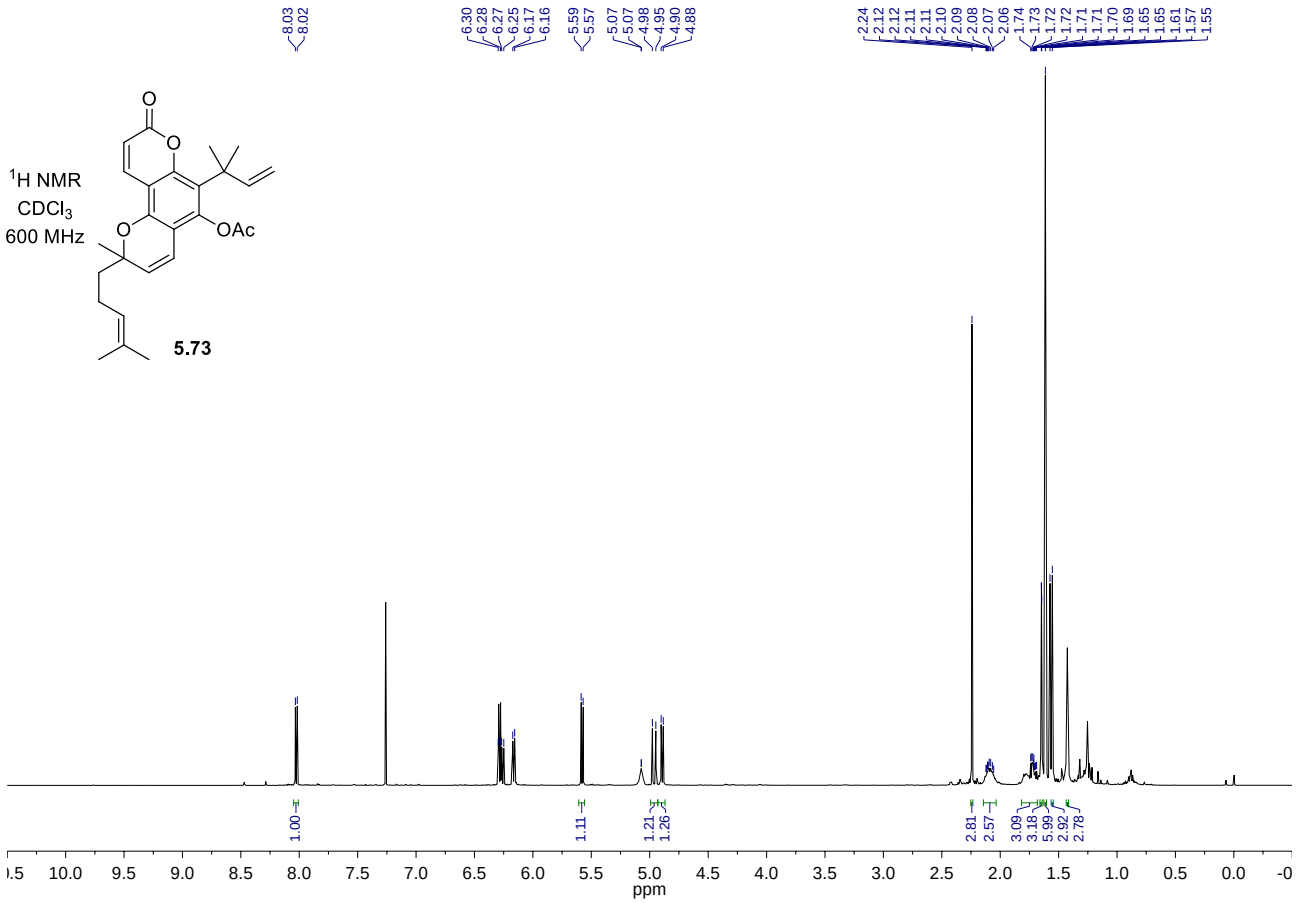
8.03
8.02
6.30
6.28
6.27
6.25
6.17
6.16
5.59
5.57
5.07
5.07
4.98
4.95
4.90
4.88
2.24
2.12
2.12
2.11
2.11
2.10
2.09
2.08
2.07
2.06
1.74
1.73
1.72
1.72
1.71
1.71
1.70
1.69
1.65
1.65
1.61
1.57
1.55
1H NMR
CDCl3
600 MHz
OAc
5.73
1.00
1.11
1.21
1.26
2.81
2.57
3.09
3.18
5.99
2.92
2.78
ppm

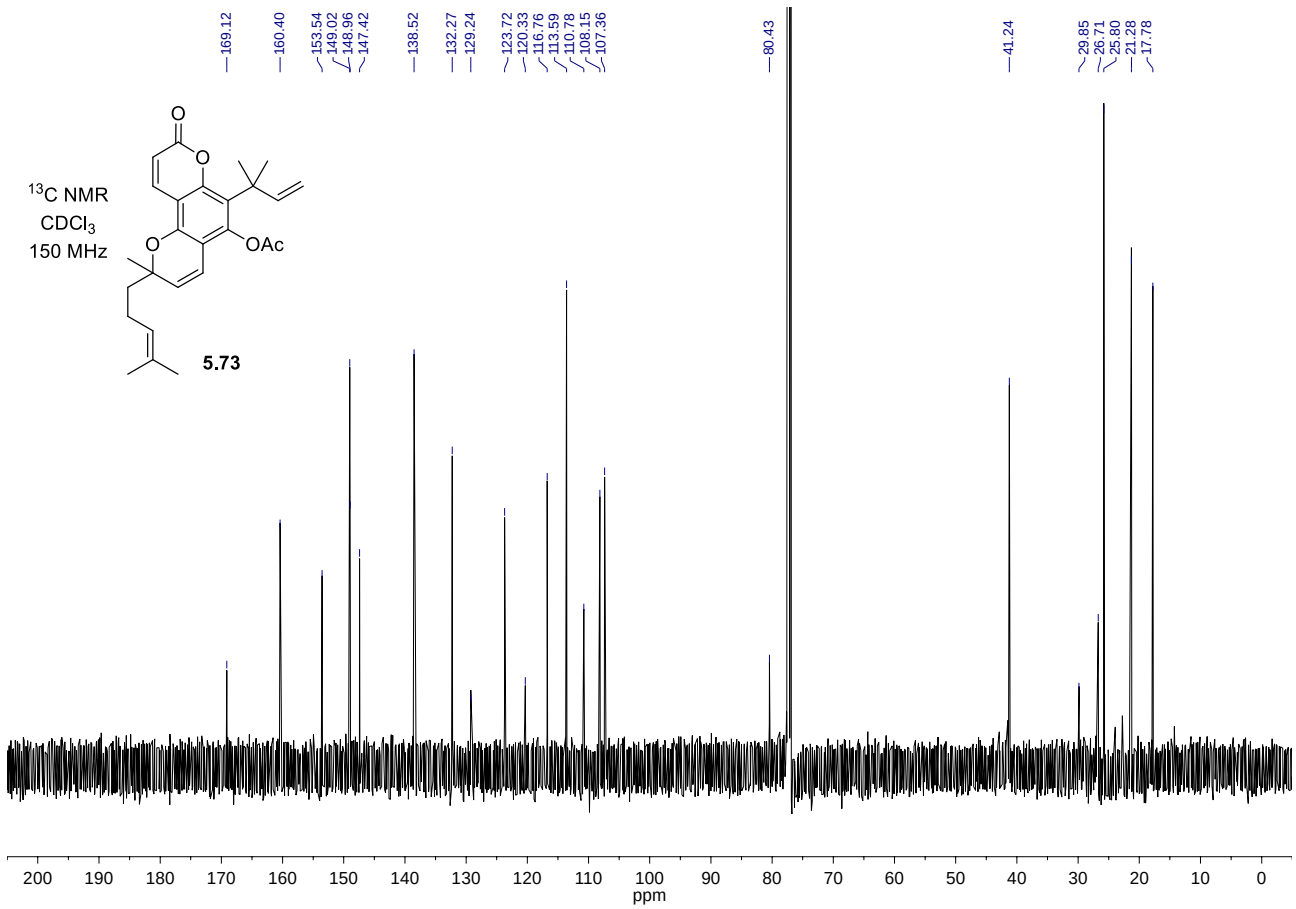
169.12
160.40
153.54
149.02
148.96
147.42
138.52
132.27
129.24
123.72
120.33
116.76
113.59
110.78
108.15
107.36
80.43
41.24
29.85
26.71
25.80
21.28
17.78
13C NMR
CDCl3
150 MHz
OAc
5.73
ppm

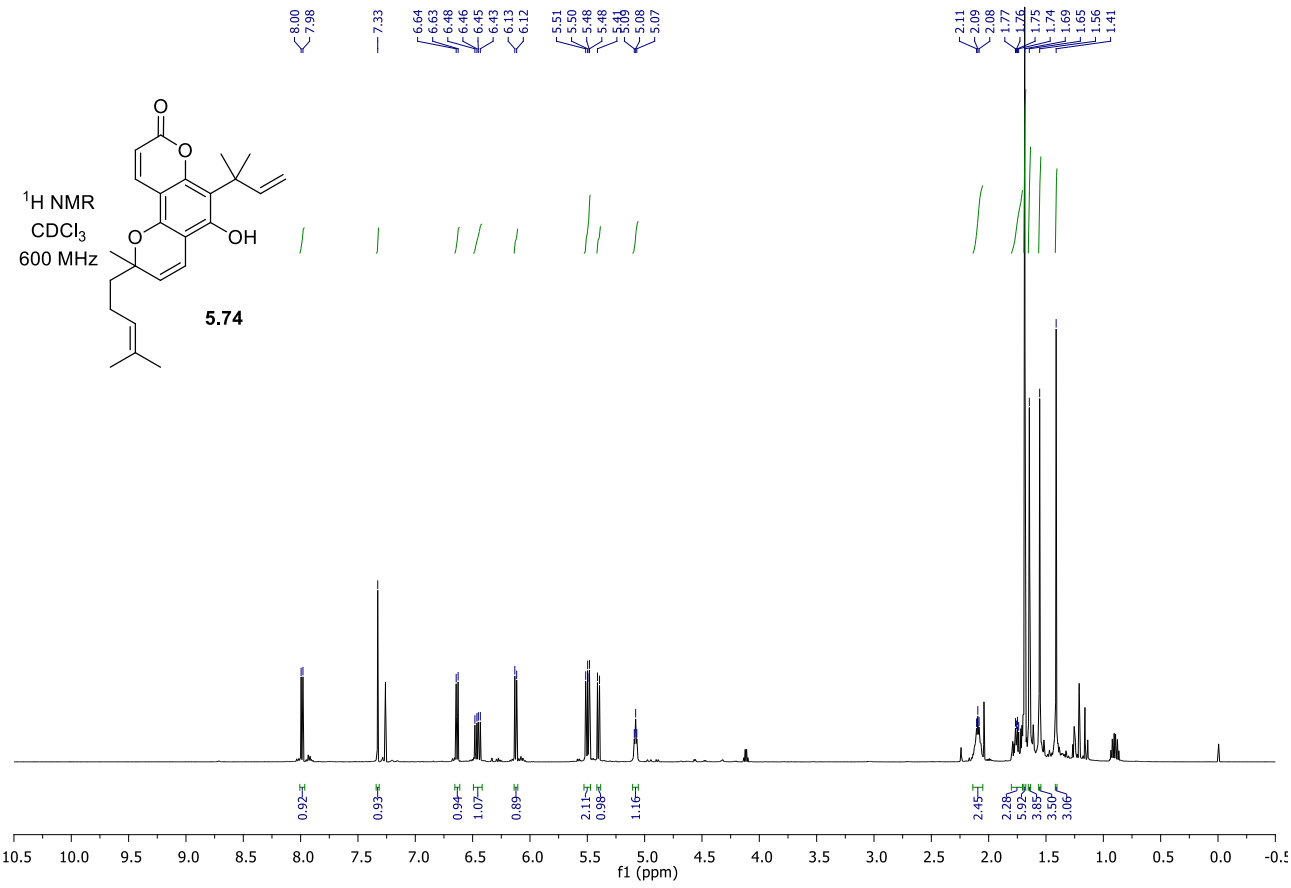
8.00
7.98
7.33
6.64
6.63
6.48
6.46
6.45
6.43
6.13
6.12
5.51
5.50
5.48
5.48
5.41
5.09
5.08
5.07
2.11
2.09
2.08
1.77
1.76
1.75
1.74
1.69
1.65
1.56
1.41
1H NMR
CDCl3
600 MHz
OH
5.74
0.92
0.93
0.94
1.07
0.89
2.11
0.98
1.16
2.45
2.28
5.92
3.85
3.50
3.06
f1 (ppm)

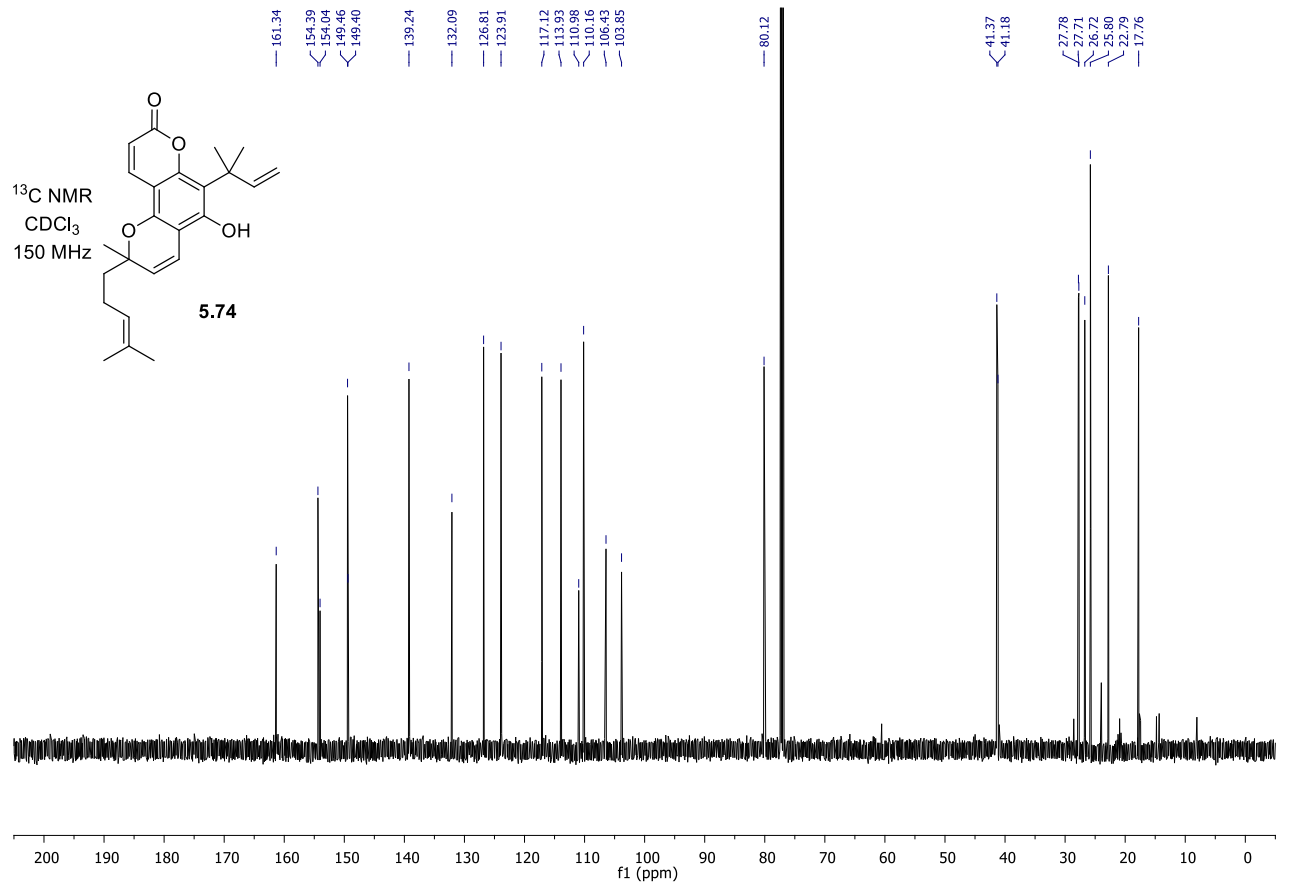
161.34
154.39
154.04
149.46
149.40
139.24
132.09
126.81
123.91
117.12
113.93
110.98
110.16
106.43
103.85
80.12
41.37
41.18
27.78
27.71
26.72
25.80
22.79
17.76
13C NMR
CDCl3
150 MHz
OH
5.74
f1 (ppm)

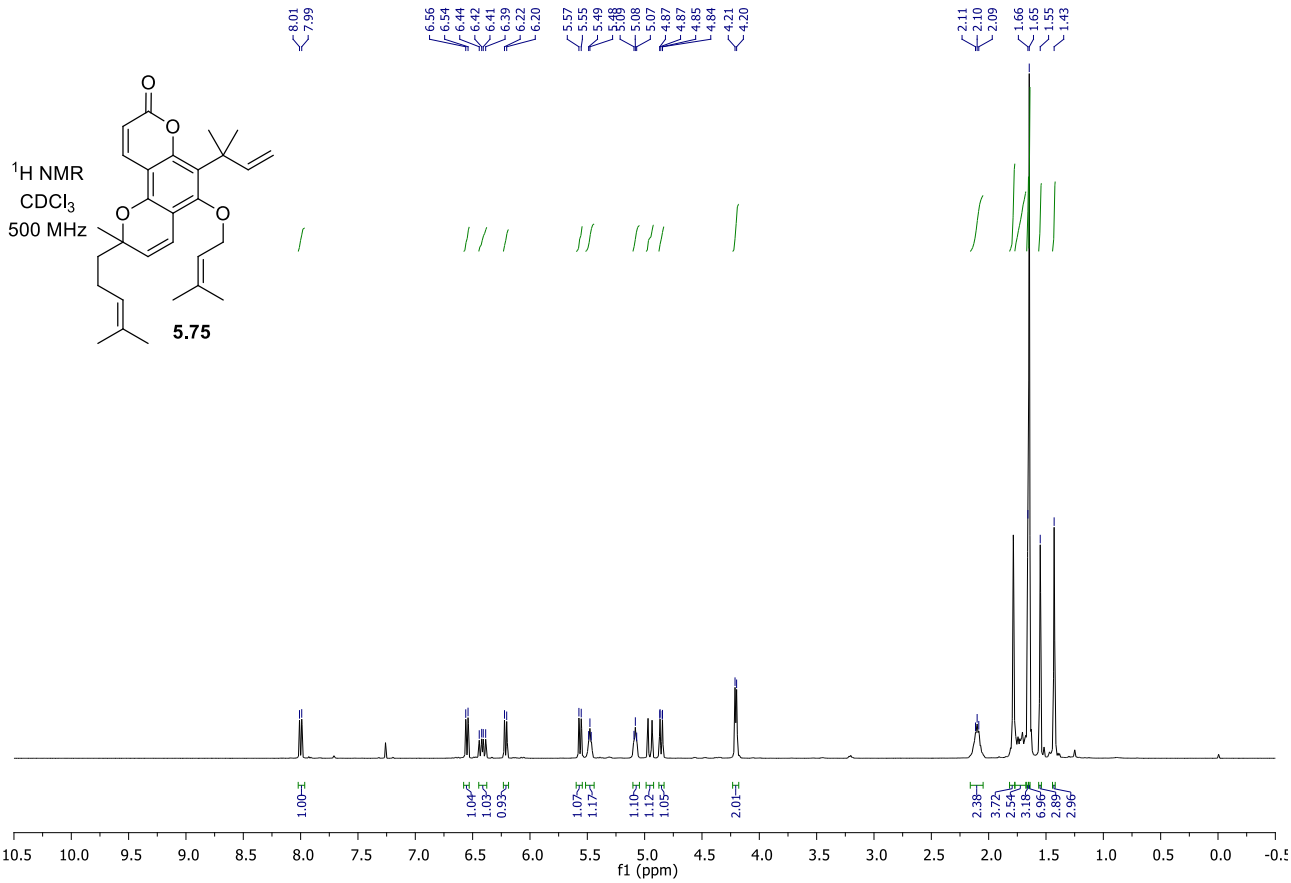
^{1}H NMR
$CDCl_3$
500 MHz
5.75
f1 (ppm)

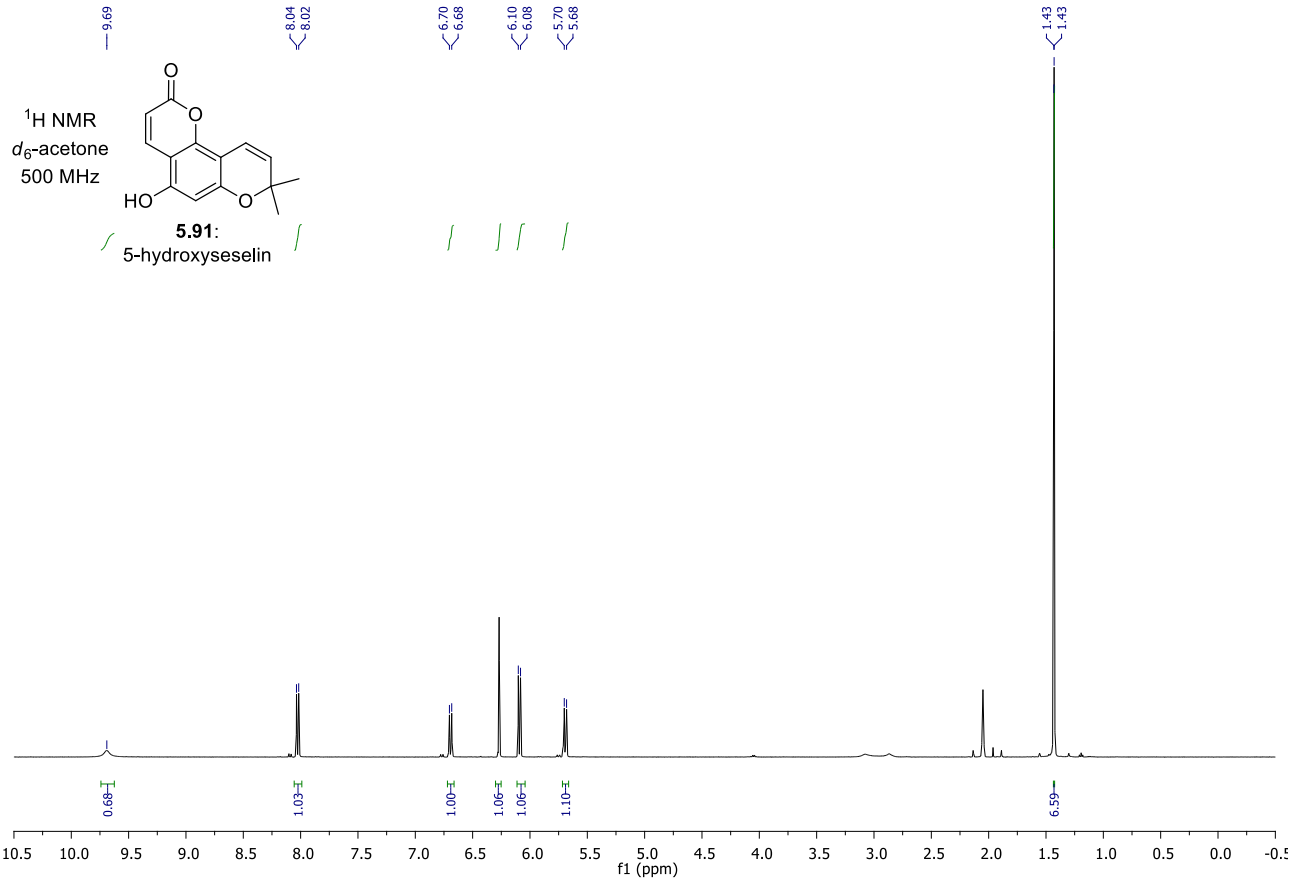
^{1}H NMR
d_6-acetone
500 MHz
HO
5.91:
5-hydroxyseselin
f1 (ppm)

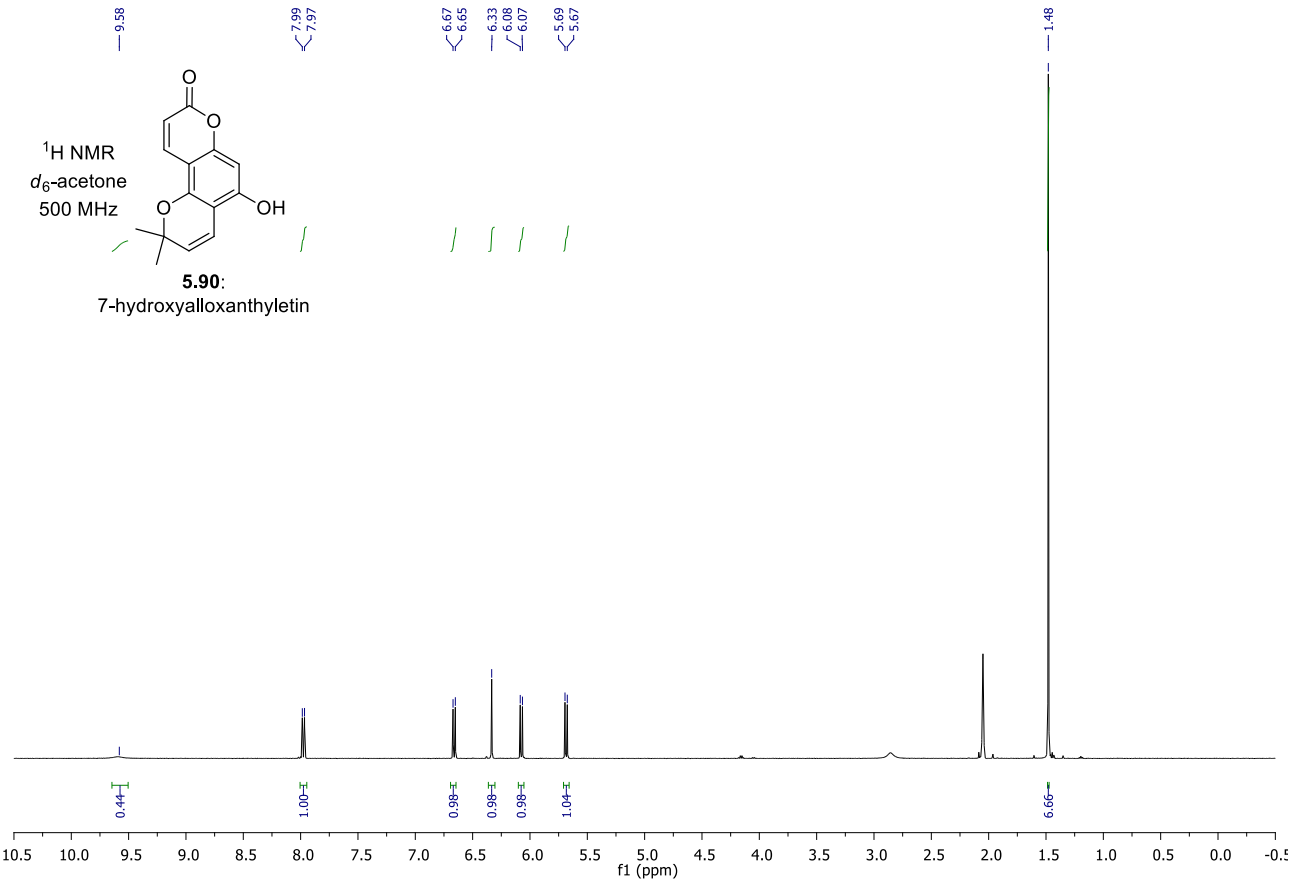

5.90:
7-hydroxyalloxanthyletin

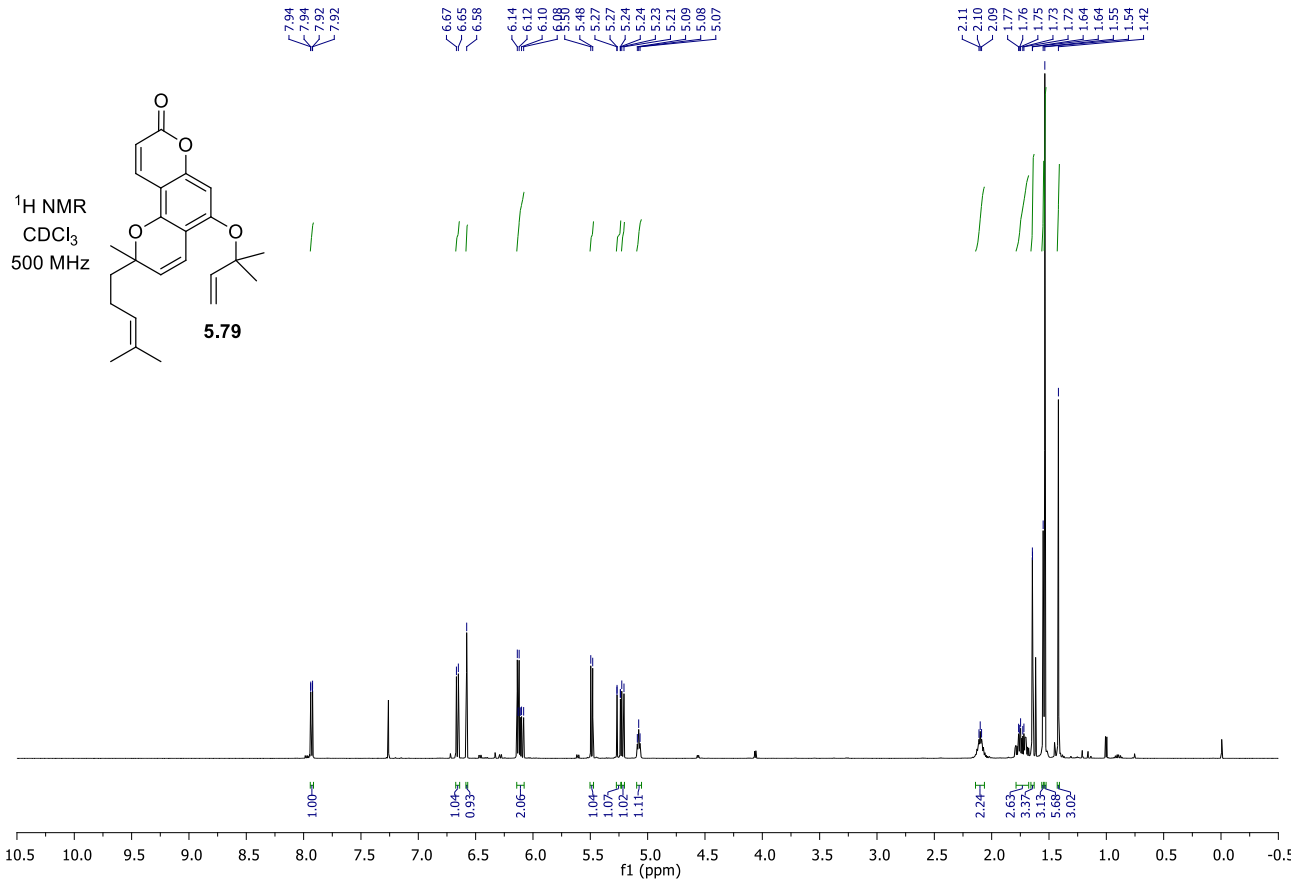
7.94
7.94
7.92
7.92
6.67
6.65
6.58
6.14
6.12
6.10
5.48
5.27
5.24
5.24
5.23
5.21
5.09
5.08
5.07
2.11
2.10
2.09
1.77
1.76
1.75
1.73
1.72
1.64
1.64
1.55
1.54
1.42
1H NMR
CDCl3
500 MHz
5.79
1.00
1.04
0.93
2.06
1.04
1.07
1.02
1.11
2.24
2.63
3.37
3.13
5.68
3.02
f1 (ppm)

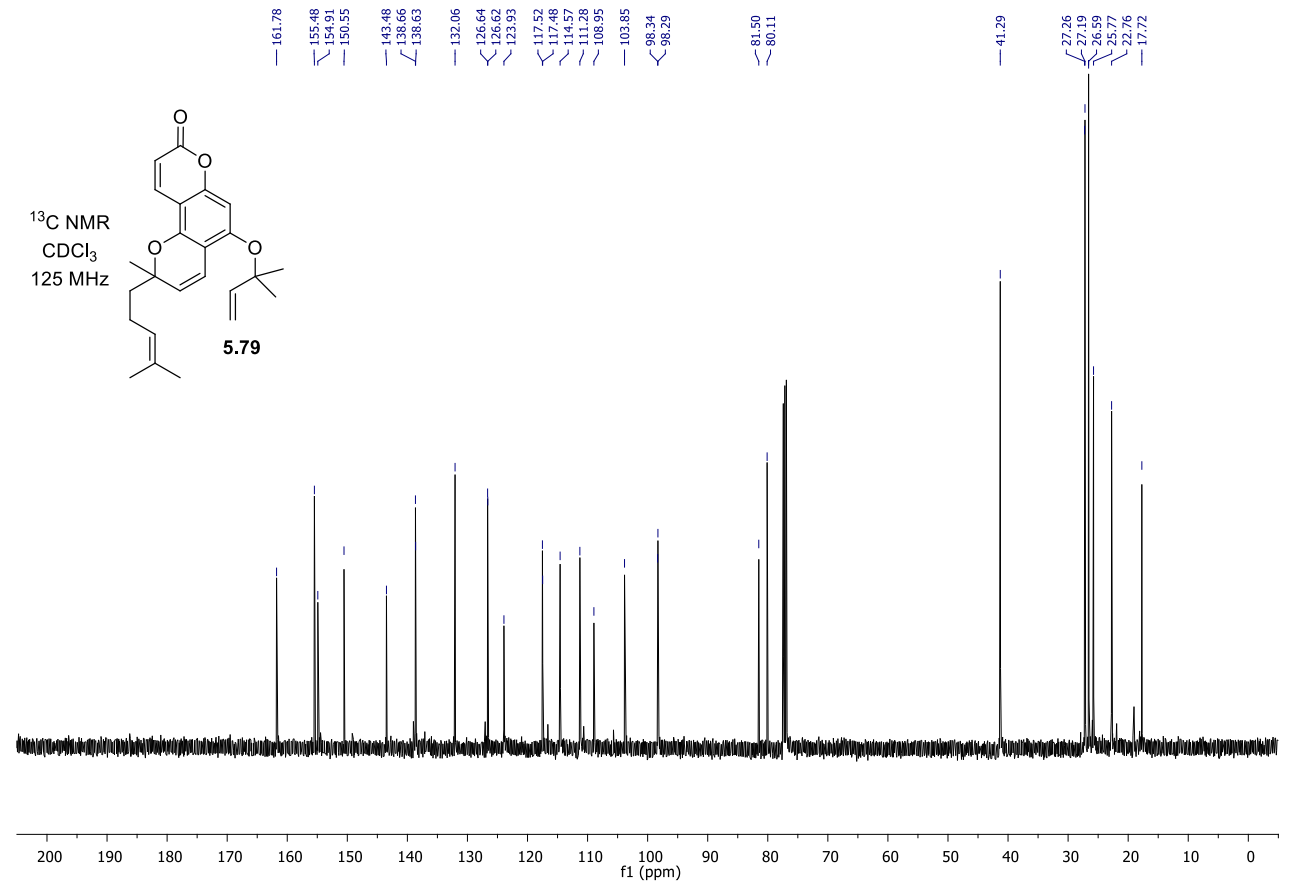
161.78
155.48
154.91
150.55
143.48
138.66
138.63
132.06
126.64
126.62
123.93
117.52
117.48
114.57
111.28
108.95
103.85
98.34
98.29
81.50
80.11
41.29
27.26
27.19
26.59
25.77
22.76
17.72
13C NMR
CDCl3
125 MHz
5.79
f1 (ppm)

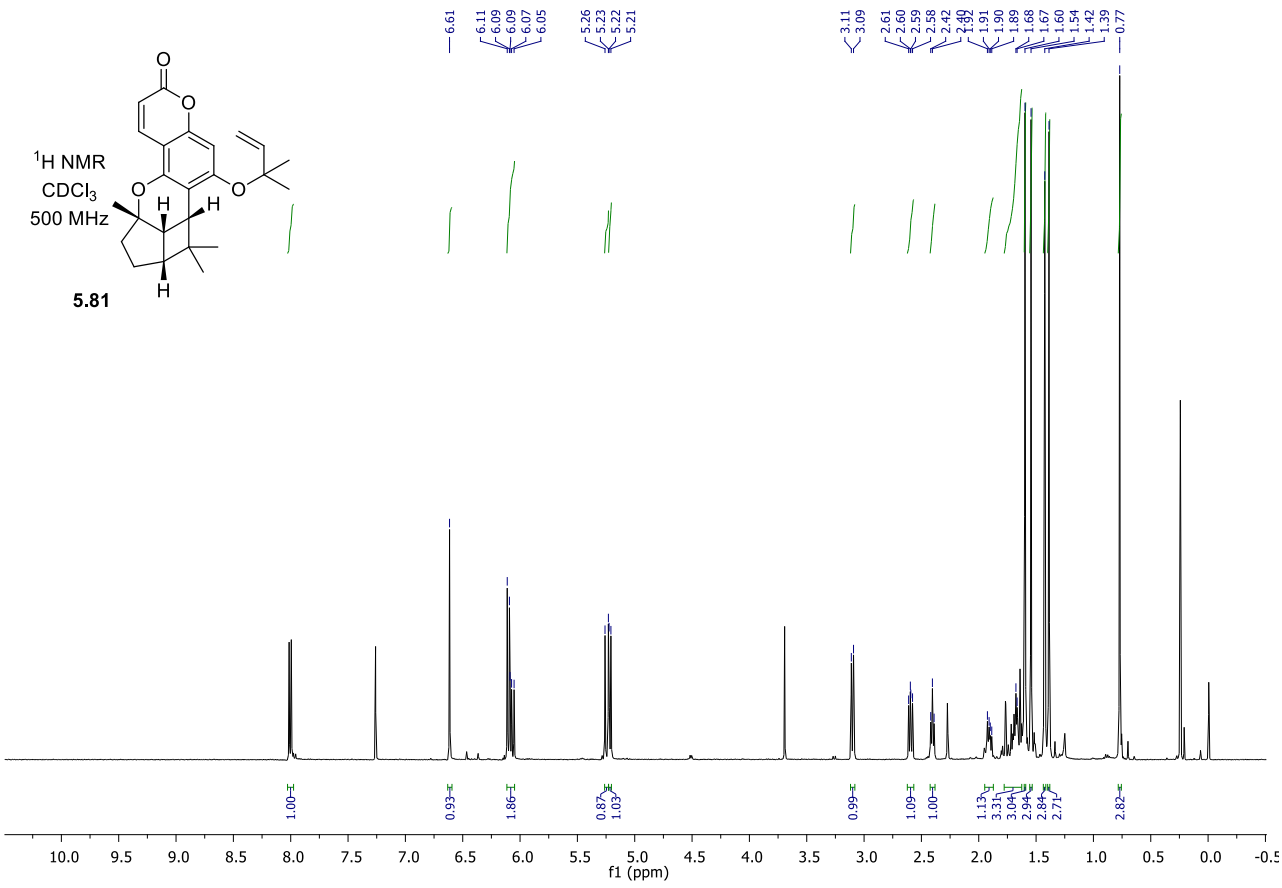
^{1}H NMR
$CDCl_3$
500 MHz
5.81
6.61
6.11
6.09
6.09
6.07
6.05
5.26
5.23
5.22
5.21
3.11
3.09
2.61
2.60
2.59
2.58
2.42
2.40
1.91
1.90
1.89
1.68
1.67
1.60
1.54
1.42
1.39
0.77
1.00
0.93
1.86
0.87
1.03
0.99
1.09
1.00
1.13
3.31
3.04
2.94
2.84
2.71
2.82
f1 (ppm)

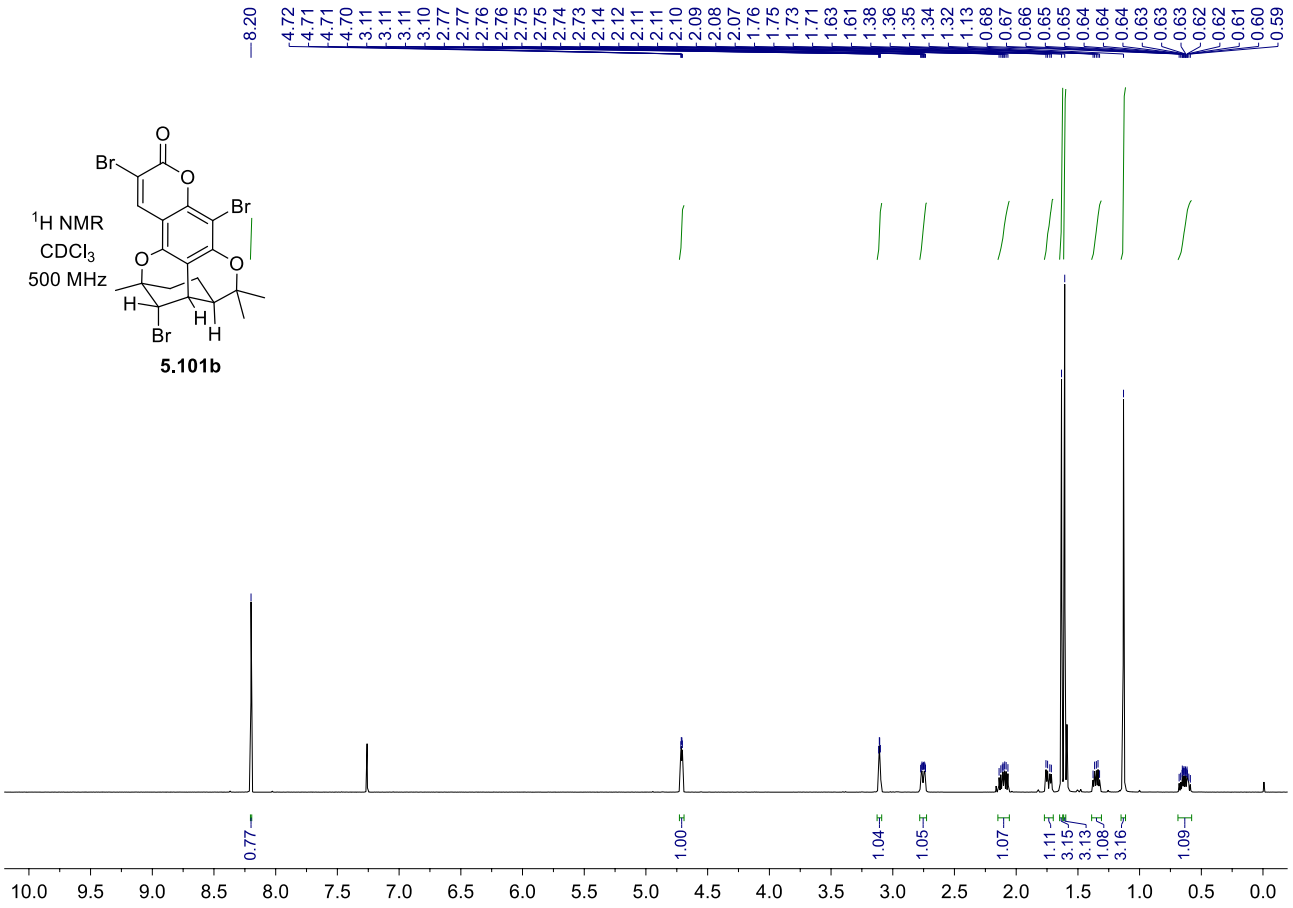
8.20
4.72 4.71 4.71 4.70 3.11 3.11 3.11 3.10 2.77 2.77 2.76 2.76 2.75 2.75 2.74 2.73 2.14 2.12 2.11 2.11 2.10 2.09 2.08 2.07 1.76 1.75 1.73 1.71 1.63 1.61 1.38 1.36 1.35 1.34 1.32 1.13 0.68 0.67 0.66 0.65 0.65 0.64 0.64 0.64 0.63 0.63 0.63 0.62 0.62 0.61 0.60 0.59
Br
O
O
Br
O
O
H
H
Br
H
1H NMR
CDCl3
500 MHz
5.101b
0.77
1.00
1.04
1.05
1.07
1.11
3.15
3.13
1.08
3.16
1.09
10.0 9.5 9.0 8.5 8.0 7.5 7.0 6.5 6.0 5.5 5.0 4.5 4.0 3.5 3.0 2.5 2.0 1.5 1.0 0.5 0.0

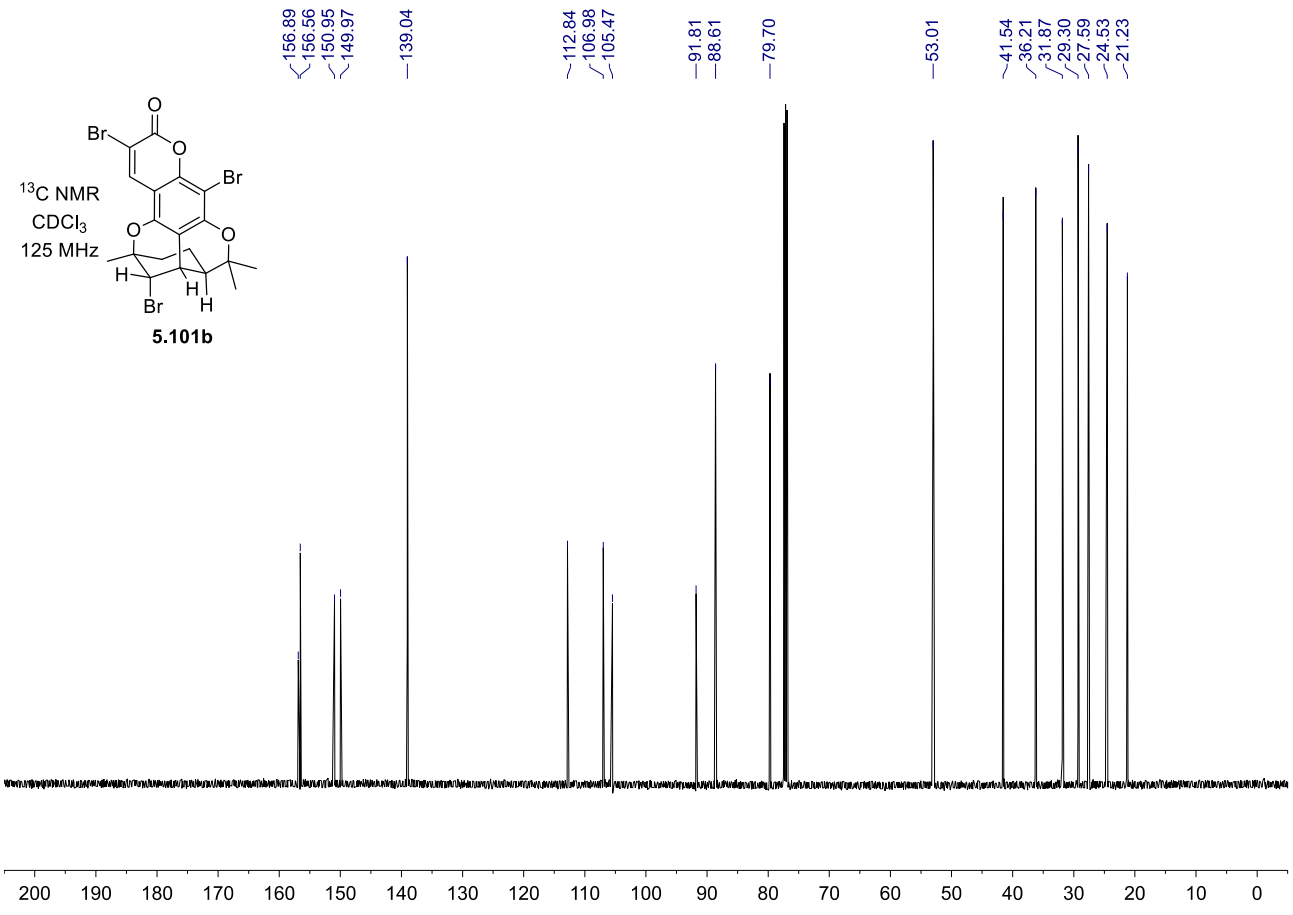
156.89
156.56
150.95
149.97
139.04
112.84
106.98
105.47
91.81
88.61
79.70
53.01
41.54
36.21
31.87
29.30
27.59
24.53
21.23
Br
O
O
Br
O
O
H
H
Br
H
13C NMR
CDCl3
125 MHz
5.101b
200 190 180 170 160 150 140 130 120 110 100 90 80 70 60 50 40 30 20 10 0

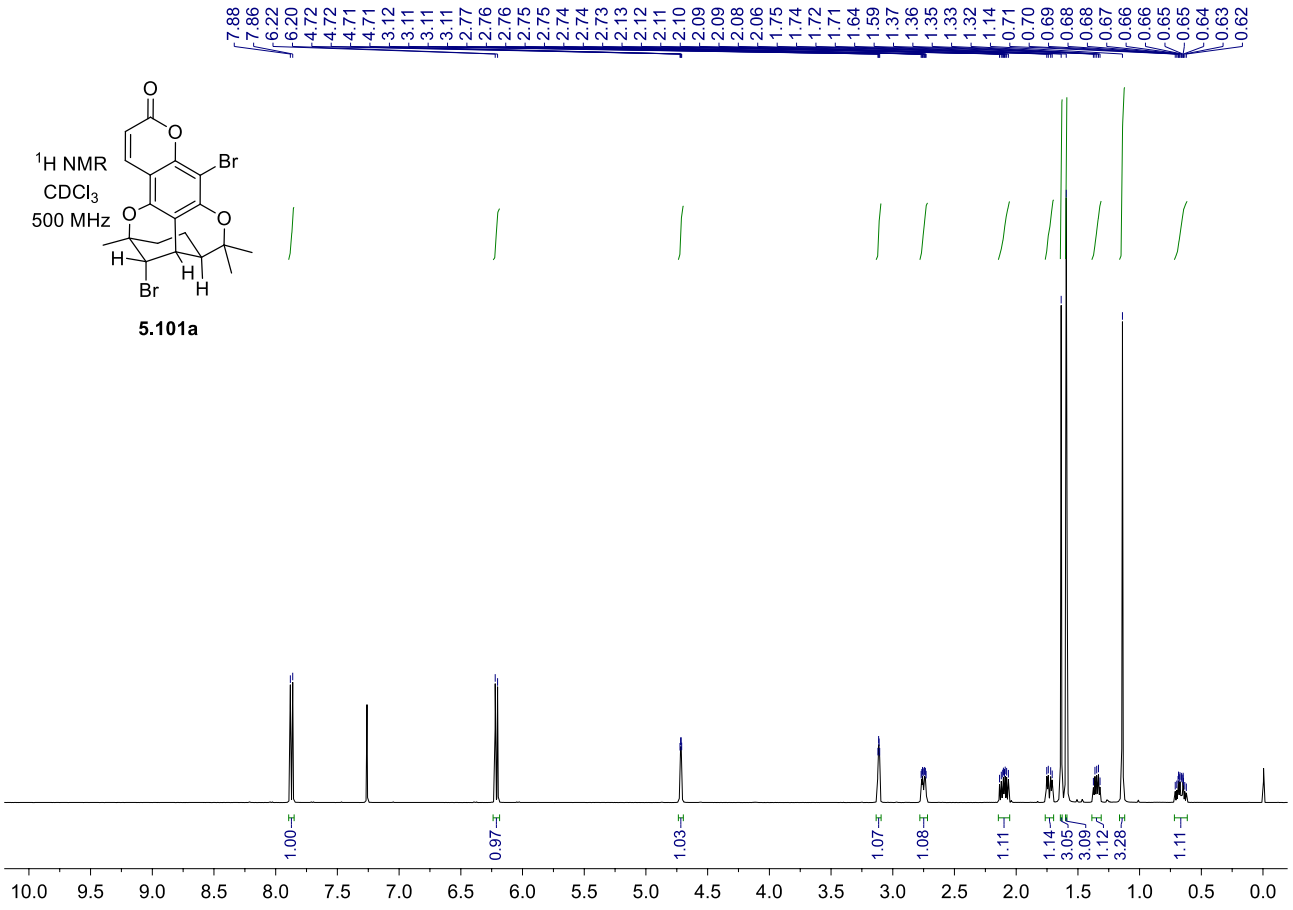
7.88
7.86
6.22
6.20
4.72
4.72
4.71
4.71
3.12
3.11
3.11
3.11
2.77
2.76
2.76
2.75
2.75
2.74
2.74
2.73
2.13
2.12
2.11
2.10
2.09
2.09
2.08
2.06
1.75
1.74
1.72
1.71
1.64
1.59
1.37
1.36
1.35
1.33
1.32
1.14
0.71
0.70
0.69
0.68
0.68
0.67
0.66
0.66
0.65
0.65
0.64
0.63
0.62
^{1}H NMR
$CDCl_3$
500 MHz
5.101a
1.00
0.97
1.03
1.07
1.08
1.11
1.14
3.05
3.09
1.12
3.28
1.11
10.0
9.5
9.0
8.5
8.0
7.5
7.0
6.5
6.0
5.5
5.0
4.5
4.0
3.5
3.0
2.5
2.0
1.5
1.0
0.5
0.0

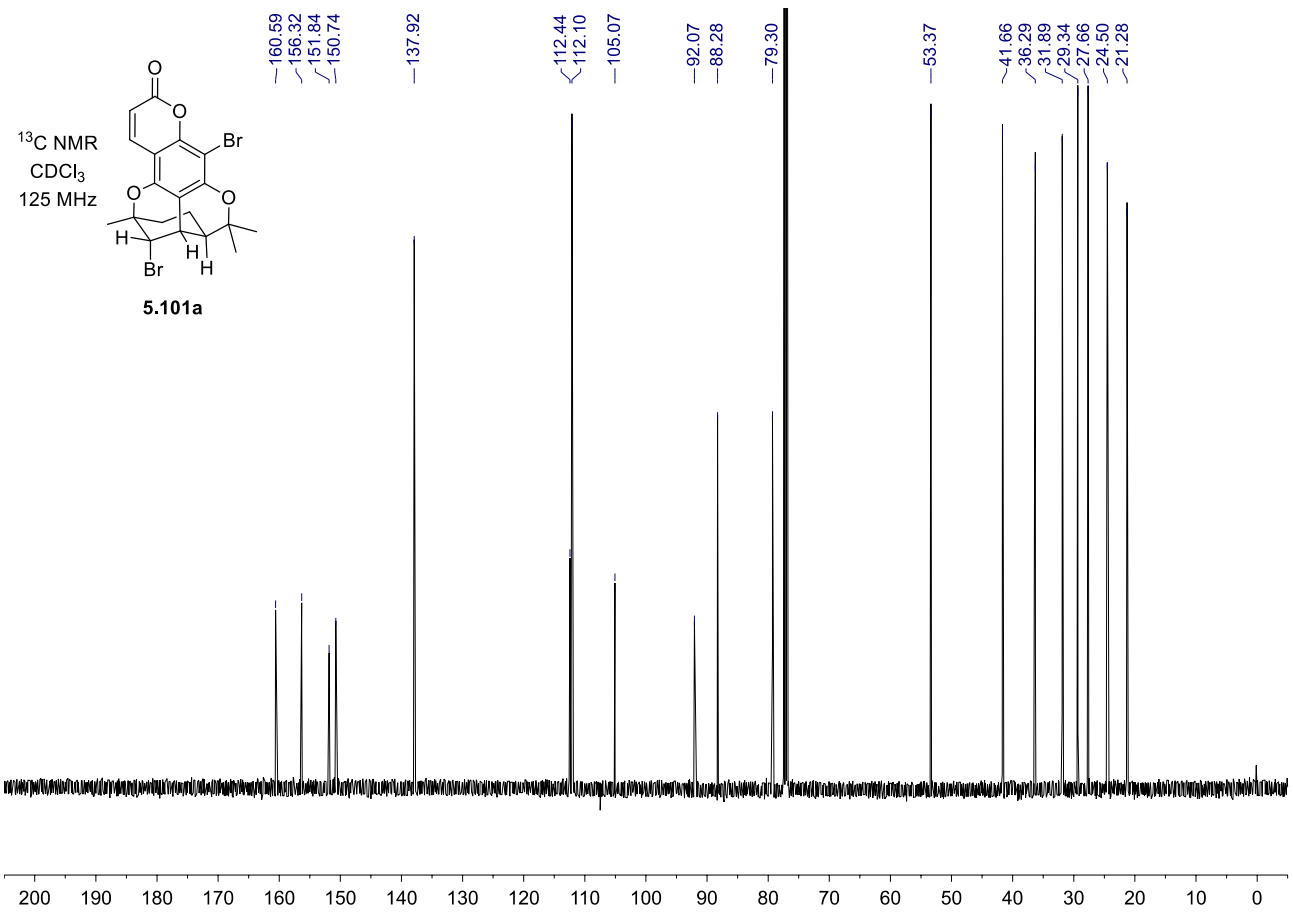
160.59
156.32
151.84
150.74
137.92
112.44
112.10
105.07
92.07
88.28
79.30
53.37
41.66
36.29
31.89
29.34
27.66
24.50
21.28
^{13}C NMR
$CDCl_3$
125 MHz
5.101a
200
190
180
170
160
150
140
130
120
110
100
90
80
70
60
50
40
30
20
10
0

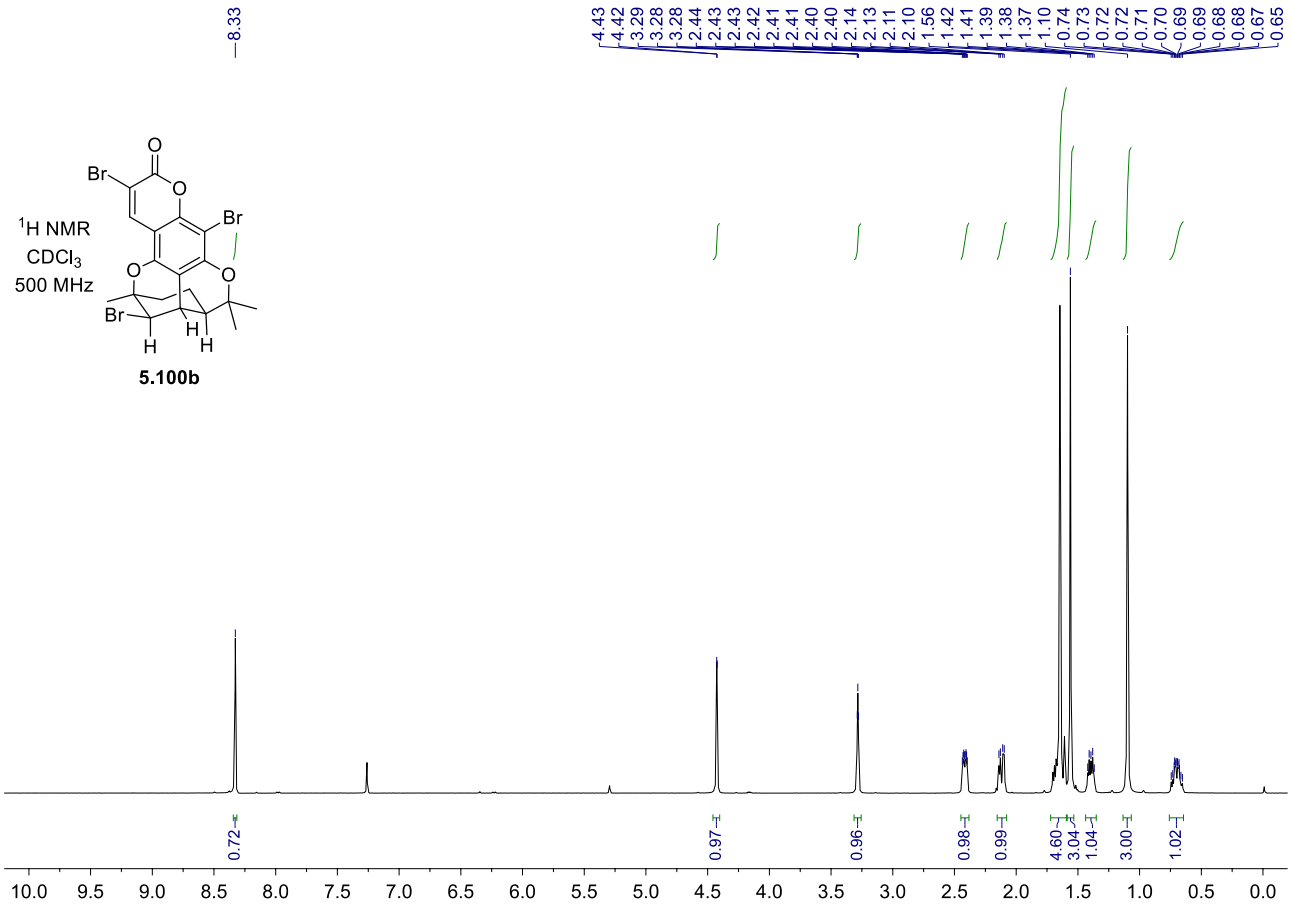
8.33
4.43
4.42
3.29
3.28
3.28
2.44
2.43
2.43
2.42
2.41
2.41
2.40
2.40
2.14
2.13
2.11
2.10
1.56
1.42
1.41
1.39
1.38
1.37
1.10
0.74
0.73
0.72
0.72
0.71
0.70
0.69
0.69
0.68
0.68
0.67
0.65
Br
O
O
Br
O
O
Br
H
H
H
^{1}H NMR
$CDCl_3$
500 MHz
5.100b
0.72
0.97
0.96
0.98
0.99
4.60
3.04
1.04
3.00
1.02
10.0 9.5 9.0 8.5 8.0 7.5 7.0 6.5 6.0 5.5 5.0 4.5 4.0 3.5 3.0 2.5 2.0 1.5 1.0 0.5 0.0

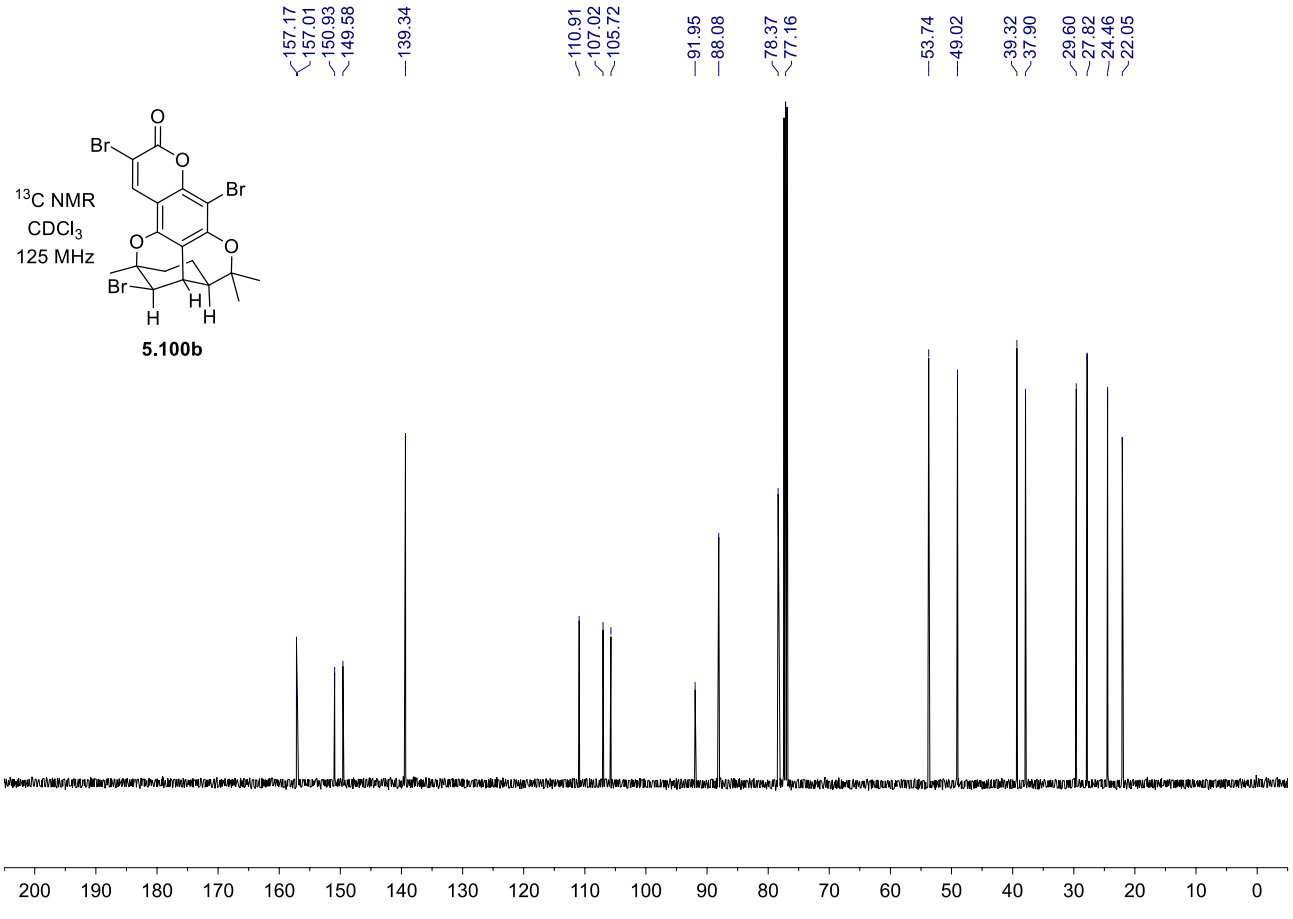
157.17
157.01
150.93
149.58
139.34
110.91
107.02
105.72
91.95
88.08
78.37
77.16
53.74
49.02
39.32
37.90
29.60
27.82
24.46
22.05
Br
O
O
Br
O
O
Br
H
H
H
^{13}C NMR
$CDCl_3$
125 MHz
5.100b
200 190 180 170 160 150 140 130 120 110 100 90 80 70 60 50 40 30 20 10 0

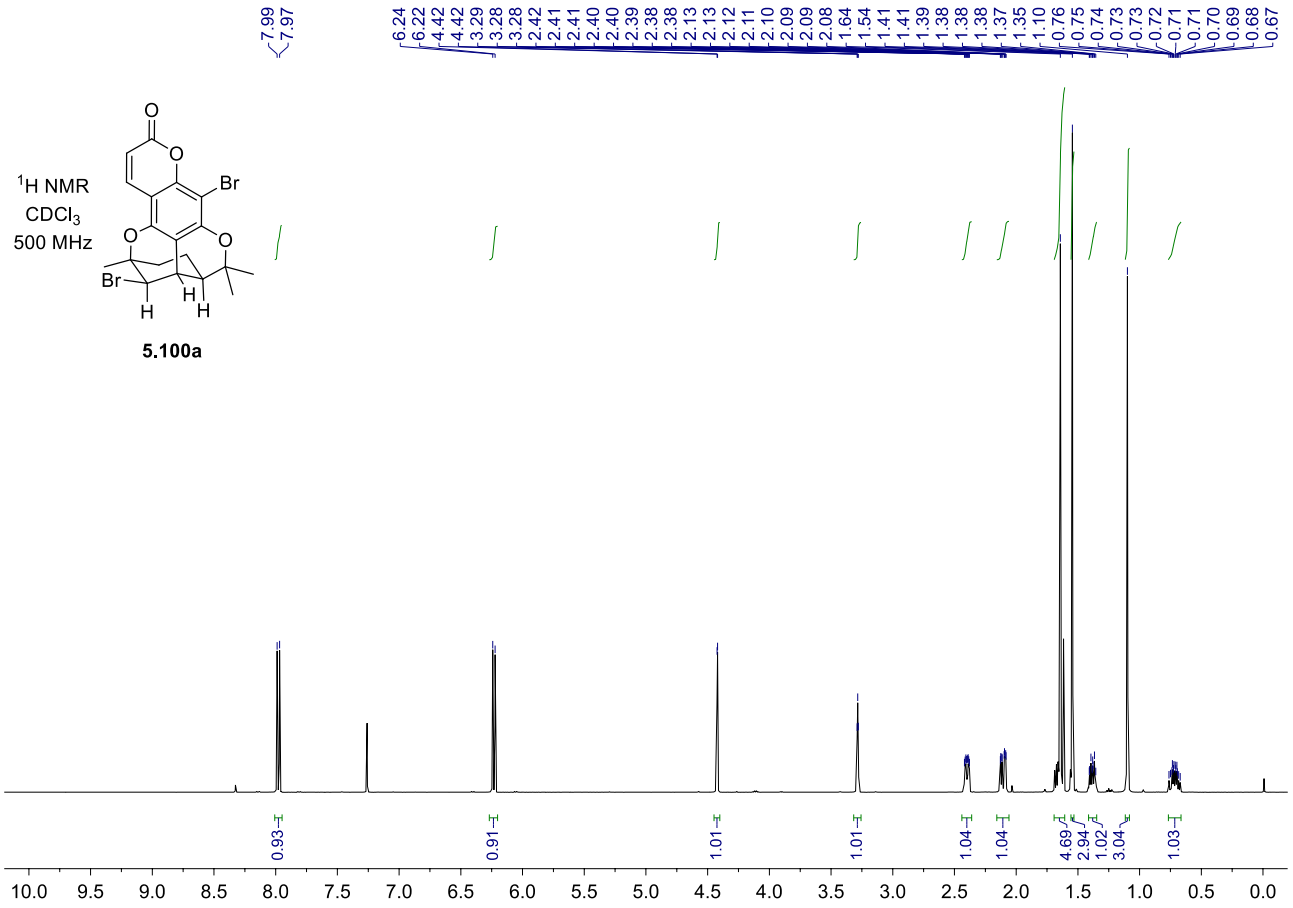
7.99
7.97
6.24
6.22
4.42
4.42
3.29
3.28
3.28
2.42
2.41
2.41
2.40
2.40
2.39
2.38
2.38
2.13
2.13
2.12
2.11
2.10
2.09
2.09
2.08
1.64
1.54
1.41
1.41
1.39
1.38
1.38
1.38
1.37
1.35
1.10
0.76
0.75
0.74
0.73
0.73
0.72
0.71
0.71
0.70
0.69
0.68
0.67
^{1}H NMR
$CDCl_3$
500 MHz
5.100a
0.93
0.91
1.01
1.01
1.04
1.04
4.69
2.94
1.02
3.04
1.03
10.0 9.5 9.0 8.5 8.0 7.5 7.0 6.5 6.0 5.5 5.0 4.5 4.0 3.5 3.0 2.5 2.0 1.5 1.0 0.5 0.0

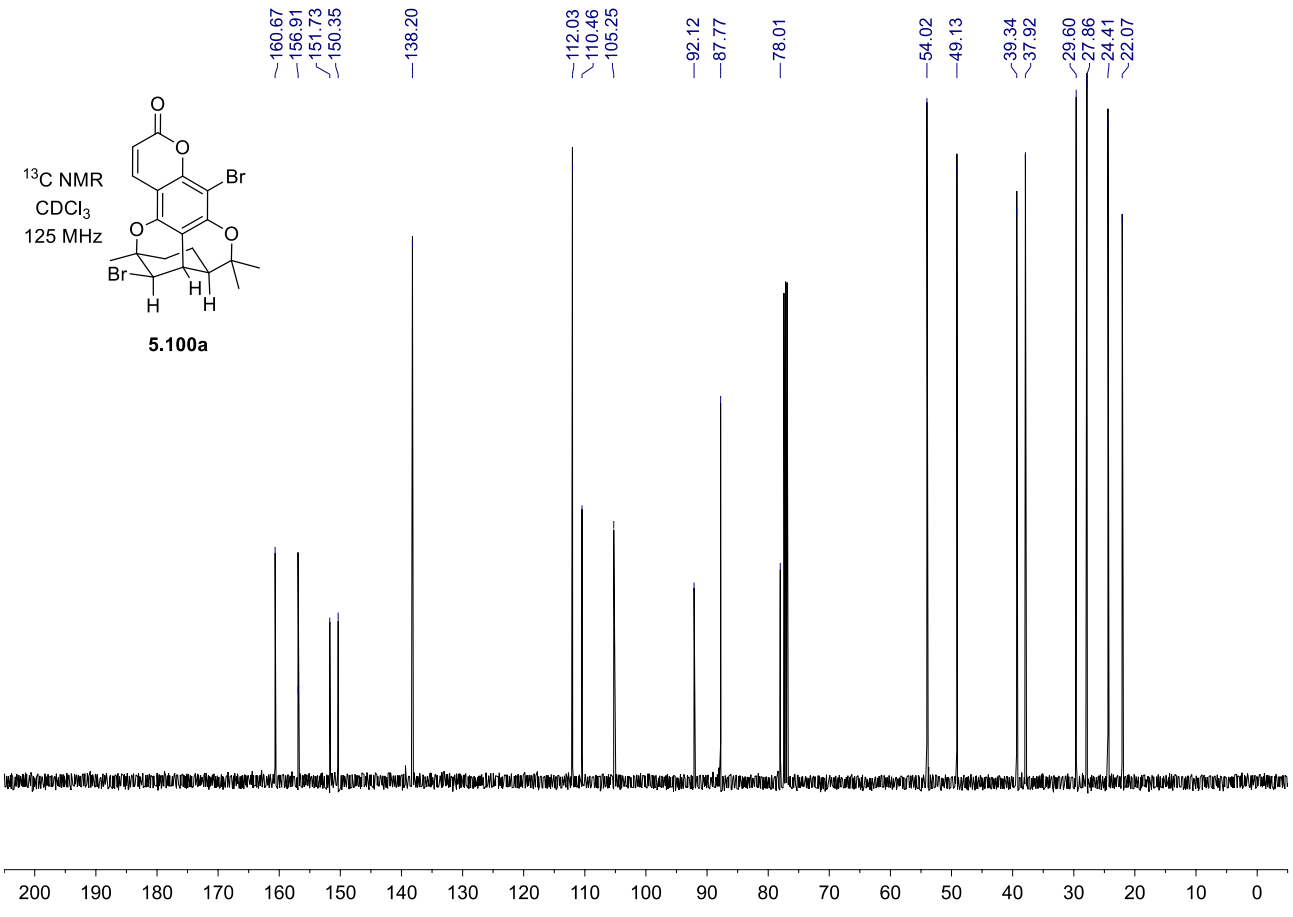
160.67
156.91
151.73
150.35
138.20
112.03
110.46
105.25
92.12
87.77
78.01
54.02
49.13
39.34
37.92
29.60
27.86
24.41
22.07
^{13}C NMR
$CDCl_3$
125 MHz
5.100a
200 190 180 170 160 150 140 130 120 110 100 90 80 70 60 50 40 30 20 10 0

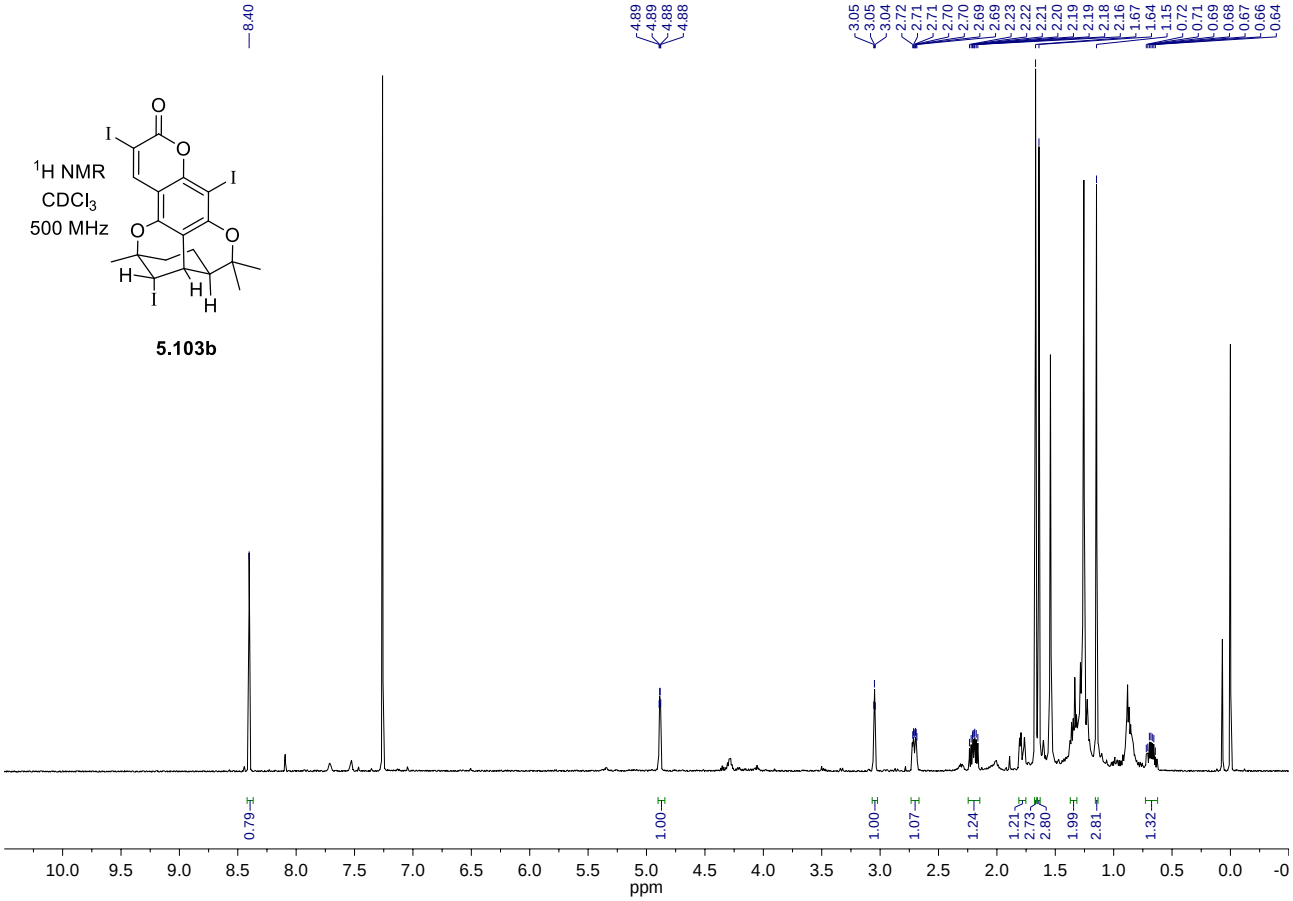
8.40
4.89
4.89
4.88
4.88
3.05
3.05
3.04
2.72
2.71
2.71
2.70
2.70
2.69
2.69
2.23
2.22
2.21
2.20
2.19
2.19
2.18
2.16
1.67
1.64
1.15
0.72
0.71
0.69
0.68
0.67
0.66
0.64
^{1}H NMR
$CDCl_3$
500 MHz
5.103b
0.79
1.00
1.00
1.07
1.24
1.21
2.73
2.80
1.99
2.81
1.32
10.0 9.5 9.0 8.5 8.0 7.5 7.0 6.5 6.0 5.5 5.0 4.5 4.0 3.5 3.0 2.5 2.0 1.5 1.0 0.5 0.0 -0
ppm

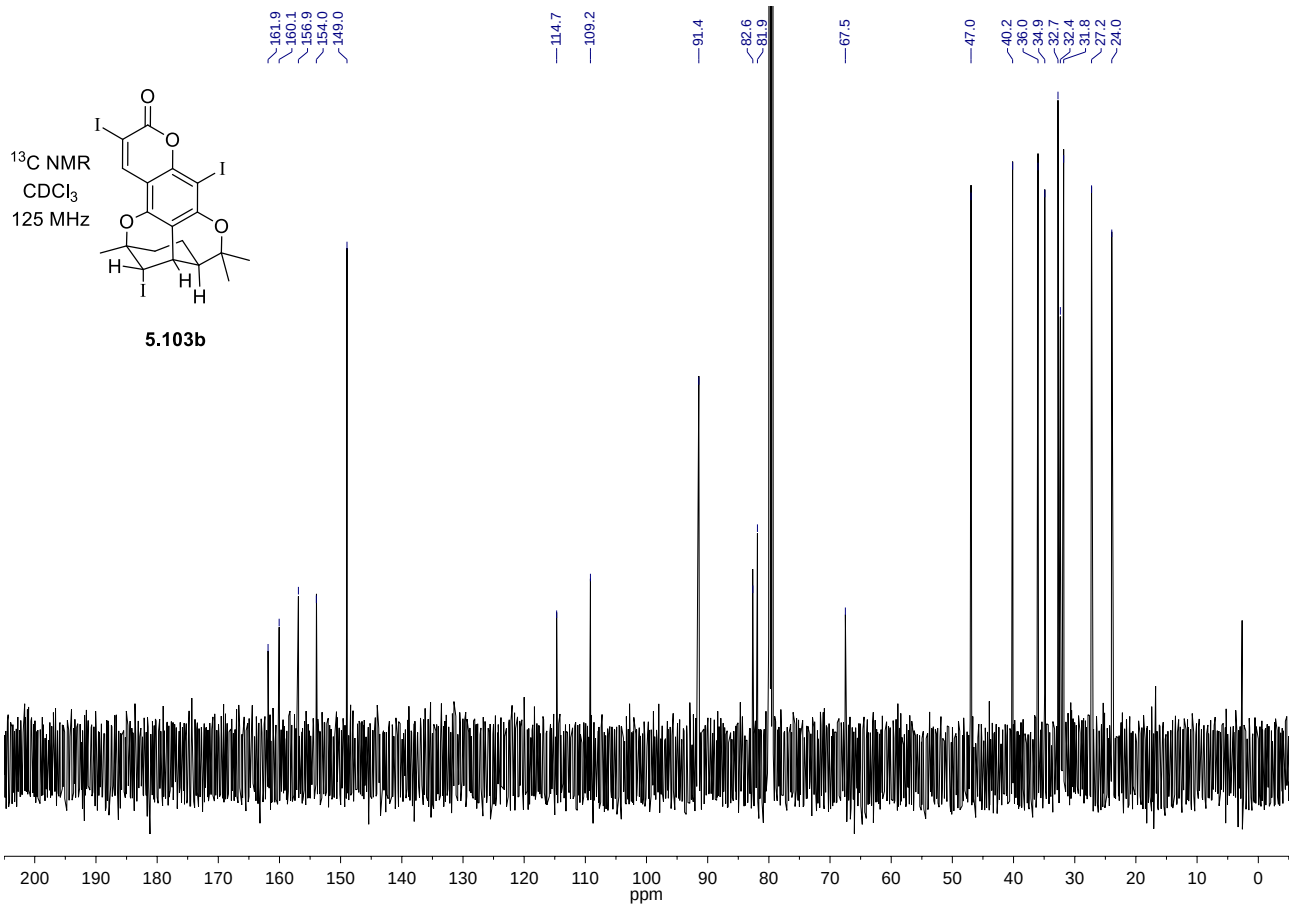
161.9
160.1
156.9
154.0
149.0
114.7
109.2
91.4
82.6
81.9
67.5
47.0
40.2
36.0
34.9
32.7
32.4
31.8
27.2
24.0
^{13}C NMR
$CDCl_3$
125 MHz
5.103b
200 190 180 170 160 150 140 130 120 110 100 90 80 70 60 50 40 30 20 10 0
ppm

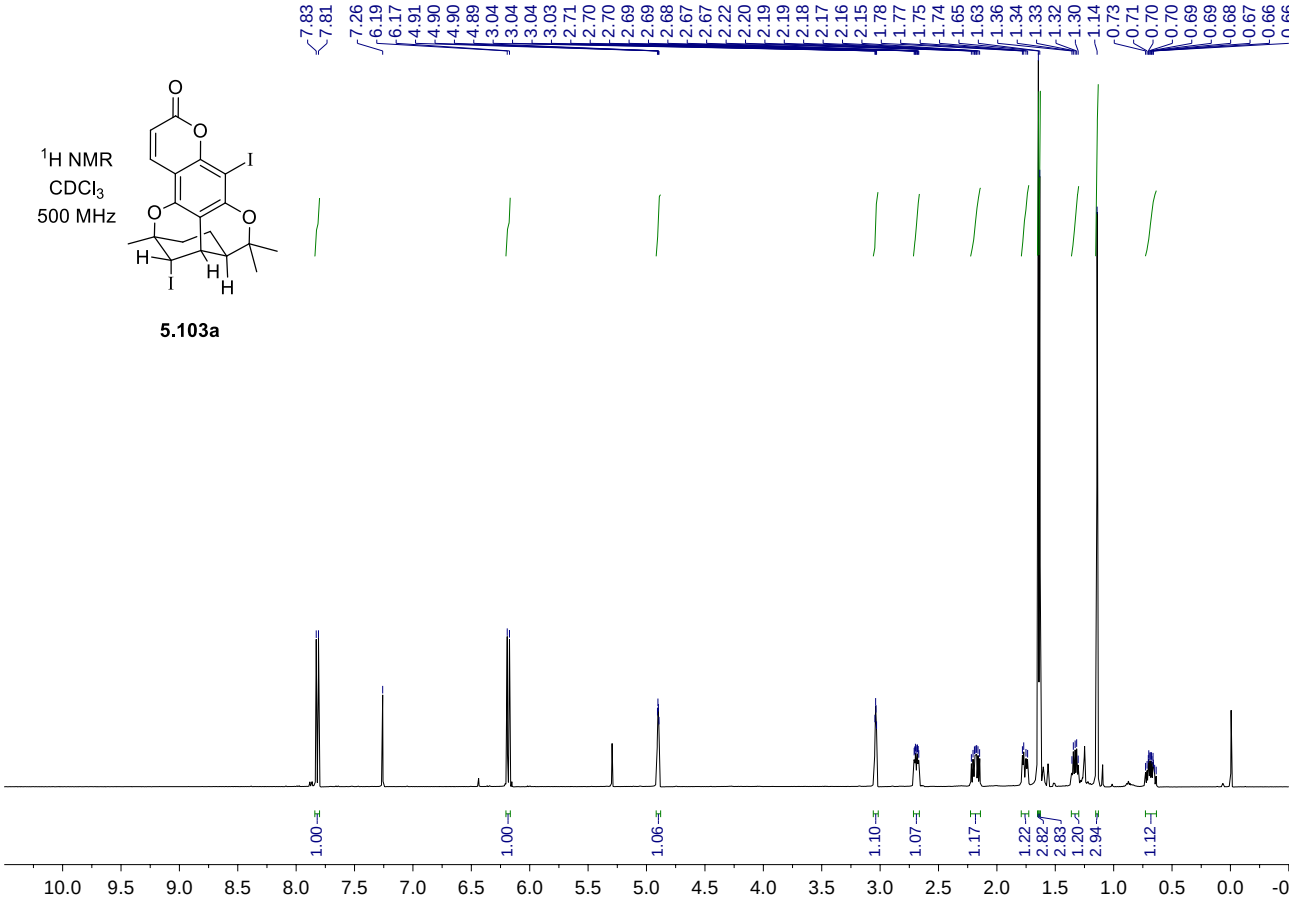
^{1}H NMR
$CDCl_3$
500 MHz
5.103a

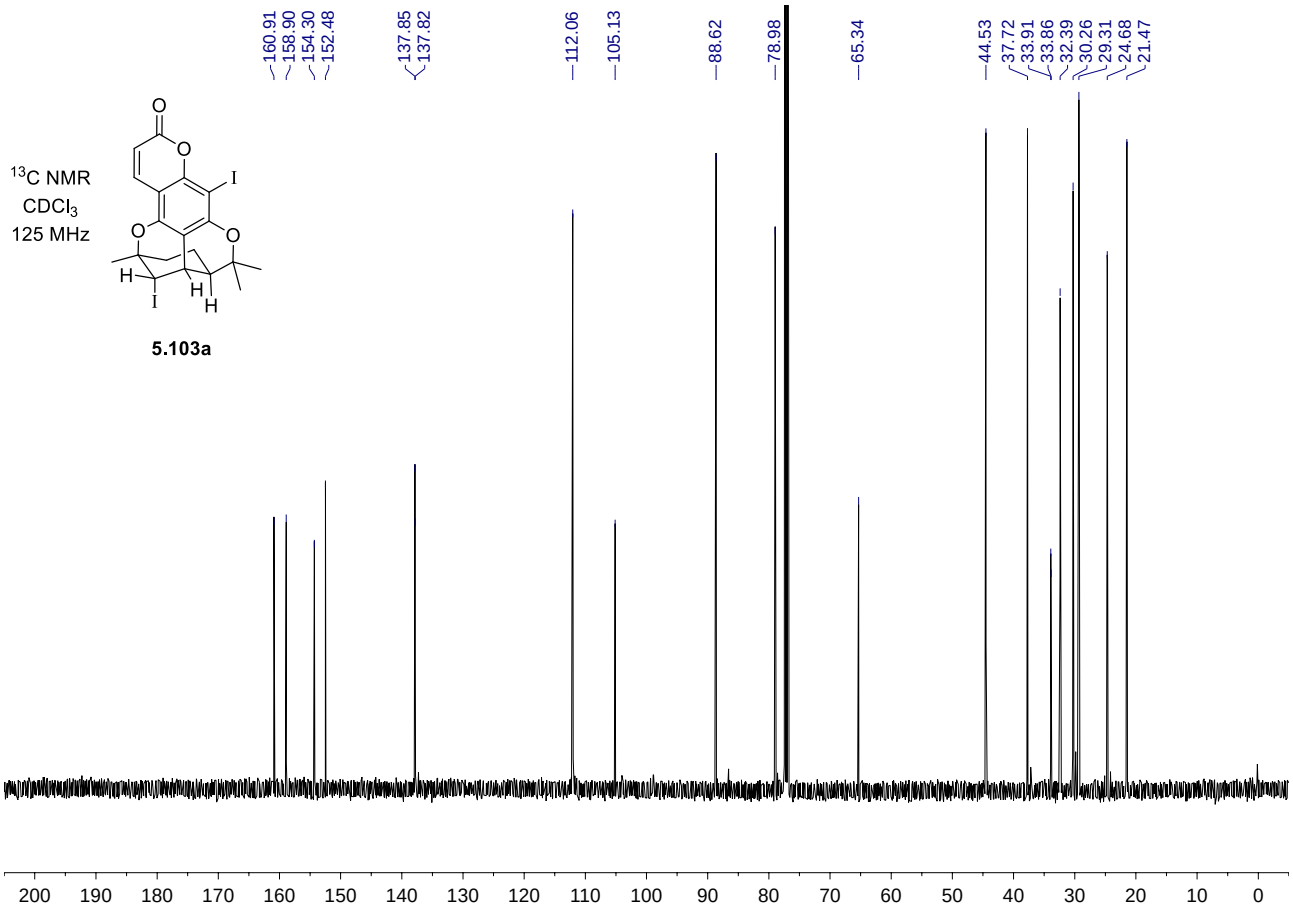
^{13}C NMR
$CDCl_3$
125 MHz
5.103a

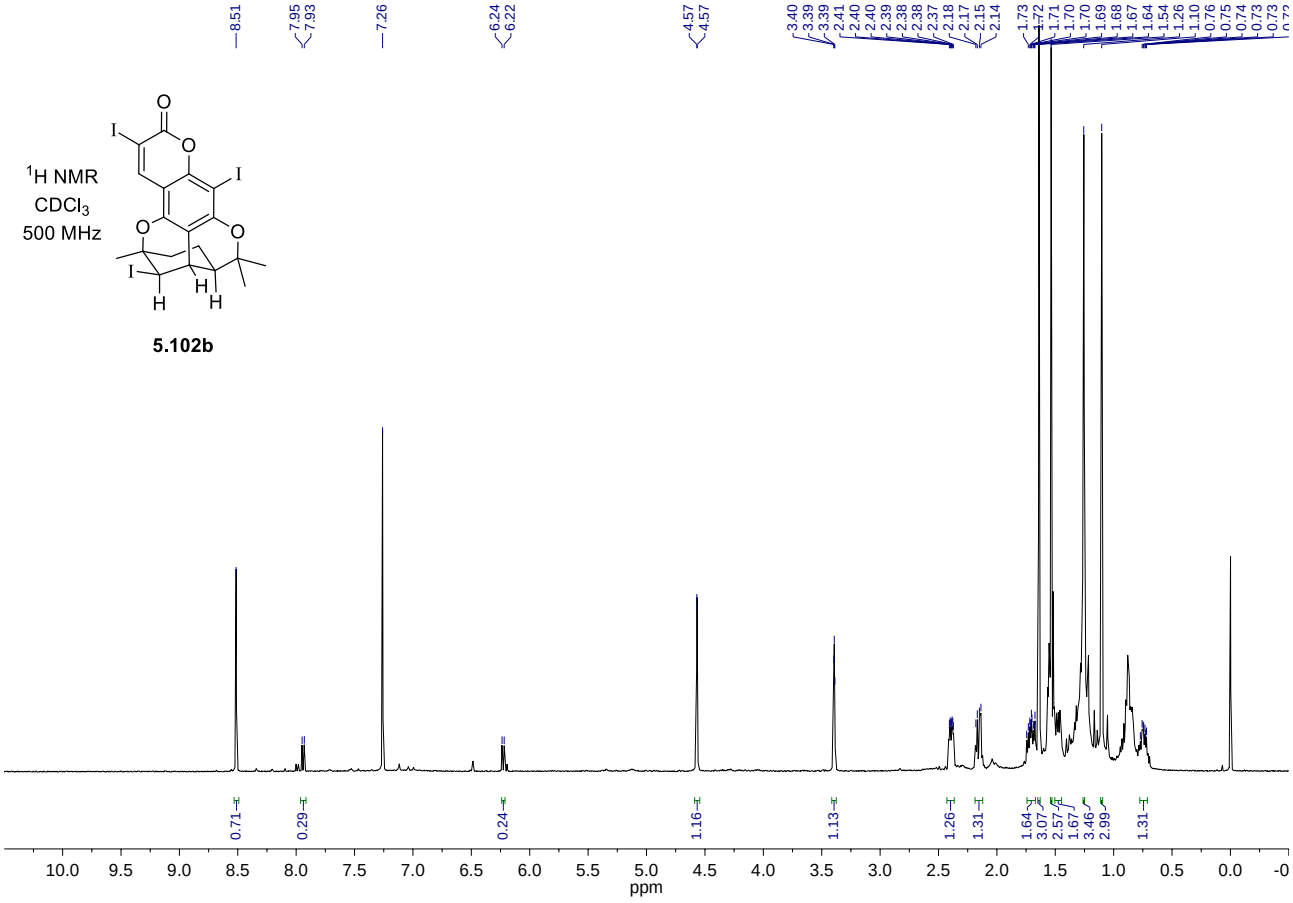

^{1}H NMR
$CDCl_3$
500 MHz

5.102b

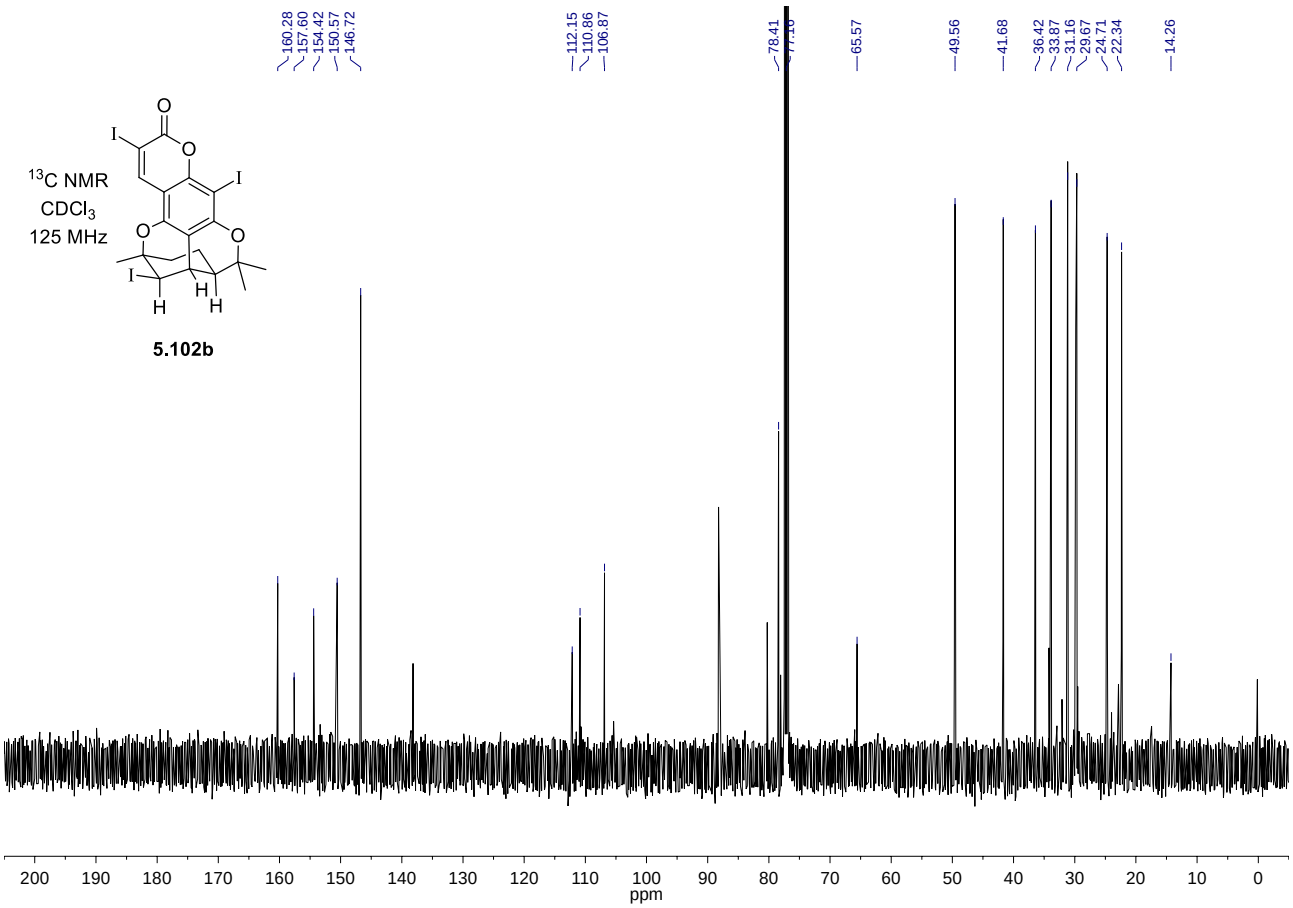

^{13}C NMR
$CDCl_3$
125 MHz

5.102b

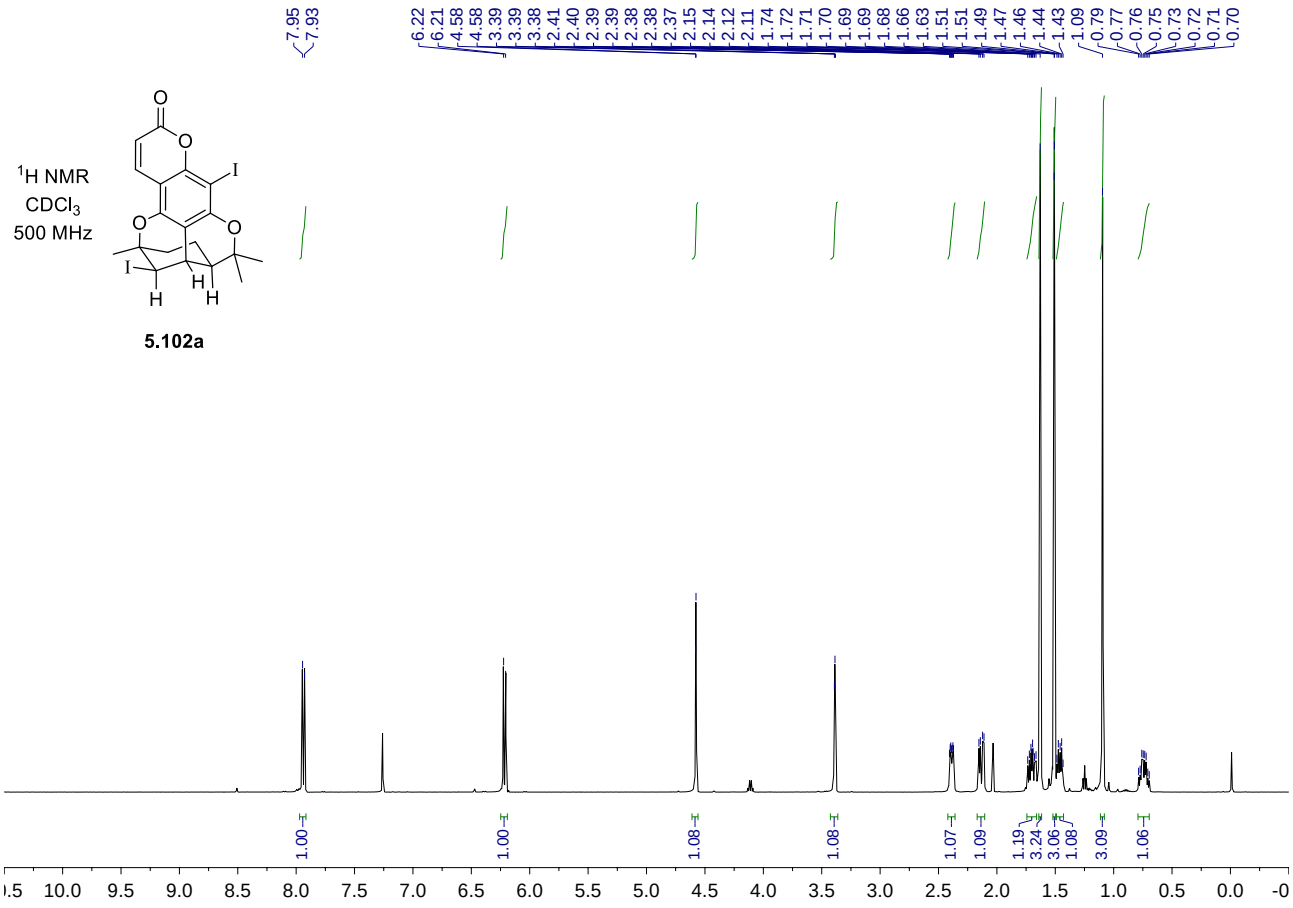
7.95
7.93
6.22
6.21
4.58
4.58
3.39
3.39
3.38
2.41
2.40
2.39
2.39
2.38
2.38
2.37
2.15
2.14
2.12
2.11
1.74
1.72
1.71
1.70
1.69
1.69
1.68
1.66
1.63
1.51
1.51
1.49
1.47
1.46
1.44
1.43
1.09
0.79
0.77
0.76
0.75
0.73
0.72
0.71
0.70
1H NMR
CDCl3
500 MHz
5.102a
1.00
1.00
1.08
1.08
1.07
1.09
1.19
3.24
3.06
1.08
3.09
1.06
10.0
9.5
9.0
8.5
8.0
7.5
7.0
6.5
6.0
5.5
5.0
4.5
4.0
3.5
3.0
2.5
2.0
1.5
1.0
0.5
0.0

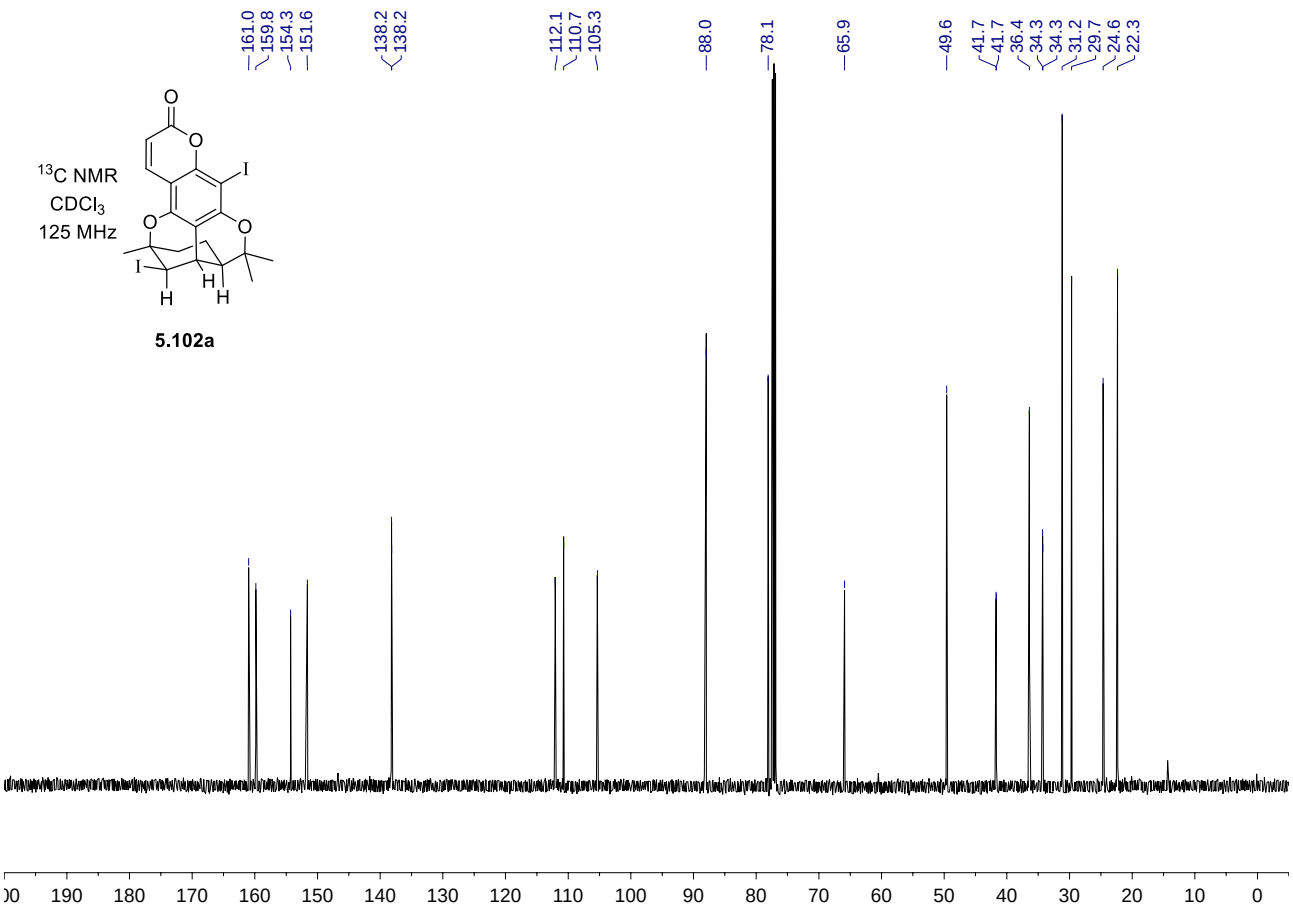
161.0
159.8
154.3
151.6
138.2
138.2
112.1
110.7
105.3
88.0
78.1
65.9
49.6
41.7
41.7
36.4
34.3
34.3
31.2
29.7
24.6
22.3
13C NMR
CDCl3
125 MHz
5.102a
190
180
170
160
150
140
130
120
110
100
90
80
70
60
50
40
30
20
10
0

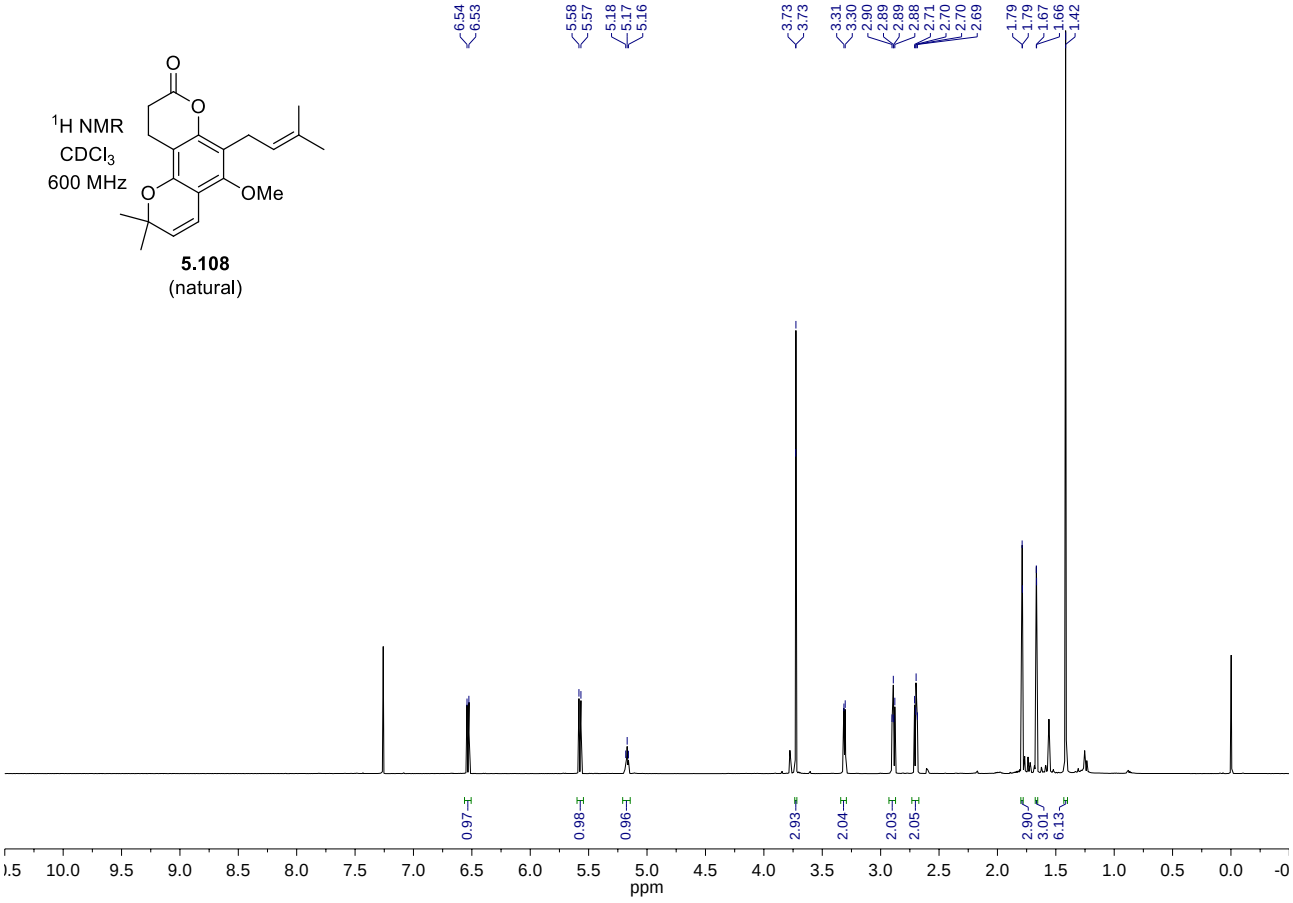
^{1}H NMR
$CDCl_3$
600 MHz
OMe
5.108
(natural)
6.54
6.53
5.58
5.57
5.18
5.17
5.16
3.73
3.73
3.31
3.30
2.90
2.89
2.89
2.88
2.71
2.70
2.70
2.69
1.79
1.79
1.67
1.66
1.42
0.97
0.98
0.96
2.93
2.04
2.03
2.05
2.90
3.01
6.13
ppm

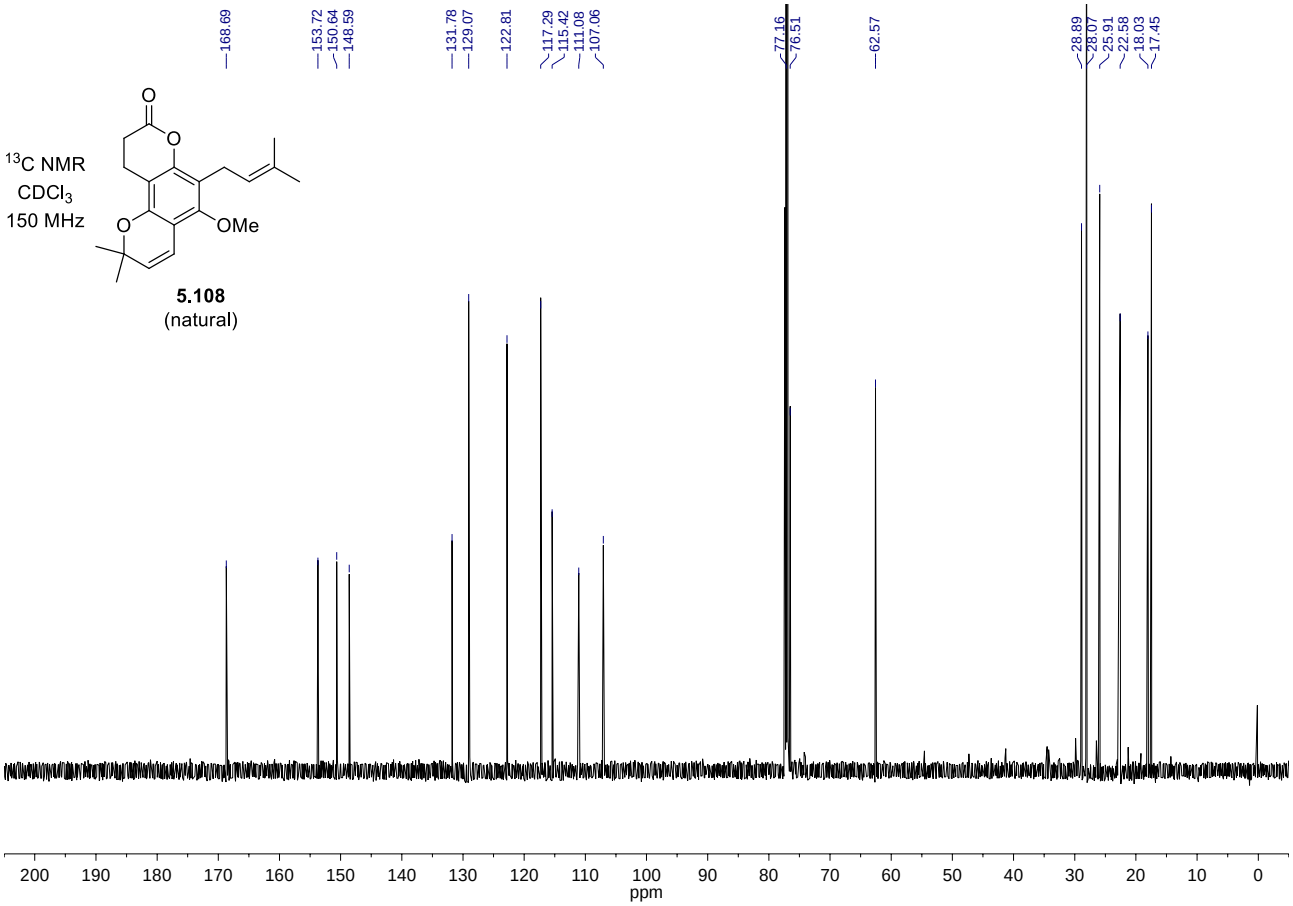
^{13}C NMR
$CDCl_3$
150 MHz
OMe
5.108
(natural)
168.69
153.72
150.64
148.59
131.78
129.07
122.81
117.29
115.42
111.08
107.06
77.16
76.51
62.57
28.89
28.07
25.91
22.58
18.03
17.45
ppm

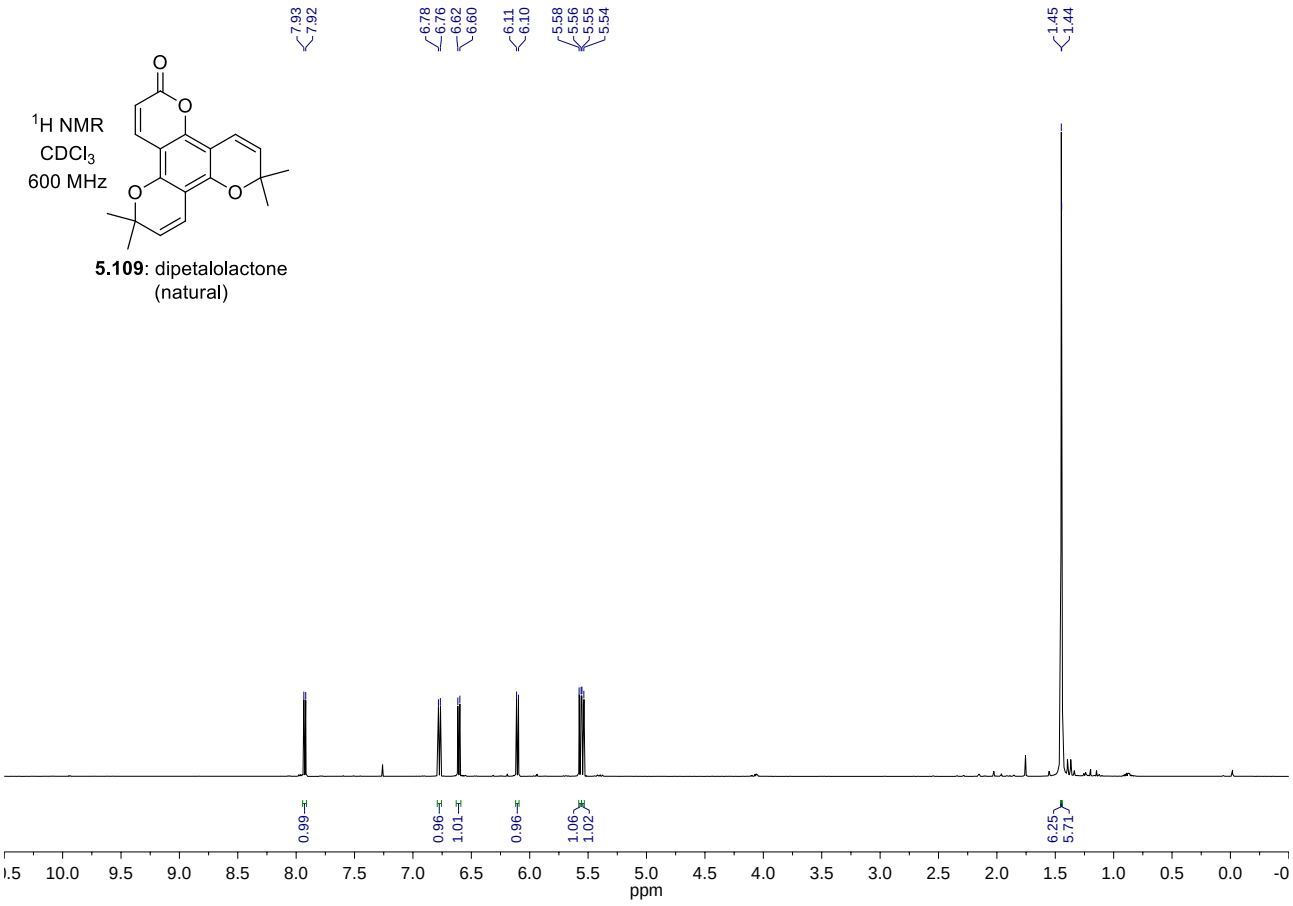

5.109: dipetalolactone
(natural)

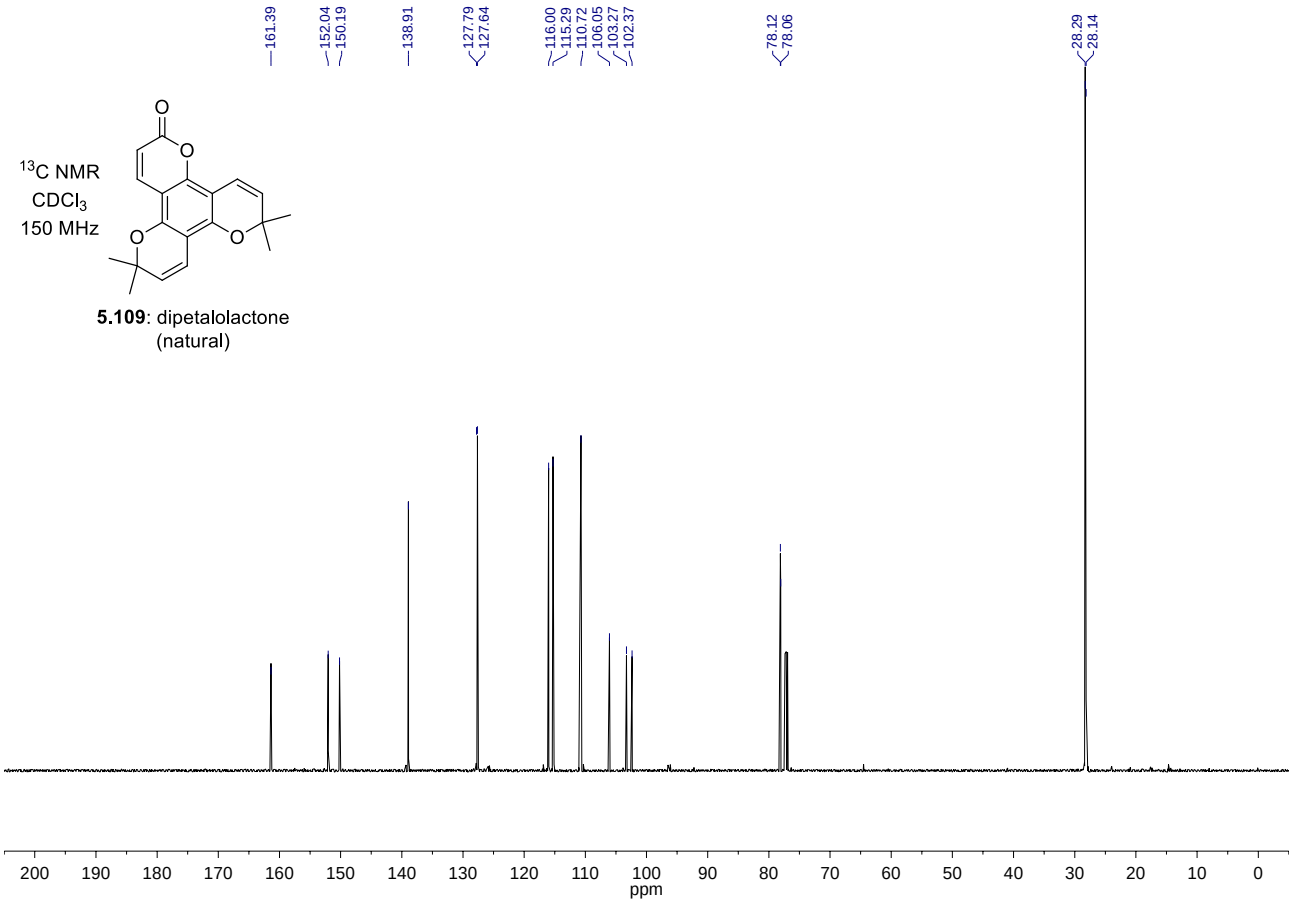

5.109: dipetalolactone
(natural)

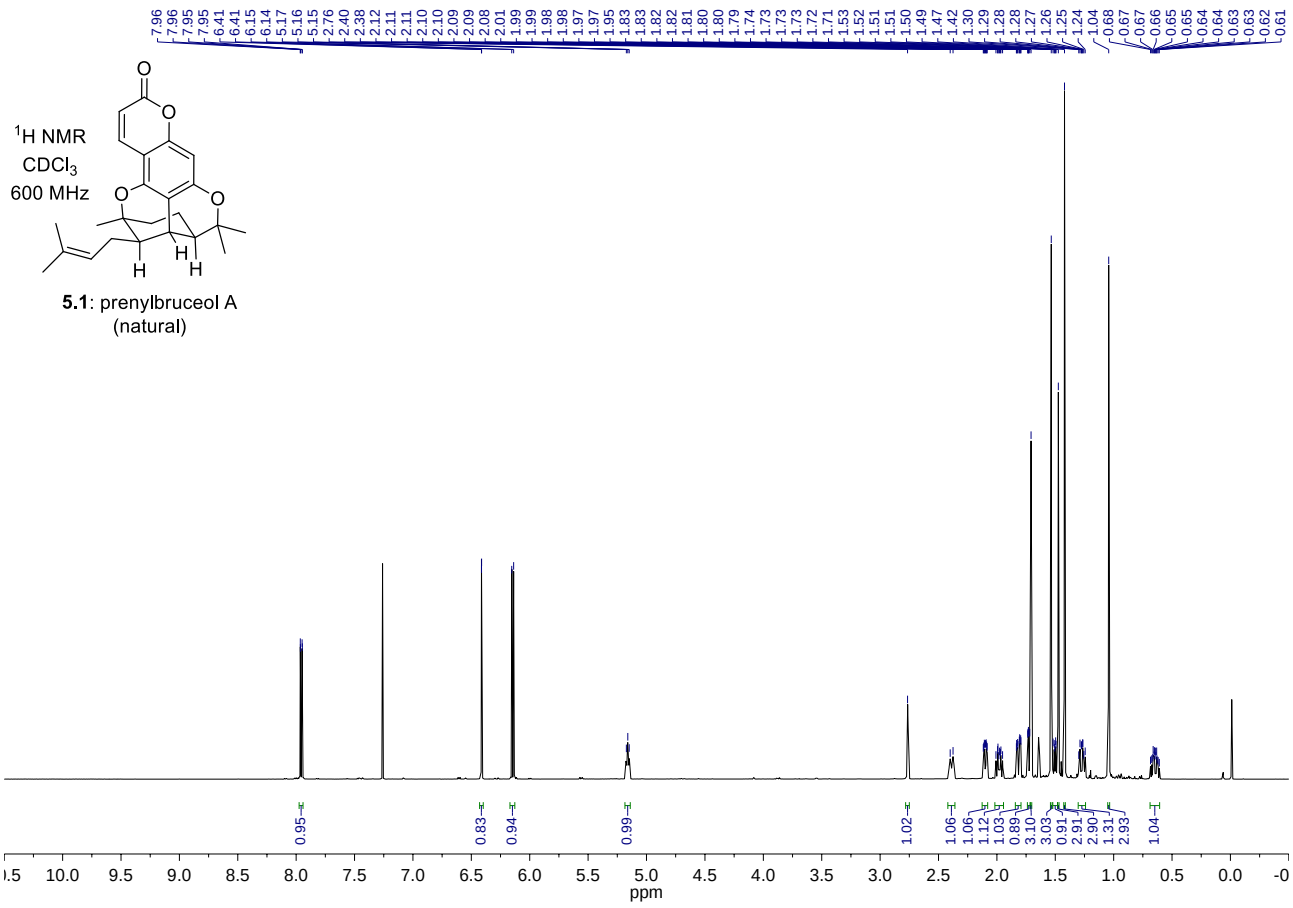
^{1}H NMR
$CDCl_3$
600 MHz
5.1: prenylbruceol A
(natural)
ppm

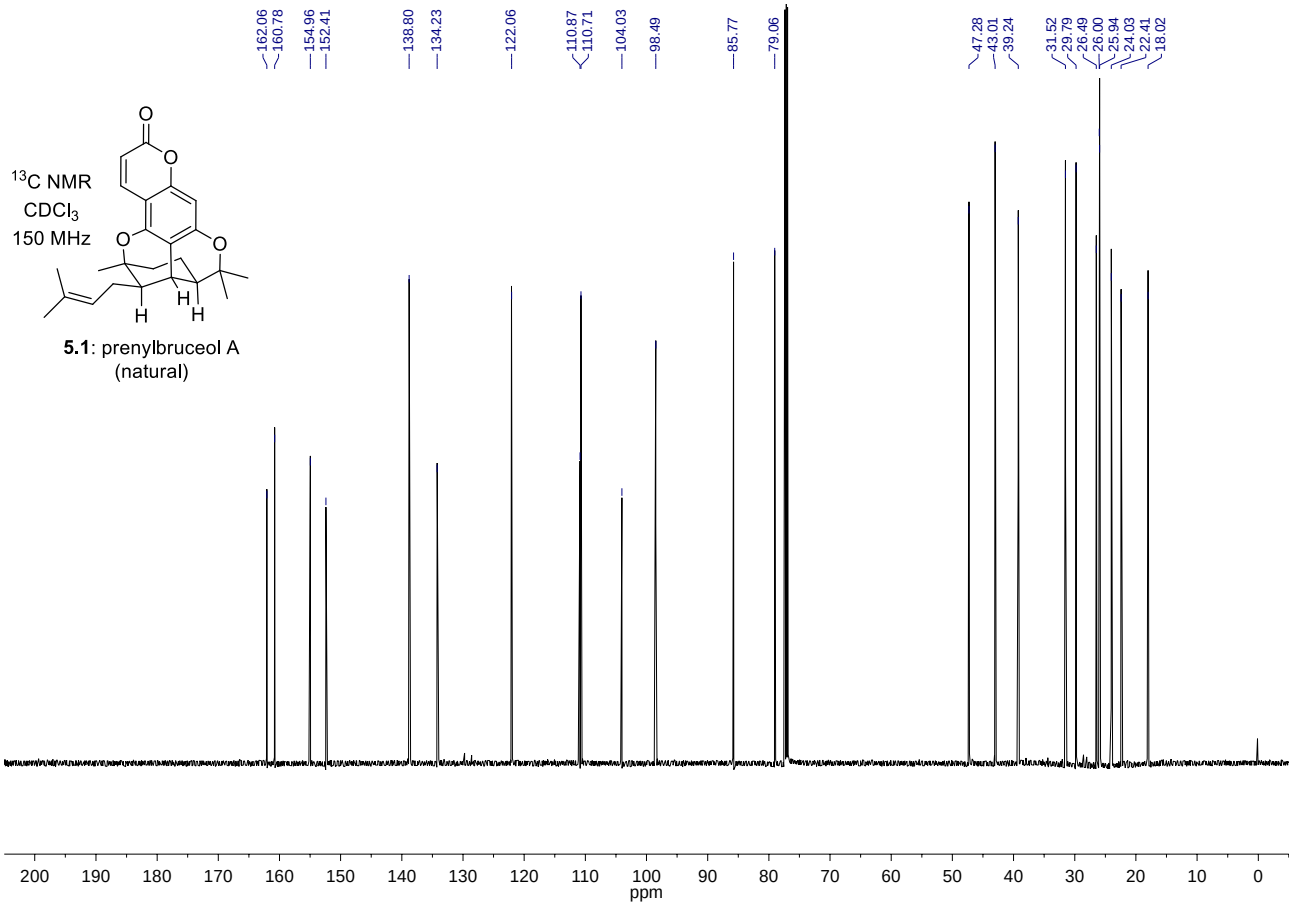
^{13}C NMR
$CDCl_3$
150 MHz
5.1: prenylbruceol A
(natural)
ppm

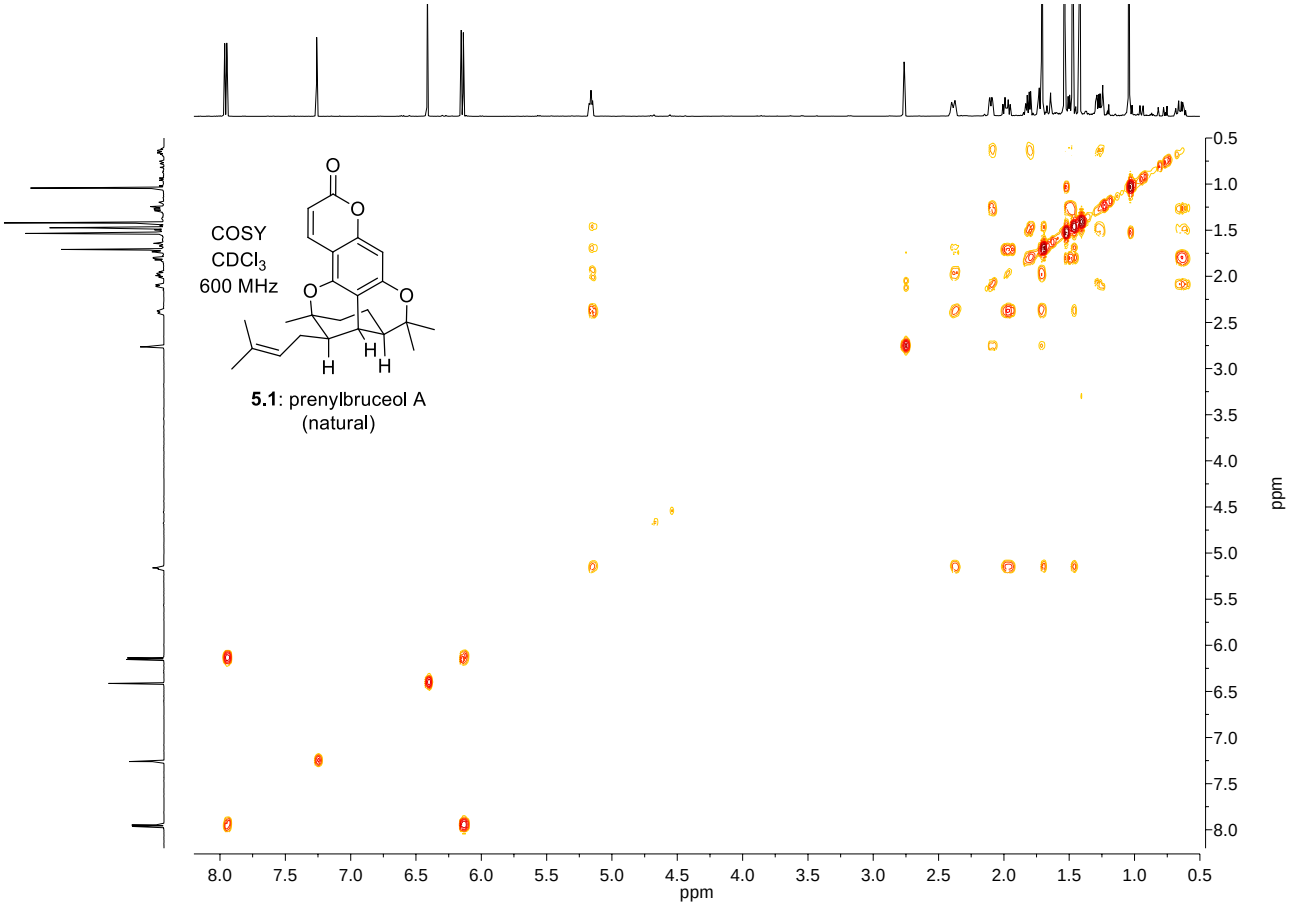
COSY
CDCl3
600 MHz
5.1: prenylbruceol A
(natural)
ppm
ppm

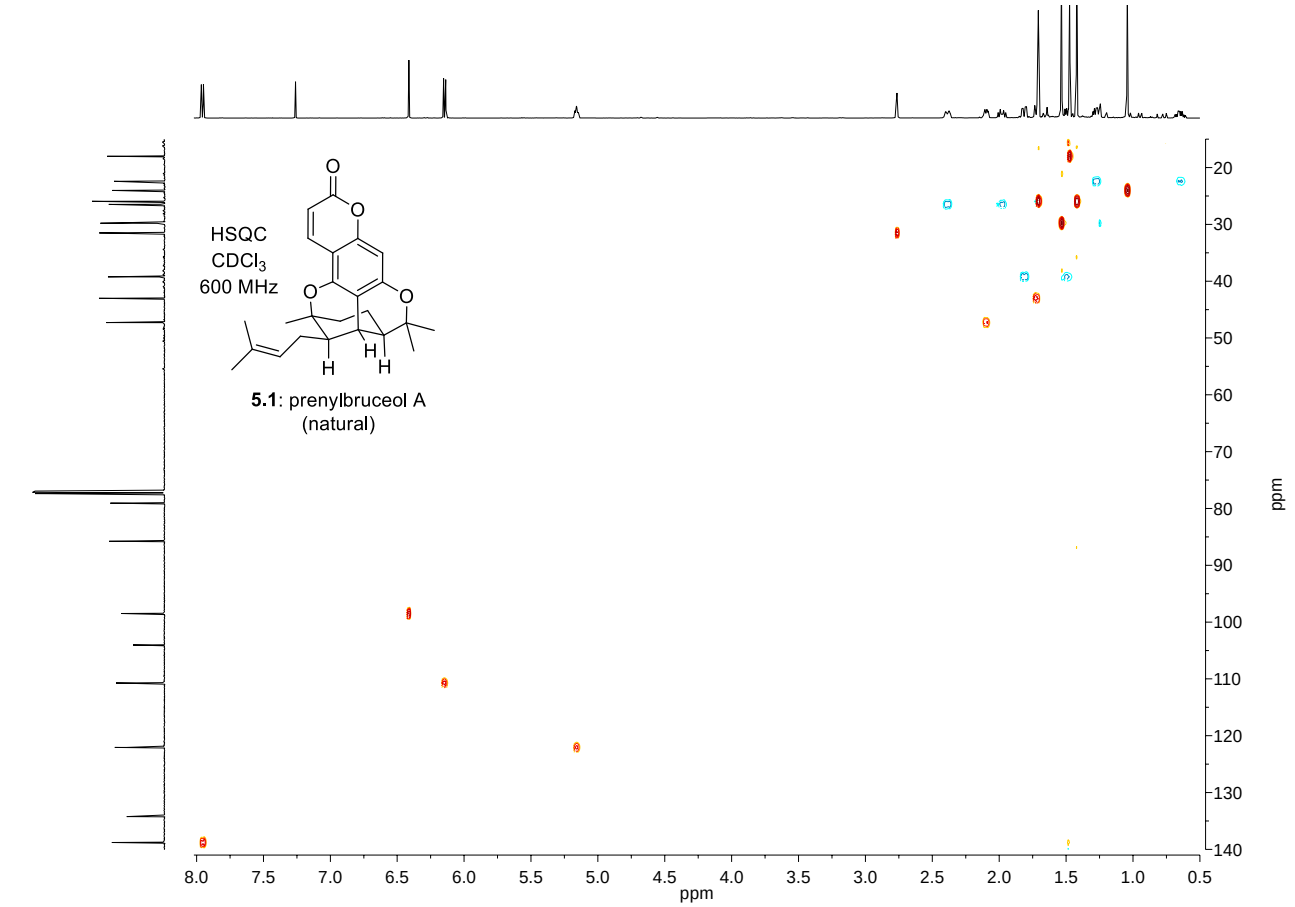
HSQC
CDCl3
600 MHz
5.1: prenylbruceol A
(natural)
ppm
ppm

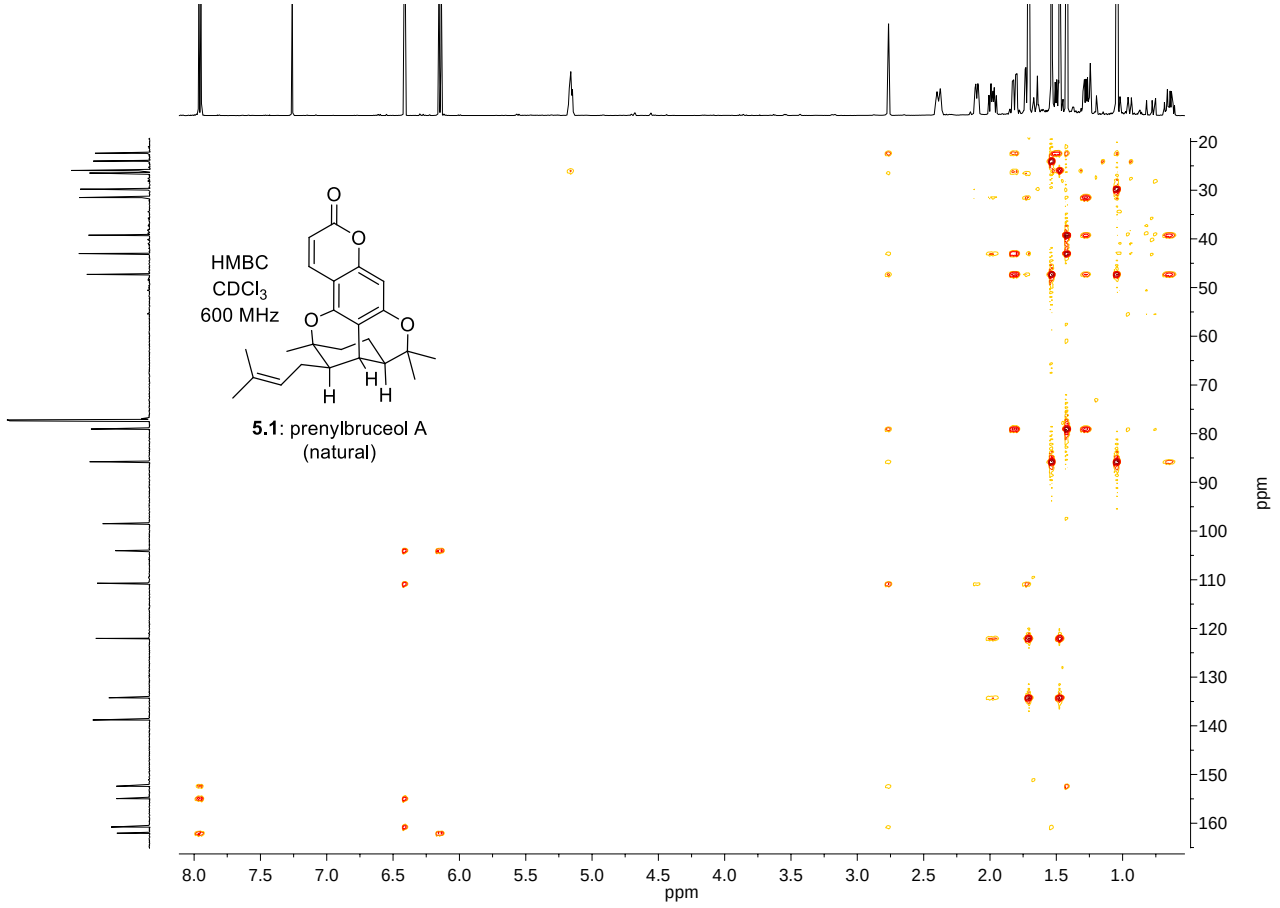
HMBC
CDCl3
600 MHz
5.1: prenylbruceol A
(natural)
ppm
ppm

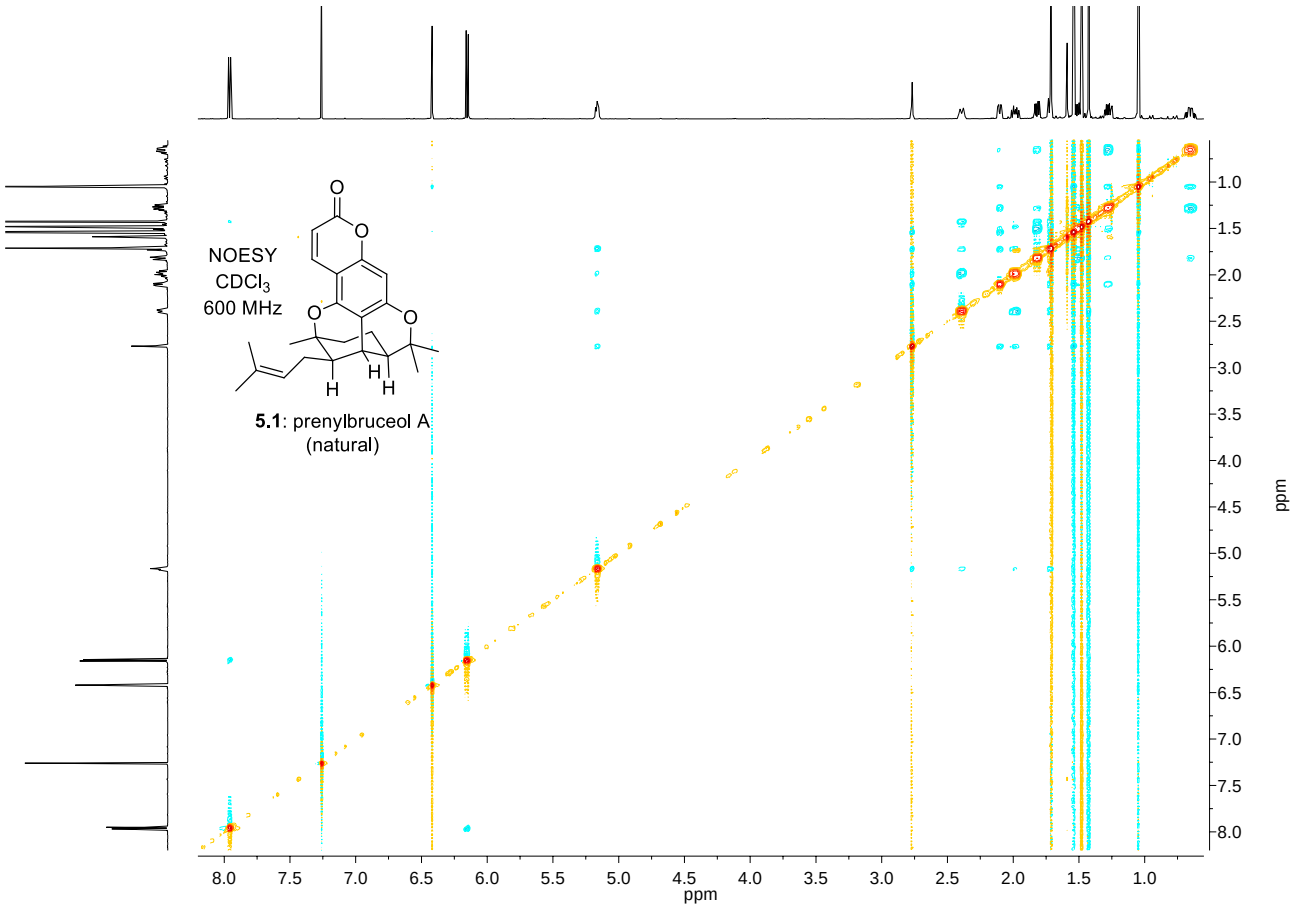
NOESY
CDCl3
600 MHz
5.1: prenylbruceol A
(natural)
ppm
ppm

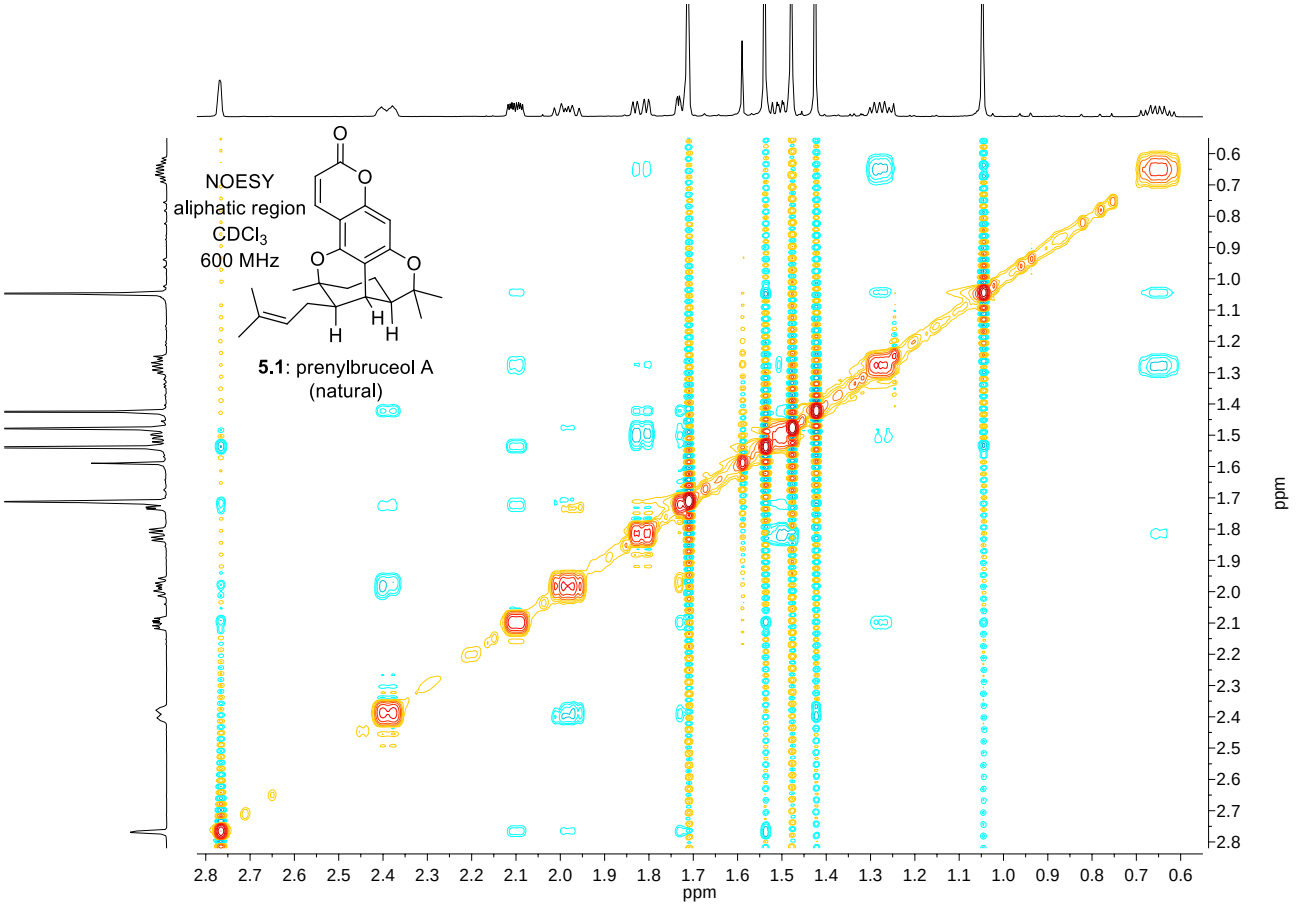
NOESY
aliphatic region
CDCl3
600 MHz
5.1: prenylbruceol A
(natural)
O
O
O
O
H
H
H
2.8 2.7 2.6 2.5 2.4 2.3 2.2 2.1 2.0 1.9 1.8 1.7 1.6 1.5 1.4 1.3 1.2 1.1 1.0 0.9 0.8 0.7 0.6
ppm
0.6 0.7 0.8 0.9 1.0 1.1 1.2 1.3 1.4 1.5 1.6 1.7 1.8 1.9 2.0 2.1 2.2 2.3 2.4 2.5 2.6 2.7 2.8
ppm

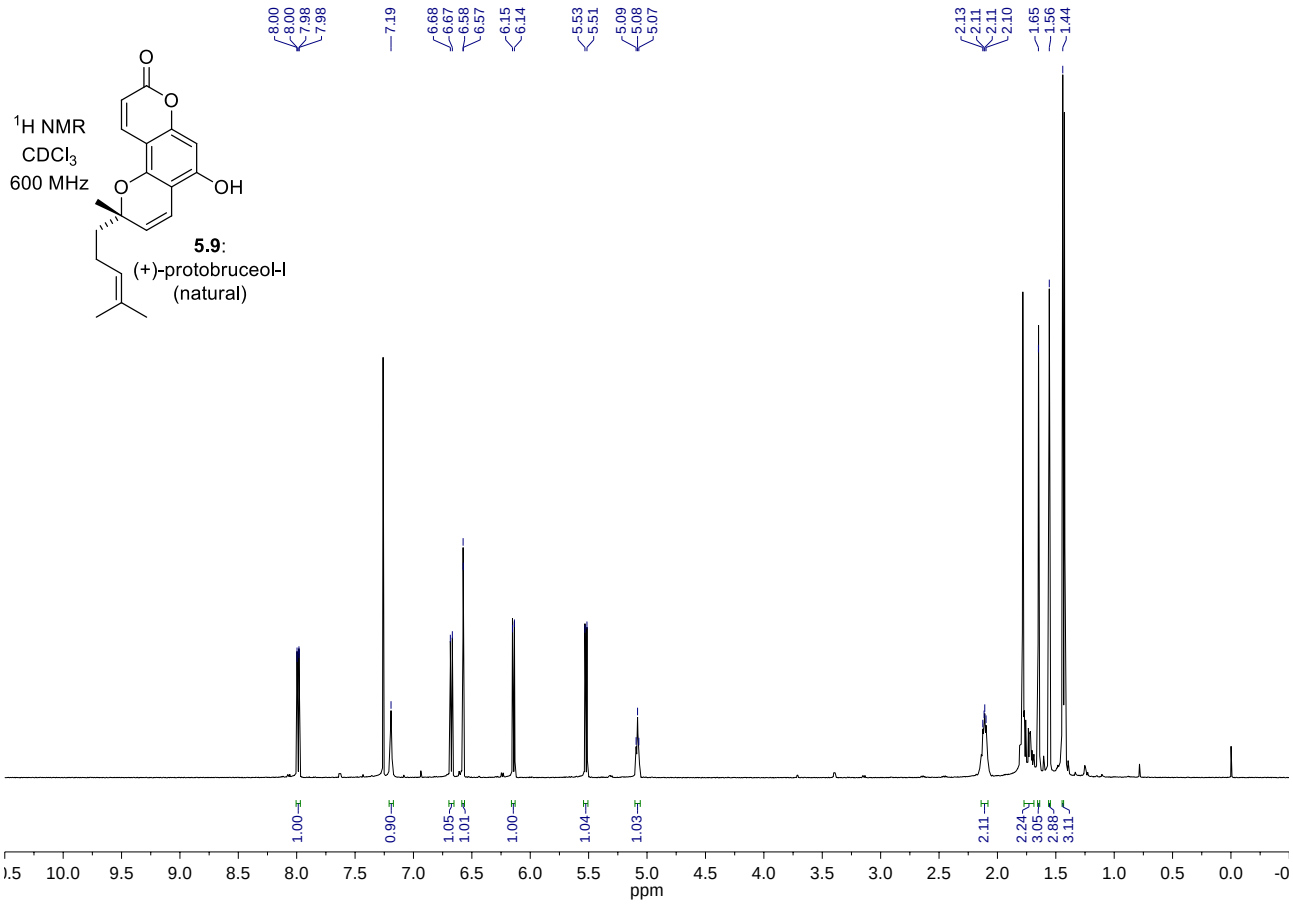
8.00
8.00
7.98
7.98
7.19
6.68
6.67
6.58
6.57
6.15
6.14
5.53
5.51
5.09
5.08
5.07
2.13
2.11
2.11
2.10
1.65
1.56
1.44
1H NMR
CDCl3
600 MHz
OH
5.9:
(+)-protobruceol-I
(natural)
1.00
0.90
1.05
1.01
1.00
1.04
1.03
2.11
2.24
3.05
2.88
3.11
ppm

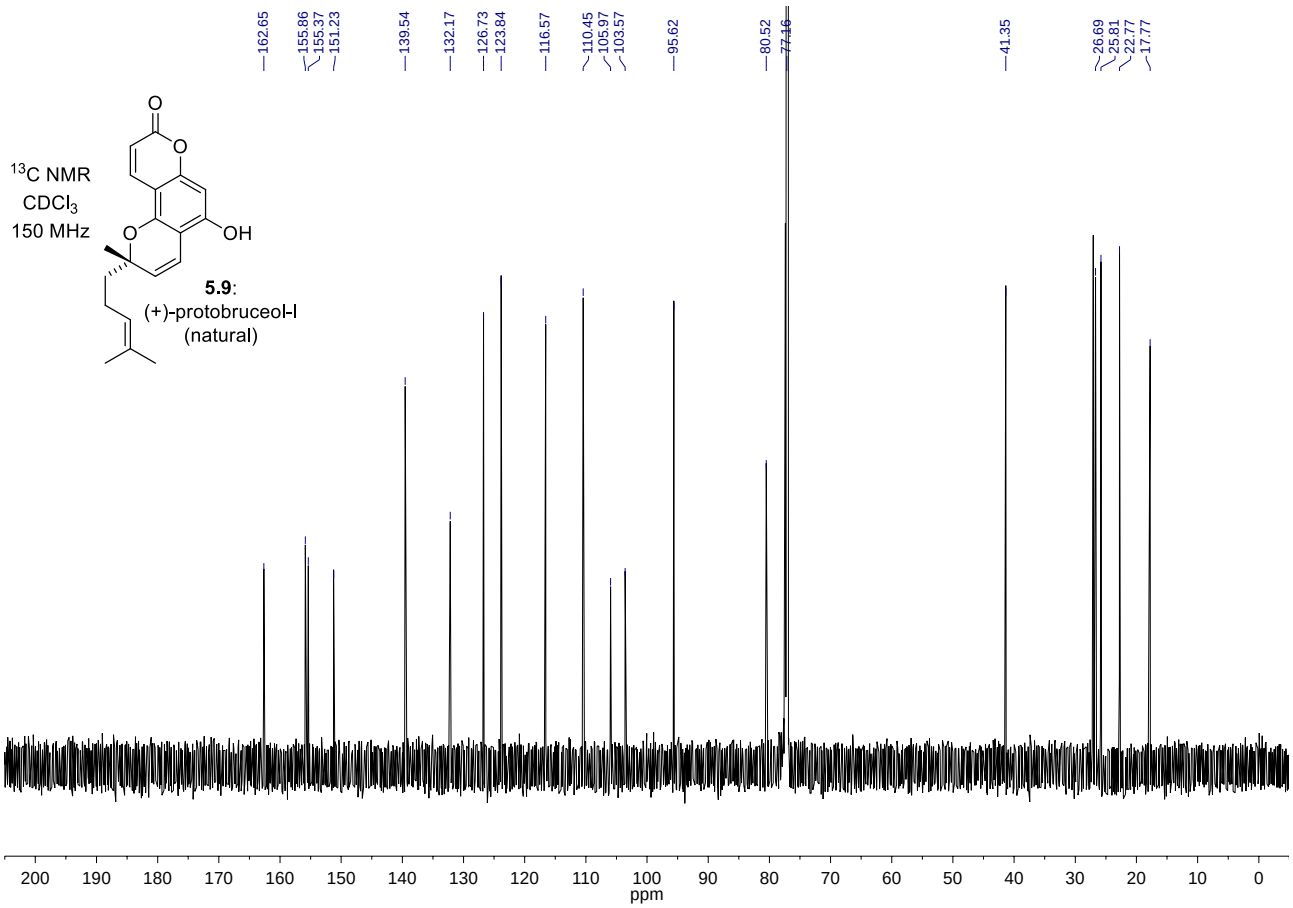
162.65
155.86
155.37
151.23
139.54
132.17
126.73
123.84
116.57
110.45
105.97
103.57
95.62
80.52
77.16
41.35
26.69
25.81
22.77
17.77
13C NMR
CDCl3
150 MHz
OH
5.9:
(+)-protobruceol-I
(natural)
ppm

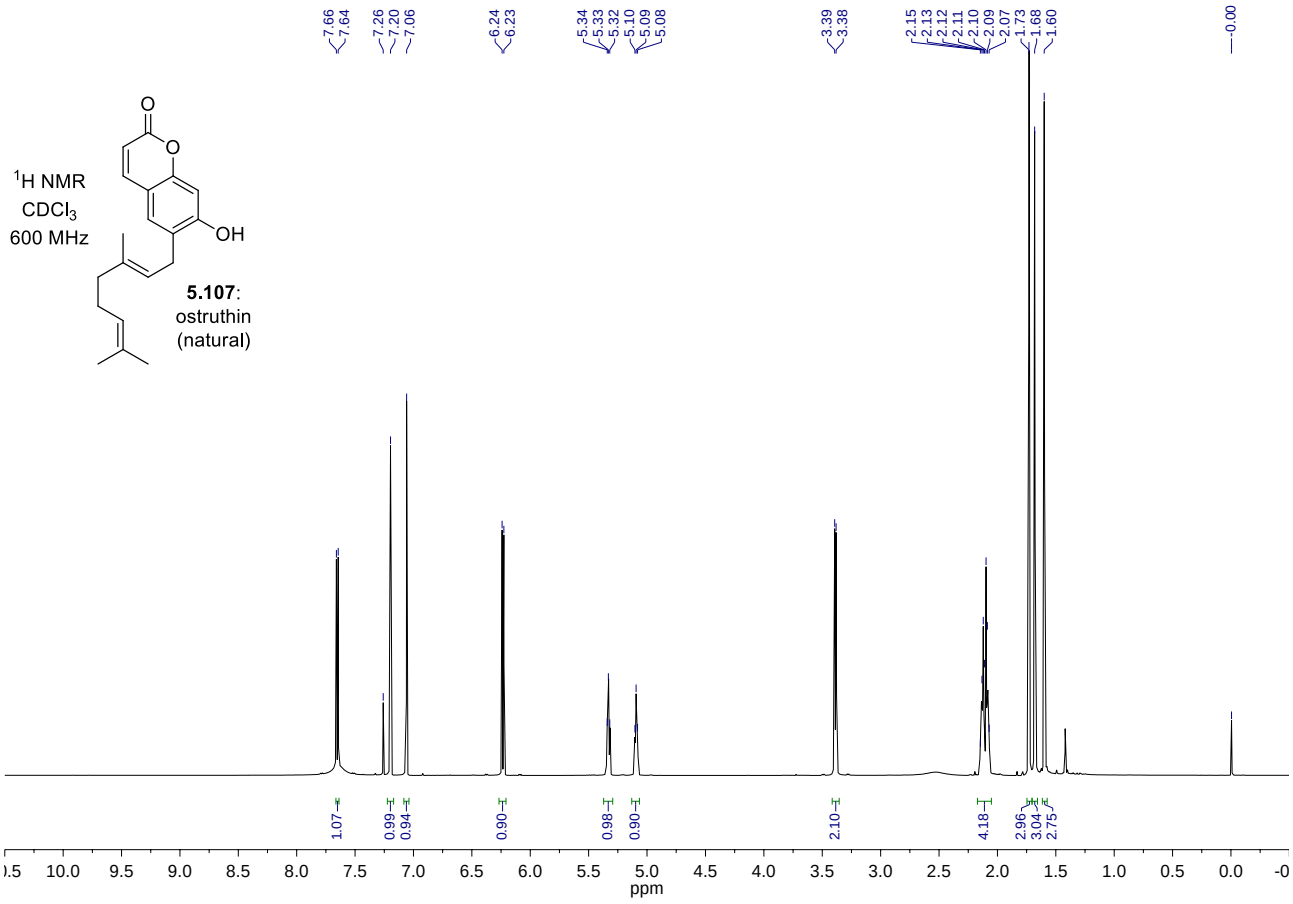
7.66
7.64
7.26
7.20
7.06
6.24
6.23
5.34
5.33
5.32
5.10
5.09
5.08
3.39
3.38
2.15
2.13
2.12
2.11
2.10
2.09
2.07
1.73
1.68
1.60
0.00
1H NMR
CDCl3
600 MHz
5.107:
ostruthin
(natural)
OH
1.07
0.99
0.94
0.90
0.98
0.90
2.10
4.18
2.96
3.04
2.75
ppm

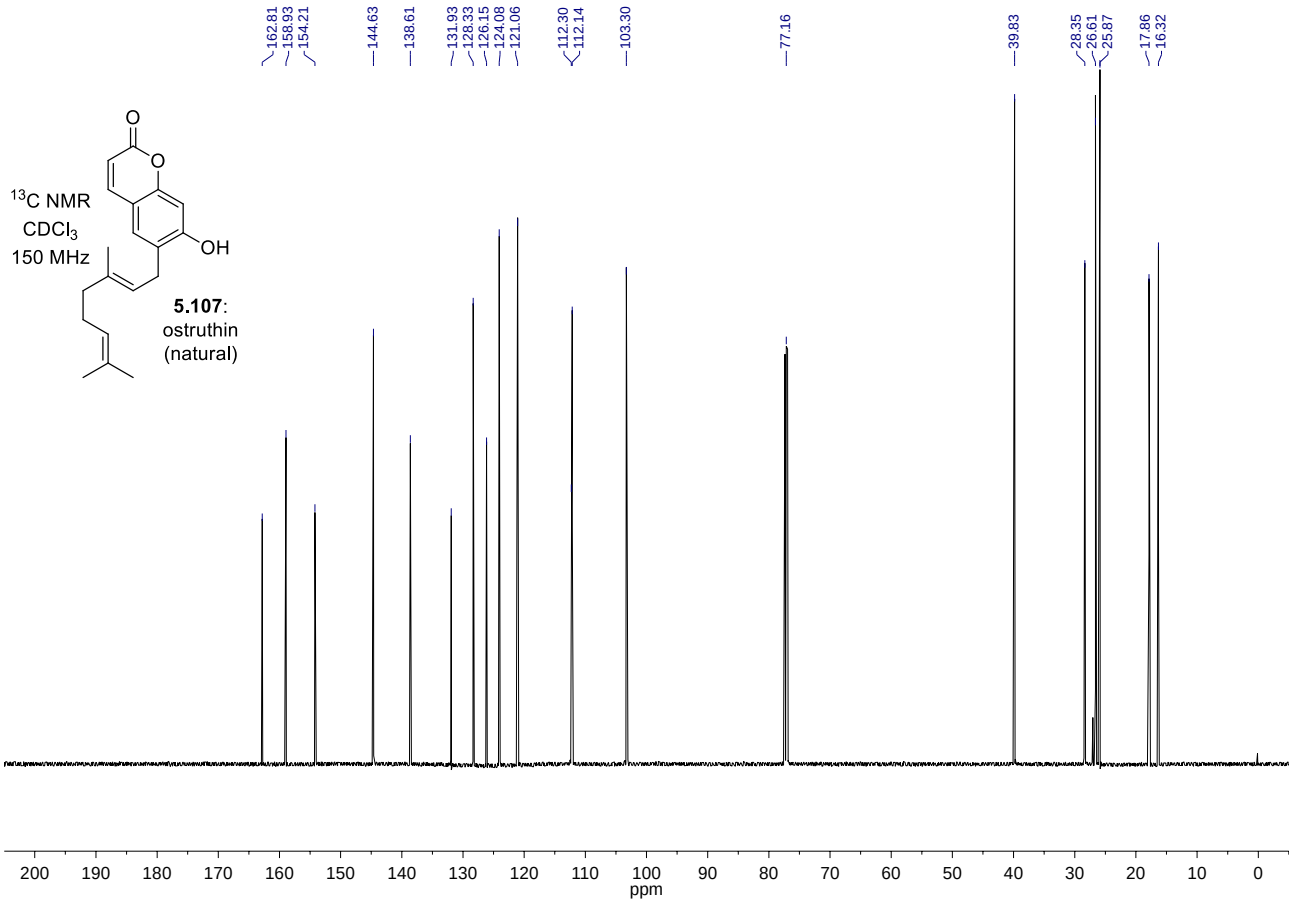
162.81
158.93
154.21
144.63
138.61
131.93
128.33
126.15
124.08
121.06
112.30
112.14
103.30
77.16
39.83
28.35
26.61
25.87
17.86
16.32
13C NMR
CDCl3
150 MHz
5.107:
ostruthin
(natural)
OH
ppm

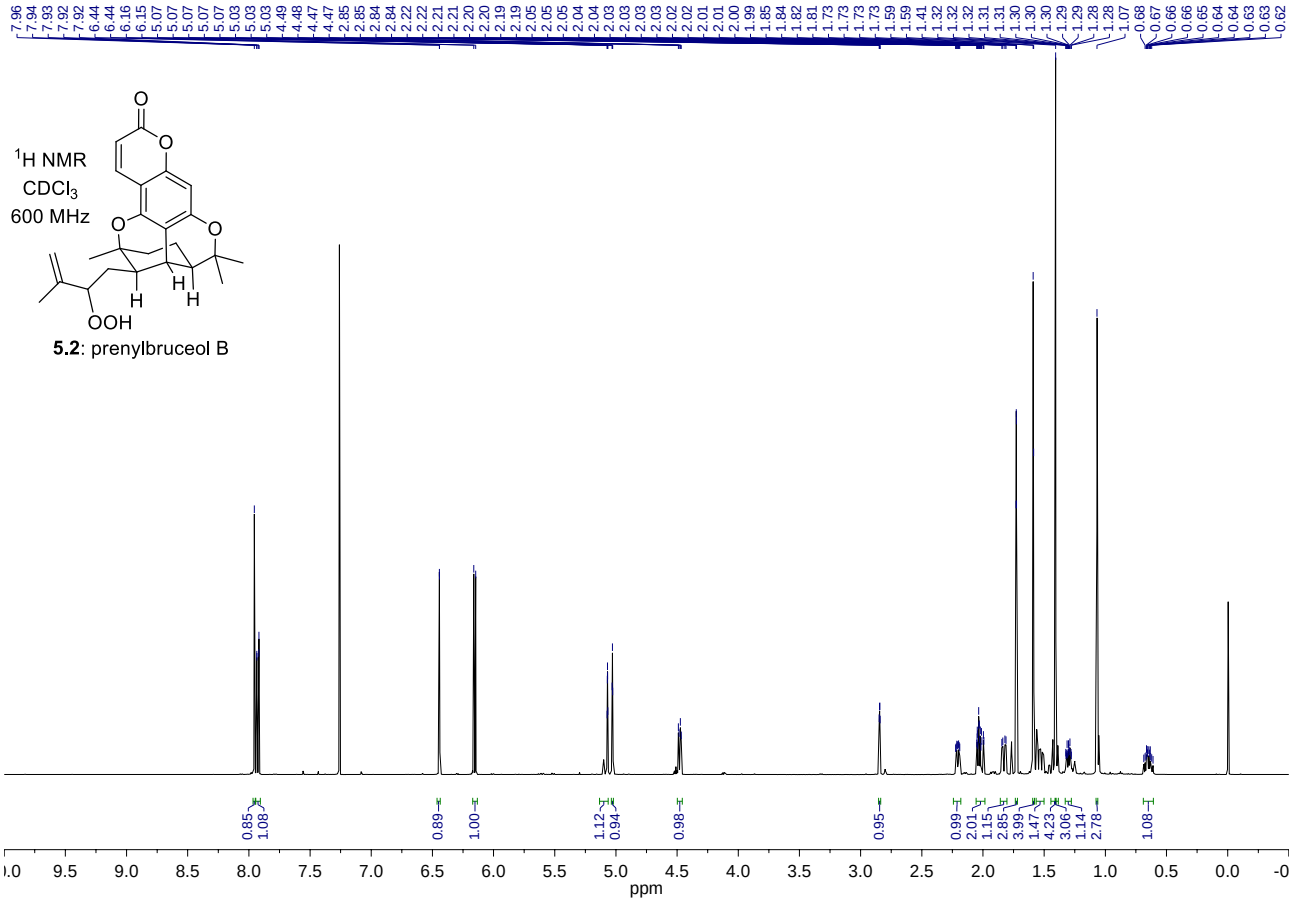
^{1}H NMR
$CDCl_3$
600 MHz
OOH
5.2: prenylbruceol B
ppm

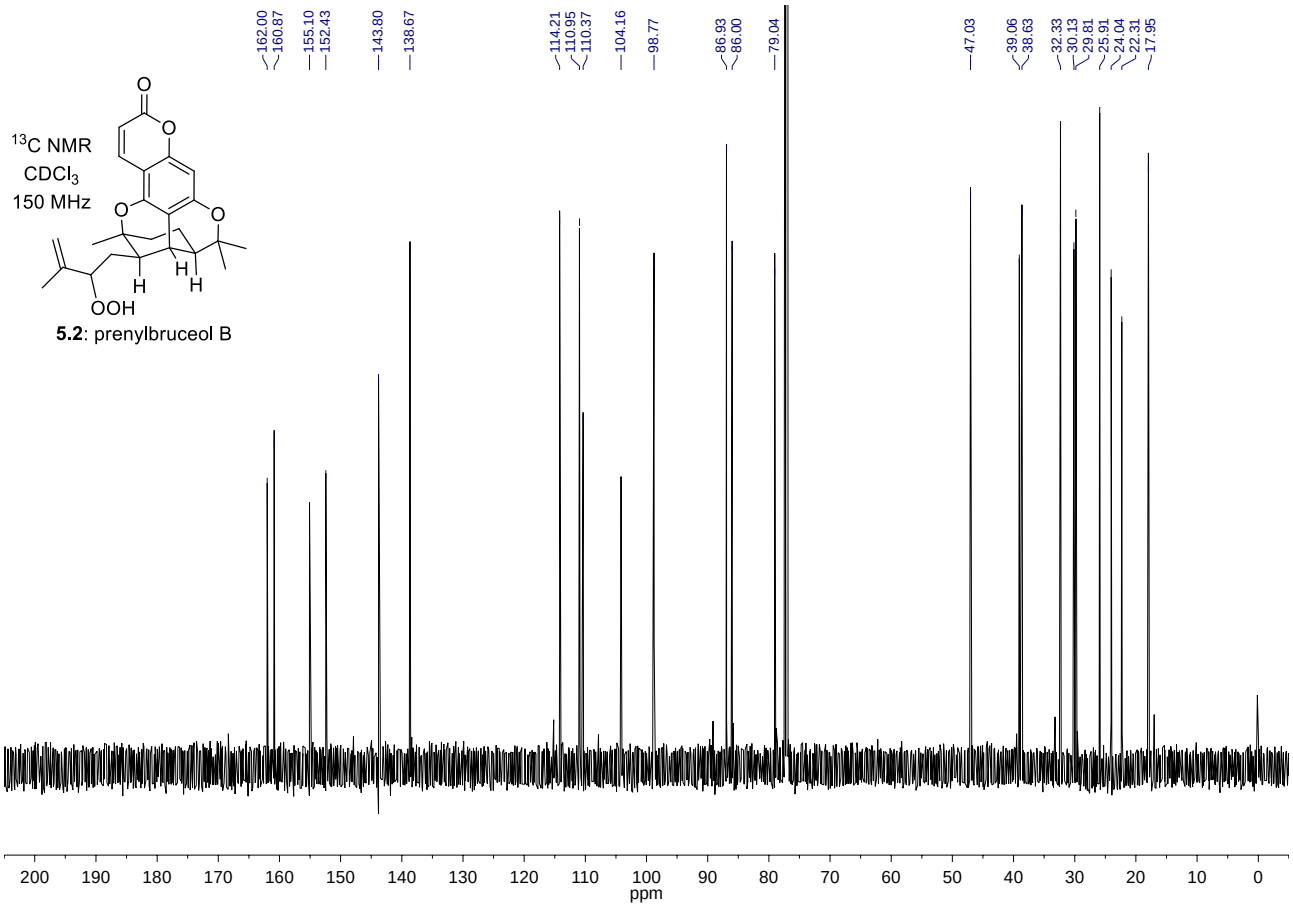
^{13}C NMR
$CDCl_3$
150 MHz
OOH
5.2: prenylbruceol B
ppm

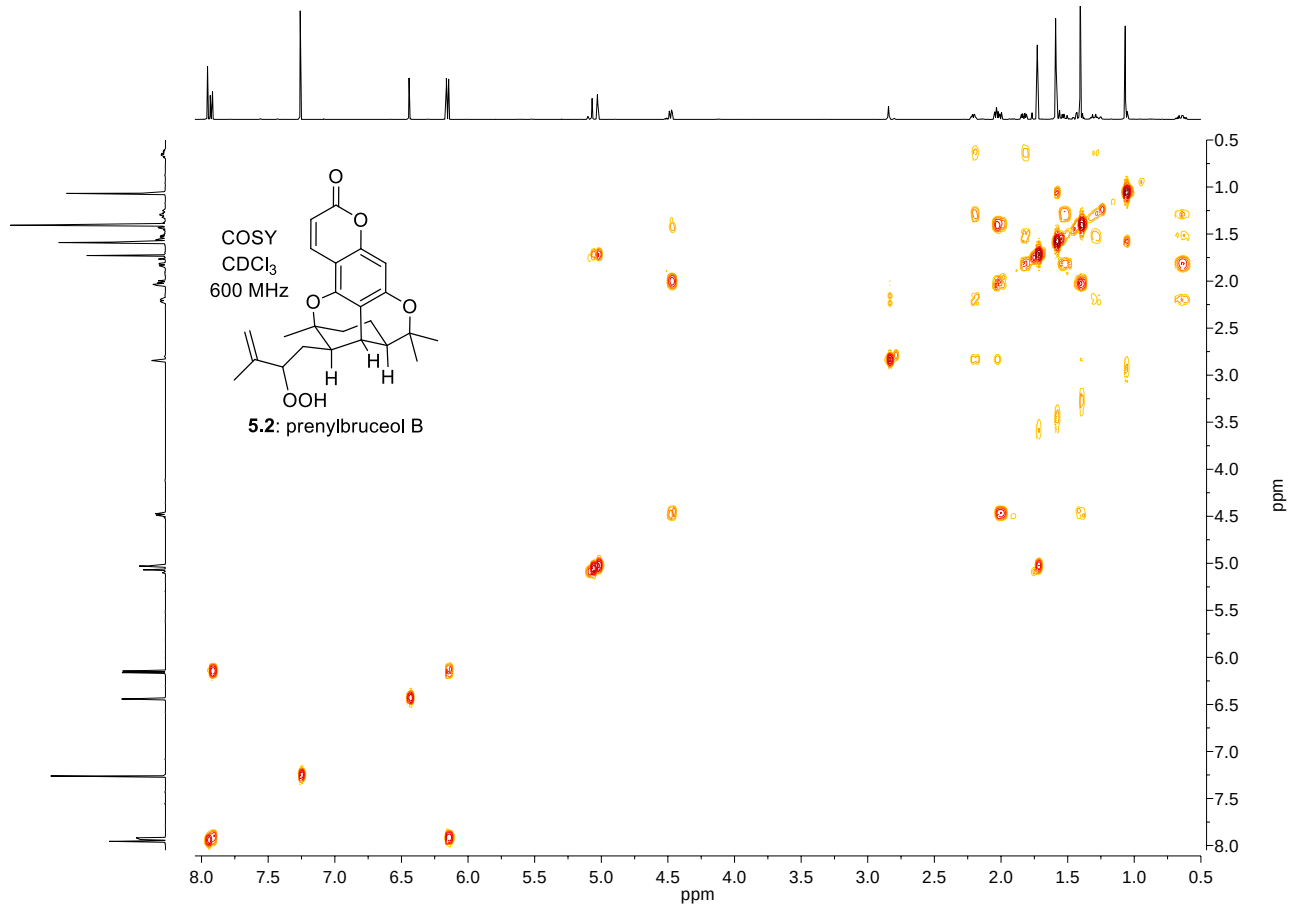
COSY
CDCl3
600 MHz
OOH
5.2: prenylbruceol B
ppm
ppm

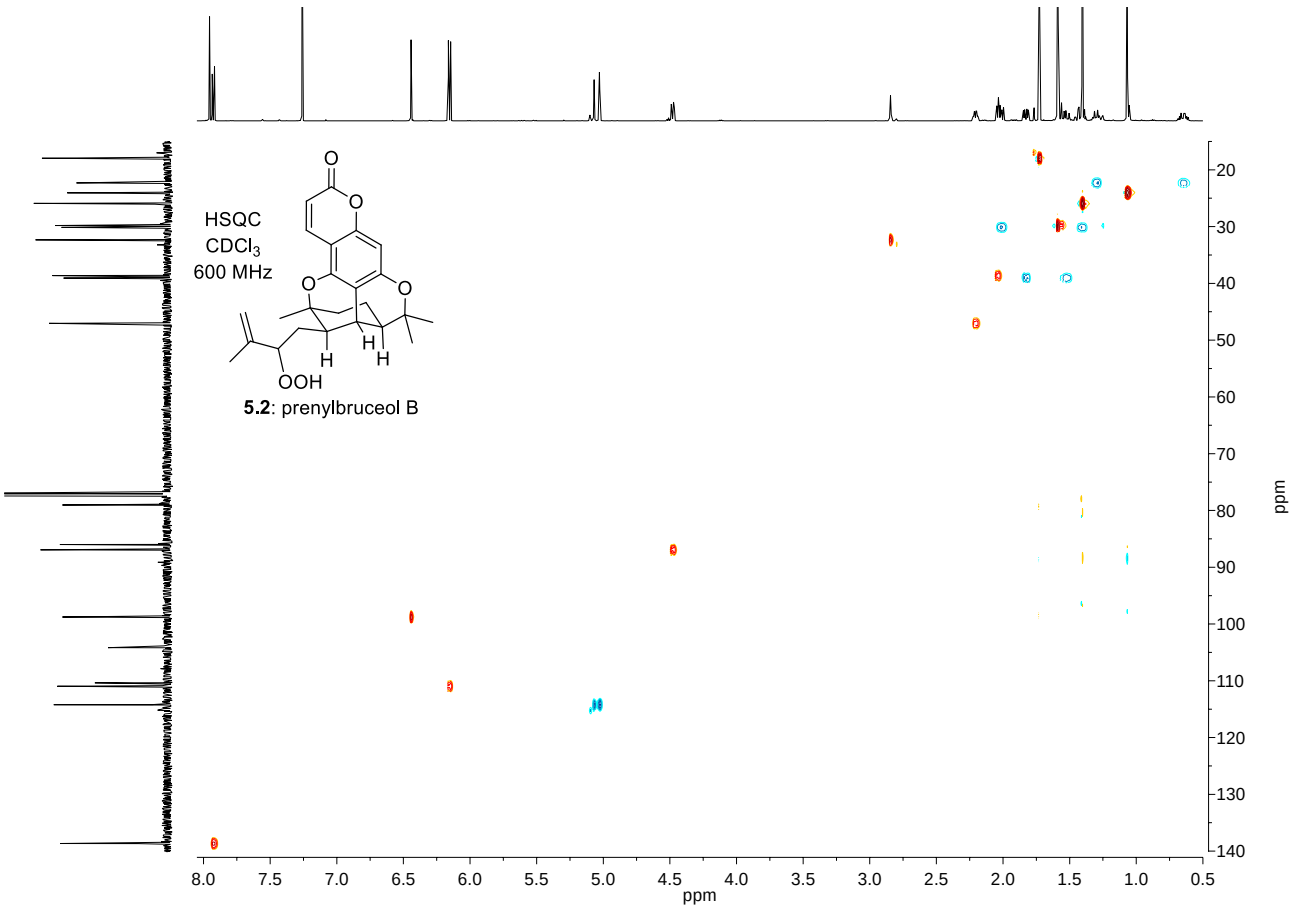
HSQC
CDCl3
600 MHz
OOH
5.2: prenylbruceol B
ppm
ppm

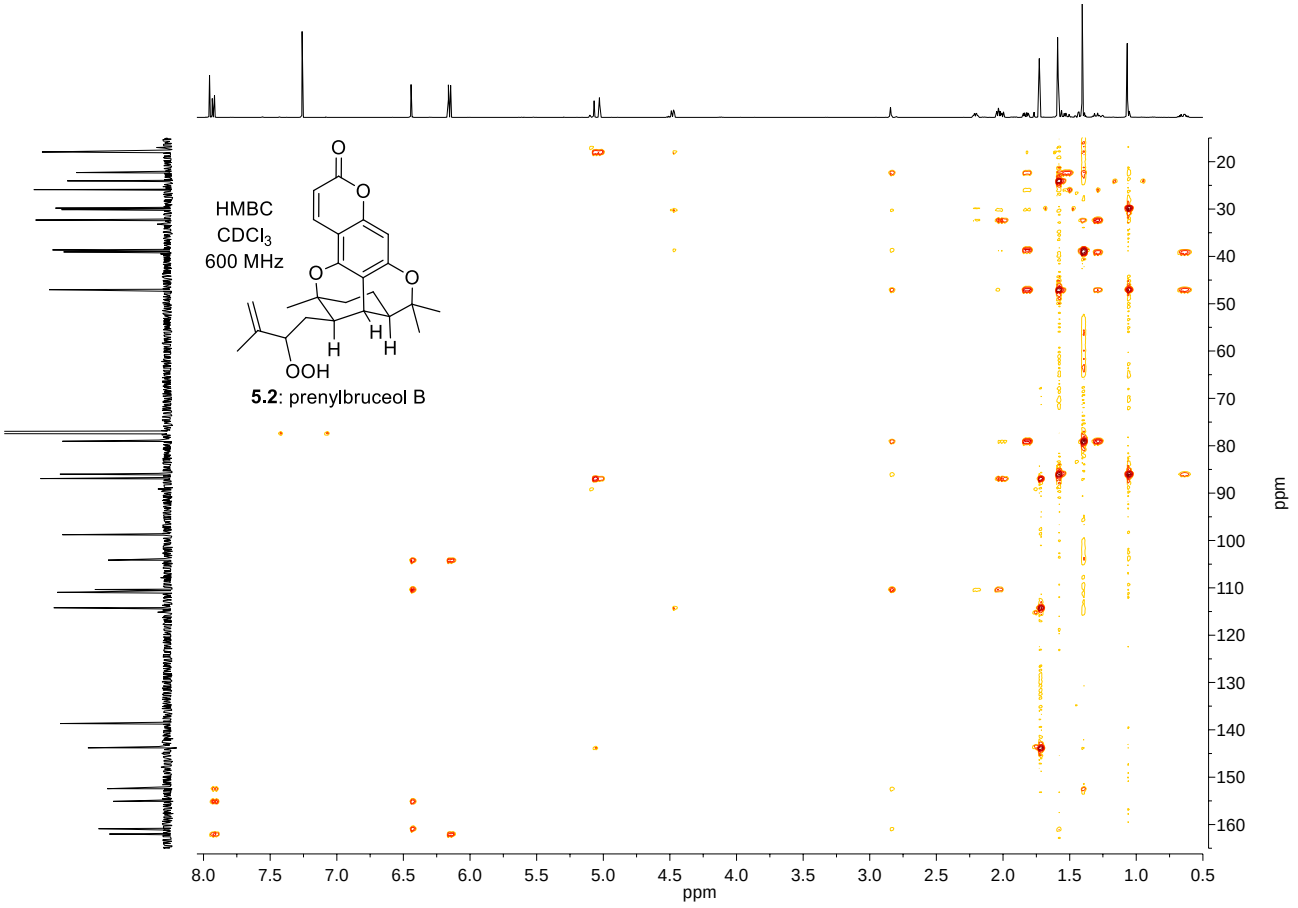
HMBC
CDCl3
600 MHz
O
O
O
O
H
H
H
OOH
5.2: prenylbruceol B
8.0
7.5
7.0
6.5
6.0
5.5
5.0
4.5
4.0
3.5
3.0
2.5
2.0
1.5
1.0
0.5
ppm
20
30
40
50
60
70
80
90
100
110
120
130
140
150
160
ppm

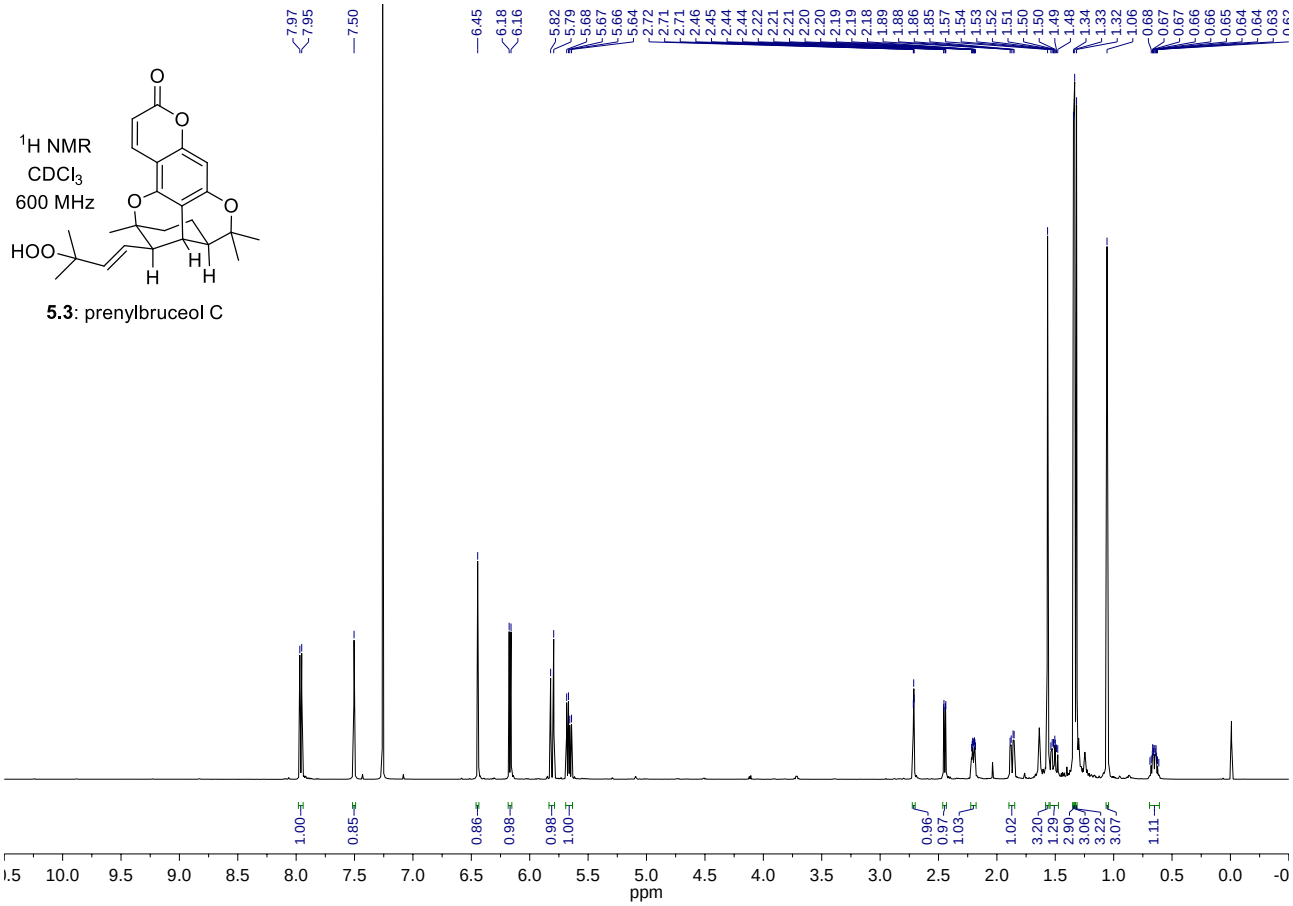
^{1}H NMR
$CDCl_3$
600 MHz
HOO
H
H
H
5.3: prenylbruceol C
ppm

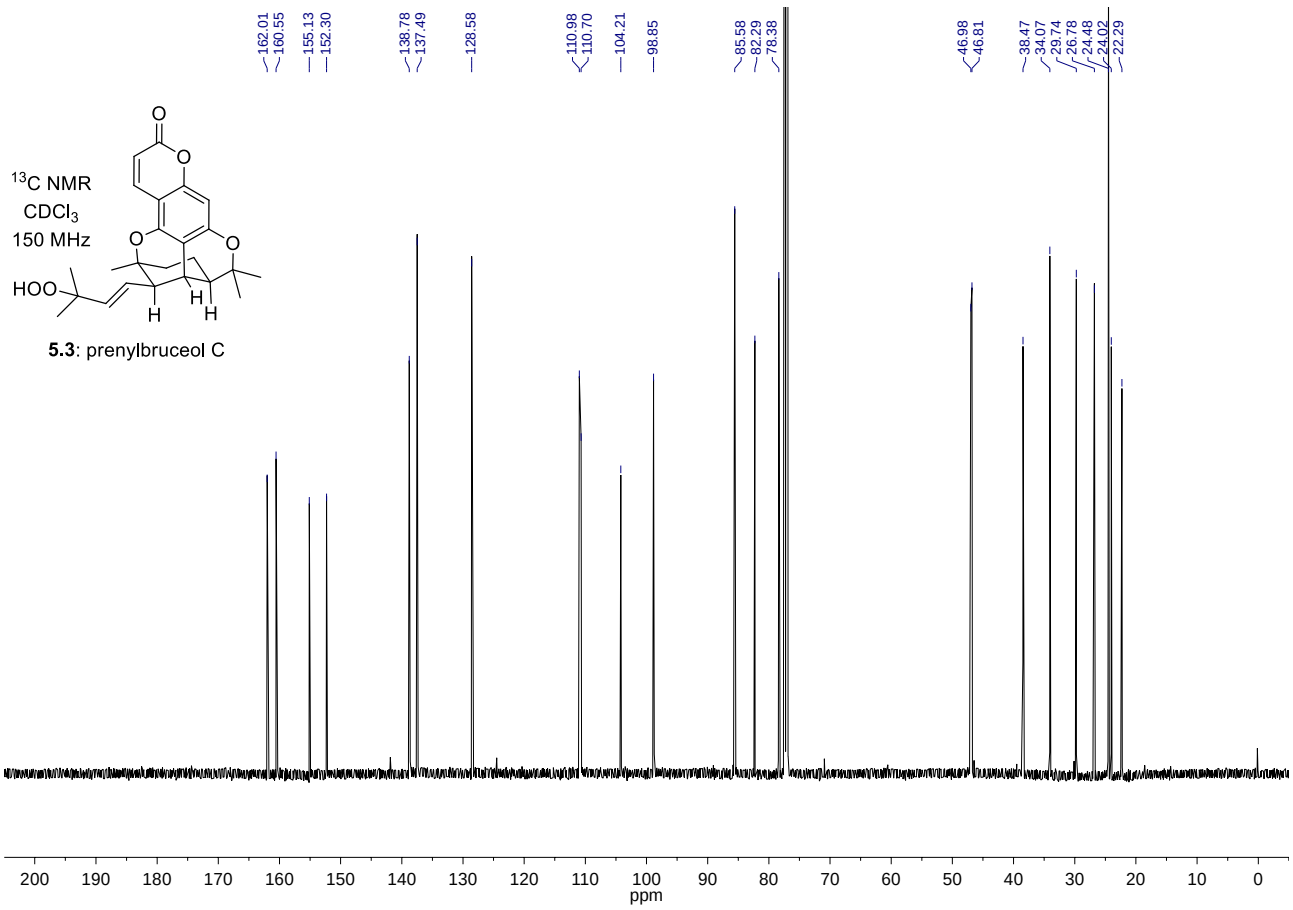
^{13}C NMR
$CDCl_3$
150 MHz
HOO
H
H
H
5.3: prenylbruceol C
ppm

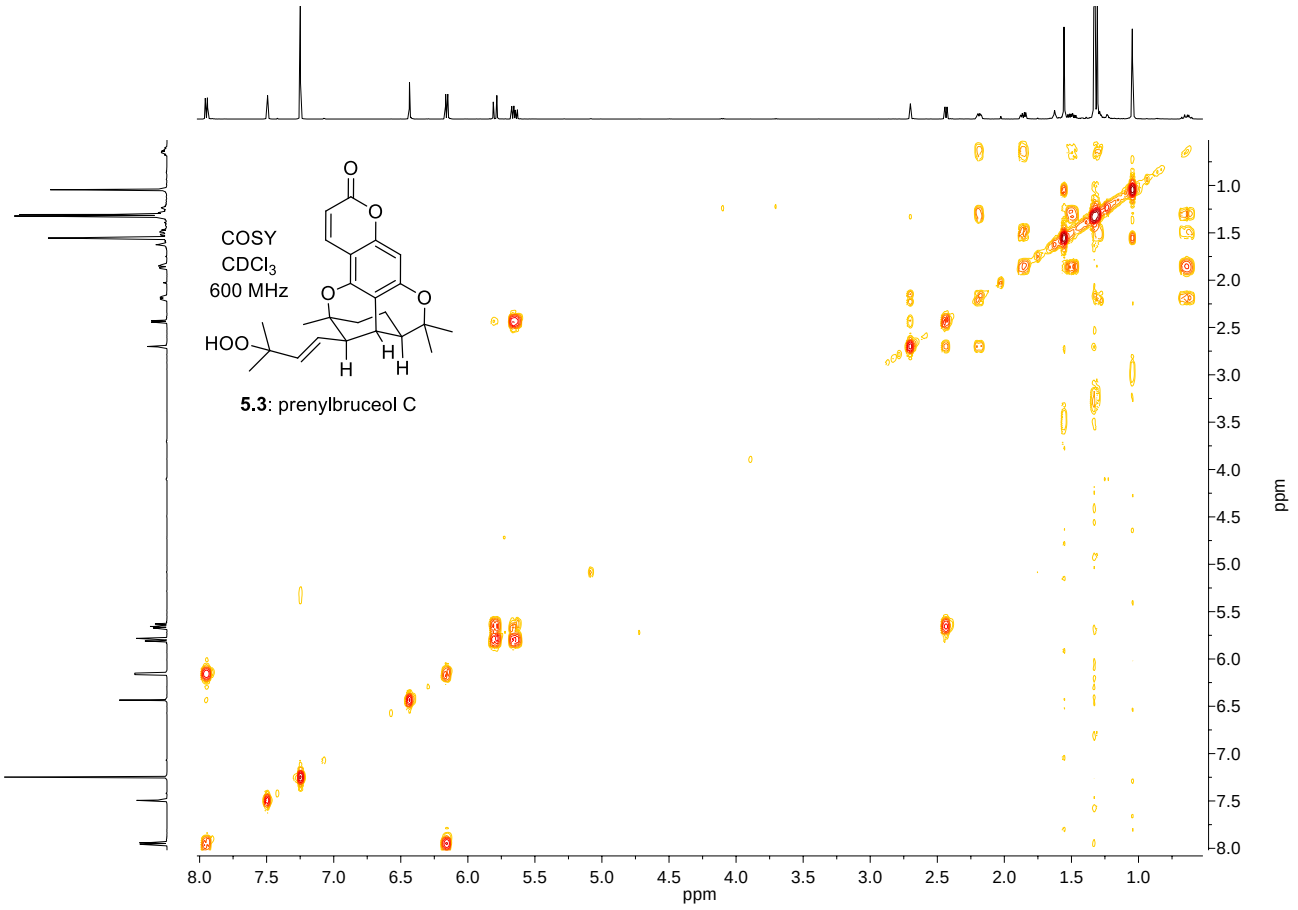
COSY
CDCl3
600 MHz
HOO
H
H
H
O
O
O
O
5.3: prenylbruceol C
ppm
ppm

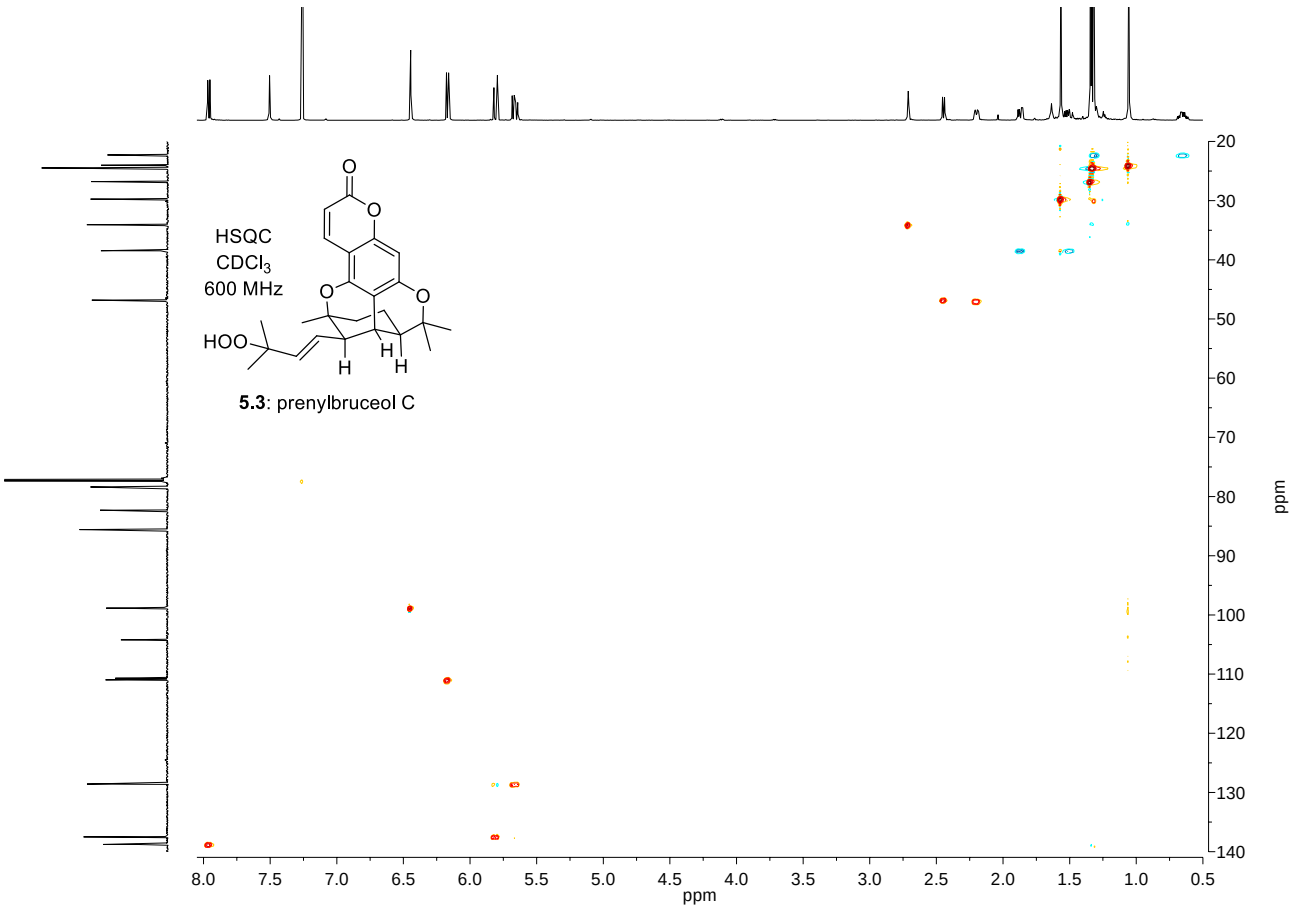
HSQC
CDCl3
600 MHz
HOO
H
H
H
O
O
O
O
5.3: prenylbruceol C
ppm
ppm

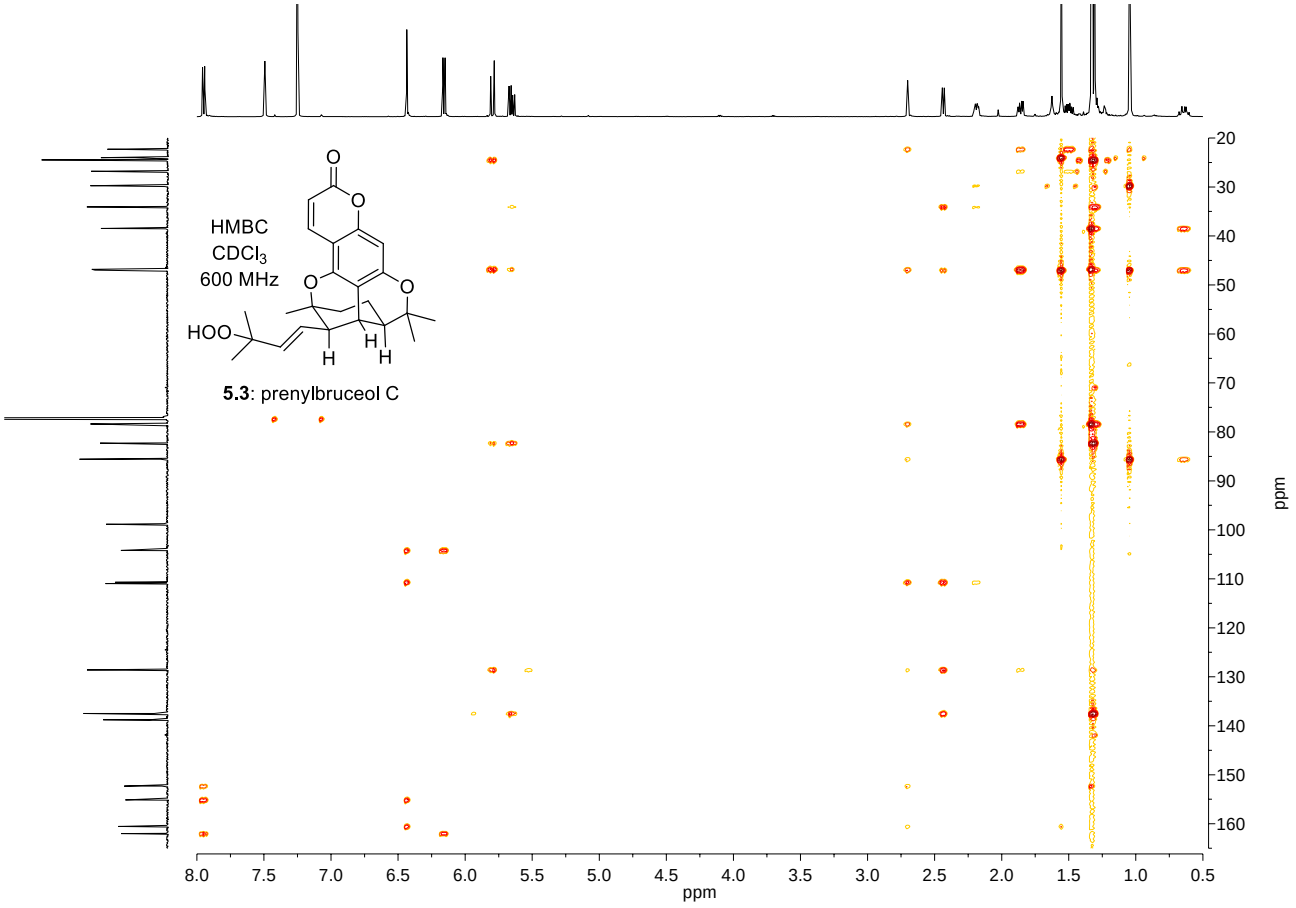
HMBC
CDCl3
600 MHz
HOO
O
O
O
O
H
H
H
5.3: prenylbruceol C
8.0
7.5
7.0
6.5
6.0
5.5
5.0
4.5
4.0
3.5
3.0
2.5
2.0
1.5
1.0
0.5
ppm
20
30
40
50
60
70
80
90
100
110
120
130
140
150
160
ppm

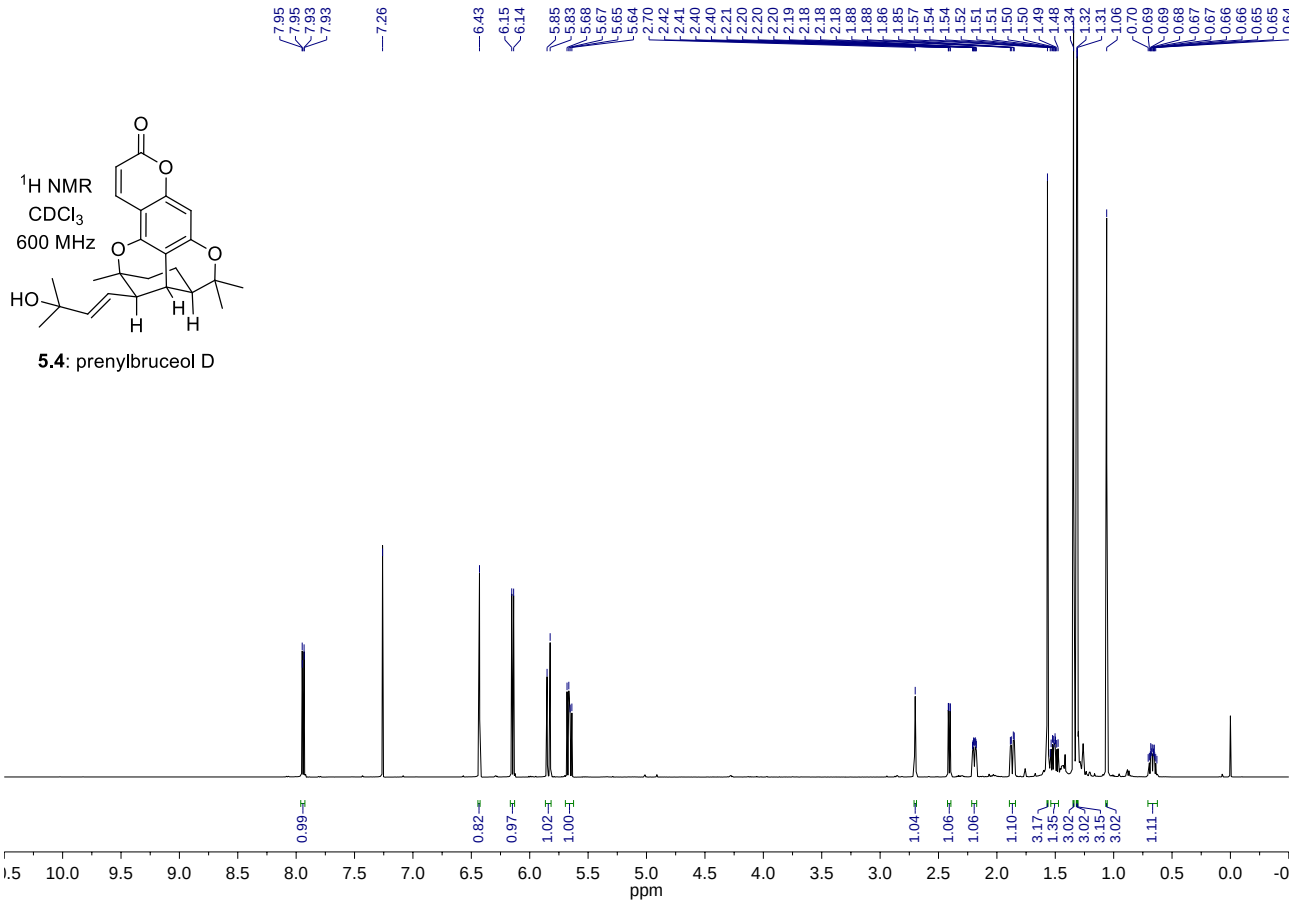

5.4: prenylbruceol D

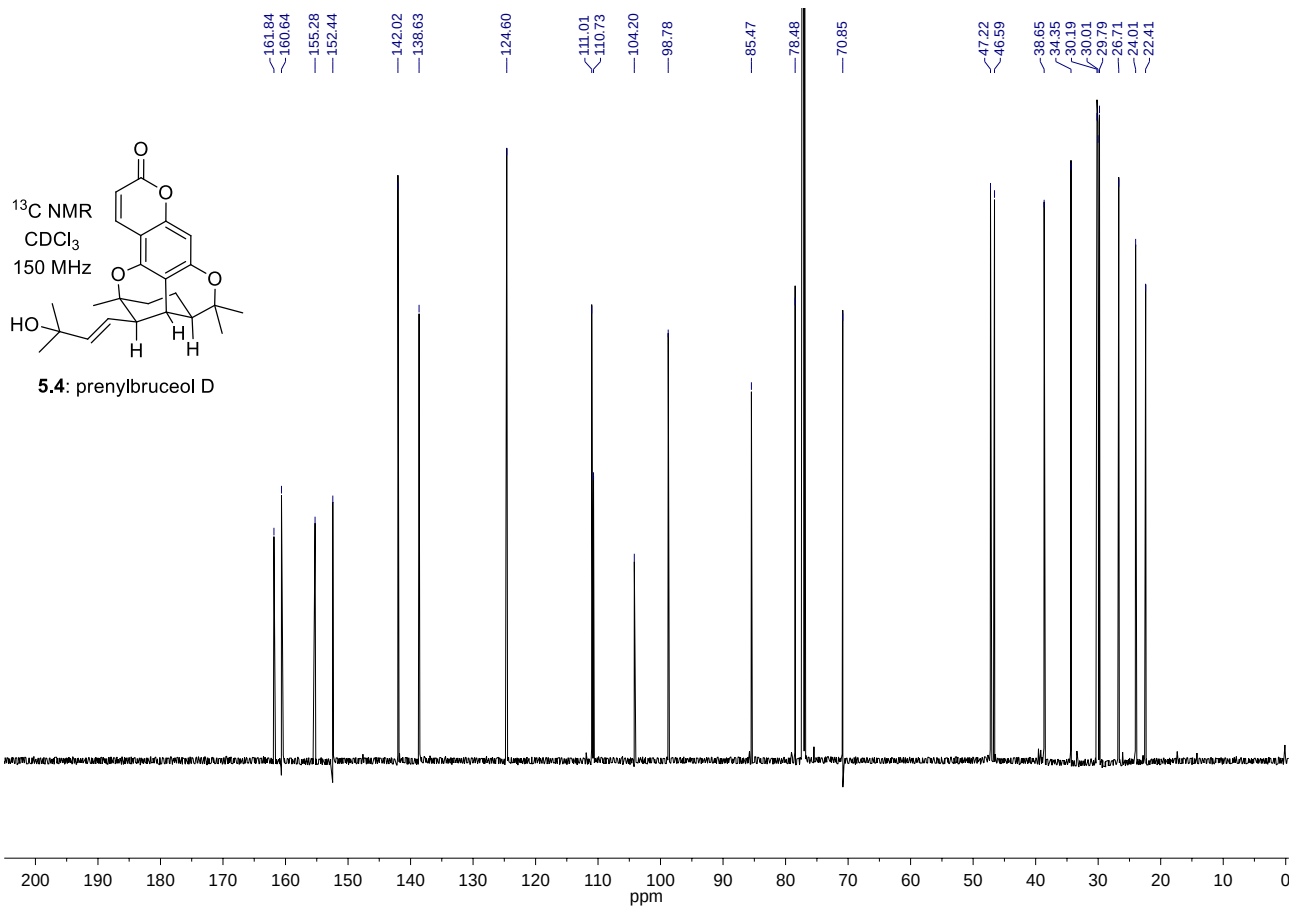

5.4: prenylbruceol D

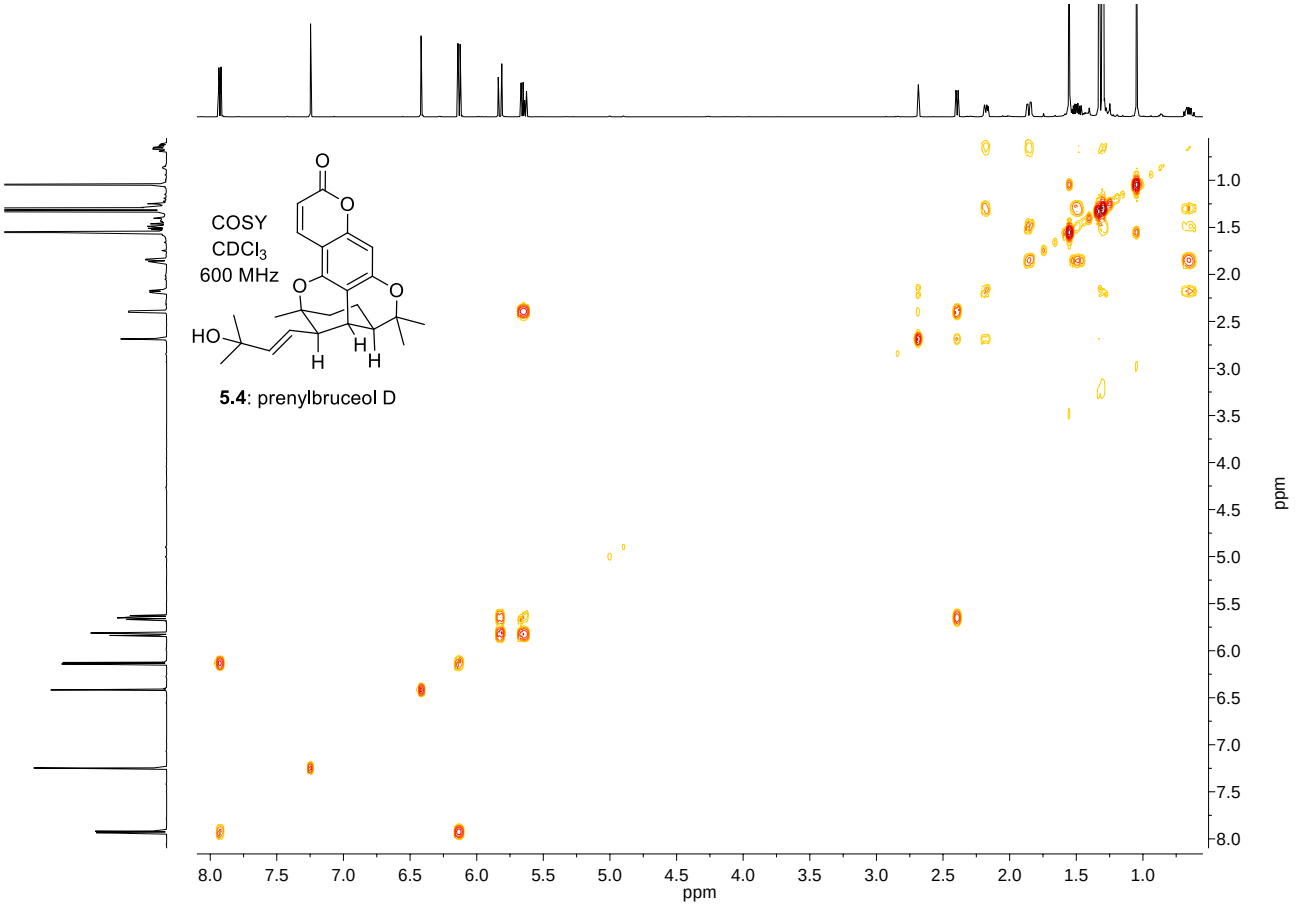
COSY
CDCl3
600 MHz
HO
H
H
H
O
O
O
O
5.4: prenylbruceol D
ppm
ppm

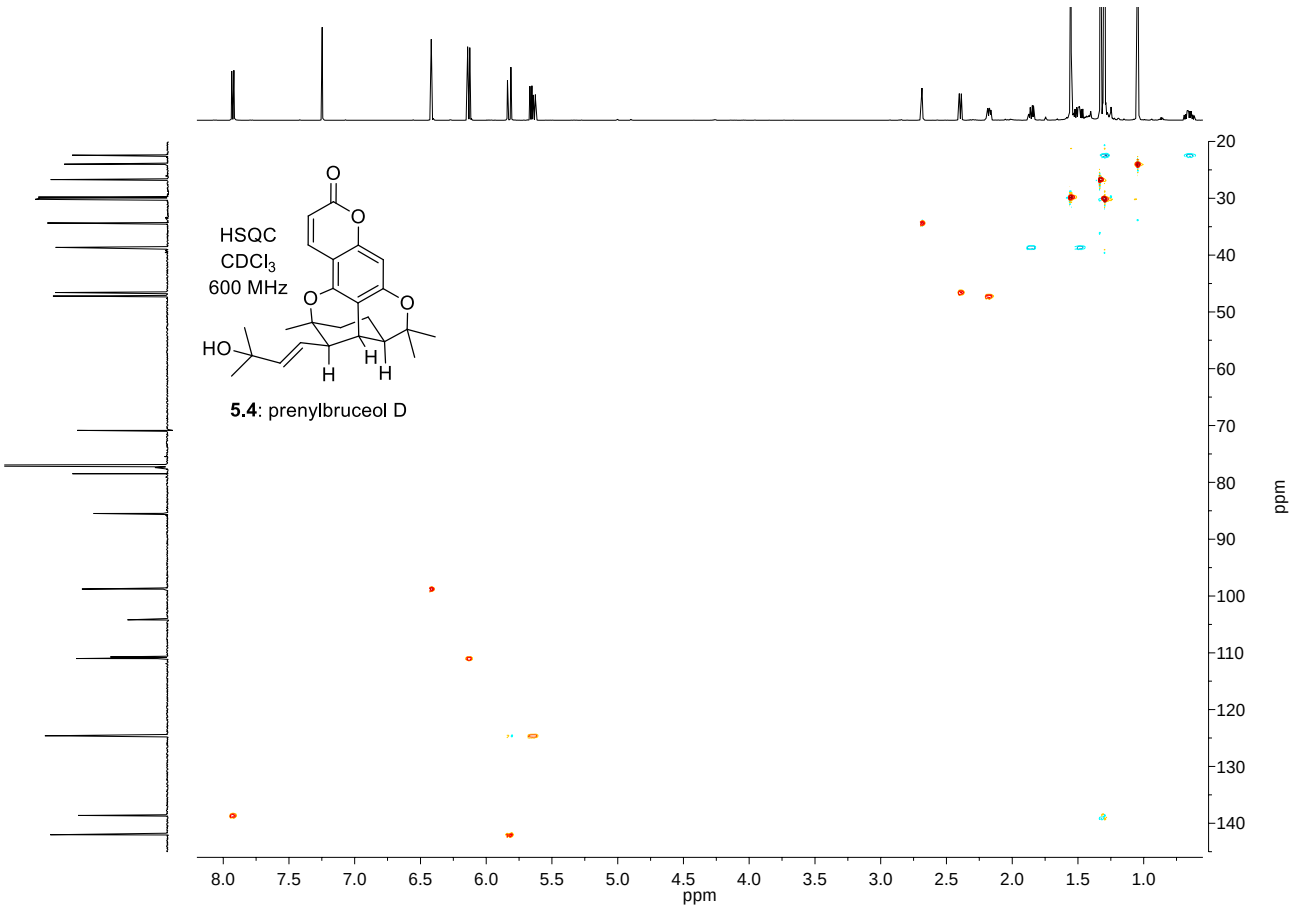
HSQC
CDCl3
600 MHz
HO
H
H
H
O
O
O
O
5.4: prenylbruceol D
ppm
ppm

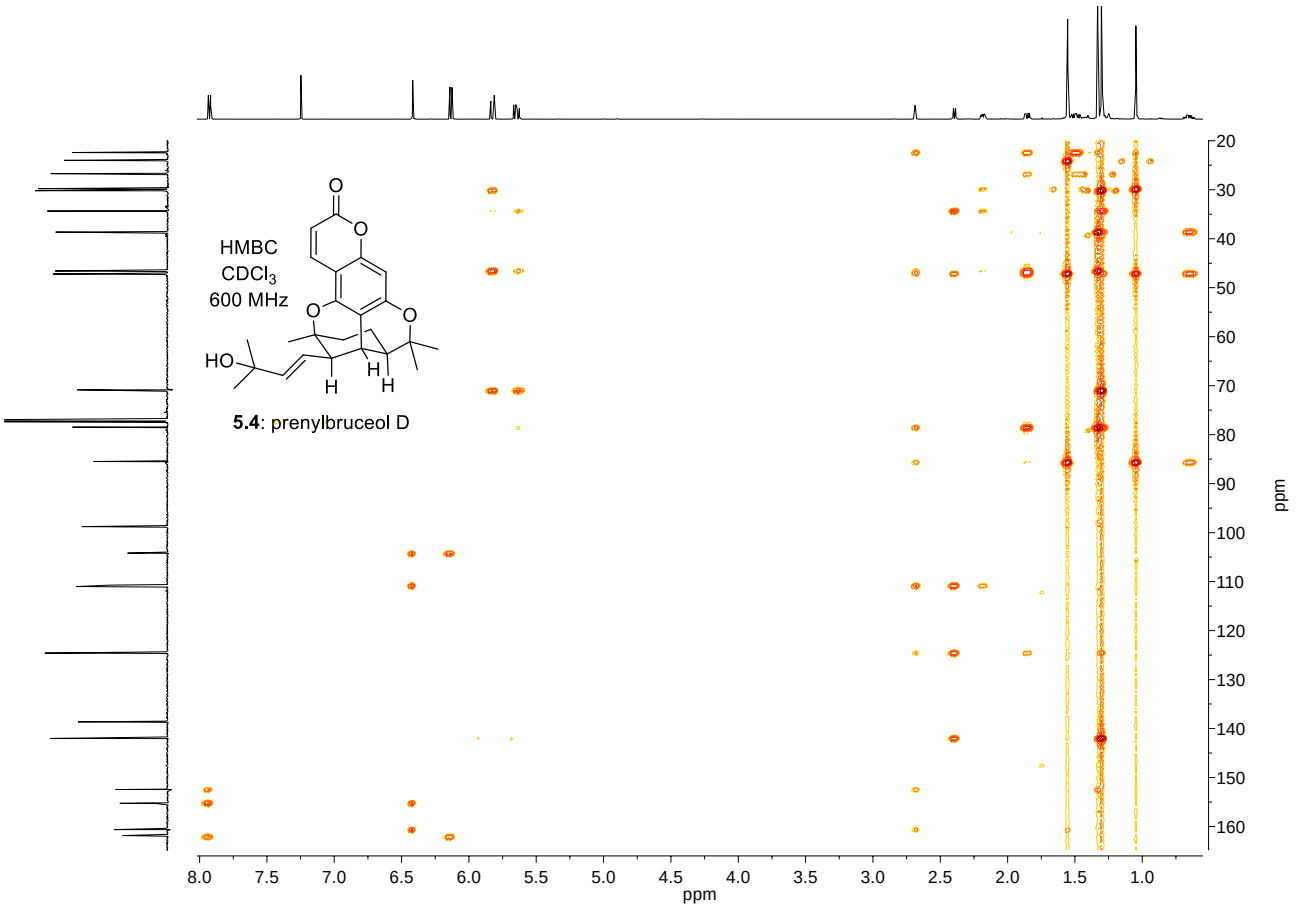
HMBC
CDCl3
600 MHz
5.4: prenylbruceol D
ppm
ppm

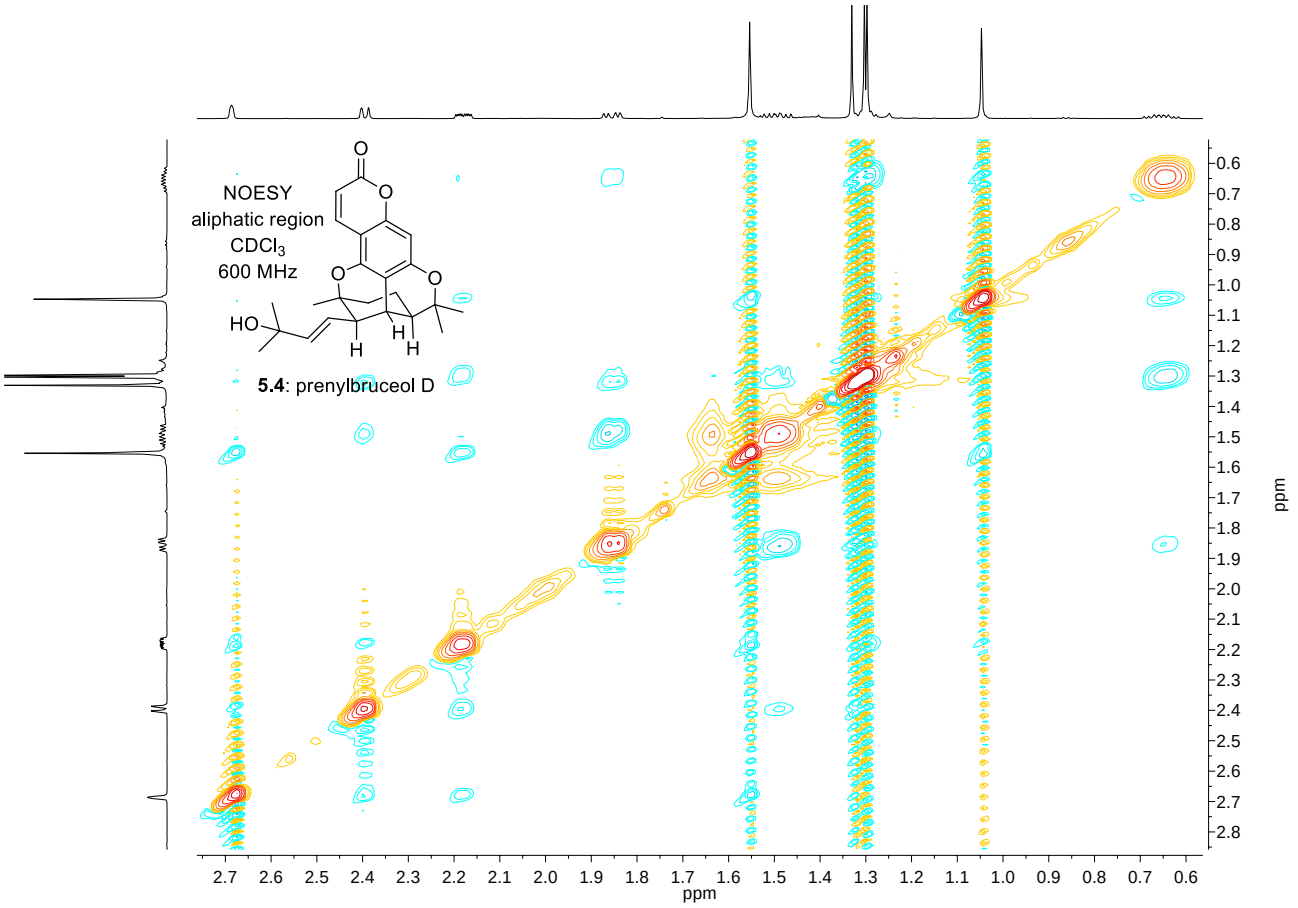
NOESY
aliphatic region
CDCl3
600 MHz
5.4: prenylbruceol D
ppm
ppm

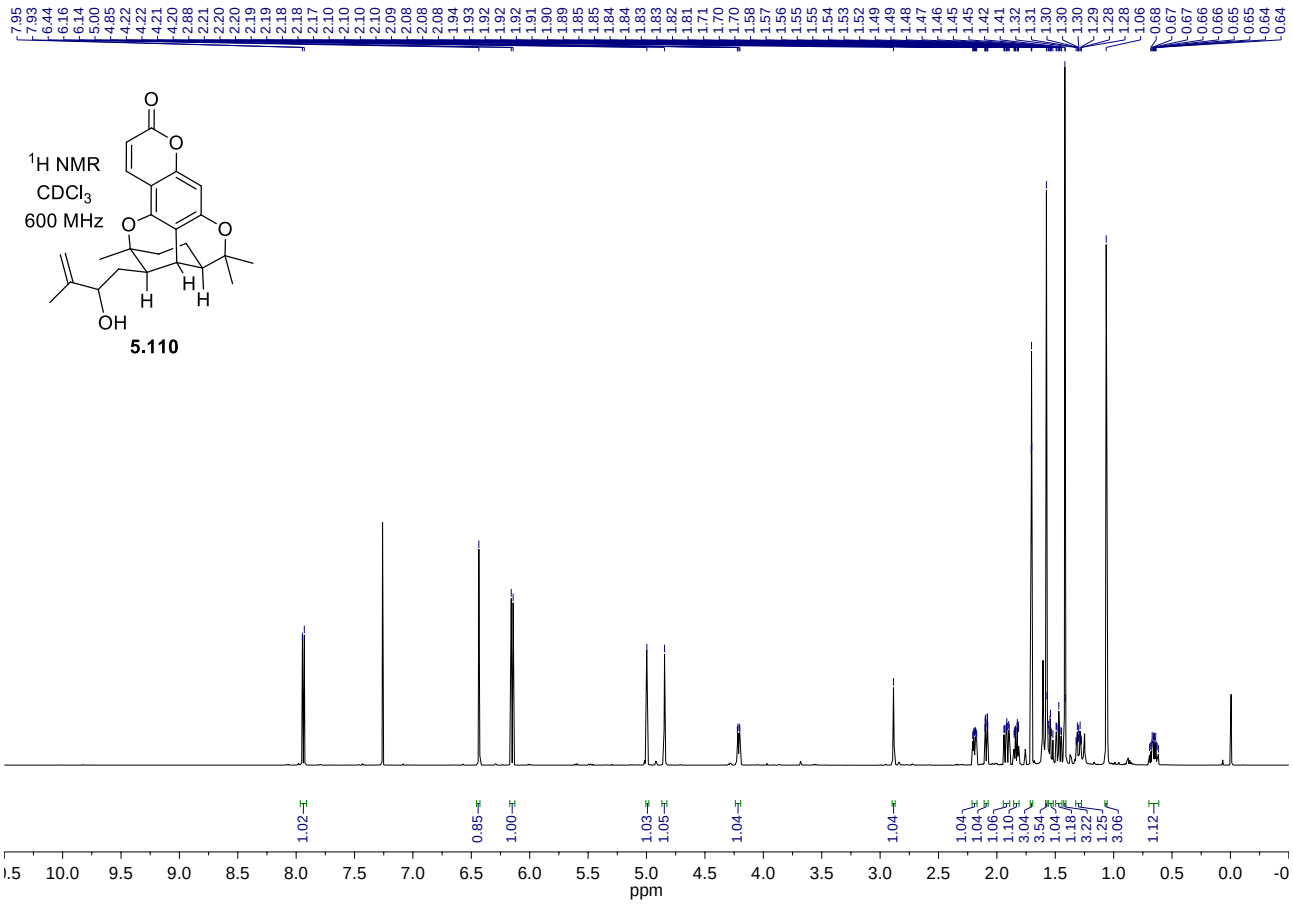
^{1}H NMR
$CDCl_3$
600 MHz
5.110
ppm

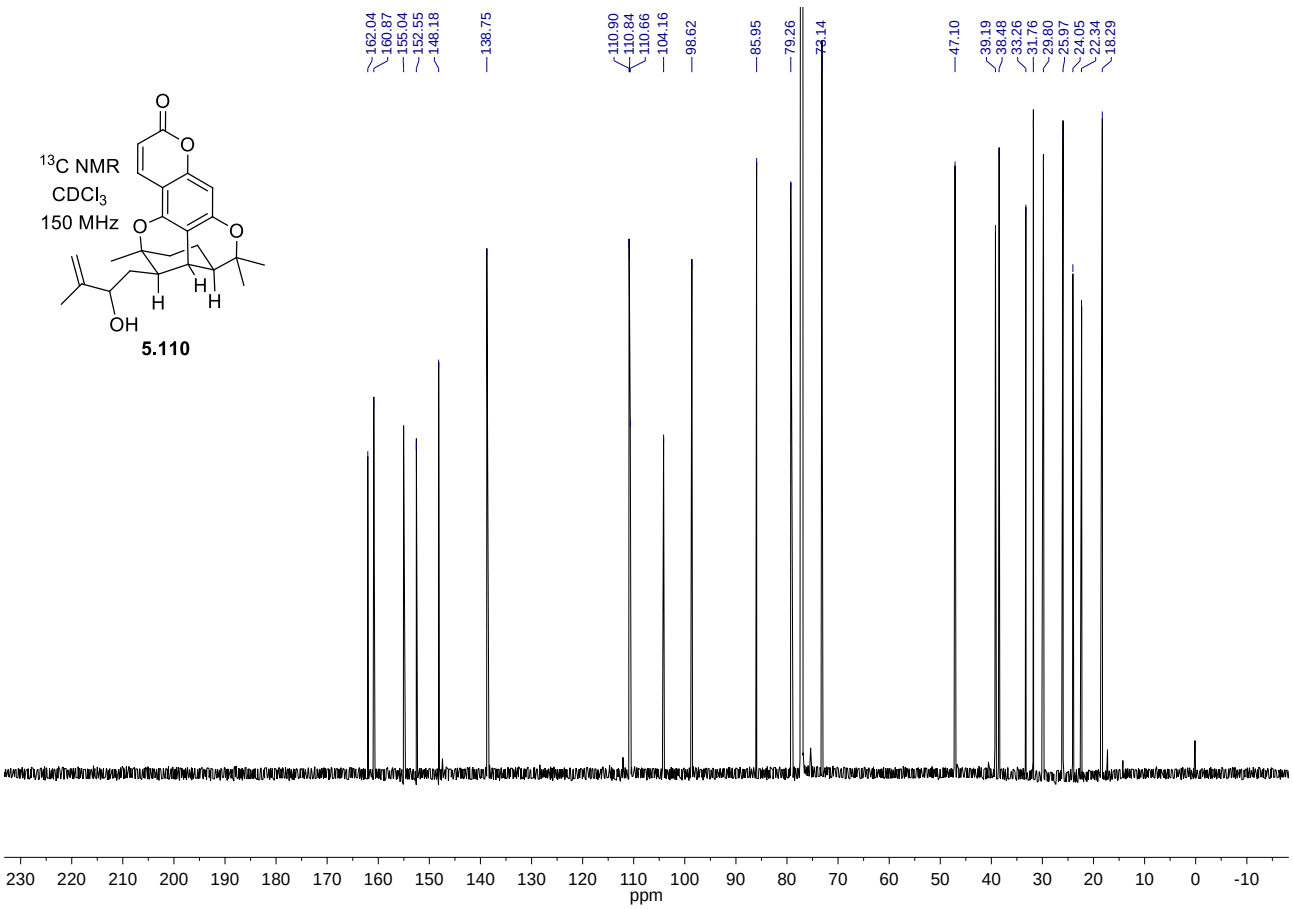
^{13}C NMR
$CDCl_3$
150 MHz
5.110
ppm

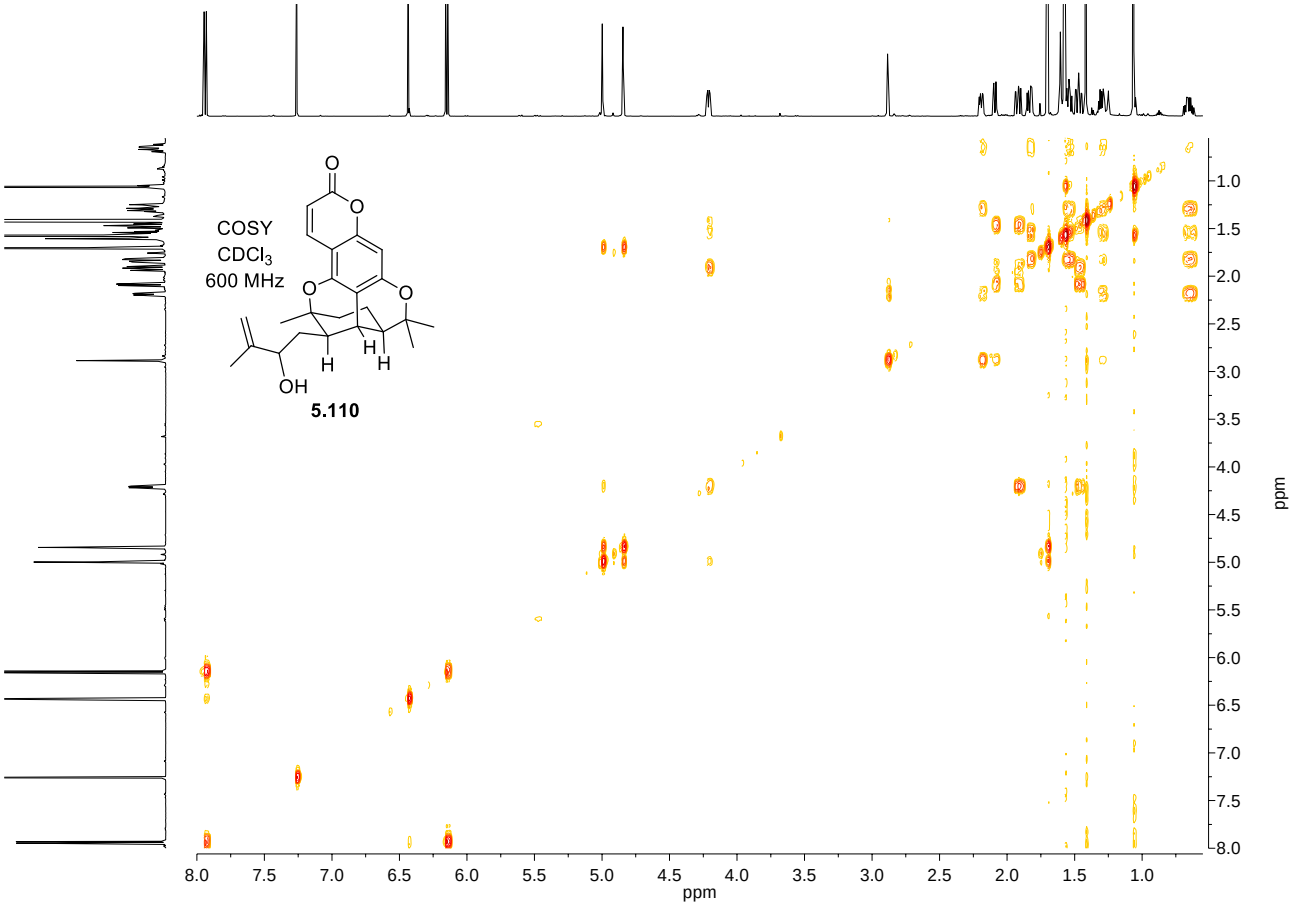
COSY
CDCl3
600 MHz
5.110
ppm
ppm

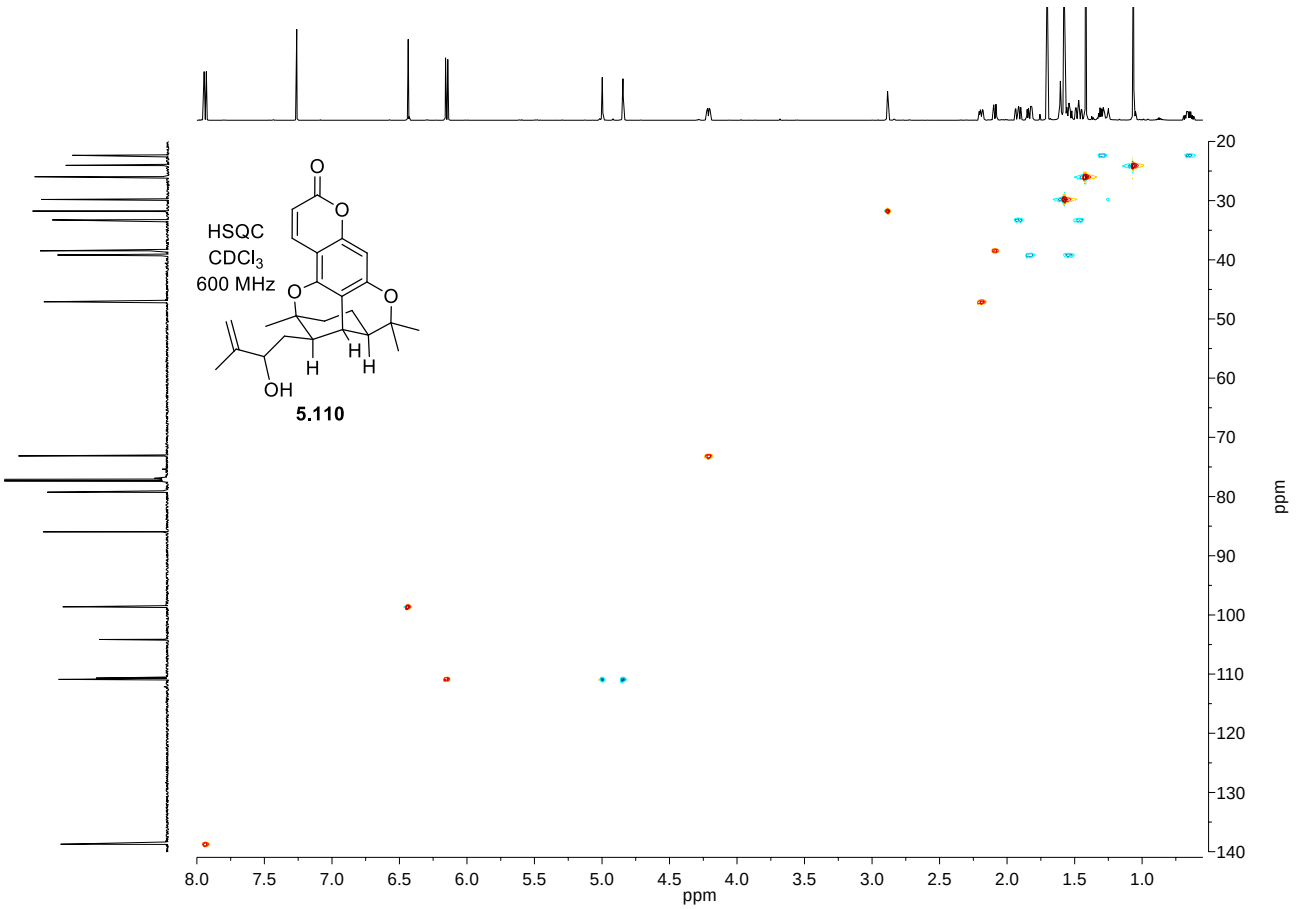
HSQC
CDCl3
600 MHz
5.110
ppm
ppm

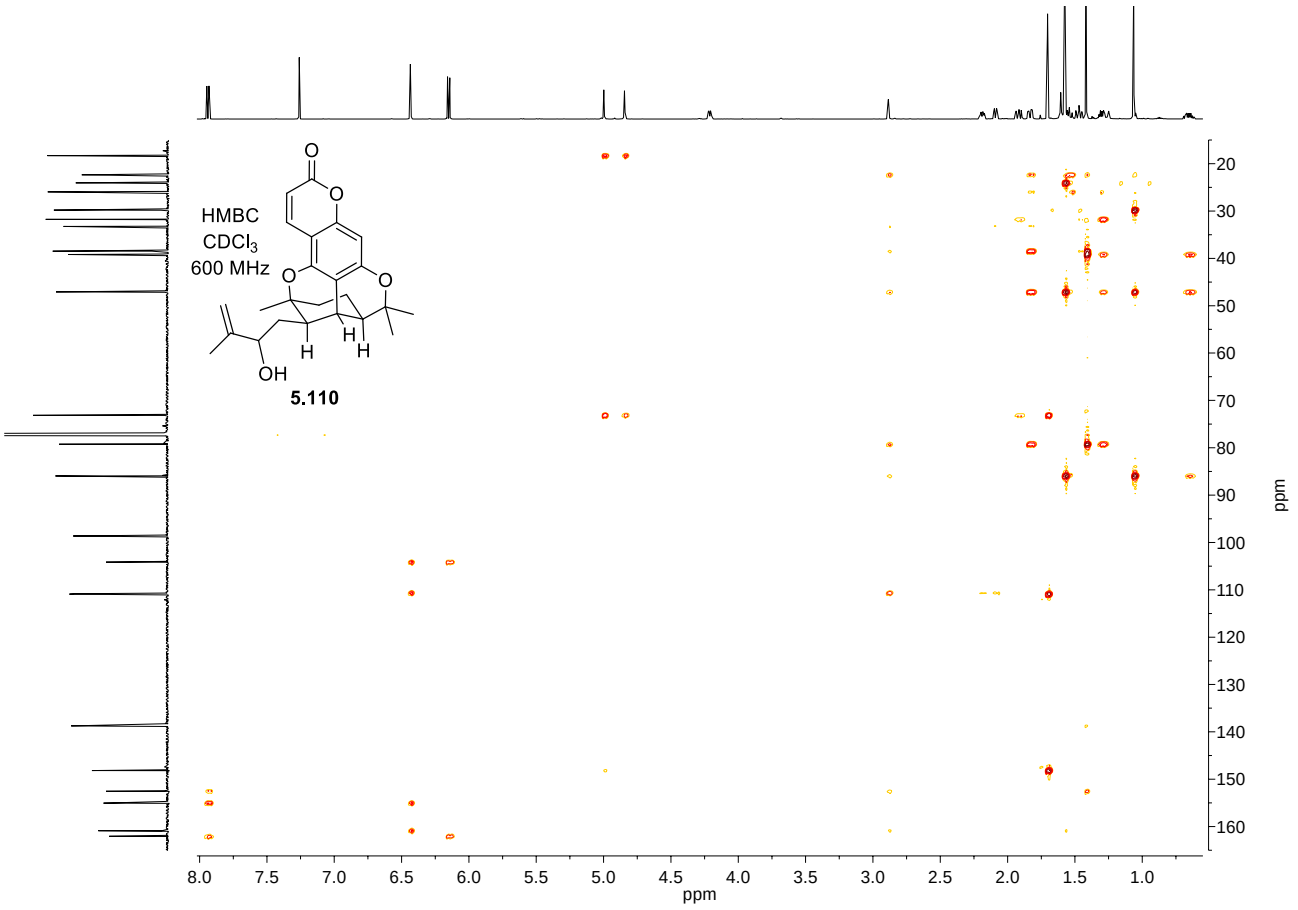
HMBC
CDCl3
600 MHz
OH
5.110
ppm
ppm

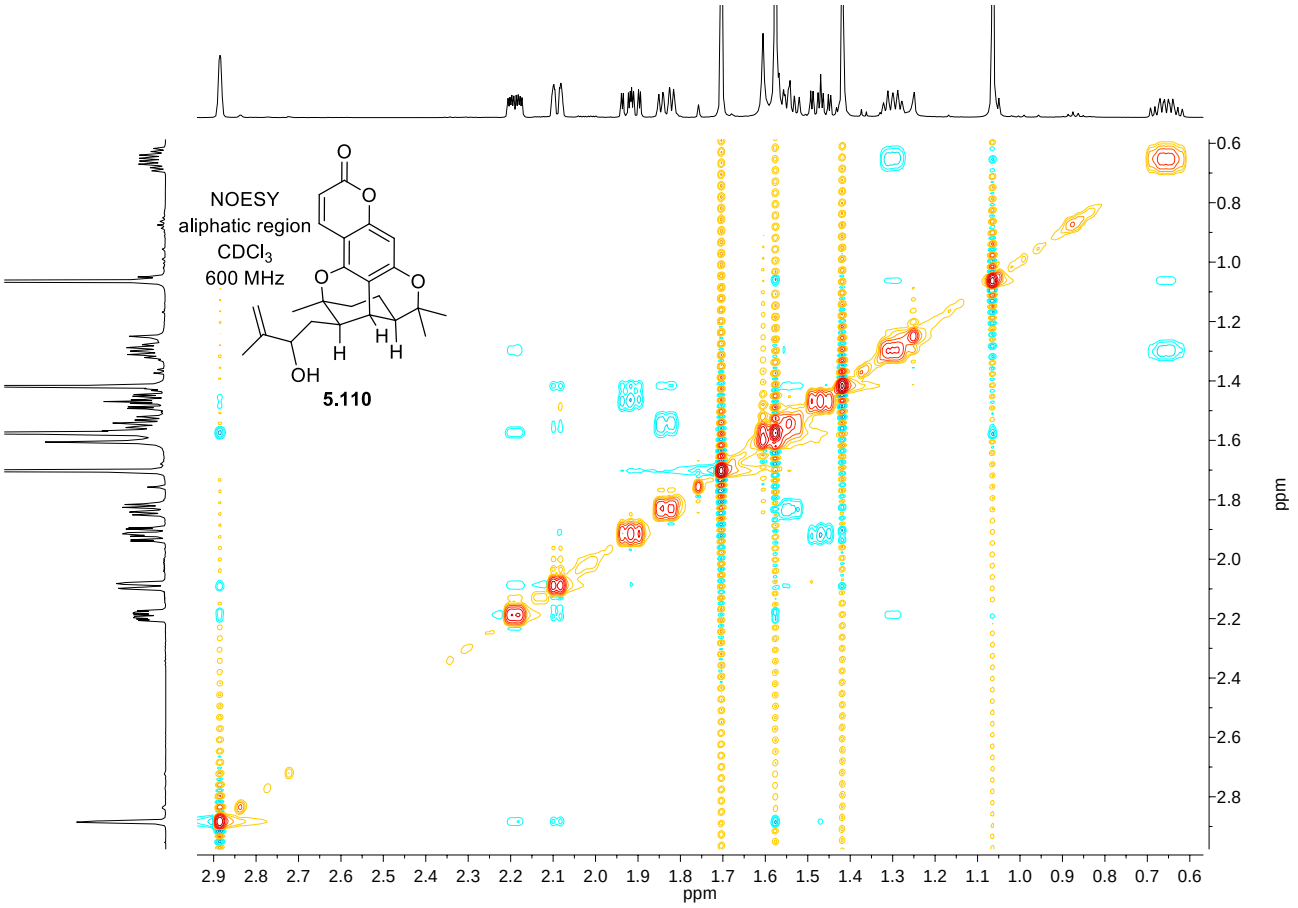
NOESY
aliphatic region
CDCl3
600 MHz
OH
5.110
ppm
ppm

5.4.4: ^{1}H and ^{13}C NMR Comparison Tables

Table 5.5: prenylbruceol B (**5.2**) ^{1}H NMR comparison

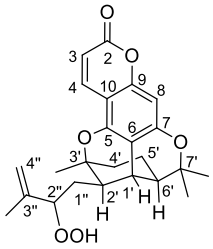

5.2: prenylbruceol B

	Waterman 1992 400 MHz ($CDCl_3$)[1]	George 2019 600 MHz ($CDCl_3$)
3	6.16 d (9.6)	6.15 d (9.6)
4	7.94 d (9.6)	7.93 dd (9.5, 0.7)
8	6.45 s	6.44 d (0.6)
1’	2.85 s	2.84 br s
2’-ax.	2.03 dd (10, 1.4)	2.04 – 2.02 m (overlapped)
3’-Me	1.42 s	1.41 s
4’-ax.	1.54 m	1.56 – 1.50 m
4’-eq.	1.84 dd (15.2, 6.1)	1.83 dd (15.2, 5.0)
5’-ax.*	0.66 ddd (26.5, 12.7, 5.9)	0.65 tdd (13.5, 11.5, 6.3)
5’-eq.	1.31 m	1.33 – 1.28 m
6’	2.21 m	2.21 ddd (11.7, 5.4, 2.8)
7’-Me	1.08 s	1.07 s
7’-Me	1.60 s	1.59 s
1’’	2.01 m	2.04 – 1.99 m (overlapped)
1’’	1.46 m	1.44 – 1.39 m (overlapped)
2’’	4.49 m	4.48 dd (10.3, 3.5)
2’’OOH	7.97 br s	7.96 s
3’’-Me	1.74 s	1.73 s
4’’	5.08 s	5.07 m
4’’	5.04 s	5.03 m

Note: CDCl3 reference to 7.27 ppm, whereas we reference to 7.26.

Table 5.6: prenylbruceol B (**5.2**) ^{13}C NMR comparison

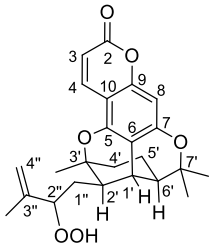

5.2: prenylbruceol B

	Waterman 1992 100 MHz ($CDCl_3$)[1]	George 2019 150 MHz ($CDCl_3$)
2	162.1	162.0
3	111.1	111.0
4	138.7	138.7
5	152.5	152.4
6	110.4	110.4
7	161.0	160.9
8	98.9	98.8
9	155.2	155.1
10	104.2	104.2
1’	26.0	25.9
2’	39.2	39.1
3’	79.1	79.0
3’-Me	32.4	32.3
4’	38.7	38.6
5’	22.4	22.3
6’	47.1	47.0
7’	86.1	86.0
7’-Me	24.1	24.0
7’-Me	29.9	29.8
1’’	30.2	30.1
2’’	87.0	86.9
3’’	143.9	143.8
3’’-Me	18.0	18.0
4’’	114.3	114.2

Note: referenced to $CDCl_3$ at 77.23, whereas we reference to 77.16

Table 5.7: prenylbruceol C (**5.3**) ^{1}H NMR comparison

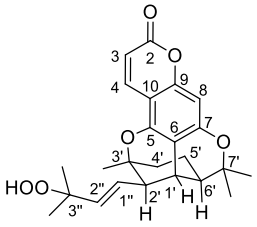

5.3: prenylbruceol C

	Waterman 1992 400 MHz ($CDCl_3$)[1]	George 2019 600 MHz ($CDCl_3$)
3	6.18 d (9.6)	6.17 d (9.6)
4	7.96 d (9.6)	7.96 d (9.6)
8	6.46 s	6.45 s
1’	2.73 s	2.71 br s
2’-ax.	2.46 dd (9.1, 1.0)	2.45 dd (9.3, 1.4)
3’-Me	1.36 s	1.34 (s, 3H),
4’-ax.	1.53 m	1.51 (ddd, *J* = 15.2, 13.1, 6.9
4’-eq.	1.89 dd (15.8, 6.4)	1.87 (dd, *J* = 15.0, 5.7
5’-ax.*	0.67 ddd (26.7, 12.8, 6.0)	0.65 (tdd, *J* = 13.5, 11.6, 6.2 Hz, 1H).
5’-eq.	1.33 m	1.34 – 1.29 m overlapped
6’	2.22 ddd	2.20 (ddd, *J* = 11.7, 5.4, 2.8 Hz
7’-Me	1.07, s	1.06
7’-Me	1.58, s	1.57
1’’	5.68 dd (15.8, 9.1)	5.66 dd (15.9, 9.3)
2’’	5.82 d	5.81 d (5.8)
3’’-OOH	7.43 br s	7.50 (br s, 1H)
3’’-Me	1.35 s	1.32
3’’-Me	1.33 s	1.33

Note: $CDCl_3$ reference to 7.27 ppm, whereas we reference to 7.26.

*Waterman has misinterpreted this multiplet, it is a tdd

Table 5.8: prenylbruceol C (**5.3**) ^{13}C NMR comparison

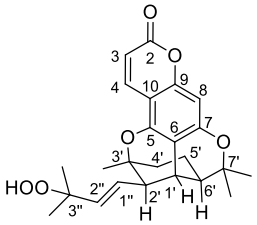

5.3: prenylbruceol C

	Waterman 1992 100 MHz ($CDCl_3$)[1]	George 2019 150 MHz ($CDCl_3$)
2	162.0	162.0
3	111.1	111.0
4	138.8	138.8
5	152.4	152.3
6	110.8	110.7
7	160.7	160.5
8	99.0	98.9
9	155.3	155.1
10	104.3	104.2
1’	34.2	34.1
2’	46.9	46.8
3’	78.5	78.4
3’-Me	26.9	26.8
4’	38.6	38.5
5’	22.4	22.3
6’	47.1	47.0
7’	85.6	85.6
7’-Me	24.6	24.0
7’-Me	29.8	29.7
1’’	128.7	128.6
2’’	137.6	137.5
3’’	82.4	82.3
3’’-Me	24.5	24.5
3’’-Me	24.6	24.5

Note: referenced to $CDCl_3$ at 77.23, whereas we reference to 77.16

Table 5.9: prenylbruceol D (**5.4**) ^{1}H NMR comparison

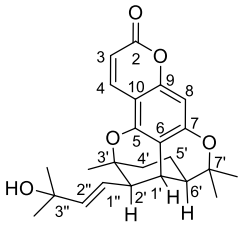

5.4: prenylbruceol D

	Waterman 1992 400 MHz ($CDCl_3$)[1]	George 2019 600 MHz ($CDCl_3$)
3	6.17 d (9.6)	6.15 d (9.6)
4	7.96 d (9.6)	7.94 dd (9.4, 0.6)
8	6.45 s	6.43 s
1’	2.70 s	2.70 br s
2’-ax.	2.42 dd (9.2, 1.0)	2.41 dd (9.2, 1.4)
3’-Me	1.35 s	1.34 s
4’-ax.	1.52 m	1.55 – 1.48 m
4’-eq.	1.88 dd (14.9, 5.5)	1.87 dd (15.3, 5.0)
5’-ax. *	0.68 ddd (26.7, 12.8, 6.0)	0.67 tdd (13.4, 11.5, 6.3)
5’-eq.	1.30 m	1.32 – 1.27 m overlapped
6’	2.21 ddd (11.6, 5.4, 2.8)	2.19 ddd (11.5, 5.4, 2.8)
7’-Me	1.07 s	1.06 s
7’-Me	1.58 s	1.57 s
1’’	5.65 dd (15.6, 9.3)	5.66 dd (15.6, 9.2)
2’’	5.85 d (15.6)	5.84 d (15.7)
3’’-Me	1.33 s	1.32 s
3’’-Me	1.32 s	1.31 s

Note: $CDCl_3$ reference to 7.27 ppm, whereas we reference to 7.26.

Table 5.10: prenylbruceol D (**5.4**) ^{13}C NMR comparison

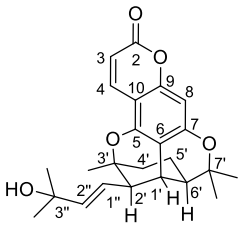

5.4: prenylbruceol D

	Waterman 1992 100 MHz ($CDCl_3$)[1]	George 2019 150 MHz ($CDCl_3$)
2	162.1	161.8
3	111.1	111.0
4	138.8	138.6
5	152.5	152.4
6	110.8	110.7
7	160.6	160.6
8	98.2	98.8
9	155.2	155.3
10	104.3	104.2
1’	34.3	34.4
2’	46.6	46.6
3’	78.5	78.5
3’-Me	26.8	26.7
4’	38.6	38.6
5’	22.4	22.4
6’	47.1	47.2
7’	85.6	85.5
7’-Me	24.1	24.0
7’-Me	29.8	29.8
1’’	124.6	124.6
2’’	142.0	142.0
3’’	71.0	70.9
3’’-Me	30.2	30.2
3’’-Me	30.1	30.0

Note: referenced to $CDCl_3$ at 77.23, whereas we reference to 77.16

Table 5.11: 1H and 13C NMR assignment of **5.108**

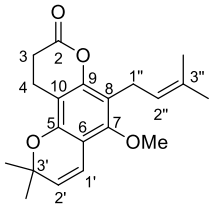

5.108
(natural)

	dihydrocoumarin (**5.108**)		
	^{1}H	^{13}C	HMBC
2	-	168.7	-
3	2.70 dd (8.2, 6.4)	28.9	2, 4, 10
4	2.89 dd (8.2, 6.5)	17.5	2, 3, 5, 6, 8, 9, 10,
5	-	148.6	-
6	-	111.1	-
7	-	153.7	-
7-OMe	3.73 s	62.6	7
8	-	115.4	-
9	-	150.6	-
10	-	107.3	-
1’	6.53 d (10.0)	117.3	5, 6, 7, 10, 3’, 3’-Me,
2’	5.57 d (10.0)	129.1	5, 6, 3’, 3’-Me
3’	-	76.5	-
3’-Me ×2	1.42 s	28.1	5, 1’, 2’, 3’, 3’-Me
1’’	3.31 d (6.6)	22.6	7, 8, 9, 2’’, 3’’, 3’’-Me
2’’	5.17 t (7.1)	122.8	1’’, 3’’-Me, 3’’-Me
3’’	-	131.8	-
3’’-Me	1.79 s	18.0	8, 2’’, 3’, 3’’-Me
3’’-Me	1.67 s	25.9	8, 2’’, 3’, 3’’-Me

5.4.5 Single Crystal X-ray Diffraction Data

General experimental

Single crystals of each sample were mounted under paratone-N oil on a nylon loop, and X-ray diffraction data were collected at 150(2) K with Mo Kα radiation (λ = 0.7107 Å) on an Oxford Diffraction X-calibur small molecule diffractometer.[20] The data sets were corrected for absorption, the structures solved by direct methods using SHELXS-2014 and refined by full matrix least-squares on F^2 by SHELXL-2014, interfaced through the programs X-Seed and/or Olex.[21] In general, all non-hydrogen atoms were refined anisotropically, and hydrogen atoms were included as invariants at geometrically estimated positions. Details of data collection and structure refinement are given below (Table SI-12 and Figures). CCDC numbers 1958707-1958710 contain the supplementary crystallographic data for this paper. These data can be obtained free of charge from The Cambridge Crystallographic Data Centre via www.ccdc.cam.ac.uk/data_request/cif.

Specific refinement details

100a. Compounds **100b** and **101a** are isomorphous but not isostructural. A small residual amount of **100b** has co-crystallised with **100a** resulting in a peak in the electron density map adjacent to atom C3. This was refined satisfactorily as a low occupancy bromine atom (2.5% occupancy) at this position consistent with co-crystallisation.

Table 5.12: X-ray experimental data for **101a**, and **100a**

Compound	**101a**	**100a**
Data code	Br2epicitran	Br2citran
CCDC #	1958708	1958709
Empirical formula	$C_{19}H_{18}Br_2O_4$	$C_{19}H_{17.98}O_4Br_{2.02}$
Formula weight	470.15	472.13
Crystal system	triclinic	monoclinic
Space group	P-1	$P2_1/c$
a/Å	7.0199(2)	11.3644(6)
b/Å	8.2476(2)	8.7153(5)
c/Å	15.7704(4)	17.5002(11)
α/°	88.837(2)	90
β/°	78.506(2)	90.885(5)
γ/°	76.606(3)	90
Volume/Å^3	870.10(4)	1733.09(17)
Z	2	4
ρ_{calc}g/cm^3	1.795	1.809
μ/mm^{-1}	4.680	4.757
F(000)	468.0	939.0
Crystal size/mm^3	0.40 × 0.30 × 0.11	0.47 × 0.32 × 0.23
2θ range for data collection/°	6.966 to 58.762	7.172 to 58.756
Reflections collected	30830	20229
Independent reflections	4360 [R_{int} = 0.0573]	4303 [R_{int} = 0.0361]
Data/restraints/parameters	4360/0/229	4303/1/239
Goodness-of-fit on F^2	1.057	1.044
Final R indexes [I>=2σ (I)]	R_1 = 0.0367, wR_2 = 0.0719	R_1 = 0.0323, wR_2 = 0.0684
Final R indexes [all data]	R_1 = 0.0567, wR_2 = 0.0777	R_1 = 0.0464, wR_2 = 0.0738
Largest diff. peak/hole / e Å^{-3}	0.72/-0.50	0.97/-0.57

Table 5.13: X-ray experimental data for **100b**.

Compound	**100b**
Data code	Br3citran
CCDC #	1958710
Empirical formula	$C_{19}H_{17}O_4Br_3$
Formula weight	549.05
Crystal system	monoclinic
Space group	$P2_1/c$
a/Å	11.2865(2)
b/Å	8.9228(2)
c/Å	18.4922(4)
α/°	90
β/°	95.950(2)
γ/°	90
Volume/Å^3	1852.26(7)
Z	4
ρ_{calc}g/cm^3	1.969
μ/mm^{-1}	6.556
F(000)	1072.0
Crystal size/mm^3	0.44 × 0.30 × 0.18
2θ range for data collection/°	7.094 to 58.538
Reflections collected	21055
Independent reflections	4533 [R_{int} = 0.0388]
Data/restraints/parameters	4533/0/238
Goodness-of-fit on F^2	1.044
Final R indexes [I>=2σ (I)]	R_1 = 0.0315, wR_2 = 0.0620
Final R indexes [all data]	R_1 = 0.0475, wR_2 = 0.0672
Largest diff. peak/hole / e Å^{-3}	0.80/-0.58

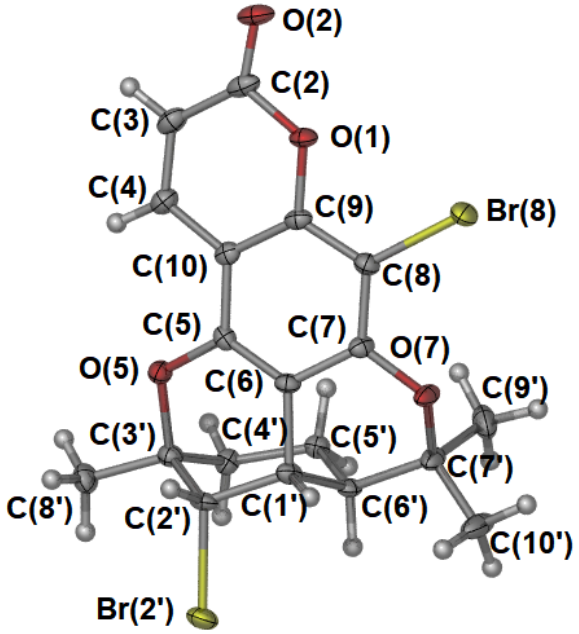

Figure 5.8: A representation of the structure of **101a** with ellipsoids presented with 50% probability level. Carbon - grey; hydrogen - white; oxygen - red; and bromine - yellow. Single crystals were grown from a petrol/ethyl acetate mixture.

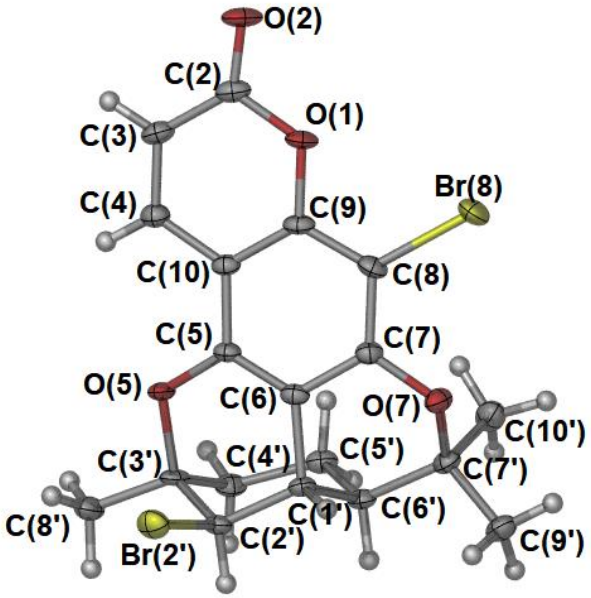

Figure 5.9: A representation of the structure of **100a** with ellipsoids presented with 50% probability level. Carbon - grey; hydrogen - white; oxygen - red; and bromine - yellow. The disorder arising from co-crystallisation is not shown. Single crystals were grown from a petrol/ethyl acetate mixture.

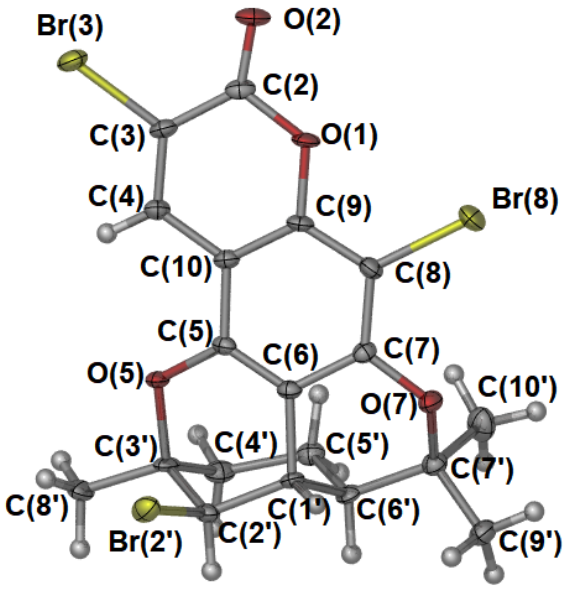

Figure 5.10: A representation of the structure of **100b** with ellipsoids presented with 50% probability level. Carbon - grey; hydrogen - white; oxygen - red; and bromine - yellow. Single crystals were grown from a petrol/ethyl acetate mixture.

5.5 References

[1] Sarker, S. D.; Armstrong, J. A.; Gray, A. I.; Waterman, P. G. *Phytochemistry* **1994**, *37*, 1287.

[2] Ghisalberti, E. L. *Phytochemistry* **1998**, *47*, 163.

[3] For a review of natural product artifacts: Capon, R. J. *Nat. Prod. Rep.* **2020**, *37*, 55.

[4] Herz, W.; Grisebach, H.; Kirby, G. W.; Gotlieb, O. R.; Herrman, K.; Murray, R. D. H.; Ohloff, G.; Pattenden, G. *Progress in the Chemistry of Organic Natural Products, Vol 35*, **1978**, Wien Springer-Verlag (New York).

[5] Hata, K.; Koawa, M. *Yakagaku Zasshi*, **1967**, *88*, 283.

[6] Saki, Y.; Moringa, K.; Okegawa, O.; Sakai, S.; Amaya, Y.; Ueno, A.; Fukushima, S. *Yakagaku Zasshi* **1971**, *91*, 1313.

[7] Markwell-Heys, A. W.; Kuan, K. K. W.; George, J. H. *Org. Lett.* **2015**, *17*, 4228.

[8] Chan, J. A.; Freyer, A. J.; Carté, B. K.; Hemling, M. E.; Hofmann, G. A.; Mattern, M. R.; Mentzer, M. A.; Westley, J. W. *J. Nat. Prod.* **1994**, *57*, 1543.

[9] Markwell-Heys, A. W.; George, J. H. *Org. Biomol. Chem.* **2016**, *14*, 5546.

[10] Mei, Q.; Wang, C.; Zhao, Z.; Yuan, W.; Zhang, G.; *Beilstein J. Org. Chem.* **2015**, *11*, 1220.

[11] Cairns, N.; Harwood, L. M.; Astles, D. P. *J. Chem. Soc. Perkin Trans I* **1994**, 3101.

[12] Murray, R. D. H.; Jorge, Z. D. *Tetrahedron*, **1984**, *40*, 3129.

[13] Farmer, J. L.; Hunter, H. N.; Organ, M. G. *J. Am. Chem. Soc.* **2012**, *134*, 17470.

[14] Snyder, S. A.; Treitler, D. S. *Angew. Chem. Int. Ed.* **2009**, *48*, 7899.

[15] Stratakis, M.; Orfanopoulos, M. *Tetrahedron Lett.* **1997**, *38*, 1067.

[16] Dale, J. A.; Dull, D. L.; Mosher, H. S. *J. Org. Chem.* **1969**, *34*, 2543.

[17] Shibuya, M.; Ito, S.; Takahashi, M.; Iwabuchi, Y. *Org. Lett.* **2004**, *6*, 4303.

[18] More, J. D.; Finney, N. S. *Org. Lett.* **2002**, *4*, 3001.

[19] Ruchti, J.; Carreira, E. M. **2014** *J. Am. Chem. Soc.* 136, *48*, 16756

[20] CrysAlisPro, CrysAlis171.NET, Verson 1.171.34.44, Oxford Diffraction Ltd: Oxfordshire, U.K., **2010**.

[21] (a) G. M. Sheldrick, Phase Annealing in SHELX-90: Direct Methods for Large Structures. *Acta Crystallog.*, **1990**, A46, 467. (b) G. M. Sheldrick, SHELXL-2014, University of Göttingen, Göttingen, Germany, **2014**. (c) L. J. Barbour, X-Seed – A Software Tool for Supramolecular Crystallography, *J. Supramol. Chem.* **2001**, *1*, 189. (d) O. V. Dolomanov, L. J. Bourhis, R. J. Gildea, J. A. K. Howard, and H. Puschmann, *J. Appl. Cryst*. **2009**, *42*, 339.